NOAA Technical Report NOS OES 003

LONG ISLAND SOUND OCEANOGRAPHY PROJECT

SUMMARY REPORT, VOLUME 2:

RESIDUAL CIRCULATION AND THERMOHALINE STRUCTURE

Silver Spring, Maryland
January 1994

noaa National Oceanic and Atmospheric Administration

U.S. DEPARTMENT OF COMMERCE
National Ocean Service
Office of Ocean and Earth Sciences
Marine Analysis and Interpretation Division
Coastal and Estuarine Oceanography Branch

Office of Ocean and Earth Science
National Ocean Service
National Oceanic and Atmospheric Administration
U.S. Department of Commerce

The Office of Ocean and Earth Sciences provides for the understanding of the coastal and ocean environment through the conduct of applied research and development in geophysics; the measurement, analyses, and product development of ocean and lake water levels; the collection, analyses, product development, and dissemination of coastal and global marine data; and the synthesis and interpretation with numerical and mechanistic modeling of global marine data sets. The Office cooperates with the U.S. Navy in conducting oceanographic activities for defense and mixed defense-civil sector purposes and applications.

It plans, develops and coordinates NOAA participation in Federally conducted oceanographic programs and activities, and facilitates cooperative programs, projects and activities with the oceanographic research community. It monitors and analyzes oceanographic activities between NOAA and other organizations and agencies; identifies potential conflicts, overlaps, and opportunities for joint or cooperative efforts; and develops and maintains cooperative agreements, Memoranda of Understanding and other arrangements as appropriate to resolve issues and to ensure maximum benefits from programs of mutual interest. It develops and maintains inventories of oceanographic programs, projects, systems and activities of other organizations and agencies to provide a basis for integrating current and future programs, systems and activities to ensure maximum efficiency and effectiveness in meeting national goals and requirements. The Office conducts research and development; carries out theoretical studies, data analyses, and engineering development; and formulates and executes programs encompassing technological development and application to oceanography, geophysics, geodesy, and related fields .

For the Great Lakes, coastal estuaries, sea coast and oceans, the Office plans, develops, and applies numerical and mechanistic models and produces predictions, forecasts, and analysis guidance materials of oceanographic and related marine meteorological phenomena; collects, analyzes and disseminates tide and water-level observations and associated information; and computes water-level datums for hydrographic, marine boundary and other special surveys. It evaluates and improves methods of data analysis; compares and integrates existing and new classes of data and products; provides and quality controls data sets and an array of output products; and assures science and technology transfer to and from the Office's programs and projects. The Office produces and disseminates operational marine environmental forecast and analysis guidance materials; manages and supports ocean climate studies; installs and operates real-time marine data collection systems; and formulates requirements for marine data sets and for data processing and communications systems; and designs and manages computer-based systems in support of these requirements.

NOAA Technical Report NOS OES 003

LONG ISLAND SOUND OCEANOGRAPHY PROJECT

SUMMARY REPORT, VOLUME 2:

RESIDUAL CIRCULATION AND THERMOHALINE STRUCTURE

Richard A. Schmalz, Jr.
Michael F. Devine
Philip H. Richardson

January 1994

U.S. DEPARTMENT
OF COMMERCE
Ronald H. Brown, Secretary

National Oceanic and
Atmospheric Administration
D. James Baker, Under Secretary

National Ocean Service
W. Stanley Wilson
Assistant Administrator

Office of Ocean and
Earth Sciences
Melbourne G. Briscoe

Marine Analysis and
Interpretation Division
Ledolph Baer

Coastal and Estuarine
Oceanography Branch
Bruce Parker

NOTICE

Mention of a commercial company or product does not constitute an endorsement by NOAA. Use for publicity or advertising purposes of information from the publication concerning proprietary products or the tests of such products is not authorized.

TABLE OF CONTENTS

LIST OF FIGURES

LIST OF TABLES

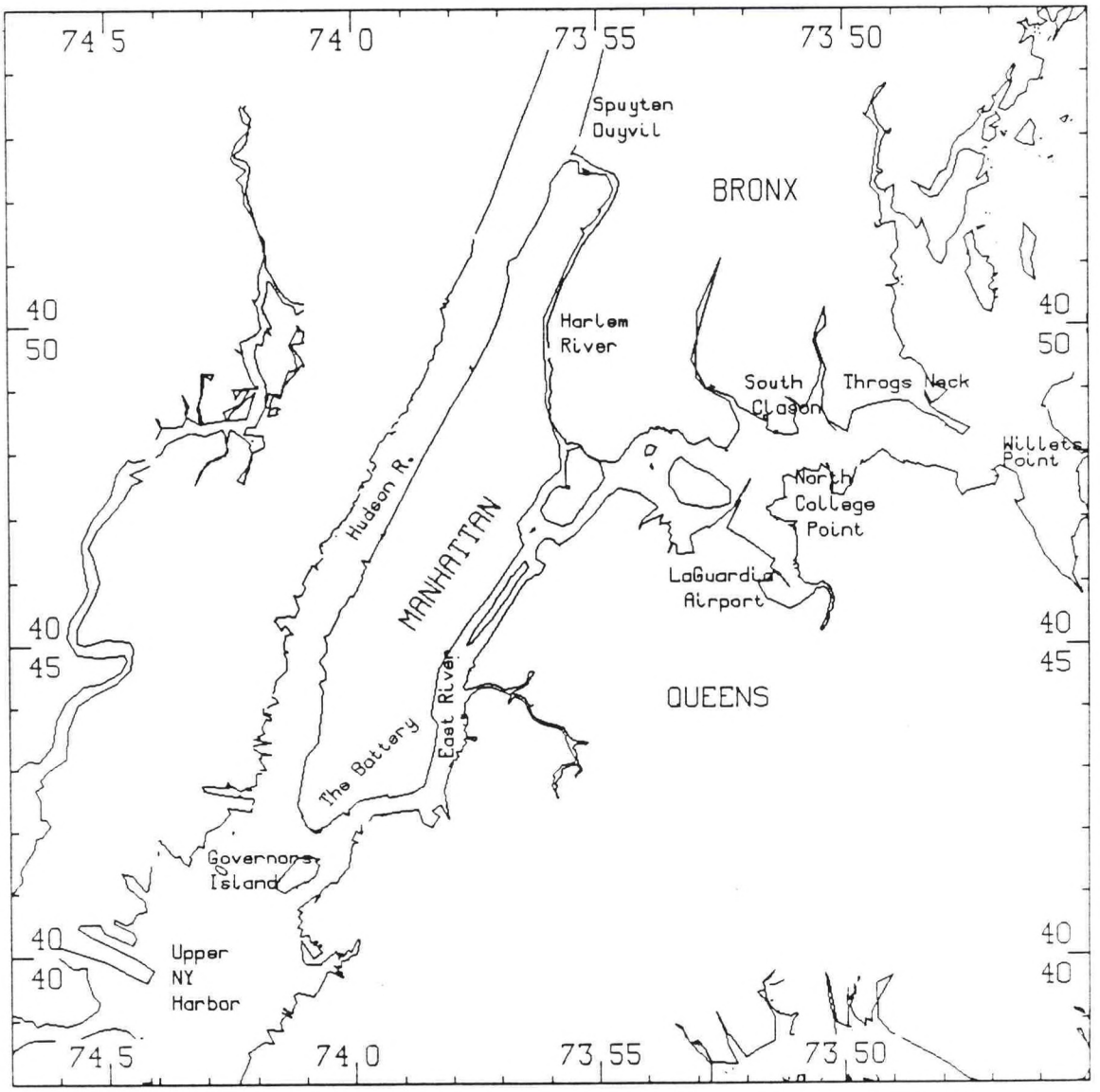

East and Harlem River Base Map

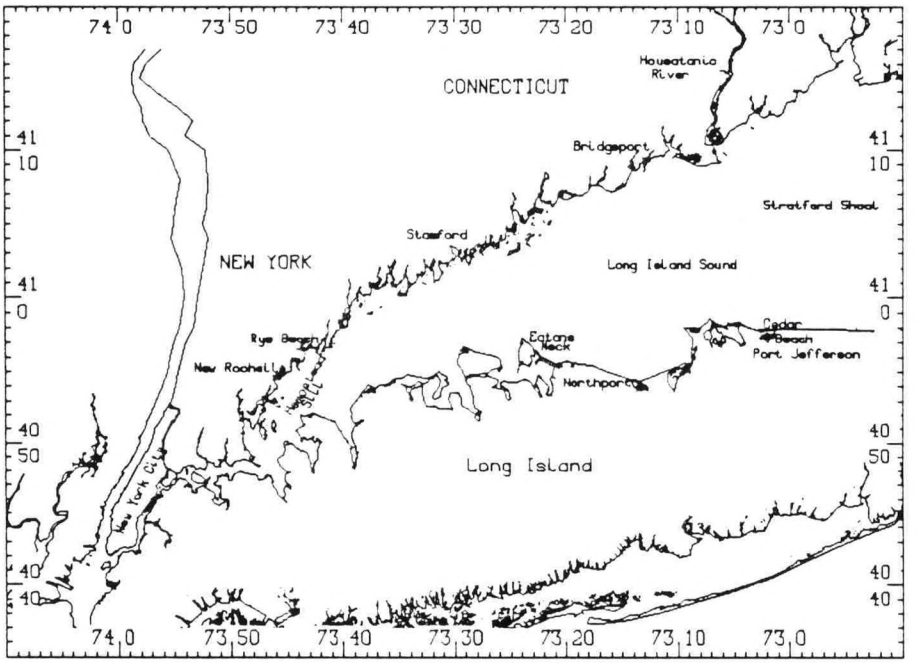

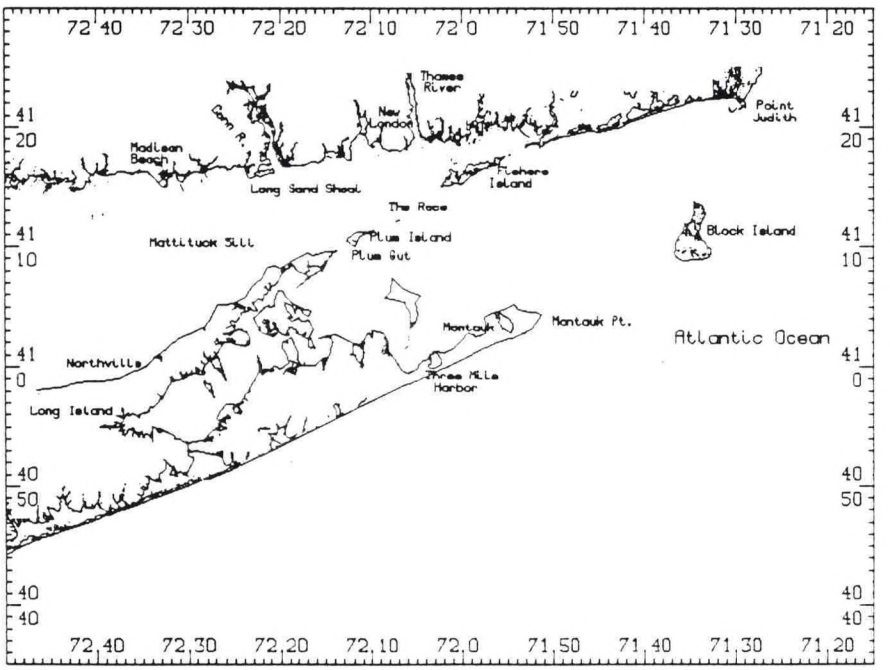

Long Island Sound Base Map

ABSTRACT

The National Oceanic and Atmospheric Administration's National Ocean Service (NOAA/NOS) Long Island Sound three-dimensional hydrodynamic model as documented in Volume 1 of this series is used to provide robust circulation patterns for water quality modeling studies supported by the United States Environmental Protection Agency (USEPA). This report, Volume 2, focuses on the simulation of the thermohaline and residual circulations in Long Island and Block Island Sounds during the period April 1988 to September 1989, which was chosen by EPA for water quality modeling. Volume 3 contains copies of scientific papers published elsewhere, primarily in peer-reviewed journals.

Model forcing data, which include water level residuals, river inflow, and winds are statistically analyzed and compared with climatological distributions developed over the thirty year period 1955 - 1984. The structure of the thermohaline and residual circulation data is assessed from the standpoint of historical observations and from the Long Island Sound Study 1988 -1990 observations. Spectral and asymptotic spatial decomposition analysis results of NOS Acoustic Doppler Current Profiles (ADCP) are presented as well as nontidal flux estimates in the East River. The evolution of the model application in terms of model modification based on model and data intercomparison and EPA East River nontidal flux targets is discussed. A skill assessment of three eighteen month simulations is performed and the most favorable eighteen month simulation results are completely compared with observations in terms of salinity and temperature time series response and salinity, temperature, and residual current vertical structure. The sensitivity of the simulated nontidal fluxes in the East River to vertical datum and offset is also discussed. Finally, conclusions on model applicability are drawn and recommendations made for possible additional observations and possible further model refinements.

MAJOR FINDINGS

The major findings of this study are summarized for climatology, thermohaline circulation, residual circulation, East River nontidal fluxes, eighteen month simulation approach and vertical datums, eighteen month simulation skill assessment, model validation, and model residual circulation sensitivity experiments.

Climatology: Monthly exceedance probability distributions for air temperature (°C) at LaGuardia Airport, NY, total freshwater inflow (cfs) to the Sound, and cross Sound water level difference (m) were developed for the 30 year period (1955-1984). Based on monthly means for the 18-month period, April 1988 - September 1989, water levels at The Battery, NY were higher with respect to Montauk, NY during the spring in 1989 than in 1988 and had exceedance probabilities of 0.4 and 0.6, respectively, relative to climatology. Freshwater inflows were much larger in the spring and summer 1989 than in 1988 with exceedance probabilities of 0.7 and 0.3, respectively. Air temperatures were extremely high during July and August 1988 with exceedance probabilities of 0.1 and 0.0, respectively, relative to climatology. In July and August 1989, the corresponding exceedance probabilities were 0.6. Calendar years 1960, 1973, 1983, 1984, and 1987 were identified as years during which large degrees of stratification could potentially develop, thereby possibly adversely effecting dissolved oxygen in western Long Island Sound.

Thermohaline circulation: Thermal stratification is usually established by late April in the western and open central Sound, and by early May in most of the eastern Sound. Thermal stratification is generally less in the eastern Sound, where tidal currents are much stronger than further west. During high Connecticut River inflow, the plume is usually confined to the Connecticut shoreline with general propagation to the west. A "C" shape in the surface salinity contours is evident in western Long Island Sound. Freshwater outflow from the East River tends to attach to the Long Island shoreline. As freshwater inflows are reduced in late summer and early fall, in much of the central and eastern Sound, the south to north rate of surface salinity increase is larger than the east to west rate. Cross-sound transfers are associated with gyres, which are intermittent in time and variable in spatial extent within the western and central basins.

Residual circulation: Highlights are summarized by region as follows.

Throgs Neck

- upper layer currents of about 3-5 cm/sec and lower layer currents of about 10 cm/sec.
- stable lower layer flow and fairly stable upper layer flow over 15 months.

Western Sound

- strong flow to the north off of Matinecock Pt. and Eatons Neck, and strong southwesterly flow in the deep channel.

- significant coherence between lower layer flows at stations near Throgs Neck and in the far western Sound.
- weak and variable residual currents at many locations in the open western Sound.

Central and Eastern Sound

- lower layer flow to the west.
- spatially and temporally variable flow in the upper layers.

The Race

- outflow at all depths through Plum Gut.
- net inflow through The Race, but with strong spatial variability.
- very steady mean flow, rotating clockwise with depth, between September and December in The Race.

Connecticut River

- convergence toward the River and a clockwise circulation around Long Sand Shoal in both the upper and lower layers.
- convergence toward the River in the upper layer during both high and low river outflow periods.
- some control of the deep flow near the River by the longitudinal pressure gradient along the Connecticut shore.

East River Nontidal fluxes: NOS analysis of NOS ADCP data indicates that the mean mass flux near Throgs Neck, NY, is on the order of 700 - 800 m^3/s into the East River for the period from June - August, 1989. It is important, however, to emphasize the uncertainties in the transport estimate. Uncertainties exist due to assignment of depth to bin numbers, assignment of areas of uniform flow, and in determining cross-sectional areas. Pritchard (personal communication) used different techniques to extrapolate NOS ADCP measurements to the surface and bottom. Assuming sustantially stronger outward flow near the surface and weaker inward flow in the deep channel below the South Clason, NY, ADCP would reduce the inward transport by about 100 m^3/s. Pritchard has assumed a linear velocity structure from top to bottom, and has obtained Stokes transports about 100 m^3/s less than calculated by NOS. All of the above uncertainties reduce the estimated transport. If the full reduction due to asymmetry is assumed to be possible, then the net transport from the Sound into the East River is in the range 200 - 800 m^3/s. This is a large uncertainty, but reflects the difficulty in estimating transport from a single ADCP that itself does not cover the full depth range.

Simulation approach and vertical datums: Due to the uncertainties in the nontidal flux estimates through the East River and since the NOS hydrodynamic model grid is only one cell wide in the East River, EPA developed a ten vertical level, fine horizontal resolution hydrodynamic model in the East River. This fine resolution model was calibrated to the vertical mean profile of the North College Point and South Clason ADCP velocity measurements during the period May - August 1989. The EPA fine resolution East River model computed monthly averaged values of the nontidal flux at Throgs Neck, NY, for: a) surface layer, b) bottom layer, and, c) water column along with the total monthly averaged values of volume fluxes at the South Clason/North College Point, NY, section and The Battery, NY, section were used as targets. The objective was for the NOS model to match these EPA fine resolution East River model nontidal flux

targets to within ± 100 m^3/s. These conditions were to be satisfied for each month during the four month period May - August 1989 for which ADCP data are available. In addition, at the Throgs Neck, NY, section, the square root of the variance of hourly volume fluxes per unit depth in the inverse frequency band from 34 to 120 hours, through NOS model level 2 near the middle of the eastward flowing upper layer and through NOS model level 6 near the middle of the westward flowing lower layer should agree with the EPA fine resolution East River model values to within 50%. Simulation 6a which used a 6.7 cm offset of mean sea level relative to NAVD (1988) met all targets and established the mean sea level offset for three 18-month simulations (NOS 5/93, NOS 6/93, and NOS 6/93R).

Simulation skill assessment: Each of these simulations was performed on the National Institute of Standards and Technology CRAY YMP-2/216 in 9 two-month segments. The skill assessment was based on the following six factors: 1) monthly compliance with the EPA total nontidal flux estimates at Throgs Neck, NY, 2) monthly compliance with the EPA upper and lower layer nontidal flux estimates at Throgs Neck, NY, 3) calibration and verification period rms salinity differences between simulations and all vertical profiles, 4) calibration and verification period salinity stratification index based on all vertical profiles, 5) calibration and verification period rms temperature differences between simulations and all vertical profiles, and 6) calibration and verification period temperature stratification index based on all vertical profiles. Simulation NOS 6/93 was determined to be the superior simulation and served as the thermohaline and residual circulation component of the model validation.

Model validation: Based on a simulation of September 1988, the tidal component of the model was validated. Rms differences at 13 tide stations between simulated and reconstructed water levels are order 10 cm. Simulated currents at level 5 agree to within 20% of the reconstructed ranges in both horizontal velocity components. The thermohaline and residual circulation validation consists of a nine month calibration (April - December 1988) and a separate nine month verification (January - September 1989). For NOS 6/93, the magnitude of the rms differences (psu) between 227 observed and computed salinity profiles are of the same order for the calibration and verification periods at stations A2 (0.70, 0.97) , at H6 (0.56, 0.55), and at M3 (0.73, 0.69) in western, central, and eastern Long Island Sound, respectively. For stratification index (psu), the comparisons between periods at station A2 (0.60, 0.74), at station H6 (0.37, 0.49), and at station M3 (0.42, 0.51) are all of the same order. In general, the longitudinal salinity gradients both at the surface and near bottom of the Sound are well represented, thus insuring a reasonable representation of the density flow component due to salinity changes. In NOS 6/93, the magnitude of the rms differences (°C) between observed and computed temperature profiles are of the same order for the calibration and verification periods at stations A2 (0.69, 0.85) , at H6 (0.67, 0.57), and at M3 (0.58, 0.31) in western, central, and eastern Long Island Sound, respectively. For the stratification index (°C), the comparisons between periods are at station A2 (0.69, 0.85), at station H6 (0.67, 0.57), and at station M3 (0.58, 0.31) all of the same order. In general, the longitudinal temperature gradients both at the surface and near bottom of the Sound are well represented in the model, thus insuring a reasonable representation of the density flow component due to temperature changes. Simulated near surface and near bottom salinity and temperature fileds are compared with observation

derived fields for the specific periods April 4 - 7, 1988, June 13 - 16, 1988, and August 2 - 4, 1988. During April 4 - 7, the location of the surface salinity 26.0 psu contour is very similar in both the observations and model. In addition, the structure of the Connecticut River surface plume is well represented. The location of the simulated bottom salinity 27.0 psu contour corresponds closely to observations. For temperature during April 4 - 7, the location of the surface waters between 5.5 and 6.0 °C in the central Sound in the simulation, appears to be in general agreement with the observations. The location of the simulated bottom cold water pool (less than 4.0 °C) in the central Sound is very similar to the observations. During June 13 - 16, the extent of the Connecticut River plume indicated in the surface simulation field is in close agreement with the observations. In the near bottom salinity fields, the influence of the Connecticut River is more closely confined to the Connecticut shoreline in the observations than that shown in the simulation. For temperature during June 13 - 16, the fine scale, near surface, thermal gyres indicated in the observations are smoothed in the simulation due to interpolation. However, the simulated longitudinal gradient (12.5 - 18.0 °C) is in close agreement with the observations. Simulated and observed bottom temperature structures are in close agreement. During August 2 - 4, the extent of the Connecticut River plume indicated in the simulation agrees very well with that indicated in the observations, while the simulated near surface salinity fields in western Long Island Sound are slightly saltier by order 0.5 psu than observed. In the near bottom salinity fields, the locations of both the 28.5 psu and 30.0 psu contour lines are very close in the simulation and observations. For temperature during August 2 - 4, the extent of the simulated 25.0 °C pool in the central Sound is similar to that indicated in the observations along the Long Island Sound shoreline. The NOS 6/93 simulated residual currents are in reasonable agreement with the observations except for the v-component in The Race (Stations 11, 12, and 13), where the simulated currents are much stronger than the observations. In this region of large spatial gradients in topography, model resolution may be inadequate.

Model residual circulation sensitivity experiments: To estimate the astronomical tide and density components of the residual circulation, a simulation was performed for April 1988 using the NAVD (1988) vertical datum and with water level residuals and local winds set to zero (Schmalz, 1993b). Simulated near surface and near bottom monthly averaged residual circulation fields indicate the presence of a pair of cyclonic gyres in the central and western basins. Additional simulations for April 1988 using the NGVD (1929) and mean sea level datums, did not alter these circulation patterns (Schmalz, 1993a). Simulations in which wind effects were included indicated that the structure of the near surface gyres is very sensitive to local wind forcings. Winds with a west to east component tend to either eliminate or significantly reduce the spatial extent of the central basin gyre. Winds with a east to west component tend to pinch the central basin gyre.

1. INTRODUCTION

In conjunction with the United States Environmental Protection Agency (USEPA), the National Oceanic and Atmospheric Administration's (NOAA), National Ocean Service (NOS), was commissioned to develop and apply a three-dimensional hydrodynamic model to Long Island Sound. NOAA/NOS conducted extensive hydrographic measurements in Long Island and Block Island Sounds (Earwaker, 1990) to provide model validation and forcing data. The ultimate objective of the modeling effort in support of EPA is to provide residual circulation over annual time scales (1-3 years) in order to enable water quality simulation for Sound-wide planning studies. A supplemental NOS model objective is to develop a comprehensive tidal simulation set in order to further elucidate tidal dynamics and produce a updated tidal atlas.

Volume 1 in this series presents the application and documentation of the model to Long Island Sound. This report, Volume 2, focuses on the validation of the model for thermohaline and residual circulation. Volume 3 contains copies of scientific papers published elsewhere, primarily in peer-reviewed journals.

This report is organized in the following manner. Section 2 presents a statistical analysis of the model forcing data, which includes water level residuals, wind, and river inflows. Climatological distributions of water level residuals, river inflows , and air temperature are developed for the thirty year period 1955 - 1984 in order to determine how the eighteen month period April 1988 -September 1989, during which extensive hydrographic measurements were made, compares with the climatology. Section 3 reviews historical salinity and temperature data. In addition, the Long Island Sound Study salinity and temperature data acquired by the State University of New York (SUNY) and the University of Connecticut (UCONN) are interpreted to provide a more complete understanding of the seasonal thermohaline response in Long Island Sound. Section 4 considers historical near surface and bottom drifter data and Long Island Sound Study current meter data acquired by SUNY and NOS ADCP data. General aspects of the residual circulation are developed as well as spectral analysis and asymptotic decomposition of NOS ADCP data. Nontidal flux estimates in the East River based on NOS ADCP measurements are given and discussed in terms of overall accuracy. In Section 5, the evolution of the NOS Long Island Sound hydrodynamic model is presented. The incorporation of additional freshwater sources as well as the determination of offsets to the 1988 North American Vertical Datum (NAVD 1988), to meet EPA nontidal flux estimates in the East River is presented. A skill assessment of three eighteen month simulations is performed. Section 6 initially considers the astronomic tide calibration during September 1988. Next the most favorable simulation results are compared with available salinity, temperature, and residual current observations. Sensitivity of simulated East River nontidal fluxes to vertical datum and offsets are also shown. In Section 7, recommendations are developed for possible additional observations and future model enhancements.

2. MODEL FORCING DATA

As documented in Volume 1, a three-dimensional hydrodynamic model has been developed for Long Island Sound and has been calibrated to the eighteen month period, April 1988 through September 1989. It was during this time period that extensive hydrographic data were available.

The model forcing data include river flow into the Sound, wind, and water level residuals. In this study, five rivers from the state of Connecticut, along with five New York streams were included. Three rivers, the Connecticut River, the Housatonic River and the Thames River are emphasized. The wind data are from La Guardia, NY. The water level residual data are from The Battery, NY, and from Montauk, NY. Forcing data from the eighteen month calibration period have been analyzed. A summary of this analysis is presented in Section 2.2. In order to assess how representative this eighteen month period is with regard to forcing variables, thirty years of historical data (1955-1984) were obtained. The climatological characterization is presented in Section 2.1.

The data from both time periods were obtained from the same sources. The river flow data were obtained from the United States Department of the Interior, Geological Survey (USGS). The values recorded for each month are an average of the daily averaged values. The air temperature values (monthly average at La Guardia, NY) were compiled from records on file at the National Climatic Data Center in Asheville, North Carolina. The water level data (monthly average water levels at The Battery, NY and at Montauk, NY) were obtained from the Ocean and Lake Levels Division of the National Ocean Service.

2.1. Climatological Characterization

Table 2.1 summarizes the thirty years (1955-1984) of climatology from Long Island Sound. For each data type, for each month of the year, there is a minimum value, a maximum value, and the thirty year mean value.

Air temperature follows a typical seasonal cycle. Air temperatures are at a minimum during January and reach a peak during July and August. The thirty year mean January temperature of -0.59°C corresponds to 31°F. The lowest January mean temperature (on record) was -5.39°C (22.3°F). The thirty year mean July temperature is 24.69°C (76.4°F) and the maximum July (mean) was 27.17°C (81°F).

The USGS estimated the total river flow into the Sound based on the recorded values of the Thames, Housatonic, and the Connecticut Rivers. To the sum of these three river flows, the USGS added 5.5% to account for the remaining Connecticut rivers. In addition to this amount the USGS added 280.0 cfs; 80.0 cfs accounted for Long Island streams and 200.0 cfs accounted for the New York streams. Table 2.1 gives a good idea of the seasonal variability of river flow into Long Island Sound. For example, the maximum daily average July inflow of 39832 cfs would correspond to the monthly average inflow during the spring (March, April). Generally, the inflow is moderate during the winter, increases greatly during the spring, and dwindles

during the summer. The mean April flowrate is 68065.0 cfs, with peak flows reaching over 100,000 cfs. The mean flowrate drops off to about 10,000 cfs during the summer (July, August, September).

The cross sound water level difference is defined as the average water level at Montauk minus the average water level at The Battery, NY. To calculate the monthly cross sound difference, the mean sea level (5.65 ft (1.72 m) at The Battery, NY and 4.89 ft (1.49 m) at Montauk, NY) is subtracted from the mean water level at The Battery, NY and at Montauk, NY. Then, the mean sea level at both stations is adjusted to the 1988 North American Vertical Datum (NAVD (1988)) by subtracting 0.123 m at The Battery, NY and 0.148 m at Montauk, NY. Then, the difference (Montauk, NY minus The Battery, NY) for the cross sound difference in meters is taken.

Table 2.1. Long Island Sound Climatology (1955-1984)

	Air Temperature(°C)			Total Inflow (cfs)			Cross Sound Difference (m)		
	Min	Max	Mean	Min	Max	Mean	Min	Max	Mean
January	-5.39	3.44	-.59	4869.3	62208.5	25807.3	-.083	.094	.014
February	-5.00	4.83	.67	10798.3	60140.7	28161.4	-.068	.076	.007
March	1.06	7.61	4.84	23152.4	92254.9	43134.8	-.113	.027	-.023
April	8.39	13.11	10.83	32816.2	104672.3	68065.0	-.098	.030	-.041
May	12.78	19.50	16.50	16316.0	72948.4	41019.4	-.104	.000	-.045
June	18.78	23.61	21.68	7886.5	66681.7	22139.1	-.086	.000	-.044
July	22.89	27.17	24.69	5228.0	39831.9	12339.6	-.107	.021	-.039
August	22.44	25.94	24.14	4763.8	48968.3	11216.1	-.080	.018	-.039
September	18.06	23.11	20.11	4267.9	24523.9	10050.8	-.107	.009	-.043
October	11.22	16.94	14.17	5069.7	56574.8	16797.5	-.098	.042	-.034
November	5.94	11.44	8.50	7454.0	61237.9	23383.1	-.116	.103	-.007
December	-1.11	6.28	2.45	13256.5	62081.9	28112.7	-.068	.085	.008

Generally, there is a higher water level at The Battery, NY relative to Montauk, NY during the spring and summer months. This elevation difference reaches a peak by May and June, with average cross sound differences of -0.045 m and -0.044 m, respectively. The elevation difference diminishes during the fall and winter.

2.2. Forcing Variables for 1988 through 1989

Table 2.2 describes the Connecticut River inflow over the eighteen month calibration period. Table 2.3 describes the Thames River inflow and Table 2.4 describes the Housatonic River inflow. Of the three rivers, the Connecticut is the largest. In general, the flowrate of the

Connecticut River is on the order of five to ten times greater than the flowrate of either the Thames River or the Housatonic River. The Thames River and the Housatonic River are roughly equivalent, with the Housatonic River generally having a slightly higher rate of flow. The remaining Connecticut and New York streams are almost negligible compared to these three rivers. Table 2.2 shows the Connecticut River having a generally high rate of flow into the Sound through the late spring and summer months of 1989. This can also be seen in Figure 2.1. The most extreme spike in May 1989 reaches almost 100,000 cfs. Figure 2.2 shows the distribution of Connecticut River flowrates over the eighteen month period. Tables 2.3 and 2.4 indicate that the Thames and Housatonic Rivers follow a similar pattern of larger than normal flowrates through 1989.

Table 2.2. Connecticut River Flow (cfs) - April 1988 through September 1989

Month	Year	Min	Max	Mean	Standard Deviation	Exceedence Probability
April	1988	14200.0	62800.0	34306.7	17666.4	0.83
May	1988	11300.0	74300.0	27396.8	17620.6	0.53
June	1988	4340.0	16600.0	8023.7	3197.3	0.83
July	1988	10300.0	28300.0	9482.3	6374.7	0.33
August	1988	3730.0	29100.0	8052.3	5043.7	0.30
September	1988	4860.0	27100.0	9888.2	5509.3	0.17
October	1988	3480.0	16100.0	7289.4	3309.3	0.67
November	1988	8980.0	49600.0	26559.3	7948.2	0.17
December	1988	8120.0	26900.0	13985.2	5134.7	0.57
January	1989	4040.0	14500.0	8065.8	2481.3	0.87
February	1989	3630.0	22700.0	8598.2	4936.5	0.93
March	1989	4130.0	60200.0	16790.6	16480.0	0.90
April	1989	20100.0	101000.0	42853.3	21042.0	0.80
May	1989	20100.0	99700.0	48861.3	24527.4	0.07
June	1989	12900.0	59000.0	28410.0	11807.2	0.10
July	1989	6780.0	18500.0	10217.1	2905.3	0.20
August	1989	5310.0	42000.0	15609.7	9998.3	0.10
September	1989	4640.0	22200.0	10374.0	5125.4	0.13

Included in these tables are, for each month, the minimum value, the maximum value, the mean value, and the standard deviation. Also included is the exceedence probability. The mean value, for that month, was compared with the mean values over the thirty year historical period. The exceedence probability is the probability of finding a year in which the value (for that month) is greater than the value from the simulation period. In other words, an exceptionally high mean flowrate would correspond to an exceedence probability of close to 0.0. An exceptionally small

rate of flow, such as 2871.3 cfs for the Thames River in March 1989, would correspond to an exceedence probability close to 1.0 (in this case, exactly 1.0). Exceedence probabilities were calculated not only for river flow (Connecticut, Housatonic, and Thames), but for windspeed, air temperature, and cross sound average water level difference as well.

Table 2.3. Thames River Flow (cfs) - April 1988 through September 1989

Month	Year	Min	Max	Mean	Standard Deviation	Exceedence Probability
April	1988	1600.0	7840.0	2919.7	1520.5	0.93
May	1988	2110.0	6030.0	3290.0	896.4	0.40
June	1988	394.0	2140.0	998.5	565.2	0.90
July	1988	235.0	7780.0	1492.1	1909.3	0.20
August	1988	221.0	1520.0	560.3	303.3	0.50
September	1988	274.0	5970.0	935.5	1620.9	0.37
October	1988	261.0	1740.0	788.3	335.2	0.67
November	1988	953.0	15400.0	4678.1	3498.1	0.10
December	1988	1910.0	5970.0	2982.6	948.3	0.40
January	1989	1660.0	3200.0	2172.9	392.8	0.73
February	1989	1290.0	10000.0	2985.4	2033.3	0.70
March	1989	1730.0	5530.0	2871.3	950.6	1.00
April	1989	2960.0	10800.0	6288.7	2191.8	0.30
May	1989	3650.0	14400.0	7600.6	2961.8	0.00
June	1989	1950.0	11900.0	5354.7	2211.5	0.10
July	1989	1000.0	3360.0	1805.5	462.1	0.13
August	1989	589.0	10700.0	5969.8	2884.3	0.03
September	1989	610.0	3049.8	1677.9	830.4	0.07

Table 2.5 characterizes the wind at La Guardia N.Y. over the eighteen month period. Peak windspeeds are less than 35 knots for all months with the majority of hourly values less than 20 knots. This can also be seen in Figure 2.3. Figure 2.4 shows the distribution of windspeeds from April through December, 1988 and from January through September, 1989. The two distributions appear to be almost identical. Mean windspeeds tend to be greater during the fall, winter, and early spring, then diminish somewhat during the late spring and summer.

Table 2.5 also characterizes the air temperature at La Guardia, NY. Air temperatures are in degrees Celsius, and an exceedence probability is included for each month. Most notable is the summer of 1988. July and August have exceedence probabilities of 0.10 and 0.00, respectively. The year 1988 had an exceptionally warm summer. With respect to air temperature, the year 1989 was fairly typical.

Table 2.4. Housatonic River Flow (cfs) - April 1988 through September 1989

Month	Year	Min	Max	Mean	Standard Deviation	Exceedence Probability
April	1988	339.0	7080.0	3295.6	1736.9	0.90
May	1988	441.0	6170.0	2900.7	1254.8	0.77
June	1988	175.0	3210.0	1206.2	902.4	0.87
July	1988	166.0	8310.0	1900.2	2101.9	0.20
August	1988	213.0	3180.0	1172.1	829.4	0.33
September	1988	201.0	2630.0	1031.1	738.1	0.33
October	1988	190.0	2030.0	745.5	495.8	0.80
November	1988	1180.0	15600.0	5378.7	3248.1	0.07
December	1988	365.0	7540.0	3706.2	1617.3	0.47
January	1989	324.0	4350.0	2075.3	1127.3	0.77
February	1989	291.0	7920.0	2298.0	1856.8	0.83
March	1989	303.0	8420.0	2545.0	2004.6	1.00
April	1989	1910.0	8880.0	5540.0	1970.0	0.77
May	1989	3050.0	26200.0	11472.0	4898.1	0.00
June	1989	2840.0	9850.0	5672.3	1820.1	0.13
July	1989	348.0	5840.0	2173.9	1097.7	0.20
August	1989	209.0	7880.0	2101.2	2003.4	0.17
September	1989	224.0	4370.0	1630.9	1234.0	0.20

Table 2.5. La Guardia N.Y.- Wind Speed, Air Temperature

		Wind Speed (kts)				
Month	Year	Max	Mean	Standard Deviation	Air Temp (°C)	Exceedence Probability
April	1988	24.0	11.17	4.37	10.44	.57
May	1988	19.0	8.78	3.80	16.78	.50
June	1988	22.0	9.71	4.14	22.28	.40
July	1988	23.0	7.95	3.44	25.89	.10
August	1988	28.0	9.52	3.70	26.00	.00
September	1988	24.0	8.73	3.56	19.94	.53
October	1988	27.0	11.14	4.26	11.67	.97
November	1988	31.0	11.45	5.41	9.72	.23
December	1988	33.0	11.86	4.45	2.56	.57
January	1989	33.0	11.53	5.61	3.11	.03
February	1989	26.0	11.05	4.74	1.28	.43
March	1989	33.0	11.04	4.70	5.39	.37
April	1989	25.0	9.79	4.68	10.78	.53
May	1989	32.0	9.72	4.98	16.94	.50
June	1989	22.0	8.36	3.97	22.72	.13
July	1989	23.0	7.79	3.74	24.56	.57
August	1989	25.0	8.76	3.60	24.06	.57
September	1989	31.0	9.29	4.63	20.94	.30

Table 2.6 describes the water level (comparison) across Long Island Sound. The average residual values at The Battery, NY and at Montauk, NY are in feet. The cross sound difference was calculated in a way similar to the climatology (1955-1984) and is recorded in meters. Cross sound elevation difference is important because a high water level at The Battery, NY relative to Montauk, NY could induce an upper layer flow out of the East River into the Sound. May 1989 has an exceptionally large (negative) difference of -.074 meters. A high exceedence value (closer to 1.0 than to 0.0) is indicative of this type of elevation difference. The cross sound elevation difference is significantly large throughout 1989.

Figure 2.5 shows the time series of water level residuals at The Battery, NY. The largest positive residuals of over 3 ft (1.0 m) occur during October 1988. Extreme negative residuals reach about -3.0 ft (-1.0 m) in November 1988, and almost -4.0 ft in late December 1988. These events might be considered in more detail to investigate a more complete description of the meterological forcing effects in the hydrodynamic model in support of the future development of a nontidal water level atlas.

Table 2.6. Monthly Average Water Level Residuals
(The Battery, NY and Montauk, NY)

Month	Year	The Battery Residual(ft)	Montauk Residual(ft)	Cross Sound Difference(m)	Exceedence Probability
April	1988	0.391	0.358	-.037	0.47
May	1988	0.210	0.133	-.049	0.57
June	1988	0.217	0.198	-.031	0.40
July	1988	0.074	0.106	-.016	0.17
August	1988	0.183	0.206	-.019	0.23
September	1988	0.106	0.241	-.019	0.23
October	1988	0.140	0.172	-.016	0.30
November	1988	-0.099	0.004	.005	0.43
December	1988	-0.250	-0.142	.012	0.47
January	1989	-0.250	-0.194	-.004	0.70
February	1989	-0.262	-0.228	-.013	0.83
March	1989	-0.117	-0.149	-.034	0.73
April	1989	-0.156	-0.158	-.025	0.37
May	1989	0.215	0.052	-.074	0.90
June	1989	0.294	0.203	-.055	0.67
July	1989	0.222	0.185	-.040	0.67
August	1989	0.333	0.326	-.031	0.40
September	1989	0.296	0.220	-.049	0.67

Figures 2.7 and 2.8 show the distribution of hourly observations at The Battery, NY and at Montauk, NY, respectively. Overall, the distribution of water level residuals at The Battery, NY has a much wider range than does the distribution at Montauk, NY.

2.3. Analysis for Potential Stratification

Both the eighteen month calibration period and the thirty year historical period were studied to determine the likelihood of certain conditions being present which potentially either increase the demand for oxygen at the lower depths, or prevent dissolved oxygen from reaching the bottom. The two conditions which affect dissolved oxygen are stratification and pollutant loading.

A stratified condition exists when there is a significant upper layer and lower layer difference with respect to density. That is, in western Long Island Sound, a warm, fresh upper layer, and beneath it, a cool, salty lower layer. Stratification is important with regard to dissolved oxygen because at the interface between the upper layer and lower layer, little or no mixing can occur. A stratified condition thereby reduces the transport of oxygen to the lower depths. Stratification is brought about by high spring and summer river inflow and is sustained during the summer by high surface temperatures.

A high pollutant loading condition is most likely to occur when high river flow coincides with a very small (large negative value) elevation difference. Since the cross sound difference is defined as the water level at Montauk, NY minus the water level at The Battery, NY, a loading condition implies a high water level at The Battery, NY. This type of elevation difference should induce an upper layer flow from the East River into Long Island Sound. We are primarily looking for loading conditions which occur during the winter and spring months.

Each year of the thirty years of climatology was examined for the presence of potentially critical conditions. As with the eighteen month simulation period, an exceedence probability was obtained for each month of each year. For the years 1955 through 1984, the exceedence probability is based on comparison with the other twenty nine years of historical data. Based upon these probabilities, several years which seem likely to present critical conditions were identified.

Table 2.7 summarizes physical conditions for 1983. The river inflow from March through June is very heavy. April 1983 not only has an estimated inflow of 91116 cfs, but has a cross sound difference of -0.098 m, the largest (most negative) elevation difference of any April we have studied. June, July, August, and September are all warm. These conditions offer excellent potential for stratification.

Several other years are worthy of further consideration. The year 1960, with its early spring high temperature and river inflow offers a good chance for stratification. The years 1973, 1983, and 1984 all offer potential for both loading and stratification. Any of these years, with the potential for extreme conditions, could be the subject of future study in support of water quality management activities.

Table 2.7. River Flow, Elevation Difference, and Air Temperature for 1983

		Air Temp		Cross Sound Difference		Total Inflow	
		(°C)	EP	(m)	EP	(cfs)	EP
January	1983	1.33	.21	.012	.61	27520.1	.31
February	1983	1.67	.38	-.019	.93	33829.0	.24
March	1983	6.22	.14	-.049	.85	60151.3	.10
April	1983	10.94	.48	-.098	1.00	91115.5	.10
May	1983	14.94	.93	-.052	.67	59581.6	.07
June	1983	22.50	.28	-.059	.74	29661.8	.14
July	1983	25.72	.10	-.022	.30	9604.1	.55
August	1983	24.83	.21	-.043	.67	8959.5	.52
September	1983	21.50	.10	-.046	.64	6316.7	.79
October	1983	14.11	.48	-.059	.79	10017.7	.66
November	1983	8.89	.45	-.016	.64	29936.1	.24
December	1983	1.72	.69	-.013	.82	60636.6	.03

2.4. 1987 Water Quality Year

Dissolved oxygen levels in Western Long Island Sound were observed to be very low for the year of 1987. This prompted further investigation of the physical conditions which existed that year. Physical conditions for the water quality year of 1987 are summarized in Table 2.8.

Table 2.8. 1987 Water Quality Year

		Air Temperature		Cross Sound Difference		Total Inflow	
		(°C)	EP	(m)	EP	(cfs)	EP
October	1986	14.44	.40	*-.013	.27	15004.6	.37
November	1986	7.72	.77	*.002	.47	28480.2	.27
December	1986	4.06	.27	*.015	.40	44030.9	.17
January	1987	.39	.33	.027	.43	23895.5	.47
February	1987	.61	.50	.024	.23	15433.1	.90
March	1987	7.00	.10	-.049	.80	35749.0	.60
April	1987	11.50	.40	-.104	1.00	105464.0	.00
May	1987	17.39	.37	-.055	.73	23084.1	.93
June	1987	22.78	.13	-.031	.43	17796.7	.53
July	1987	25.39	.17	-.034	.57	13383.5	.30
August	1987	23.33	.80	-.040	.57	7993.1	.57
September	1987	20.06	.50	-.059	.80	18724.7	.07

* Water Level at Montauk, NY was estimated from Montauk Point data

The heavy river inflow during April of 105464 cfs is the highest estimated inflow of any of the years we have studied. There is excellent potential for stratification to be well established early on in spring. That stratification would have been well maintained by the warm temperatures of June and July 1987.

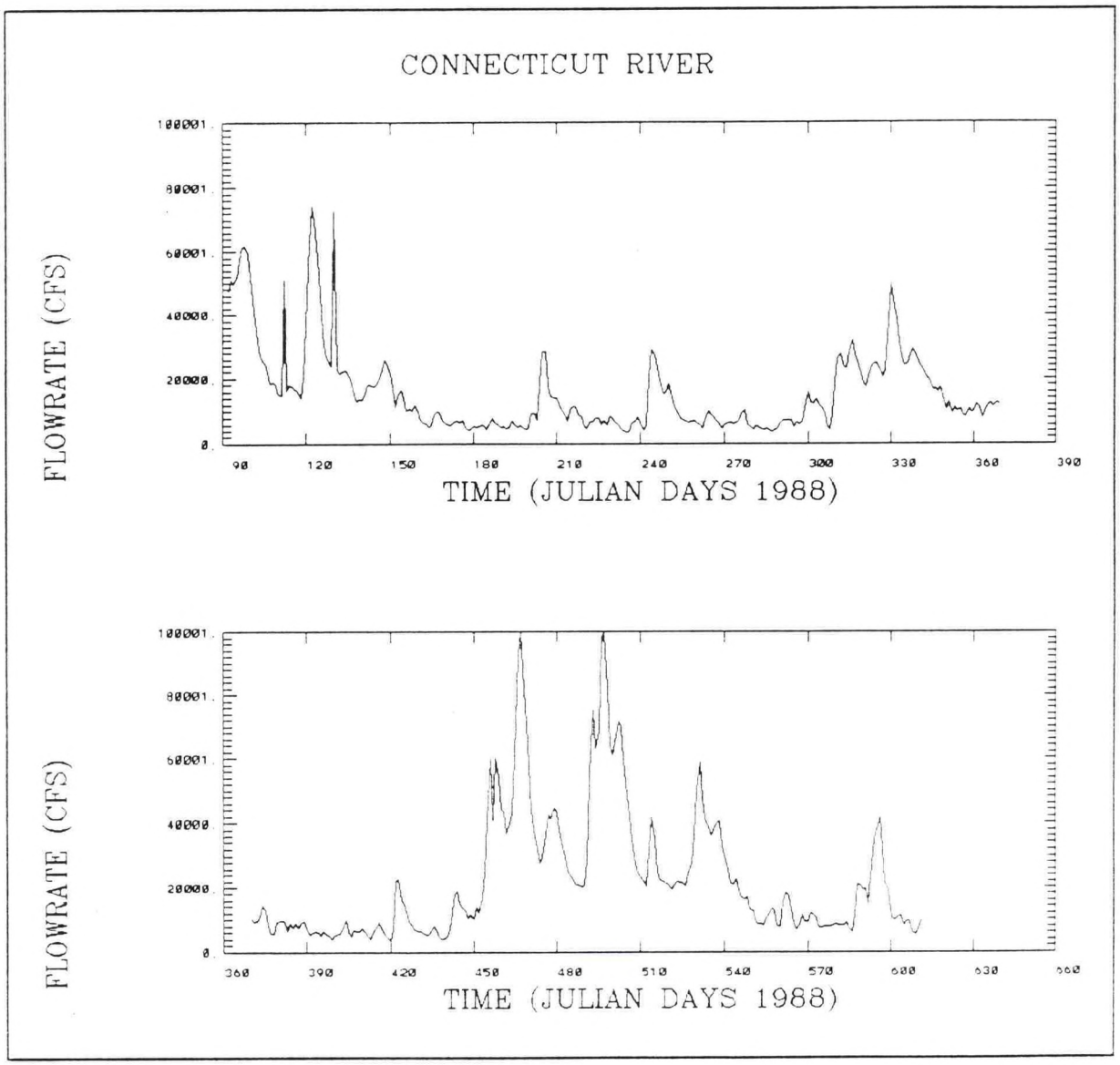

Figure 2.1. Connecticut River Daily Flowrates (April 1988 - September 1989)

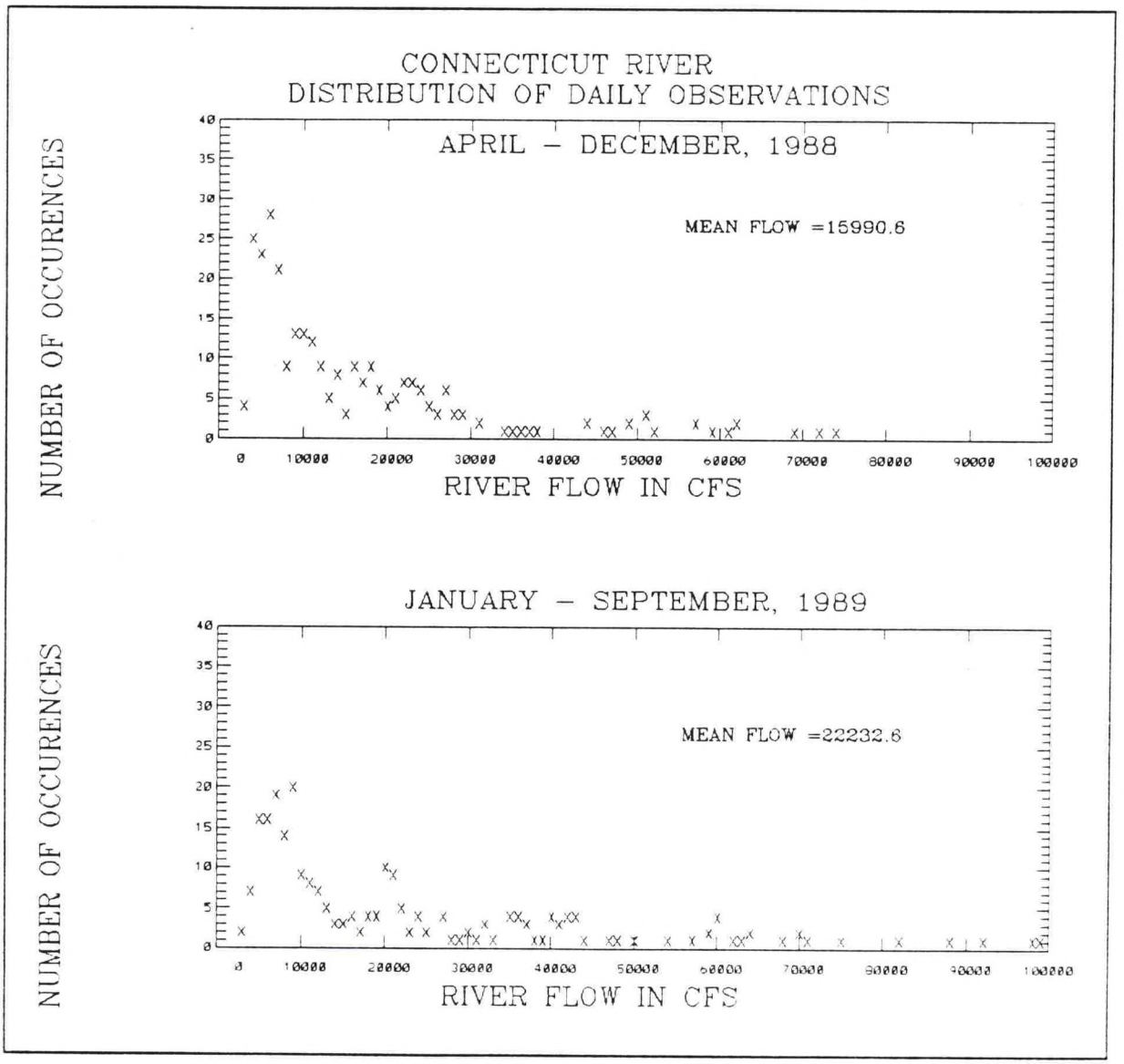

Figure 2.2. Connecticut River Daily Flowrate Distribution (April 1988 - September 1989)

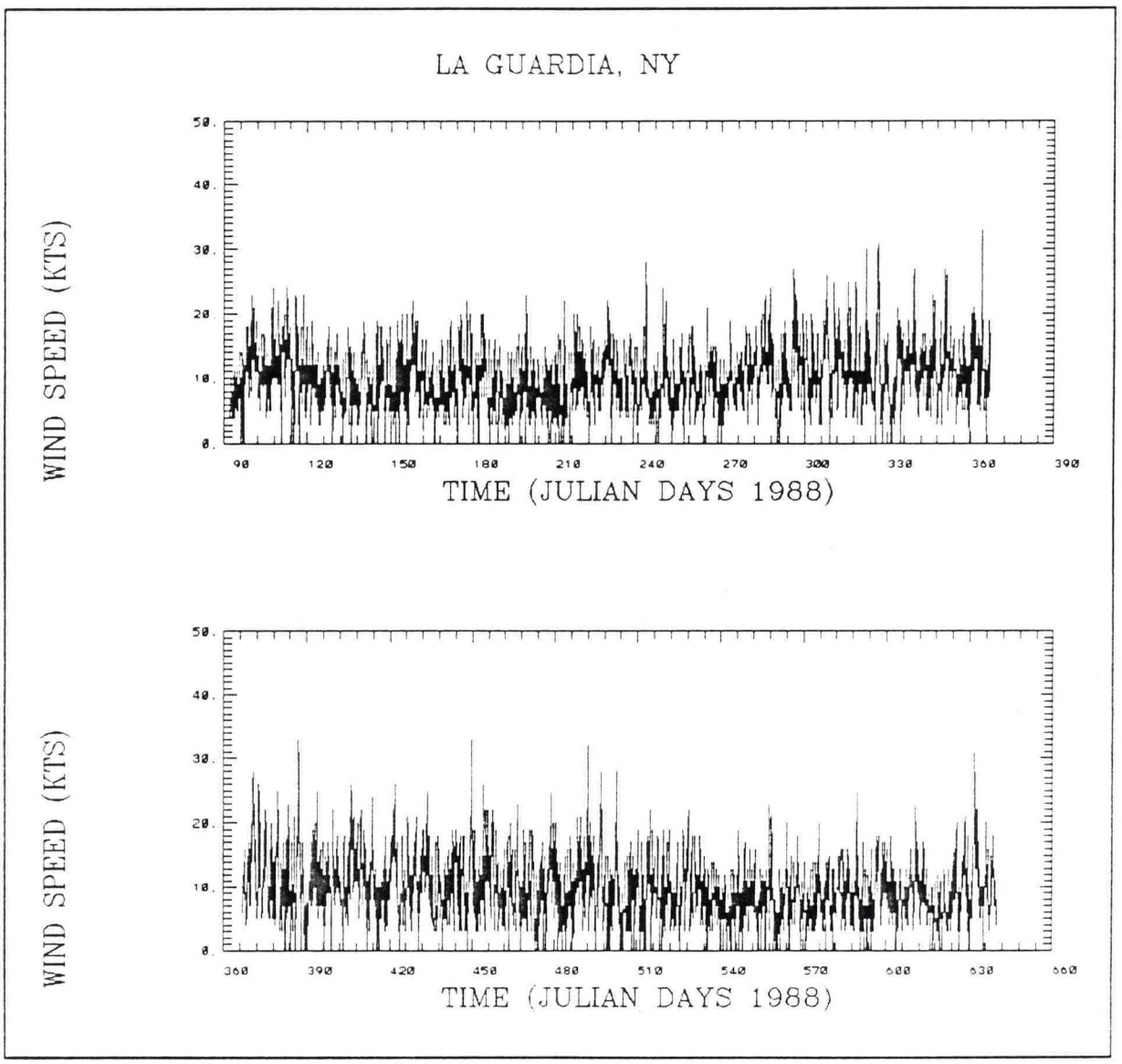

Figure 2.3. LaGuardia, NY, Hourly Windspeeds

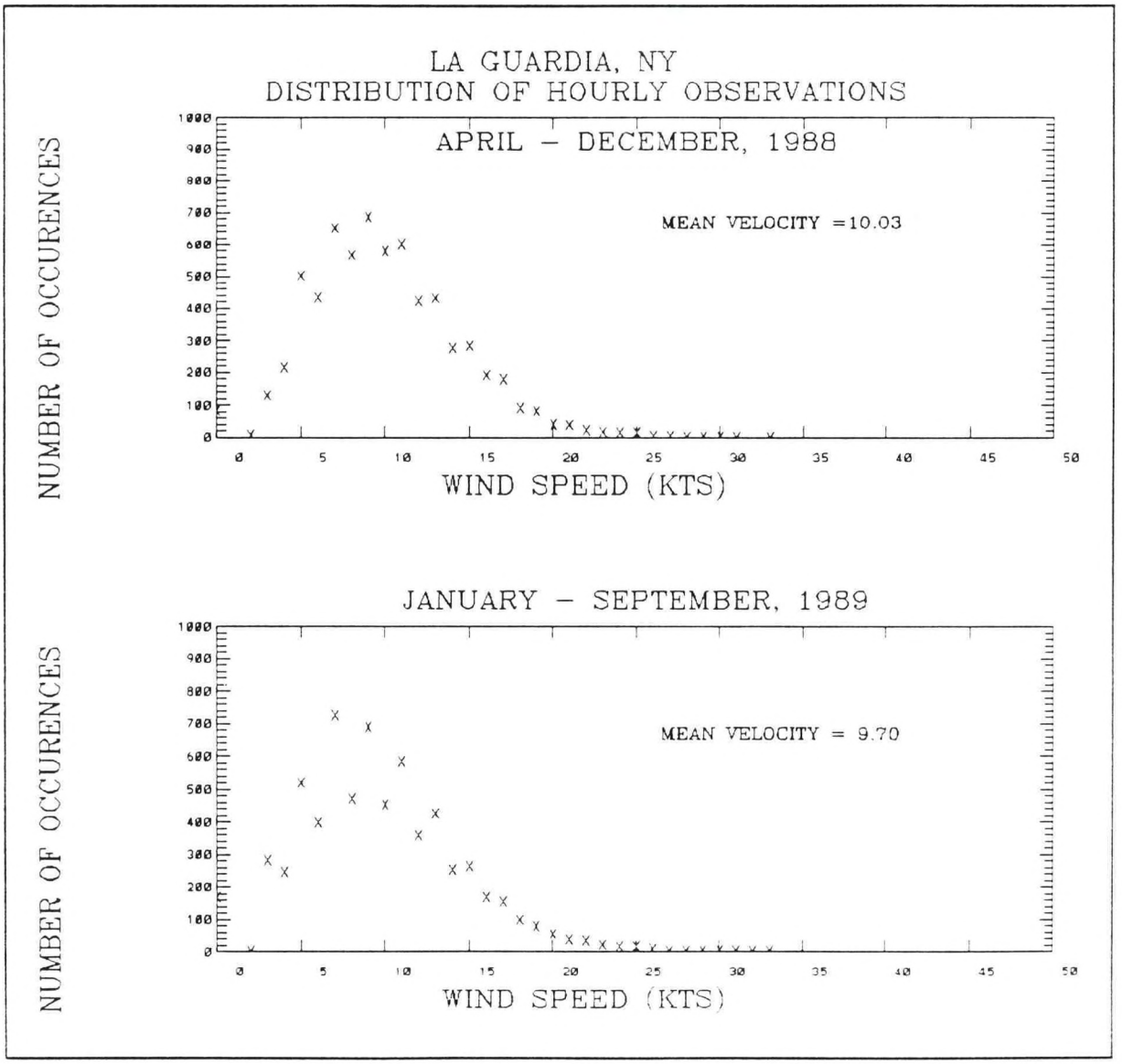

Figure 2.4. LaGuardia, NY, Hourly Windspeed Distribution

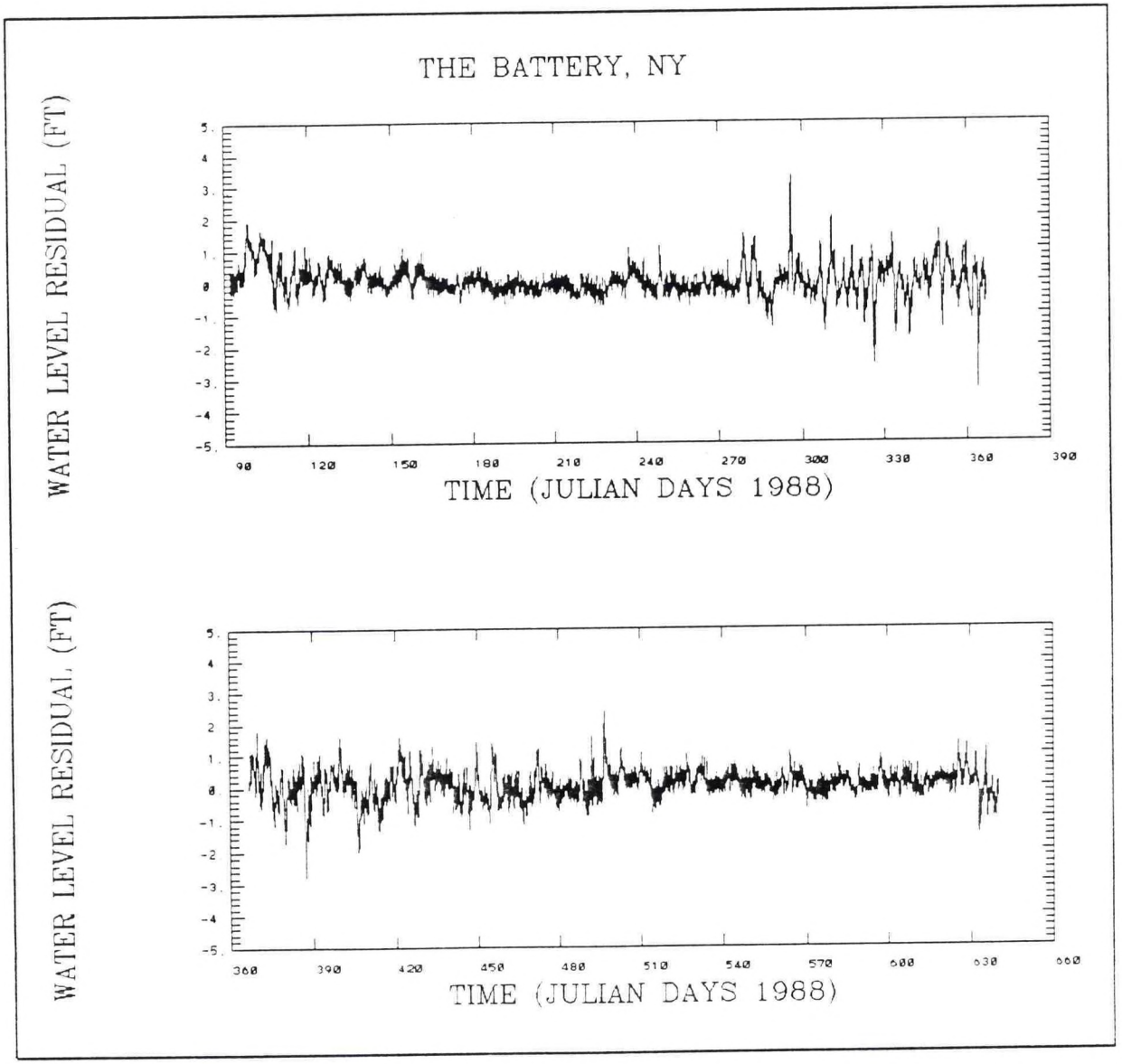

Figure 2.5. The Battery, NY, Hourly Water Level Residuals

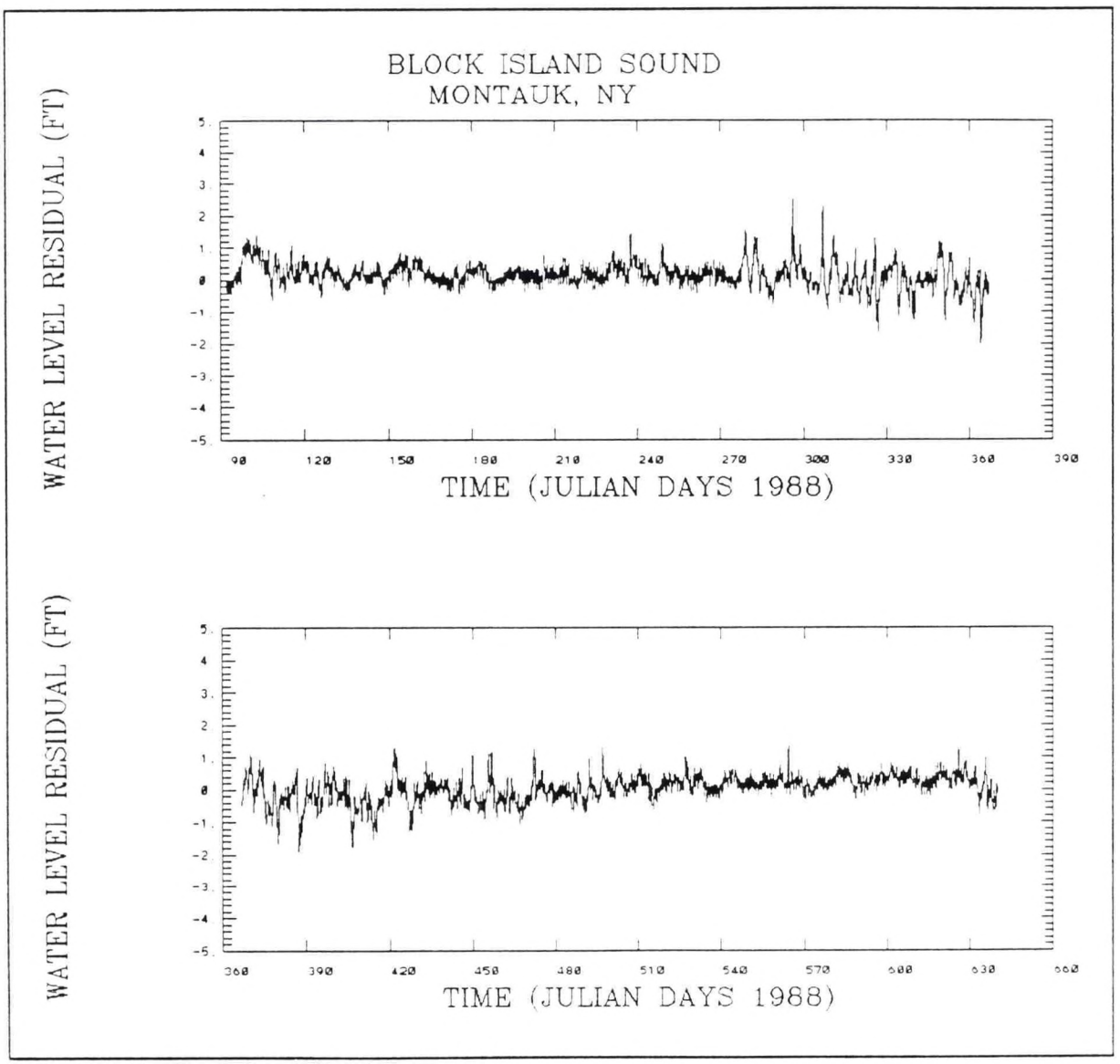

Figure 2.6. Montauk, NY, Hourly Water Level Residuals

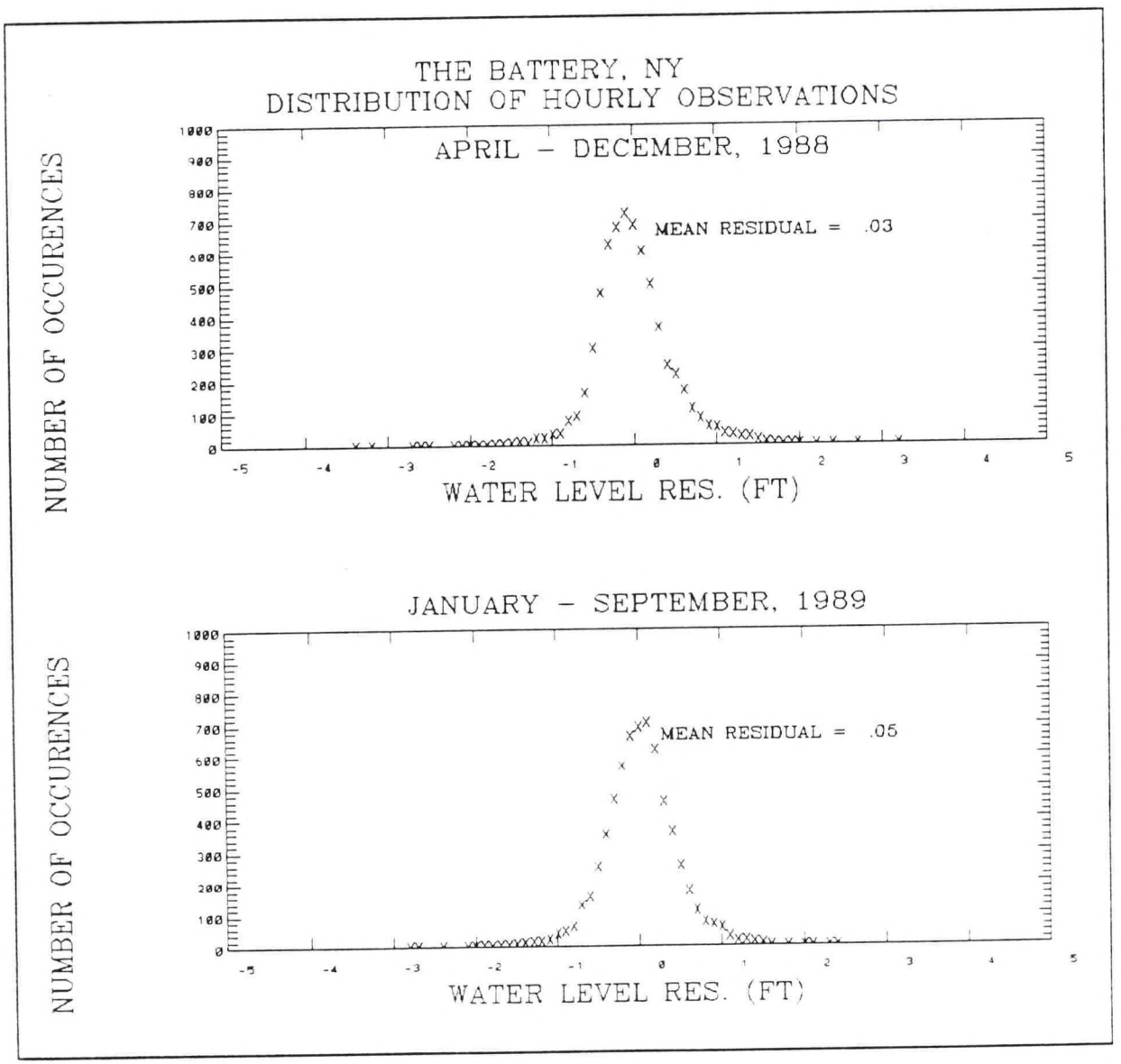

Figure 2.7. The Battery, NY, Hourly Water Level Residual Distribution

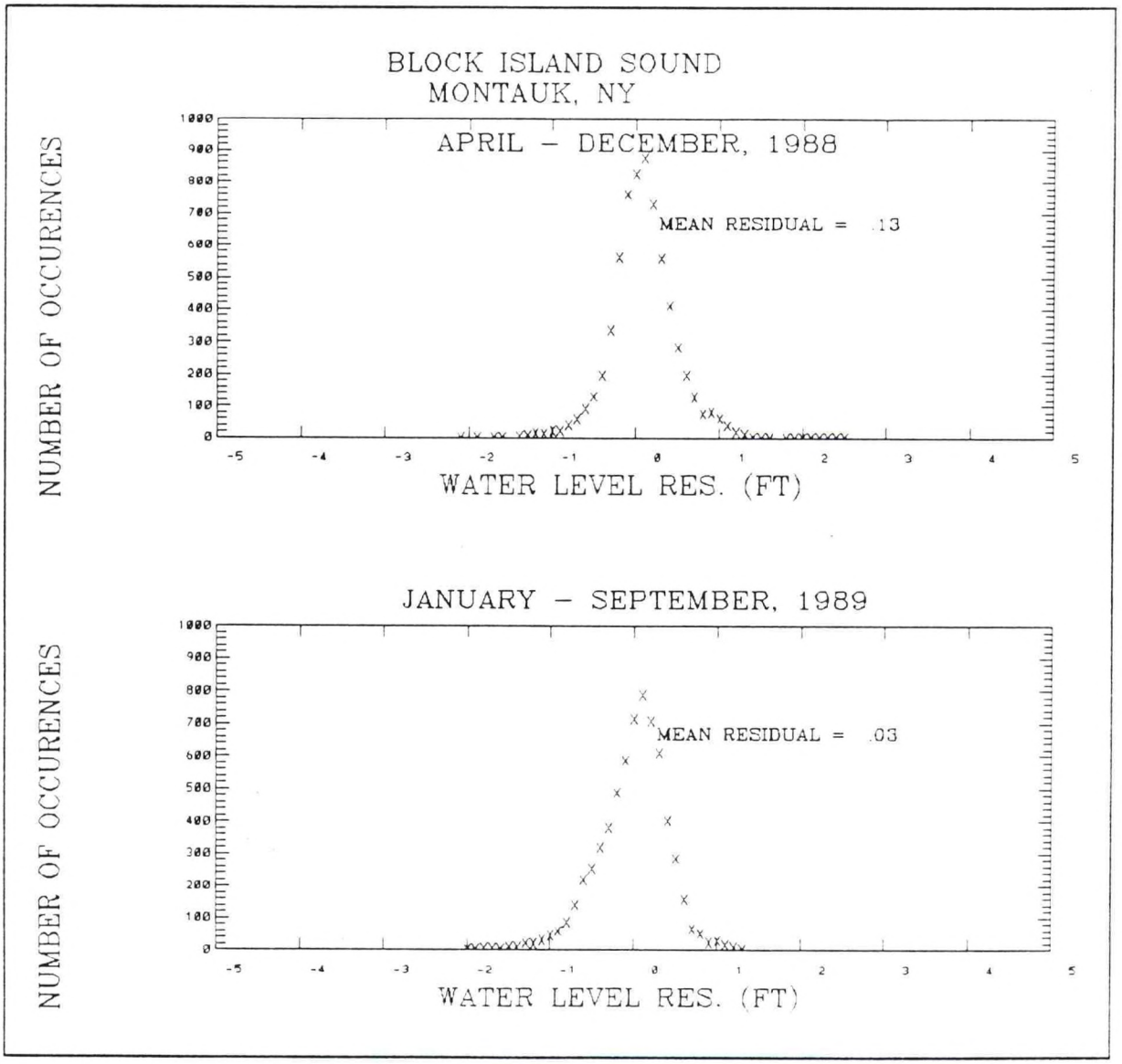

Figure 2.8. Montauk, NY, Hourly Water Level Residual Distribution

3. THERMOHALINE OBSERVATIONAL DATA AND INTERPRETATION

An extensive program of temperature and salinity measurements was carried out in Long Island Sound by NOS, SUNY and UCONN. Detailed sections of temperature and salinity covering the whole Sound were taken between April and September 1988. First, the general pattern of temperature and salinity from historical records is considered. Next, a detailed consideration of conditions during the April - September 1988 period of intensive observations is presented.

3.1. General Structure and Annual Patterns

The first comprehensive studies of the thermohaline structure in Long Island Sound were carried out in the 1950's by Riley (1952, 1956); the general temporal and spatial patterns were established at this time. Riley (1956) studied the average near surface and near bottom temperature and salinity in mid-Sound monthly cycle over a two year period. The annual cycle of temperature and thermal stratification emerged fairly clearly. Systematic thermal stratification began in late April to early May in both years. It did not persist into the fall, but disappeared in late August, presumably due to convective overturning. Some salinity stratification was present in all seasons, along with an annual cycle related to spring runoff of fresh water into the Sound. Stratification was strongest during these runoff periods.

Riley found that vertical salinity stratification was weak, averaging 1 - 2 psu, and that summertime thermal stratification was small, generally 1 - 2 °C. In winter, slight positive thermal gradients were common. An exception to the salinity structure was the region around the mouth of the Connecticut River, where a 2 - 4 m thick lens of low salinity water could have values 10 - 20 psu lower than the water underneath. The average east-west salinity change at the surface was about 4 psu (from about 25.5 psu near Throgs Neck to 29.5 psu at The Race) while at the bottom it was almost 5 psu (from less than 26 psu to about 30.5 psu). The longitudinal gradient was greatest at the eastern and western ends, and relatively slight in the middle. Horizontal gradients were strong near the Connecticut and Housatonic Rivers. The latter, however, had pronounced gradients only during periods of high runoff.

3.2. The Thermohaline Pattern in 1988

Extensive temperature and salinity observations were taken by SUNY and UCONN from April to September, 1988. We will look at horizontal and vertical patterns in April, June, August, and September to examine the development of seasonal stratification, the influence of fresh water inflow, and the late summer convective overturning.

<u>April 1988</u>

Figures 3.1 and 3.2 show near-surface and near bottom horizontal isopleths of temperature, salinity and sigma-t. Vertical cross-sections along the thalweg, and in the western (Stations H1 to H7), central (Stations K1 to K4) , and eastern (Stations B1 to B4) Sound are shown in Figures 3.3 - 3.6. Station locations are shown in the figure on page A-1.

The surface salinity increases from west to east from about 25 to 29 psu, with, in most areas, little vertical stratification, although the upper horizontal section shows strong evidence of outflow from the Connecticut and Housatonic Rivers. The salinity is more than 5 psu lower near the river than farther south. The near-bottom salinity has a north to south mid-Sound maximum except in the far western Sound. Seasonal stratification has not yet begun, but there is some thermal stratification in the far western Sound, although there is no systematic west-to-east gradient. The warmest surface water is in the far western Sound, while the coldest near bottom temperatures are in the central Sound. The section along the thalweg confirms the varying patterns of temperature and salinity stratification in different parts of the Sound.

The vertical cross-section in the western Sound (Figure 3.4) shows moderate stratification in both temperature and salinity, attributable to the upper layer inflow of warmer, fresher water from the East River, which enters the Sound on the Long Island side (Wilson and Bokuniewicz, 1990). In the upper layers the water becomes warmer and fresher from north to south. The temperature gradient is slightly reversed in the lower layers, with a near-bottom pool of cold, salty water along the southern slope. Moderate stratification is also present in the central Sound (Figure 3.5). The deep water is colder than in the west. The magnitude of the vertical salinity gradient is similar to the western section, but fresher water is found near both the Connecticut and Long Island coasts. In the eastern Sound (Figure 3.6), the most prominent feature is the shallow lens of fresher water from the Connecticut River. There is little thermal stratification, except near Connecticut. Unlike the central and western sections, there is no deep cold pool.

June 1988

Figures 3.7 - 3.12 show temperature, salinity and sigma-t patterns for mid-June. Thermal stratification is well established in most of the Sound. The surface temperatures have warmed by 8 - 14 °C and the bottom temperatures by 7 - 10 °C, giving a top to bottom gradient of 4 - 5 °C through most of the central and western Sound. This is a considerably larger gradient than was found by Riley (1956). Thermal stratification was established by late April in the western and open central Sound, and by early May in most of the eastern Sound. Thermal stratification is generally less in the eastern Sound, where tidal currents are much stronger than farther west. The surface temperature section shows evidence of pronounced thermally controlled gyres in the central and eastern Sound, and there are strong thermal gradients in most areas. Surface temperatures often vary by several degrees in a few kilometers. As in April, the coldest bottom temperatures are in the central Sound.

Salinity stratification is very weak in the western Sound, and similar to April in the central Sound. The west to east gradient is similar overall, but there is an extensive region of weak reversal in the upper fifteen meters. The water in Block Island Sound is 1 psu or more saltier than in April at all depths.

The vertical cross section in the western Sound (Figure 3.10) does not have lighter water to the south, as it did in April. The near-bottom pool of cold water is still present. In the central cross-section (Figure 3.11), water at intermediate depths tends to become colder and saltier from

south to north, with a reversal near Connecticut. Thermal stratification in the eastern cross-section is much less than farther west, and there is no evidence of Connecticut River outflow.

August - September 1988

By early August (Figures 3.13 - 3.18), all levels of the central and western Sound have warmed by more than five degrees from mid-June. Thermal stratification is strong, except in the extreme western Sound; the thermocline begins three to five meters below the surface in most regions. Gyres are still present in the western and central Sound, but are weaker than in June. Thermal stratification continues to be much weaker in the far eastern Sound, due to considerably lower surface temperatures. Note in Figure 3.15 that, due to missing data, the section along the thalweg extends only through part of the eastern Sound. The west to east salinity gradient is smaller than in June, with salinity in the far western Sound over 26 psu. In much of the central and eastern Sound, the south to north rate of surface salinity increase is larger than the east to west rate. At mid and lower depths, the weak salinity gradient reverses through parts of the central Sound. These reversals were associated by Wilson (1976) with reversals in the estuarine circulation, and together with the gyral structures found in the surface temperature in June, indicate how complex and variable the residual circulation in the central Sound can be.

The north to south section in the western Sound (Figure 3.16) shows a weak south to north increase in salinity and a strong temperature structure. The lightest near-surface water is in the south-central part of the section, with density isopleths sloping upward from south to north through most mid and upper depths. In the central Sound (Figure 3.17) there is a somewhat larger vertical salinity gradient than in April or June; deep salinities are higher. The thermal structure shows a stronger thermocline; as in the west, almost all regions are 6 - 7 °C warmer. In the eastern section (Figure 3.18), salinity is higher than in June at all depths. The vertical thermal gradient continues to be weak, with near-surface temperatures more than five degrees lower than in the western and central Sound.

Figures 3.19 and 3.20 show north to south temperature sections in the central Sound for mid-August and mid-September, respectively. By mid August, the vertical temperature structure has greatly weakened. The top to bottom temperature gradient, which was more than 5 °C except in the shallow far north, has decreased to less than 3 °C almost everywhere. There is a notable thermocline only in the southern portion. By mid-September, the thermal structure is gone. Other data indicate that it had disappeared by early September.

3.3. Summary of Thermohaline Structure

Thermal stratification is usually established by late April in the western and open central Sound, and by early May in most of the eastern Sound. However, the freshwater inflow associated with spring snow melt as well as the spring - summer surface air temperature patterns vary from year to year and directly effect the onset and degree of stratification. Thermal stratification is generally less in the eastern Sound, where tidal currents are much stronger than further west. During high Connecticut River inflow, the plume is usually confined to the Connecticut shoreline

with general propagation to the west. A "C" shape in the surface salinity contours is evident in western Long Island Sound. Freshwater outflow from the East River tends to attach to the Long Island shoreline. As freshwater inflows are reduced in late summer and early fall, in much of the central and eastern Sound, the south to north rate of surface salinity increase is larger than the east to west rate. At mid and lower depths, the weak salinity gradient reverses through parts of the central Sound. These reversals account for reversals in the estuarine circulation and indicate how complex and variable the residual circulation in the central Sound can become. Cross-sound transfers are associated with gyres, which are intermittent in time and variable in spatial extent within the western and central basins.

Long Island Sound Observations

Surface Salinity

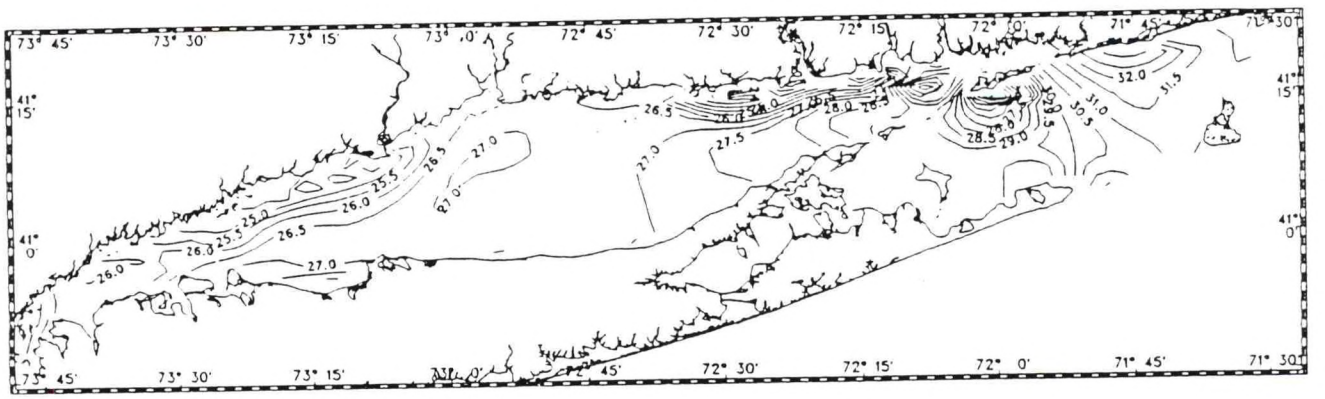

Surface Temperature [C]

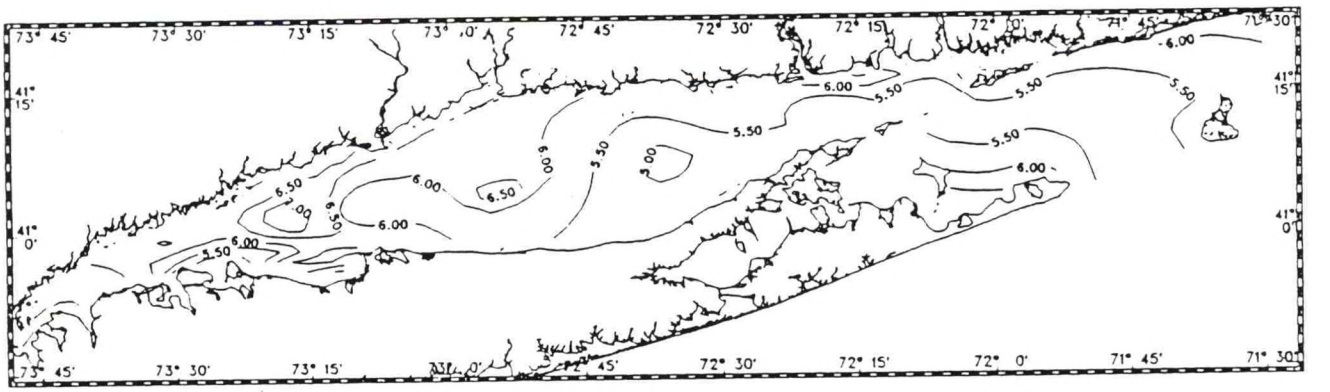

Surface Density

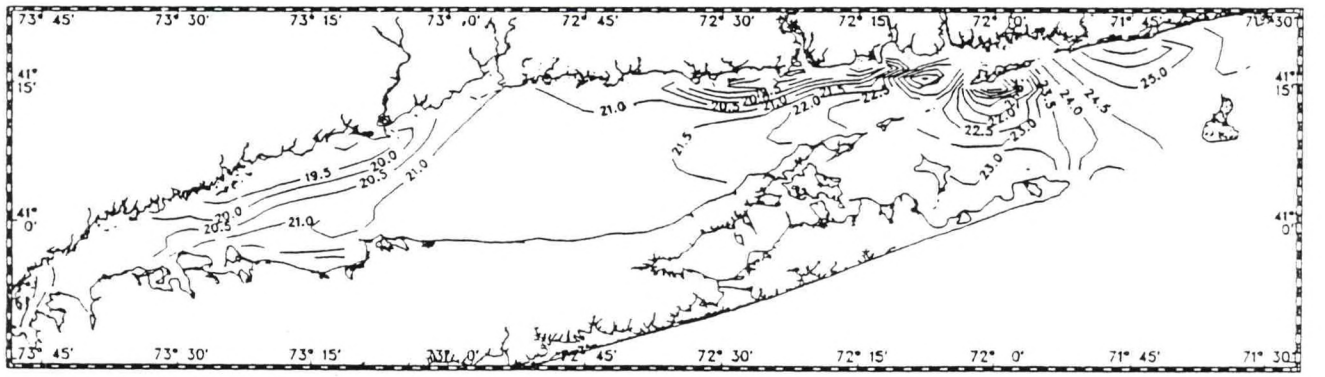

April 4 - 7, 1988

Figure 3.1. Near Surface Salinity, Temperature, and Sigma-t Maps: April 1988

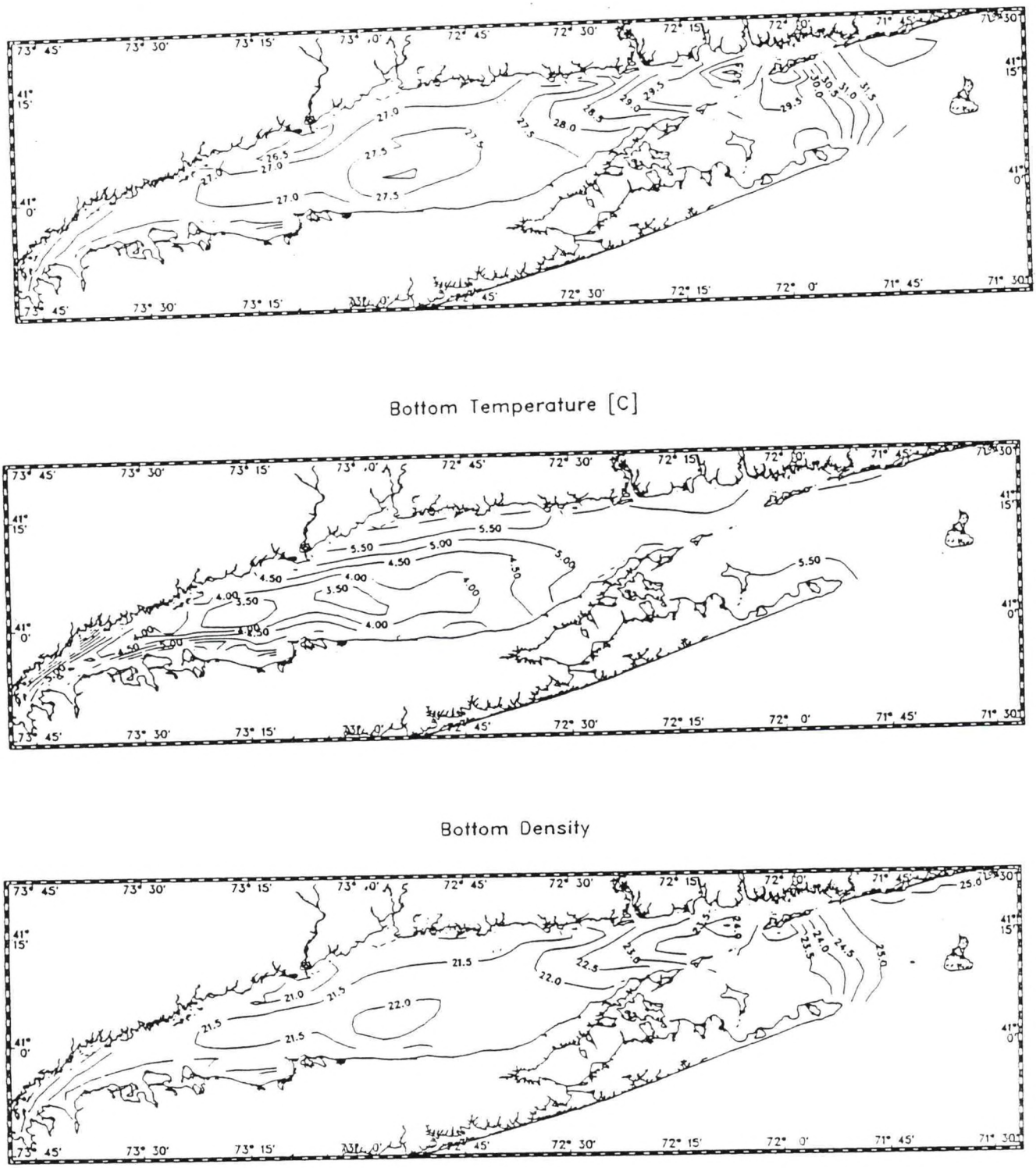

Figure 3.2. Near Bottom Salinity, Temperature, and Sigma-t Maps: April 1988

Long Island Sound Observations

West Master CTD Stations Salinity East

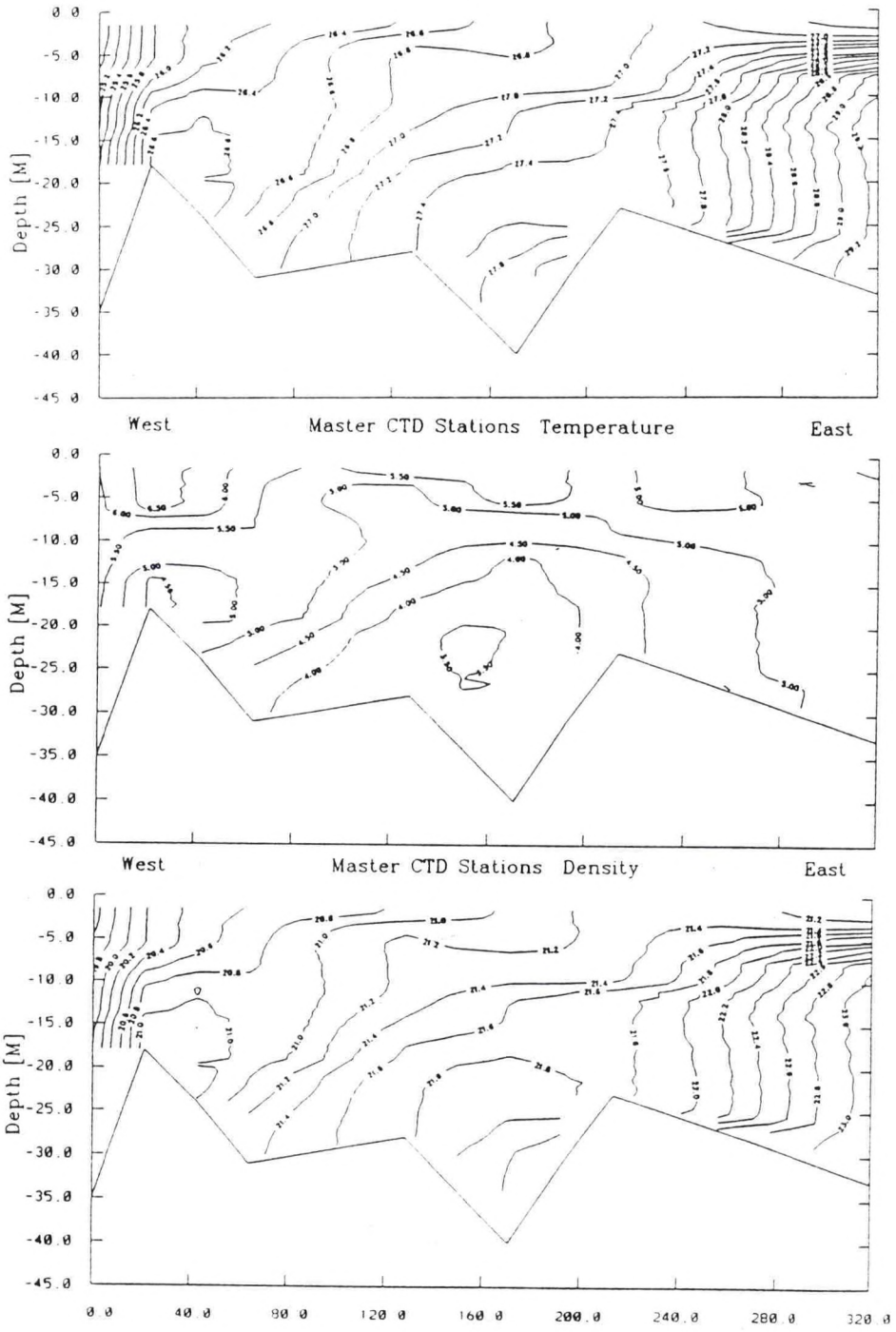

KM Distance

April 4 - 7, 1988

Figure 3.3. Longitudinal Profiles of Salinity, Temperature, and Sigma-t: April 1988

Long Island Sound Observations

North Station B1 - B4 Salinity South

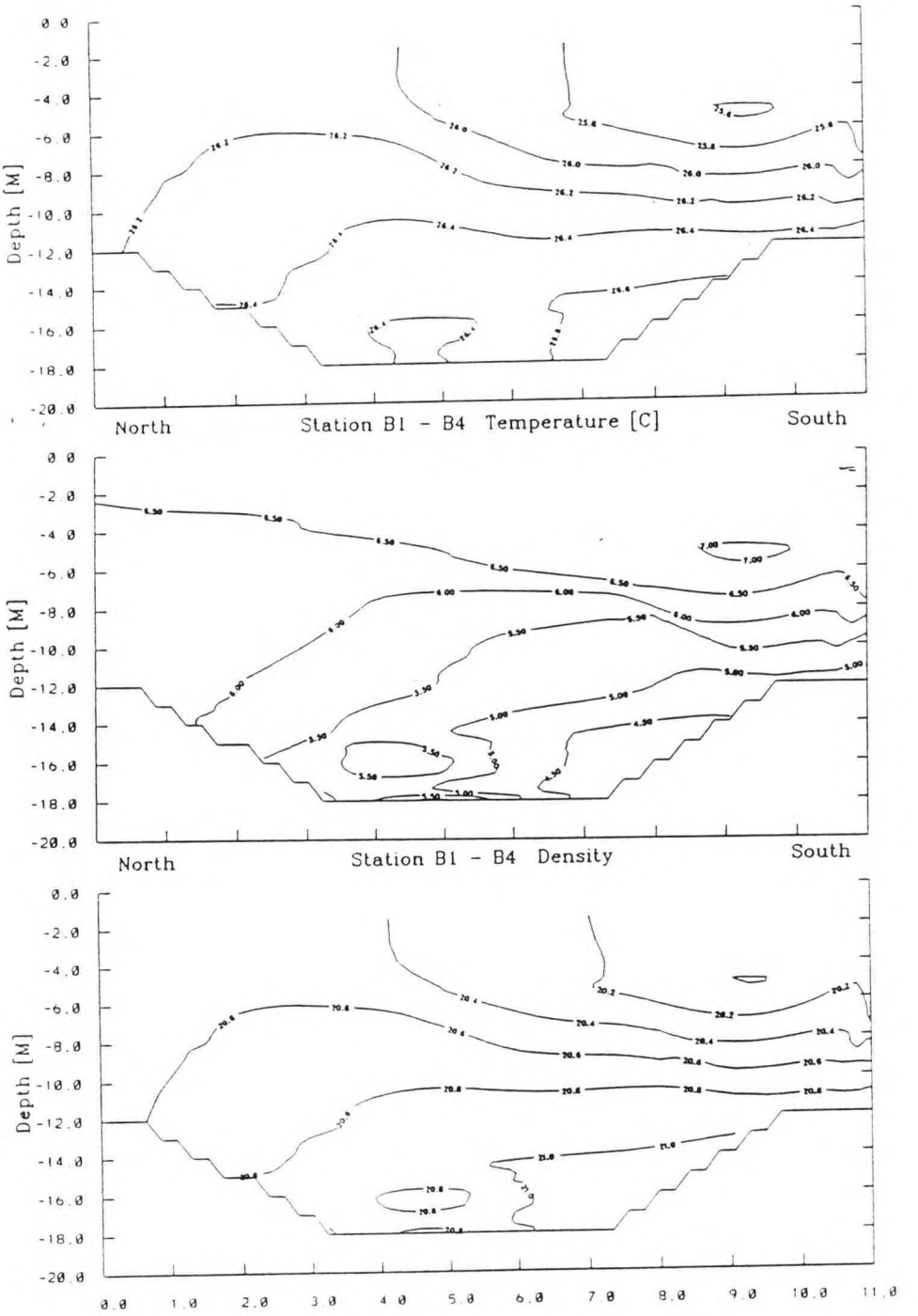

KM Distance

April 4, 1988

Figure 3.4. B1 - B4 North-South Section: April 1988

Long Island Sound Observations

North Station H1 - H7 Salinity South

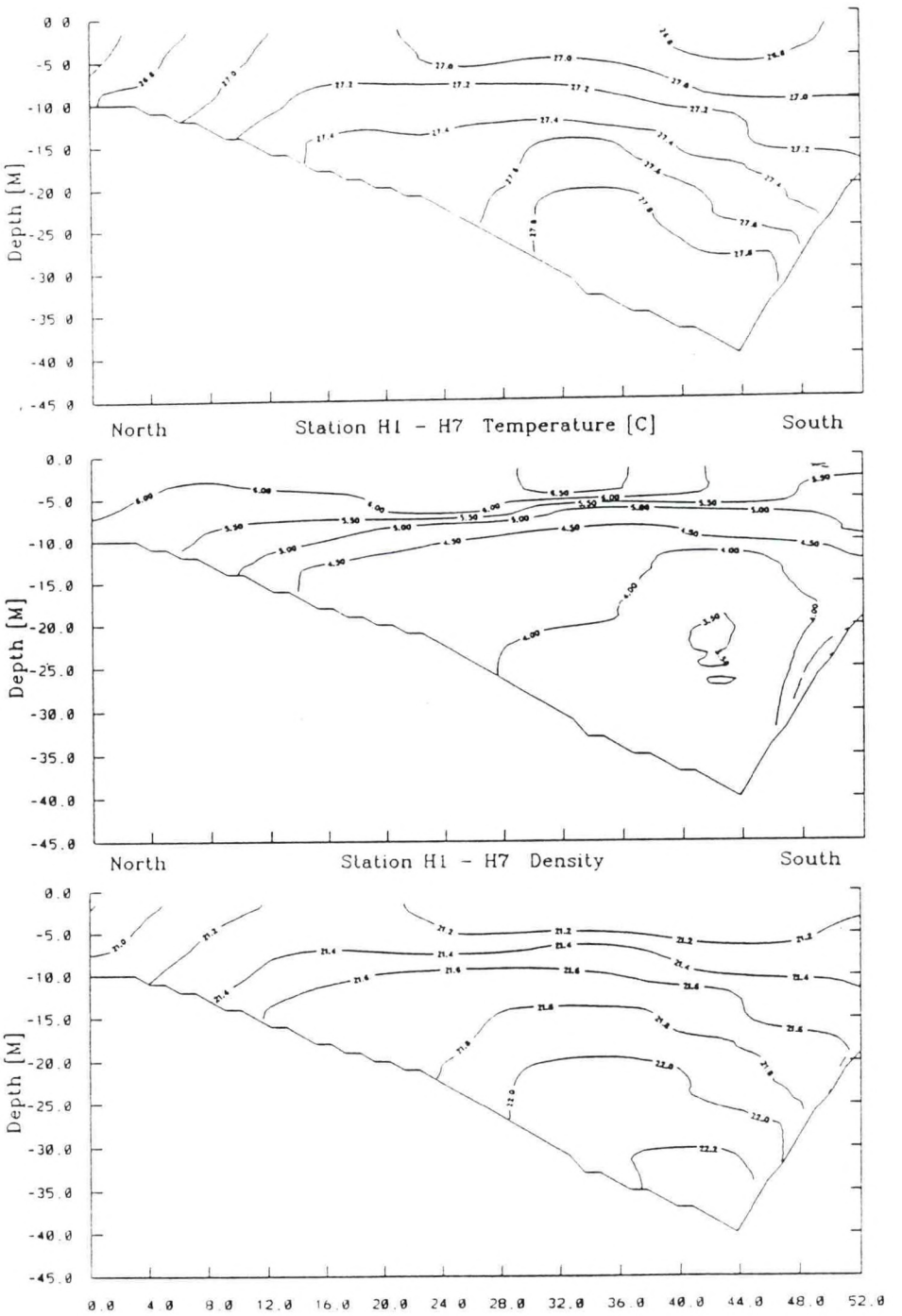

KM Distance

April 6, 1988

Figure 3.5. H1 - H7 North-South Section: April 1988

Long Island Sound Observations

North Station K1 - K4 Salinity South

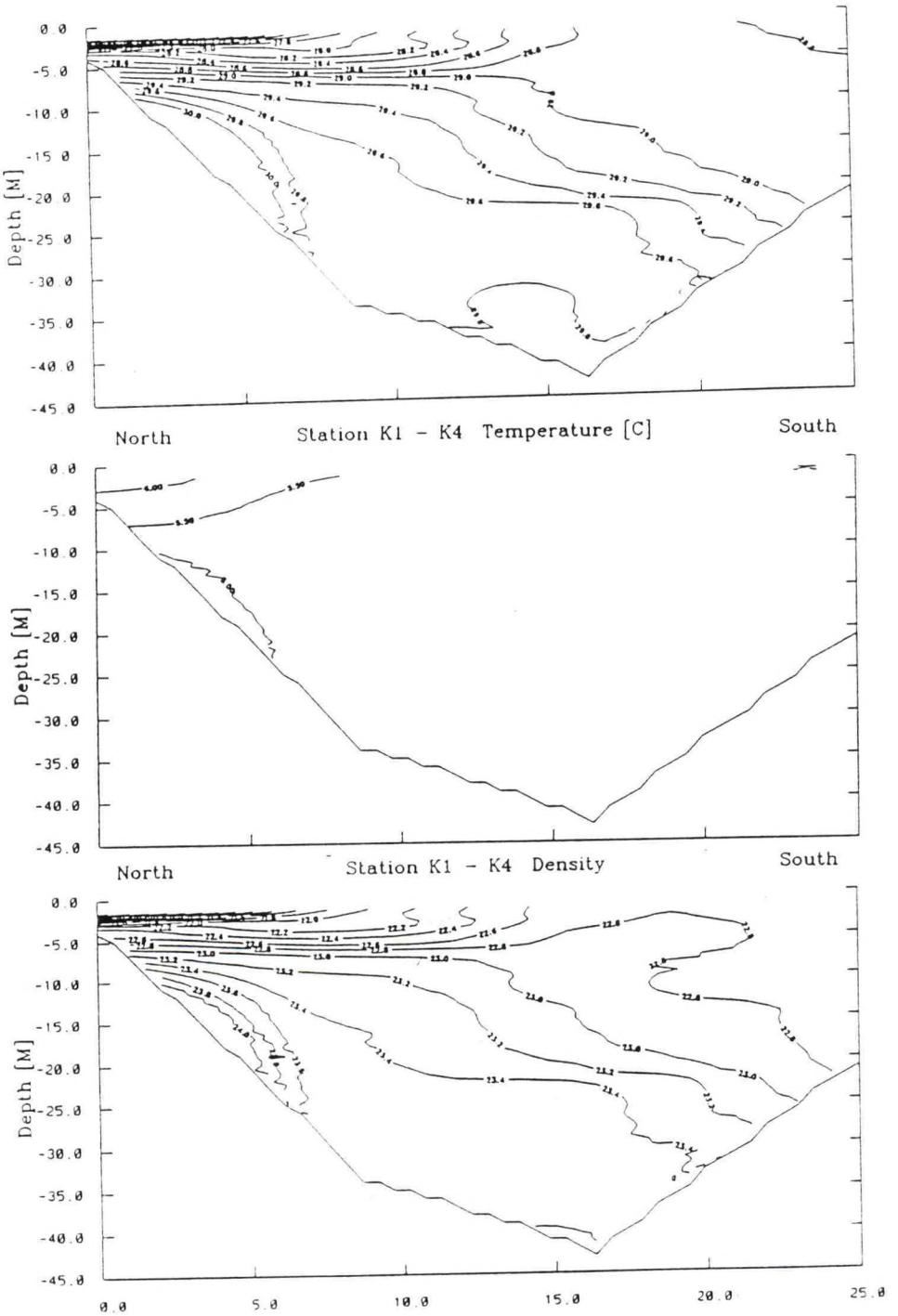

KM Distance

April 6, 1988

Figure 3.6. K1 - K4 North-South Section: April 1988

Long Island Sound Observations

Surface Salinity

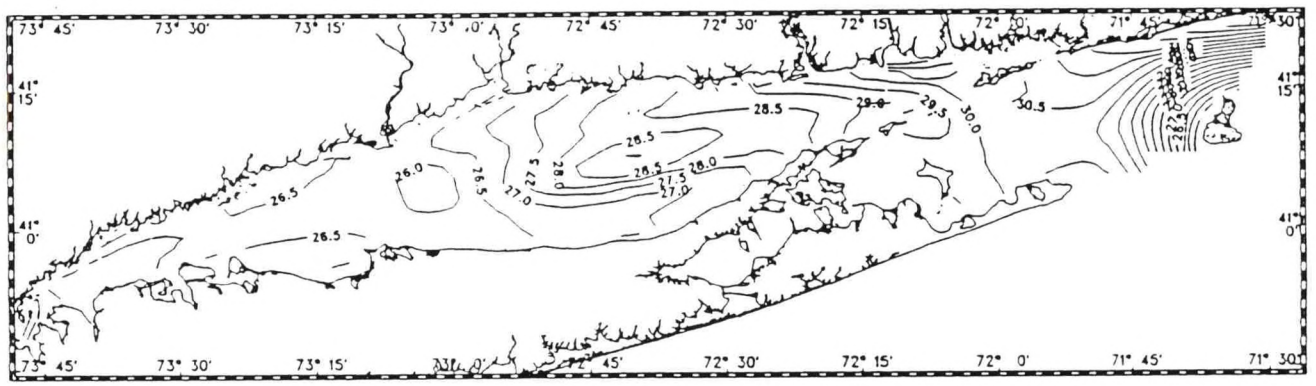

Surface Temperature [C]

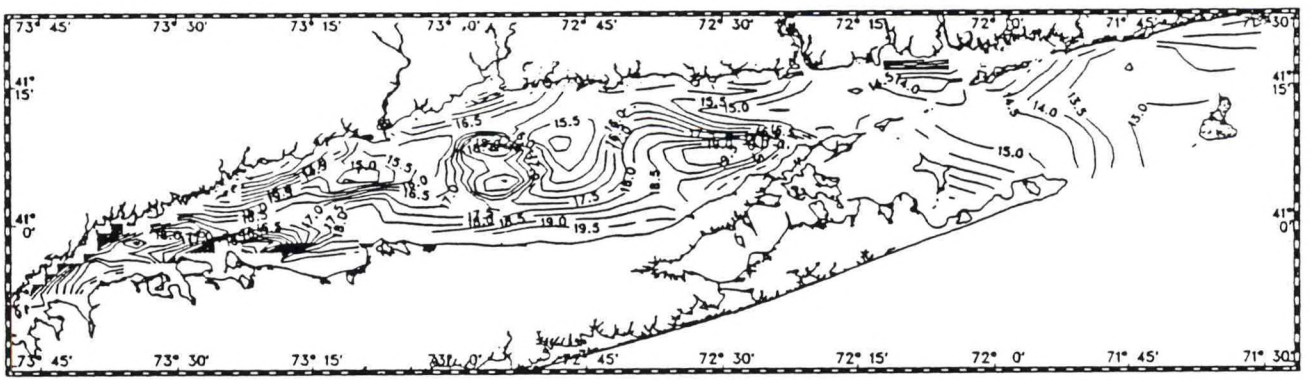

Surface Density

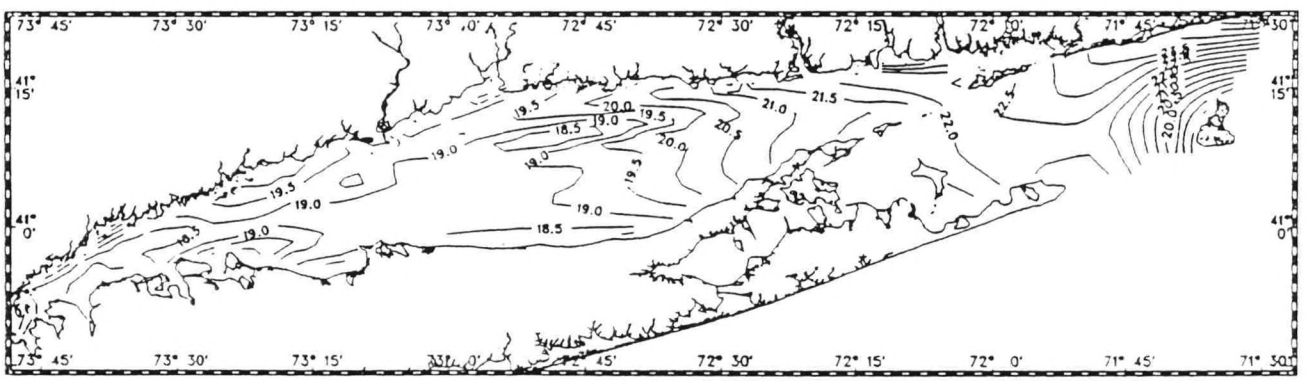

June 13 - 16, 1988

Figure 3.7. Near Surface Salinity, Temperature, and Sigma-t Maps: June 1988

Long Island Sound Observations

Bottom Salinity

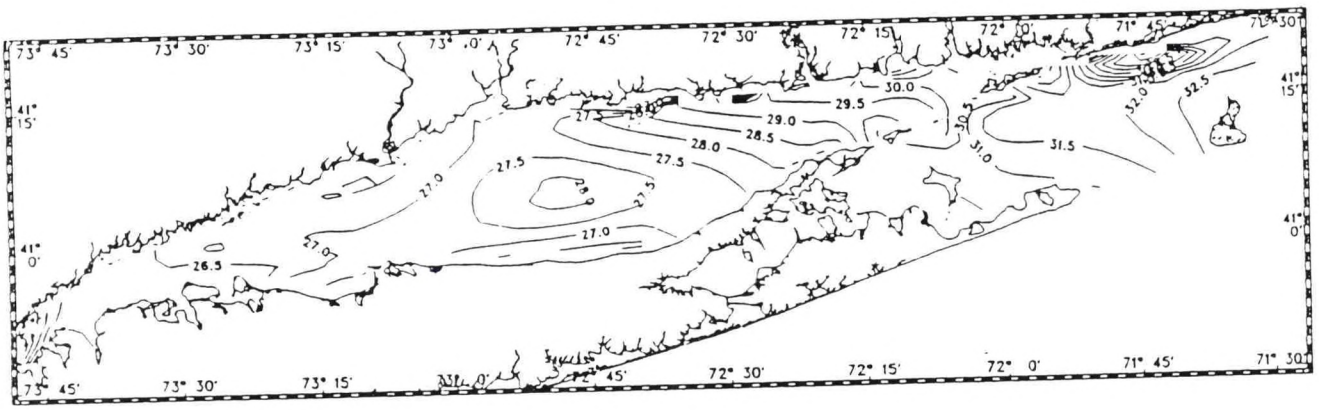

Bottom Temperature [C]

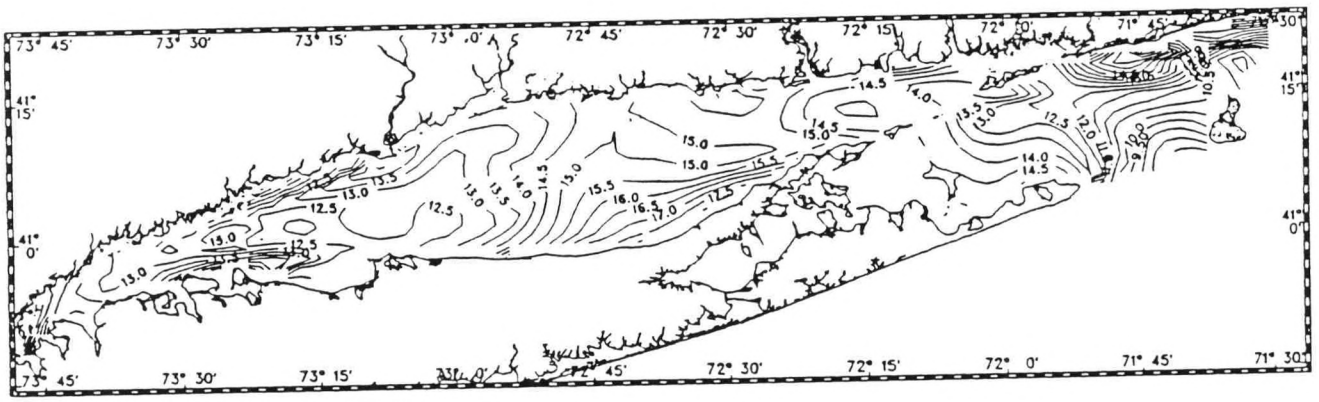

Bottom Density

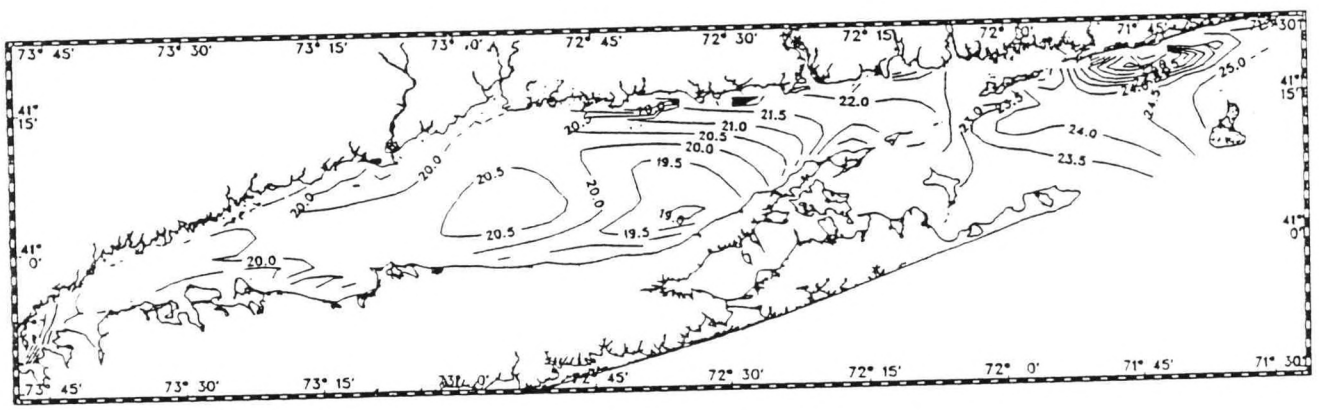

June 13 - 16, 1988

Figure 3.8. Near Bottom Salinity, Temperature, and Sigma-t Maps: June 1988

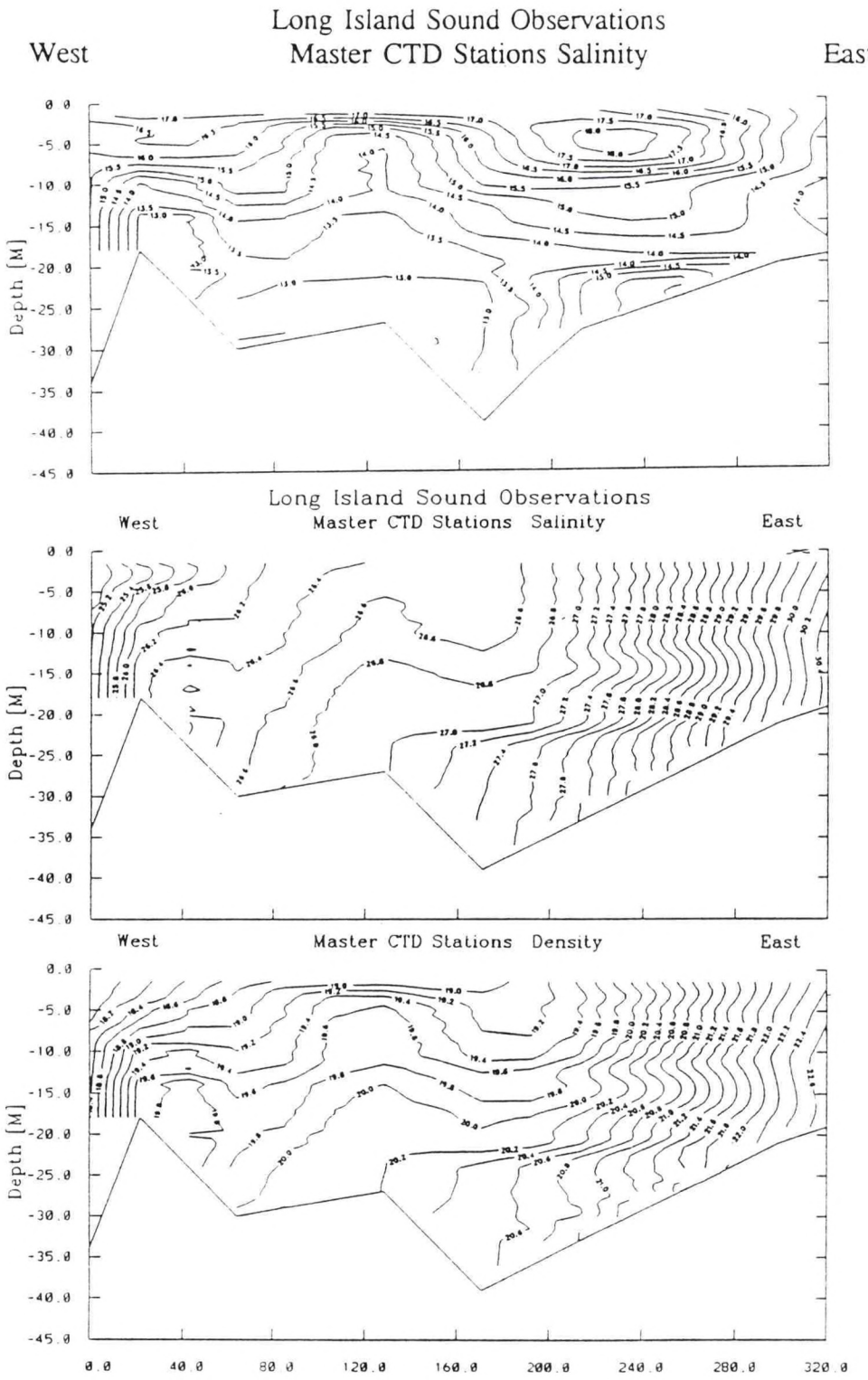

June 13 - 16, 1988

Figure 3.9. Longitudinal Profiles of Salinity, Temperature, and Sigma-t: June 1988

Long Island Sound Observations

North Station B1 - B4 Salinity South

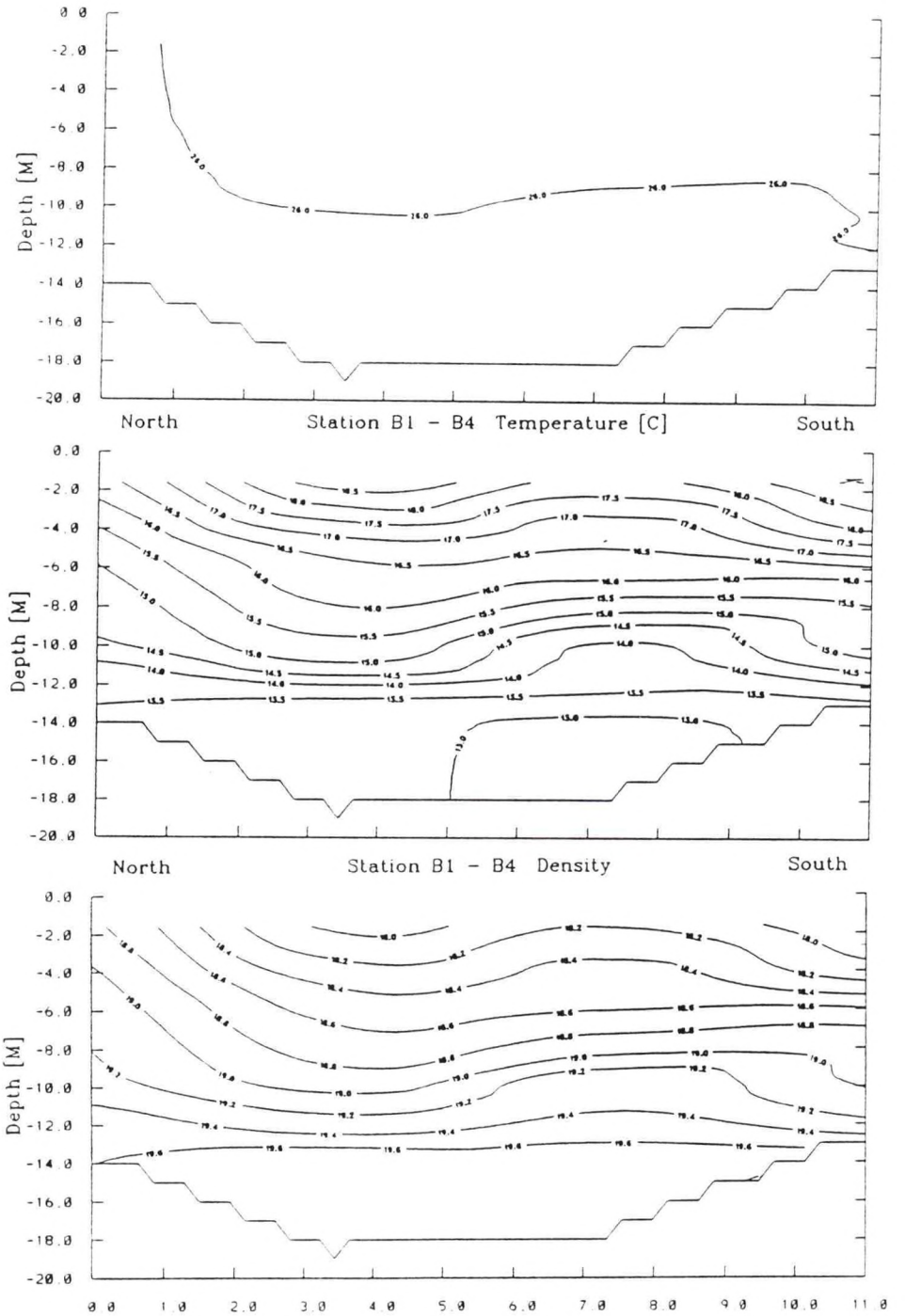

June 13, 1988

Figure 3.10. B1 - B4 North-South Section: June 1988

Long Island Sound Observations

North Station H1 - H7 Salinity South

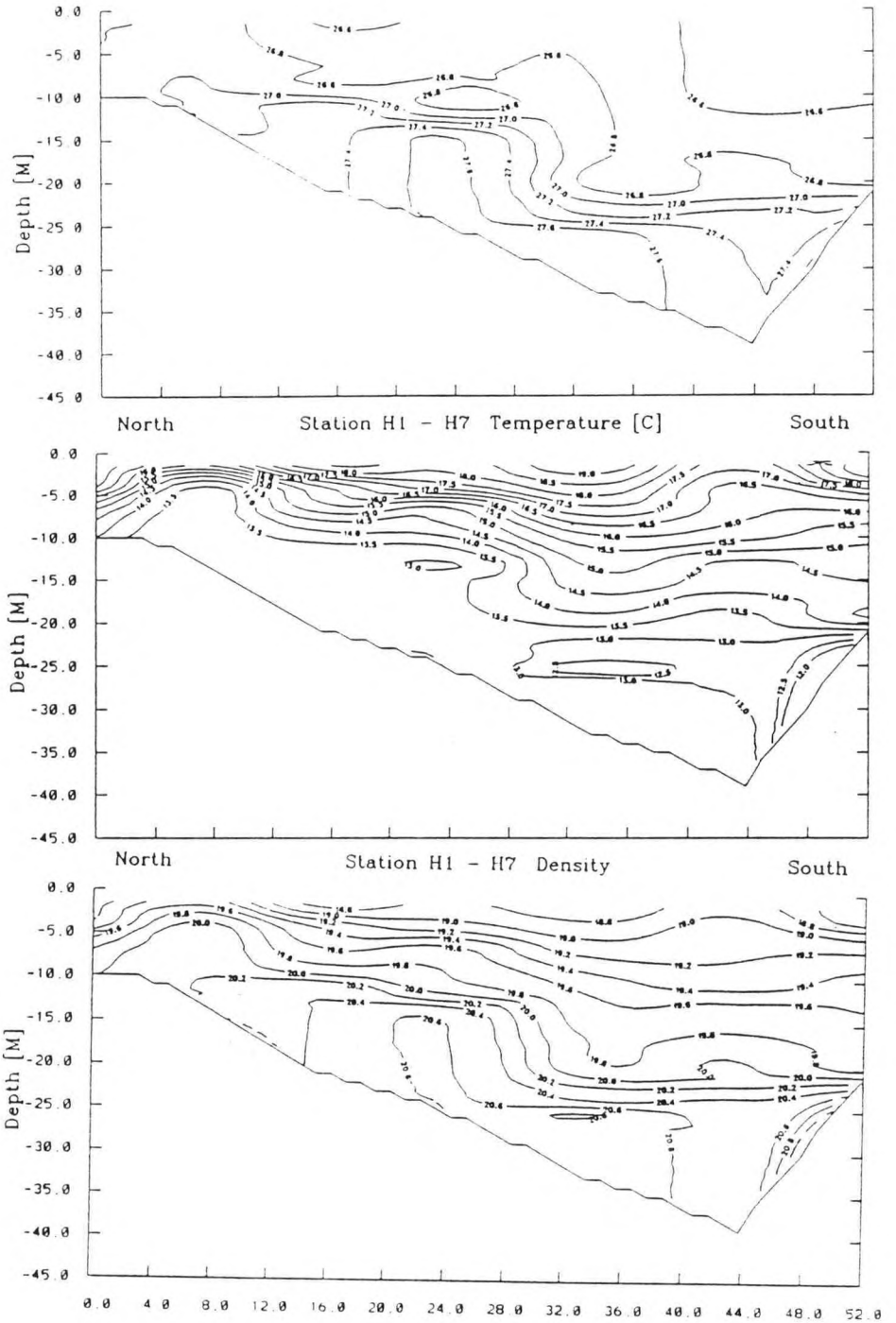

KM Distance

June 15, 1988

Figure 3.11. H1 - H7 North-South Section: June 1988

Long Island Sound Observations

North Station K1 - K4 Salinity South

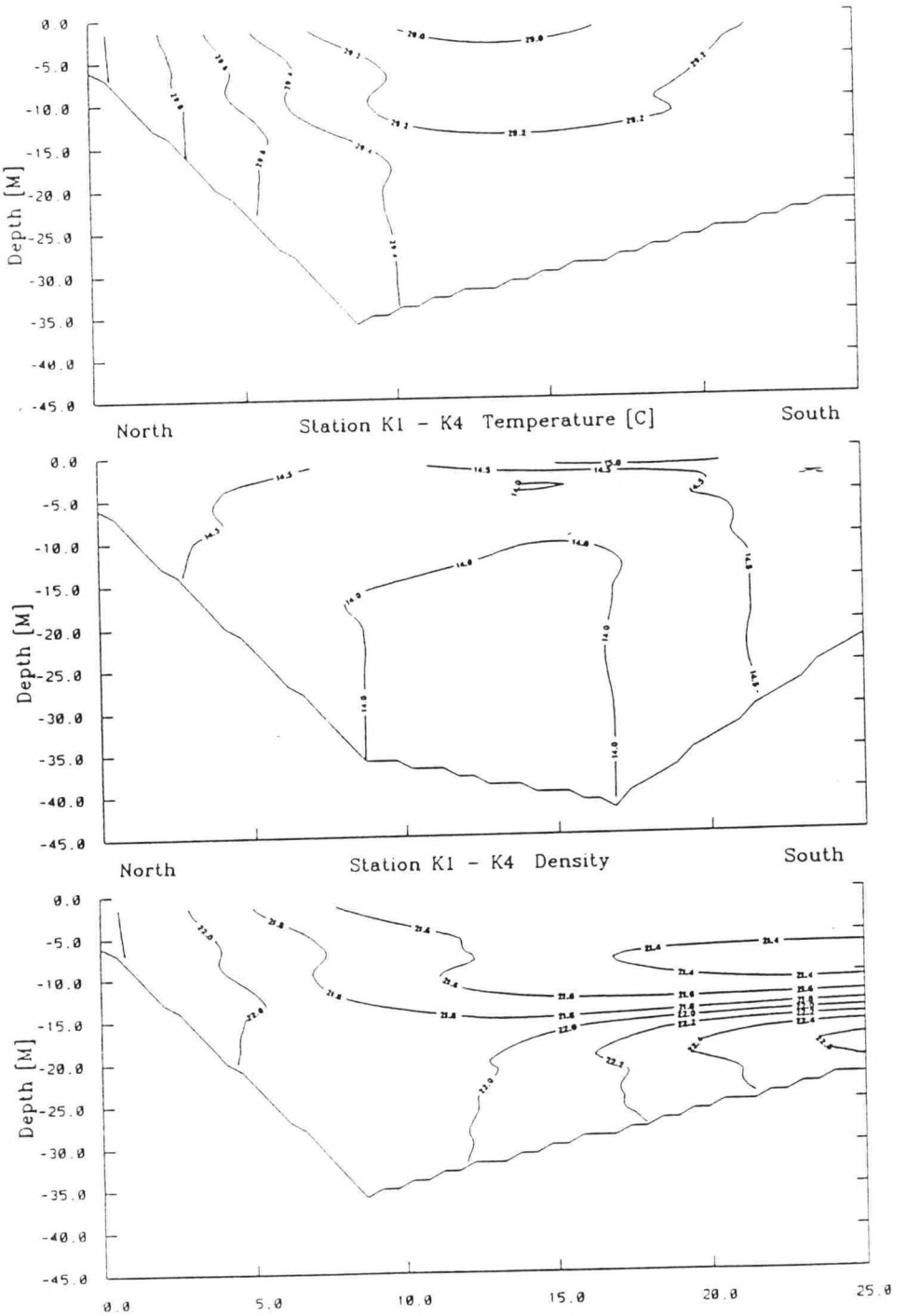

KM Distance

June 15, 1988

Figure 3.12. K1 - K4 North-South Section: June 1988

Long Island Sound Observations

Surface Salinity

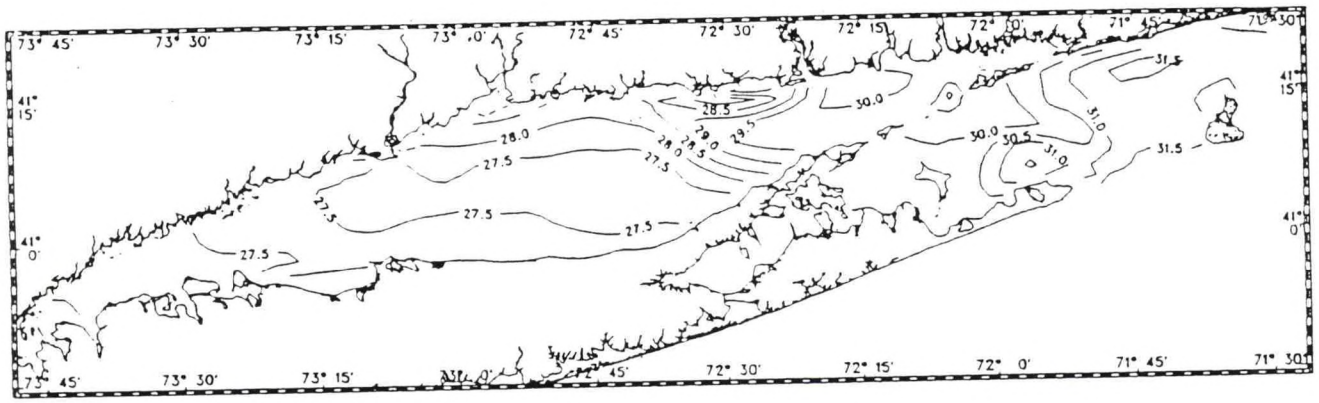

Surface Temperature [C]

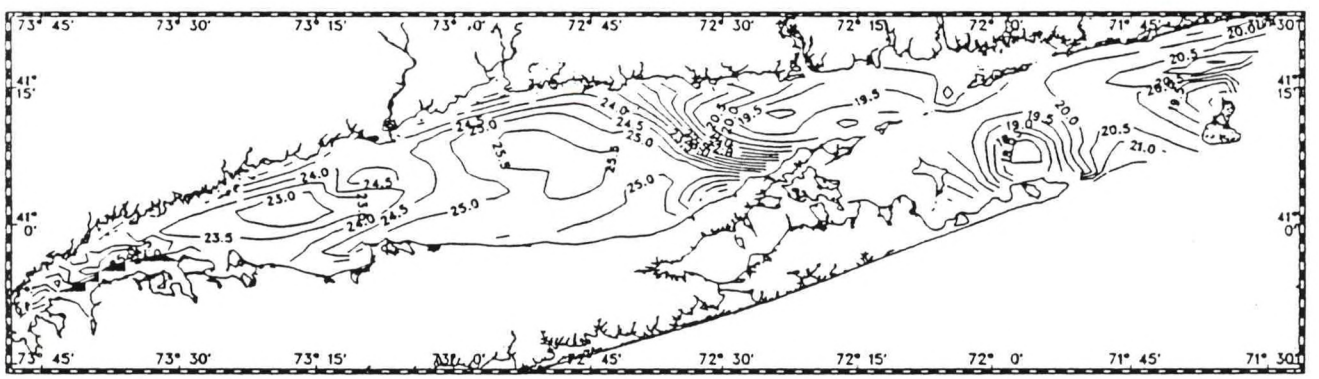

Surface Density

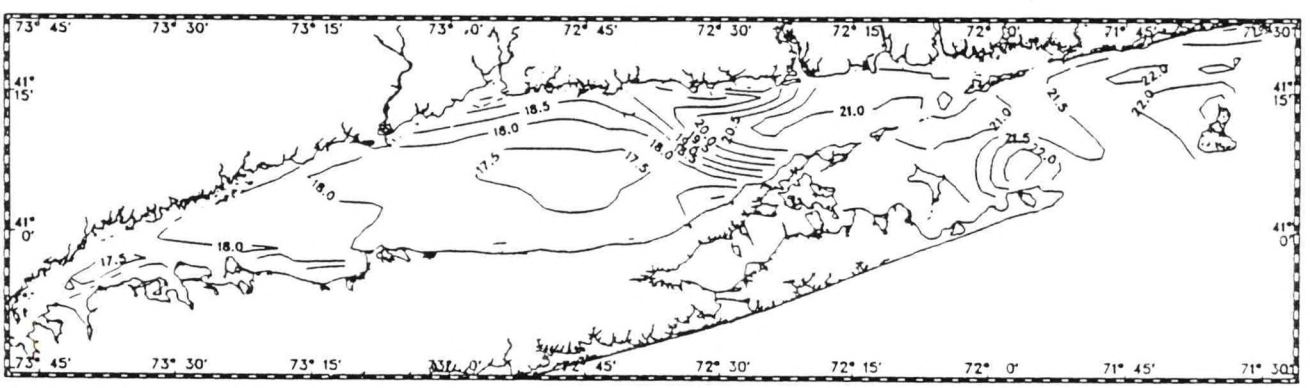

August 2 - 4, 1988

Figure 3.13. Near Surface Salinity, Temperature, and Sigma-t Maps: August 1988

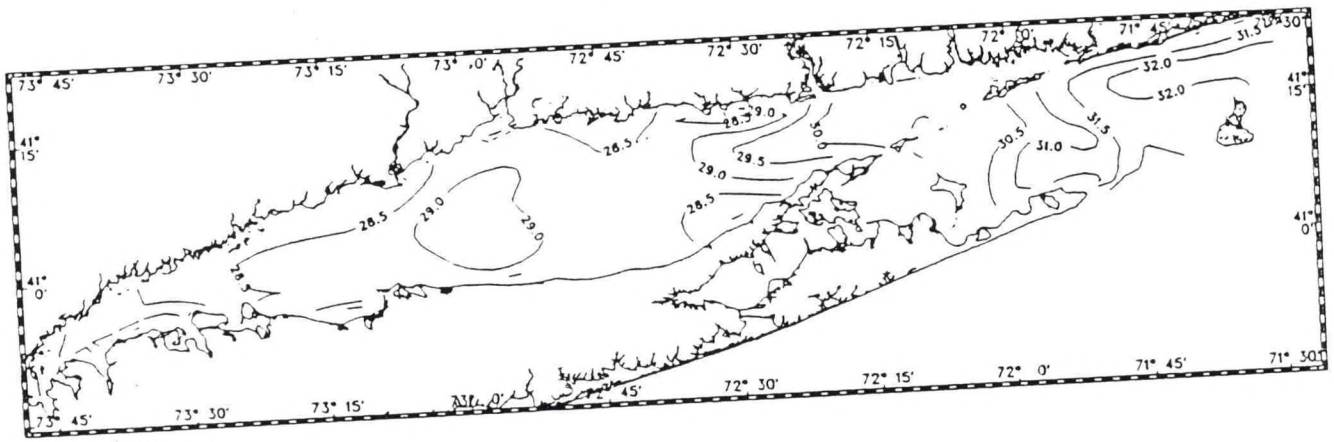

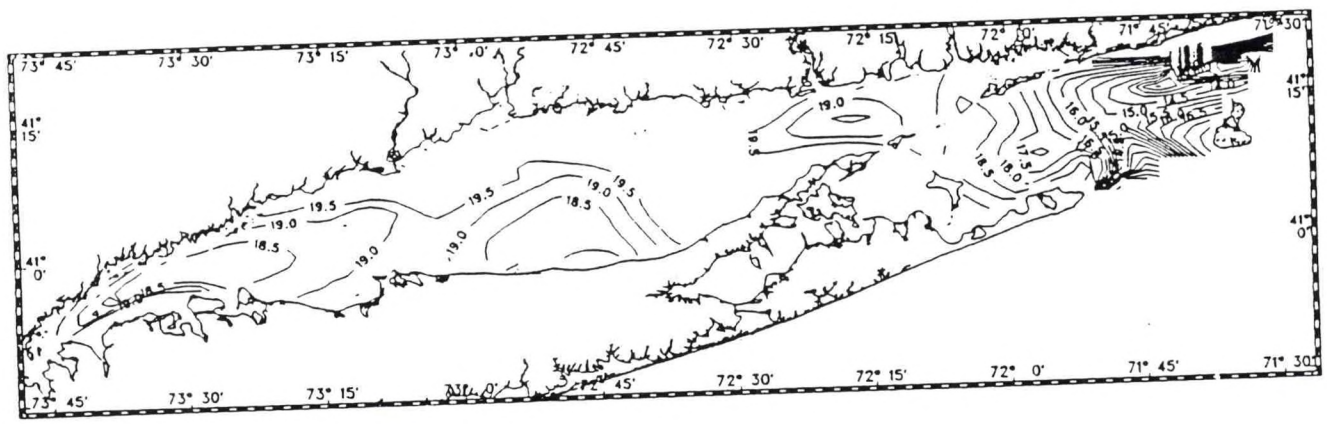

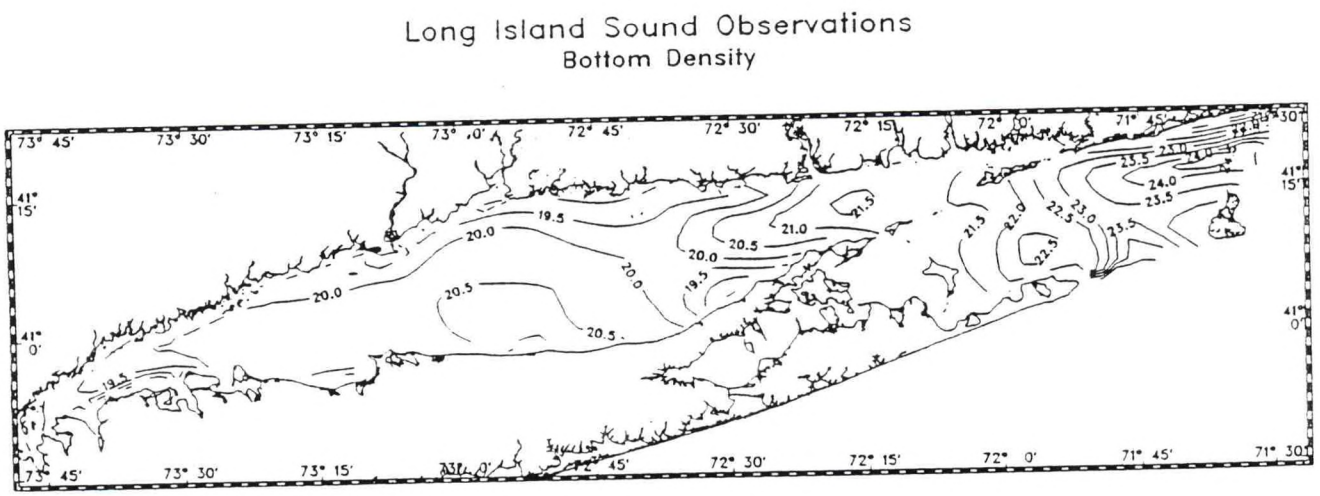

August 2 - 4, 1988

Figure 3.14. Near Bottom Salinity, Temperature, and Sigma-t Maps: August 1988

Long Island Sound Observations

West Master CTD Stations Salinity East

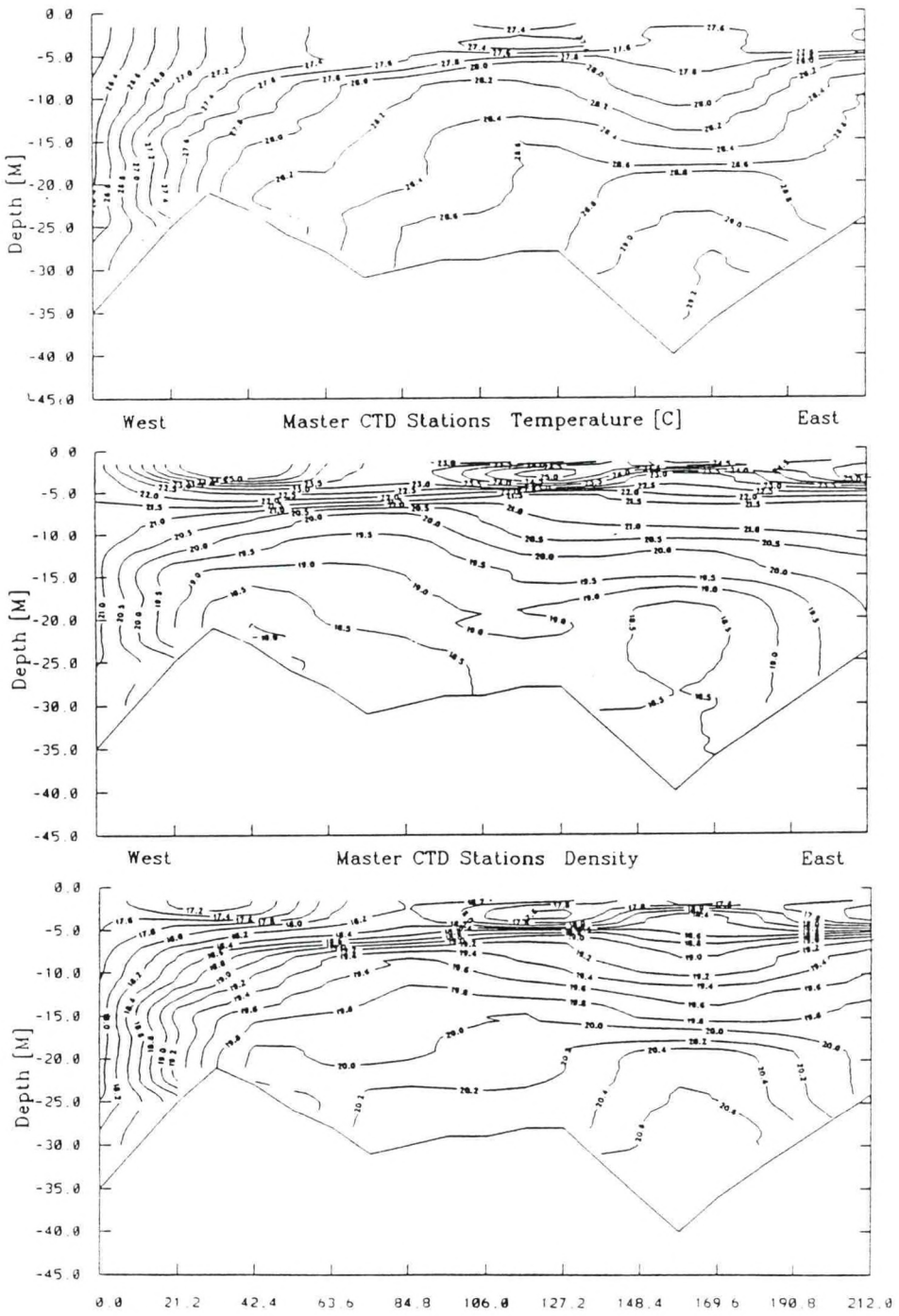

KM Distance

August 2 - 4, 1988

Figure 3.15. Longitudinal Profiles of Salinity, Temperature, and Sigma-t: August 1988

Long Island Sound Observations

North Station B1 - B4 Salinity South

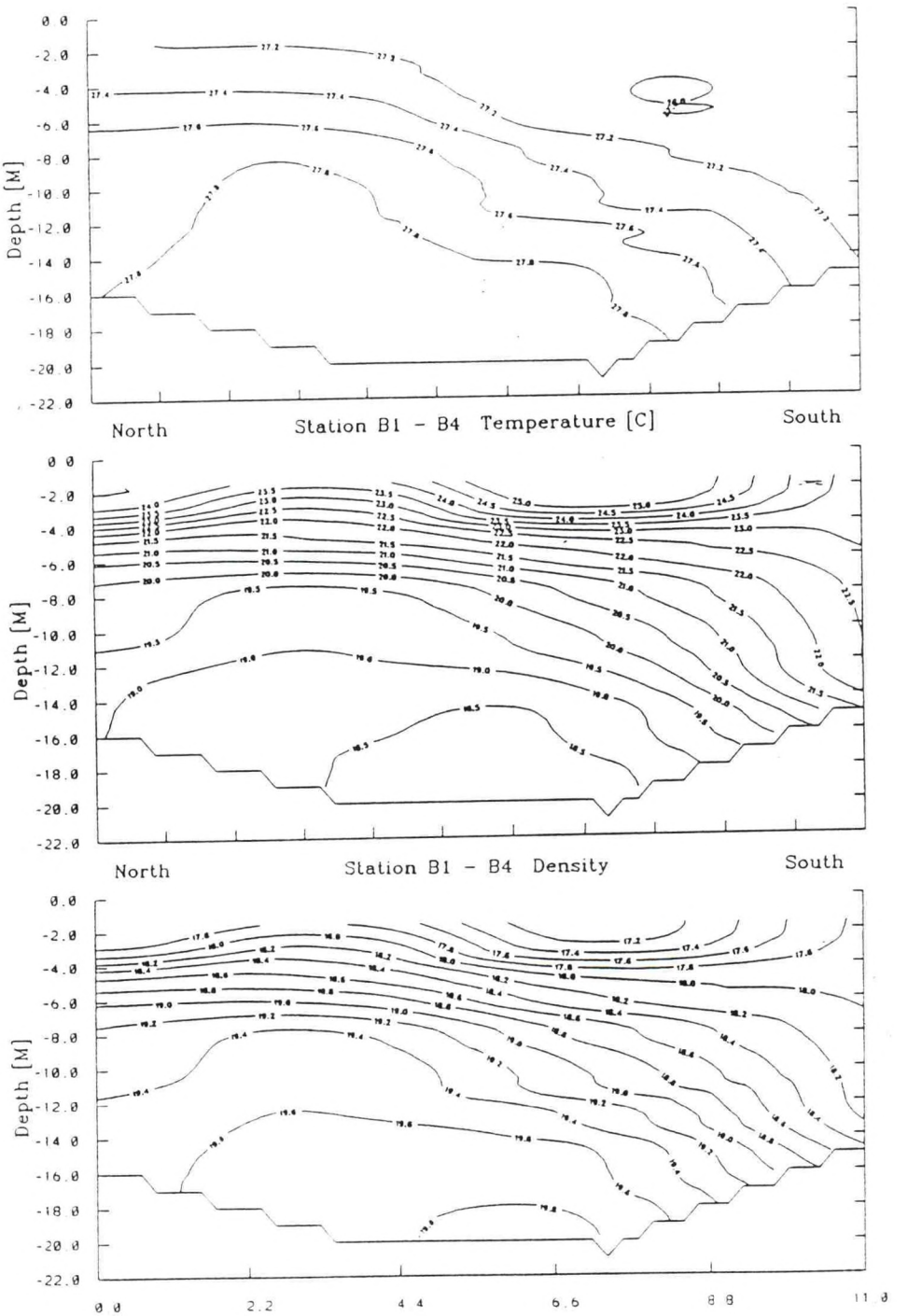

KM Distance

August 3, 1988

Figure 3.16. B1 - B4 North-South Section: August 1988

Long Island Sound Observations

North Station H1 - H7 Salinity South

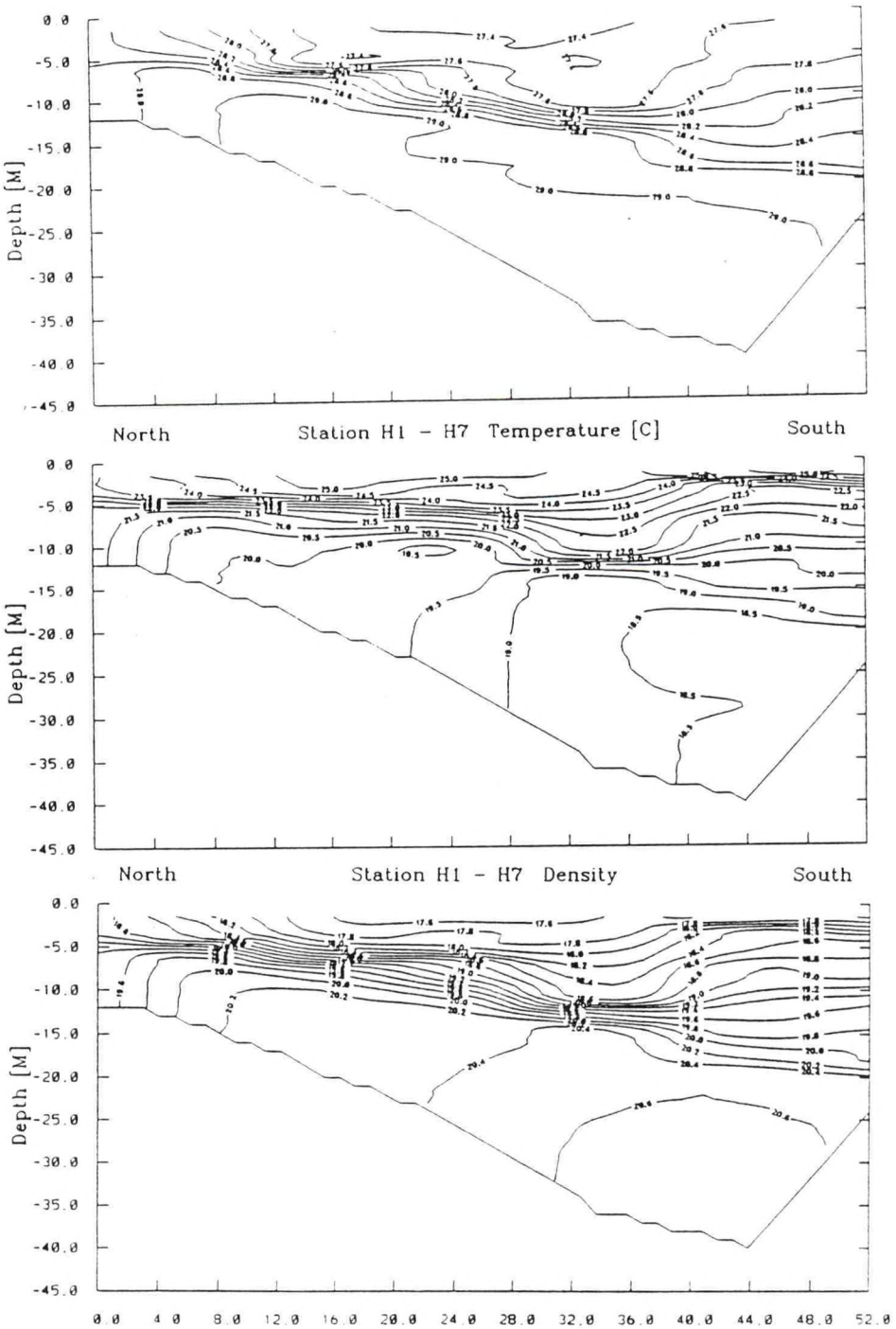

KM Distance

August 2, 1988

Figure 3.17. H1 - H7 North-South Section: August 1988

Long Island Sound Observations

North Station K1 - K4 Salinity South

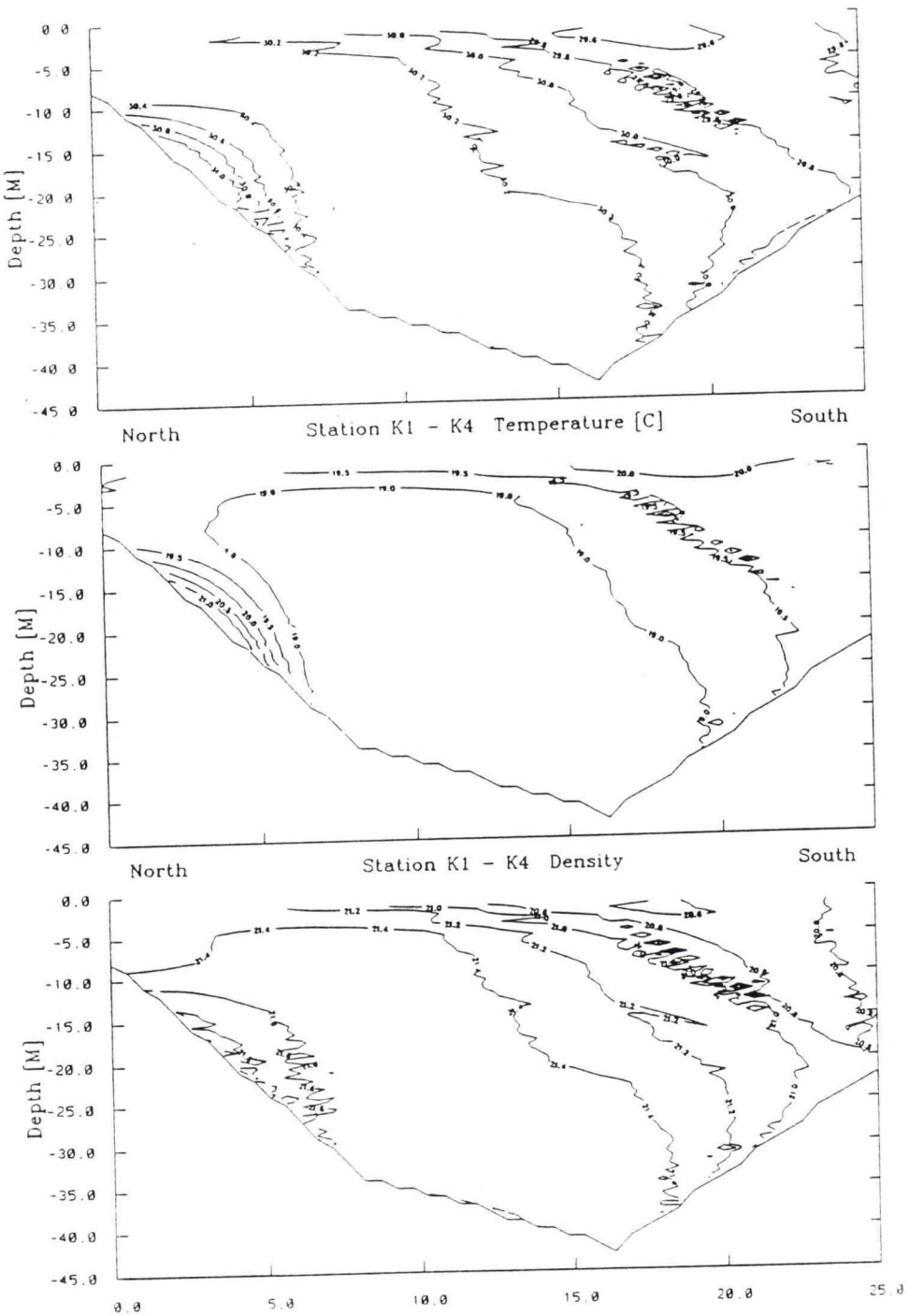

August 3, 1988

Figure 3.18. K1 - K4 North-South Section: August 1988

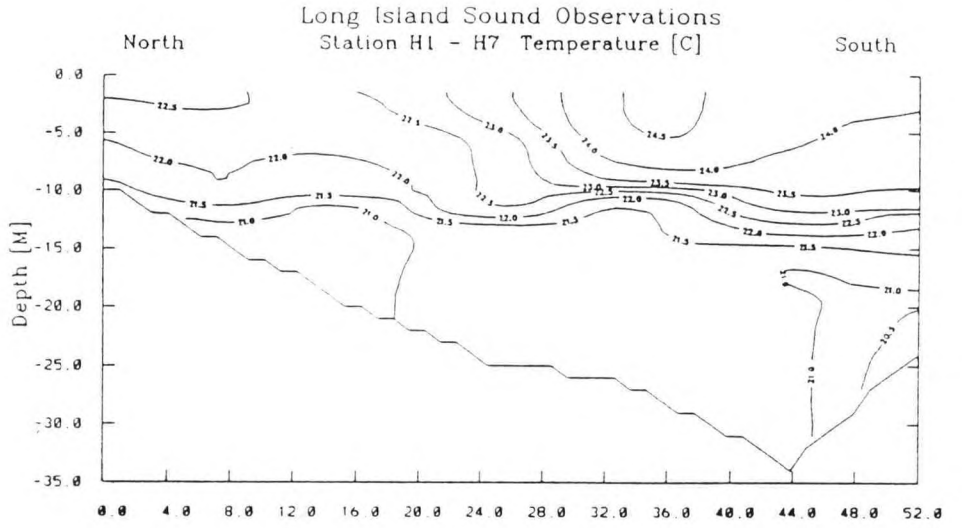

Figure 3.19. H1 - H7 North-South Section: August 17, 1988

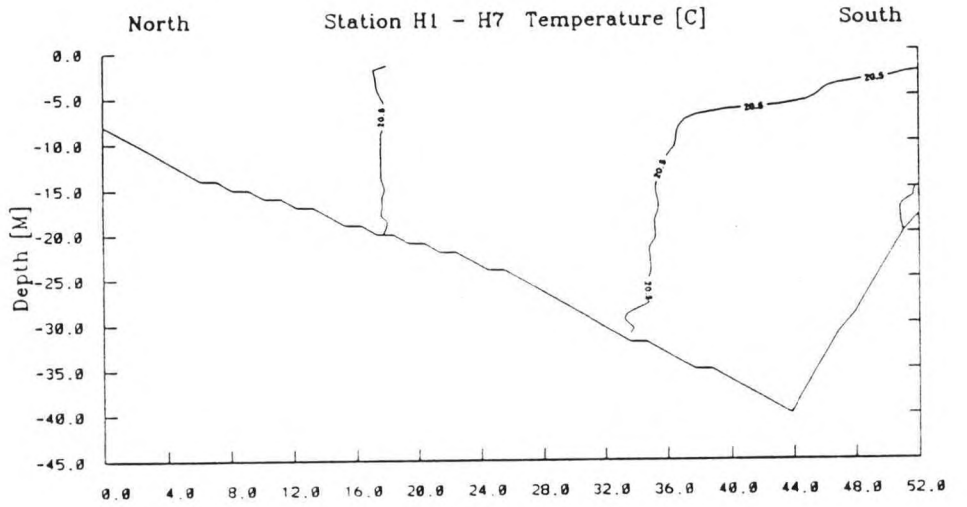

Figure 3.20. H1 - H7 North-South Section: September 16, 1988

4. RESIDUAL CIRCULATION OBSERVATIONAL DATA AND INTERPRETATION

The residual current at any point in an estuary is defined here as the net water movement after the periodic tidal current has been filtered out of the total current. This residual current accounts for all of the net transport of water. In the absence of wind, the largest part of the residual current system is usually the gravitational circulation.

The gravitational circulation in Long Island Sound is complex because of the multiple sources of fresh water to the Sound. In a simple partially mixed river system, the salinity will increase steadily along the river from the first point of measurable salinity down to the river mouth and beyond. In Long Island Sound, the greatest source of fresh water is the Connecticut River, but it directly influences only the extreme northeastern portion of the Sound. At the western end, although fresher water enters the Sound, there is believed to be a net removal of water into New York Harbor (Jay and Bowman, 1975). Salinity increases from west to east, but often in an irregular manner; in the central Sound, the west to east gradient is sometimes slightly reversed. The gravitational circulation may be correspondingly irregular.

The magnitude of gravitational circulation in Long Island Sound is much smaller than that of the tidal currents; the water movement recorded by current meters in all parts of the Sound is primarily oscillatory. There are also several other scales of motion that can obscure or confuse a pure estuarine-type circulation. Long-term barotropic pressure gradients can generate an additional net transport of water. The wind can set up strong near surface currents and compensating lower layer currents that can interact with estuarine currents over both short and long time scales. Other important residual flows can be generated by the interaction of tidal currents with complex topography, particularly near The Race (Ianello, 1981) and north of topographic projections into the Sound such as Matinecock Pt. and Eatons Neck (Wilson, personal communication). These residual flows result from the relative vorticity (rotation) of water columns being increased or decreased as they move into deeper or shallower regions or around topographic barriers, and are often associated with small-to moderate-scale eddies.

4.1. Previous Observations and Analyses

The large-scale gravitational circulation in Long Island Sound, with a general eastward flow of lower salinity water in the upper layer and a westward flow of higher salinity water in the lower layer, has been extensively studied only since the 1950's, when it was analyzed as part of a series of reports on the Sound by Riley (1952, 1956). Some long-term measurements were made earlier (LeLacheur and Sammons, 1932), and non-tidal currents were qualitatively attributed to wind and fresh water runoff, but no analysis was given.

Riley (1956) deduced from temperature and salinity records and some current meter measurements that a two layer circulation exists throughout most of the Sound, becoming progressively stronger from west to east. The net transport increases from about 3,000 m^3/s to 15,000 m^3/s in cross-sections through the central and eastern Sound to nearly 20,000 m^3/s

through The Race. In the western Sound he calculated that eastward transport is about 1,100 - 1,300 m^3/s and that westward transport is very weak. Despite this coherent general picture, his cross-sections, using data from all periods, show large changes in average residual velocity over short distances. This indicates that the flow may not be very stable in space or time, except possibly in the deep central channel.

Riley (1956) also hypothesized that weak gyral circulations are present in the broad middle region of the Sound in addition to the general east-west flow. Residual drift calculations indicated the possible presence of a weak, counterclockwise gyre in the western half of the Sound, perhaps related to outflow from the Housatonic and from New Haven harbor. A clockwise gyre was thought to be present in the central Sound.

The hypothezised general longitudinal or east-west pattern of flow has been confirmed by several drift bottle studies (Larkin and Riley, 1967; Paskausky and Murphy, 1976), which also showed the importance of wind and seasonal effects. In during predominantly south and southwest winds, most surface drifters landed on the Connecticut shore, while during the west-northwest winds of fall to spring most landings were on the Long Island shore. The prevailing surface current direction was eastward, but many bottles were recovered to the south and west of their release point. The bottom drift was always westward, but bottles released at the eastern end of the Sound penetrated beyond the Mattituck Sill into central Long Island Sound only during the winter, when a pronounced northward component of drift was also observed.

Gordon and Pilbeam (1975) studied the near bottom circulation in central Long Island Sound, using current meter records from 28 stations. They found a general westward drift, with velocities decreasing from east to west. There is a shoreward component to the flow at depths of less than 20 meters. There are large fluctuations in the non-tidal velocity, with durations of up to 10 days or more, but these are not correlated with any meteorological factors, or with variations in freshwater outflow. Fluctuations are largest in the winter.

Garvine (1977, 1986) studied the part of Long Island Sound that is near the Connecticut River outflow. He found that the river plume often extends 10 km or more from shore, and a similar distance up and down the coast, but that it is confined to the upper 2 - 4 m of water. Circulation in the shallow plume itself is intense, but away from the plume ambient water dynamics appear to be little affected by the freshwater outflow. The fresh water from the Connecticut River must mix with Long Island Sound water and ultimately leave the Sound, but this process has not been observed in detail.

4.2. The 1988-1990 Circulation Survey

The circulation survey in Long Island Sound was conducted by NOS, SUNY and UCONN. The NOS field program extended over the periods March 1988 - September 1989 and May - July 1990 included the following components:

(1) ADCP current measurements at 25 locations in Long Island Sound, Block Island Sound and the East River,
(2) Water level measurements from both permanently installed water level stations and stations that were installed specifically for this study, and
(3) Temperature and conductivity measurements taken in conjunction with several cruises.

In addition to the NOS ADCP measurements, SUNY made six series of current measurements in Long Island Sound. Each series consists of a section of three or four locations, with current meters at three to four depths at each location. The measurement durations ranged from 10 to 40 days.

Both SUNY and UCONN conducted temperature and salinity measurement programs. They made vertical profiles every two to four weeks from April to September 1988 at over 40 locations in Long Island Sound and conducted several longitudinal cruises of the Sound.

Tables 4.1 and 4.2 present the locations and depths of all NOS and SUNY current meters, respectively. The locations of stations at which data used in this report were obtained are illustrated in Figure 4.1. Additional details of the measurement program are given in NOS Oceanographic Circulation Survey Report No. 10 (Earwaker, 1990). Note that the ADCP station numbers generally increase from west to east, with the exception of 24, 2 and 3 in the East River and 20, 21 and 22 near the Connecticut River. The six SUNY transects are numbered 1 to 6 from west to east, with N, NC, SC and S used to denote north to south position in each transect.

The ADCPs deployed in Long Island Sound were mounted on bottom platforms and measured currents in bins of one meter thickness from the bottom up to the water surface. Four acoustic beams were used, and 100 or more individual returns were averaged to produce the velocity recorded by the system. Because of the high number of returns for each velocity reading, the standard error of the reading is generally reduced to less than 1 cm/sec. The effective uncertainty of each reading is then the uncertainty of the instrument itself, conservatively estimated by the manufacturer to be 1 cm/sec.

Because of the large amount of data acquired by each ADCP, only selected depths were completely processed and analyzed, generally five to 10 at each location. Depth intervals ranged from 2 meters at shallow stations to 10 meters at the deepest stations. If pressure data were not available, sounded depths were used to obtain an approximate depth below mean low water.

When the acoustic beam return bin is near the surface, the velocity record can be contaminated by the side lobe signal from the instrument. Even though the ADCP transducer is designed to suppress these spurious signals, the echo from the sea surface is so strong, due to the large impedance mismatch between air and water, that it can overcome the suppression. Bins near the sea surface may be contaminated. For this reason, following the recommendations of the manufacturer, we do not use data from bins that are less than 15% of the distance from the surface to the bottom-mounted ADCP.

Table 4.1. NOS ADCP Station Summary

STATION	LOCATION LATITUDE (N)	LONGITUDE (W)	DEPLOYMENT PERIOD(S)	STATION DEPTH (FT)	NO. BINS
1	40°48.64	73°47.13	03/30/88 - 04/30/88	57	16
			05/05/88 - 07/10/88	52	20
			07/12/88 - 04/24/89		20
			06/05/89 - 10/03/89		20
2	40°47.98	73°50.81	04/24/89 - 08/22/89	52	25
3	40°48.06	73°51.28	04/24/89 - 06/05/89	65	22
4	40°50.41	73°45.96	05/03/88 - 06/07/88	116	48
	40°50.43	73°45.94	04/24/89 - 06/05/89	110	48
5	40°55.19	73°38.97	05/03/88 - 06/07/88	63	32
6	40°56.25	73°39.49	05/03/88 - 06/07/88	63	32
7	40°59.73	73°24.60	05/07/90 - 07/17/90	147	50
8	41°01.32	73°08.37	07/14/88 - 09/13/88	138	50
9	41°01.64	72°54.73	08/02/88 - 09/13/88	128	60
10	41°04.73	72°33.91	05/06/90 - 07/18/90	74	35
11	41°09.91	72°12.77	06/09/88 - 07/13/88	180	90
	41°09.91	72°12.72	09/14/88 - 10/20/88	186	70
12	41°13.55	72°05.52	06/07/88 - 07/12/88	285	128
	41°13.52	72°05.53	09/14/88 - 12/29/88	282	100
	41°13.32	72°05.58	08/24/89 - 10/02/89	278	100
13	41°14.16	72°03.36	06/08/88 - 07/13/88	253	80
	41°14.00	72°03.58	12/07/88 - 03/14/89	264	80
14	41°08.65	71°58.76	02/10/89 - 03/16/89	88	27
15	41°14.65	71°46.43	02/10/89 - 03/15/89	126	41
16	41°07.26	71°41.69	12/30/88 - 02/08/89	98	44
17	41°16.99	71°32.71	12/30/88 - 02/08/89	130	50
20	41°15.40	72°15.37	03/17/89 - 04/20/89	84	27
21	41°13.95	72°22.33	03/17/89 - 04/20/89	112	40
22	41°14.48	72°25.30	03/17/89 - 04/20/89	55	22
23	40°46.69	73°56.31	06/06/89 - 08/22/89	66	30
24	40°42.36	73°59.85	06/06/89 - 08/22/89	60	25

Table 4.2. SUNY Station Summary

STATION	LOCATION LATITUDE (N)	LOCATION LONGITUDE (W)	DEPLOYMENT PERIOD(S)	INSTRUMENT DEPTH (FAB*)
1N	40°57.1	73°40.3	03/28/88 - 05/02/88	+8
1N			03/28/88 - 05/02/88	+16
1N			03/28/88 - 05/02/88	+24
1NC	40°56.2	73°39.5	03/28/88 - 05/02/88	+8
1NC			03/28/88 - 05/02/88	+21
1NC			03/28/88 - 05/02/88	+36
1NC			03/28/88 - 04/22/88	+47
1SC	40°55.3	73°39.0	03/28/88 - 04/17/88	+7
1SC			03/28/88 - 05/02/88	+20
1SC			03/28/88 - 04/30/88	+35
1SC			03/28/88 - 04/19/88	+46
1S	40°54.8	73°38.3	03/28/88 - 05/02/88	+6
1S			03/28/88 - 05/02/88	+18
1S			03/28/88 - 05/02/88	+30
2N	41°02.1	73°26.6	05/02/88 - 05/31/88	+27
2N			05/02/88 - 05/31/88	+47
2NC	41°00.9	73°25.5	05/10/88 - 06/01/88	+30
2NC			05/02/88 - 05/28/88	+69
2SC	40°59.2	73°24.8	05/03/88 - 06/01/88	+50
2SC			05/03/88 - 05/31/88	+87
2S	40°58.4	73°24.3	05/02/88 - 05/30/88	+29
3N	41°07.3	73°10.2	07/14/88 - 08/08/88	+10
3N			07/14/88 - 08/08/88	+20
3NC	41°05.0	73°10.2	07/14/88 - 08/09/88	+10
3NC			07/14/88 - 08/09/88	+25
3NC			07/14/88 - 08/09/88	+47
3SC	41°03.3	73°09.3	07/14/88 - 08/09/88	+11
3SC			07/14/88 - 08/09/88	+50
3SC			07/14/88 - 07/24/88	+68
3S	40°59.8	73°08.1	07/14/88 - 08/08/88	+32
3S			07/14/88 - 08/08/88	+50
3S			07/14/88 - 08/08/88	+70
4N	41°10.8	72°57.8	08/10/88 - 09/06/88	+13
4N			08/10/88 - 09/06/88	+33
4NC	41°08.5	72°56.9	08/10/88 - 09/06/88	+10
4NC			08/10/88 - 09/06/88	+25
4NC			08/10/88 - 09/06/88	+50

* FAB = Feet above bottom

Table 4.2. (Cont.) SUNY Station Summary

STATION	LOCATION LATITUDE (N)	LONGITUDE (W)	DEPLOYMENT PERIOD(S)	INSTRUMENT DEPTH (FAB*)
4SC	41°06.2	72°56.2	08/10/88 - 09/06/88	+10
4SC			08/10/88 - 09/06/88	+24
4SC			08/10/88 - 09/06/88	+46
4S	41°04.1	72°55.5	08/10/88 - 09/06/88	+30
4S			08/10/88 - 09/06/88	+50
4S			08/10/88 - 09/06/88	+70
4S			08/10/88 - 09/06/88	+90
5N	41°14.7	72°25.0	09/08/88 - 09/16/88	+10
5N			09/08/88 - 10/12/88	+40
5C	41°12.5	72°24.3	09/08/88 - 10/13/88	+15
5C			09/10/88 - 10/13/88	+60
5C			09/08/88 - 10/13/88	+100
5C			09/08/88 - 10/14/88	+138
5S	41°09.2	72°21.8	09/09/88 - 10/14/88	+35
5S			09/08/88 - 10/13/88	+60
6N	41°15.4	72°16.6	09/09/88 - 10/12/88	+15
6N			09/21/88 - 10/12/88	+45
6C	41°13.5	72°15.9	09/09/88 - 10/12/88	+9
6C			09/09/88 - 10/12/88	+49
6C			09/09/88 - 10/09/88	+89
6C			09/08/88 - 10/11/88	+129
6S	41°11.0	72°14.5	09/09/88 - 10/14/88	+50
6S			09/09/88 - 10/14/88	+85
6S			09/09/88 - 10/13/88	+110
5N	41°14.7	72°25.0	06/02/88 - 06/30/88	+41
5C	41°12.2	72°24.5	06/02/88 - 06/30/88	+60
5C			06/02/88 - 06/30/88	+135
5S	41°09.0	72°22.0	06/01/88 - 06/30/88	+10
5S			06/01/88 - 06/29/88	+60
5S			06/01/88 - 06/29/88	+90
6N	41°15.4	72°16.7	06/02/88 - 06/30/88	+45
6C	41°13.4	72°15.8	06/02/88 - 06/30/88	+10
6C			06/02/88 - 06/30/88	+50
6C			06/02/88 - 06/30/88	+124
6S	41°11.2	72°14.4	06/02/88 - 07/05/88	+50
6S			06/02/88 - 07/05/88	+85

* FAB = Feet above bottom

The data from each of the processed ADCP bins and SUNY current meters are subjected to a 39-hour Doodson filter to remove the principal tidal frequencies, followed by a 5-hour smoothing filter. Mean currents and standard deviations in the along-mean and cross-mean directions are calculated for selected 30-day periods, or for the duration of the deployment if a 30-day record is not available. These mean residuals are considered in detail below as well as plots of speed and direction as a function of time to examine temporal variability. Initially, however, we will look at the general structure of the residual circulation.

4.3. The Overall and Regional Mean Circulation

Although researchers have sometimes treated the circulation in Long Island Sound as a single system, it is such only to a limited extent. There are general patterns of near surface and near bottom flow throughout the length of the Sound, but these undergo considerable cross-Sound variation. The East River, the topographic constrictions of the Western Narrows, river outflows, and the strong tidal flow through the Race each create distinct dynamic regions in the Sound. First we look at the dynamics of the Sound as a whole and illustrate the main features of the near bottom and near surface circulation by means of charts of the western and eastern Sound. Next we will examine the vertically averaged flow and upper layer transport, followed by details of each important region.

Near Bottom and Near Surface Mean Circulation Patterns

The near bottom circulation in Long Island Sound has a simpler pattern and is easier to interpret than the near surface circulation. This is because wind and density changes more easily affect the upper layers.

The mean residual flow in the lower layers of the western Sound is shown in Figure 4.2. Unlike the depths given in the rest of the report, this and the following figure give the height of each record above the bottom, with a "+" sign added. The length of the arrows is equal to one day's translation. The data in this and the following three figures is taken between March 1988 and July 1990, and includes records from all four seasons. As is discussed in more detail below, this sometimes obscures important temporal variations, although many stations showed quite stable flow over periods of many months.

The lower layer flow at Throgs Neck is almost directly southward and toward the East River at around 10 cm/sec. This mean flow also persisted over the entire 15 month deployment of the Throgs Neck ADCP. The deep flow at the other ADCP stations in the far western Sound is also toward the East River, but at progressively decreasing velocities. The net deep flow at two of the SUNY stations has a strong northward component. These records were taken during April and May 1988, and might be related to fresh water outflow from rivers in New York and Connecticut, which would tend to set up a return flow in the lower layers.

The two deep ADCP stations in the central Sound (Figure 4.2) support the idea (Gordon and Pilbeam, 1975) of a steady westward drift in the deep layers of the open central and eastern

Sound. There are no data in shallower locations nearer to the Connecticut shore. Previous studies (Gordon and Pilbeam, 1975) have measured a northward component to the mean net flow near the Connecticut shore.

The bottom flow through The Race is strongly into the Sound (westward) at almost 18 cm/sec at one station and about 11 cm/sec at the other, but with a 45 degree difference in direction. The deep flow through Plum Gut is still outward, although much weaker than the upper layer flow. The deep flow in the Connecticut River region shows a convergence toward the river and a clockwise circulation around Long Sand Shoal. This is clear evidence of a local topography and river dominated circulation that is quite different from that in the open Sound.

Figure 4.3 shows average near surface residual currents in the western Sound. The numbers at the heads of the arrows indicate depth below the sea surface. At Throgs Neck (Station 1) the upper layer flow is from the East River into the Sound (eastward) at about 3 cm/sec. The flow is stronger nearer to the surface (about 5 cm/sec) where, however, the acoustic signal from the ADCP may have been contaminated by side lobe signals. The velocity varied somewhat, but a mean eastward flow of this order, including stronger upper layer flow, was present during the entire 15-month period that measurements were made at Throgs Neck. Even near the surface, the mean eastward flow has only half the magnitude of the mean westward flow. The upper layer flow 3 km to the northeast near Hart Island is toward the southeast, indicating local control by topography and, possibly, wind. Farther to the east, there is an indication of an upper layer counterclockwise gyre in the far western Sound, as alluded to by Wilson (personal communication). The near surface stations near 73° 40' W support the idea that much of the low salinity water from the East River, which is advected eastward primarily in the southern part of the Sound, may recirculate back in a localized cyclonic gyre, and not penetrate toward the central Sound. This also indicates that the near surface flow south of Hart Island may be highly spatially variable, since there should be continuity between the flow through Throgs Neck and the eastward flow in the station closest to Hempstead Harbor.

Farther to the east, the section in Figure 4.3 near 73° 25' W shows strong topographic control by Eatons Neck, just east of Huntington Bay. This strong northward flow may be locally controlled by vorticity generated within a few km of Eatons Neck, or it may be part of another recirculating gyre.

In the open central Sound, stations near 73° 05' W show the eastward drift which is thought to be characteristic of near surface flow in much of the central and eastern Sound. Near 72° 55' W however (Figure 4.3), one station has a net current to the west and one to the north-northwest. This supports the deduction of Wilson (1976) that eastward drift can be interrupted or reversed in portions of the central Sound. Wilson's analysis assumes lateral homogeneity, while density records (Riley, 1956; Wilson, 1990) show distinct lateral inhomogeneities due in large part to outflows from the rivers of Connecticut. These can be expected to contribute to lateral inhomogeneities and temporal variations in the residual drift.

In the region of The Race, there is strong near surface outflow through Plum Gut (over 20 cm/sec), while the upper layer flow in The Race is northeastward, more toward Fisher's Island at the northern and eastern boundary of The Race than out of the Sound. The magnitude of the net flow varies by a factor of 3 between the two stations in The Race even though they are less than three kilometers apart, which shows that there are strong spatial gradients in the region.

In the area near the Connecticut River, current records taken at widely different times indicate a near surface convergence toward the River and a clockwise circulation around Long Sand Shoal similar to that near the bottom. Only one record (from a station located more or less between the Connecticut River - Long Sand Shoal and The Race regions) shows an eastward drift. This indicates that moderate-scale features can generate local circulations that interrupt or overcome any general tendency toward an upper layer eastward drift.

An examination of Figures 4.2 and 4.3 confirms that the residual circulation in Long Island Sound is complex. An estuarine circulation exists, but local factors overwhelm or replace it in large parts of the Sound. The data in the broad central region of the Sound are sparse and do not give a consistent picture of the upper layer circulation, while confirming lower layer westward flow only in the main east-west channel. In The Race and Connecticut River regions, local factors are often dominant.

Vertically Averaged Flow and Upper Layer Transport Patterns

The vertical resolution of the ADCP Stations allows vertical averages of the flow to be computed; this is also true for SUNY Stations 1NC and 1SC. The vertically averaged flow gives the intensity of the net transport at a given location, which can be thought of as a local transport vector. These vectors are shown in Figure 4.4. Figure 4.4 also gives upper layer transport perpendicular to SUNY Transects 1-4. The mean velocity at the ADCP Stations in the western and central Sound is primarily westward, while the computed upper layer transport is toward the east. The upper layer transport is typical of what would be expected in a partially mixed estuary, but the mean velocity at the ADCP Stations are typical only of their specific locations. Most of the ADCP Stations west of The Race were located in the deep channel that runs roughly east-west along the Sound. These stations give a fairly consistent picture of the flow regime in the channel, with generally strong westerly flow at depth giving a net westward mean velocity.

At ADCP Stations 1 and 4 the mean velocity is westward toward the East River at about 5 cm/sec, while the mean velocity at ADCP Station 6, SUNY Stations 1NC and 1SC along SUNY Section 1 is also westward, averaging about 1.6 cm/sec. The implied total transport at the narrow section through Throgs Neck is about 300 - 400 m^3/s. The extrapolated transport across the much wider Section 1 is about 3,000 m^3/s. This must be much more than the actual net inflow; there are no substantial sinks other than the East River for transport through Section 1. It implies that there are pronounced transport asymmetries at Section 1. Wilson (1990) hypothesizes that there is a net eastward transport in the southern part of the far western Sound which could provide an appropriate mass balance.

The mean velocity at ADCP Station 7 in the western Sound is about 4 cm/sec toward the southwest. In the central Sound, the mean is 2.3 cm/sec toward the west-northwest at ADCP Station 8, and 2.6 cm/sec toward the west at ADCP Station 9. If the component of these flows along the axis of Long Island Sound were extrapolated to a section across the Sound, the resultant net westward transport would be over 20,000 m^3/s. Again, this must be much larger than actually occurs; the net flow in the central Sound cannot be more than a few hundred m^3/s in either direction because of the limited fresh water input. The flow regime in the main east-west channel of the Sound, where ADCP Stations 7 - 9 are located, must therefore be quite different from that occurring elsewhere. In particular, the strong westward flow in the deep layers is probably unique to the channel. Earlier deep current measurements (Gordon and Pilbeam, 1976) near the longitude of ADCP Station 9 showed flow with a strong westward component only in the southern third of the Sound. It is also possible that a large counterclockwise gyre, as hypothesized by Riley, may exist, with net eastward flow in the northern part of the cross-sections, but this cannot be confirmed by the data. Current meters farther to the east (Gordon and Pilbeam, 1976) showed a deep northward flow in the shallower northern part of the Sound.

Strong spatial gradients in velocity are present in the vicinity of The Race. The transport at ADCP Station 12 is almost directly into the Sound, and almost perpendicular to that at ADCP Station 13. The mean major direction of the flooding tidal current is toward the west-northwest at both stations, almost the average of the directions of the transport vectors. The flow through Plum Gut is mostly outward, although the large parallel component shows the strong spatial gradients that must exist across this opening which is less than 5 km wide. Overall, the transport data indicate a clockwise circulation between Plum Gut and The Race. However, because the outflow through Plum Gut is less than 5,000 m^3/s, this recirculation is only a fraction of the 20,000 m^3/s that Riley (1956) and Wilson (1976) deduced are exchanged through The Race itself.

The normal component of flow in the upper layers of a given cross-section gives an estimate of the magnitude of the water exchange at the section, although it gives no information on net transport. A net flow toward the east in the upper layers will be approximately balanced by a westward flow in the lower layers. Any net transport is only a small fraction of the total water exchange and cannot be calculated from upper layer data alone. The water exchange shows the rate at which advection is replacing water from one part of the Sound with water from another. Advection related to gravitational circulation, and tidal mixing, are the main mechanisms by which dissolved constituents and pollutants are transferred between regions.

The arrows at the top of Figure 4.4 indicate the approximate net upper layer transport at each of the Sections 1-4 in thousands of cubic meters/sec. The transport at Section 1 is slightly to the west, but if the mid-depth meter at SUNY Station 1S is included, the calculated transport is about 900 m^3/s to the east. As we discuss below, there is no systematic reversal of flow with depth at any of the Section 1 stations. The data indicate that the circulation in the far western Sound is strongly asymmetric, and that flow varies more across the Sound than vertically. The eastward transport at the three stations in the central and western Sound ranges from about 4,000

- 6,000 m^3/s. This is somewhat larger than, but in general agreement with, the transport deduced by Riley (1956). In agreement with Wilson (1976), the results indicate that the east-west circulation does not strengthen steadily to the east, but is subject to local influences.

Throgs Neck and the Western Sound Mean Circulation

The Throgs Neck ADCP (NOS Station 1) was deployed from the end of March 1988 until September 1989, except for May 1989 and short periods in May and July 1988. It was located in 15 meters of water near the center of a channel that is about one km wide and 10-15 m deep. The channel is oriented almost directly north-south but turns east-west about 1 km south of the station at the boundary between Long Island Sound and the East River.

The mean residual speed and direction, plus the along-mean (A.M.) and cross-mean (C.M.) components of the standard deviation of the mean, are given in Tables 4.3 and 4.4 for NOS ADCP and SUNY current measurements, respectively, for the 30-day period beginning March 30, 1988, along with similar data for the rest of the Sound. The along-mean standard deviation (S.D.) is the square root of the along-mean variance, and indicates the expected departure of an individual residual from the mean. The variability of the mean itself is given by the standard error, S.E.. Note S.E. = S.D./$\sqrt{n}$, where n is the number of degrees of freedom in the record. In Long Island Sound the autocorrelation function of the along-mean component goes to zero in about 1.5 - 2.5 days. Roughly then, each two day record adds a degree of freedom. For the 30-day residual records in this report, n = 15 and $\sqrt{n}$ = 3.9, so that the standard error of the longshore mean is about one-fourth of the standard deviation. This is particularly important in considering whether a small mean current, or a moderate one with high variance, is significantly different from zero.

Mean vectors at three depths are shown in Figure 4.5 in the western Sound for all ADCP stations and SUNY current meter stations, where 15 days or more of data were obtained. The reversal of flow with depth is clear, as is the stronger southward flow in the lower layer relative to the northward flow in the upper layer. If the current is decomposed into two components, one with a zero average depth and the other with no depth variation, we can consider it as consisting of a gravitational circulation component of maximum amplitude about 8 cm/sec in each layer and a net depth-independent flow of 3 cm/sec to the south into the East River. Stratification in the area is weak but, with the longitudinal density gradient, is sufficient to support the gravitational circulation.

The variance of the flow is greater in the lower layer than in the upper on an absolute basis, but less fractionally. At mid-depths (5 meters) both direction and speed are variable. This is generally the case near a level of flow reversal, where mean speeds are small.

Three ADCP stations were occupied in the narrowing portion of Long Island Sound west of Stratford Shoal. Of these, Station 4 is located in a hydrographically and topographically complex location near Hart Island, while Station 6 is in the open part of western Long Island Sound and

Station 7 is north of Eatons Neck. SUNY deployed current meters in two cross-sections in the western Sound.

The results at Station 4 indicate a more complex flow than at Station 1, which is less than 3 km to the south-southwest. The flow is toward the southeast in the upper layer, and veers with depth to become generally south-southwestward in the lower layers. Local influences play a major role at this station, although the flow in most of the lower layer is similar to Station 1. There is more directional variability at Station 4, and the mean flow near the bottom is, unexpectedly, not significantly different from zero.

ADCP Station 6 and SUNY Stations 1SC, 1NC and 1N in the far western Sound show weak net flow. In all cases, the standard deviations of the velocities are comparable in size to the velocities themselves, particularly when the instrument uncertainty of 1 cm/sec is considered, although only near the surface at Station 6 is the standard error larger than the mean. A backing with depth is evident at ADCP Station 6 and SUNY Station 1SC, with flow toward the northeast in the upper layer at Station 1SC, and weakly to moderately toward the west to south-southwest in most of the lower layers. The flow at Stations 1N and 1NC is toward the southwest-northwest quadrant at all depths. Station 6 was in place during May 1988, while SUNY section 1 was in place during April 1988. The flow at Station 6 during May 1988 was quite similar to Station 1SC during April, showing weak flow and a counterclockwise rotation with depth. Station 6 and Station 1NC were less than 1 km apart, but show a different residual pattern.

SUNY Station 1S has a pronounced flow to the north at mid-depth and near the bottom; there are no data near the surface. This flow is associated with the shallow isobaths projecting outward from Matinecock Pt. However, Station 1S is relatively shallow (12 m), and the northerly flow there may also be part of the proposed recirculation of lower-salinity water back toward the western end of the Sound. The mean salinity increased north of Long Island from early April to early May 1988, and a lens of high salinity water extended along the central axis of the Sound from about SUNY section 1 to the vicinity of Execution Rocks.

SUNY Section 2 is oriented north-northwest from Eatons Neck, where shallow isobaths extend well out into the Sound. Many analyses (Pingree and Maddock, 1979; Robinson, 1983) have shown that tidal flow past a headland sets up local residual eddies. The strong flow toward the north and north-northeast at Stations 2SC and 2S indicates that such an eddy is present near Eatons Neck. The strong flow at Station 2S has a very low variance, indicating a steady, permanent feature. The weaker flow at Station 2SC is much more variable. ADCP Station 7, close to SUNY Station 2SC but occupied two years later, shows similar but weaker flow toward the north to north-northeast in the upper layers. In the lower layers, however, there is strong flow toward the southwest. This represents a continuation and intensification of the deep westward flow from the central and eastern sound, a flow which must clearly be greatly modified between SUNY Sections 1 and 2.

Table 4.3. NOS Station Residual Currents. Numbers in parenthesis denote station depth (m).

Station	Start Date	Depth (m)	Speed (cm/s)	Dir. (°T)	Stand. Dev. A.M. (cm/s)	Stand. Dev. C.M. (cm/s)
1 (15)	03/30/88	3	2.8	334	0.8	0.7
		5	1.8	232	1.1	1.6
		7	5.2	189	2.3	0.9
		9	8.7	178	2.5	0.6
		11	10.0	175	2.3	0.5
		13	9.0	179	2.1	0.3
4 (34)	05/03/88	7	3.1	131	1.6	1.3
		12	3.9	185	1.7	2.2
		17	5.9	196	2.4	1.8
		22	7.1	198	2.2	1.7
		27	6.1	203	2.2	0.8
		30	0.7	201	2.5	0.9
6 (17)	05/03/88	3	0.3	21	2.0	1.4
		6	2.6	247	1.8	1.4
		9	3.4	230	2.7	1.3
		12	2.4	209	2.3	1.8
		14	1.4	173	1.1	2.4
7 (45)	05/07/90	8	3.6	28	1.5	1.8
		13	2.6	247	2.3	1.9
		18	1.3	354	3.6	2.4
		23	3.6	204	4.7	3.9
		28	9.7	208	5.5	5.2
		33	11.9	217	5.7	5.3
		38	11.5	223	5.4	4.7
8(41)	08/10/88	9	2.4	23	2.9	2.6
		14	2.9	326	2.6	3.1
		19	3.0	277	2.1	1.3
		24	3.4	270	2.4	2.2
		29	3.4	281	2.9	2.8
		34	2.3	281	2.9	2.0
		37	4.1	14	2.0	2.6
9 (39)	08/10/88	7	3.2	88	4.8	1.9
		12	0.5	50	2.4	3.0
		17	2.9	279	4.3	1.4
		22	5.2	276	3.8	1.4
		27	6.4	271	3.0	1.5
		32	5.0	267	2.9	0.7
10 (22)	05/06/90	7	2.1	120	2.0	3.3
		12	2.4	195	2.4	2.0

Table 4.3. (Cont.) NOS Residual Currents

Station	Start Date	Depth (m)	Speed (cm/s)	Dir. (oT)	Standard Deviation A.M. (cm/s)	Standard Deviation C.M. (cm/s)
10 (22)	05/06/90	17	4.0	227	2.3	2.8
		19	5.1	236	2.3	2.1
11 (56)	09/14/88	12	23.1	109	4.2	1.5
		18	20.8	115	4.0	1.1
		24	18.3	122	3.6	1.2
		30	14.7	128	2.8	1.7
		36	11.1	129	2.2	2.0
		42	7.9	123	2.2	2.0
		48	5.9	104	2.6	1.7
		52	4.8	101	2.7	2.0
12 (86)	09/14/88	14	15.5	38	3.1	2.1
		24	13.5	20	2.2	1.7
		34	11.6	4	1.6	1.5
		44	10.5	344	1.4	1.4
		54	10.9	320	1.9	1.3
		64	13.9	300	2.3	1.3
		74	17.6	288	2.5	1.6
		82	15.0	289	2.5	1.6
13 (80)	12/06/88	18	4.9	50	3.4	4.3
		28	2.0	282	5.5	1.1
		38	7.2	247	4.1	3.3
		48	9.8	242	2.8	3.6
		58	10.4	245	2.3	3.5
		68	11.4	265	2.1	3.2
20 (25)	03/18/89	8	3.2	240	2.0	0.9
		13	3.8	244	1.9	0.8
		18	3.6	253	2.1	0.8
		21	3.7	257	2.2	0.7
21 (34)	03/18/89	7	13.6	223	3.6	2.5
		12	6.7	229	2.7	0.8
		17	2.7	247	2.8	0.8
		22	2.8	278	1.7	1.3
		27	3.5	304	1.0	1.2
		30	5.6	321	1.3	1.7
22 (19)	03/18/89	3	2.7	65	8.9	8.8
		6	8.6	87	3.8	1.2
		9	8.5	92	2.2	0.8
		12	8.0	89	1.9	0.9
		15	5.9	88	1.6	0.7

Table 4.4. SUNY Residual Currents. Note residuals are for 30 days from start date, unless beginning and ending dates are given. Numbers in parenthesis denote station depth (m).

Station	Start Date	Depth (m)	Speed (cm/s)	Dir. (oT)	Standard Deviation A.M. (cm/s)	Standard Deviation C.M. (cm/s)
1N (10)	03/30/88	3	0.8	285	1.2	2.2
		5	1.9	301	1.4	2.6
		8	2.4	313	2.0	2.4
1NC (17)	03/30/88	3	2.9	224		
		6	3.5	237	1.5	1.7
		11	2.2	265	2.5	1.5
		15	1.9	284		
1SC (17)	03/30/88 - 04/18/88	3	2.1	40	1.8	1.1
		6	1.1	311	1.2	1.5
		11	1.9	266	3.4	1.8
		15	0.7	228	2.0	1.7
1S (12)	03/30/88	7	8.2	10	2.1	1.4
		10	5.2	345	1.9	2.1
2N (17)	05/02/88	9	4.6	261	1.1	0.3
2NC (24)	05/02/88	3	2.9	301	5.1	4.0
2SC (29)	05/02/88	3	6.8	18	3.1	3.3
		14	2.9	21	1.2	1.9
2S (12)	05/02/88	3	14.6	21	1.6	1.1
3N (9)	07/14/88 - 08/08/88	3	2.8	44	1.9	1.7
		6	3.2	80	1.6	0.6
3NC (18)	07/14/88 - 08/09/88	4	1.4	59	3.8	1.8
3S (24)	07/14/88 - 08/08/88	3	4.6	98	3.0	1.0
4N (13)	08/10/88 - 09/07/88	3	2.5	61	2.6	1.0
		9	1.7	18	1.7	1.3
4SC (23)	08/10/88 - 09/06/88	3	0.9	18	3.1	2.4

Table 4.4. (Cont.) SUNY Residual Currents

Station	Start Date	Depth (m)	Speed (cm/s)	Dir. (oT)	Standard Deviation A.M. (cm/s)	Standard Deviation C.M. (cm/s)
4S (31)	08/10/88 - 09/06/88	4	2.0	236	2.2	3.3
5N (17)	09/09/88	5	9.9	89	1.5	0.6
5C (46)	09/09/88	4	8.1	259	5.0	1.2
		28	5.0	303	4.6	4.7
		41	8.0	250	2.5	0.6
5S (30)	09/09/88	19	4.3	320	1.5	1.9
6N (18)	09/09/88	4	2.9	295		
		13	9.1	249	1.9	0.6
6C (43)	09/09/88	4	2.8	89	2.6	1.8
		16	5.0	156	1.1	3.6
		28	5.5	270	5.6	2.0
		40	8.2	240	2.6	2.2
6S (42)	09/09/88	8	10.8	102	3.3	4.3
		16	6.5	87	2.6	4.4
		27	9.9	205	2.7	2.6

The deep flow at SUNY Station 2N is toward the west, as would be expected, but the flow at SUNY Station 2NC is anomalous, being toward the west-northwest in the upper layers, and toward the north-northeast in the lower. This anomalous flow may be associated with a region of low salinity water that was observed south of the Connecticut coast during early May 1988. The low salinity water in this part of the Sound is primarily due to spring outflow from the Housatonic River, which enters Long Island Sound about 30 km east of section 2. Salinity increased from east to west in much of this region during this period and also had significant north-south gradients.

Central and Eastern Long Island Sound Mean Circulation

The water movement data are relatively sparse in this broad region, comprising only ADCP Stations 8-10 and SUNY Sections 3 and 4. Tables 4.3 and 4.4 and Figure 4.6 show the residual flows at these ADCP and SUNY Stations. The data at ADCP Stations 8 and 9 and SUNY Section 4 are for August - September 1988, those at SUNY Section 3 are for July - August 1988, while those at ADCP Station 10 are for May - June 1990.

Station 8 north of Old Field Pt. shows strong flow toward the east-northeast in the upper layers, with flow toward the west to west-northwest in the lower two-thirds of the water column. The meters at Stations 3S and 3NC, which are both within 5 meters of the surface, also have flow to the east to east-northeast, but at much lower speeds. The flow at the shallow Station 3N is east to east-northeast at both depths. Although the Housatonic River is less than 10 km to the east, Station 3N indicates that there is a general west to east drift near the Connecticut shore during this low-outflow period. Overall, there is a well-developed gravitational circulation in the deeper parts of this region. As is often the case, the shallow station near the Connecticut shore shows a different pattern.

Station 9, about 20 km to the east, again shows evidence of a well-developed gravitational circulation. Both Stations 8 and 9 were placed in the deep east-west channel in the southern part of the Sound where gravitational circulation would tend to be best developed. In contrast, the somewhat shallower Station 4S, less than 3 km away from Station 9, shows residual flow to the west in the upper layer. The upper layer variance at both stations is quite high; however, in both cases the standard deviations are of greater magnitude than the speeds. Station 4SC has weak flow to the north, while the shallower Station 4N has flow toward the northeast to east-northeast in the upper and lower layers, not very different from the flow at 3N. In general, the SUNY Section 4 stations show a very different pattern than ADCP Station 9; there is no gravitational circulation evident. The greatest variability is in the upper layer; there are no lower layer data at the deep Stations 4S and 4SC, and the mean flow in the lower layer at Station 9 is stronger than the upper layer flow, with less relative variability. ADCP Station 10, about 35 kilometers east of Station 9 and Section 4, has flow toward the west-southwest through the lower half of the water column; flow in the upper layer is toward the east-southeast. There is a small gravitational circulation component at this station, but the predominant feature is the strong deep inward flow.

Riley's (1956) historical data shows the irregular nature of residual flow in the upper layers of the central Sound. The combined historical and new data indicate that any gyral circulations in the central Sound are variable and irregular. Near surface waters in the western Sound can take a month or more to be advected out of the Sound even with a well-developed gravitational circulation, which is by no means always the case. River inflow and runoff, which provide the fresh water that drives the density circulation, are highly variable, with strong spring and intermittent peaks. Waters from high and low runoff periods mix into the central and eastern Sound over periods of weeks to months. This is consistent with an irregular, variable residual circulation.

Mean Circulation at The Race

Three ADCPs were deployed in this cross-section, at Station 11 in Plum Gut and Stations 12 and 13 in The Race. Each of the three stations gathered several months of data. We will consider periods beginning in mid-September 1988 for Stations 11 and 12, and early December 1988 for Station 13.

Mean residual currents for Stations 11, 12 and 13 are presented in Tables 4.3 and 4.4 and Figure 4.7. The flow through Plum Gut is out of the Sound at all depths, with directions varying from east to southeast, and velocities generally decreasing from top to bottom. The variance is relatively small in the upper layers, and is proportionately larger near the bottom. Station 12 has upper layer flow that is only slightly out of the Sound; the current turns continuously counterclockwise with depth to flow strongly into the Sound in the lower layers. Station 13 is only about 3 km away from Station 12 and at a similar depth, but exhibits very different flow characteristics. The current nearly reverses with depth, being toward the northeast in the upper layer and toward the west-southwest in most of the lower. Upper layer velocities are much lower than at Station 12, but with higher variance. In the lower 40 meters there is a flow out of the Sound that varies only slightly with depth. Variance is relatively low at all depths at Station 12, indicating that the pattern of rotation of the currents with depth is a persistent phenomenon. These data show that the spatial scale of variation in The Race is very small. Distances of less than 3 km produce pronounced variations in the residual flow. The variability in the tidal current is also very large. Station 13 has tidal current velocities almost twice as great as Station 12.

Ianello (1981) examined tidally-induced residuals in eastern Long Island Sound, The Race, and western Block Island Sound, and concluded that they can account for net currents of up to 5 cm/sec. These residual currents are generated by the strong non-linearities associated with high tidal current variability in the region of The Race. Robinson (1983) concludes that significant net currents can be produced by the interaction of strong rotational effects (vorticity) in the flow and rapidly varying topography.

Extensive temperature and salinity measurements made by UCONN show that there are often significant gradients in density in the vicinity of The Race. Salinity changes by as much as 2 psu and temperature by as much as several °C over a spring tidal cycle. Changes during winter and at neap tide are much smaller. Even small salinity changes, in conjunction with the large depths and strong mixing in The Race, could support a strong gravitational circulation. Station 11 (like Throgs Neck) can be thought of as consisting of a barotropic (depth independent) outflow of about 15 cm/sec superimposed on a gravitational circulation of about 10 cm/sec in each layer. This is also the case at Station 12, where the total current undergoes a counterclockwise rotation with depth, but with speeds always 10 cm/sec or greater. This can be roughly decomposed into a gravitational current oriented northeast to southwest and a barotropic current toward the northwest. The overall dynamics are complicated by inertial effects, which can also produce depth-varying flows (Ianello, 1981).

Paskausky (1977) analyzed short-period current meter records in Plum Gut and The Race and deduced from the depth-averaged current that a clockwise gyre exists in the region, with outward flow through Plum Gut and inward flow through The Race. The ADCP data support this deduction, although spatial gradients in this region are so large that the horizontal extent of such flows cannot be reliably estimated.

Mean Circulation in the Connecticut River Region

Three NOS ADCP Stations (20, 21 and 22) were deployed south of the Connecticut River during a period of rapidly increasing outflow (March and April 1989). SUNY Sections 5 and 6 were deployed in June and September 1988, when outflow was much less.

Tables 4.3 and 4.4 and Figure 4.7 show the mean residual currents for the ADCP and SUNY Stations in the vicinity of the Connecticut River. ADCP Station 20, located about 10 km east of the Connecticut River, has weak flow toward the south-southwest in the upper layer and moderate flow toward the west-southwest in the lower layers. Station 22, located about 10 km west of the Connecticut River, exhibits a very different structure; the flow is toward the east-northeast in the uppermost layer but is almost due east through most of the water column. The very high variance in the uppermost flow may indicate sporadic influence from the Connecticut River. Together, Stations 20 and 22 imply a convergence of the deep flow toward the river.

Station 21 has strong southwestward flow out from the Connecticut River in the upper layers, with the current turning clockwise with depth to flow toward the northwest in the lowest layers. If a barotropic flow of about 3 cm/sec toward the west is subtracted, most of the remaining flow consists of a flow that reverses from south to north with depth. This is the pattern of a seasonal, estuarine-type circulation in the river that has been found to extend 10 or more km out into the Sound during high runoff conditions (Garvine, 1986). The deep convergence toward the river indicated at Stations 20 and 22 may be part of this circulation. The variances are generally moderate at Stations 20 - 22, indicating that these features are persistent.

SUNY Station 5N, which is very close to Station 22 but occupied six months earlier during low-flow conditions, indicates that near surface flow to the east in the upper layers is a persistent feature. A shorter record at 14 m depth, not shown in Figure 4.7, indicates that the deep eastward circulation persists as well, and that this relatively shallow region near the Connecticut coast has a local runoff and topography-controlled circulation independent of that in the open Sound to the south. Station 6N, near Station 22 to the east of the Connecticut River, indicates that the general flow to the west is also present during a low-runoff period. Variances are low at both stations, indicating that the flows are steady as well as persistent.

The flow at station 5C is generally westward at all depths, but quite variable in the upper layers. The flow at 5C and 5N may indicate the presence of a strong clockwise gyre around Long Sand Shoal, which runs in a generally east-west direction between 5N and 5C. The relationship of this gyre to the Connecticut River outflow and related near-coastal circulations is not clear.

The near surface flow at Stations 6C and 6S is moderately to strongly eastward, as would be expected. The flow in the lower layers at 6C also is not surprising, being unsteadily westward in the lower layer, veering to be steadily to the southwest 3 meters from the bottom. The deep flow at 6S, however, is toward the south-southwest, indicating a possible relationship to the outflow through Plum Gut.

Gravitational circulation is well developed in this region only at the central station 6C, away from the influences of The Race, the Connecticut River and Long Sand Shoal. Even here, the flow is quite variable. At the other ADCP and SUNY locations these more local factors are influential to dominant. There are probably at least three distinct local circulation regimes associated with the Connecticut River and Long Sand Shoal, while the influence of The Race extends well into the region, if only because of the tidal excursion.

Summary

In the previous sections, the overall near surface and near bottom residual circulation in Long Island Sound, plus details in the several regions of the Sound, have been considered. Some of the highlights for each region are:

(a) Throgs Neck
- upper layer currents of about 3-5 cm/sec and lower layer currents of about 10 cm/sec.
- stable lower layer flow and fairly stable upper layer flow over 15 months.

(b) Western Sound
- strong flow to the north off of Matinecock Pt. and Eatons Neck, and strong southwesterly flow in the deep channel.
- significant coherence between lower layer flows at stations near Throgs Neck and in the far western Sound.
- weak and variable residual currents at many locations in the open western Sound.

(c) Central and Eastern Sound
- lower layer flow to the west.
- spatially and temporally variable flow in the upper layers.

(d) The Race
- outflow at all depths through Plum Gut.
- net inflow through The Race, but with strong spatial variability.
- very steady mean flow, rotating clockwise with depth, between September and December in The Race.

(e) Connecticut River
- convergence toward the River and a clockwise circulation around Long Sand Shoal in both the upper and lower layers.
- convergence toward the River in the upper layer during both high and low river outflow periods.
- some control of the deep flow near the River by the longitudinal pressure gradient along the Connecticut shore.

4.4. Residual Circulation Time-dependencies

Gordon and Pilbeam (1975) found that time histories of residual speed and direction are in general difficult to relate to external parameters. Nevertheless, the time records are informative, and comparison among two or more locations can yield some insight into the relationship, or lack of it, between adjacent stations. In this section we examine records and statistics at some representative ADCP stations in the lower layer, where variations are smoother than near the surface. Some of the observed month-to-month variations are briefly discussed. Where appropriate, other variables such as residual water level, salinity structure, river runoff and wind are also considered. In conclusion, an overall summary of the characteristics of the residual circulation in different regions of the Sound is provided.

Table 4.5 gives the along-mean (A.M.) and cross-mean (C.M.) correlation coefficients. In addition, the mean speed, direction, and standard deviations of the along-mean (A.M.) and cross-mean (C.M.) components are given. For the records given, a correlation of about 0.5 is significant at the 95% confidence level.

Table 4.5. NOS ADCP Statistical Analysis. Numbers in parenthesis denote analyzed depth (m). Note x-y denotes Station x correlated with Station y.

		Mean		Standard Deviation		Correlation	
Station	Start Date	Speed (cm/s)	Dir. (°T)	A.M. (cm/s)	C.M. (cm/s)	A.M. (cm/s)	C.M. (cm/s)
1 (4)	05/04/88	11.2	181	2.5	0.7		
4 (7)		6.4	204	2.0	0.7		
6 (5)		2.5	212	2.4	1.7		
1-4						.68	.36
1-6						.75	.39
4-6						.36	.60
8 (7)	08/10/88	2.3	282	2.8	2.1		
9 (7)		5.0	267	2.9	0.7		
8-9						.48	.07
11 (6)	06/08/88	4.2	87	3.0	2.8		
12 (10)		16.1	292	8.8	1.9		
11-12						-.83	-.39
12 (12)	12/08/89	19.4	289	1.9	1.2		
13 (12)		11.4	258	2.0	2.5		
12-13						.37	.15

Throgs Neck and the Far Western Sound

During May 1988, ADCP units were simultaneously deployed at Throgs Neck, at Station 4 south of Hart Island, and at Station 6 north of Matinecock Point. Figure 4.8 shows residual speed and direction for a depth in the lower layer at each location from early May to early June (Julian Days 128-156).

The direction of flow is very steady at Throgs Neck and mostly steady at Station 4. There are large shifts in direction at Station 6, but a substantial part of this is associated with periods of very weak flow. Throughout much of this period, changes at station 4 and 6 follow those at Station 1. The correlation coefficients between Stations 1 and 4 and between 4 and 6 indicate considerable spatial coherence in the western end of the Sound, although, surprisingly, Stations 4 and 6 are not significantly correlated. Time lagged correlation coefficients at all the pairs of stations in Figure 4.8 are lower than at zero lag, although sometimes only slightly so for the first few hours. May is a transition month meteorologically, and winds at LaGuardia Airport were highly variable throughout the month. There is no significant coherence between the wind and either the residual tide level or the deep current.

On a month-to-month basis, although the magnitudes change, both the estuarine circulation and the net transport into the river persist at Station 1 in all seasons. The upper layer flow is more variable than the lower-layer flow. The upper layer flow is 4 cm/sec higher in August than in December, while the maximum variation in the lower layer flow, despite higher velocities, is 2 cm/sec. At Station 4, the mean residual flow in May 1989 was similar in strength throughout the lower layer, in contrast to the weak mean flow at the lowest station during May 1988.

The Central Sound

In the central Sound, ADCP Stations 8 and 9 were deployed from mid-July to early September 1988. The stations are about 20 kilometers apart along the main channel. Figure 4.9 shows residual speed and direction 5 meters off the bottom at each station from early August to early September. The mean flow at each location is toward the west, more weakly so at Station 8. The along-current standard deviation is higher than the mean speed, indicating a high degree of variability. The large apparent directional changes at both stations occurred during periods of very weak residual flow. The along-mean speeds are moderately correlated, although not quite significantly so. This indicates that, in this part of the Sound, a substantial part of both the barotropic and baroclinic variations are relatively local, despite the expectation of spatial coherence along the deep, main channel.

The Race and Plum Gut

At the other end of the Sound, three ADCPs were deployed in the region of The Race. Figure 4.10 shows June - July 1988 residuals (Julian Days 164-192) in the lower layers at Stations 11 (Plum Gut) and 12 (The Race). The most striking event at Station 12 is the sharp decline in speed and the backing from steady flow to the west to very weak flow to the east in the lower

layer from days 170-177. At Station 11 the direction of the lower layer flow is variable, first veering from north to east, then backing to the northeast. The two stations are negatively correlated; a stronger/weaker outflow through Plum Gut is associated with a stronger/weaker inflow through The Race, which is consistent with a gyral recirculation. There were no large anomalies in residual sea level or wind in this period; river outflow was undergoing a normal decrease after the yearly maximum in April and May. However, salinity in the upper 10 meters at several shallow stations in or near The Race was 1-3 ppt lower on June 23, 1988 (Julian Day 175) than during six other observations in the May - September 1988 period.

Figure 4.11 shows December 1988 residuals in the lower layer at the proximate Stations 12 and 13 in The Race. Directions are quite stable in the lower layers at Station 12, although some veering is present early in the record when velocities increase from low values. The direction of the residual flow is somewhat less stable at Station 13 than at Station 12.

On a month-to month basis, considering first Station 12, upper layer and near bottom velocities were much higher in June - July 1988 than in September - December 1988; the direction at 50 m changed by almost 30 degrees. The 30 day mean flows were almost constant from September to December. The largest change was in the direction of flow in the uppermost layer. The difference between June - July and September - December can be at least partly attributed to the change from high-flow to low-flow conditions; a greater input of fresh water would be expected to increase the intensity of the gravitational circulation. However, keeping in mind the large differences between the nearby Stations 12 and 13, some of the difference could also be due to the second deployment being in a slightly different position than the first. The general pattern of flow at Station 11 was the same in June - July and September - October and shows no obvious effects of changes in river outflow.

Station 13 was quite stable from December to February in the lowest 40 meters, but showed some changes in direction of flow in the upper layers. The near surface mean current set to the left of the wind at both Stations 12 and 13. Both the wind and the top layer current veered from September-October to December at Station 12, and from December to February at Station 13.

4.5. Spectral Analysis of ADCP Data

Spectral analysis of a current meter record shows the distribution of the energy of the record by frequency. It can also reveal the underlying time dependence of the data by exhibiting the frequencies at which energy is concentrated. Coherence spectra exhibit the correlation between two time series as a function of frequency. The phase spectrum shows how the phases of two records are related as a function of frequency. Coherence and phase spectra can be run between two current meter records or between a current meter record and another variable such as wind speed, sea level or sea level slope. Spectra of residual records reveal time dependence at less than tidal frequencies. If tidal currents are retained, their strong spectral peaks will tend to dominate the much weaker lower frequency peaks.

A smoothed periodogram was computed as a spectral estimate using a data interval of 12 hours, so that the high frequency cutoff was one cycle/day. In fact, there was very little spectral energy in any of the residual records for periods of less than two days, which would be expected for data subjected to a 39 hour filter. In addition, coherence and phase spectra were run between selected pairs of current meter records, and between current meter records and residual sea level, rate of change of residual sea level, and wind speed. Simple correlations were also computed between all the records. Results are discussed below for lower layer spectra at Throgs Neck, in the central Sound, and in the Race. The (u,v) components are directed in the east and north directions, respectively.

Throgs Neck

A 90 day spectral analysis for the lower layer at Station 1 (Throgs Neck) was performed on the v component. The net residual current in the lower layer at Throgs Neck is almost directly southward. There are strong peaks near the Neap-Spring period, about 14 days, and at around 25 days. This latter peak relates to the monthly oscillation in the tidal current due to M_2 and N_2. There are small, barely significant peaks in the 3 - 10 day band that probably reflect the various scales of meteorological variation. The residual current at Station 1 does not correlate well with either residual sea level or residual sea level slope at Willets Point.

The Central Sound

The deep residual current at Station 9 in the central Sound is almost due west (Figure 4.2). A lower layer spectrum for the u component for August 1988 at Station 9 exhibits a strong spectral peak near a period of 9 days as well as weak meteorological perturbations. The record was not well correlated with east-west wind speed at LaGuardia, NY, residual sea level at Bridgeport, CT or residual sea level slope at Bridgeport, CT. Residual sea level slope at Bridgeport, CT did show a broad spectral peak between about 4 and 10 days, and was highly coherent with the lower layer at Station 9 in the 9 - 13 day period range, but was about 120 degrees out of phase.

The complexities in the spectral record at Station 9 reflect the complexity of the residual circulation in the central Sound. A considerably longer record would be needed to try to better analyze and resolve the spectral peaks and to see whether tidal modulation was present.

The Race

A lower layer spectrum was calculated for the u component for a 30 day period in December-January 1988-89 at a station in the northeast part of The Race near Fishers Island (see Figure 4.2, Station 13). Most of the deep residual energy at this Station is in the east-west direction. There is a strong spectral peak near a period of 4-5 days. This is approximately the cycle of mid-latitude meteorological variation in the winter. There is again no evidence of tidal modulation.

The results of the spectral analyses for all the major areas of the Sound clearly show the importance of both meteorological variation and tidal modulation in generating spectral peaks. Stations in all regions show the effects of Neap-Spring tidal modulation, but influences often vary greatly from one station to another and from upper to lower layers. Meteorological effects were somewhat more consistent, being present in almost all records. The peaks exhibited considerable variability through the Sound due to the different locations and seasons. The most pronounced meteorological peak in all the records is the 5 day peak at both the stations in The Race during December, which is a reflection of the greater intensity of winter weather systems.

Coherence and phase of jointly analyzed records can also be important, but only at frequencies where both records have significant energy. Most of the pairs of current records have high coherence at some high frequencies (periods of less than two days), but since there is very little energy in the residual records at these frequencies, the coherence is not significant.

Overall, the spectral results confirm the complexity of the circulation in the Sound. The spectral records in Long Island Sound do not show a consistent picture. They vary considerably in the degree to which they exhibit meteorological peaks and Neap-Spring modulation. Nevertheless, it is clear that the meteorological and tidal factors are important in Long Island Sound, and further investigation of the relationships is definitely warranted.

4.6. Asymptotic Singular Decomposition Analysis of the Total Circulation

The asymptotic singular decomposition (ASD) method is a powerful technique for exhibiting the most important features of a complex data set. ASD analysis, closely related to orthogonal function analysis and principal component analysis, focuses on the most characteristic features of a large data array, features that may be hidden by the array's size and complexity. ASD decomposes the data set into a series of mutually orthogonal functions. The order of the function will generally be related to the number of zero crossings in the principal spatial variable. Details of the method can be found in Sullivan (1980).

For a current record dominated by semidiurnal tides, with smaller but important residual currents, the first order ASD function will generally vary only moderately with depth, and will oscillate semidiurnally with time. It will contain not only the oscillating tidal current, but any barotropic residual current that may be present. The second order ASD function will contain the gravitational circulation. It will reverse direction with depth and will oscillate with time, but in a more complex way than the first order function.

All of the important information about a given ADCP record will usually be contained in the first and second order functions. This is one of the principal objectives of ASD analysis. The third and fourth order ASD functions are also derived by the ASD procedure, but they contain high-frequency, depth-varying oscillations which are not directly related to any large-scale physical process. The energy in these higher modes is always much smaller than that in the first order process, and usually much smaller than the second order process as well. They will not

be directly considered in the analysis below, except for references to the percent variance (approximately proportional to kinetic energy) they contain.

The ASD procedure is carried out for either the u (east) or the v (north) component. If one of them is dominant, it is sufficient to analyze only that component; otherwise both u and v must be considered.

Throgs Neck

Table 4.6 and Figures 4.12 - 4.17 represent the decomposition of a 15 day and a two day record of the v component at Throgs Neck. They illustrate all of the major features of the ASD procedure. Figures 4.12 and 4.14 show the space and time variation over 15 days of the first mode. It varies slowly in space, and oscillates semidiurnally in time. Using Table 4.6, the magnitude of the first mode is obtained by multiplying the single value given in Table 4.6 by the spatial magnitude from Figure 4.12, and multiplying this product by the temporal magnitude from Figure 4.14. The average maximum first mode magnitude is then about (4481)(-0.32)(.035) = -50 cm/sec, a flooding tidal current out of the Sound and toward the East River. The ebbing current is slightly weaker. From Figure 4.15, which shows the temporal oscillation over a two day period, there is clearly a net transport by the first mode out of the Sound and toward the East River. This is present throughout the longer 15 day record.

Figure 4.13 and Figures 4.16 - 4.17 illustrate the second mode. The average maximum amplitude near the surface is about (1164)(0.4)(.035) = 16 cm/sec.

Table 4.6. ASD Statistics: ADCP Station 1 v-component

Start Time: July 6, 1989 0.0 hours, Stop Time: July 21, 1989 0.0 hours, Bins: 1 - 13

Description of Statistical Property	Component 1	Component 2
Single value	4481.07	1164.19
Variance explained around 0	92.949%	99.2228%
Variance explained around the mean	92.6013%	99.1845%
G Factor	12.0833	10.6773
Estimate of Standard Deviation	7.6677	2.6595
Estimate of Standard Deviation	7.3652	2.4452

The first and second modes together explain 99.4% of the variance, which is very high. The third and fourth modes contribute only 0.4%. Over 90% of the energy at Throgs Neck is in the v component, and essentially all of this energy is contained in the first two modes.

Figures 4.15 and 4.17 show the time oscillation of the first and second modes over a two day period. Note the ordinates in Figures 4.15 and 4.17 do not correspond to those in Figures 4.14 and 4.16, respectively, since these ordinates are obtained from an independent 2 day analysis, which is not shown here, but is analogous to the 15 day analysis of Table 4.6. The second mode also oscillates semidiurnally, but with overtides and higher frequencies superimposed. From Figure 4.16 we see that this mode is usually unidirectional at a given depth, varying from a maximum to near zero. The minima occur near the time of maximum flooding currents, but with considerable irregularity.

The Central Sound

Almost all of the energy at Station 9 is contained in the u component. Table 4.7 and Figures 4.18 - 4.21 show the first and second modes of this component. The first mode contains 94% of the variance while the second mode contains about 4%. The semidiurnal oscillation of the first mode is very smooth at this location in the open central Sound, where overtides are very small. The second mode also varies semidiurnally, with minimum speeds near the time of maximum flooding currents, but with much more high frequency variability than the first mode. Maximum first mode current speeds average about 40 cm/sec. The second mode maximum near the surface is about 10 cm/sec, but with considerable variation including one strong reversal.

Table 4.7. ASD Statistics: ADCP Station 9 u-component

Start Time: August 16, 1988 0.0 hours, Stop Time: August 31, 1988 0.0 hours, Bins: 1 - 32

Description of Statistical Property	Component 1	Component 2
Single value	6418.52	1269.9
Variance explained around 0	93.9995%	97.6791%
Variance explained around the mean	93.8567%	97.6238%
G Factor	30.0798	19.0096
Estimate of Standard Deviation	6.267	3.9629
Estimate of Standard Deviation	6.1668	3.3353

The Race

Most of the main features of Station 12 are exhibited by the u component, which contains about two-thirds of the total energy. Table 4.8 and Figures 4.22 - 4.25 exhibit this component. The first mode declines noticeably more with depth than shallow stations in other regions, the near bottom value being only about half of the near surface value. This corresponds to a similar observed decline in tidal current amplitude derived from a harmonic analysis. There is a fairly smooth semidiurnal oscillation with a moderate net transport to the east. This, combined with

a pronounced northward transport by the first mode of the v component, gives a net flow to the north-northeast. The direction of the second mode is mostly steady at a given depth, with only a few weak reversals in direction. It oscillates at much higher frequencies than the first mode, possibly reflecting inertial effects. A quarter-diurnal variation is also evident. The first (94%) and second (5%) modes together account for 99% of the variance. The average maximum magnitude of the first mode is about 90 cm/sec near the surface and about 45 cm/sec near the bottom. The average maximum second mode amplitude near both the surface and the bottom is about 25 cm/sec.

The ASD method has been shown to be very useful in analyzing Long Island Sound ADCP data. It exhibits depth variations concisely, and shows up short and long term variability in the gravitational circulation. It also shows where gravitational circulation is absent or anomalous. It would be still more useful if time averages of each mode could be calculated at every depth. This would quantify any barotropic net transport contained in the first mode.

Table 4.8. ASD Statistics: ADCP Station 12 u-component

Start Time: December 10, 1988 0.0 hours, Stop Time: December 25, 1988 0.0 hours
, Bins: 1 - 70

Description of Statistical Property	Component 1	Component 2
Single value	18336.8	4463.4
Variance explained around 0	93.6381%	99.1861%
Variance explained around the mean	93.5545%	99.1754%
G Factor	65.5466	60.1727
Estimate of Standard Deviation	12.3834	4.4627
Estimate of Standard Deviation	12.2917	4.3965

4.7. Nontidal Fluxes in the East River

Longuet-Higgins (1969) considered the Lagrangian transport to represent the total net transport by time varying ocean currents. The Lagrangian transport is composed of two parts: the Eulerian transport and the Stokes transport. The Eulerian transport is computed by integrating the velocity normal to the cross section from the bottom to the mean sea level. The Stokes contribution is found from the correlation of the surface current and the water level. The Lagrangian current is just the vertical integral of the velocity normal to the section from the bottom to the time varying free surface.

Method

The following steps are used to compute the transports at the South Clason, NY, ADCP and the Throgs Neck, NY, ADCP:

1) Select bins representative of the vertical structure of the current,

2) Establish the depth of the ADCP stations so that the bins can be related to depth below mean sea level,

3) Filter the NOS ADCP data for each bin using a 3-hour Fourier filter,

4) Phase shift the water level at Willets Point, NY, by an appropriate amount for College Point adjacent to South Clason, NY, and assume no phase shift at Throgs Neck opposite Willets Point, NY,

5) Define the width associated with each bin level and compute a cross sectional conveyance area for each bin (width times the bin level thickness),

6) Compute the Eulerian transport as the vertical integral of the instantaneous 3-hour filtered current from the bottom to mean sea level,

7) Compute the Stokes transport as the product of the instantaneous surface elevation, surface current and the surface width of the cross section,

8) Compute the Lagrangian transport as the sum of the Eulerian and Stokes, and

9) Filter the hourly Lagrangian transport with a 36-hour Fourier filter to determine the hourly tidally averaged transport.

Assumptions

NOS determined from the ship's log and correction for the tide at the time of sounding that the station depth of the South Clason, NY, ADCP was 15.5 meters below mean sea level. This would place the center of the first bin at about 12.5 meters depth. Mean sea level would be near the top of bin 13 according to these calculations. NOS investigated a number of ADCP parameters including vertical velocity, error velocity, echo amplitude and percent good pings. These parameters usually give an indication of the location of the surface which is not evident in the horizontal velocity structure. The acoustic beam is reflected at the surface producing a mirror image of the surface bins. If there is a significant surface vertical velocity, it will exhibit an apparent change of sign. This is due to the fact that the reflected beam will be traveling in the opposite vertical direction to the incident beam. Statistics of the vertical gradient and curvature of the vertical velocity revealed that the maximum gradient peaked on the average between the base of bin 13 and the top of bin 14. Echo amplitude and error velocity gave further

but less conclusive evidence of the mean surface at the same location. The percent good pings is an indicator of what fraction of incident pulses return on the sound path. The surface signature (Figure 4.26) is seen already in bin 13 where the percent drops below 100% on an intermittent basis. Bin 14 exhibits extensive dropout indicating that the surface is present in that bin more than in bin 13. Bins 15, 16, 17 are substantially similar to 14, 13, 12, respectively. The surface is most certainly between bin 13 and bin 14.

Figure 4.27 shows the results of calculations of the Lagrangian transport as a function of the assumed bin at mean sea level. The effect of the shift of the vertical grid is marked. It can be seen that the Stokes transport is rather independent of the bin location indicating that the tidal current is not a strong function of depth. However, it is important to accurately establish the depth in order for the Eulerian transport to be accurately estimated. The total conveyance area at South Clason, NY, was 11,420 m^2 based on NOS bathymetric data and 11,810 m^2 based on US Army Corps of Engineers echo sounding data.

NOS assumed in its calculations that the currents at the ADCP were representative for the entire width of the channel. This is not supported with direct evidence. Substantial asymmetries are present in the towed ADCP data from a section northeast of Throgs Neck, NY.

Results

Figure 4.28 shows the time varying NOS computed transports at South Clason, NY. The into sound and out of sound transports are computed by summing all outgoing water and summing all incoming water and represent the rectified tidal transports. The difference between them is the net Lagrangian transport in the center of the figure. The sum of the Stokes and Eulerian transports at the top of the figure equals the net Lagrangian transport. Most of the temporal variability in the net transport is due to the Eulerian current as would be expected. Some variation in the Stokes current is due to the additional effects of wind on water level and barotropic currents.

Similar procedures used at South Clason, NY, have been followed for computation of transports at Throgs Neck and transport estimates computed for both locations are given in Table 4.9.

Table 4.9. NOS Nontidal Flux Estimates at South Clason, NY, and Throgs Neck, NY
14 May - 13 July 1989

	South Clason, NY	Throgs Neck, NY
Type	Flux (m^3/s)	Flux (m^3/s)
Stokes	-326	-294
Eulerian	-473	-435
Net	-799	-730

Since the transport estimates are nearly the same, this tends to confirm that the transports are computed in a consistent manner. Figure 4.29 illustrates the temporal variability of the decompositon of the Throgs Neck, NY, transport and can be compared to Figure 4.28 at South Clason, NY. Figure 4.30 compares the decomposed fluxes. The agreement of the means and the time varying Stokes is obvious. As obvious is the fact that the time varying Eulerian transports can differ significantly. The detailed intercomparison of model transports and data derived transports must be viewed with this in mind. The hydrodynamic model cannot be expected to track either data set better than data sets track each other. The differences in the computation of the two data sets are related to time-invariant assumptions and the lateral variability (asymmetry) at each station.

Conclusions

The analysis of NOS data indicate that the mean mass flux near Throgs Neck, NY, is on the order of 700 - 800 m^3/s into the East River for the period from June - August, 1989. Temporal differences in nearby ADCP stations provides a method to establish how accurately the model can be compared temporally to data derived transports.

It is important, however, to emphasize the uncertainties in the transport estimate. The depth used is a minimum; if the depth were one meter greater, which is well within the range of uncertainty, the calculated transport would decrease by 100 m^3/s, due to a thicker outflowing layer.

There is evidence of cross-sound asymmetry at Throgs Neck, NY; towed ADCP results indicate that the cross channel mean velocity may be 2 cm/sec less into the East River than that indicated by the ADCP. This would reduce the Throgs Neck, NY, estimate by 300 m^3/s, but would leave unexplained the resulting discrepency between Throgs Neck, NY, and South Clason, NY.

Pritchard (personal communication) and others have used different techniques than those employed here to extrapolate ADCP results to the surface and bottom. Assuming substantially stronger outward flow near the surface and weaker inward flow in the deep channel below the South Clason, NY, ADCP would reduce the inward transport by about 100 m^3/s.

Pritchard has also used other methods than those employed here to compute the Stokes transport. He has assumed a linear velocity structure from top to bottom, and has obtained Stokes transports about 100 m^3/s less than calculated above.

All of the above uncertainties reduce the estimated transport. If the full reduction due to asymmetry is assumed to be possible, then we conclude that the net transport from the Sound into the East River is in the range 200 - 800 m^3/s. This is a large uncertainty, but reflects the difficulty in estimating transport from a single ADCP that itself does not cover the full depth range.

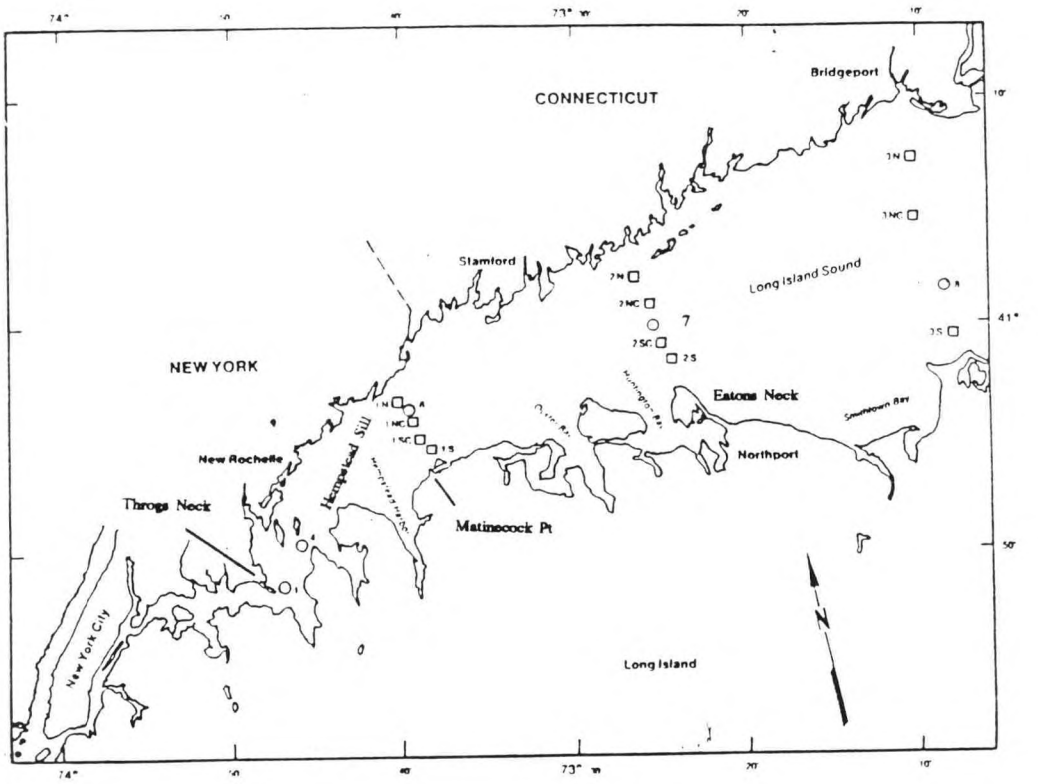

Stations in the western Sound

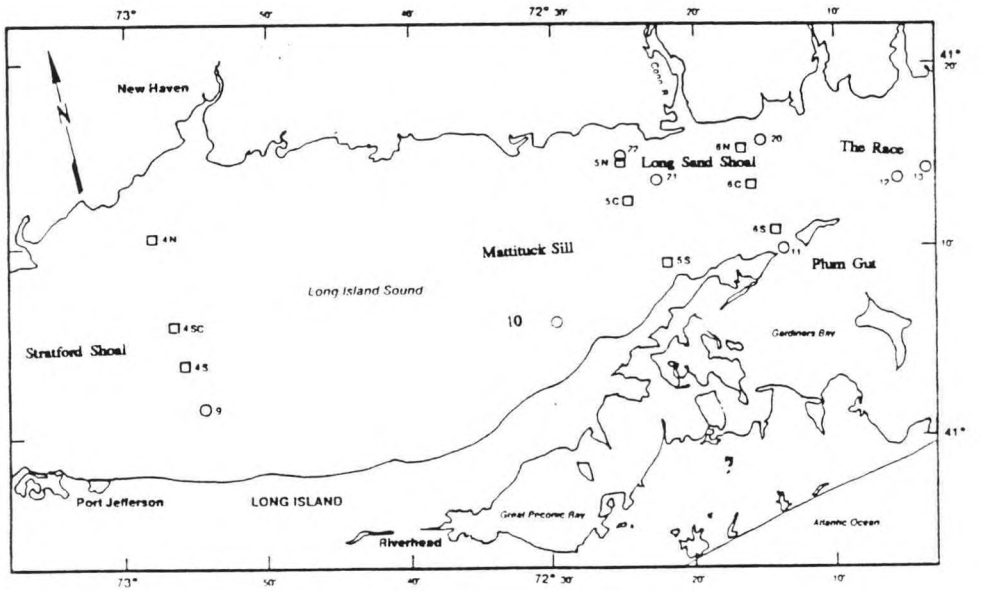

Stations in the central and eastern Sound

Figure 4.1. NOS ADCP and SUNY Current Meter Station Locations

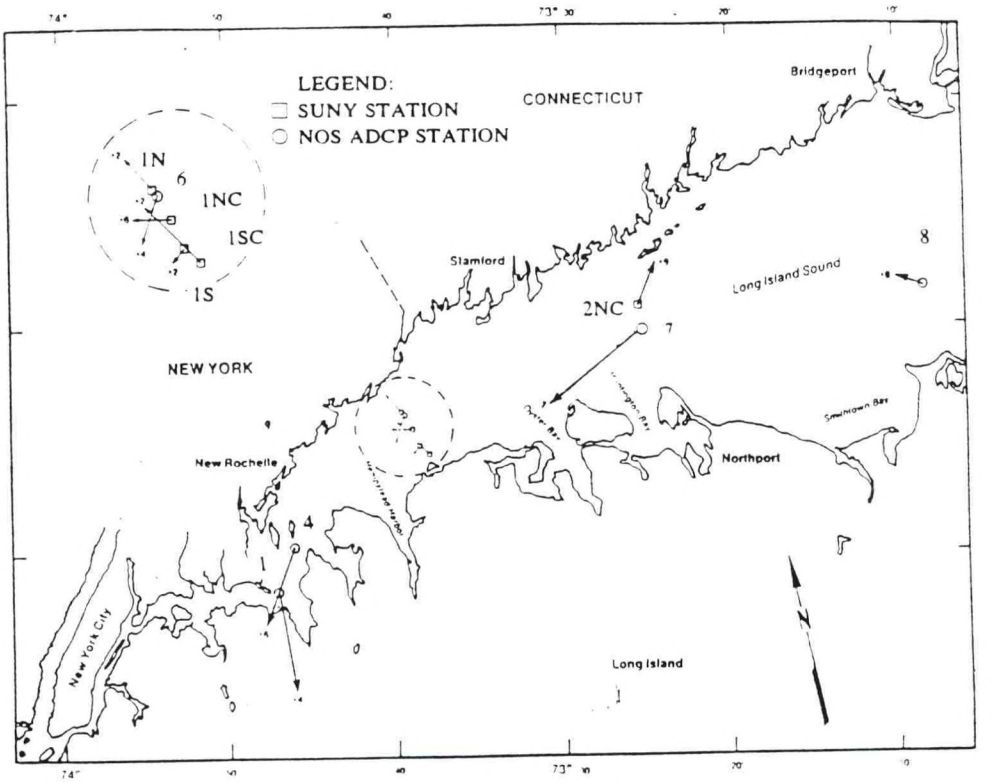

Western Sound

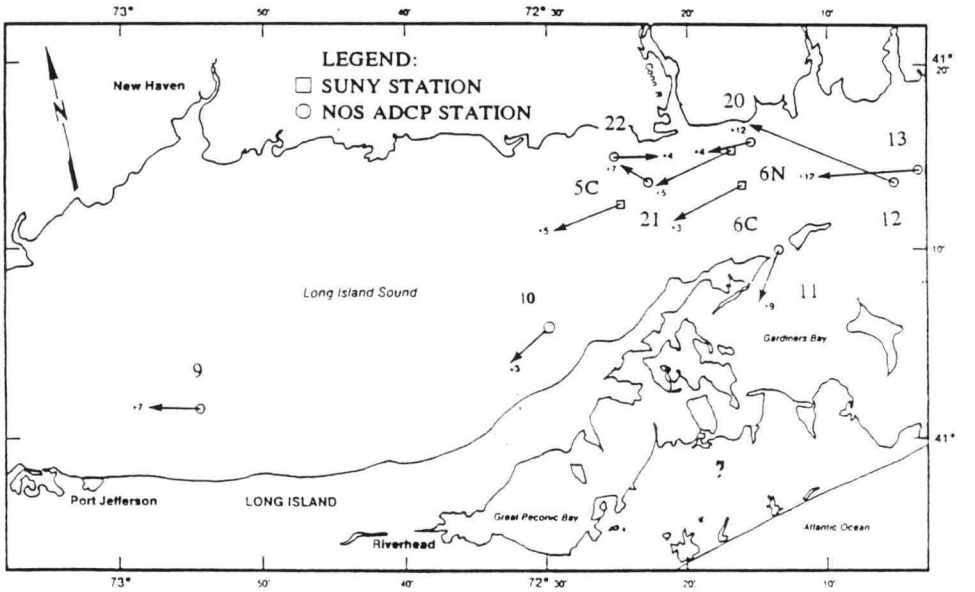

Central and Eastern Sound

The length of the arrows represent a one day translation. The height of the current above the bottom in meters is indicated at the head of the arrow.

Figure 4.2. NOS ADCP and SUNY Near-bottom Residual Currents

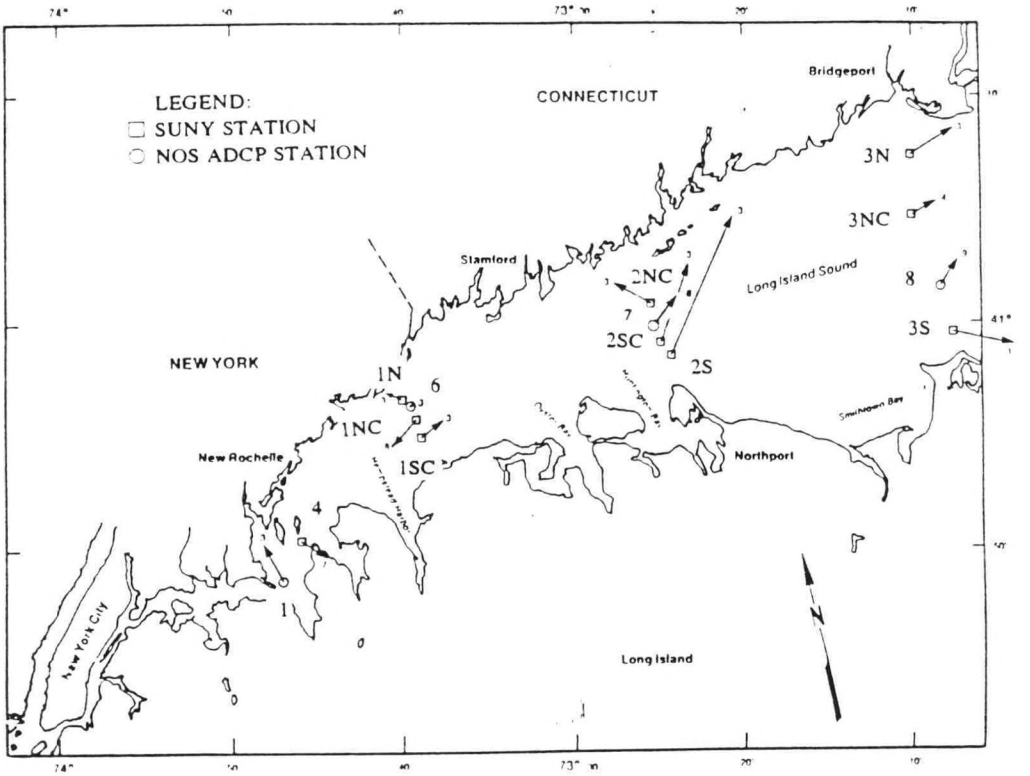

Western Sound

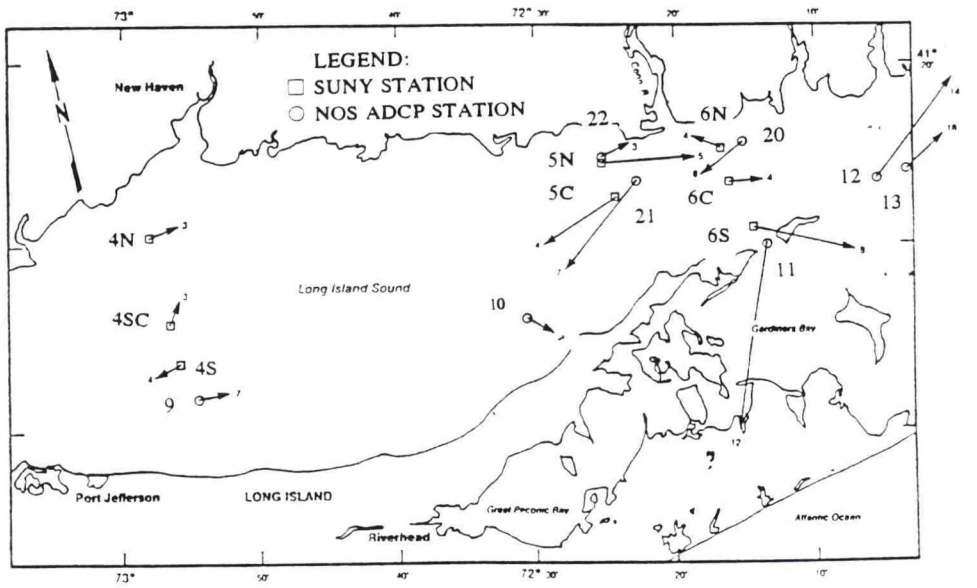

Central and Eastern Sound

The length of the arrows represent a one day translation. The depth of the current above the bottom in meters is indicated at the head of the arrow.

Figure 4.3. NOS ADCP and SUNY Near-surface Residual Currents

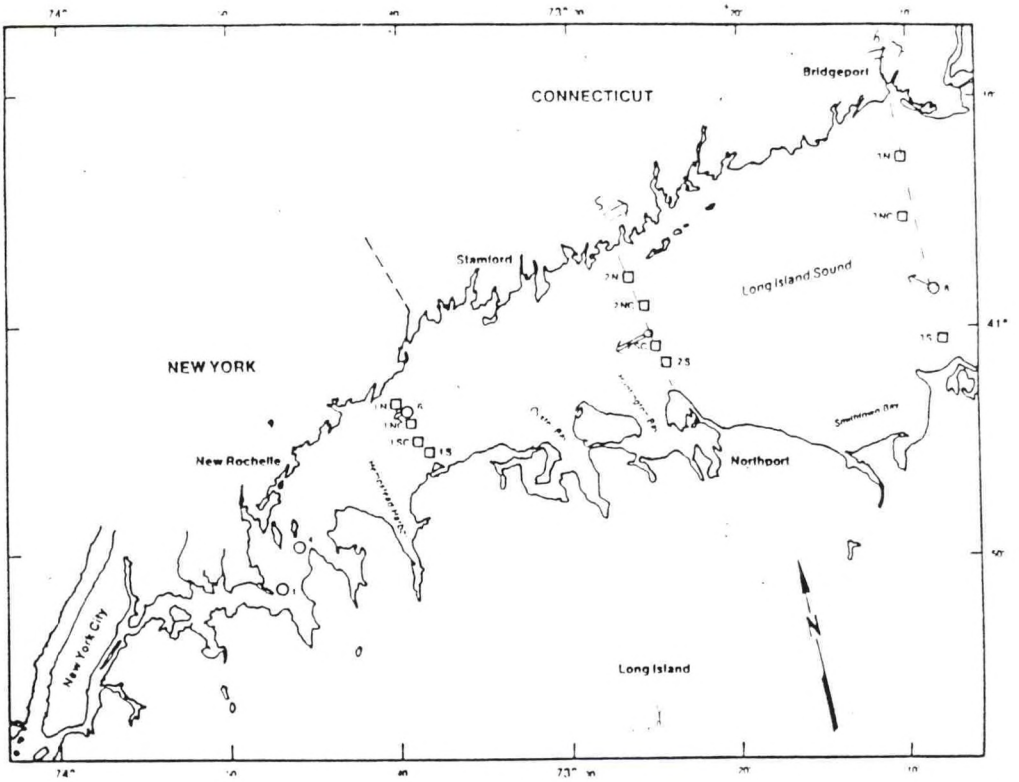

Western Sound

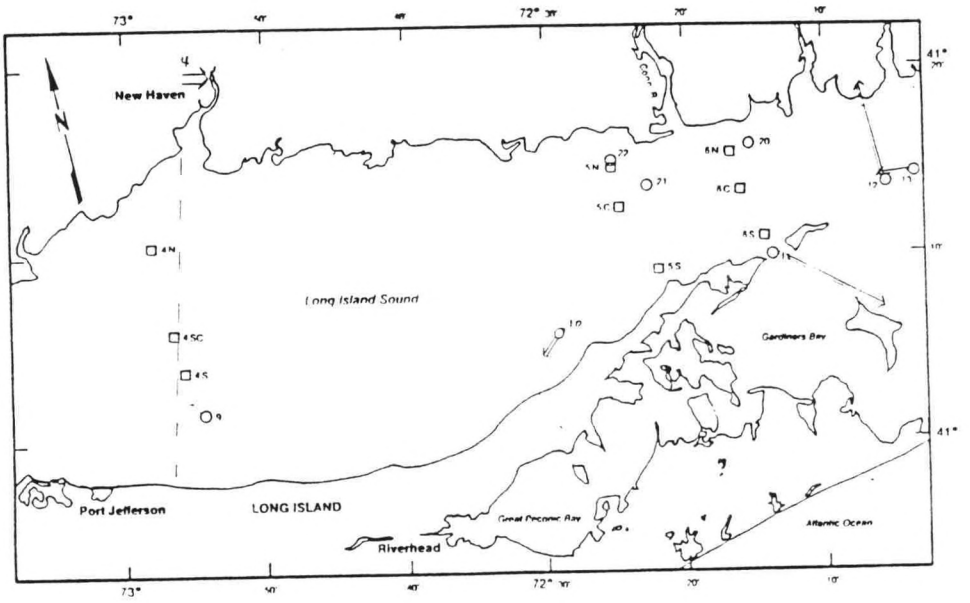

Central and Eastern Sound

Figure 4.4. Mean Velocity and Upper Layer Transport

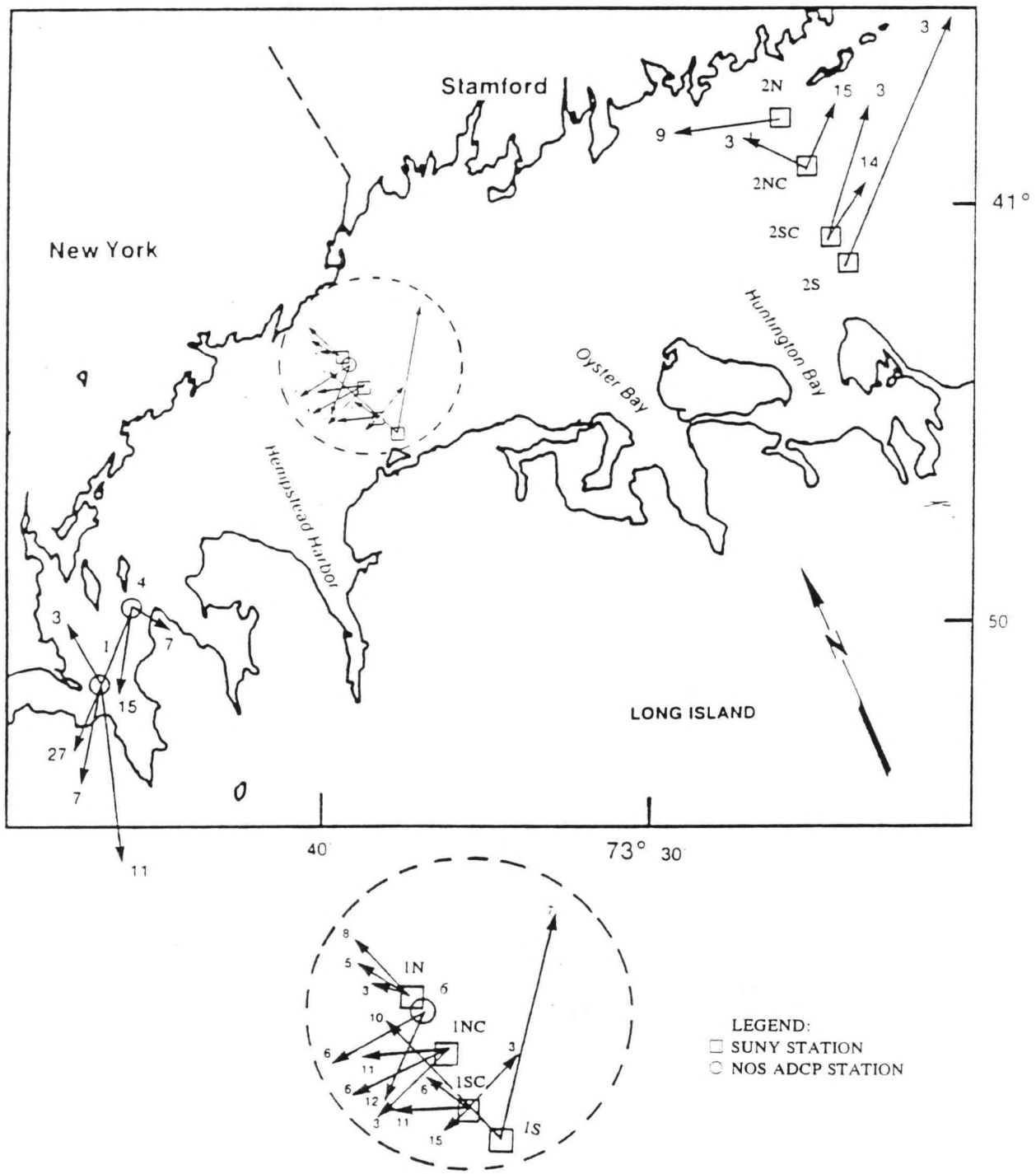

The length of the arrows represents a one day translation. The depth of the current in meters is indicated at the head of the arrow.

Figure 4.5. Residual currents at ADCP and SUNY stations in the western Sound

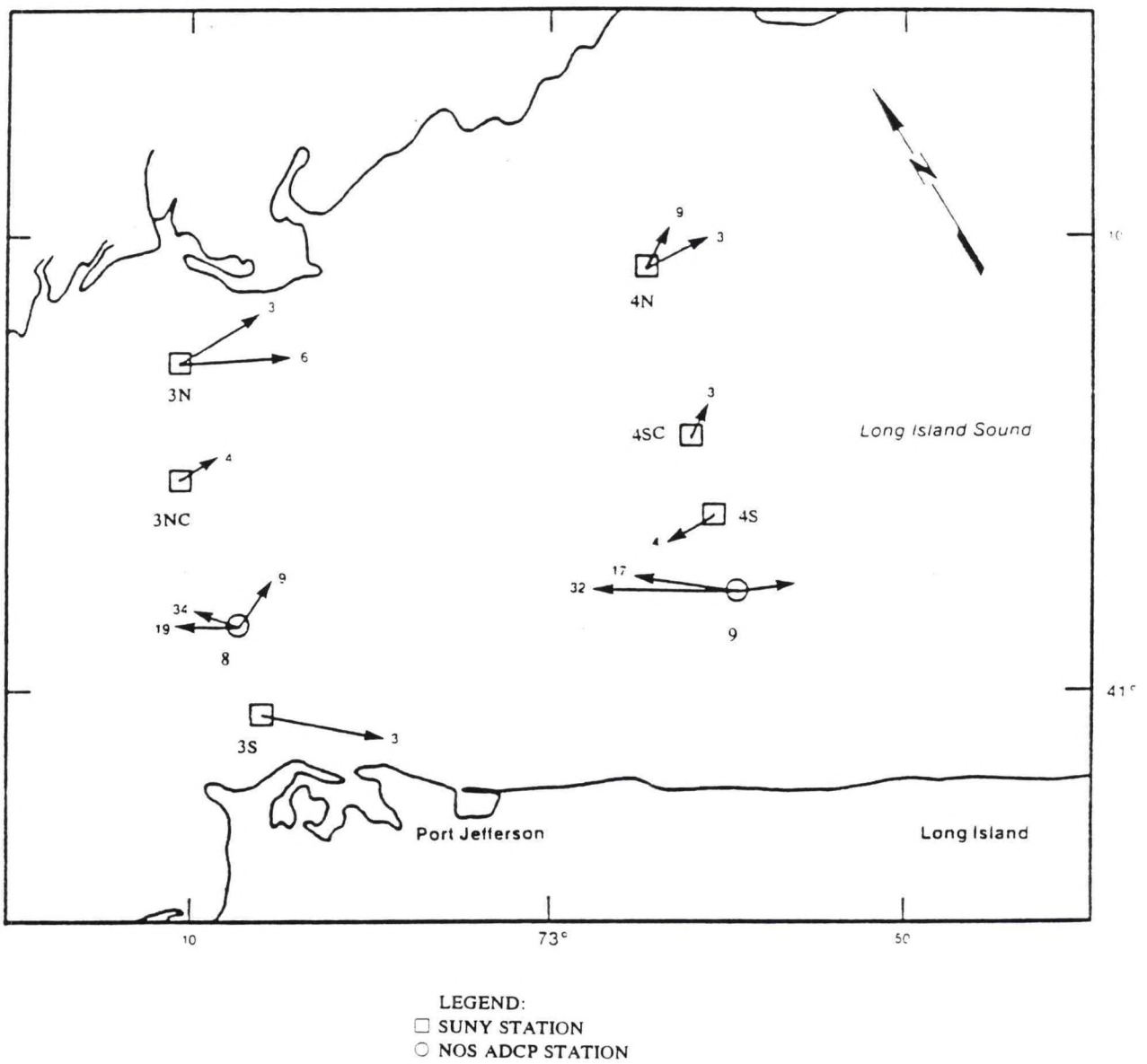

The length of the arrows represents a one day translation. The depth of the current in meters is indicated at the head of the arrow.

Figure 4.6. Residual currents at ADCP and SUNY stations in the central Sound

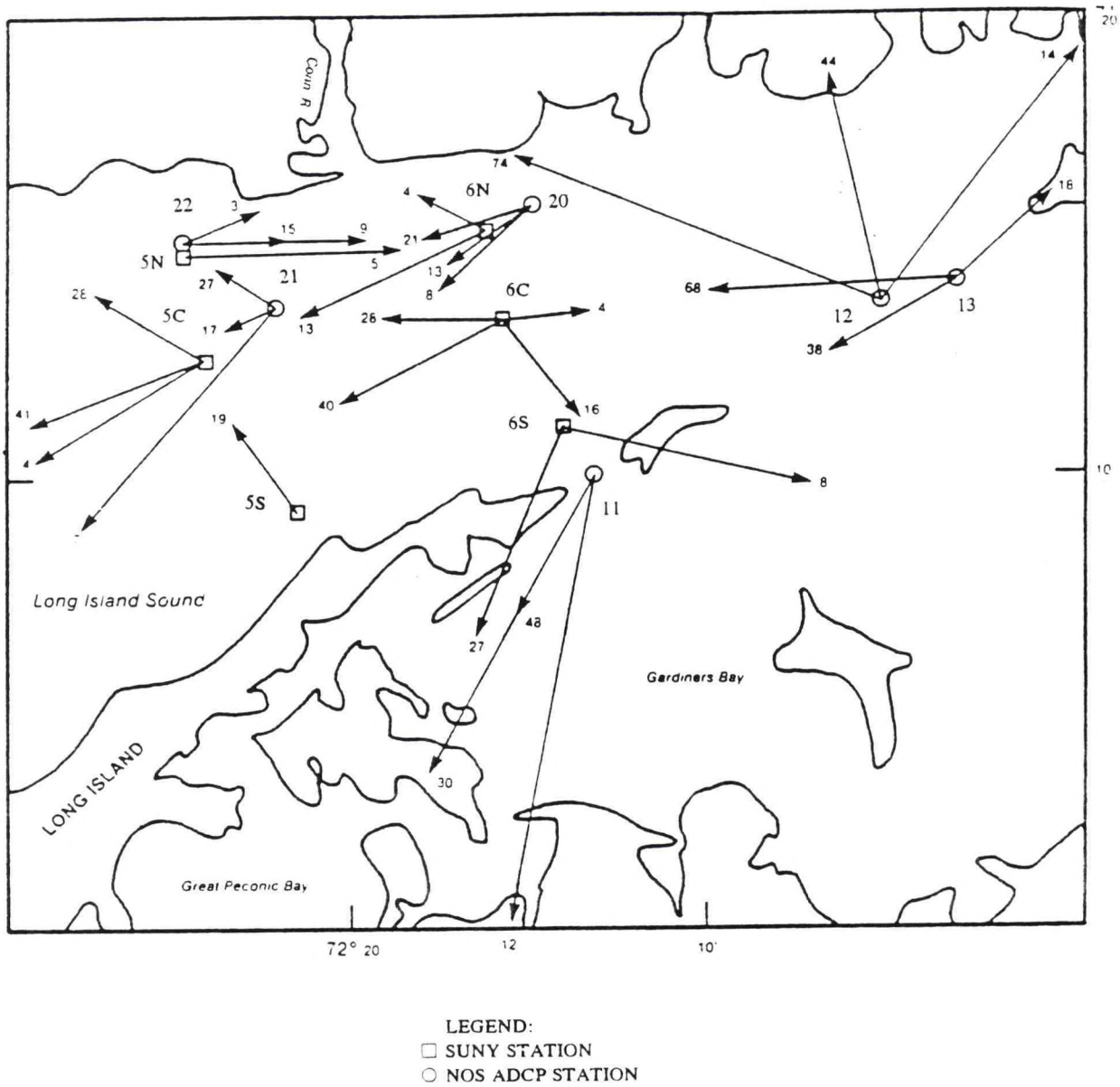

The length of the arrows represents a one day translation. The depth of the current in meters is indicated at the head of the arrow.

Figure 4.7. Residual currents at ADCP and SUNY stations in the eastern Sound

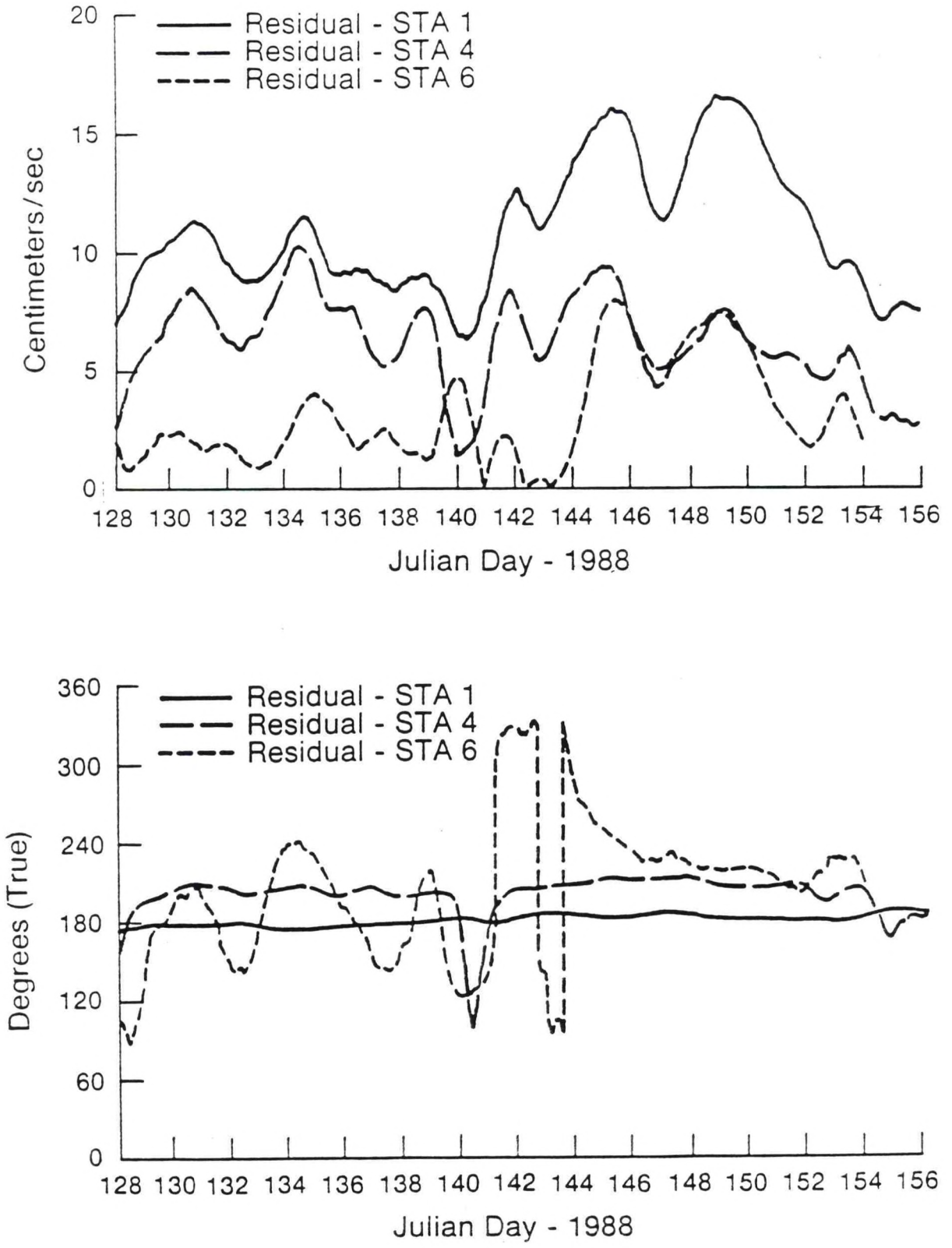

Figure 4.8. Lower layer residual currents at Stations 1 (3 m above bottom), 4 (5 m above bottom), and 6 (3 m above bottom)

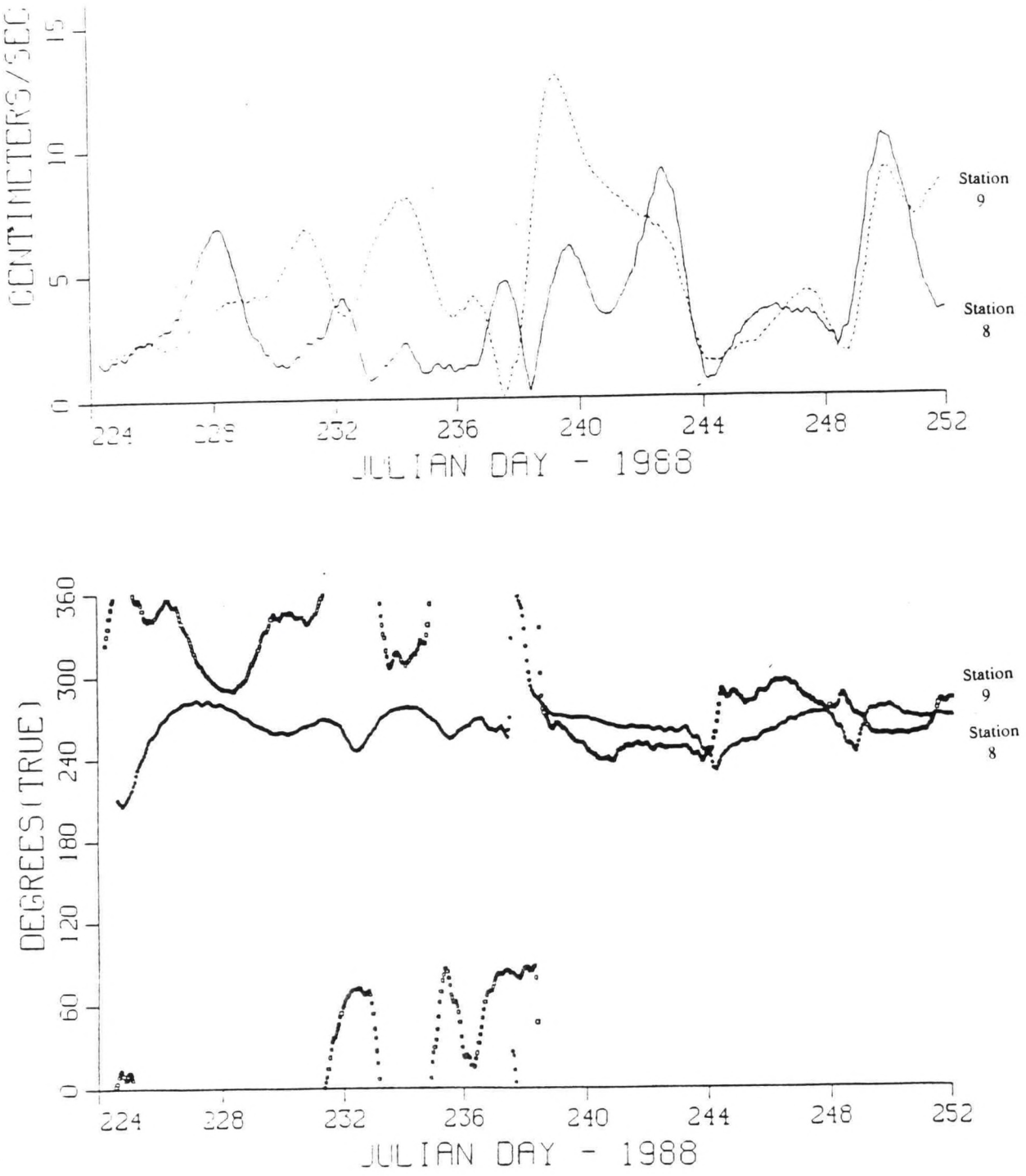

Figure 4.9. Lower Layer Residual Flow (5 m above bottom) at ADCP Stations 8 and 9

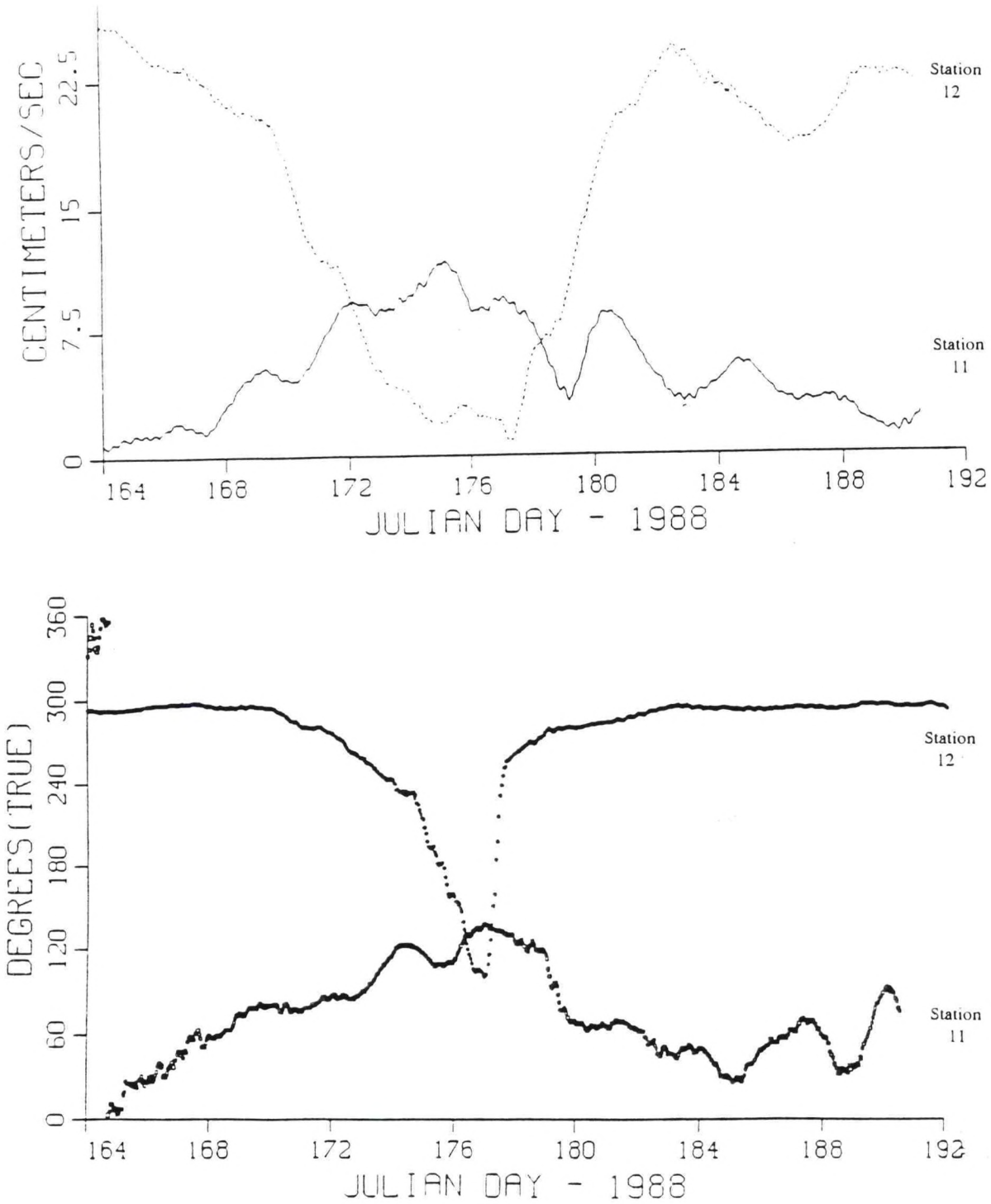

Figure 4.10. Lower Layer Residual Flow at Station 11 (8 m above bottom) and at Station 12 (12 m above bottom)

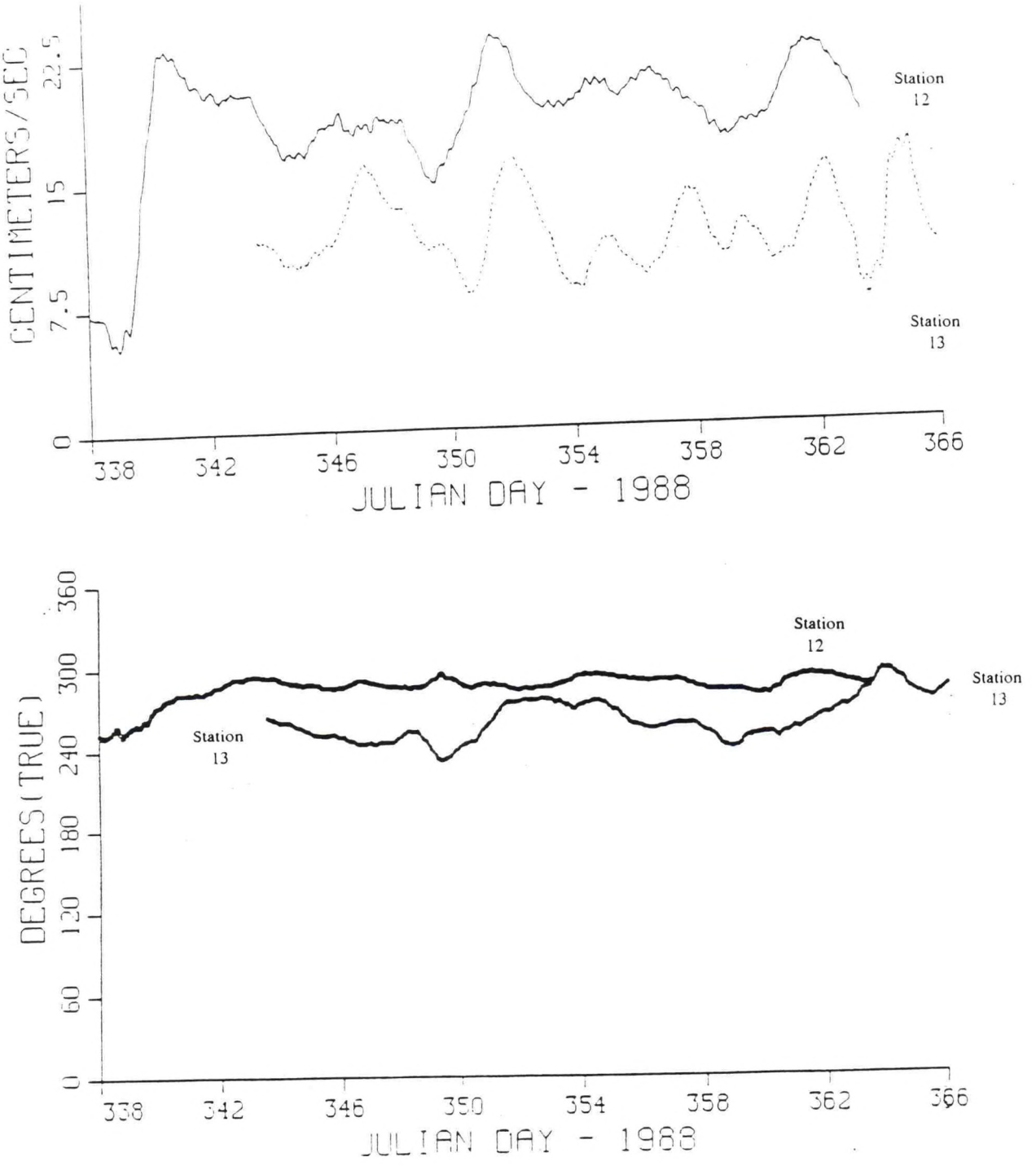

Figure 4.11. Lower Layer Residual Flow (12 m above bottom) at Stations 12 and 13

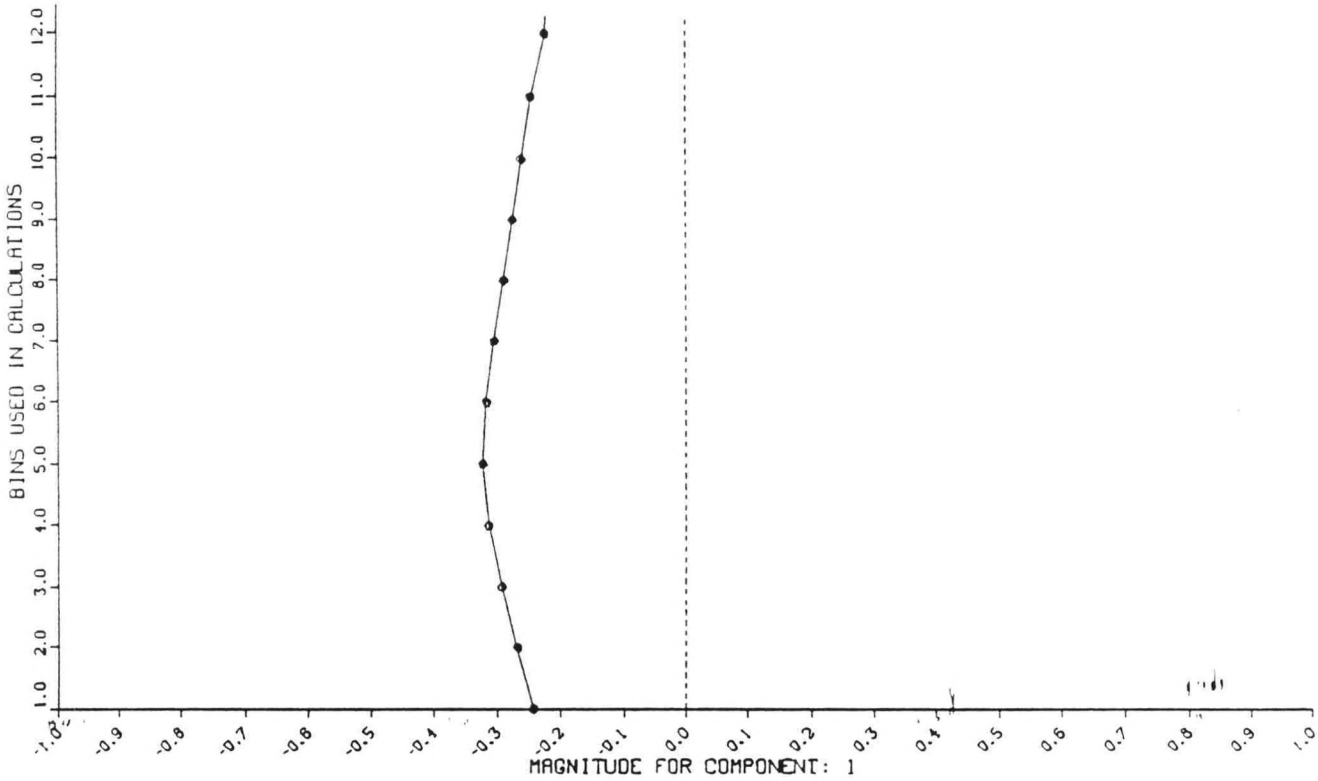

Figure 4.12. ASD Spatial Decomposition: Station 1 v-component mode 1

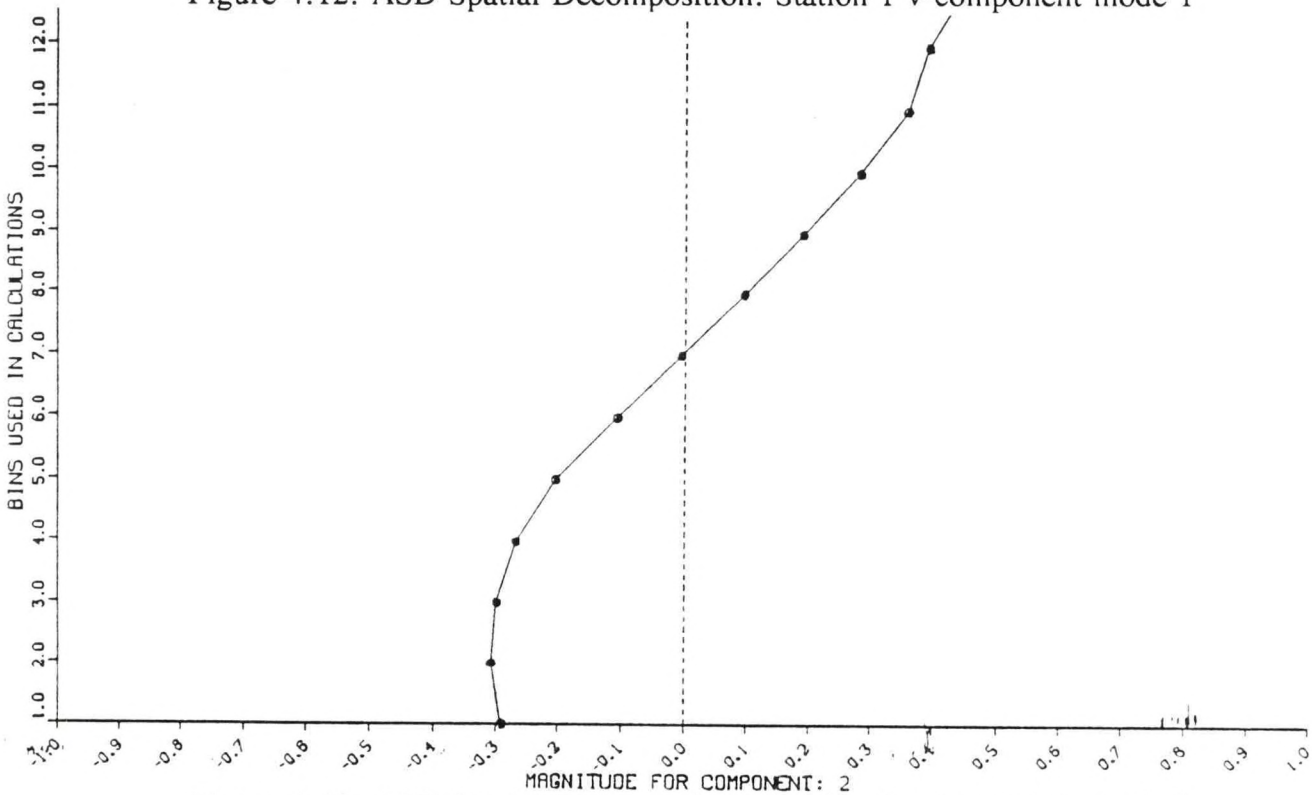

Figure 4.13. ASD Spatial Decomposition: Station 1 v-component mode 2

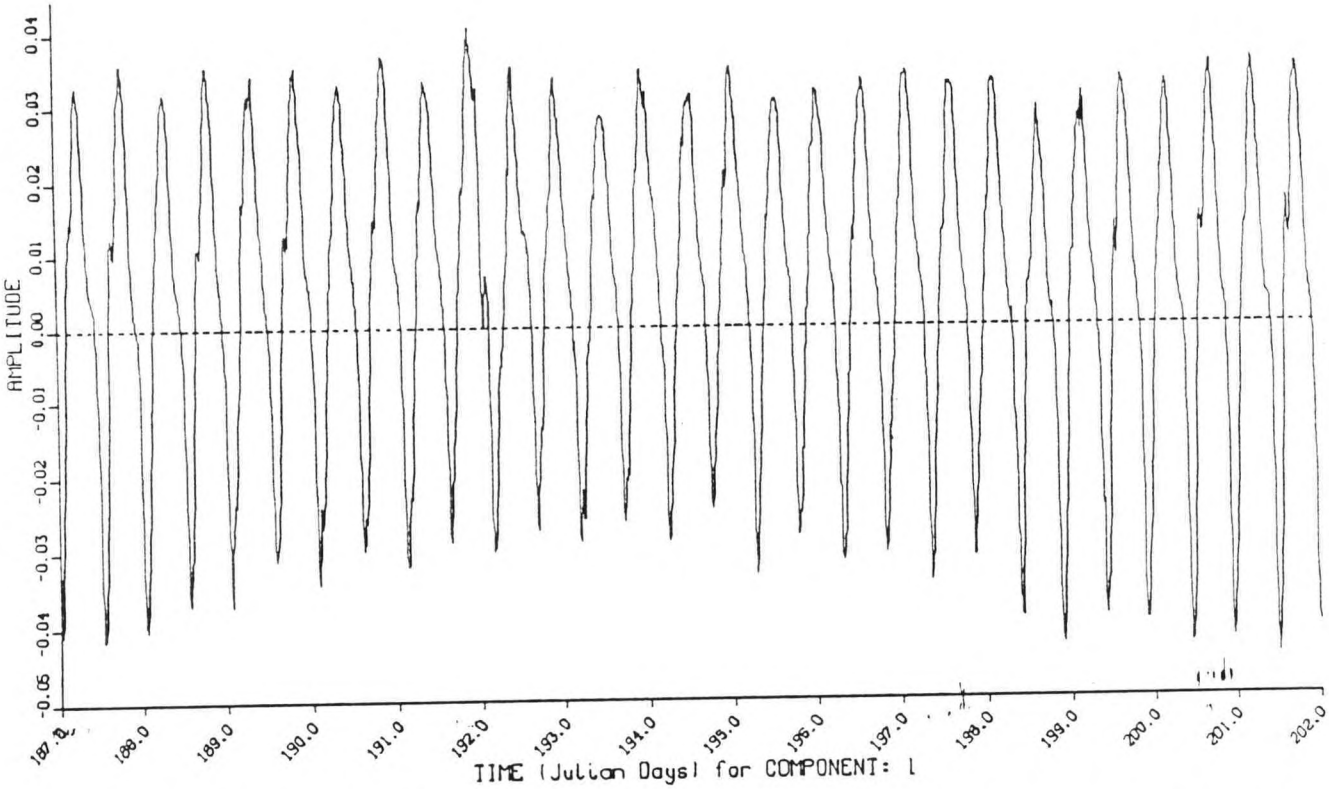

Figure 4.14. ASD 15-Day Temporal Decomposition: Station 1 v-component mode 1

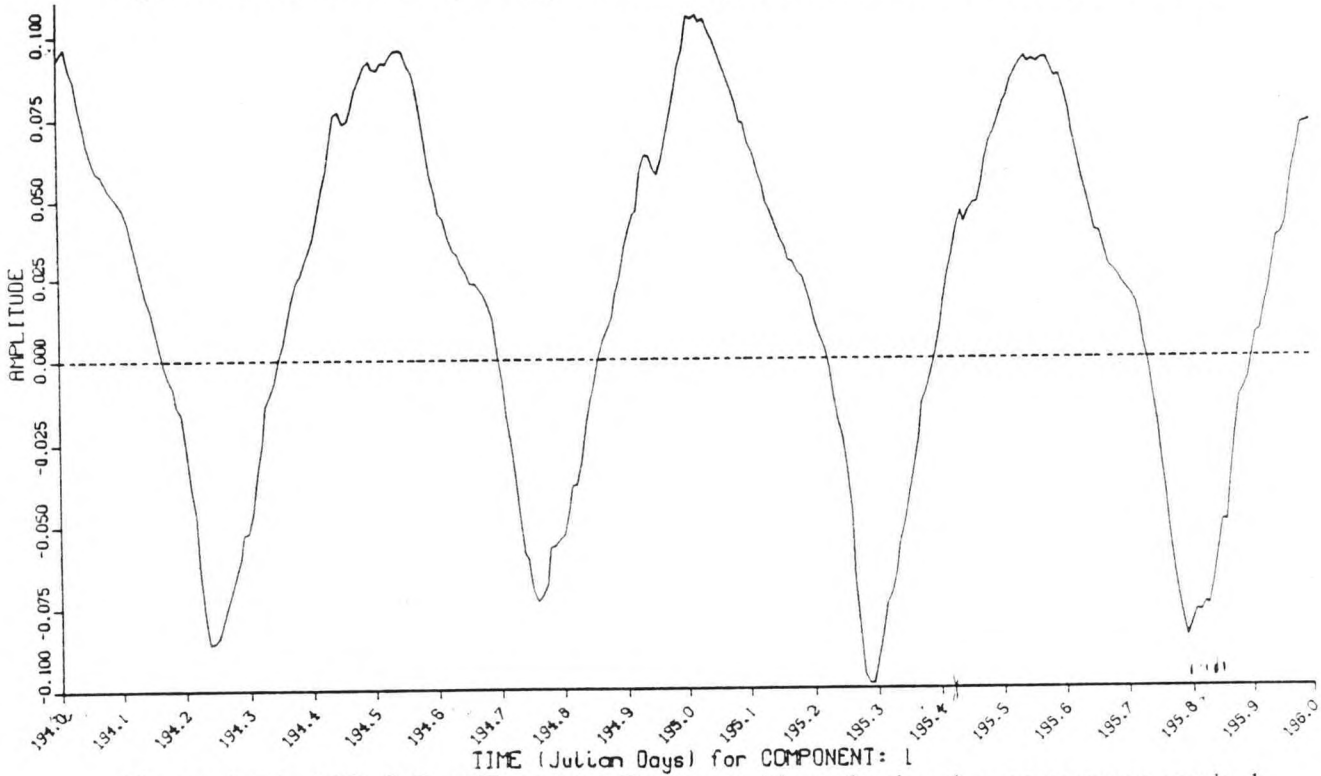

Figure 4.15. ASD 2-Day Temporal Decomposition: Station 1 v-component mode 1

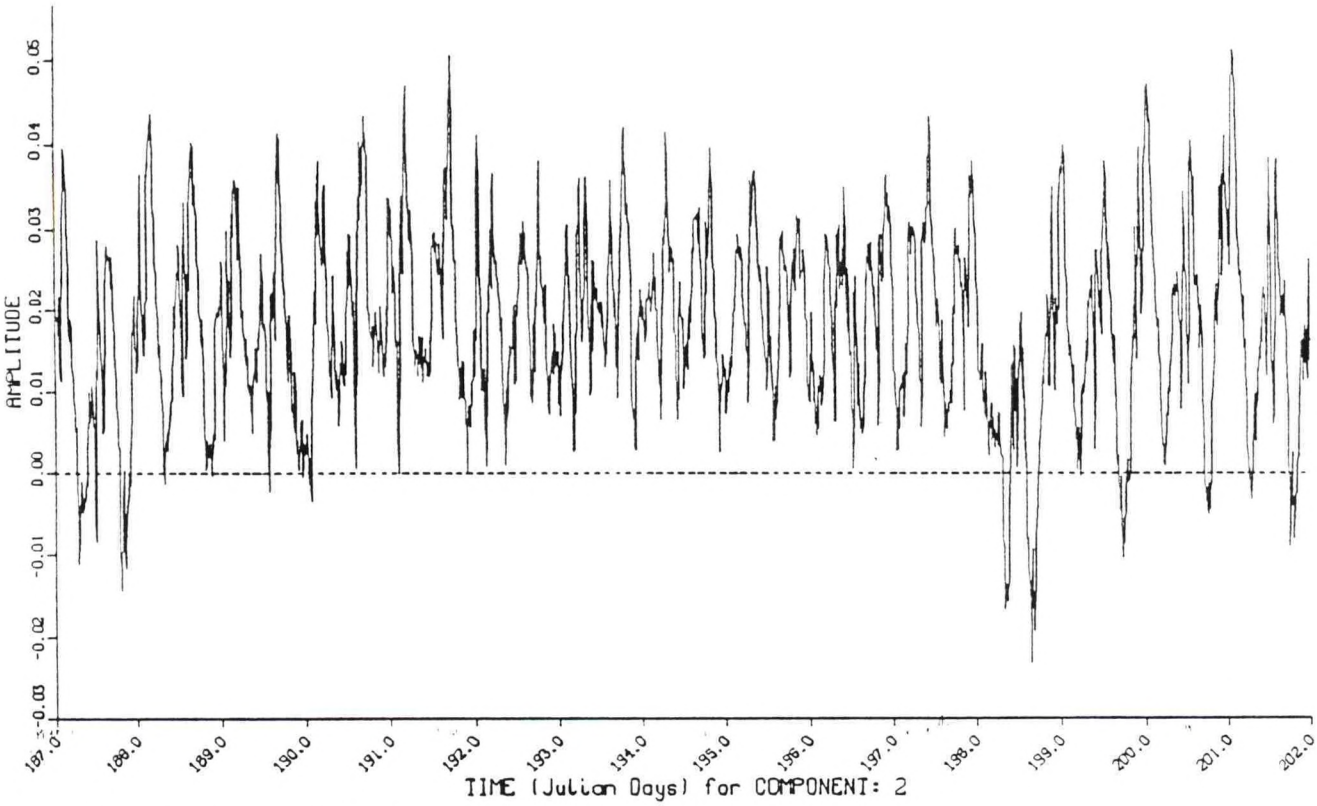

Figure 4.16. ASD 15-Day Temporal Decomposition: Station 1 v-component mode 2

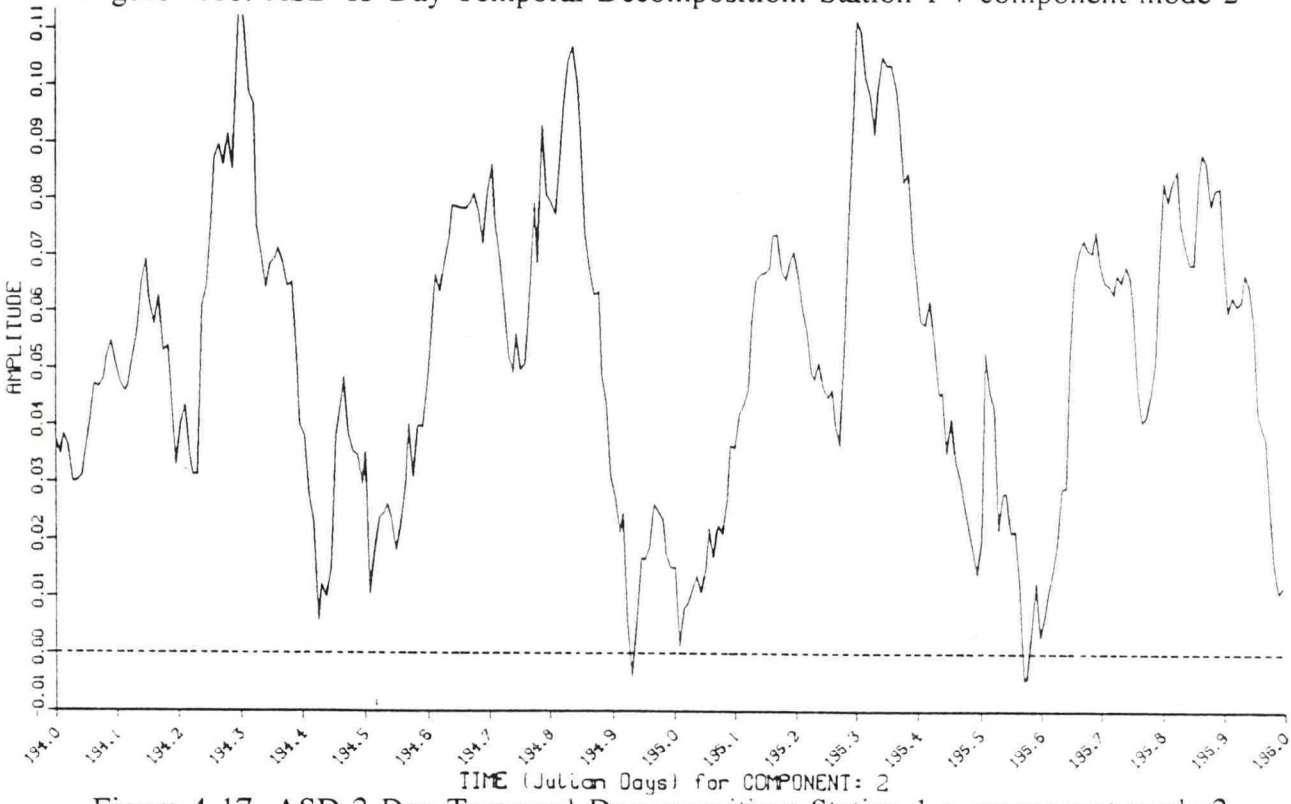

Figure 4.17. ASD 2-Day Temporal Decomposition: Station 1 v-component mode 2

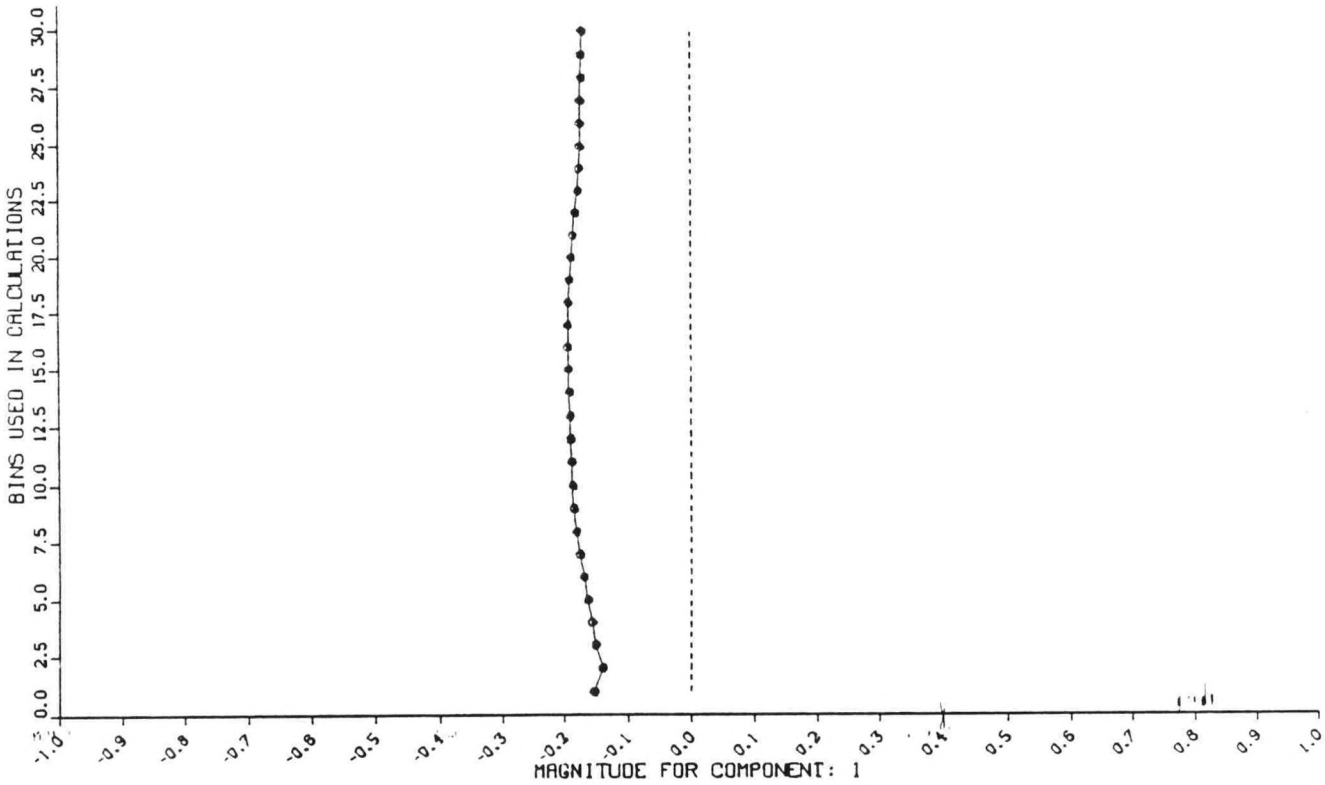

Figure 4.18. ASD Spatial Decomposition: Station 9 u-component mode 1

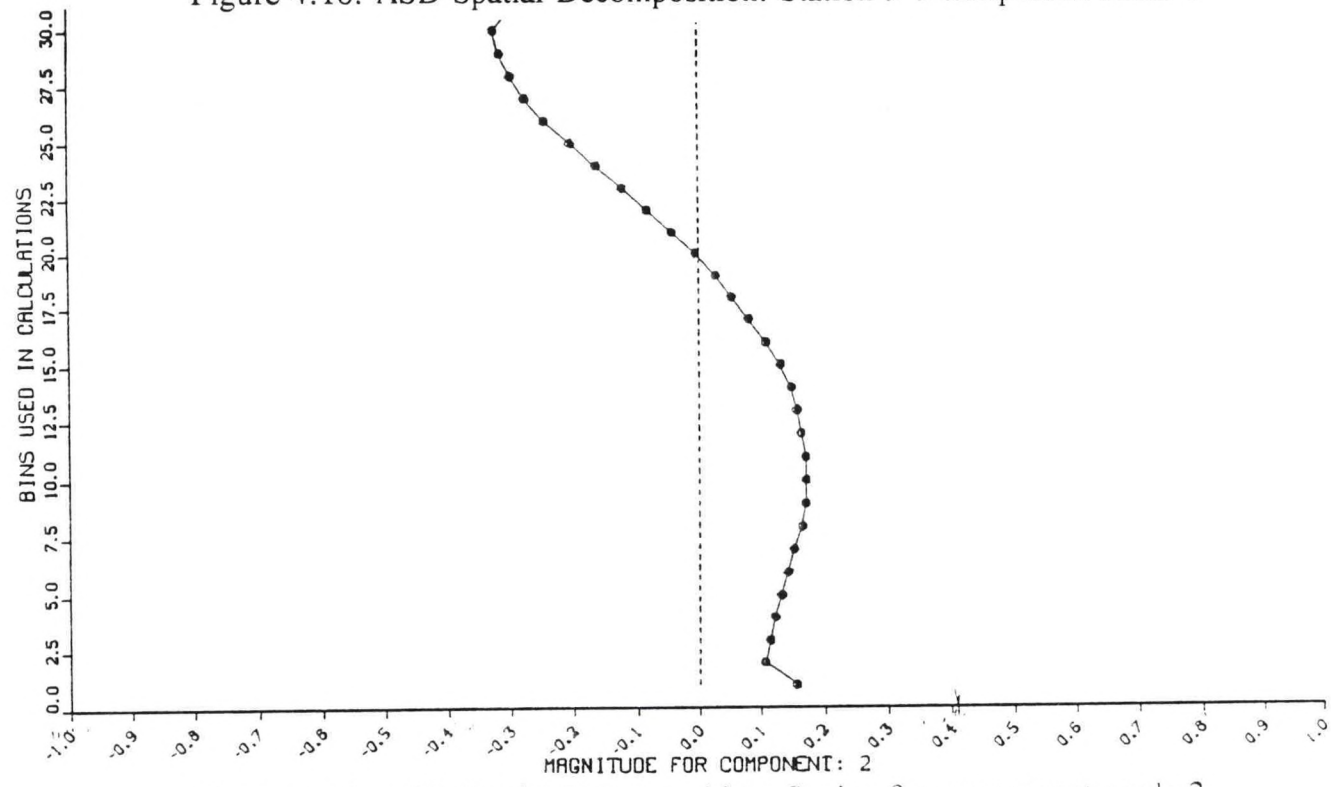

Figure 4.19. ASD Spatial Decomposition: Station 9 u-component mode 2

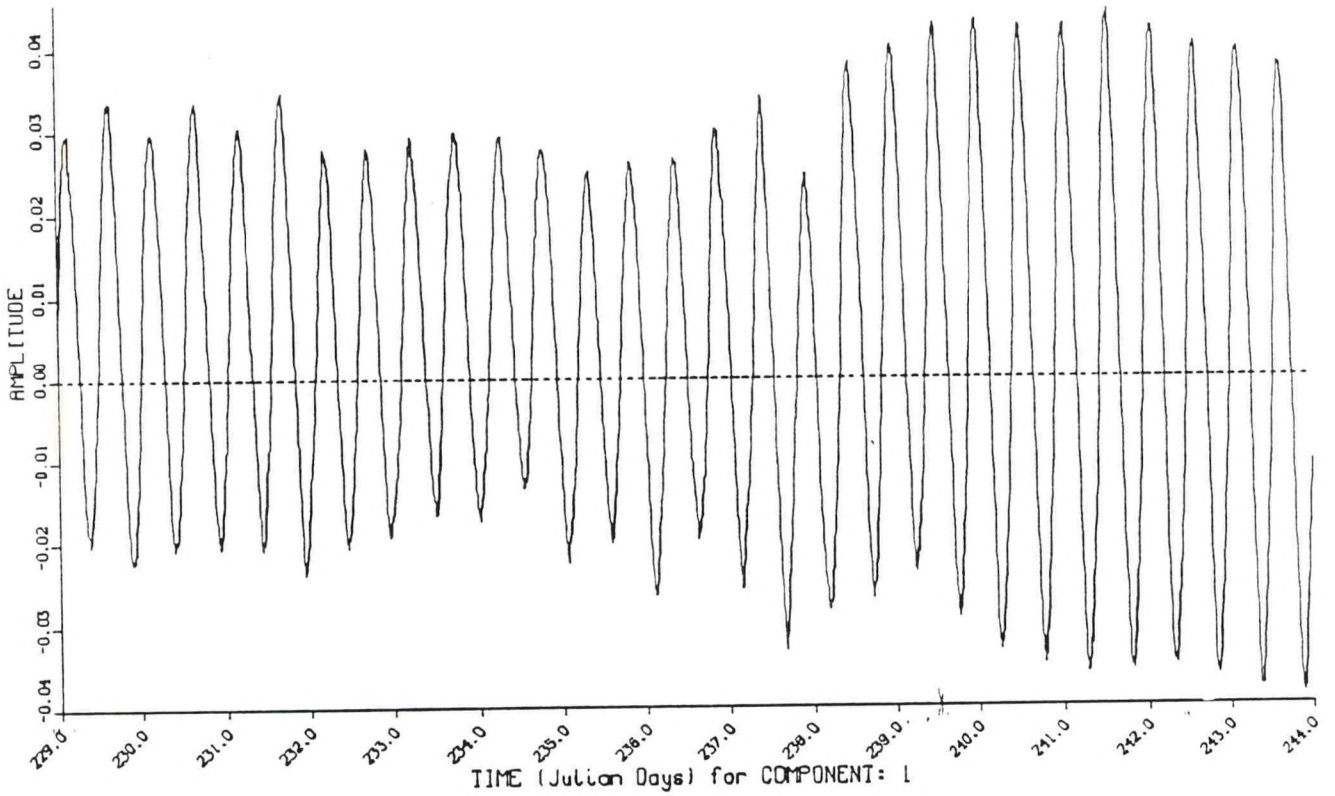

Figure 4.20. ASD 15-Day Temporal Decomposition: Station 9 u-component mode 1

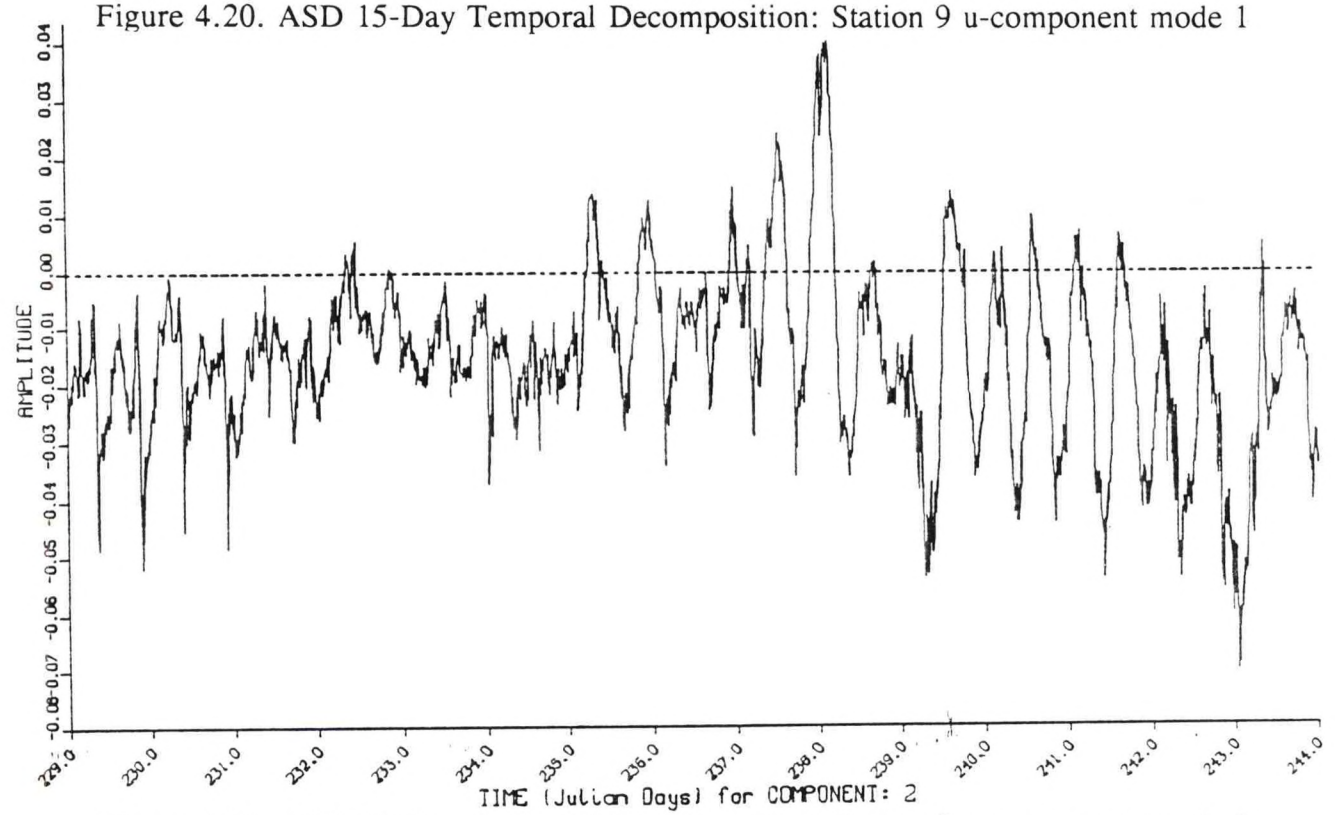

Figure 4.21. ASD 15-Day Temporal Decomposition: Station 9 u-component mode 2

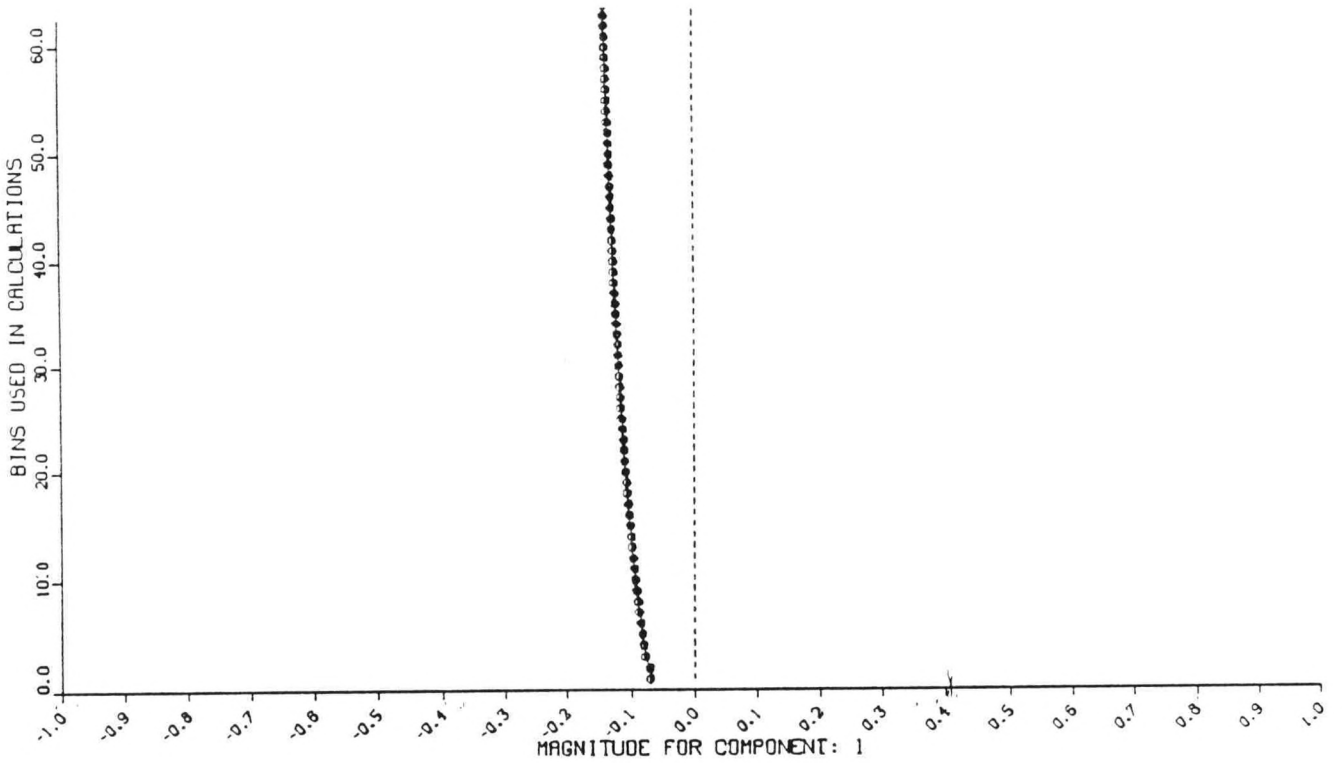

Figure 4.22. ASD Spatial Decomposition: Station 12 u-component mode 1

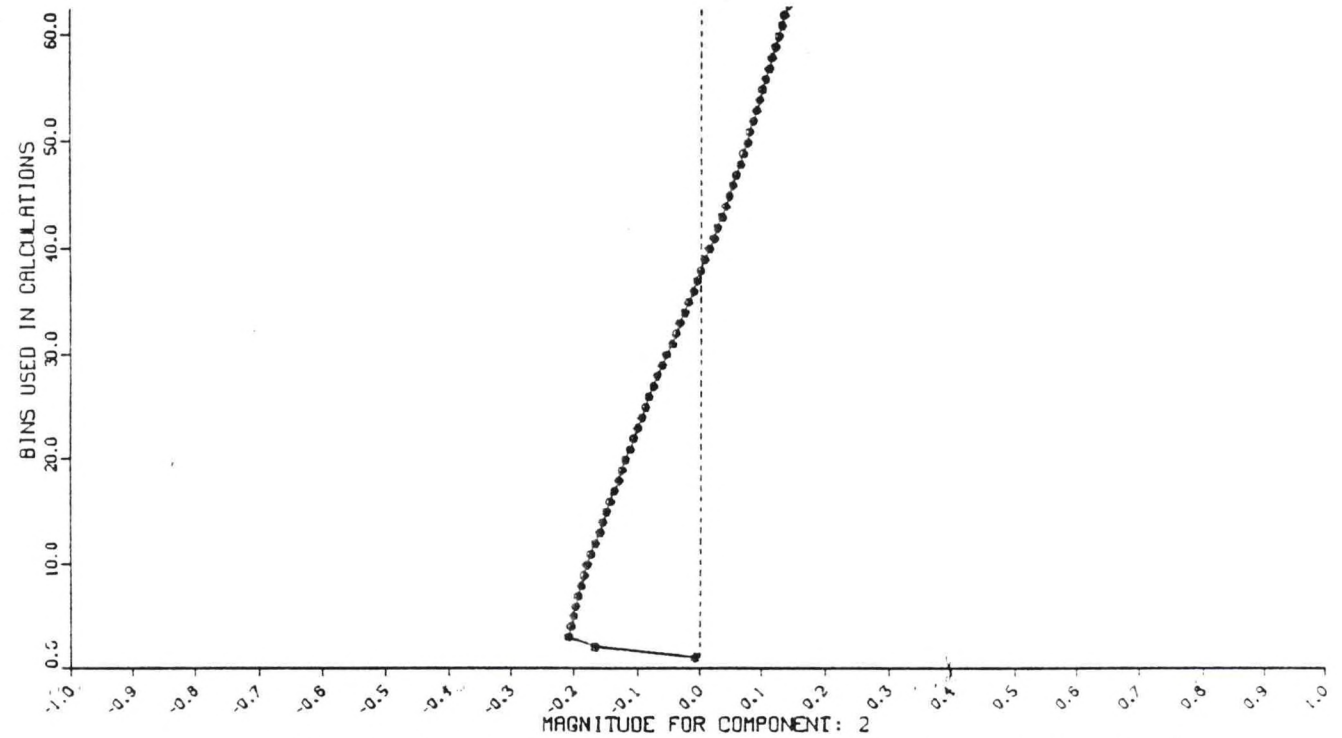

Figure 4.23. ASD Spatial Decomposition: Station 12 u-component mode 2

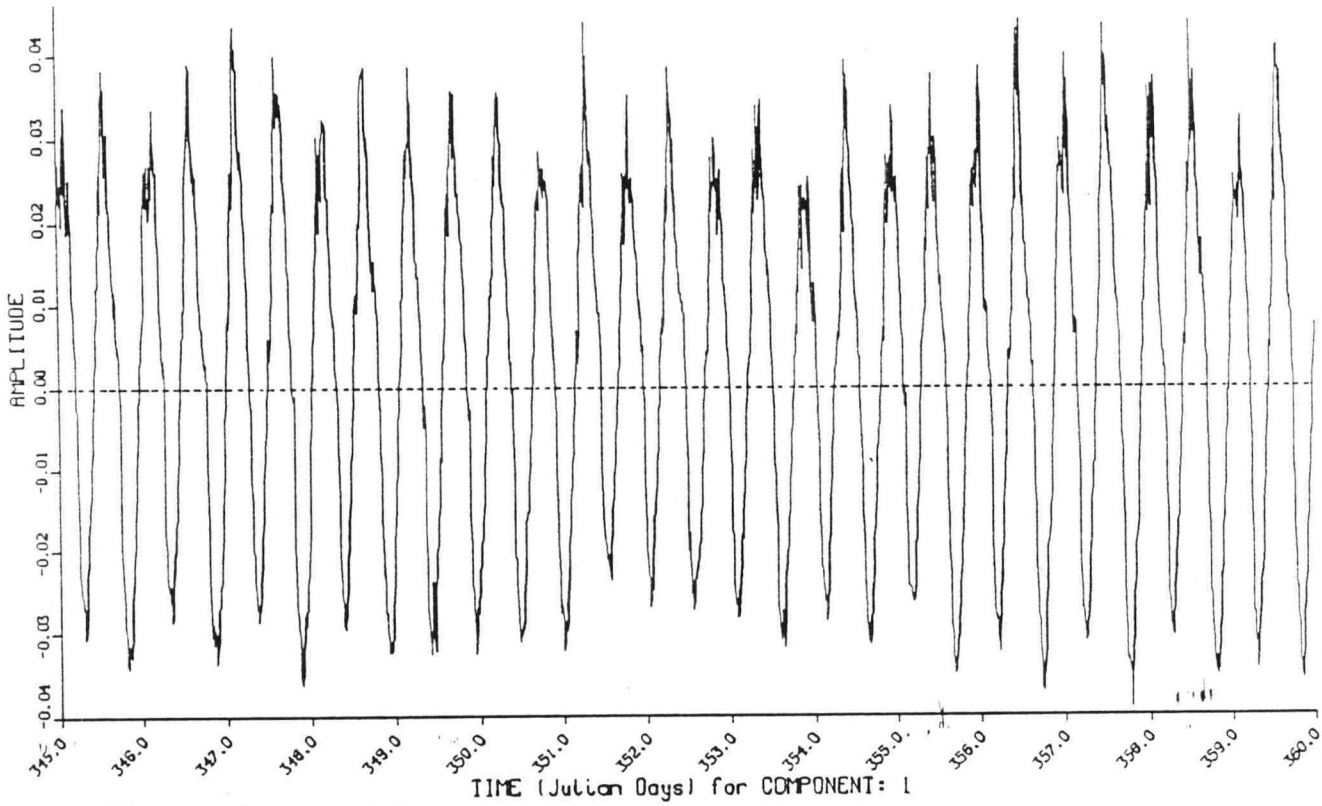

Figure 4.24. ASD 15-Day Temporal Decomposition: Station 12 u-component mode 1

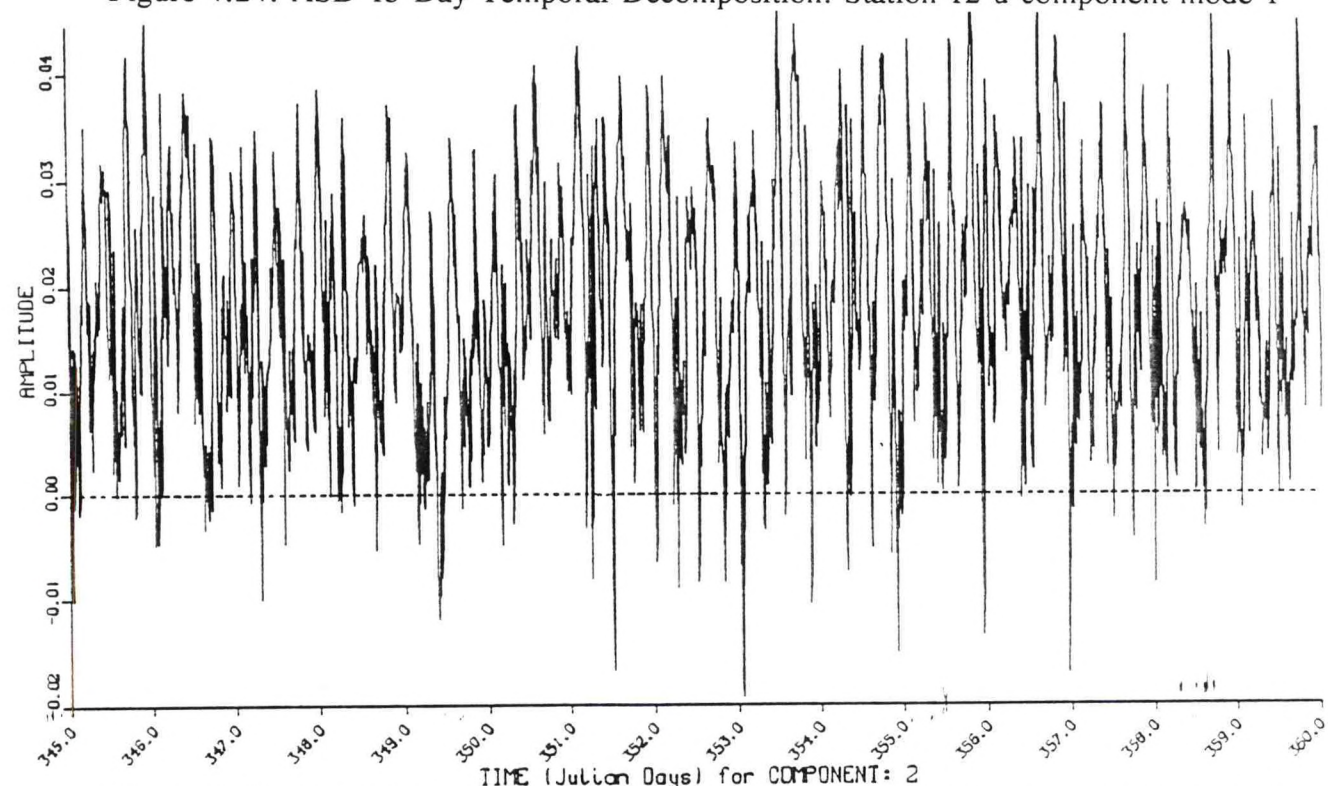

Figure 4.25. ASD 15-Day Temporal Decomposition: Station 12 u-component mode 2

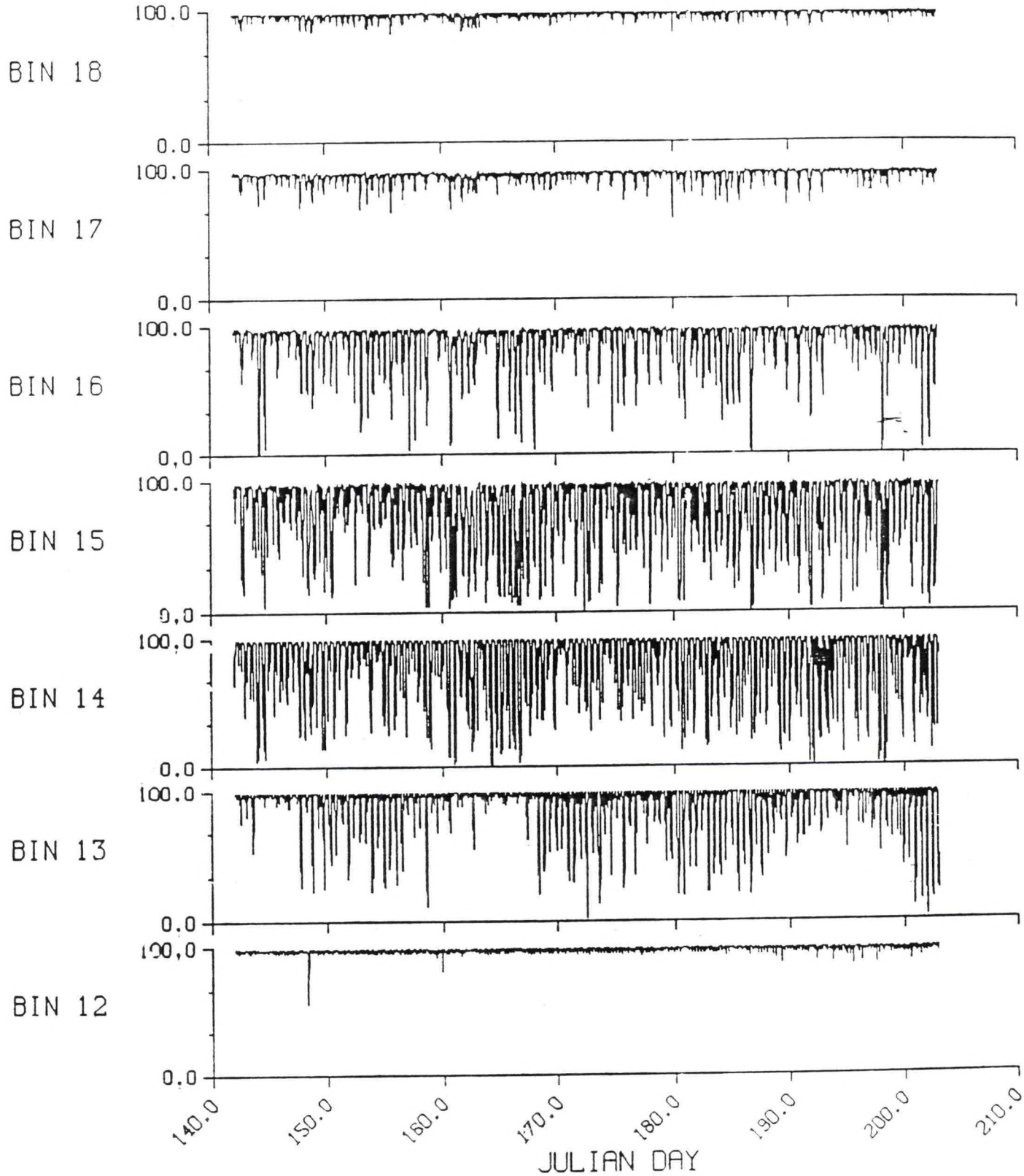

Figure 4.26. Multiple Bin Percent Good Pings: ADCP Station 2, South Clason, NY

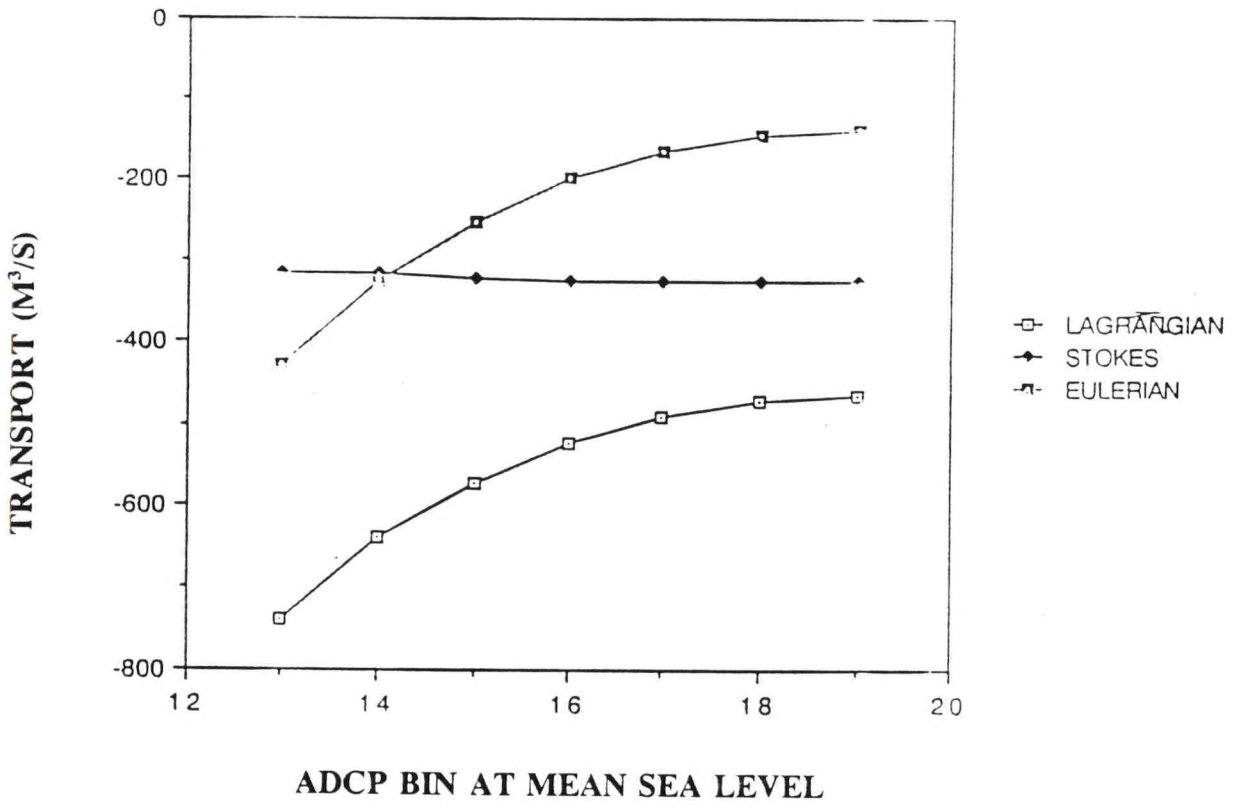

Figure 4.27. Transport versus Surface Bin: ADCP Station 2, South Clason, NY

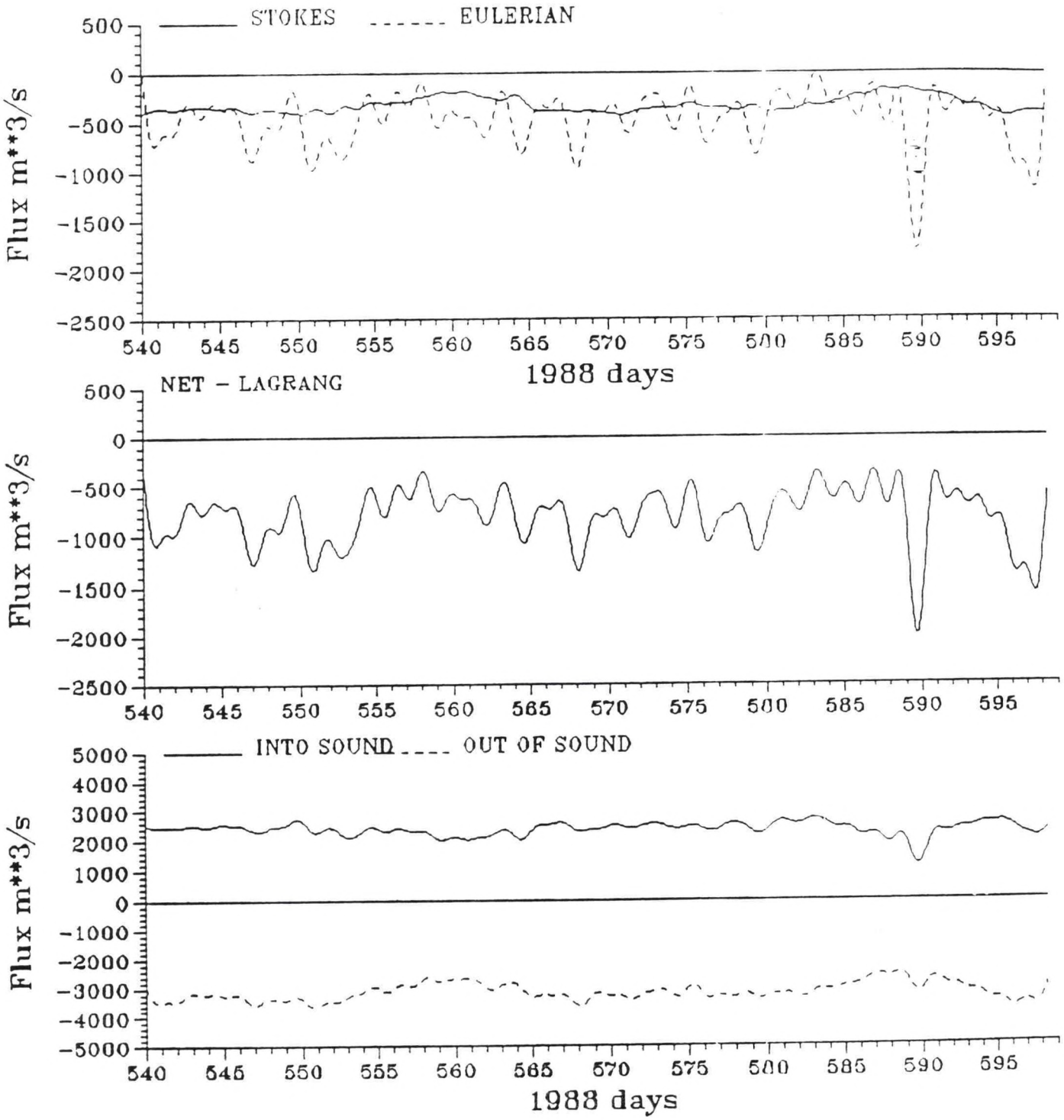

Figure 4.28. 36-Hour Filtered Mass Fluxes: ADCP Station 2, South Clason, NY

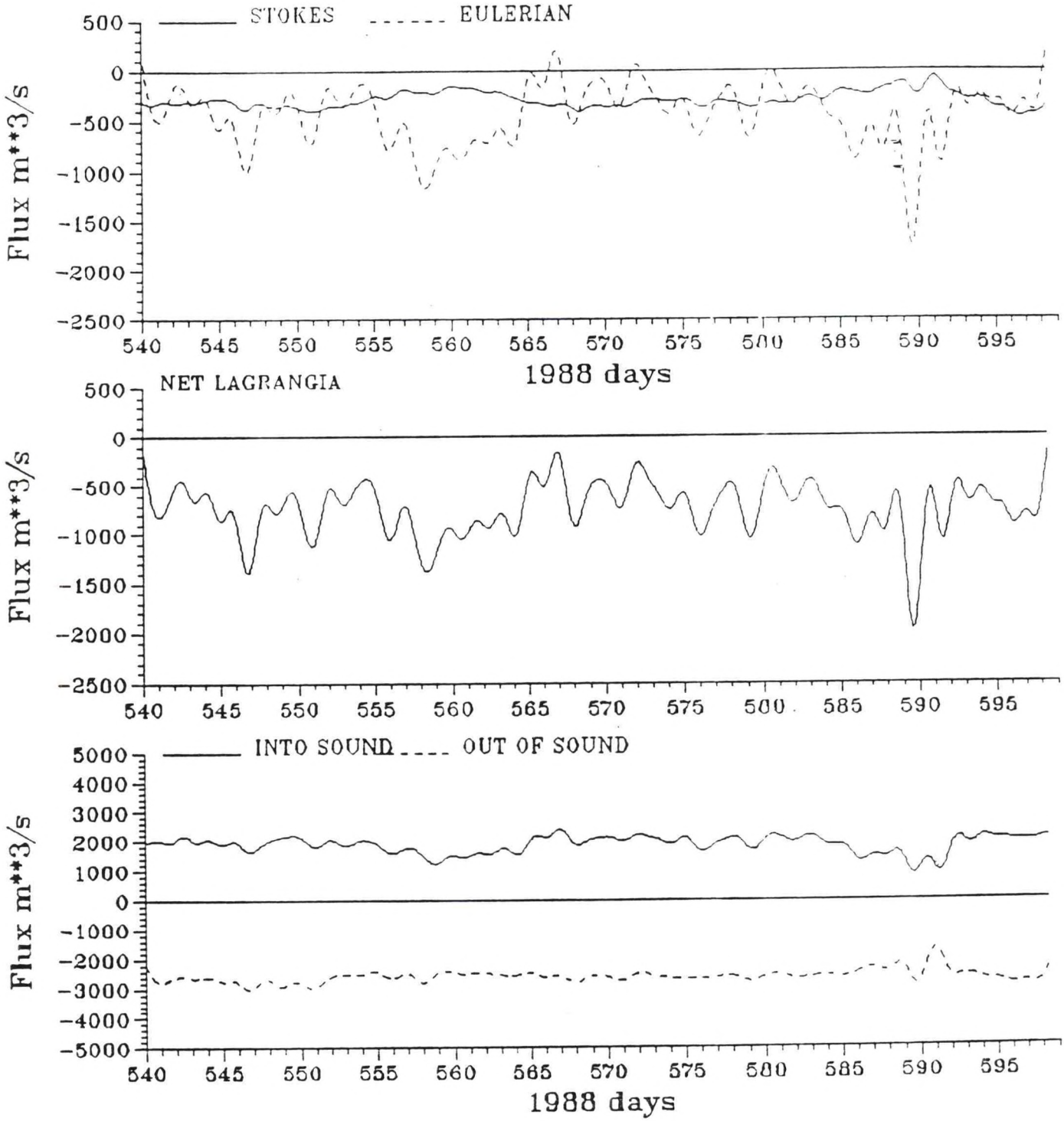

Figure 4.29. 36-Hour Filtered Mass Fluxes: ADCP Station 1, Throgs Neck, NY

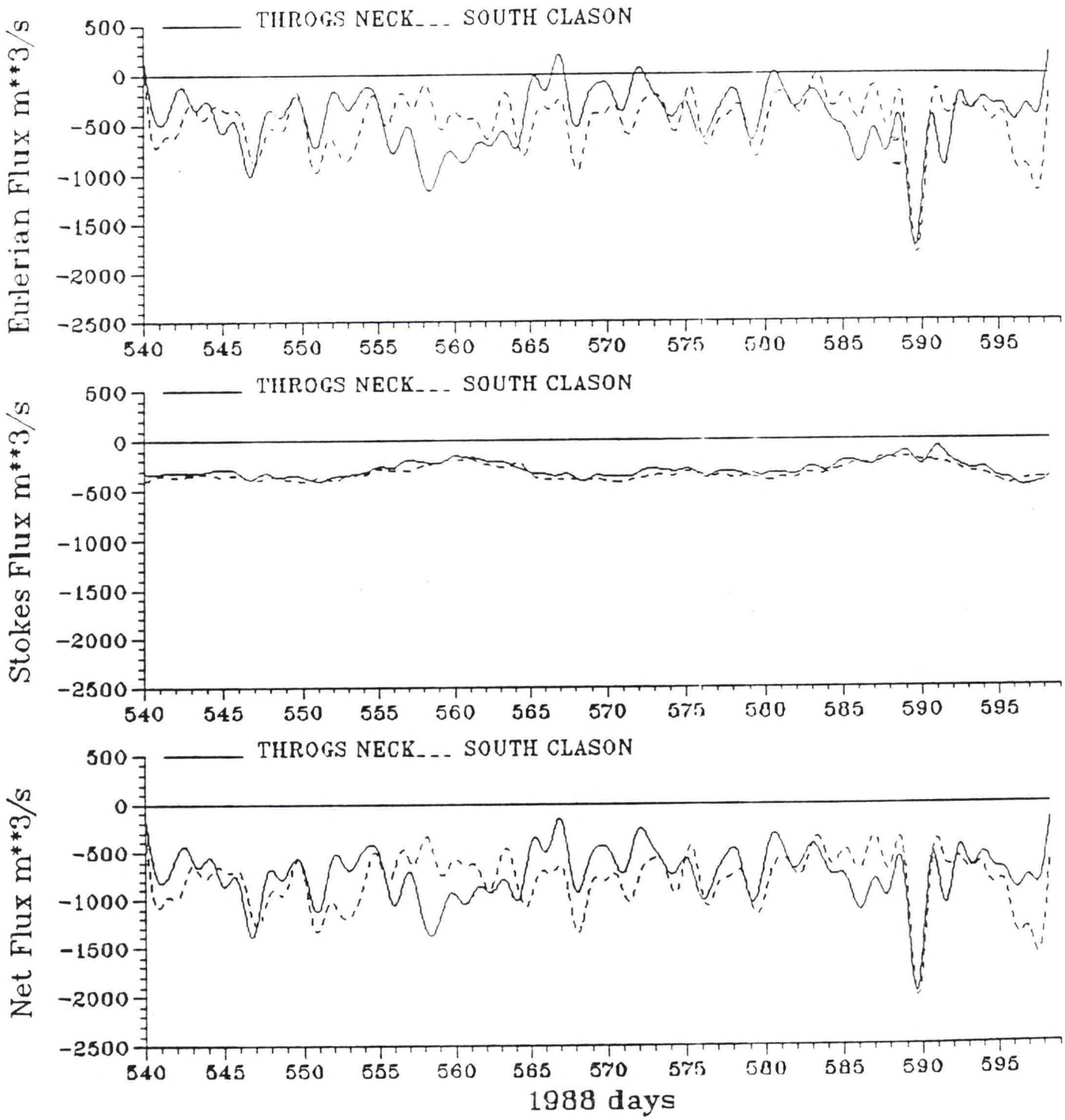

Figure 4.30. Comparison of Computed Nontidal Fluxes at ADCP Station 1, Throgs Neck, NY and ADCP Station 2, South Clason, NY

5. MODEL EVOLUTION

Two complementary perspectives provided the focus for the NOS hydrodynamic model evolution. The first focus is on tidal elevations and currents over a lunar month in order to support the development of improved NOS navigation products such as an updated tide and current atlas for Long Island Sound. The second perspective is on long term (12-18 months) residual circulation for use in EPA water quality modeling studies. The model evolution from each perspective is briefly outlined in this chapter. While detailed discussions of the modeling work are deferred until Section 6, the reader may desire to consult Figure 6.1 now for the form of the computational grid.

5.1. NOS Modeling Perspective

From the NOS perspective, the proper representation of the astronomic tide over a lunar month (29.53 days) is the primary focus. However, since the astronomic tide forcing will be used in the long term simulations, it is also important from the EPA perspective to insure that tidal elevations and currents are representative over the lunar month. In order to validate the hydrodynamic model a simulation of the astronomic tide from 1 - 30 September 1988 was performed in August 1990. Wind and water level residuals were set to zero, however, river flows were considered. Initial salinity and temperature conditions were developed as outlined in Chapter 4 of Volume 1 (Schmalz, 1994a). The model was run in prognostic mode and density effects were dynamically included. This simulation provided the basis for the development of a model-based tidal elevation and near-surface current atlas. Such an atlas is intended to
improve on the previous Long Island Sound tidal current atlas, which was based on observational data alone. The development of a model-based atlas is outlined in Wei (1993).

5.2. EPA Modeling Perspective

Since the ultimate EPA objective is to describe pollutant transport and their interactions, the hydrodynamics is assessed on its ability to simulate observed salinity and temperature fields over time periods of constituent interaction scales (yearly). Short term (storm) events are of less interest. It is the long term seasonal cycles of salinity and temperature that are of major concern. If the hydrodynamic model can reproduce the observed salinity and temperature behavior over an entire year, then the computed residual circulation should be representative and the associated water quality modeling physically relevant. To simulate the salinity and temperature as accurately as possible, it is necesary to include meteorologicalin addition to astronomical tide forcing terms. These meteorological terms consist of wind, freshwater inflows, and water level residual forcings. By adding the water lever residual to the astronomical tide, the total observed water level signal is obtained. In performing this addition, care was taken to insure that the appropriate harmonic constant set and water lever residual were used. Since severe dissolved oxygen problems have occurred in western Long Island Sound, the ability of the hydrodynamic model to accurately simulate nontidal transports between the East River and the western Sound is deemed to be a second major concern.

Initial Simulations

To apply the hydrodynamic model for water quality studies, several modifications were made to the model as it was configured for the astronomic tide simulation. The grid in western Long Island Sound was modified to include additional areas in the western embayments in order to more closely represent the total storage volume. Additional astronomic tide simulations indicated that by including the western embayments rms deviations between simulated and reconstructed water levels were approximately 1 - 2 cm larger than in the previous water level comparisons. These increased deviations were considered to be insignificant for water quality computations. Using the mean sea level as the model datum, the first eighteen month simulation was performed in May 1991 and is designated as the NOS 5/91 eighteen month simulation. Subsequent eighteen month simulation are designated by using this same month/year of performance convention. Although Wei (1992) confirmed the validity of the boundary condition approach using seasonal timescales, in the NOS 5/91 simulation surface salinity in the western Long Island Sound was systematically 1 psu larger than observations during the spring and summer periods of 1988 and 1989, thereby underestimating the along thalweg salinity gradient.

To improve the simulated salinity in the western Sound, additional freshwater inflows (five New York streams, six sewage treatment plants (STPs) in the East River and seventeen combined sewer overflows (CSOs)) were included as well as the Harlem River, which was represented by seven grid cells with cell widths tapered from 2032 m at the confluence with the East River to 150 m at Spuyten Duyvil, NY (Schmalz, 1992). An additional astronomic tide simulation revealed that the incorporation of the Harlem River did not significantly alter tidal amplitude and phase relationships in either the East River or western Long Island Sound. The horizontal diffusivity, k_H , given in Equation (2.13) in Volume 1 (Schmalz, 1994a) was multiplied by a factor of five in the East River, thus increasing the horizontal viscosity and diffusivity to account for shoreline boundary layer effects. In addition, upwind differencing of the horizontal advection terms in the salinity and temperature equations was used in the Harlem and State of Connecticut rivers in order to minimize negative salinities associated with central differencing in regions of large gradients. While salinity results were improved significantly using these modifications in the next eighteen month simulation (NOS 9/91), the simulated nontidal fluxes (369 - 1081 m^3/s) at Throgs Neck, NY, were substantially larger than the previous values of order 300 m^3/s. In addition, within the East River section of the grid, the vertical transports averaged over the $2M_2$ tidal periods, exhibited cell to cell upwelling and downwelling making duplication of the NOS hydrodynamic model salinity computations by the EPA water quality model difficult.

In order to further advance the hydrodynamic modeling, several additional steps were undertaken for the next run (NOS 4/92). Upon further investigation, EPA decided that the $2M_2$ tidal cycle averaging scheme was not appropriate in regions of large gradients in topography. All quantities were therefore averaged over a one hour period. This resulted in an order of 25 increase in data to be transferred from the NOS hydrodynamic model to the EPA water quality model. For the complete eighteen month period, approximately 3.2 gigabytes of information was required to be

transferred. In order to ensure for the most efficient transfer, the IEEE 32 bit binary format was utilized directly instead of ASCII data coding schemes.

The vertical datum used in the model was changed from mean sea level to the 1988 North American Vertical Datum, NAVD (1988), instead of the 1929 National Geodetic Vertical Datum, NGVD (1929) to utilize the most recent vertical control information. The geometry of the Harlem River was modified to more closely reflect the true prototype conditions in the vicinity of the East River confluence. In the revised eighteen month simulation (NOS 4/92) simulated salinities were not significantly altered in western Long Island Sound; i.e., the longitudinal salinity gradient was maintained. Nontidal fluxes in the Harlem River were significantly reduced to order 30 m^3/s, which are more in line with estimated values. The nontidal fluxes at Throgs Neck, NY, were reduced from order 800 m^3/s to 100 m^3/s. In order to improve the agreement in temperature, spatial interpolation of surface temperature data was performed more frequently than monthly intervals during the summer months in the eighteen month simulation NOS 8/92.

East River Nontidal Flux Targets

Since ADCP measurements were made at only one point in the cross-section at Throgs Neck, NY, and also in the South Clason/North College Point, NY, section, it was felt that, as noted in Section 4, considerable uncertainties in the resulting volume flux estimates through the East River would exist. Uncertainties exist in assigning areas of flow uniformity, in assigning bin numbers to distance above bottom, and in determining cross-sectional areas. Since the NOS hydrodynamic model grid is only one cell wide and the grid is folded in the East River, EPA developed a ten vertical level, fine horizontal resolution hydrodynamic model in the East River. This fine resolution model was calibrated to the vertical mean profile of the North College Point and South Clason ADCP velocity measurements during the period May - August 1989. Nontidal fluxes at each section for each of the ten levels were computed by summing over the cells in each section. At Throgs Neck, NY, the summation was performed over six grid cells. Based on the sigma level thicknesses in each model, EPA model levels 1,2,9,and 10 were matched to NOS model levels 1,2,6, and 7, respectively, while EPA model levels 3 plus 4 , 5 plus 6, and 7 plus 8 were assigned to NOS model levels 3,4,and 5, respectively. Using this assignment, hourly time series of cross-section fluxes were computed from the EPA simulation and provided target fluxes for the NOAA/NOS hydrodynamic model. Upper layer and lower layer fluxes at Throgs Neck, NY, were computed as the sum of levels 1-2 and 3-7, respectively. Hourly nontidal flux variances at the Throgs Neck, NY, section in a prescribed inverse frequency band (discussed below) were determined by using the recursive Martin filter with 30 weights as discussed by McClain and Walden (1979). The frequency response of the Martin filter with 30 weights was sufficient and equivalent to the frequency response of the cosine Lanczos filter with 60 weights. Using the Martin filter with 30 weights instead of the more traditional cosine Lanczos filter with 60 weights allowed an additional 60 hours of fluxes to be considered. The EPA cell fluxes were computed at each of the above seven levels using the described assignments and then adjusted to NOS level thickness. The series were then summed and then the filtered variance of the sum was computed. Finally, the variance was scaled to the NOS cell width at Throgs Neck, NY.

Using this procedure, the results from the NOS simulation could be directly (without any further manipulation) compared to these targets.

The EPA fine resolution East River model computed monthly averaged values of the volume flux at Throgs Neck, NY, when summed over: a) surface layer, b) bottom layer, and, c) water column are given in Table 5.1 along with the total monthly averaged values of volume fluxes at the South Clason/North College Point, NY, section and The Battery, NY, section. The objective was for the NOS model to match these EPA fine resolution East River model nontidal fluxes to within $\pm$ 100 m^3/s. These conditions were to be satisfied for each month during the four month period May - August 1989 for which ADCP data are available. In addition, at the Throgs Neck, NY, section, the square root of the variance of hourly volume fluxes per unit depth in the inverse frequency band from 34 to 120 hours, through NOS model level 2 near the middle of the eastward flowing upper layer and through NOS model level 6 near the middle of the westward flowing lower layer should agree with the EPA fine resolution East River model values shown in Table 4.1 to within 50%. Note that NOS model levels 3,4,and 5 are twice as thick as EPA model levels 1,2,6, and 7. Thus the variances in Table 5.1 per unit depth decrease from top to bottom in the water column as one might expect. The inverse frequency band 34 - 120 hours was selected based on the boundary condition sampling interval and calibration period duration. It was felt that the models could not be expected to represent fluctuations with periods greater than 5 days in duration due to the salinity and temperature boundary condition sampling interval of order 15 days.

Table 5.1. EPA Fine Resolution Model Target Nontidal Fluxes. Targets for monthly-averaged volumetric flowrates (m^3/s). Note: "-" means toward New York Harbor.

	May	June	July	August
		Throgs Neck Cross Section		
Total	-282	-380	-262	-324
Upper	241	228	209	121
Lower	-522	-609	-471	-444
		N. College to S. Clason Cross Section		
Total	-273	-373	-255	-318
		The Battery Cross Section		
Total	-353	-440	-336	-385

Targets for the square root of variance at Throgs Neck, NY, for May-August 1989 in NOS model layers. (EPA variance adjusted by ratio of layer depths and channel widths: NOS/EPA)

NOS Level	1	2	3	4	5	6	7
EPA	83	59	98	82	69	30	24

Target Simulations

All simulations used a one month spin-up and were run over the five month period April - August 1989. The EPA fine resolution East River model salinity and temperature time series and water surface elevations were used at The Battery, NY, and Spuyten Duyvil, NY. The EPA fine resoultion East River model used the average of the water levels at The Battery, NY, over the period 10 April - 31 August, 1989. This average was then subtracted from the water surface elevation time series at The Battery, NY, Spuyten Duyvil, NY, and Willets Point, NY. Then the following offsets (0.0 cm, 6.0 cm, and 3.6 cm) were applied to The Battery, NY, Spuyten Duyvil, NY, and Willets Point, NY, respectively. In the NOS hydrodynamic model, NAVD (1988) was used as the model datum and offsets to mean sea level with respect to this datum were applied. The offsets applied at The Battery, NY, and Spuyten Duyvil, NY, were 0.0 cm and -0.4 cm, respectively. In this manner, equivalent water surface elevations were used at these two western boundary locations. The mean sea level offset relative to NAVD (1988) was adjusted from 2.5 - 7.2 cm at the Block Island Sound open boundary. The salinity at the Block Island Sound open boundary was increased from 30 to 31 psu on day 1 for months July - October 1989. Two different geometries for the East and Harlem River System were considered. The initial "L" shaped geometry was utilized as well as a revised geometry to more closely match the EPA fine resolution grid in surface area and volume. The "L" shape was not changed in the revised geometry. Two freshwater inflow (STP and CSO) sets were used. The set initially developed was revised to correspond to the inputs used in the EPA fine resolution East River model.

The initial set of target simulations is summarized in Table 5.2 in terms of a measure of each simulation's success in meeting the East River nontidal flux targets. Note that there is a total of 20 flux targets (total fluxes at Throgs Neck, North College/South Clason, and The Battery, NY, and upper and lower layer fluxes at Throgs Neck, NY, for each of the four months). There are two variance targets relative to the entire four month period for NOS model layers 2 and 6. The final simulation set results are evaluated in Table 5.3. Simulation 6a successfully met all the East River nontidal flux targets as shown in Table 5.4. In general, the variances are similar in both models, with the NOS model in general showing greater variability, especially in the surface level. Of interest is to compare the difference in water levels (η), top (S_1) and bottom salinities (S_7 or S_{10}), and top (T_1) and bottom temperatures (T_7 or T_{10}) between The Battery, NY, and Throgs Neck, NY, at opposite ends of the East River. These differences are given in Table 5.5 for the ten level EPA fine resolution East River model and in Table 5.6 for simulation 6a using the seven level NOS model. In comparing these tables, it should be noted that in Table 5.5, the differences for salinity and temperature are for prescribed inflow conditions only, while in Table 5.6 both inflow and outflow conditions are averaged. In the case of salinity, one would expect the salinity in most cases to be higher northeast of The Battery, NY, than at the boundary itself. Since on outflow, these higher salinities would be felt at The Battery, NY, the NOS monthly averages, which contain the outflow conditions, should be higher than the EPA fine resolution model values. This is true during most months with July 1989 being an exception. During this month, it is possible that the Harlem River salinity was such as to lower The Battery, NY,

Table 5.2. Summary of Initial Set of Target Simulations

Note: All simulations (except 1) were run over the period April - August 1989. A one month spin-up period was used.
D corresponds to the elevation offset relative to NAVD (1988) used at Block Island Sound open boundary.
S corresponds to the salinity on 1 July 1989 imposed along the Block Island Sound open boundary.

Simulation	Description	Flux Targets Not Met Out of 20	Variance Targets Not Met Out of 2
1	NOS 4/92 18-month simulation, D=0.0 cm, original CSO and geometry S=30.0 psu	18	1
2	D=5.2 cm, original CSO S=31.0 psu	1	1
3	D=5.7 cm, revised geometry S=31.0 psu	7	1
4	D=7.2 cm, original CSO and geometry, s=31.0 psu	2	1
5	D=6.9 cm, original CSO and geometry, s=31.0 psu	2	1
6	D=6.7 cm, original CSO and geometry, s=31.0 psu	1	1
7	D=5.7 cm, original CSO and new geometry with two cells revised, s=31.0 psu	3	1

Table 5.3. Summary of Final Set of Target Simulations

Note: All simulations were run over the period April - August 1989. A one month spin-up period was used.
D corresponds to the elevation offset relative to NAVD (1988) used at Block Island Sound open boundary.
S corresponds to the salinity on 1 July 1989 imposed along the Block Island Sound open boundary.

Simulation	Description	Flux Targets Not Met Out of 20	Variance Targets Not Met Out of 2
2	D=5.2 cm, original CSO S=31.0 psu	1	1
6	D=6.7 cm, original CSO S=31.0 psu	1	1
6a	D=6.7 cm, revised CSO S=30.0 psu	0	0
6b	D=6.7 cm, revised CSO S=31.0 psu	1	1

Table 5.4. Comparison of NOS Run 6a with EPA Flux Targets

Monthly-averaged volumetric flowrates (m^3/s) with targets. Note: "-" means toward New York Harbor. Difference is NOS minus EPA.

	Source	May	June	July	August
		Throgs Neck Cross Section (3,5)			
Total	NOS	-279	-386	-351	-344
	Diff.	3	-6	-89	-20
Upper	NOS	332	228	191	63
	Diff.	91	0	-18	-58
Lower	NOS	-611	-614	-542	-407
	Diff.	-89	-5	-71	37
		N. College to S. Clason Cross Section (7,2)			
Total	NOS	-287	-393	-353	-352
	Diff.	-14	-20	-98	-34
		The Battery Cross Section (16,2)			
Total	NOS	-341	-441	-396	-401
	Diff.	12	-1	-60	-16

Square root of variance at Throgs Neck, NY, (3,5) for May-August 1989 in NOS model layers. % Diff = 100 ¦ NOS - EPA ¦/EPA (EPA variance adjusted by ratio of layer depths and channel widths: NOS/EPA)

NOS Layer	1	2	3	4	5	6	7
NOS	165	86	78	69	49	22	18
% Diff.	---	46	--	--	--	27	-

Table 5.5. EPA Hydrodynamic Model (η,S,T) Monthly Averages: May - August 1989

Note 1 and 10 denote top and bottom.

The Battery, NY					
Month	η (m)	S_1 (psu)	S_{10} (psu)	T_1 (°C)	T_{10} (°C)
May	0.002	11.4	19.1	14.7	13.2
June	0.026	12.8	22.1	19.8	18.3
July	0.004	18.1	23.3	22.7	21.4
August	0.038	19.8	24.9	23.4	22.5
Willets Point, NY					
Month	η (m)	S_1 (psu)	S_{10} (psu)	T_1 (°C)	T_{10} (°C)
May	0.021	23.5	25.5	12.6	10.8
June	0.060	24.0	25.0	16.5	14.7
July	0.036	23.8	24.8	20.2	18.8
August	0.086	24.5	25.5	21.4	20.0
Difference between Willets Point, NY, and The Battery, NY					
Month	η (m)	S_1 (psu)	S_{10} (psu)	T_1 (°C)	T_{10} (°C)
May	0.019	12.1	6.4	-2.1	-2.4
June	0.034	11.2	2.9	-3.3	-3.6
July	0.032	5.7	1.5	-2.5	-2.6
August	0.048	4.7	0.6	-2.0	-2.5

Table 5.6. NOS Run 6a (η,S,T) Monthly Averages: May - August 1989

Note 1 and 10 denote top and bottom.

The Battery, NY					
Month	η (m)	S_1 (psu)	S_7 (psu)	T_1 (°C)	T_7 (°C)
May	-.052	12.6	19.2	14.1	13.0
June	-.032	13.5	20.9	20.0	18.0
July	-.054	17.1	22.2	23.0	21.0
August	-.020	20.4	24.0	23.1	22.2
Willets Point, NY					
Month	η (m)	S_1 (psu)	S_7 (psu)	T_1 (°C)	T_7 (°C)
May	-.019	22.0	24.0	13.1	12.0
June	0.022	22.8	24.6	17.8	17.0
July	0.007	23.6	24.8	20.6	20.0
August	0.050	24.3	24.9	22.1	21.7
Difference between Willets Point, NY, and The Battery, NY					
Month	η (m)	S_1 (psu)	S_7 (psu)	T_1 (°C)	T_7 (°C)
May	0.033	9.4	4.8	-1.0	-1.0
June	0.054	9.3	3.7	-2.2	-1.0
July	0.061	6.5	2.6	-2.4	-1.0
August	0.070	3.9	0.9	-1.0	-0.5

salinity values on outflow. In the case of temperature, similar arguments cannot in general be made because of the relative uniformity in spatial gradients at both the surface and bottom in the vicinity of The Battery, NY. Due to the different datums employed in the two models, 58 mm should be added to the NOS water levels at The Battery, NY, to obtain the EPA prescribed water levels at this location. Note the difference in water levels at The Battery, NY, and Willets Point, NY, does not depend on the datum employed. The discrepancy in the two models in monthly averaged water surface elevation differences between these two locations ranges from 17 - 29 mm.

Final Eighteen Month Simulations

After meeting the above targets, the three final eighteen month simulations (NOS 5/93, NOS 6/93 and NOS 6/93R) were performed. Each simulation was performed on the National Institute of Standards and Technology (NIST) CRAY YMP-2/216 in 9 two-month segments. The EPA provided total nontidal flux estimates at The Battery, NY, Spuyten Duyvil, NY, and Throgs Neck, NY, for the corresponding eighteen month period based upon a simulation using their fine resolution East River model. In addition, upper and lower layer nontidal flux estimates were provided by EPA at Throgs Neck, NY. The objective was to compare NOS hydrodynamic East River nontidal flux estimates with those provided by EPA in order to determine if the models was still in reasonable agreement with the previous nontidal flux targets. In addition, for salinity and temperature, the first nine months (April - December 1988) were considered as a calibration period, while the second nine months (January - September 1989) were used as an independent verification period. Characteristics of each of the three NOS eighteen month simulations are presented initially, followed by salinity, temperature, and nontidal flux comparisons.

For the NOS 5/93 simulation, the most recent CSO flows used in the EPA fine scale East River model were employed in the original East and Harlem River geometry. A 6.7 cm offset to mean sea level relative to NAVD (1988) was used at the Block Island Sound open boundary along with the salinity boundary conditions of target simulation 6a. Montauk Point water level residuals were used along the Block Island Sound open boundary during the period April - September 1988, while Montauk water level residuals were used for the following 12 months. Salinity, temperature, and water surface elevation time series at The Battery, NY, and Spuyten Duyvil, NY, equivalent to those used in the EPA fine scale East River model were used.

For the NOS 6/93 simulation, the following several modifications to the NOS 5/93 simulation were made. Montauk water level residuals were used in place of Montauk Point water level residuals during the April - September 1988 period in order to improve the correspondence in nontidal fluxes at Throgs Neck, NY, between the two models. Surface salinities at the Block Island Sound open boundary were lowered from 32 psu to 31 psu at day 1 of September 1988 through May 1989 in order to improve model and CTD data salinity agreement. The 1 August 1988 temperature boundary condition along the Block Island Sound open boundary was adjusted by increasing the sea surface temperature by 2 °C to 19.3 °C and decreasing the stratification from 8 °C to 4 °C in order to improve the model and CTD data temperature agreement in Block Island Sound.

The NOS 6/93R simulation was restarted from the NOS 6/93 simulation after 10 months on February 1, 1989. Surface salinities at the Block Island Sound open boundary were lowered from 32 psu to 31 psu on March 1, 1989 only. Surface salinities on April 1 and May 1, 1989 were kept at 32 psu. These modifications insured that the Block Island Sound open boundary salinity conditions corresponded exactly to the April 1 - September 1, 1989 period used in the target simulations. In addition, this simulation allowed the sensitivity of the nontidal fluxes at Throgs Neck, NY, to changes in salinity on the Block Island Sound open boundary to be assessed.

In order to assess the salinity and temperature response, each SUNY CTD cast was edited and quality controlled by Professor Emeritus D.W. Pritchard. While UCONN CTD casts were not as thoroughly considered, all casts were edited and reviewed at NOS in consultation with Pritchard. Downcast data for 227 CTD casts were used in the model versus data comparisons. Error tolerances were estimated by Pritchard to be ($\pm$ 0.05 psu, $\pm$ 0.05 °C) and ($\pm$ 0.1 psu, $\pm$ 0.05 °C) for SUNY and UCONN data, respectively. At each CTD depth for each simulation, a model value is computed based on linear interpolation and the squared difference determined. An rms difference between the observed CTD and model profile is computed as the square root of the mean of the sum of these differences at each CTD depth. The complete simulated vertical model profiles are compared with observed CTD profiles for each of these simulations at master stations A2, B3, D3, F3, H6, I2, and M3 in Tables 5.7 and 5.8 for salinity and temperature, respectively. The stations as listed above progress from west to east. Stations A2 and B3 are in the western Sound, D3, F3, and H6 are in the central Sound, and I2 and M3, lie in the eastern Sound. Sound wide averages are computed by considering all stations and weighting the station averages by the number of observations at each station. Results are also shown for the NOS 4/92 simulation, which employed no offset to mean sea level relative to NAVD (1988). By increasing the water level at the Block Island Sound open ocean boundary, the higher open ocean boundary salinity tends to intrude from the eastern to the western Sound. Therefore, for NOS 5/93, NOS 6/93, and NOS 6/93R, rms differences are larger by 0.2 psu over the entire Sound during the first nine months. During the second nine months, for NOS 5/93, in the central Sound rms differences were order 0.5 psu larger, while in the western Sound rms differences were 0.8 psu larger than obtained for NOS 4/92. The magnitude of these differences caused some concern. However, by lowering the salinity along the Block Island Sound open boundary, the rms differences during the last nine months were reduced by approximately 0.5 psu from 0.8 psu to 0.3 psu. Rms temperature differences given in Table 5.8, were order 0.8 °C for each of the three simulations (NOS 5/93, NOS 6/93, and NOS 6/93R) and represent an improvement of order 0.2 - 0.3 °C from results obtained in NOS 4/92. This improvement was due to the incorporation of additional surface temperature fields during the summer months as forcing.

In order to compare the stratification, the following index is developed.

$$S.I. = |(|(S_o^s - S_o^b)| - |(S_m^s - S_m^b)|)| \qquad (5.1)$$

where ,

$S.I.$ $\equiv$ Stratification Index ,

S_o^s $\equiv$ Observed surface salinity or temperature ,

S_m^s $\equiv$ Model surface salinity or temperature ,

S_o^b $\equiv$ Observed bottom salinity or temperature , and

S_m^b $\equiv$ Model bottom salinity or temperature .

Table 5.7. Average RMS Salinity Differences between NOS 18-month Model Simulations and Data. Note number of observations in parenthesis following station.

April-December 1988

Station	NOS 4/92 Salinity Difference (PSU)	NOS 5/93 Salinity Difference (PSU)	NOS 6/93,6/93R Salinity Difference (PSU)
A2 (22)	0.67	0.83	0.70
B3 (20)	0.45	0.50	0.43
D3 (19)	0.34	0.45	0.40
F3 (20)	0.31	0.44	0.39
H6 (16)	0.34	0.60	0.56
I2 (10)	0.36	0.75	0.59
M3 (14)	0.55	0.54	0.73
WT. AVE.	0.44	0.58	0.53

January-September 1989

Station	NOS 4/92 Salinity Difference (PSU)	NOS 5/93 Salinity Difference (PSU)	NOS 6/93, 6/93R Salinity Difference (PSU)
A2 (15)	0.68	1.45	0.97, 1.09
B3 (15)	0.58	1.26	0.80, 0.93
D3 (15)	0.51	1.15	0.70, 0.81
F3 (14)	0.49	0.99	0.54, 0.64
H6 (16)	0.54	1.06	0.55, 0.72
I2 (16)	0.46	0.95	0.45, 0.62
M3 (15)	0.76	0.71	0.69, 0.80
WT. AVE.	0.57	1.08	0.67, 0.80

Table 5.8. Average RMS Temperature Differences between NOS 18-month Model Simulations and Data. Note number of observations in parenthesis following station.

April - September 1988

Station	NOS 4/92 Temperature Difference (°C)	NOS 5/93 Temperature Difference (°C)	NOS 6/93,6/93R Temperature Difference (°C)
A2 (22)	0.77	0.57	0.69
B3 (20)	1.42	1.09	1.06
D3 (19)	1.41	0.91	0.75
F3 (20)	1.25	0.91	0.57
H6 (16)	1.08	0.82	0.67
I2 (10)	1.06	0.70	0.65
M3 (14)	1.02	0.68	0.58
WT. AVE.	1.15	0.82	0.72

January - September 1989

Station	NOS 4/92 Temperature Difference (°C)	NOS 5/93 Temperature Difference (°C)	NOS 6/93,6/93R Temperature Difference (°C)
A2 (15)	1.05	0.78	0.85, 0.76
B3 (15)	1.15	0.87	1.25, 0.82
D3 (15)	1.20	0.86	0.92, 0.86
F3 (14)	1.44	1.07	0.96, 1.05
H6 (16)	1.20	0.79	0.57, 0.75
I2 (16)	0.97	0.51	0.35, 0.49
M3 (15)	0.71	0.53	0.31, 0.52
WT. AVE.	1.09	0.78	0.74, 0.74

Table 5.9. Average Salinity Stratification Index
Note number of observations in parenthesis following station.

April - December 1988

Station	NOS 4/92 Salinity Index	NOS 5/93 Salinity Index	NOS 6/93,6/93R Salinity Salinity Index
A2 (22)	0.69	0.65	0.60
B3 (20)	0.37	0.29	0.31
D3 (19)	0.43	0.34	0.34
F3 (20)	0.44	0.32	0.27
H6 (16)	0.39	0.36	0.37
I2 (10)	0.34	0.33	0.36
M3 (14)	0.47	0.37	0.42
WT. AVE.	0.46	0.46	0.39

January - September 1989

Station	NOS 4/92 Salinity Index	NOS 5/93 Salinity Index	NOS 6/93,6/93R Salinity Index
A2 (15)	0.70	0.69	0.74, 0.74
B3 (15)	0.49	0.52	0.57, 0.53
D3 (15)	0.64	0.47	0.46, 0.46
F3 (14)	0.90	0.69	0.72, 0.66
H6 (16)	0.75	0.53	0.49, 0.53
I2 (16)	0.58	0.69	0.61, 0.66
M3 (15)	0.44	0.53	0.51, 0.55
WT. AVE.	0.64	0.59	0.58, 0.59

Table 5.10. Average Temperature Stratification Index
Note number of observations in parenthesis following station.

April - December 1988

Station	NOS 4/92 Temperature Index	NOS 5/93 Temperature Index	NOS 6/93,6/93R Temperature Index
A2 (22)	1.04	0.69	0.69
B3 (20)	2.00	1.20	1.06
D3 (19)	1.37	0.81	0.75
F3 (20)	1.51	0.63	0.57
H6 (16)	1.11	0.70	0.67
I2 (10)	0.98	0.71	0.65
M3 (14)	1.08	0.94	0.58
WT. AVE.	1.34	0.82	0.72

January - September 1989

Station	NOS 4/92 Temperature Index	NOS 5/93 Temperature Index	NOS 6/93,6/93R Temperature Index
A2 (15)	0.70	0.90	0.85, 0.83
B3 (15)	1.45	1.28	1.25, 1.22
D3 (15)	1.33	0.93	0.92, 0.94
F3 (14)	1.27	0.97	0.96, 0.93
H6 (16)	0.87	0.56	0.57, 0.53
I2 (16)	0.88	0.34	0.35, 0.28
M3 (15)	0.40	0.33	0.31, 0.34
WT. AVE.	0.98	0.75	0.74, 0.72

Stratification at the master stations is given in Tables 5.9 and 5.10 for salinity and temperature, respectively. In the case of salinity, the stratification index remains nearly constant at 0.4 - 0.5psu during the first nine months, and at 0.6 psu during the second nine months for all simulations. For temperature, due to the improved temporal surface forcing, the stratification index is 0.7 -0.8 °C in NOS 5/93, NOS 6/93, and NOS 6/93R, which represents a reduction of 0.2 °C from the index exhibited by NOS 4/92. With respect to salinity, the rms difference between model and observation and stratification index are approximately 0.6 psu and 0.5 psu, respectively for NOS 6/93. For temperature, the corresponding values are order 0.7 °C.

Nontidal fluxes as averaged over the complete eighteen month period are given in Table 5.11 for the EPA fine resolution East River model and for each of the three NOS eighteen month simulations. Agreement in total nontidal at Throgs Neck, NY, is order 20 m^3/s, while agreement at The Battery, NY, and Spuyten Duyvil, NY, are order 40 m^3/s. At Throgs Neck, NY, both the upper and lower layer nontidal fluxes for each of the three NOS simulations correspond to the EPA fine resolution East River model to order 30 m^3/s, which is equal to the order of the agreement in the total nontidal fluxes. The monthly compliances for each of the three NOS simulations with the nontidal fluxes estimated from the EPA fine resolution East River model are summarized in Table 5.12. In each of the three NOS simulations, as shown in Table 5.13, in six of the eighteen months, the difference in average total nontidal flux at Throgs Neck, NY, computed by the two models is larger than 100 m^3/s. The difference in either the monthly averaged upper or lower layer nontidal fluxes computed by the two models is larger than 100 m^3/s in either ten or eleven of the eighteen months as may be seen from Table 5.13. If we focus on the four month EPA fine resolution East River model calibration period (May - August 1989), all three NOS simulations meet the EPA total nontidal flux targets at Throgs Neck, NY, North College Point, NY, and The Battery, NY, for all four target period months. All three NOS simulations meet the upper and lower layer flux targets at Throgs Neck, NY, for all months with the exception of May 1989, only. The variance target in the lower layer for the inverse frequency period 34 -120 hours is met by all three NOS simulations. The upper layer variance target for the inverse frequency period 34 -120 hours is met by the NOS 5/93 simulation and exceeded by 1% in the NOS 6/93 and by 4% in the NOS 6/93R simulations, respectively.

In order to determine the skill of each of the three NOS simulations, the following skill assessment factors were considered: 1) monthly compliance with the EPA total nontidal flux estimates at Throgs Neck, NY, 2) monthly compliance with the EPA upper and lower layer nontidal flux estimates at Throgs Neck, NY, 3) calibration and verification period rms salinity differences between simulations and all vertical profiles, 4) calibration and verification period salinity stratification index based on all vertical profiles, 5) calibration and verification period rms temperature differences between simulations and all vertical profiles, and 6) calibration and verification period temperature stratification index based on all vertical profiles. The skill assessment approach consisted of a straight ranking of each simulation with respect to each factor. This approach attempted to develop an objective procedure for selecting the most appropriate simulation for input to water quality modeling. A rank of from 1 - 3 was assigned for each of the above six factors as exhibited (for nontidal fluxes in Table 5.13, for rms

Table 5.11. Average Nontidal Fluxes April 1988 - September 1989

Source	East River[1] Throgs Neck, NY (m3/s) Total (m^3/s)	Upper (m^3/s)	Lower (m^3/s)
EPA	-310	259	-568
NOS 5/93	-351	206	-557
NOS 6/93	-295	237	-532
NOS 6/93R	-297	238	-535

Source	East River[2] The Battery, NY (m^3/s)	Harlem River[3] Spuyten Duyvil, NY (m^3/s)
EPA	310	34
NOS 5/93	404	-1
NOS 6/93	353	-7
NOS 6/93R	355	-7

Note:

1 Plus direction from East River into Western Long Island Sound
2 Plus direction from East River into New York Harbor
3 Plus direction from Harlem River into Hudson River

Table 5.12. NOS Eighteen Month Simulations Compliance with EPA Nontidal Flux Estimates April 1988 - September 1989

Simulation	Flux Estimates Not Met Out of 18	Flux Distribution Estimates Not Met Out of 18
NOS 5/93	6	11
NOS 6/93	6	10
NOS 6/93 R	6	10

Table 5.13. Nontidal Flux Analysis at Throgs Neck, NY
Plus direction from East River into Western Long Island Sound

Month/Source	Total	Upper	Lower
April 1988/			
EPA	-278	227	-505
NOS 5/93	-511	12	-523
NOS 6/93	-385	72	-457
May 1988/			
EPA	-235	149	-384
NOS 5/93	-501	55	-556
NOS 6/93	-407	113	-519
June 1988/			
EPA	-268	176	-444
NOS 5/93	-452	63	-514
NOS 6/93	-249	201	-450
July 1988/			
EPA	-299	135	-435
NOS 5/93	-401	228	-629
NOS 6/93	-251	310	-561
August 1988/			
EPA	-328	153	-481
NOS 5/93	-292	331	-623
NOS 6/93	-172	430	-602
September 1988/			
EPA	-266	187	-452
NOS 5/93	-411	94	-504
NOS 6/93	-228	221	-449
October 1988			
EPA	-254	298	-551
NOS 5/93	-237	274	-511
NOS 6/93	-206	303	-509
November 1988/			
EPA	-367	375	-742
NOS 5/93	-268	427	-696
NOS 6/93	-239	450	-689
December 1988/			
EPA	-314	465	-780
NOS 5/93	-233	368	-601
NOS 6/93	-210	383	-592

Table 5.13.(Continued) Nontidal Flux Analysis at Throgs Neck, NY
Plus direction from East River into Western Long Island Sound

Month/Source	Total	Upper	Lower
January 1989/			
EPA	-370	373	-743
NOS 5/93	-244	274	-518
NOS 6/93	-222	296	-518
February 1989/			
EPA	-343	402	-745
NOS 5/93	-340	133	-473
NOS 6/93, NOS 6/93R	-318 -318	134 134	-452 -452
March 1989/			
EPA	-399	286	-684
NOS 5/93	-495	49	-544
NOS 6/93, NOS 6/93R	-472 -495	55 51	-528 -546
April 1989/			
EPA	-369	260	-629
NOS 5/93	-360	237	-597
NOS 6/93, NOS 6/93R	-339 -371	235 203	-574 -574
May 1989/			
EPA	-286	234	-520
NOS 5/93	-249	427	-676
NOS 6/93, NOS 6/93R	-249 -253	400 411	-649 -664
June 1989/			
EPA	-378	233	-611
NOS 5/93	-369	273	-642
NOS 6/93, NOS 6/93R	-382 -372	245 266	-627 -638
July 1989/			
EPA	-251	213	-464
NOS 5/93	-338	215	-553
NOS 6/93, NOS 6/93R	-347 -341	206 213	-553 -554
August 1989/			
EPA	-315	121	-436
NOS 5/93	-337	87	-424
NOS 6/93, NOS 6/93R	-342 -339	65 82	-406 -421
September 1989/			
EPA	-257	366	-623
NOS 5/93	-287	160	-447
NOS 6/93, NOS 6/93R	-291 -288	152 155	-443 -444

differences in Tables 5.7 and 5.8, and for stratification indicies in Tables 5.9 and 5.10) in eachof the three NOS simulations. A rank of 1 corresponded to the superior measure. For a given factor, if the simulations were judged to tie, then the total of the two ranks was divided equally between the simulations. Results are presented in Table 5.14, in which the lowest score represents the best simulation. Note the ranks across each row in Table 5.14 sum to six and the sum of all total scores equals thirty six. The difference between the score obtained for the NOS 6/93 and the NOS 6/93R eighteen month simulations was only one point, with this point being

Table 5.14. NOS 18-month Simulation Skill Assessment Results

Note: Lowest score represents best skill.

Factor	NOS 5/93	NOS 6/93	NOS 6/93R
Total Flux	3	1.5	1.5
Flux Distr.	2	2	2
RMS Salinity	3	1	2
RMS Temperature	3	1.5	1.5
S.I. Salinity	3	1.5	1.5
S.I. Temperature	3	1.5	1.5
TOTAL SCORE	17	9	10

decided by the rms salinity rank. The net Sound wide difference in the weighted average rms salinity from Table 5.7 was 0.13 psu. All three simulation residual circulation results were provided to EPA for use in water quality studies as described by Schmalz (1994b). In Section 6, for the eighteen month simulation, NOS 6/93, the simulated salinity and temperature time series are reviewed and compared to observed vertical profiles at the master stations. In addition, residual current model-data comparisons at NOS ADCP stations are investigated.

6. MODEL VALIDATION

In this section, details of the hydrodynamic model validation are presented from two perspectives. Initially the NOS perspective involving an astronomic tide plus density simulation is presented. From the EPA perspective, a complete intercomparison of the NOS 6/93 eighteen month simulation with observational data is discussed. The model grid shown in Figure 6.1 is used in Long Island and Block Island Sounds in both simulations. The Harlem River [cells (10,3) - (10,8)] is not included in the astronomic tide simulation.

6.1. Astronomic Tide Plus Density Simulation: September 1988

In order to validate the tidal component of the hydrodynamic model, a simulation of the astronomic tide from 1 - 30 September 1988 was performed using a 300 second internal mode and 30 second external mode time step or 10:1 mode split. The model was run in prognostic mode and density effects were dynamically included. Water levels were reconstructed at The Battery, NY, and along the open boundary in Block Island Sound as shown in Table 6.1. Harmonic constituents for each of the tidal constituents used in this reconstruction are given in Table 6.2. Average daily streamflows were input for the five major State of Connecticut rivers (Norwalk River, Mill and Quinnipiac Rivers, Housatonic River, Connecticut River, and Thames Rivers). Average daily streamflows were less than 10,500 cfs on the Connecticut River for all but the first eight days. Sewage treatment plant, combined sewer overflows, and New York State streams were not considered. Water level residuals and wind magnitudes were set to zero. A spatially uniform bottom roughness, z_o = 1 cm was employed except within the Connecticut rivers, wherein z_o = 4 cm was used.

Table 6.1. Water Surface Elevation Open Boundary Specification

Boundary Description	Type	Grid Location	Astronomic Tide Station	Residual Tide Station
The Battery, NY	S	(16,2)	851-8750	851-8750
Montauk Pt., NY	I	(83-92,20)	851-0321,845-9449	851-0560
Block Island South, RI	S	(92,19-23)	845-9449	851-0560
Block Island North, RI	S	(97,29-36)	845-5083	851-0560
Spuyten Duyvil, NY	S	(10,9)	851-8903	851-8750

S = Astronomic tide specified using tidal signal in column 4
I = Astronomic tide interpolated as a linear function of distance using column 4 signals 851-0321 and 845-9449

Table 6.2. Harmonic Constants for Water Surface Elevation Stations at Open Boundaries

	The Battery, NY 851-8750		Montauk Pt, NY 851-0321		Spuyten Duyvil, NY 851-8903	
Const	Ampl. (ft)	Phase (κ' °)	Ampl. (ft)	Phase (κ' °)	Ampl. (ft)	Phase (κ' °)
M_2	2.167	237.60	1.212	216.60	1.764	261.10
S_2	.450	258.20	.265	233.30	.340	281.50
N_2	.483	221.50	.267	204.90	.378	241.50
K_1	.331	106.50	.257	90.40	.268	117.10
M_4	.048	335.40	.052	188.20	.062	333.70
O_1	.175	110.90	.118	131.60	.130	129.70
M_6	.095	93.20	.051	118.80	.079	115.30
MK_3	.000	.00	.000	.00	.000	.00
S_4	.037	77.70	.005	323.60	.015	103.30
MN_4	.000	.00	.000	.00	.000	.00
ν_2	.102	214.90	.052	206.50	.073	244.10
S_6	.000	.00	.005	60.90	.000	.00
μ_2	.065	246.60	.000	.00	.000	.00
$2N_2$	.064	205.50	.036	193.20	.050	221.80
OO_1	.000	.00	.005	49.20	.006	104.50
λ_2	.039	243.50	.008	224.30	.012	270.60
S_1	.043	62.20	.000	.00	.000	.00
M_1	.012	108.70	.008	111.00	.009	123.40
J_1	.013	104.30	.009	70.00	.010	110.80
Mm	.000	.00	.000	.00	.000	.00
Ssa	.067	27.40	.000	.00	.067	27.40
Sa	.271	133.80	.000	.00	.271	133.80
MSf	.000	.00	.000	.00	.000	.00
Mf	.000	.00	.000	.00	.000	.00
ρ_1	.000	.00	.004	149.30	.005	135.20
Q_1	.042	123.50	.023	152.00	.025	135.90
T_2	.027	258.40	.016	232.60	.020	281.70
R_2	.000	.00	.002	233.90	.003	281.20
$2Q_1$	.000	.00	.003	172.40	.003	142.30
P_1	.107	109.40	.085	93.50	.089	117.50
$2SM_2$	.000	.00	.000	.00	.000	.00
M_3	.000	.00	.000	.00	.000	.00
L_2	.081	241.10	.038	199.50	.049	280.80
$2MK_3$	.000	.00	.000	.00	.000	.00
K_2	.131	259.70	.072	234.60	.092	281.00
M_8	.000	.00	.002	123.20	.012	203.10
MS_4	.055	308.60	.000	.00	.000	.00

Table 6.2. (Cont.) Harmonic Constants for Water Surface Elevation Stations at Open Boundaries

	Vail Beach, RI 845-9449		Pt Judith, RI 845-5083	
Const	Ampl. (ft)	Phase (κ' °)	Ampl. (ft)	Phase (κ' °)
M_2	1.451	215.80	1.495	220.10
S_2	.304	232.40	.302	237.30
N_2	.368	203.00	.336	209.00
K_1	.256	86.20	.225	85.50
M_4	.066	90.10	.094	89.60
O_1	.123	129.70	.135	118.20
M_6	.051	115.70	.034	96.40
MK_3	.000	.00	.000	.00
S_4	.003	92.70	.001	345.80
MN_4	.000	.00	.000	.00
ν_2	.071	204.80	.065	210.55
S_6	.001	245.30	.004	235.50
μ_2	.035	195.90	.036	199.80
$2N_2$	.049	190.30	.045	197.90
OO_1	.005	42.60	.006	52.90
λ_2	.010	223.50	.010	228.10
S_1	.000	.00	.000	.00
M_1	.009	107.90	.010	101.80
J_1	.010	64.40	.011	69.20
Mm	.000	.00	.000	.00
Ssa	.000	.00	.000	.00
Sa	.000	.00	.000	.00
MSf	.000	.00	.000	.00
Mf	.000	.00	.000	.00
ρ_1	.005	148.40	.005	132.20
Q_1	.024	151.50	.026	134.50
T_2	.018	232.70	.018	237.50
R_2	.002	232.20	.002	237.10
$2Q_1$	.003	173.20	.004	150.80
P_1	.085	86.60	.075	85.90
$2SM_2$	.000	.00	.000	.00
M_3	.000	.00	.000	.00
L_2	.041	228.60	.042	231.20
$2MK_3$	.000	.00	.000	.00
K_2	.083	232.00	.082	236.90
M_8	.005	51.30	.011	118.10
MS_4	.000	.00	.000	.00

Water Surface Elevation Comparisons

Simulated water levels are compared in Table 6.3 with reconstructed water levels at 15 stations as shown in Figure 6.2 as summarized in terms of root mean square (rms) difference over the complete simulation period. Since the model requires approximately one tidal cycle (12.5 hours) to spin up, agreement between model predicted levels and reconstructed levels is closer than indicated in Table 6.3. Agreement over the entire Sound is on the order of 10 cm. In considering the comparisons, it is instructive to note that the model predicted level is computed at the center of 2032 m square computational cell, whereas water levels are measured at a single location. Note in Table 6.3, The Battery, NY and Pt. Judith, RI are on the grid boundary and the simulated and reconstructed water levels should in theory exactly match. In practice due to slight differences in the methods used to compute the series and to roundoff errors, the differences are not exactly zero. The agreement in the eastern Sound is order 5 cm except at Plum Island, NY. This may be due to the use of a more consistent model and observation harmonic constituent set. Bridgeport, CT and New London, CT are the only internal tide stations for which the observed time series is sufficient in length to determine the long period constituents. These long term constituents were not included at the other stations and not used for tidal forcing along the Block Island Sound open ocean boundary. In constrast, at The Battery, NY, the long term constituents were included in the tidal forcing and are not included in the majority of western Sound tide stations. Simulated water levels were computed with respect to mean sea level (assumed spatially invariant) and tide gage water level series were reconstructed from the harmonic constants directly without the specification of a mean component.

Table 6.3. September 1988 Astronomical Tide Simulation Water Level vs Reconstructed Tide

	Comparison Summary	
Station	Sta. ID	RMS Difference (cm)
The Battery, NY	851-8750	3
Willets Point, NY	851-6990	11
Rye Beach, NY	851-8091	11
Bridgeport, CT	846-7150	11
Cedar Beach, NY	851-4422	10
Madison Beach, CT	846-4041	12
Northville, NY	851-2987	10
New London, CT	846-1490	5
Montauk, NY	851-0560	6
Plum Island, NY	851-1236	11
Fisher Island, NY	851-0719	5
Three Mile Hbr, NY	851-1171	8
Montauk Pt, NY	851-0321	7
Vail Beach, RI	845-9449	6
Pt. Judith, RI	845-5083	1

Current Comparisons

Simulated horizontal current component time series are compared with reconstructed currents for the ADCP stations shown in Figure 6.3. The current station time series were reconstructed directly from the harmonic constants with no mean component specified. Harmonically analyzed ADCP station bin depths are converted to corresponding model sigma levels as shown in Table 6.4. Sigma level 5 is used in order to avoid near surface and near bottom reflection interference in the observations. The ratio of the rms difference between simulated and reconstructed currents (cms) and the average reconstructed current range (cms) is presented by component in Table 6.5. Simulated horizontal currents at level 5 agree to within 20% of the reconstructed ranges in the (u,v) components. While additional grid resolution is warranted in regions of topographic variability, the overall tidal characteristics of Long Island Sound have been successfully simulated as further confirmed via harmonic analyses as shown by Wei (1993). Note differences between the average cell depth and the station depths indicated in Table 6.4.

Table 6.4. ADCP Station Comparison Summary

ADCP Station	Depth (m - MSL) Grid Cell	Harmonically Analysed Sigma Levels		Model Level Range
1	1	77	(-.26, -.5, -.74)	3-5
4	34	16	(-.62, -.85)	5-6
8	42	39	(-.33, -.81)	3-6
9	39	36	(-.29, -.55)	3-4
11	56	30	(-.42, -.85)	4-6
12	86	63	(-.38, -.85)	3-6
13	81	46	(-.41, -.85)	4-6
14	27	21	(-.17, -.54, -.83)	2-6
15	38	35	(-.26, -.53, -.87)	3-6
16	30	32	(-.25, -.58, -.85)	3-6
17	40	44	(-.23, -.55, -.88)	3-6
20	26	10	(-.33, -.83)	4-6
22	17	12	(-.26, -.56, -.85)	3-6

Since changes in topography occur over space scales less than 2 km in the vicinity of The Race (Stations 11,12, and 13) and in western Long Island Sound (Stations 1 and 4), it is to be expected that model predicted currents may not correspond to the reconstructed current values as closely as in regions of milder topographic variability. In order to obtain reconstructed levels at required model sigma levels, linear interpolation in sigma was performed. If this was not possible near the surface, the nearest data level was extrapolated. The no flow data value (0,0) at $\sigma = -1$ was added to the measurement vertical profile. As a result, for sigma levels near the

Table 6.5. September 1988 Astronomical Tide Simulation Horizontal Current versus Reconstructed Current Level 5 Comparison Summary

ADCP	RMS Diff/Recstr. Range U (cms)	RMS Diff/Recstr. Range V (cms)	Harmonic Analysis Length (Days)
1	+ 13.3 / 10	+ 21. / 80	29
4	+ 6.2 / 30	+ 13.7 / 40	29
8	+ 10. / 90	+ 5.2 / 5	29
9	+ 9.5 / 40	+ 2.6 / 5	29
11	- 42.6 / 150	21.5 /100	29
12	+ 33.3 / 100	+ 46. / 60	29
13	- 21.6 / 206	19.2 /100	29
14	41.3 /100	5.2 / 15	29
15	+ 10.4 / 80	+ 7.6 / 12	29
17	+ 17.6 / 75	8.4 / 10	15
20	9.7 /110	10.7 / 60	29
22	+ 10.9 /100	9.2 / 20	29

+/- Model signal stronger/weaker than reconstructed current

bottom, a linear sigma interpolation was used as opposed to the logarithmic law of the wall profile. The selection of model level 5 (σ = -0.6) is used to minimize interpolation error. Except at the stations noted above, predicted current components are within approximately 10-20 percent of reconstructed levels.

Table 6.6. September 1988 Astronomical Tide Simulation Salinity and Temperature versus CTD Data Comparison

Station	Julian Date (1988)	RMS Salinity Difference (PSU)	RMS Temperature Difference (°C)
A1	270.46	2.29	1.28
A2	270.44	0.47	1.50
F3	272.32	0.75	2.01
H6	272.48	1.50	1.47
J3	252.59	0.76	1.26
K3	251.59	1.14	0.66
M5	251.39	0.44	0.33
RMS AVE		1.05	1.22

Point Salinity and Temperature Comparisons

Predicted salinity and temperature at stations shown in Figure 6.4 are compared with observed digitized CTD profiles in terms of rms difference as shown in Table 6.6. In computing the rms difference, linear interpolation of the model predicted results to the corresponding sigma level of the data was performed. If interpolation was not possible, nearest model level values were used. In general, average rms differences, are on the order of 1 psu and 1.2 °C for salinity and temperature, respectively. These areal averages are based on a single digitized CTD cast over the one month period at each station.

6.2. Eighteen Month Complete Forcing Calibration and Verification: April 1988 - September 1989

Based on the criteria discussed in the previous chapter, the NOS 6/93 eighteen month simulation was selected for further evaluation and analysis. Detailed salinity and temperature point comparisions are initially considered for the nine month calibration (April - December 1988) and verification (January - September 1989) periods, respectively. Characteristics of salinity and temperature fields are compared with observational patterns analyzed in Chapter 3. Residual circulation comparisons are next considered at ADCP locations. A classification of the gyral structure of the simulated monthly near surface residual circulation is next developed. Finally, the sensitivity of the East River nontidal fluxes to vertical datum and mean sea level offset is presented.

Point Salinity Comparisons

Simulated near surface and near bottom time series over the calibration period April - September 1988 are compared with observed CTD profiles in Figures 6.5 - 6.10 at stations A2, B3, D3, H6, I2, and M3, respectively. Station locations progress from western to eastern Long Island Sound as noted in Figure 6.4. Each horizontal axis tick corresponds to a Julian Day. Each "x" in the time series plots corresponds to the value of the observed CTD cast. At each CTD depth a model value is computed based on linear interpolation and the squared difference determined. An rms difference between the observed CTD and model profile is computed as the square root of the mean of the sum of these differences at each CTD depth. In order to compare the stratification, the following two measures are used.

$$STR.D = (S_o^s - S_o^b) \tag{6.1a}$$

$$STR.M = (S_m^s - S_m^b) \tag{6.1b}$$

where ,

$STR.D$ ≡ Data Stratification Measure ,
$STR.M$ ≡ Model Stratification Measure ,
S_o^s ≡ Observed surface salinity or temperature ,
S_m^s ≡ Model surface salinity or temperature ,
S_o^b ≡ Observed bottom salinity or temperature , and
S_m^b ≡ Model bottom salinity or temperature .

Calibration period simulated versus observed vertical profiles are compared for stations A2, B3, H6, and M3 in the initial panels in Figures A.1 - A.4, respectively, in Appendix A. CTD data versus model profile comparisons for this same period are summarized in the upper half of Tables A.1 - A.8 at master stations A2, B3, D3, F3, H6, I2, J2, and M3, respectively, in Appendix A. Date time and depth of the CTD cast are given in columns 2 - 4. Of interest is to investigate the uniformity of the cast depths, to insure that measurements were made at approximately the same location each time. For the most part, cast depths are nearly equal. Rms error, surface data, surface model, bottom data, bottom model values are given in columns 5 - 9, respectively. The two stratification measures are given in columns 10 and 11. In studying these tables, we locate in column 9, the time of maximum salinity stratification in the data and note the corresponding model stratification given in column 10. The difference in stratification between model and observation may be found by subtraction.

Simulated near surface and near bottom time series over the verification period January - September 1989 are compared with observed CTD profiles in Figures 6.11 - 6.16 at stations A2, B3, D3, H6, I2, and M3, respectively. The verification period model versus observed CTD profiles are compared at stations A2, B3, H6, and M3 in the end panels of Figures A.1 - A.4, respectively, in Appendix A. Observed CTD measurements versus model profile comparisons are summarized in the lower half of Tables A.1 - A.8 at stations A2, B3, D3, F3, H6, I2, J2, and M3, respectively, in Appendix A. In order to assess the model's ability in representing maximum stratification at master stations, compute the difference between model and data at times of maximum stratification in the data and assemble the differences in Table 6.7 below. In general, peak stratification coincides with spring runoff and is larger in 1989 than in 1988. At most stations, the maximum stratification is underpredicted by the model by order 0.5 psu in 1988 and 1.0 psu in 1989. Stratification is represented by the model better in the Central Sound (Stations D3, F3, and H6), than in either the western Sound (Stations A2 and B3) or the eastern Sound (Stations I2 and M3). In general, the magnitude of the rms differences between observed and computed salinity profiles are of the same order for the calibration and verification periods at stations A2 (0.70, 0.97) , at H6 (0.56, 0.55), and at M3 (0.73, 0.69) in western, central, and eastern Long Island Sound, respectively. For the Chapter 5 stratification index, the comparisons between periods at station A2 (0.60, 0.74), at station H6 (0.37, 0.49), and at station M3 (0.42, 0.51) are all of the same order. In general, the longitudinal salinity gradients both at the surface and near bottom of the Sound are well represented in the model, thus insuring a reasonable representation of the density flow component due to salinity changes.

Salinity Field Comparisons

Initially, four monthly averaged simulated near surface, 2 meter depth, and near bottom, 2 meter above, spatial patterns are shown in Figure 6.17 for July 1988, in Figure 6.18 for January 1989, in Figure 6.19 for March 1989, and in Figure 6.20 for July 1989. The characteristic "C" shape of the near surface isohalines is well represented by the model. Of interest is to note the much larger stratification in western and central Long Island Sound in July 1989 than in July 1988. This is due to the significantly larger freshwater spring inflows that occurred in 1989 relative

to 1988. Stratification for January and March 1989 is of the same order as July 1988. These fields serve to demonstrate the model's ability to evolve the freshwater inflows and represent the longitudinal and north-south salinity gradients.

Next, simulated near surface and near bottom spatial patterns are compared with observation derived fields for the specific periods April 4 - 7, 1988, June 13 - 16, 1988, and August 2 - 4, 1988, which have been previously discussed in Chapter 3. Observed near surface fields are shown in Figure 6.21 with the corresponding model fields depicted in Figure 6.22. Near bottom fields are shown in Figure 6.23 and in Figure 6.24 for observations and simulation, respectively. Observation contours for surface salinity during June 13-16 in Block Island Sound cannot be adequately resolved relative to the spatial gradients in the observations. However, station spatial density in Long Island Sound is sufficient to resolve major circulation features.

During April 4 - 7, the location of the surface salinity 26.0 psu contour is very similar for both the observations and model. In addition, the structure of the Connecticut River surface plume is well represented. The location of the simulated bottom salinity 27.0 psu contour corresponds closely to observations. The location of the simulated bottom salinity 29.0 psu contour is further west by 5 seconds of longitude in the model than in the observations. The "C "shape is visible in both model and observation contours in eastern Long Island Sound in the bottom salinity fields.

During June 13 - 16, the extent of the Connecticut River plume indicated in the surface simulation field is in close agreement with the observations. While the location of the surface salinity 27.0 psu contour is further west in the model than in the observations, the difference in the simulated and observed fields is within 0.5 psu. In the near bottom fields, the location of the 28.0 psu contour in the simulation corresponds very closely to the location of the 27.0 psu contour in the observations. The location of the intersection of the 30.0 psu contour with the Connecticut shoreline is almost the same in both the model and observations. However, the influence of the Connecticut River is more closely confined to the Connecticut shoreline in the observations than that shown in the simulation.

During August 2 - 4, the extent of the Connecticut River plume indicated in the simulation agrees very well with that indicated in the observations. The location of the 27.5 psu contour in the observations relative to the position of the same contour line in the simulation, indicates the simulated near surface salinity fields in western Long Island Sound are slightly saltier by order 0.5 psu than observed. In the near bottom fields, the locations of both the 28.5 psu and 30.0 psu contour lines are very close in the simulation and observations. In the simulated field a tongue of 29.5 - 30.0 psu water extends into the central Sound. While this tongue is not evident in the observations, the difference between simulated and observed salinities in the central Sound is less than 0.5 psu.

Point Temperature Comparisons

Simulated near surface and near bottom time series over the calibration period April - September 1988 are compared with observed CTD profiles in Figures 6.25 - 6.30 at stations A2, B3, D3, H6, I2, and M3, respectively. As for salinity, each horizontal axis tick corresponds to a Julian Day and each "x" in the time series plots corresponds to the value of the observed CTD cast. The complete model versus CTD profiles are compared for stations A2, B3, H6, and M3 in the initial panels of Figures B.1 - B.4, respectively, in Appendix B. An rms difference between the observed CTD and model profile is computed as previously for salinity. In order to compare the stratification, the same two measures previously developed above are used.

Calibration period CTD versus model profile comparisons are summarized in first half of Tables B.1 - B.13 at stations A1, A2, B3, D3, F3, H6, I2, J2, J3, K3, L1, M3, and M5, respectively, in Appendix B. Date time and depth of the CTD cast are given in columns 2 - 4. Rms error, surface data, surface model, bottom data, bottom model values are given in columns 5 - 9, respectively. The two stratification indices are given in columns 10 and 11. Simulated near surface and near bottom time series over the verification period January - September 1989 are compared with observed CTD profiles in Figures 4.31 - 4.36 at stations A2, B3, D3, H6, I2, and M3, respectively. The verification period model versus CTD profiles are compared at stations A2, B3, H6, and M3 in end panels of Figures B.1 - B.4, respectively, in Appendix B.

CTD versus model profile comparisons during this period are summarized in the lower half of Tables B.1 - B.8 at stations A2, B3, D3, F3, H6, I2, J2, and M3, respectively, in Appendix B. Employ the same approach used for salinity, in order to assess the ability of the model to represent maximum thermal stratification. The results given in Table 6.8 indicate that the stratification in 1988 is represented to order 1 °C in the central and western Sound in 1988. In 1989 the representation of the peak stratification is only within order 2 °C in these same regions. In 1988, the peak thermal stratification occurs during mid-summer in early August, while in 1989, it occurs in late May and is associated with the beginning of the summer season. In Table 6.9, the maximum stratification in sigma-t is considered. It is interesting to note in 1988, the times of maximum density stratification coincide with the times of peak thermal rather than salinity stratification in most of Long Island Sound. In 1989, the times of peak salinity, temperature, and density stratification are coincident in late May early June. In general, the magnitude of the rms differences between observed and computed temperature profiles are of the same order for the calibration and verification periods at stations A2 (0.69, 0.85) , at H6 (0.67, 0.57), and at M3 (0.58, 0.31) in western, central, and eastern Long Island Sound, respectively. For the stratification index of Chapter 5, the comparisons between periods are at station A2 (0.69, 0.85), at station H6 (0.67, 0.57), and at station M3 (0.58, 0.31) all of the same order. In general, the longitudinal temperature gradients both at the surface and near bottom of the Sound are well represented in the model, thus insuring a reasonable representation of the density flow component due to temperature changes.

Table 6.7. Maximum Observed Salinity Stratification (psu): Data (D) versus Model (M) Comparisons

	Calibration Period				Verification Period			
Station	1988 Date	D	M	D-M	1989 Date	D	M	D-M
A2	5/25	2.24	1.69	0.55	5/23	2.78	4.40	-1.62
B3	5/25	1.47	0.65	0.82	5/23	2.75	1.45	1.30
D3	6/28	1.38	1.12	0.26	5/23	3.20	1.93	1.27
F3	6/28	1.53	1.10	0.43	5/23	2.93	2.06	0.87
H6	6/29	2.28	1.75	0.53	5/23	3.72	2.81	0.91
I2	8/4	1.26	0.62	0.64	7/17	2.26	1.11	1.15
M3	4/6	2.59	2.06	0.53	5/8	4.20	6.16	-1.96

Table 6.8. Maximum Observed Temperature Stratification (°C): Data (D) versus Model (M) Comparisons

	Calibration Period				Verification Period			
Station	1988 Date	D	M	D-M	1989 Date	D	M	D-M
A2	8/15	2.87	2.46	0.41	5/23	2.79	0.77	2.02
B3	8/3	7.53	6.38	1.15	6/6	5.43	2.81	2.62
D3	8/3	5.34	4.65	0.69	5/23	7.00	4.10	2.90
F3	8/4	6.41	6.35	0.06	5/23	7.69	4.87	2.82
H6	8/2	6.89	5.94	0.95	6/20	6.02	4.31	1.71
I2	8/4	5.51	2.93	2.58	5/22	3.79	4.16	-0.37
M3	7/26	1.99	2.28	-0.29	8/7	1.54	1.54	0.00

Table 6.9. Maximum Observed Sigma-t Stratification (kg/m^3): Data (D) versus Model (M) Comparisons

	Calibration Period				Verification Period			
Station	1988 Date	D	M	D-M	1989 Date	D	M	D-M
A2	5/25	2.28	1.34	0.94	5/23	2.64	3.52	-0.88
B3	8/3	2.71	2.48	0.23	5/23	3.06	1.53	1.53
D3	8/3	2.15	1.58	0.57	5/23	3.74	2.31	1.43
F3	8/4	2.75	2.25	0.50	5/23	3.63	2.53	1.10
H6	8/2	3.03	2.41	0.62	5/23	3.87	3.05	0.82
I2	8/4	2.47	1.28	1.19	7/5	2.35	0.89	1.46
M3	4/6	2.05	1.73	0.32	5/8	3.34	4.98	-1.64

Temperature Field Comparisons

Initially, monthly averaged simulated near surface (2 meter depth) and near bottom (2 meter above bottom) spatial patterns are shown in Figure 6.37 for July 1988, in Figure 6.38 for January 1989, in Figure 6.39 for March 1989, and in Figure 6.40 for July 1989. Note the concentration of the contour lines in the bottom waters near the shorelines in July 1988 and 1989. During the fall-winter, the longitudinal and lateral temperature gradients are reduced.

Next, simulated near surface and near bottom spatial patterns are compared with observation derived fields for the specific periods April 4 - 7, 1988, June 13 - 16, 1988, and August 2 - 4, 1988, which have been previously discussed in Chapter 3. Surface observational fields are shown in Figure 6.41 with the corresponding model fields depicted in Figure 6.42. Bottom fields are shown in Figure 6.43 based on observations and in Figure 6.44 for the simulation, respectively.Observation contours for bottom temperature during June 13 - 16 in Block Island Sound cannot be adequately resolved relative to the spatial gradients in the observations. However, station spatial density in Long Island Sound is sufficient to resolve major circulation features. It should be noted that surface temperature is specified in the simulation based on bilinear interpolation in non-overlapping grid patches as outlined in Volume 1. Due to the nature of the interpolation procedure and the number of grid patches used in the interpolation, the simulated surface fields will in general be smoothed and not depict local features. However, the areal extent of waters between the 0.5 °C contours should correspond to observations.

During April 4 - 7, the location of the surface waters between 5.5 and 6.0 °C in the central Sound in the simulation, appears to be in general agreement with the observations. In addition the overall longitudinal gradient within Long Island Sound is well represented. The location of the simulated bottom cold water pool (less than 4.0 °C) in the central Sound is very similar to the observations.

During June 13 - 16, the fine scale, near surface, thermal gyres indicated in the observations are smoothed in the simulation due to the interpolation. However, the simulated longitudinal gradient (12.5 - 18.0 °C) is in close agreement with the observations. Simulated and observed bottom temperature structures are in close agreement. Note the crowding of the contour lines in both the simulated and observed fields in the near shore region off Northport in the western Sound. Also of interest is to observe, the correspondence of the simulation 14.5 °C contour line in the central Sound to the same contour line based on observations.

During August 2 - 4, the extent of the simulated 25.0 °C pool in the central Sound is similar to that indicated in the observations along the Long Island Sound shoreline. Observe a region of colder water, perhaps due to the Connecticut River plume, is indicated in the observations which is not shown in the simulation. Note in eastern Long Island Sound, the regions of the thermal front (20.5 - 25.0 °C) in the simulation and (19.5 - 25.0 °C) in the observations match very well. In the near bottom fields, the locations of both 19.5 °C contour lines in eastern and western Long Island Sound are very close in the simulation and observations. Due to data availability and the contouring procedure, the observed bottom temperature field in Block Island Sound cannot be accurately portrayed.

Residual Circulation Comparisons

Consider the residual circulation to be composed of the following components: 1) astronomic tide interaction with bottom topography, 2) density circulation induced from fresh water sources, 3) local wind (winds over Long Island and Block Island Sounds), and 4) non-local shelf wind (represented by water level residual forcings applied at The Battery, NY, Spuyten Duyvil, NY, and the Block Island Sound open boundary).

Monthly averaged simulated residual current, which in general contains all the above components, is determined in the following manner.

$$(u_k^E, v_k^E) = \left(\left\langle \frac{\langle u_k h \rangle_1}{\langle h \rangle_1} \right\rangle_2 , \left\langle \frac{\langle v_k h \rangle_1}{\langle h \rangle_1} \right\rangle_2 \right) \tag{6.2}$$

where,

(u_k^E, v_k^E) ≡ (East, North) Level k monthly averaged Eulerian residual velocity components,
(u_k, v_k) ≡ (East, North) Level k internal mode velocity components,
$(\Delta\sigma_k, \Delta x, \Delta y)$ ≡ Vertical and (East, North) grid spacings,
h ≡ Internal mode water depth,
$\langle\ \rangle_1$ ≡ Hourly average operator, and
$\langle\ \rangle_2$ ≡ Monthly average of all $\langle\ \rangle_1$ operations.

The NOS 6/93 simulated residual velocity components and standard deviations are compared with measured residual currents and their standard deviations as determined in Chapter 3 in Tables C.1 - C.11 for ADCP Stations 1, 4, 6, 8, 9, 11, 12, 13, 20, 21, and 22, respectively, in Appendix C. In general, the simulated residual currents are in reasonable agreement with the observations except for the v-component in The Race (Stations 11, 12, and 13), where the simulated currents are much stronger than the observations. In this region of large spatial gradients in topography, model resolution may be inadequate.

To estimate the astronomic tide and density components, a simulation was performed for April 1988 using the NAVD (1988) vertical datum and with water level residuals and local winds set to zero (Schmalz, 1993b). Estimated near surface and near bottom residual circulation fields are shown for astronomic tide and density in Figure 6.45. Note the presence of a pair of cyclonic gyres in the central (horizontal indicies 30 - 50) and western (horizontal indicies 20 - 30) Long Island Sound. Additional simulations for April 1988 using the NGVD (1929) and mean sea level datums, did not alter these circulation patterns (Schmalz, 1993a). Simulations in which wind effects were included indicated that the structure of the near surface gyres is very sensitive to local wind forcings. In order to further investigate the effect of the local wind on gyral structures, monthly vector averaged winds were computed (as given in Table 6.10) and the near surface flow patterns for each of the eighteen months were studied. The following initial gyral structure classification was developed:

Present = Similar to astronomic tide and density case
Absent = No gyres identified
Pinched = Central basin gyre pinched in spatial extent to the east-northeast
Reduced = Central basin and western basin gyres reduced in spatial extent
Split = Central basin gyre split into two smaller gyres with significant north-south flow in between

As suggested from Table 6.10, winds with a west to east component tend to either eliminate or significantly reduce the spatial extent of the central basin gyre. Winds with a east to west component tend to pinch the central basin gyre. In order to further illustrate some of the surface gyral structures in more detail, monthly averaged residual circulation spatial patterns near the surface (2 m depth) and near the bottom (2 m above) are shown in Figure 6.46 for July 1988, in Figure 6.47 for January 1989, in Figure 6.48 for March 1989, and in Figure 6.49 for July 1989. The figures are scaled such that all current vectors greater in magnitude than the legend value are represented by a dot at the center of the grid cell. Of particular interest, is the central

Table 6.10. Near Surface Gyral Structures in Monthly Averaged Eulerian Residual Circulation

Month	Year	Gyral Structure Classification	Wind Speed (kts)	Wind Direction (° M)
April	1988	Split	1.8	-37.4
May		Present	1.1	79.4
June		Absent	1.9	-78.0
July		Absent	2.1	-159.5
August		Absent	2.8	-144.1
Sept		Split	2.3	-84.0
Oct		Pinched	2.9	-89.5
Nov		Absent	3.4	-97.8
Dec	1988	Absent	5.1	-74.4
Jan	1989	Pinched	3.3	-72.3
Feb		Absent	3.1	-46.8
Mar		Pinched	1.5	16.4
April		Reduced	2.2	-58.8
May		Reduced	0.9	-175.5
June		Pinched	0.8	25.3
July		Reduced	0.4	-84.5
August		Absent	1.2	-49.1
Sept	1989	Pinched	0.5	78.7

basin circulation between horizontal indices 20 - 50. In the surface residual circulation, the large counter-clockwise gyre is absent in July 1988. In January 1989 and March 1989 the gyre appears pinched to the west and in July 1989 with reduced spatial extent. Localized surface eddies appear to be generated at the headland along the Long Island shoreline at horizontal index 28. The prevailing simulated monthly averaged surface circulation is from west to east, while the prevailing simulated monthly averaged near bottom circulation is in the opposite direction. This is in agreement with the generalized estuarine circulation. However, wind effects may reverse this pattern on short time scales. Note by monthly averaging both residual circulation and winds, there exists the possibility of masking significant variability on shorter time scales. In studying the hourly wind pattern for April 1988, there seems to exists a 2 to 3 day variability. In addition, sea breeze effects warrant further investigation.

Analysis of Nontidal fluxes in the East and Harlem Rivers

Since the nontidal fluxes in the East and Harlem Rivers are sensitive to the absolute water level differences over the Sound and these differences are determined in large measure by the vertical datum employed, further consideration of these datums is warranted. The Mean Sea Level (MSL) datum is determined by considering the tidal epoch (1960-1978) local mean sea levels at long term tide stations to form a equipotential surface or constitute a vertical datum over Long Island Sound, Block Island Sound, and the East and Harlem River system. The National

Table 6.11 Long Island Sound Tidal Datums

Station	MSL-NAVD (m)	MSL Determination	NGVD - NAVD (m)
851-8750 The Battery, NY	-.1233	1960 - 1978 Epoch	-.3363
851-8903 Spuyten Duyvil, NY	-.0588	1960 - 1978 Epoch 1 month compared to The Battery	-.321
851-0560 Montauk, NY	-.1484	1960 - 1978 Epoch	-.2874
845-5083 Point Judith, RI	-.1694	1960 - 1978 Epoch	-.2804

Assume: Vail Beach, RI 845-9449: MSL - NAVD(1988) = -.1589 m
Assume: MSL at Point Judith, RI equal to MSL at Newport, RI

Geodetic Vertical Datum NGVD (1929) was determined by connecting local mean sea levels at

24 locations throughout Canada and the United States to form a equipotential surface. Approximately 100,000 km of leveling was used to construct the 1929 vertical control network. The North American Vertical Datum NAVD (1988) was determined by assuming only the height of the primary tidal benchmark at Father Point, Rimouski, Quebec Canada to be fixed. An additional 625,000 km of leveling has been used to construct the vertical control network. In developing NAVD (1988), Helmert blocking was used to perform a simultaneous least-squares adjustment of the entire set of leveling observations (Zilkoski, 1992). Relationships between these tidal datums in Long Island Sound are shown in Table 6.11 above.

The water surface elevations are specified relative to these model datums at the model boundaries by using the following procedures.

$$h_I(t) = H_0^I + \sum_{j=1}^{37} f_j H_{jI} \cos\left(a_j t + (V_0 + u)_j^G - \kappa'_{jI}\right) \qquad (6.3)$$

where,

$h_I(t)$	≡	predicted elevation at time t for boundary signal I (m),
f_j	≡	node factor for constituent j for the prediction period,
$(V_0 + u)_j^G$	≡	Greenwich equilibrium argument for constituent j for the prediction period (°),
a_j	≡	constituent j speed (°/hr),
H_{jI}	≡	amplitude of constituent j (ft) for boundary signal I,
κ'_{jI}	≡	phase of constituent j (°) for boundary signal I,
t	≡	local Standard Time (hrs) from January 1, 1988, and
H^I_o	≡	mean water level relative to the vertical tide datum plus offset (m).

The above equation is used to reconstruct the predicted water level based upon the set of harmonic constants (H_{jI}, κ'_{jI}) given in Table 6.2.

The total water level for each elevation boundary signal is given by the following relationship.

$$ht_I(t) = h_I(t) + \alpha r_I(t) \qquad (6.4)$$

where,

$ht_I(t)$	≡	Total elevation at time t for boundary signal I,
$h_I(t)$	≡	Predicted elevation at time t for boundary signal I,
α	≡	Switch equal to either zero or one for boundary signal I, and
$r_I(t)$	≡	Residual elevation at time t for boundary signal I.

The following elevation boundary signals are considered: 1) The Battery, NY, 2) Spuyten

The following elevation boundary signals are considered: 1) The Battery, NY, 2) Spuyten Duyvil, NY, 3) Montauk Point, NY, 4) Point Judith, RI, and 5) Vail Beach, RI. Model datum corresponds to NAVD (1988). The total elevation signals are comprised of the following components: 1) MSL - NAVD offset , 2) reconstructed levels from harmonic constants, and 3) residuals. Note the offset at Montauk, NY, is transferred to Montauk Point, NY. The offset at Vail Beach, RI, is assumed equal to 1/2 of the sum of Montauk, NY, and Point Judith, RI, offsets. Residuals at The Battery, NY, are transferred to Spuyten Duyvil, NY. Residuals at Montauk, NY, are transferred to Montauk Point, NY, Point Judith, RI, and Vail Beach, RI.

The simulated monthly non-tidal fluxes in the East and Harlem River system are presented in Table 6.12, and the upper and lower layer fluxes given in Table 6.13 for the NOS 8/92 18-month simulation, which employed the NAVD (1988) with no offsets to mean sea level. The corresponding non-tidal fluxes are given in Table 6.14 and Table 6.15 for the NOS 6/93 eighteen month simulation, which employed a 6.7 cm offset along the Block Island Sound open boundary. In considering the sensitivity of the East River nontidal fluxes to tidal datum and offsets, note the flow area at Throgs Neck, NY, is approximately 17,000 m^2. Therefore 1 cm/s in mean cross-sectional residual velocity strength accounts for a difference of approximately 170 m^3/s.

Table 6.12. NOS 8/92 Simulation: Nontidal Fluxes in the East and Harlem River Systems

Month	Year	East River[1] Throgs Neck (m3/s)	Harlem[2] River (m3/s)	East River[3] BB (m3/s)	Balance (m3/s)
April	1988	-302	1	342	41
May		-165	-18	232	49
June		-245	-2	290	43
July		-66	-19	144	59
August		10	-25	70	55
Sept		-183	-6	240	51
Oct		-26	-21	98	51
Nov		-126	-10	191	55
Dec	1988	-222	0	269	47
Jan	1989	-170	-7	224	47
Feb		-204	-6	257	47
Mar		-232	-13	293	48
April		-188	-11	253	54
May		66	-43	31	54
June		-68	-30	152	54
July		-6	-34	86	46
August		-53	-30	139	56
Sept	1989	80	-46	21	55
AVERAGE:		-117	-18	185	50

NOTE: 1 Plus direction from East River into Western Long Island Sound
2 Plus direction from Harlem River into Hudson River
3 Plus direction from East River into New York Harbor

Table 6.13. NOS 8/92 Simulation: Upper and Lower Layer Nontidal Flux Analysis

Month	Year	East River[1] Throgs Neck (m3/s)		Harlem[2] River (m3/s)		East River[3] BB (m3/s)	
		U	L	U	L	U	L
April	1988	232	-534	-14	15	342	-
May		236	-401	-27	8	232	-
June		255	-499	-16	13	290	-
July		376	-442	-26	7	144	-
August		522	-512	-30	5	70	-
Sept		309	-492	-17	11	240	-
Oct		492	-518	-27	7	98	-
Nov		587	-713	-18	8	191	-
Dec	1988	531	-753	-11	11	269	-
Jan	1989	437	-607	-16	9	224	-
Feb		359	-564	-17	10	257	-
Mar		226	-458	-24	11	293	-
April		490	-678	-19	8	253	-
May		745	-679	-42	0	-42	73
June		541	-610	-33	3	-3	155
July		495	-502	-35	1	86	-
August		337	-390	-31	1	139	-
Sept	1989	390	-310	-46	0	-17	38

NOTE: 1 Plus direction from East River into Western Long Island Sound
2 Plus direction from Harlem River into Hudson River
3 Plus direction from East River into New York Harbor
U = Upper Layer Flow Regime
L = Lower Layer Flow Regime

Table 6.14. NOS 6/93 Simulation: Nontidal Fluxes in the East and Harlem River Systems

Month	Year	East River[1] Throgs Neck (m3/s)	Harlem[2] River (m3/s)	East River[3] BB (m3/s)	Balance (m3/s)
April	1988	-384	-2	433	47
May		-407	5	450	48
June		-249	-8	301	44
July		-251	0	309	58
August		-172	-6	233	55
Sept		-228	-11	290	51
Oct		-206	-14	271	51
Nov		-239	-12	307	56
Dec	1988	-210	-24	280	46
Jan	1989	-222	-21	289	46
Feb		-318	-11	376	47
Mar		-472	4	517	49
April		-339	-7	400	54
May		-249	-11	315	55
June		-382	-2	438	54
July		-347	0	393	46
August		-342	-1	399	56
Sept	1989	-291	-4	350	55
AVERAGE:		-295	-7	353	51

NOTE: 1 Plus direction from East River into Western Long Island Sound
2 Plus direction from Harlem River into Hudson River
3 Plus direction from East River into New York Harbor

Table 6.15. NOS 6/93 Simulation: Upper and Lower Layer Nontidal Flux Analysis

Month	Year	East River[1] Throgs Neck (m3/s)		Harlem[2] River (m3/s)		East River[3] BB (m3/s)	
	U	L	U	L	U	L	
April	1988	72	-457	-10	8	433	-
May		113	-519	-9	14	450	-
June		201	-450	-15	7	301	-
July		310	-561	-13	13	309	-
August		430	-602	-15	9	-12	245
Sept		221	-449	-16	6	290	-
Oct		303	-509	-17	4	271	-
Nov		450	-689	-17	5	-1	308
Dec	1988	383	-592	-24	1	280	-
Jan	1989	296	-518	-21	1	289	-
Feb		134	-452	-14	3	376	-
Mar		55	-527	-7	11	517	-
April		235	-574	-14	7	-2	402
May		400	-649	-19	8	-15	330
June		245	-627	-12	11	438	-
July		206	-553	-10	10	393	-
August		65	-406	-10	10	399	-
Sept	1989	152	-443	-11	7	350	-

NOTE: 1 Plus direction from East River into Western Long Island Sound
2 Plus direction from Harlem River into Hudson River
3 Plus direction from East River into New York Harbor
U = Upper Layer Flow Regime
L = Lower Layer Flow Regime

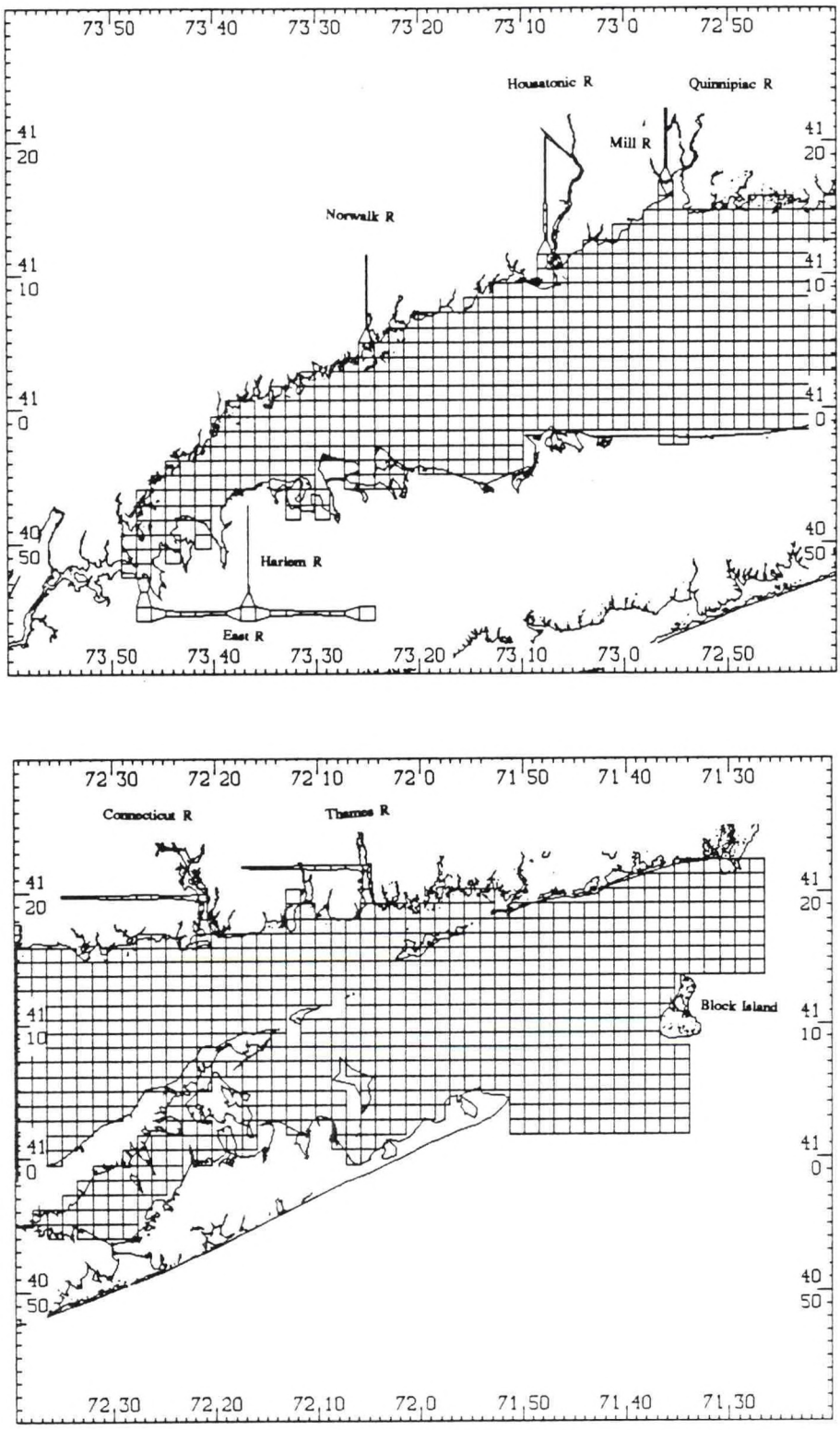

Figure 6.1. Long Island Sound Hydrodynamic Model Grid

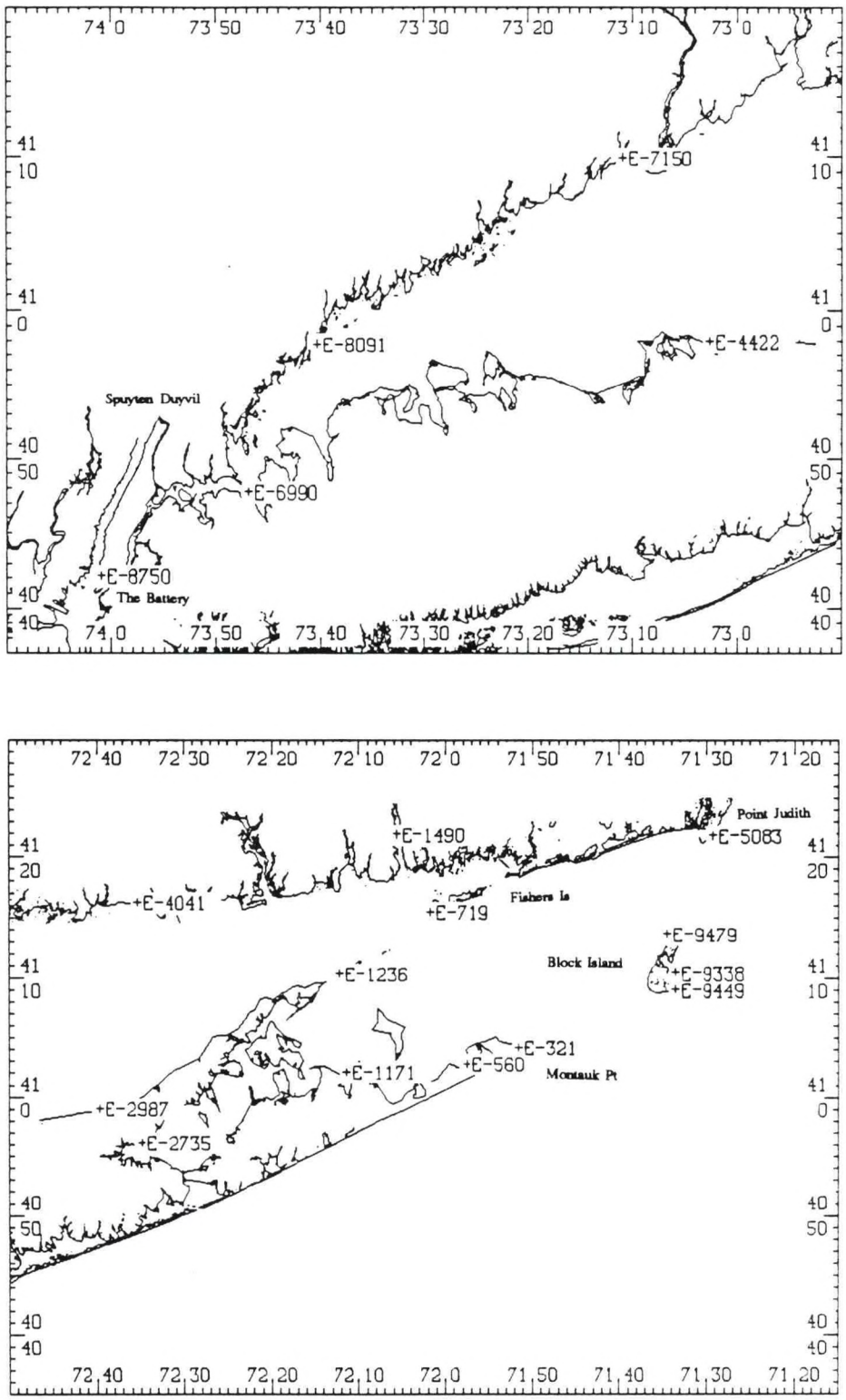

Figure 6.2 Long Island Sound Model Water Surface Elevation Validation Station Locations

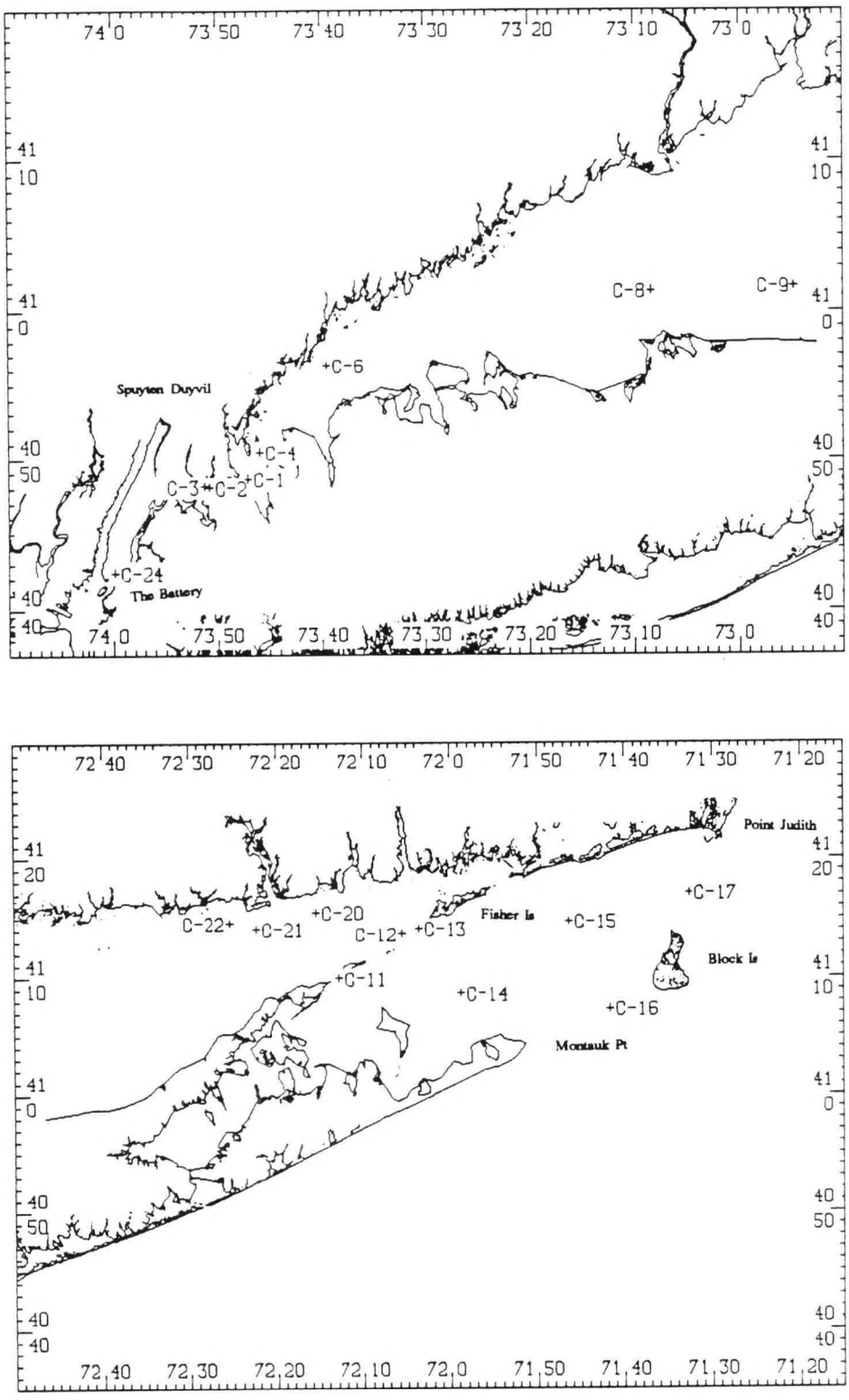

Figure 6.3. Long Island Sound Model ADCP Validation Station Locations

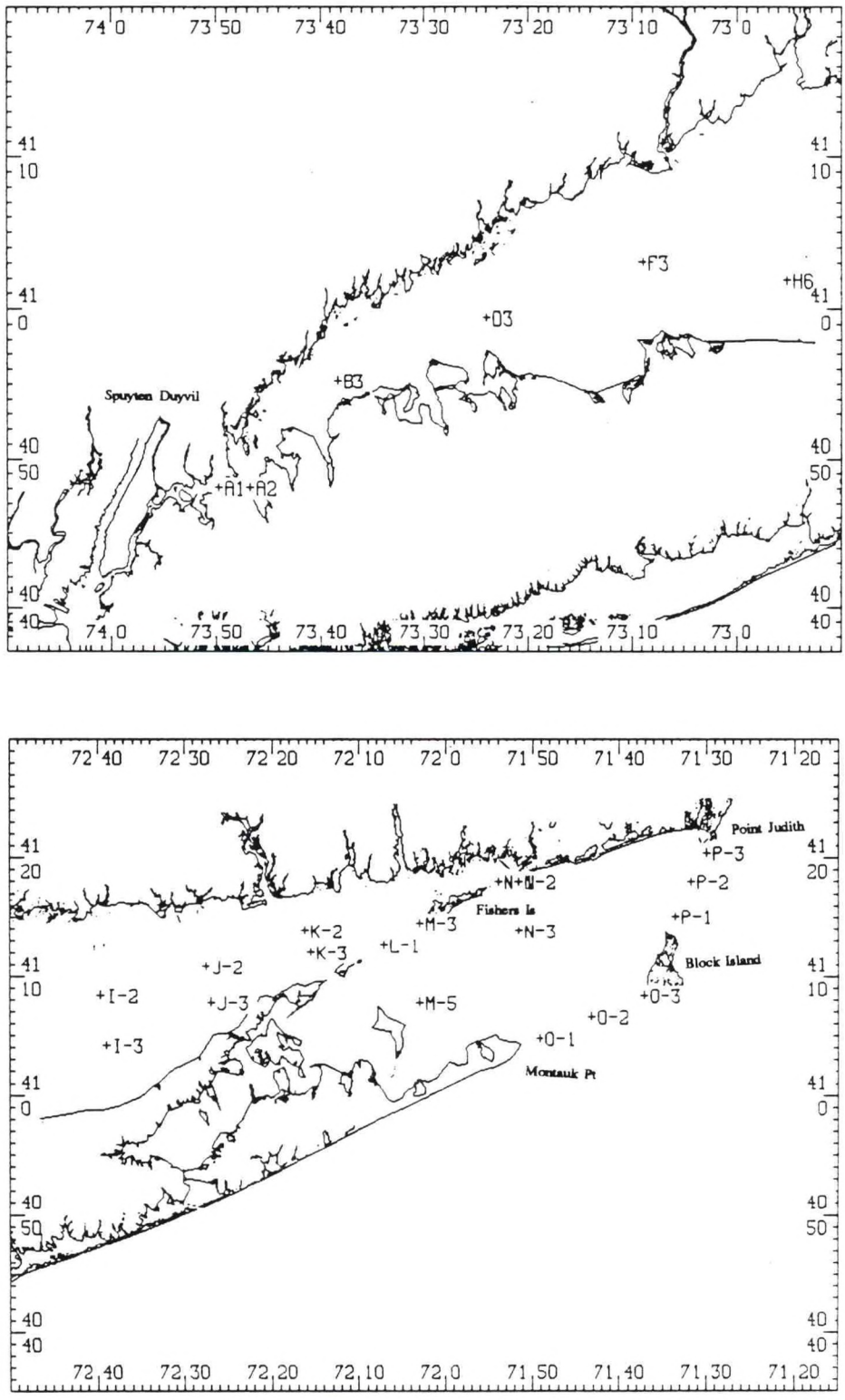

Figure 6.4. Long Island Sound Model Salinity and Temperature Validation Station Locations

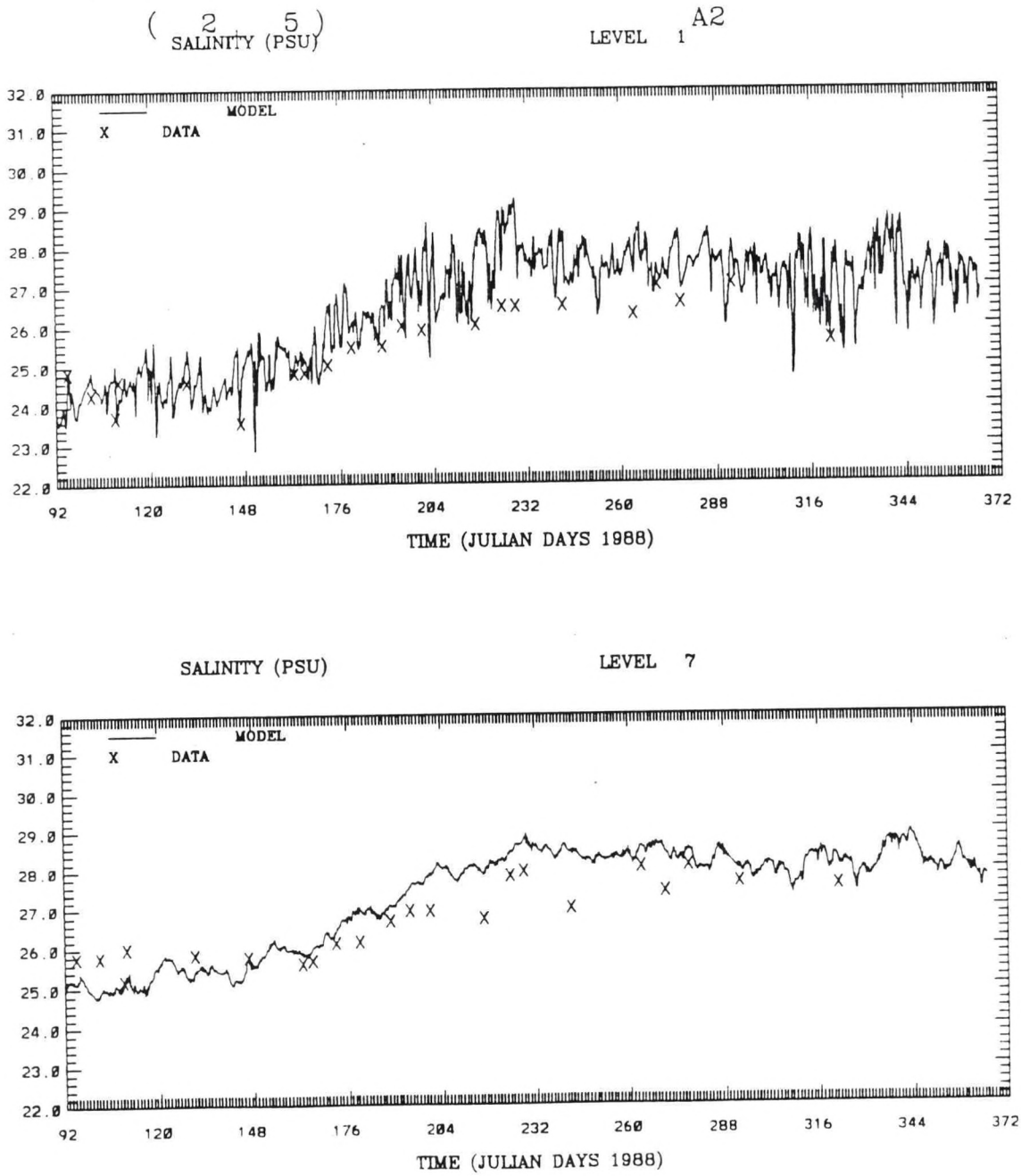

Figure 6.5. Simulated Near Surface and Near Bottom Salinity Time Series During the Calibration Period At Station: A2

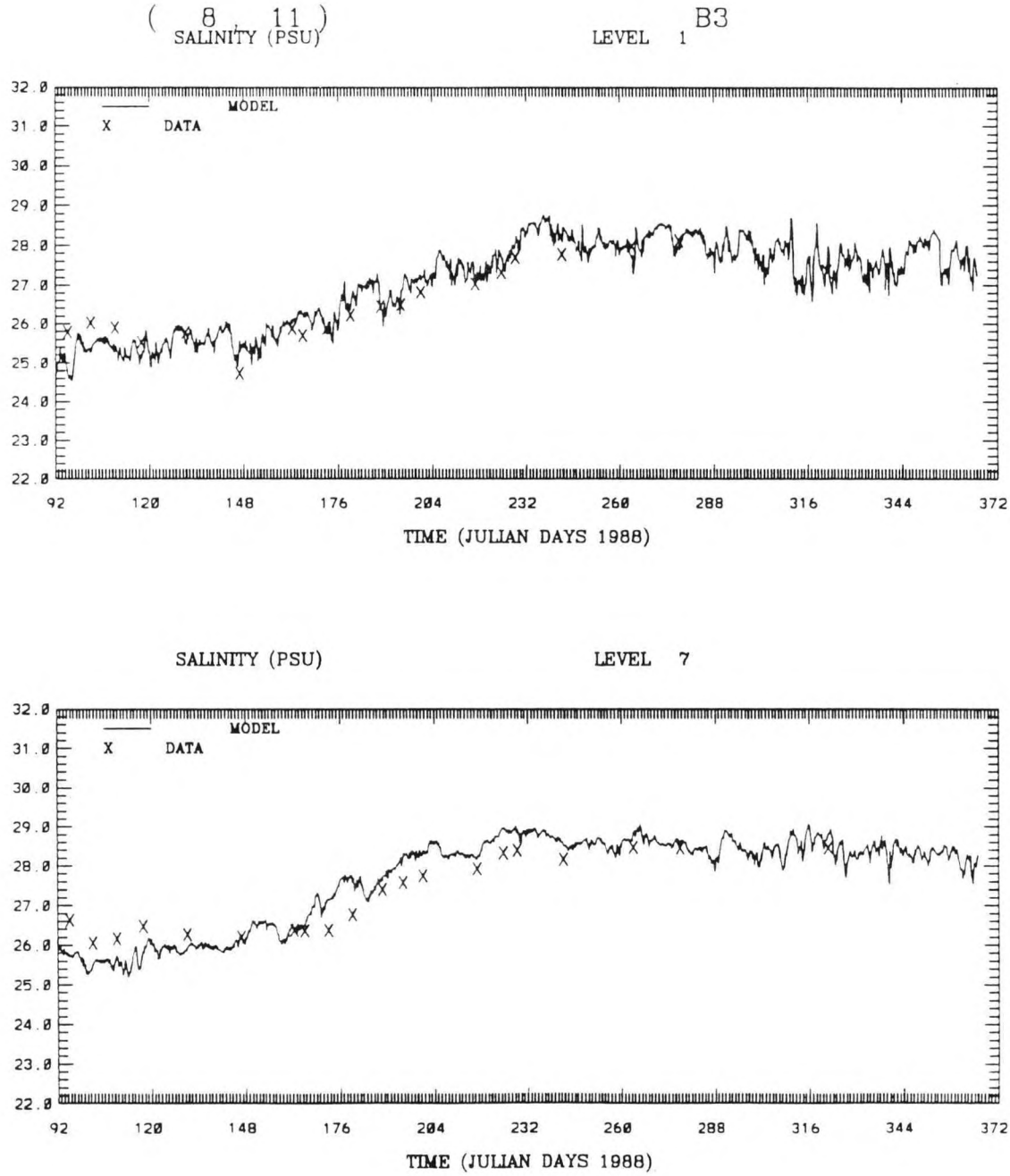

Figure 6.6. Simulated Near Surface and Near Bottom Salinity Time Series During the Calibration Period At Station: B3

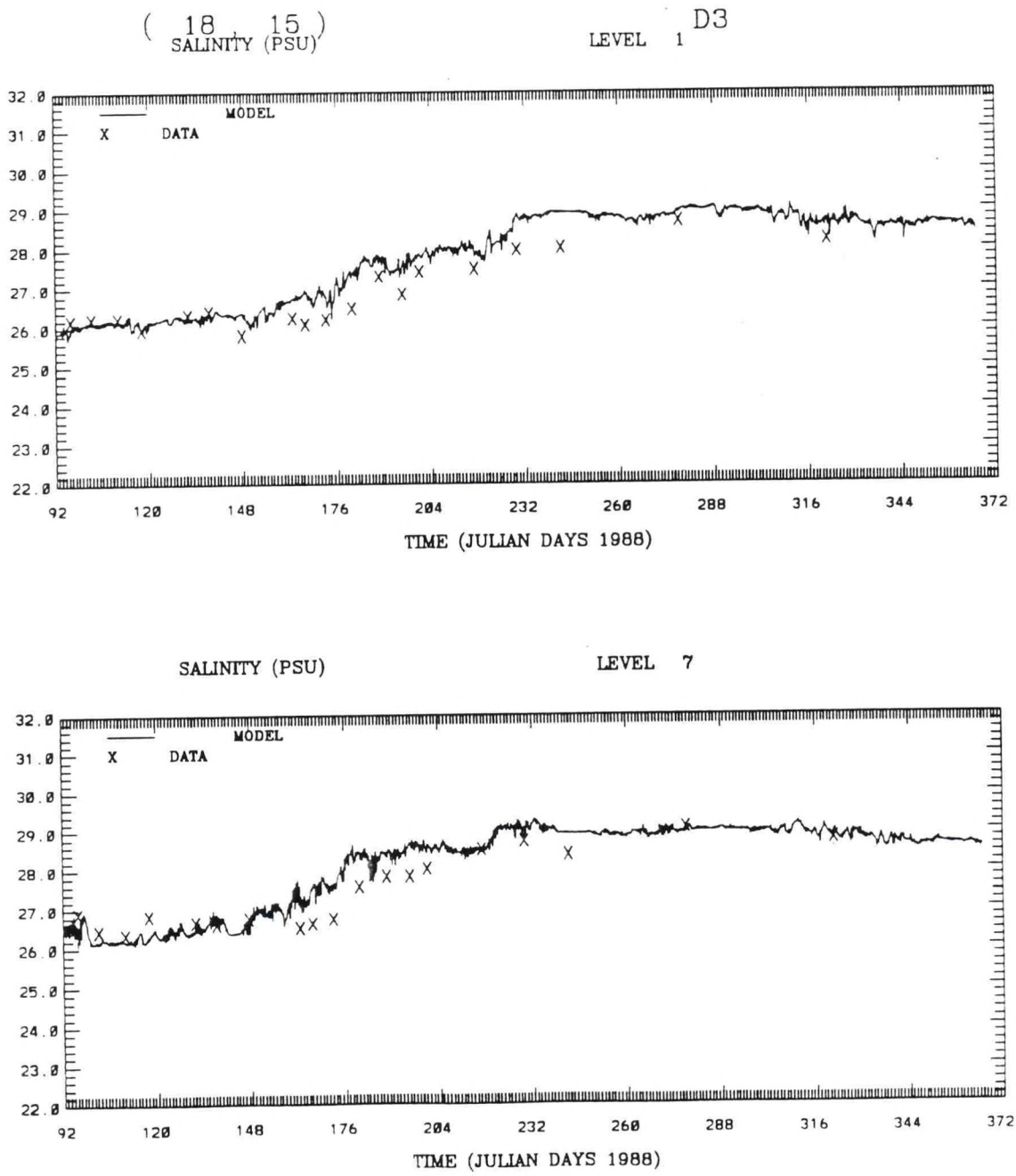

Figure 6.7. Simulated Near Surface and Near Bottom Salinity Time Series During the Calibration Period At Station: D3

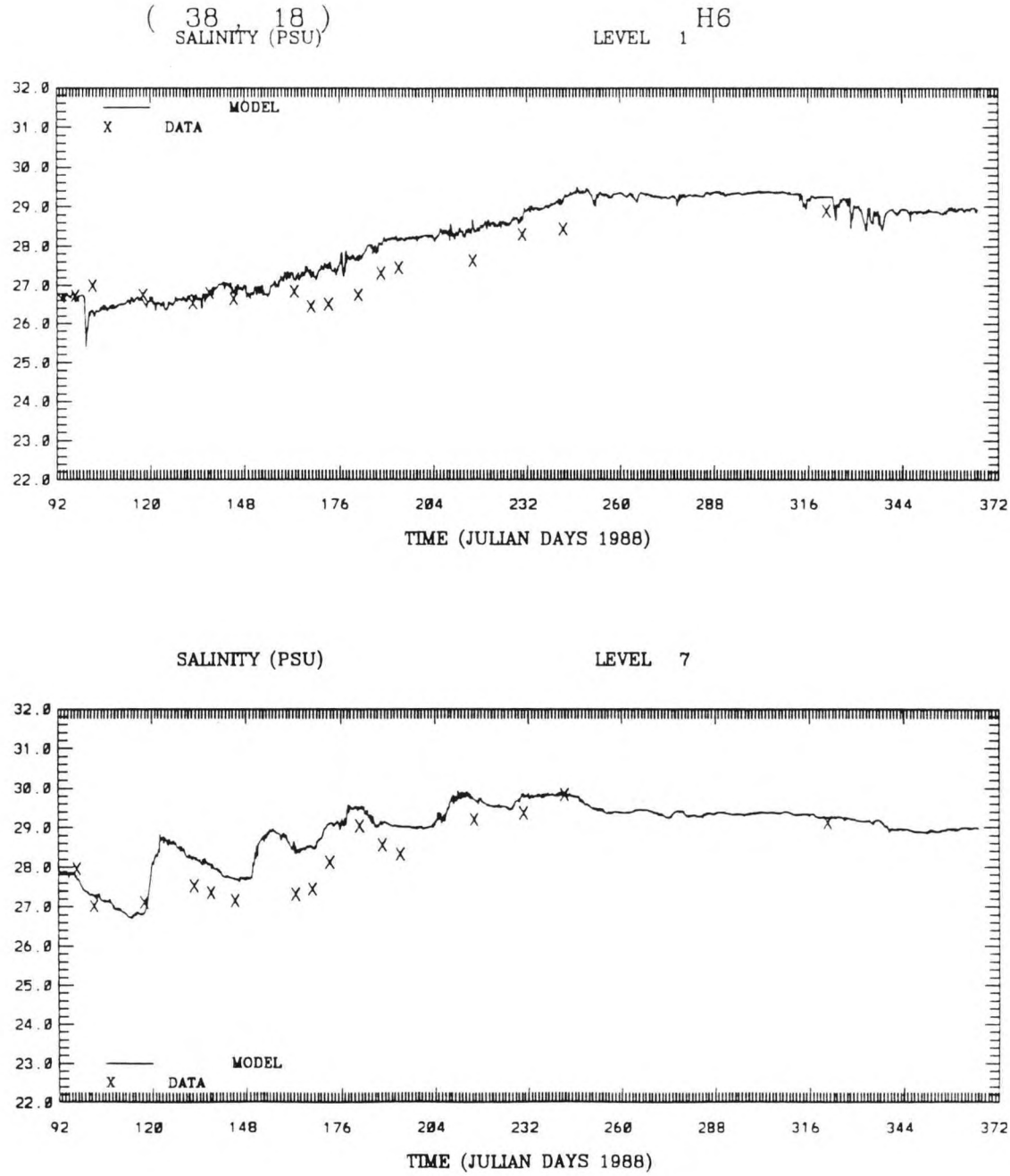

Figure 6.8. Simulated Near Surface and Near Bottom Salinity Time Series During the Calibration Period At Station: H6

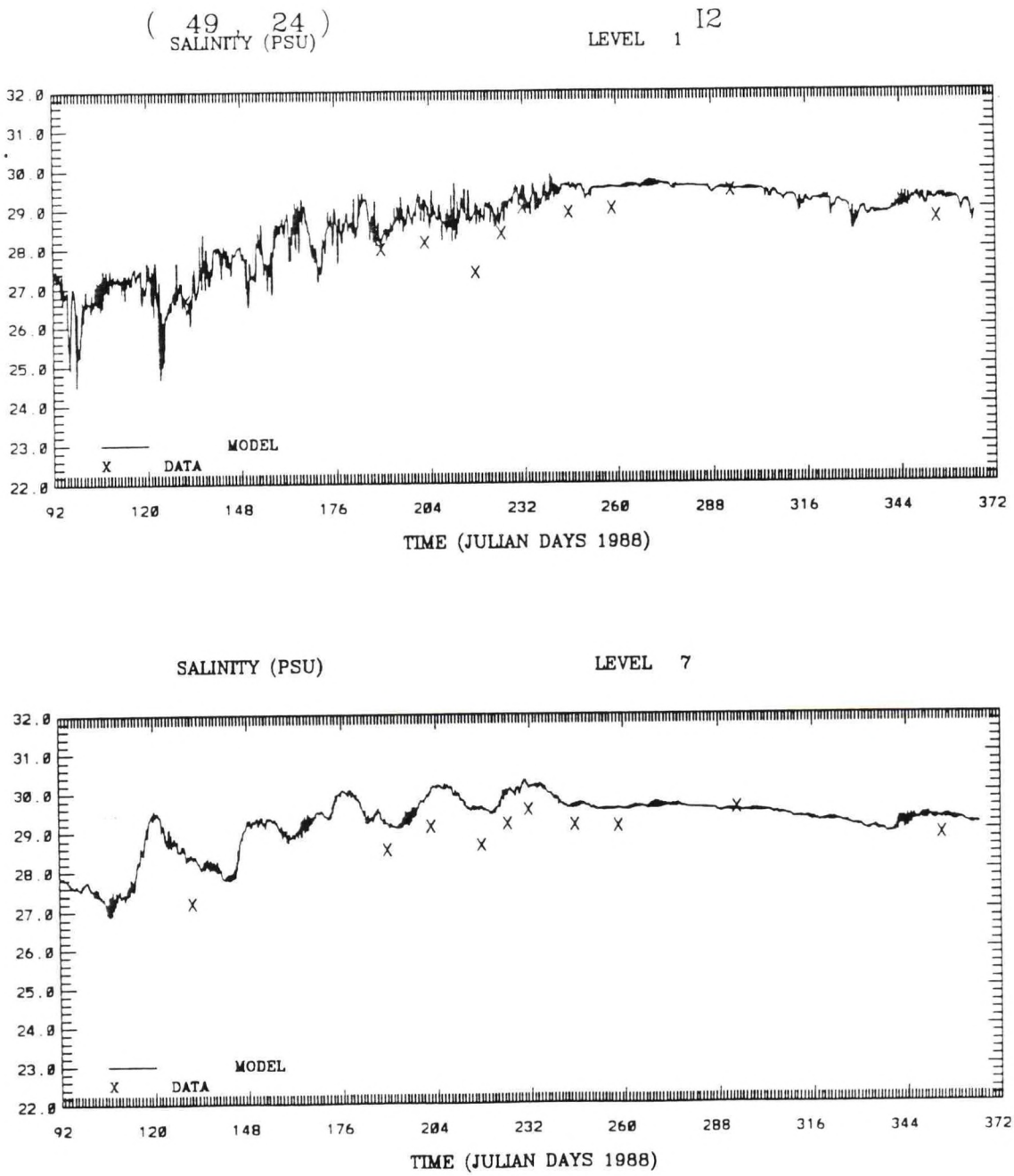

Figure 6.9. Simulated Near Surface and Near Bottom Salinity Time Series During the Calibration Period At Station: I2

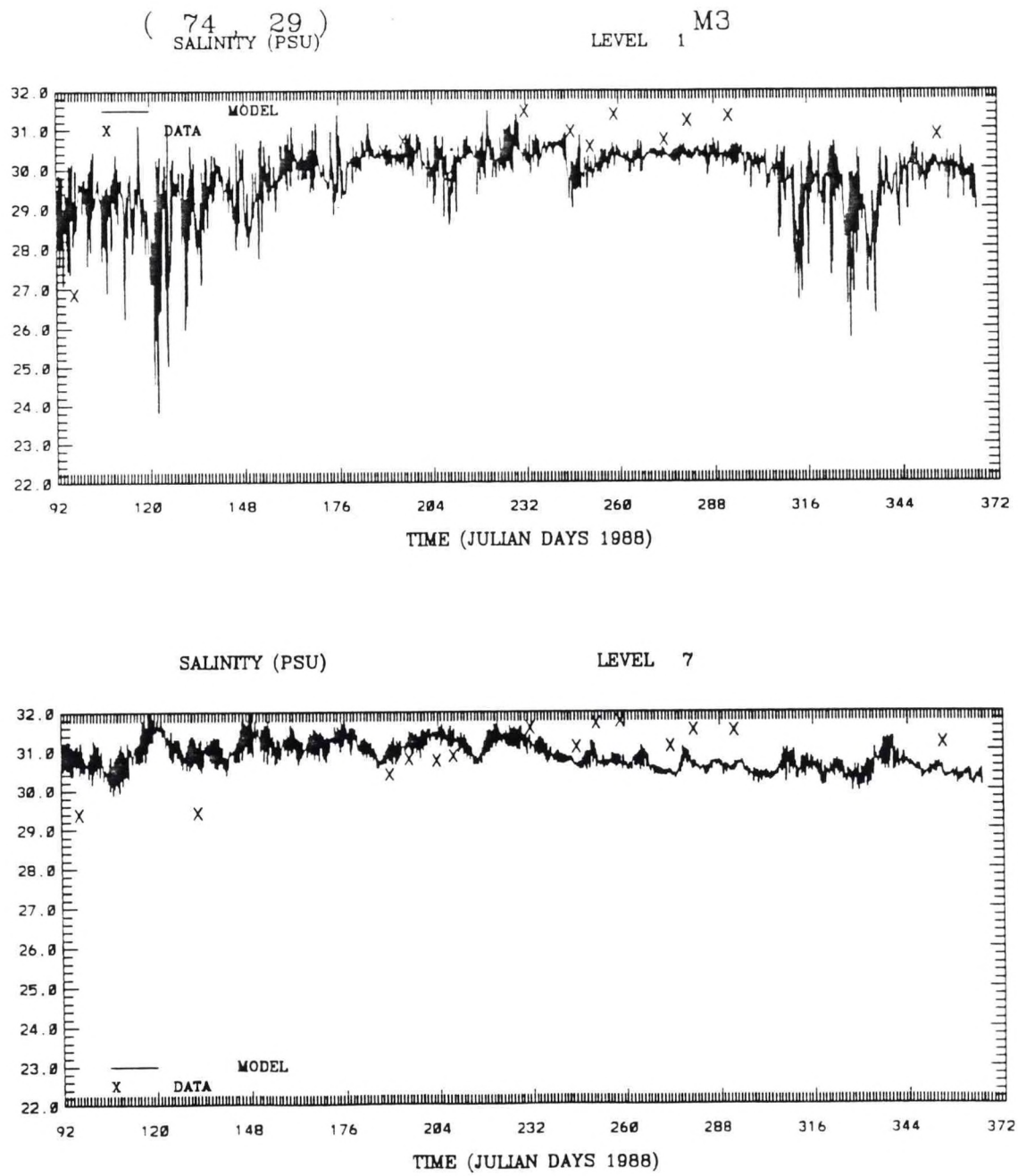

Figure 6.10. Simulated Near Surface and Near Bottom Salinity Time Series During the Calibration Period At Station: M3

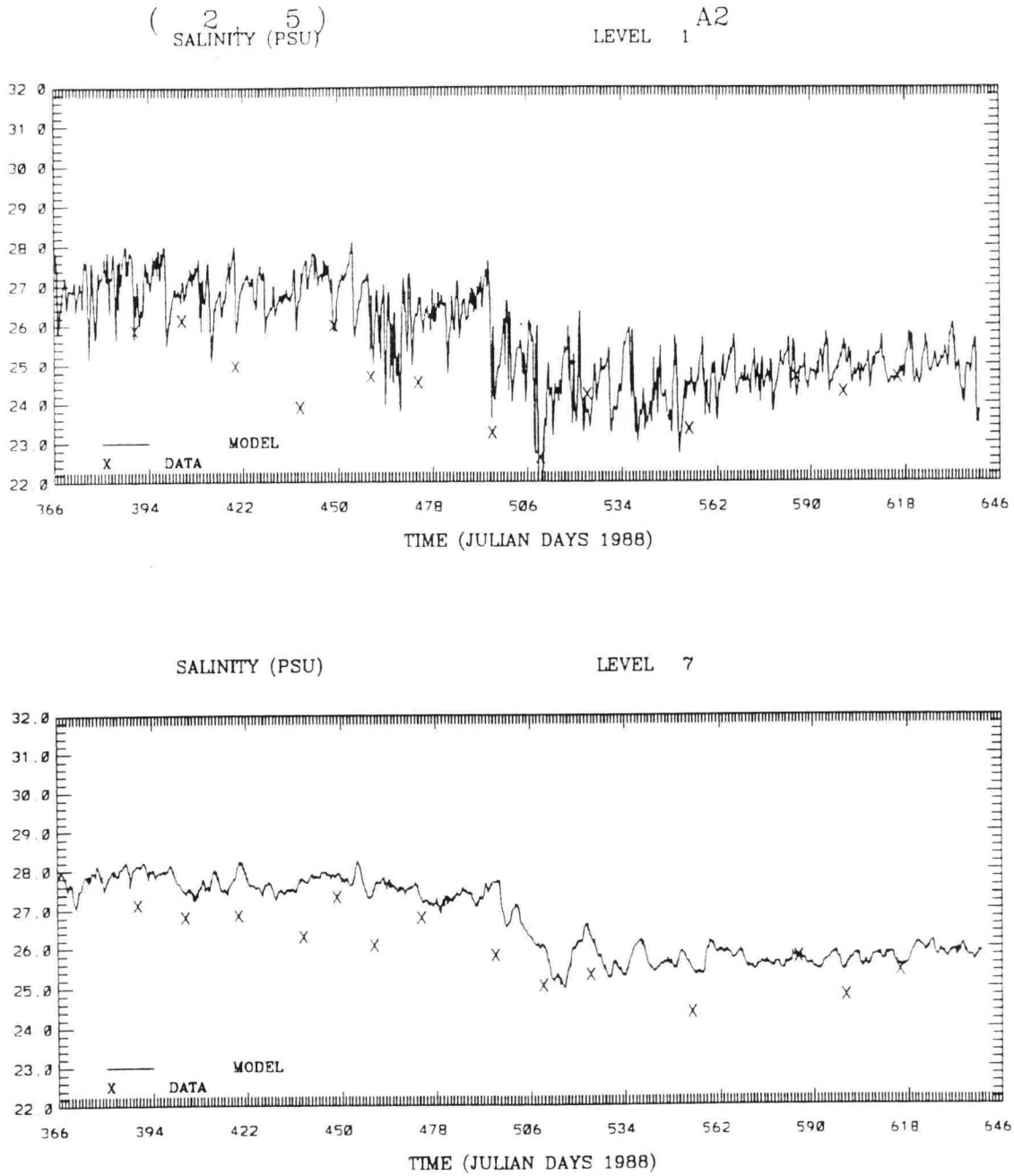

Figure 6.11. Simulated Near Surface and Near Bottom Salinity Time Series During the Verification Period At Station: A2

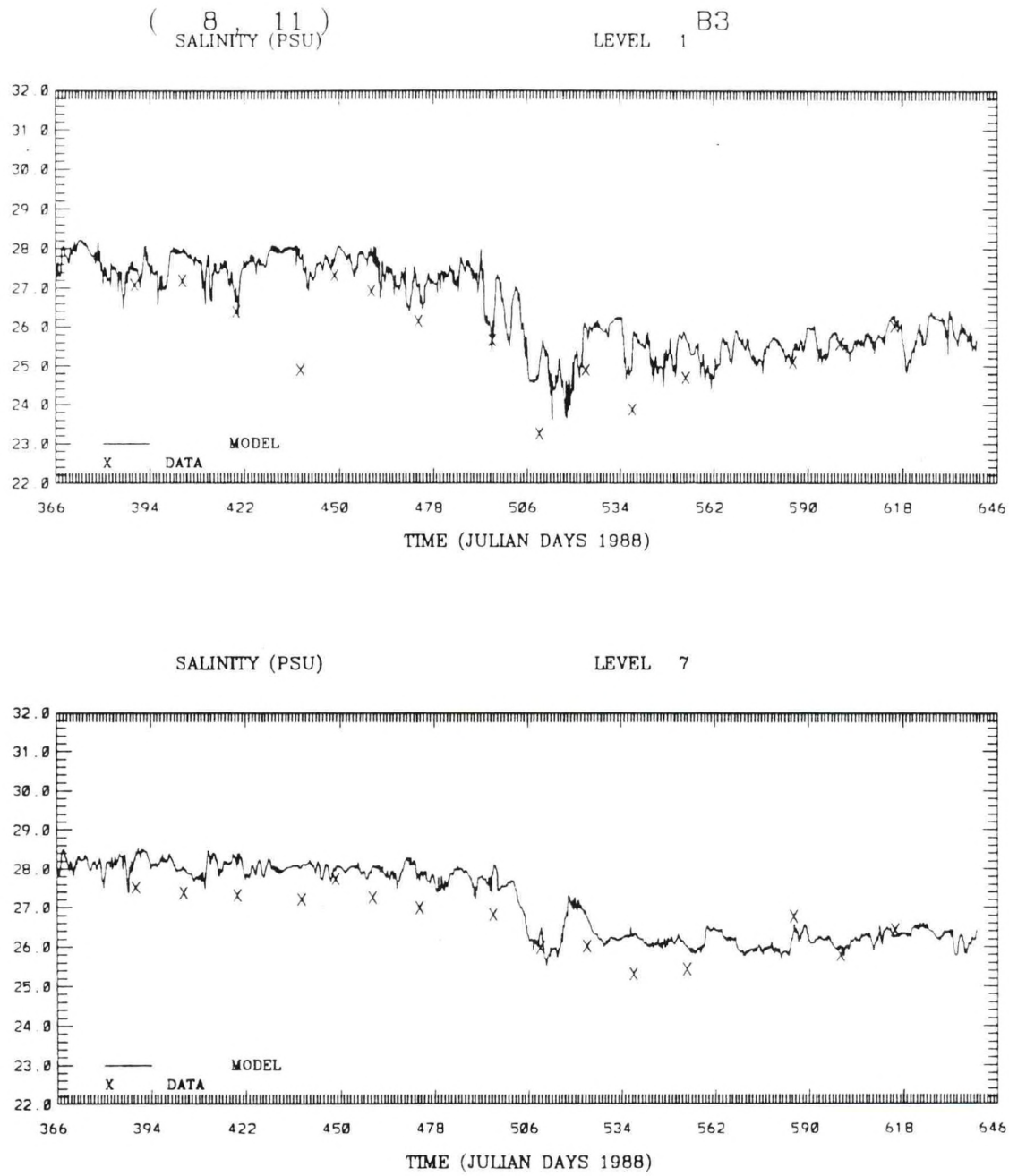

Figure 6.12. Simulated Near Surface and Near Bottom Salinity Time Series During the Verification Period At Station: B3

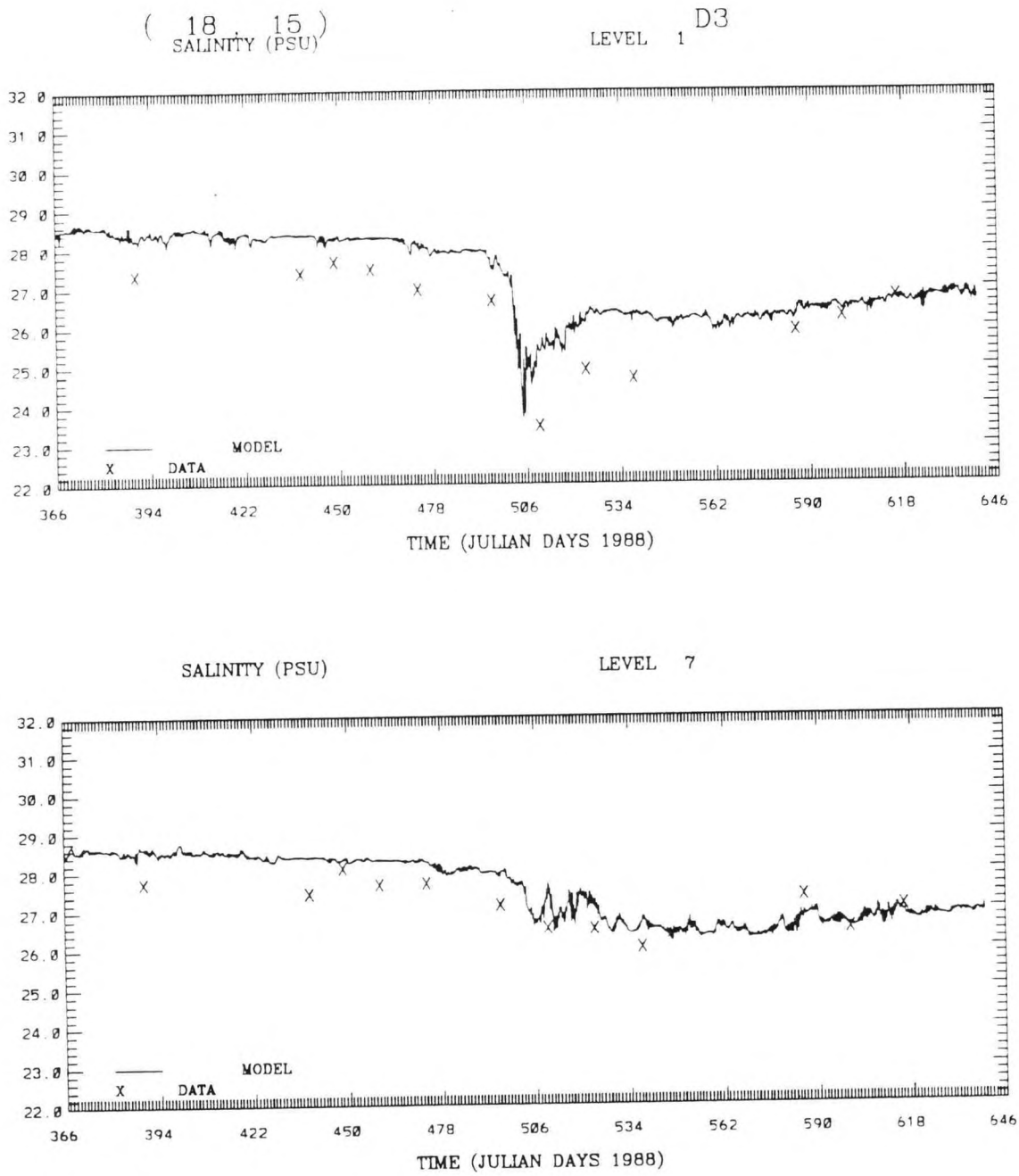

Figure 6.13. Simulated Near Surface and Near Bottom Salinity Time Series During the Verification Period At Station: D3

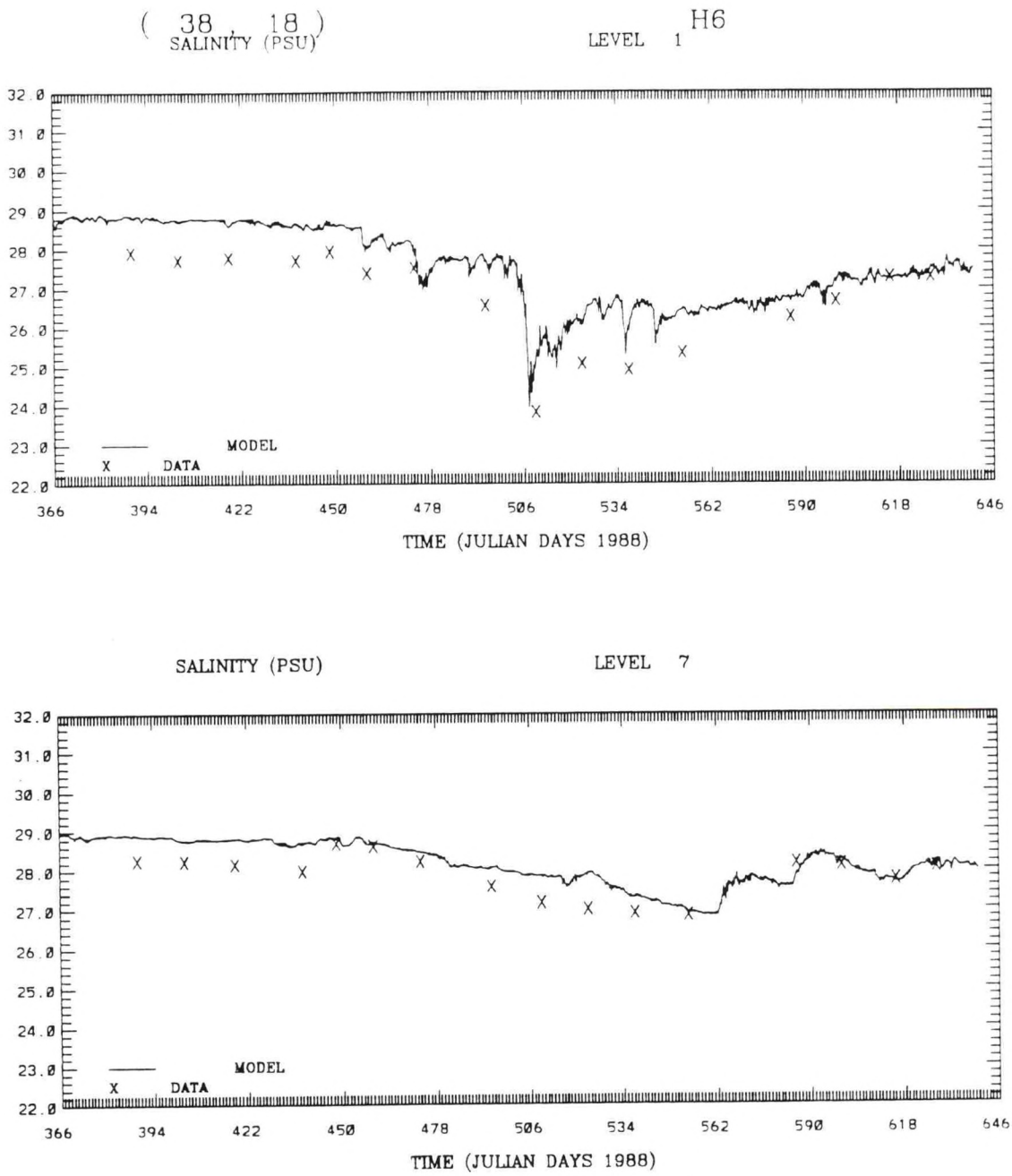

Figure 6.14. Simulated Near Surface and Near Bottom Salinity Time Series During the Verification Period At Station: H6

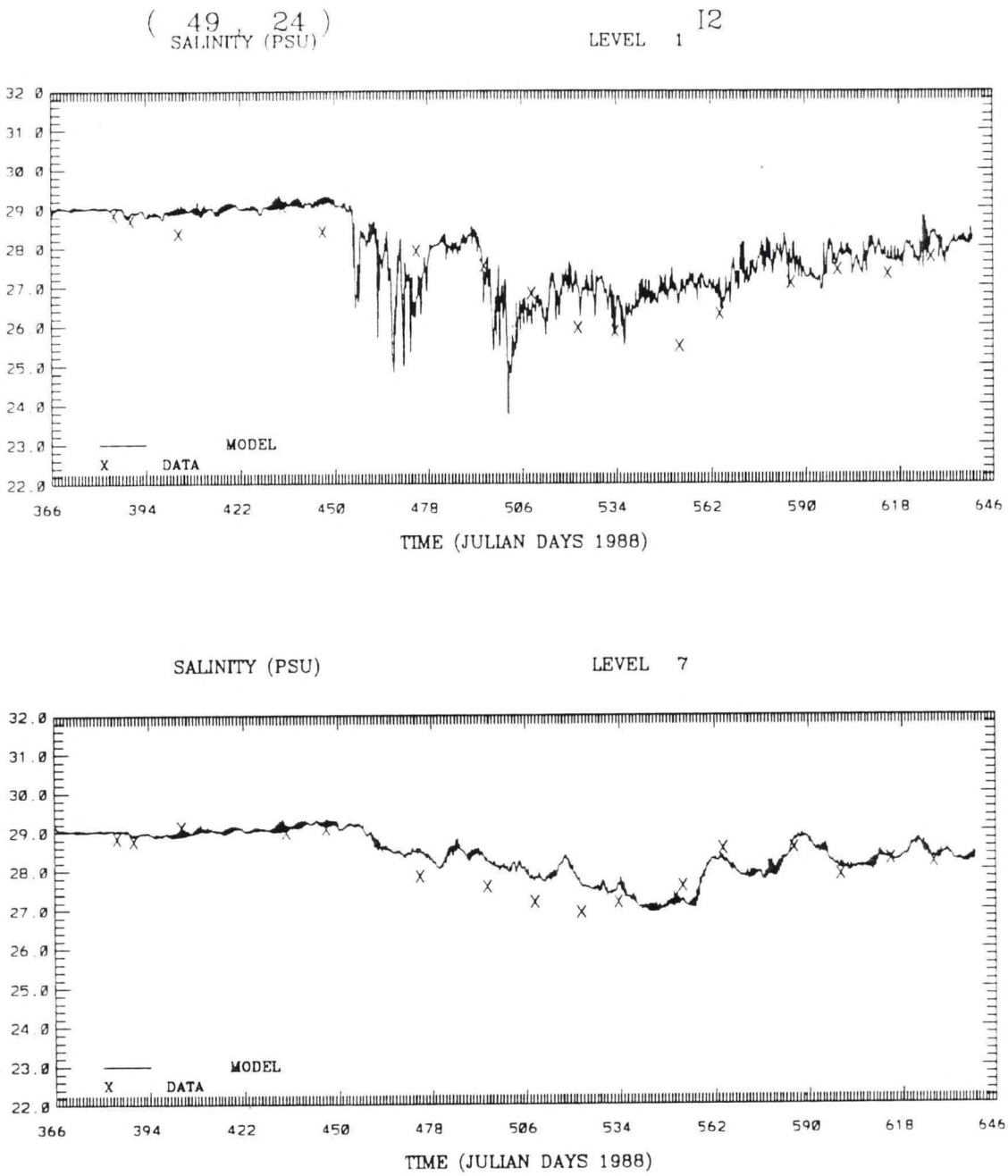

Figure 6.15. Simulated Near Surface and Near Bottom Salinity Time Series During the Verification Period At Station: I2

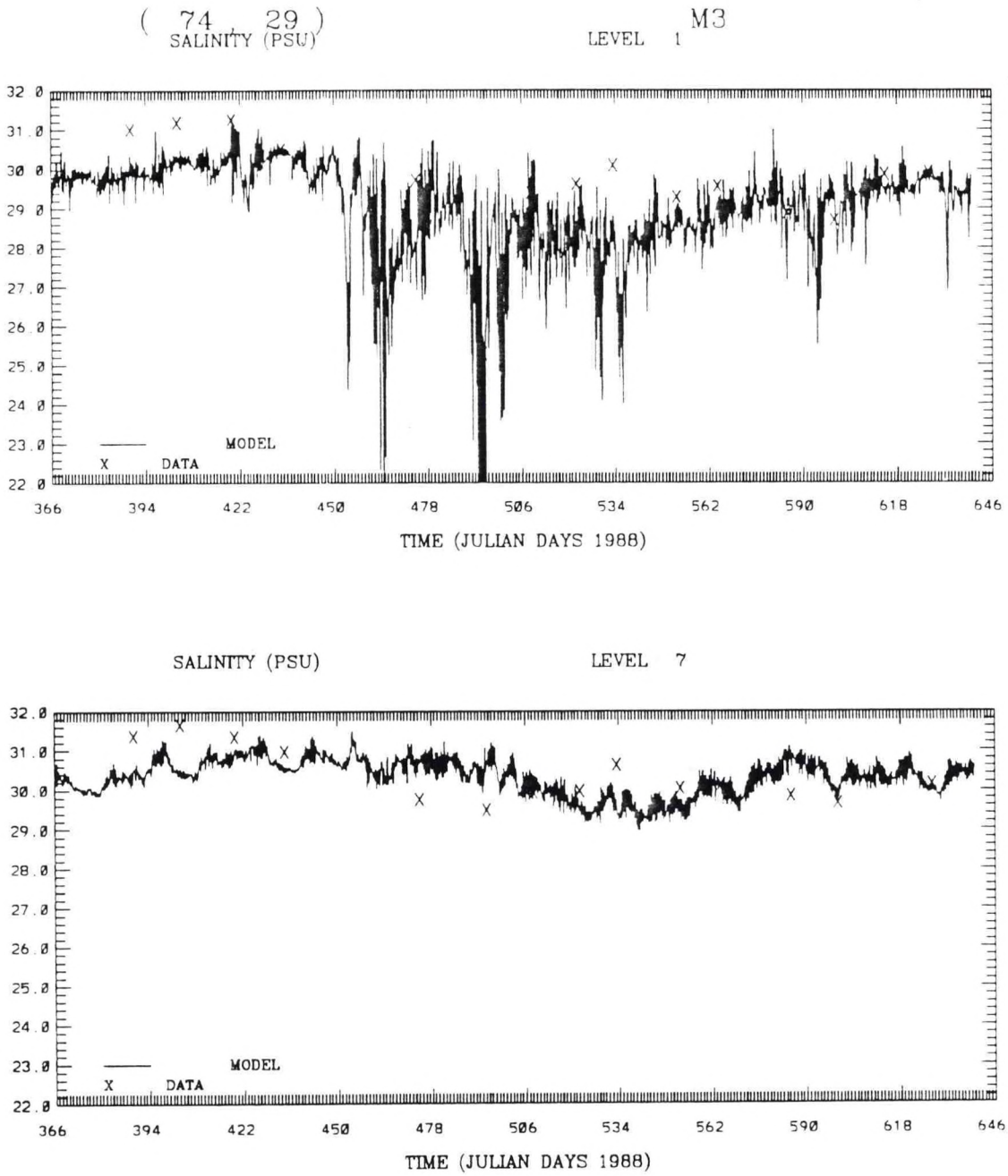

Figure 6.16. Simulated Near Surface and Near Bottom Salinity Time Series During the Verification Period At Station: M3

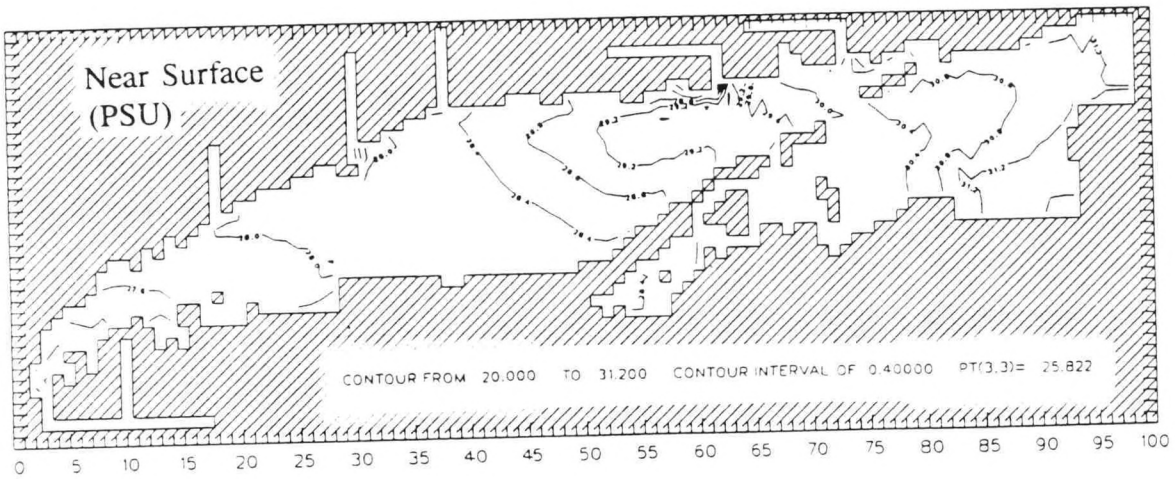

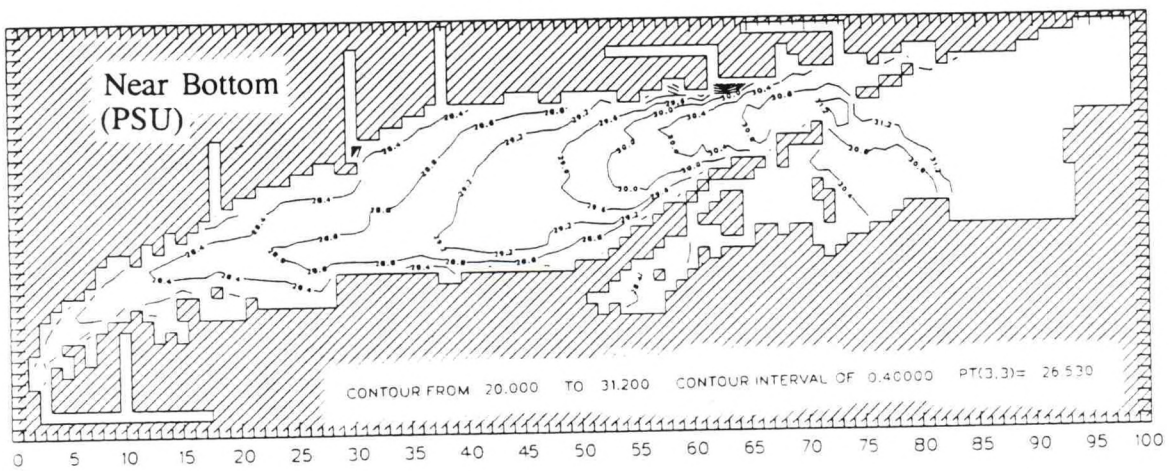

Figure 6.17. Simulated Near Surface and Near Bottom Salinity Distributions: July 1988

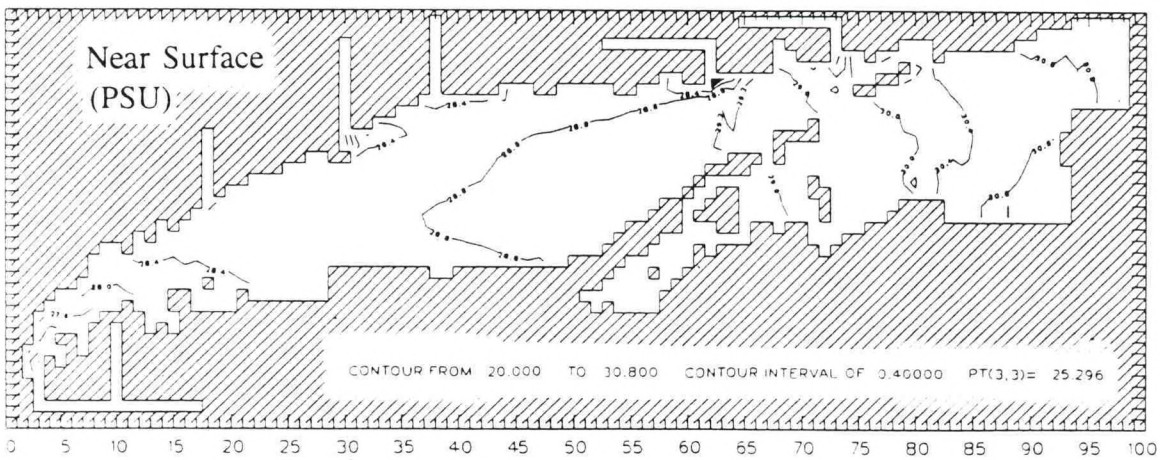

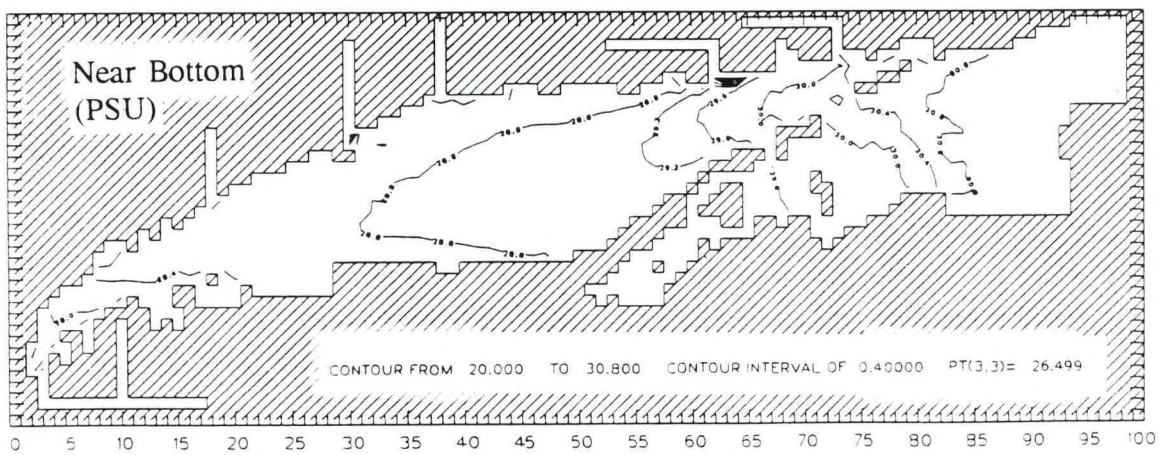

Figure 6.18. Simulated Near Surface and Near Bottom Salinity Distributions: January 1989

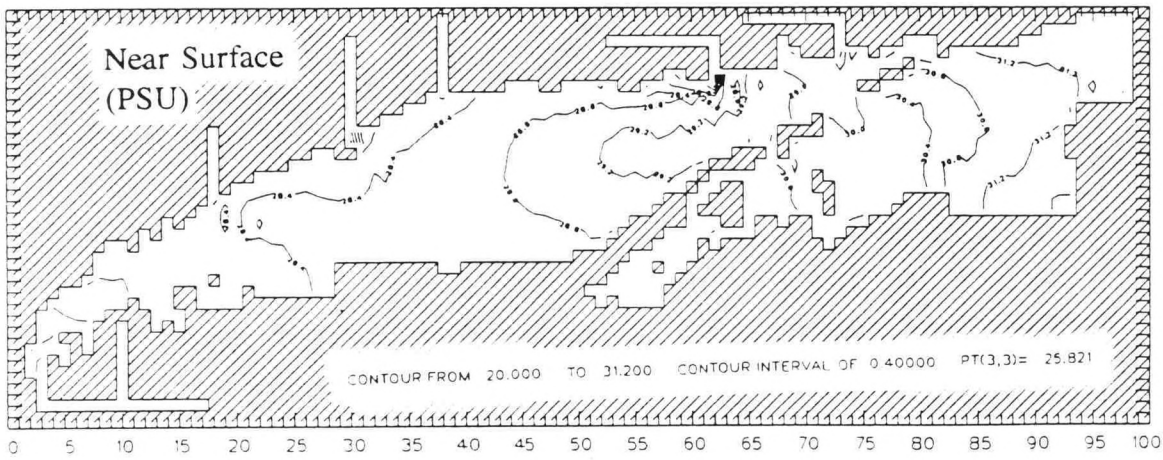

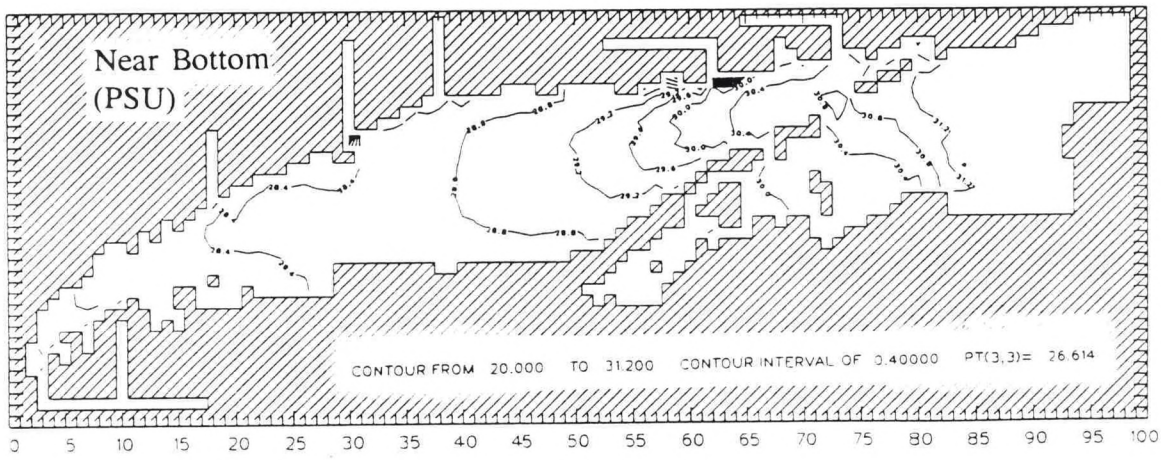

Figure 6.19. Simulated Near Surface and Near Bottom Salinity Distributions: March 1989

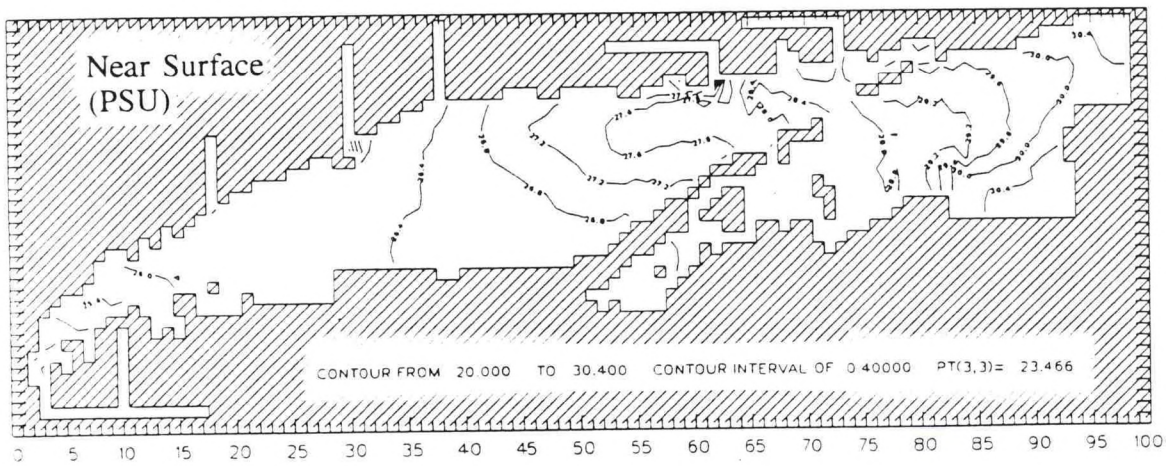

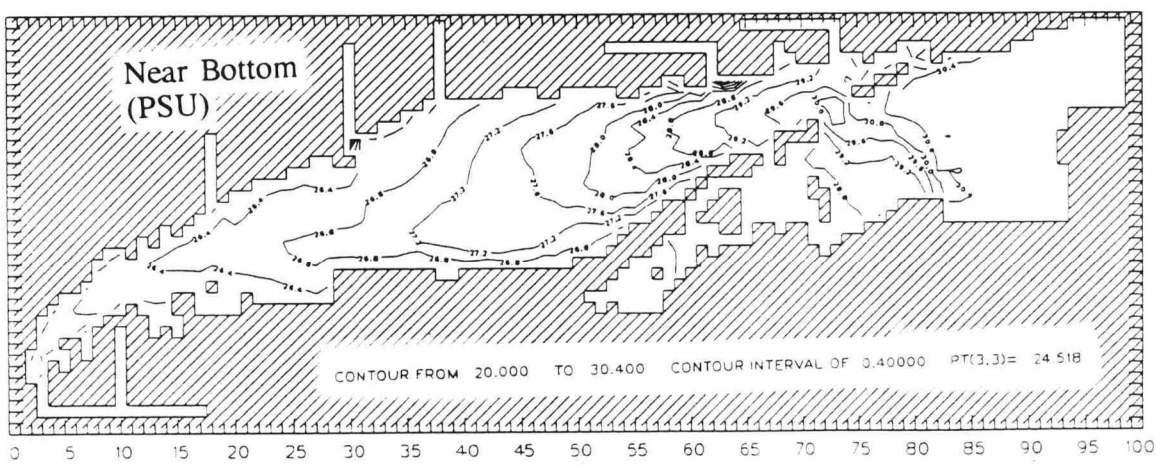

Figure 6.20. Simulated Near Surface and Near Bottom Salinity Distributions: July 1989

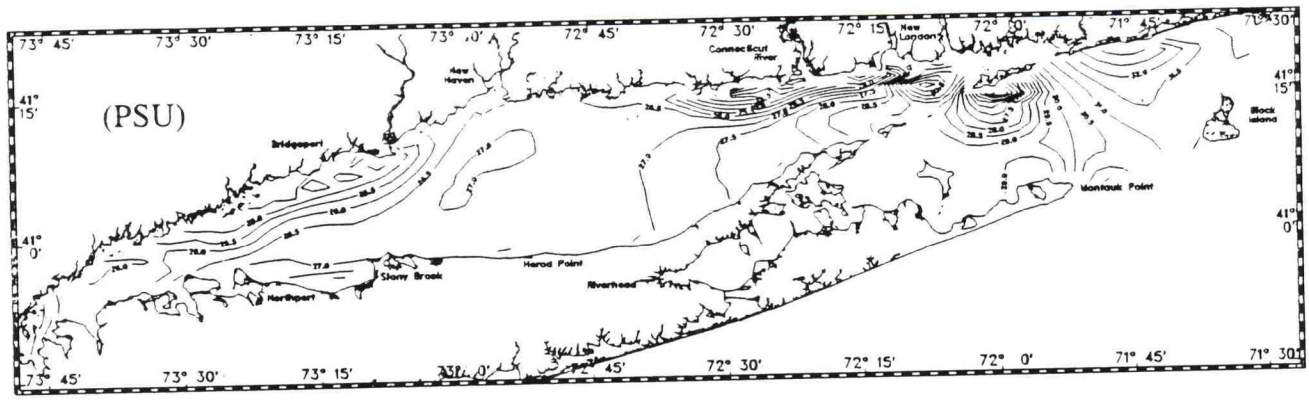

April 4 - 7, 1988

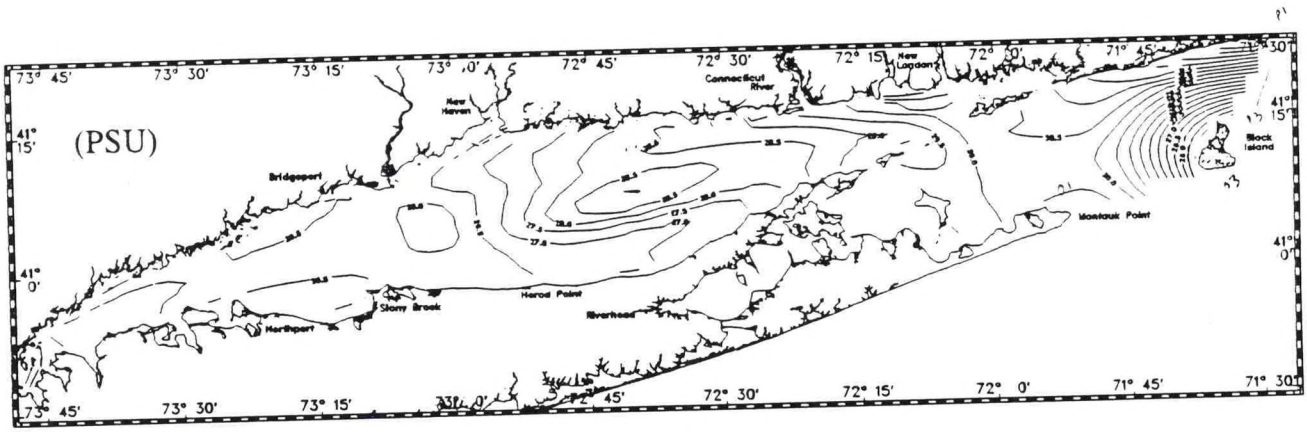

June 13 - 16, 1988

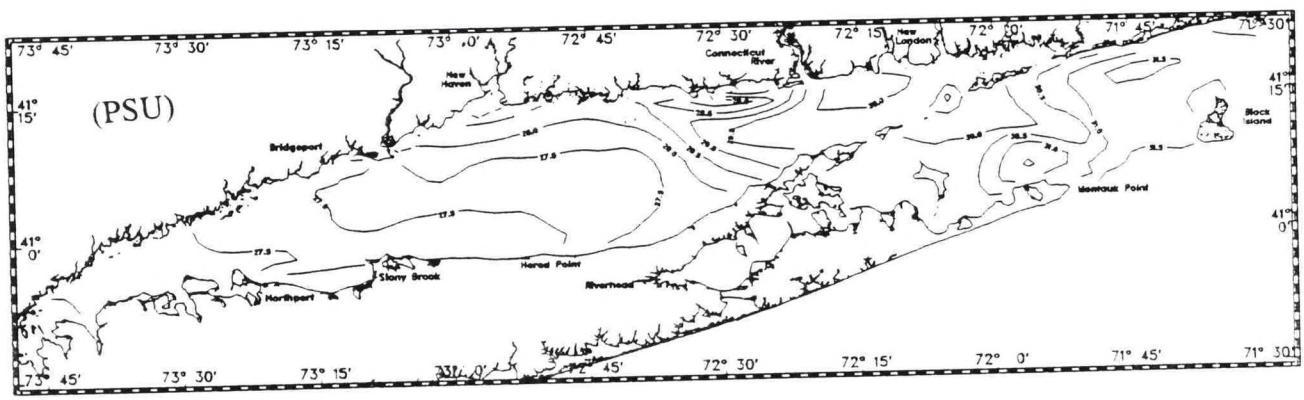

August 2 - 4, 1988

Figure 6.21. Observed Near Surface Salinity Fields:
April 4-7, June 13-16, and August 2-4, 1988

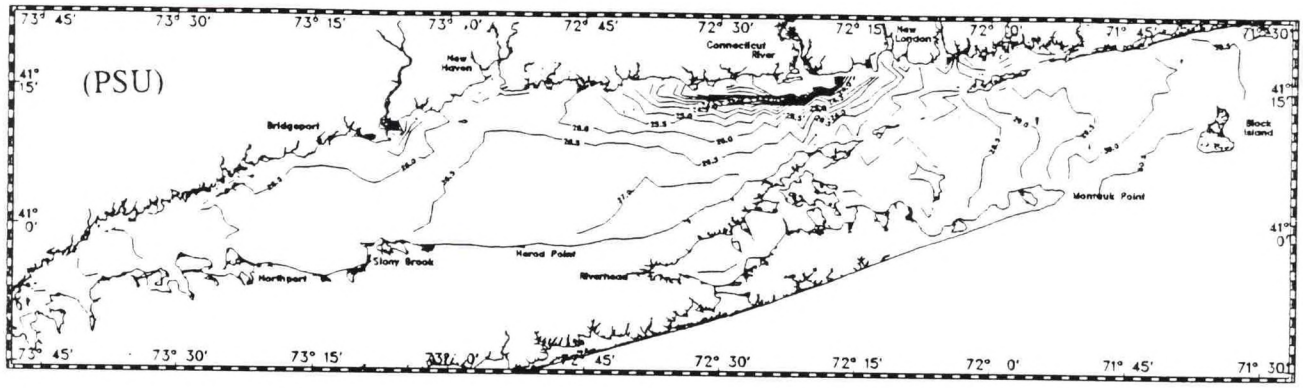

April 4 - 7, 1988

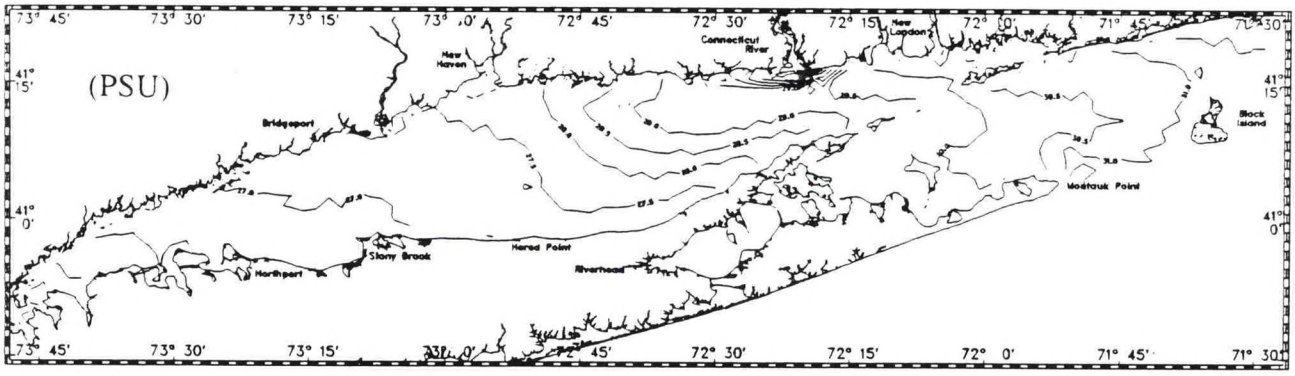

June 13 - 16, 1988

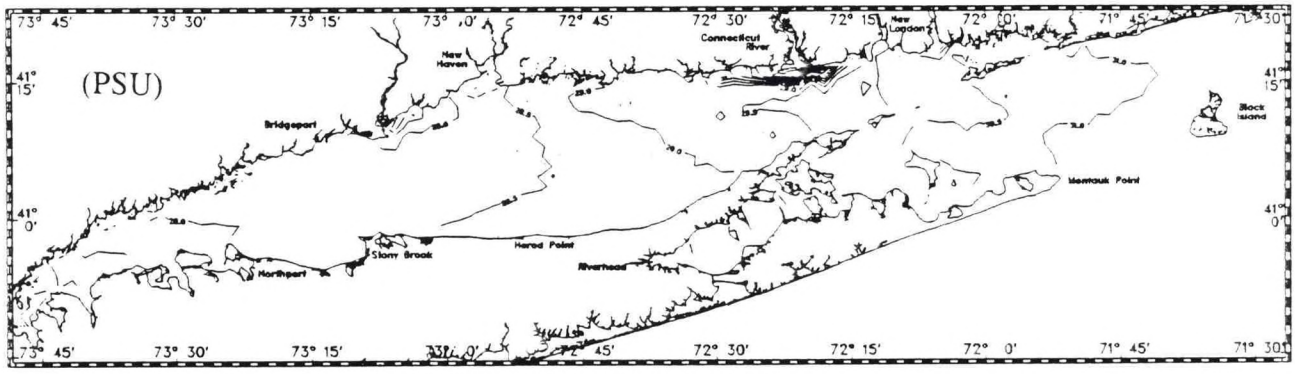

August 2 - 4, 1988

Figure 6.22. Simulated Near Surface Salinity Fields:
April 4-7, June 13-16, and August 2-4, 1988

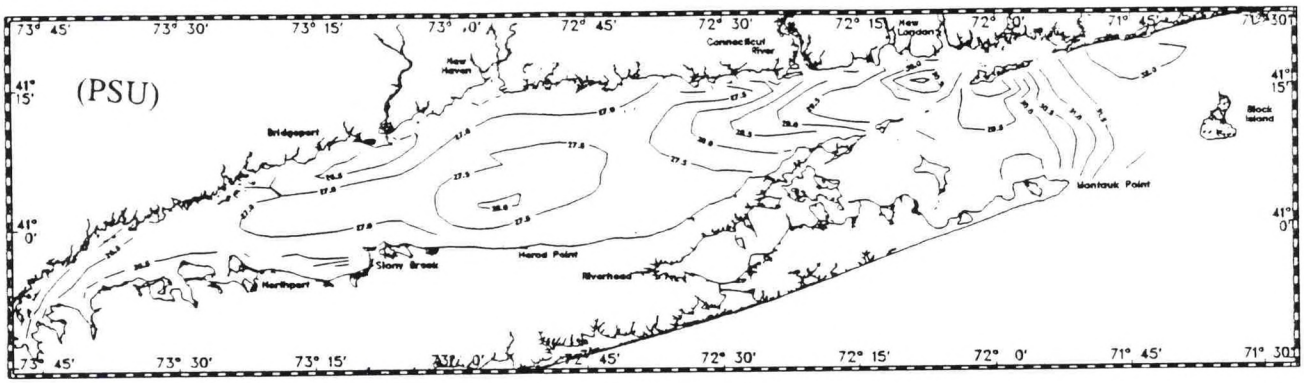

April 4 - 7, 1988

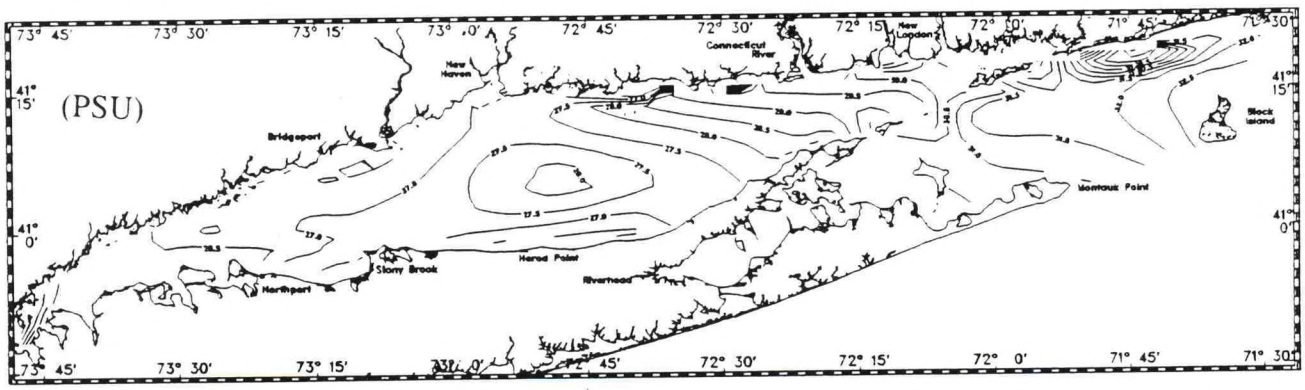

June 13 - 16, 1988

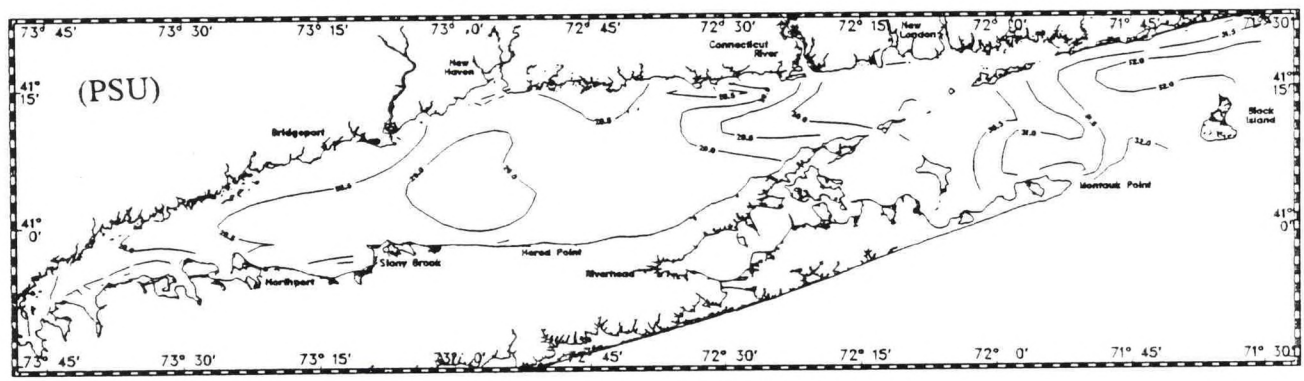

August 2 - 4, 1988

Figure 6.23. Observed Near Bottom Salinity Fields:
April 4-7, June 13-16, and August 2-4, 1988

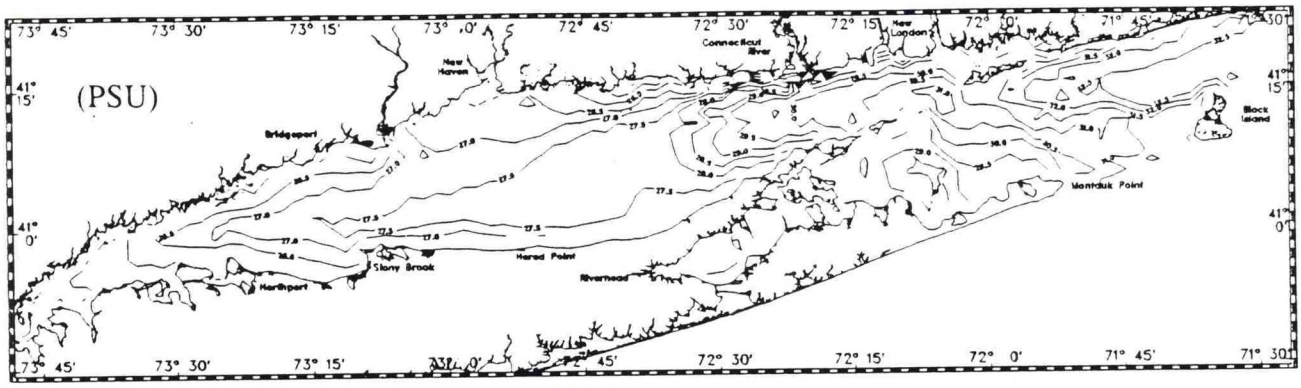

April 4 - 7, 1988

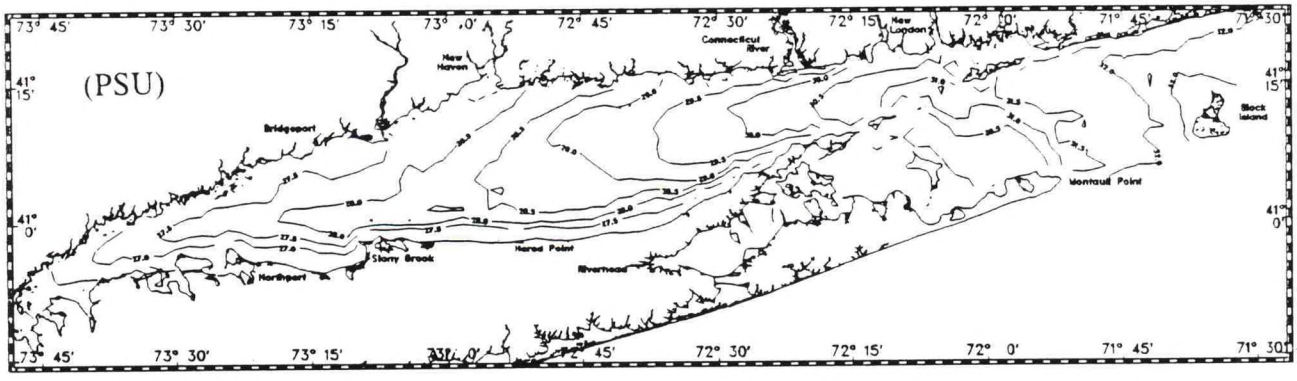

June 13 - 16, 1988

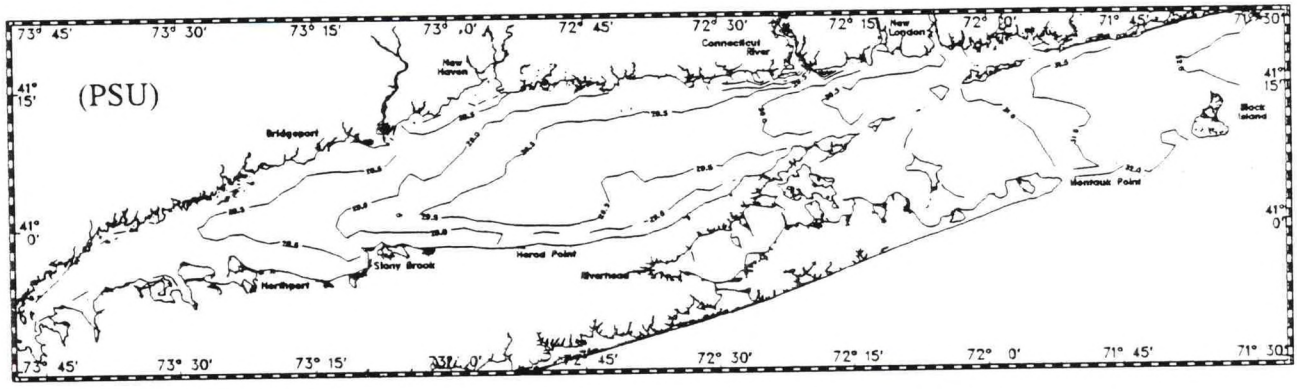

August 2 - 4, 1988

Figure 6.24. Simulated Near Bottom Salinity Fields:
April 4-7, June 13-16, and August 2-4, 1988

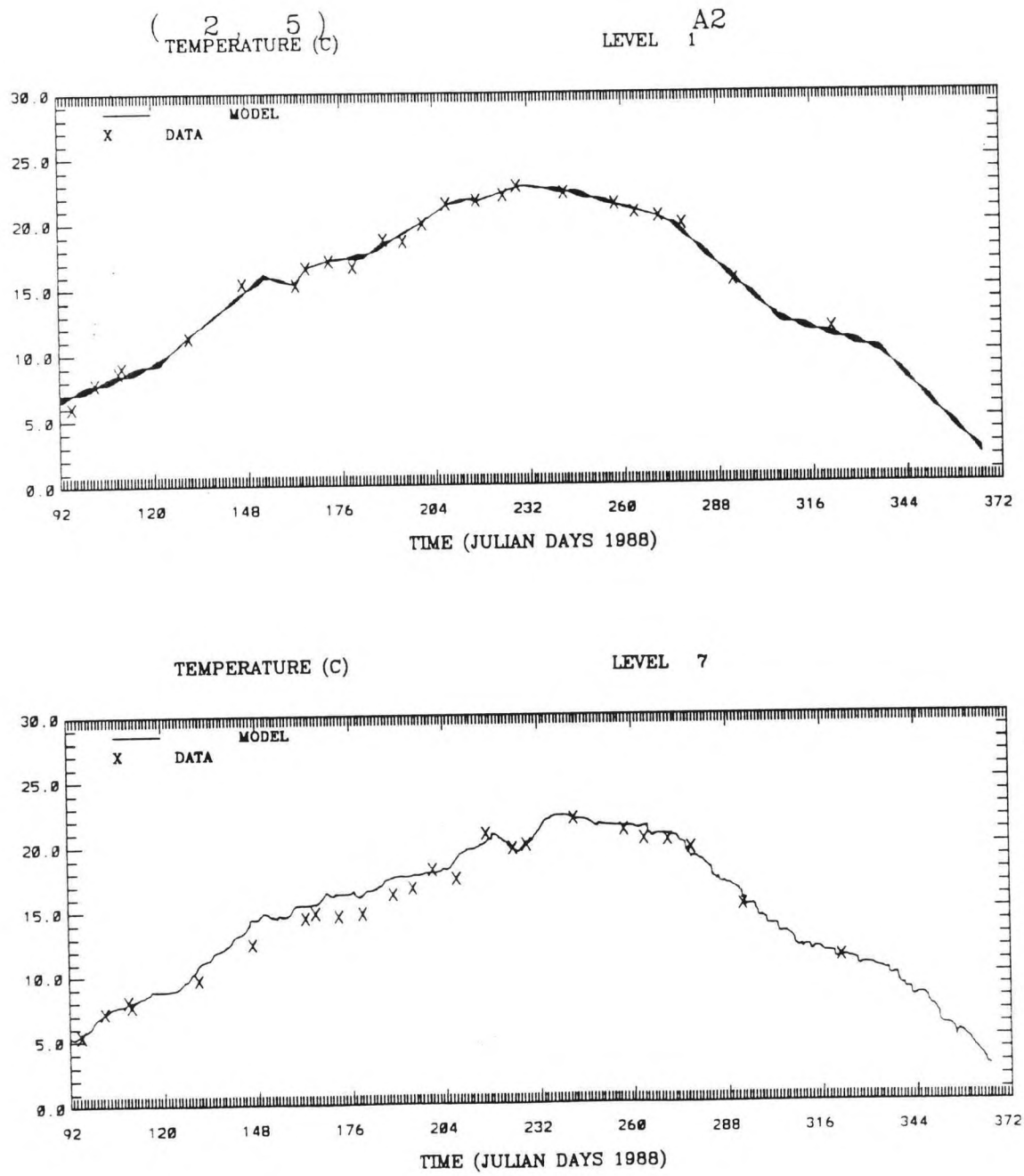

Figure 6.25. Simulated Near Surface and Near Bottom Temperature Time Series During the Calibration Period At Station: A2

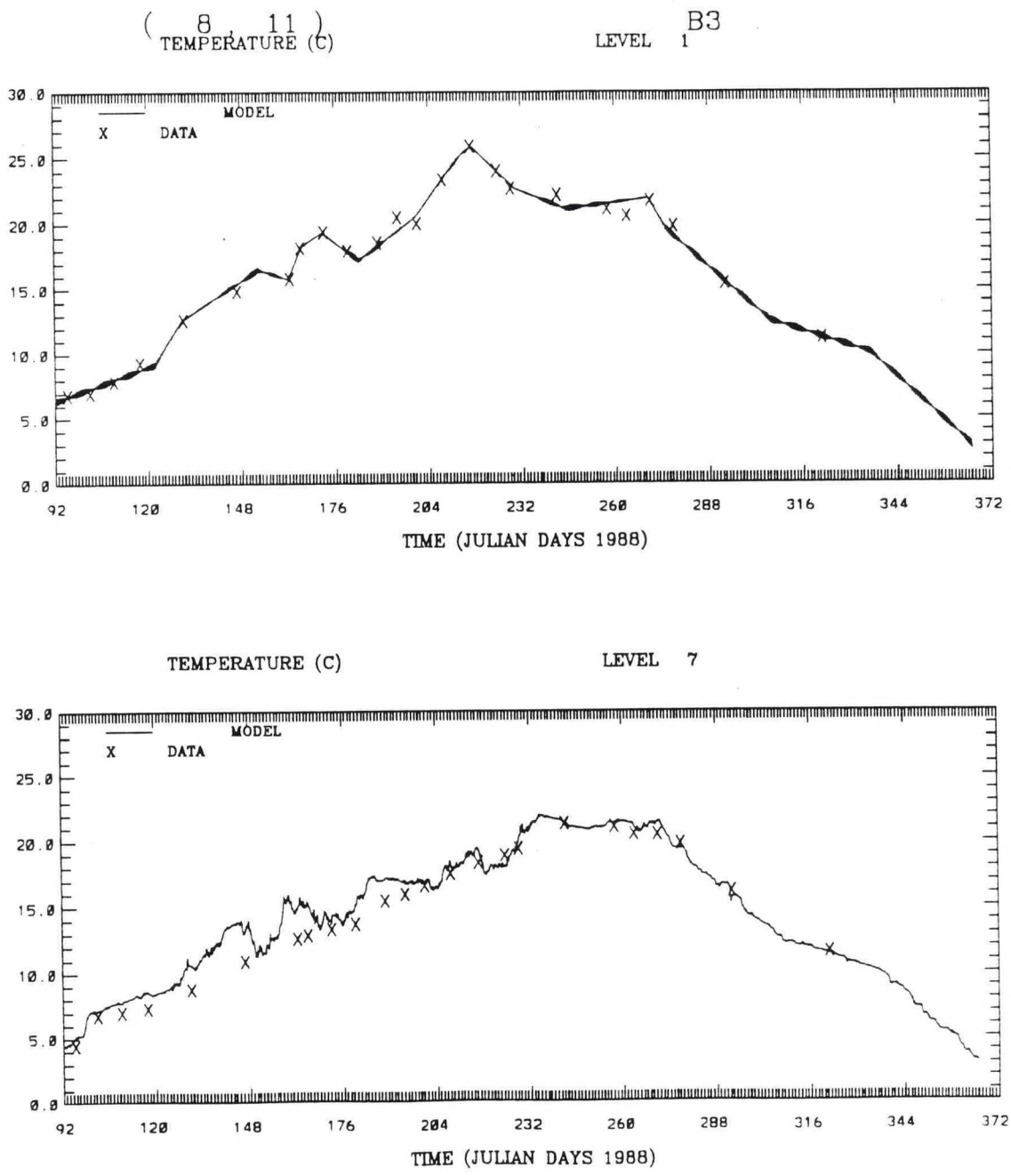

Figure 6.26. Simulated Near Surface and Near Bottom Temperature Time Series During the Calibration Period At Station: B3

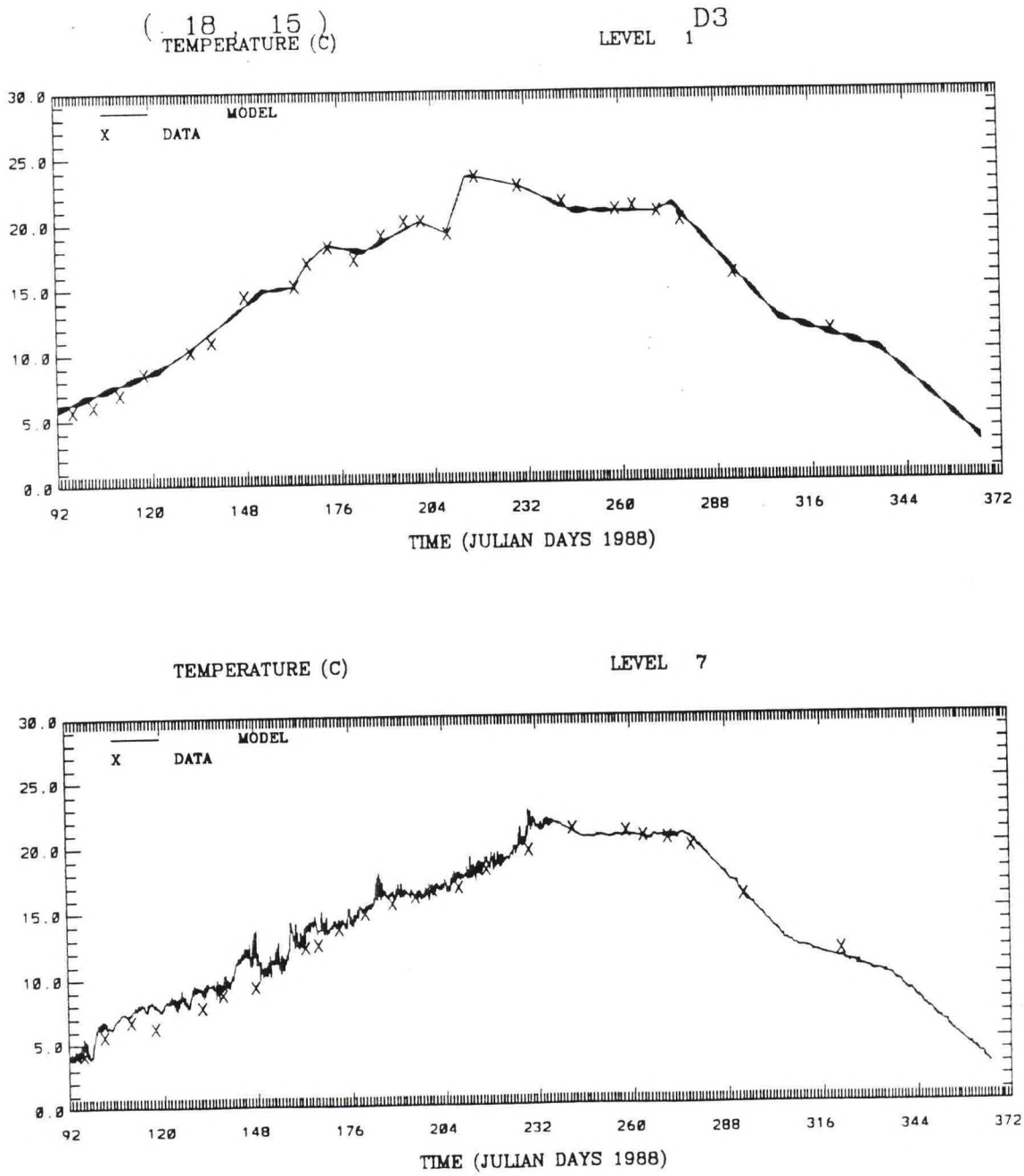

Figure 6.27. Simulated Near Surface and Near Bottom Temperature Time Series During the Calibration Period At Station: D3

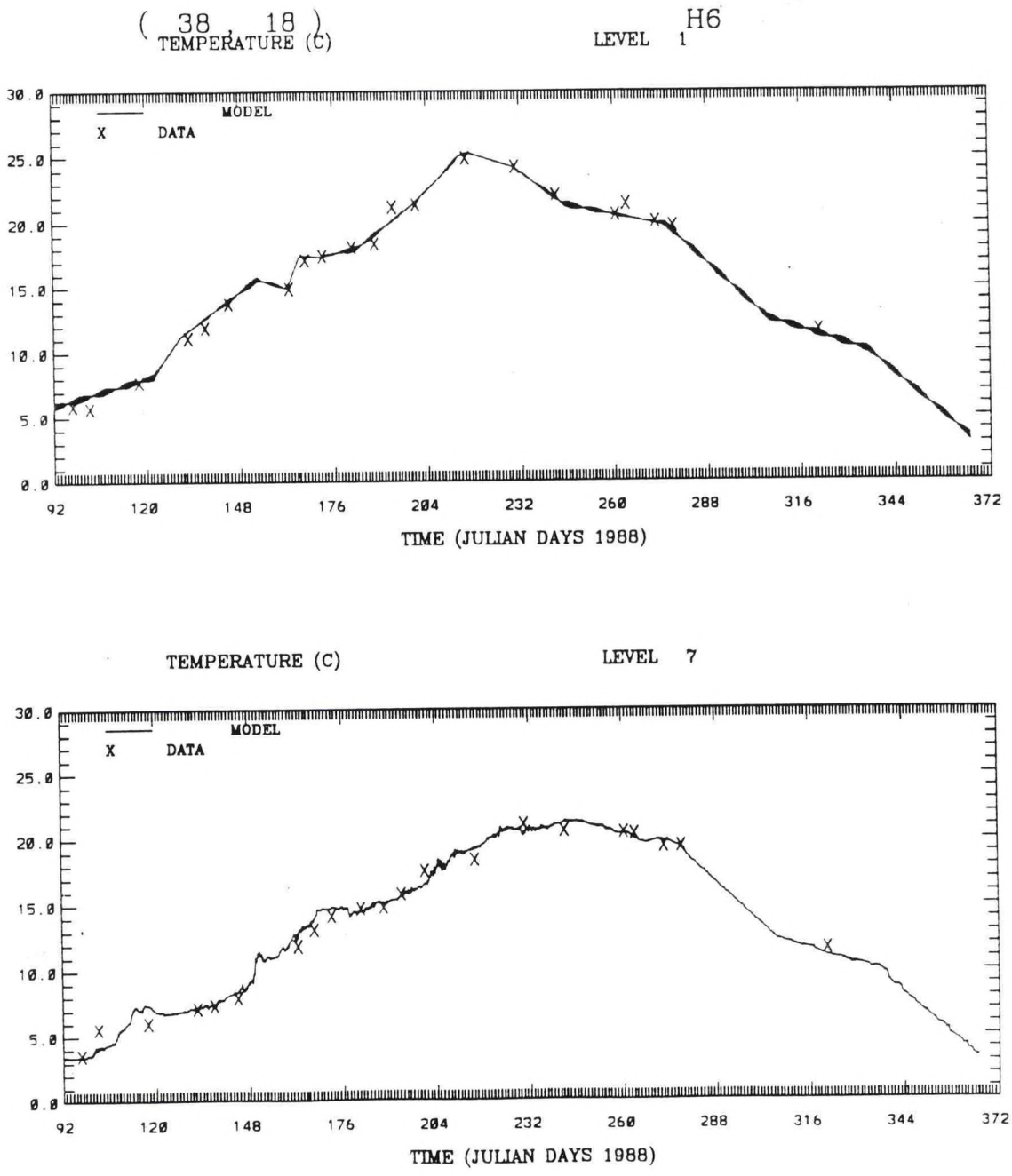

Figure 6.28. Simulated Near Surface and Near Bottom Temperature Time Series During the Calibration Period At Station: H6

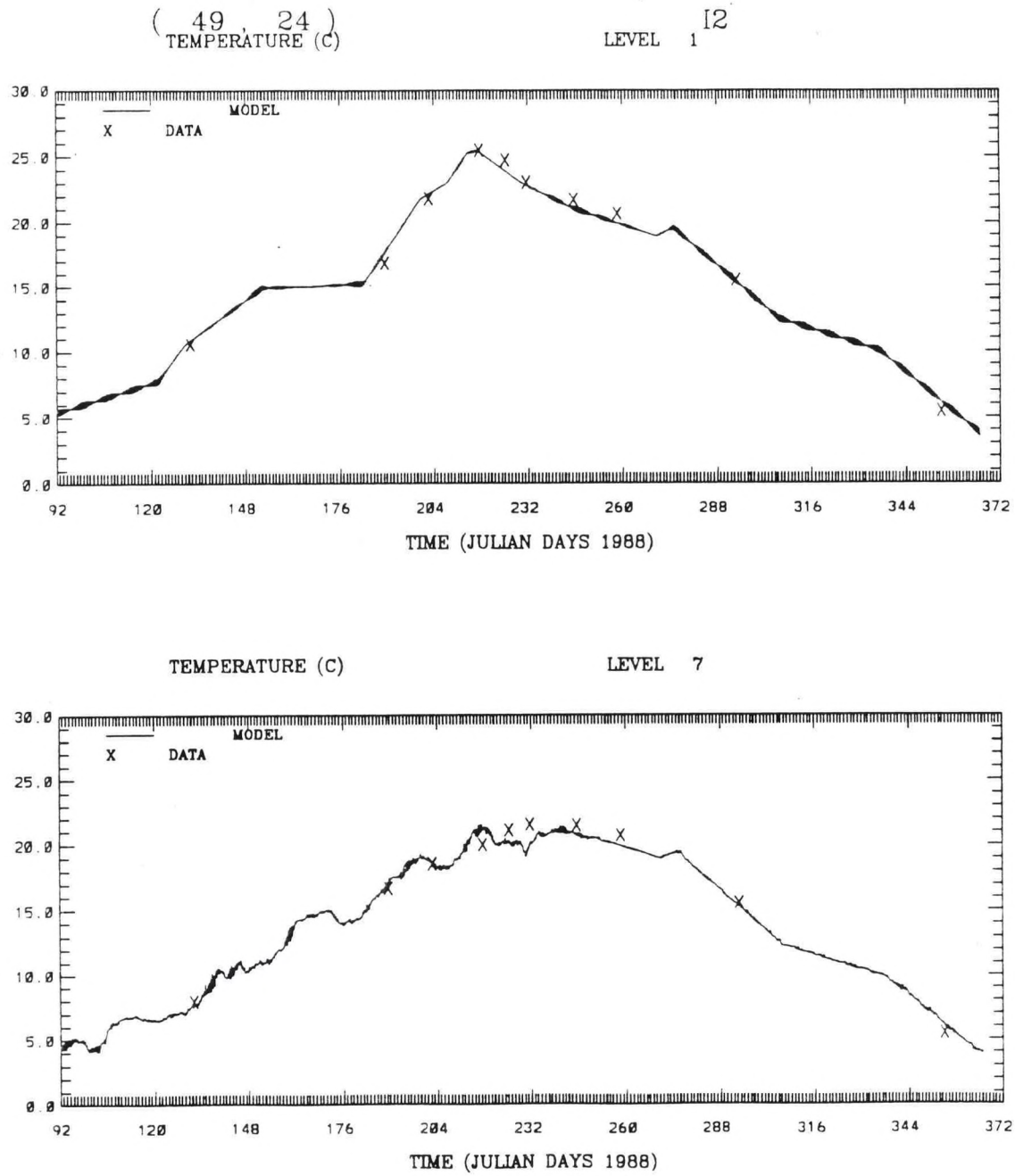

Figure 6.29. Simulated Near Surface and Near Bottom Temperature Time Series During the Calibration Period At Station: I2

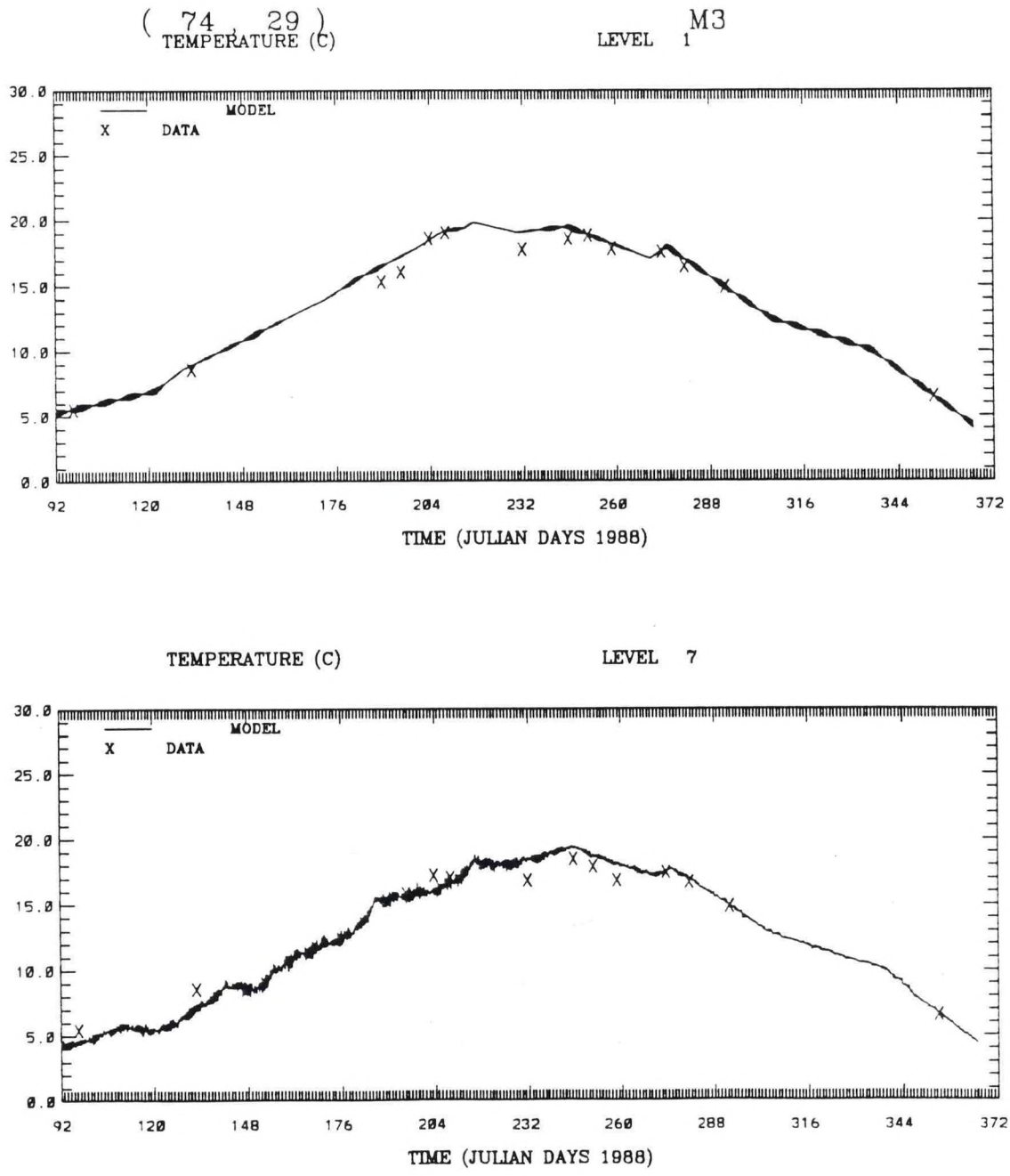

Figure 6.30. Simulated Near Surface and Near Bottom Temperature Time Series During the Calibration Period At Station: M3

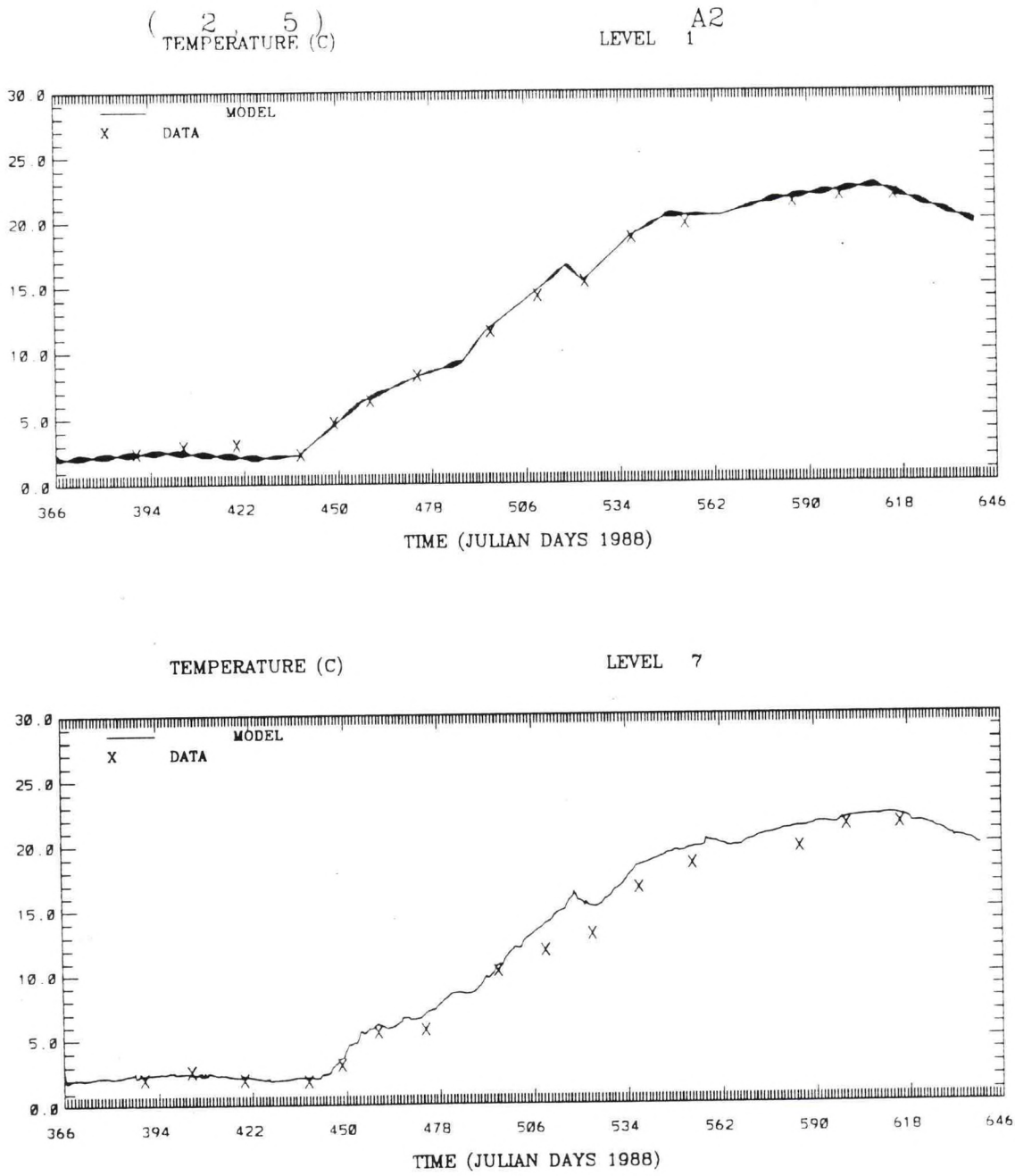

Figure 6.31. Simulated Near Surface and Near Bottom Temperature Time Series During the Verification Period At Station: A2

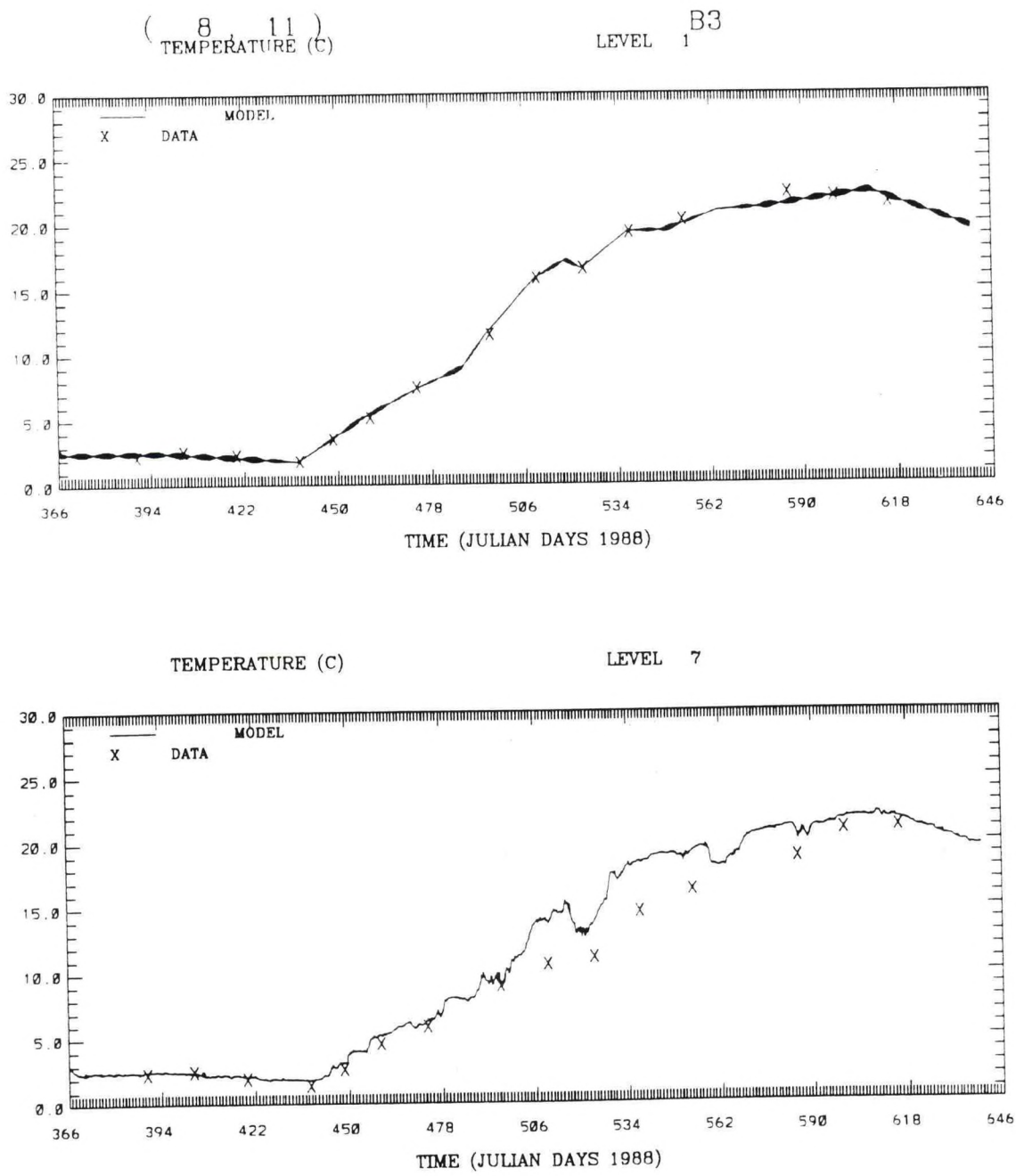

Figure 6.32. Simulated Near Surface and Near Bottom Temperature Time Series During the Verification Period At Station: B3

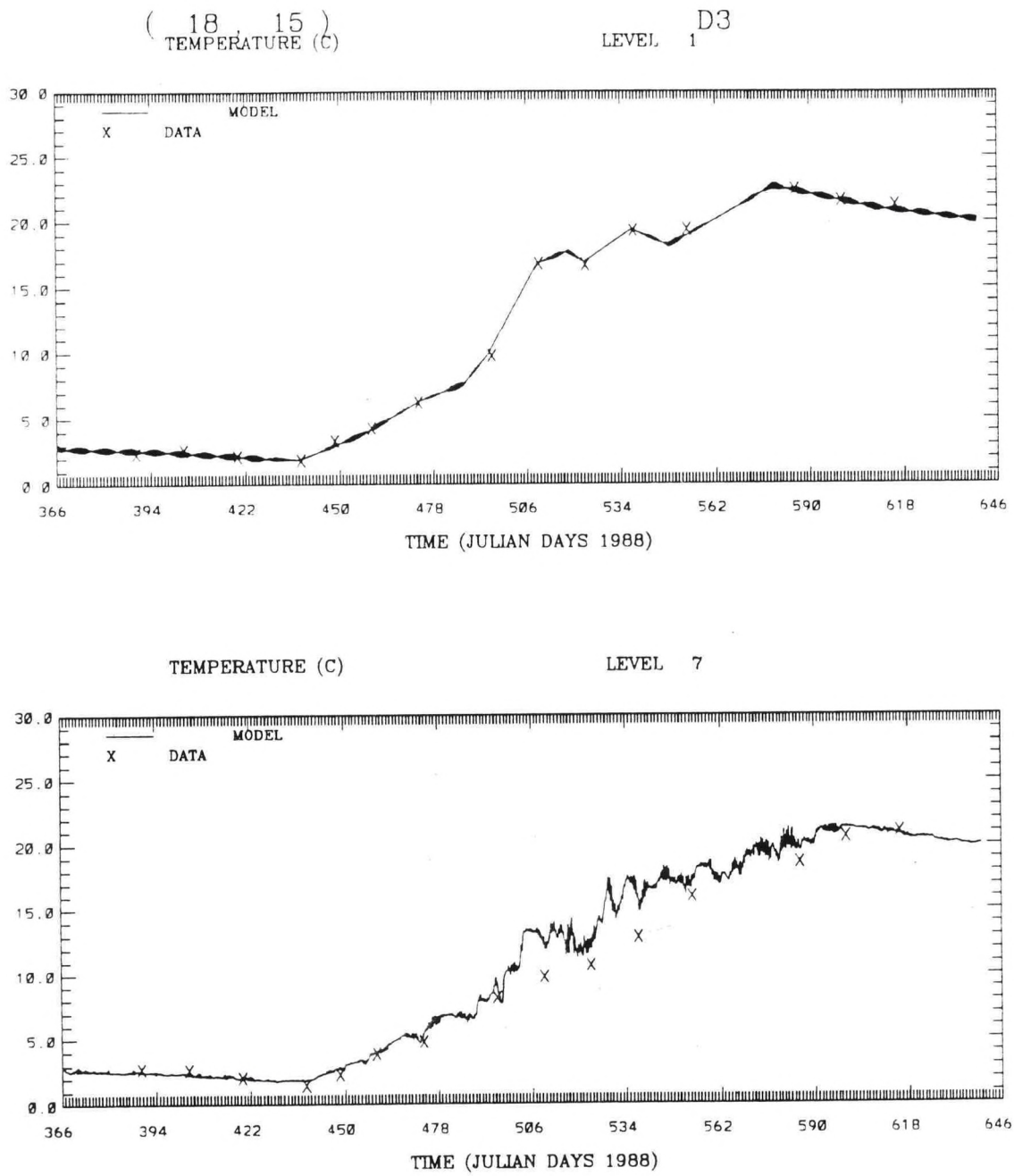

Figure 6.33. Simulated Near Surface and Near Bottom Temperature Time Series During the Verification Period At Station: D3

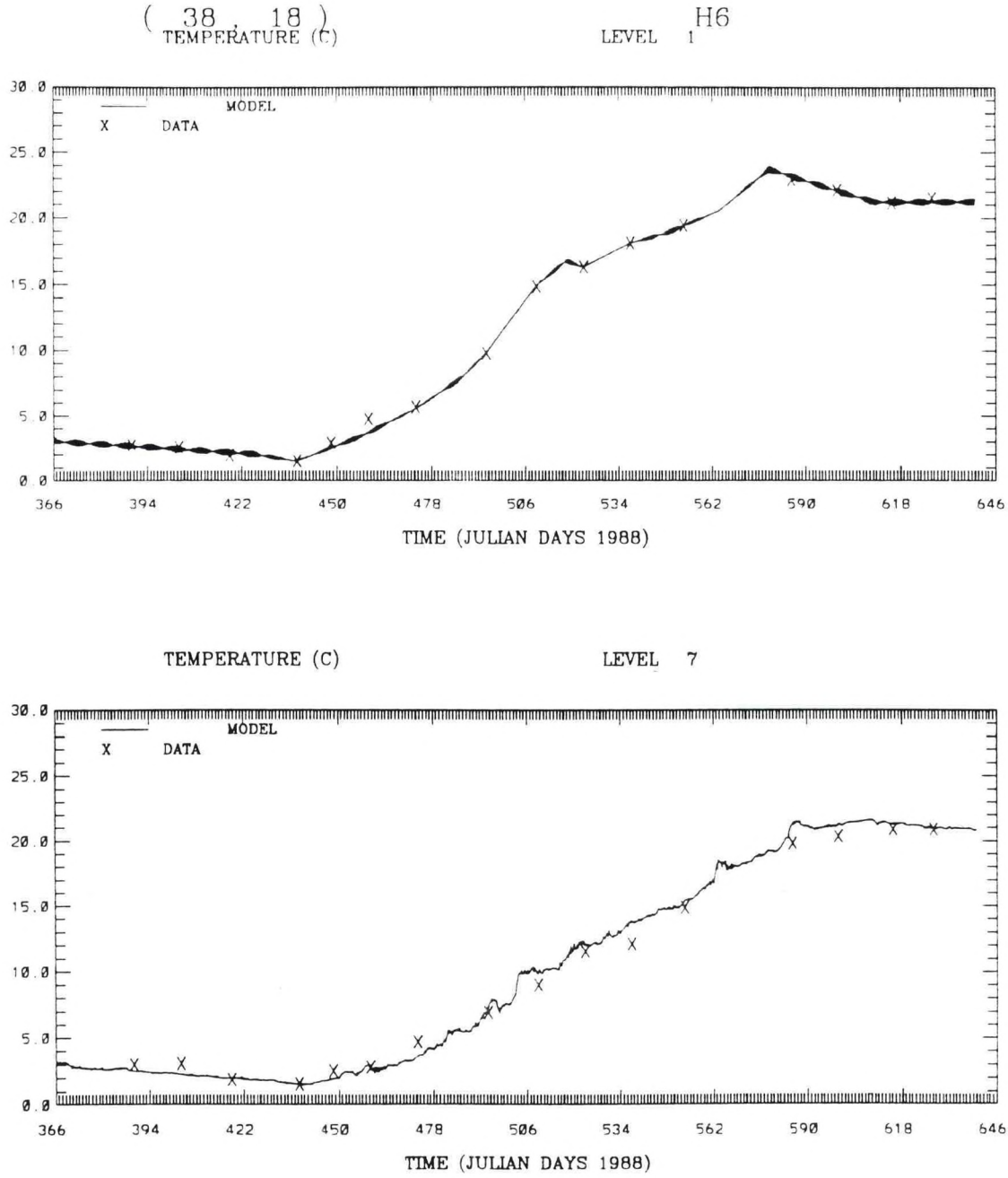

Figure 6.34. Simulated Near Surface and Near Bottom Temperature Time Series During the Verification Period At Station: H6

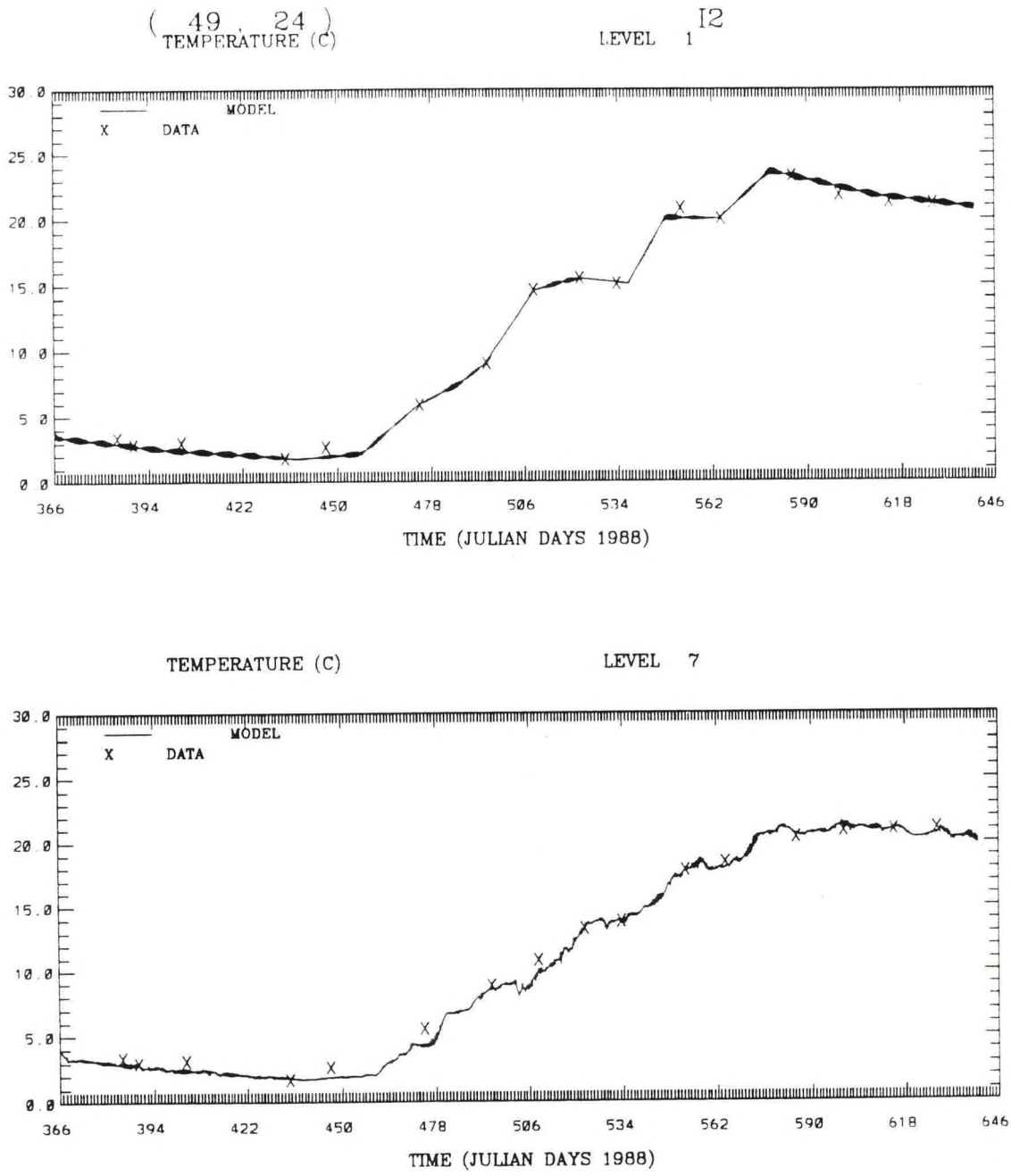

Figure 6.35. Simulated Near Surface and Near Bottom Temperature Time Series During the Verification Period At Station: I2

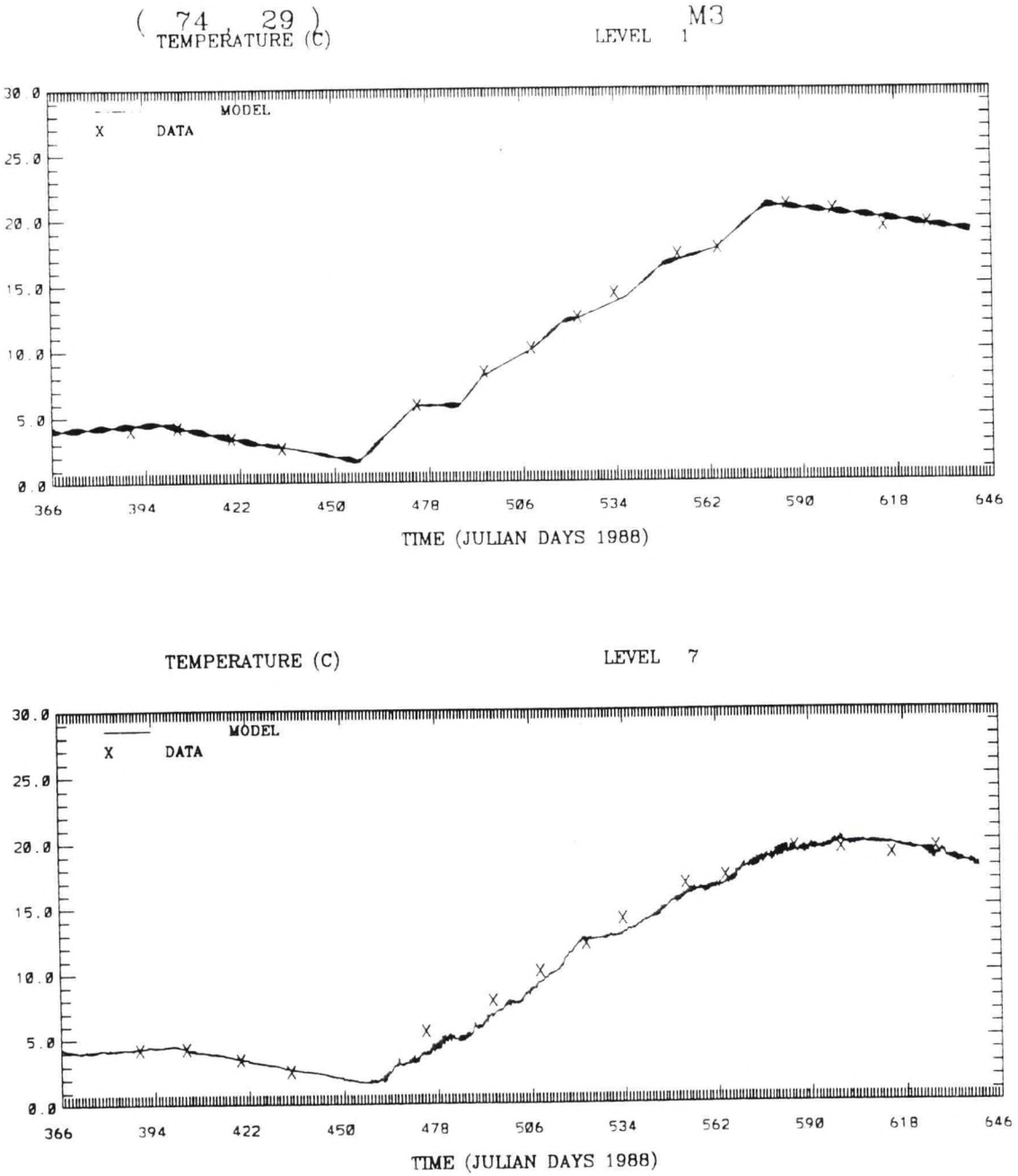

Figure 6.36. Simulated Near Surface and Near Bottom Temperature Time Series During the Verification Period At Station: M3

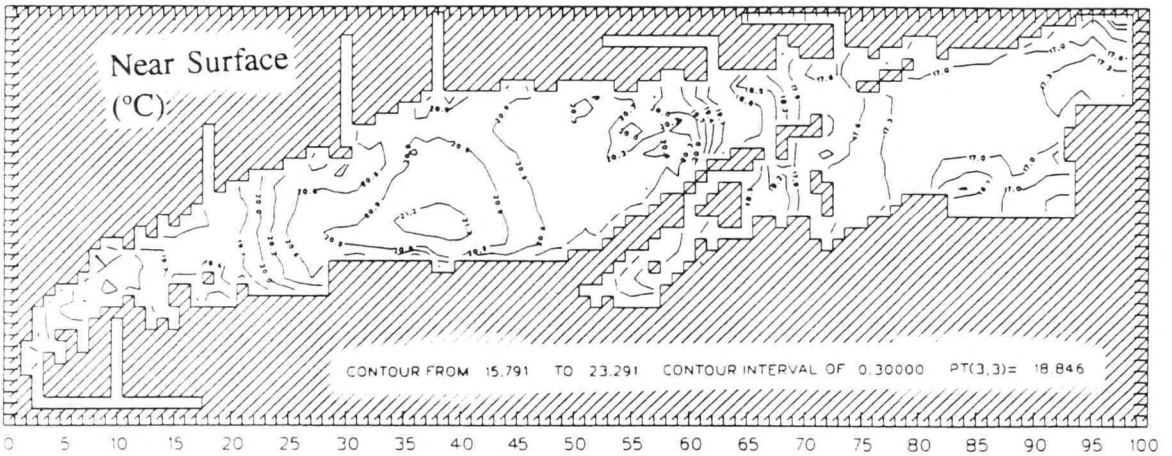

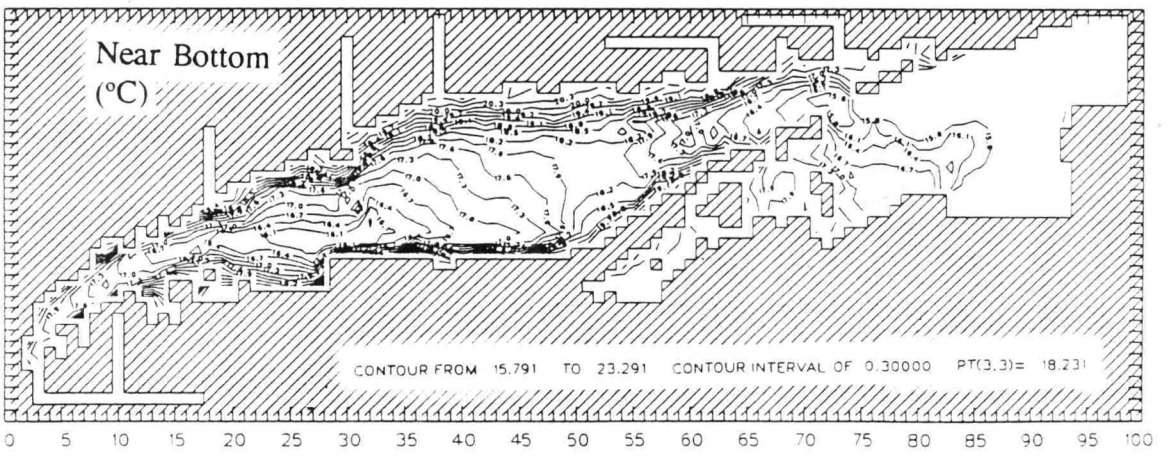

Figure 6.37. Simulated Near Surface and Near Bottom Temperature Fields: July 1988

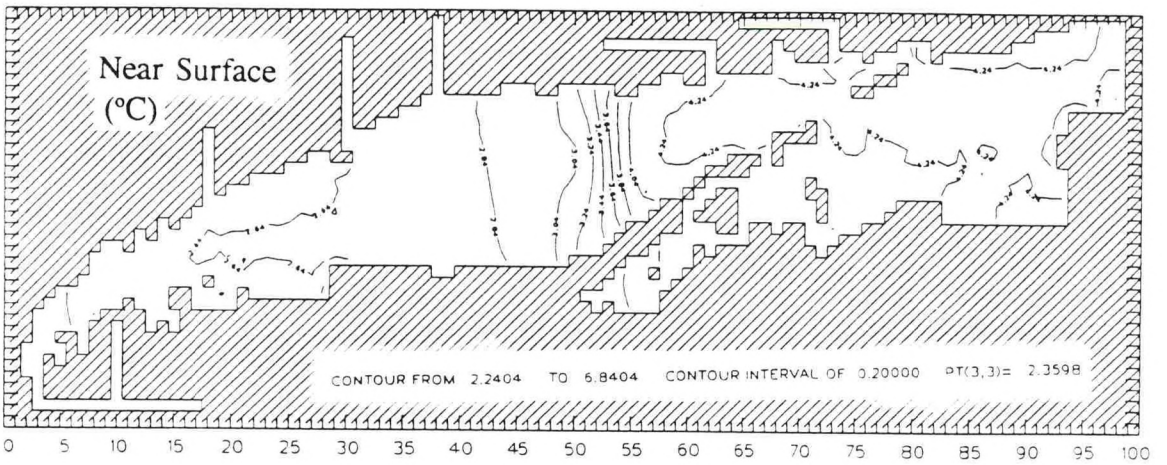

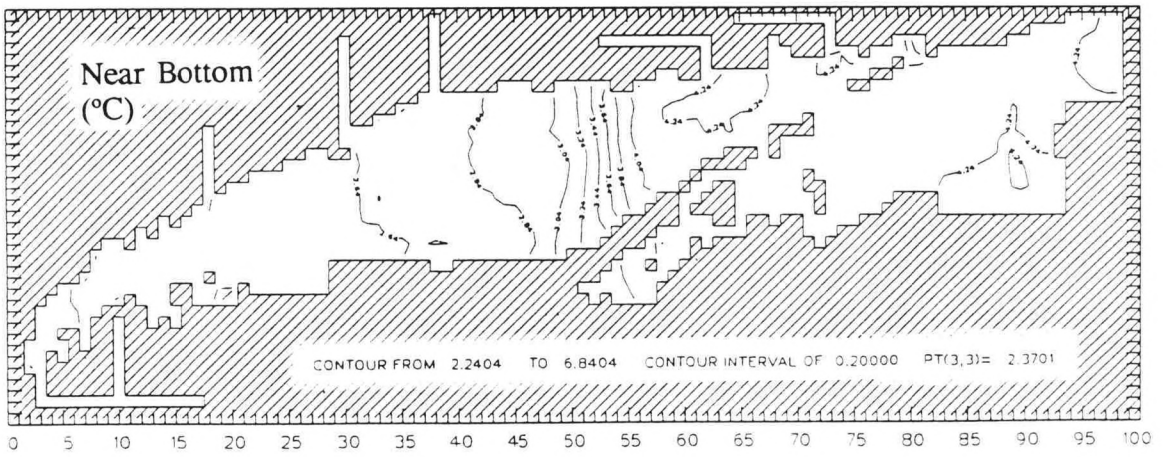

Figure 6.38. Simulated Near Surface and Near Bottom Temperature Fields: January 1989

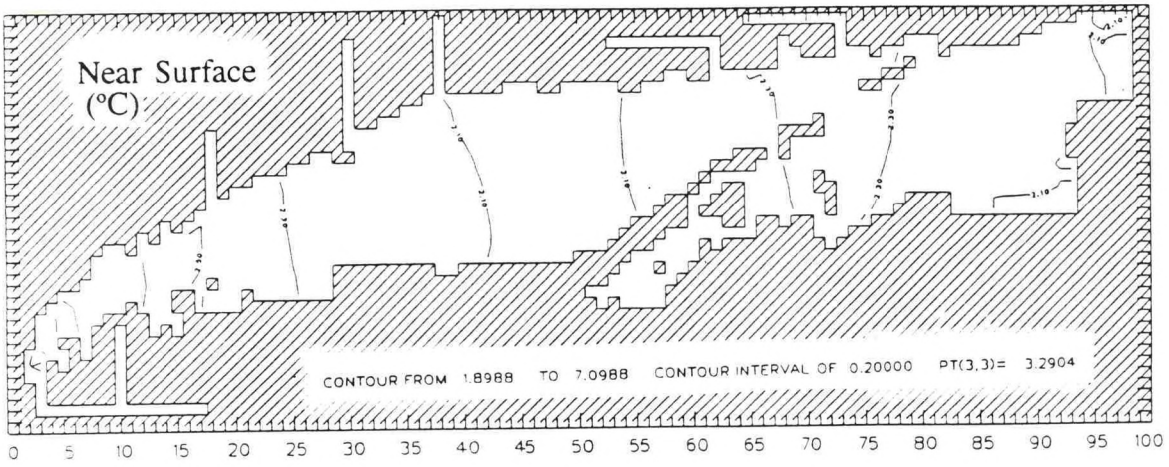

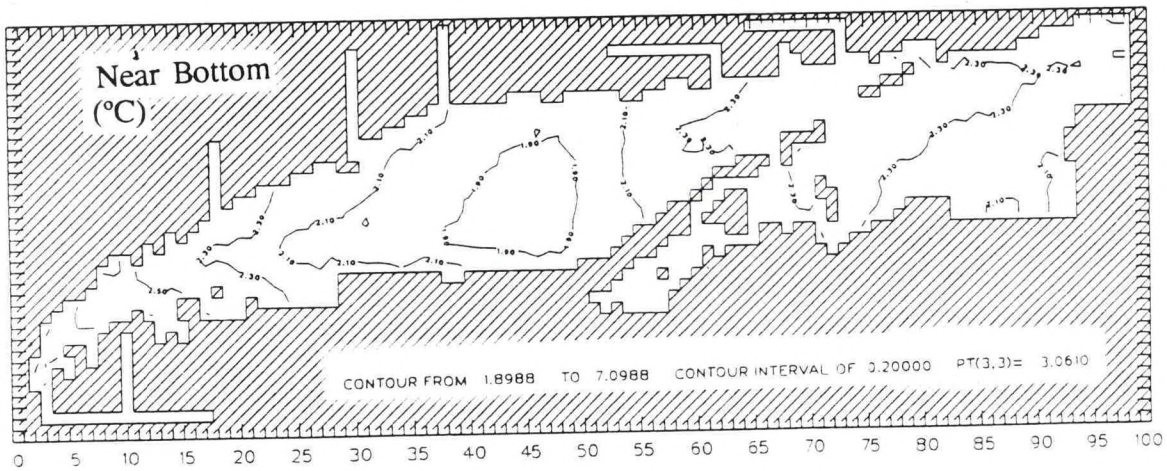

Figure 6.39. Simulated Near Surface and Near Bottom Temperature Fields: March 1989

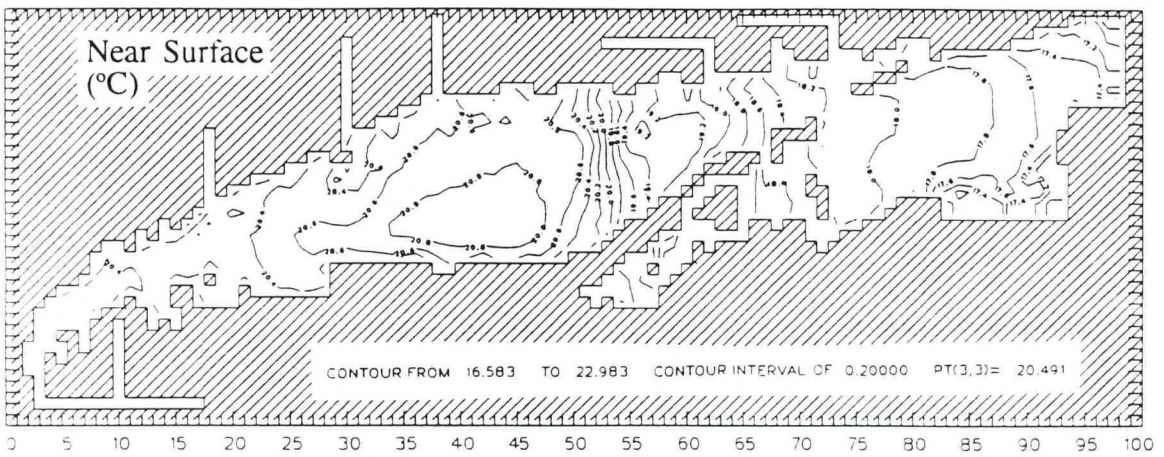

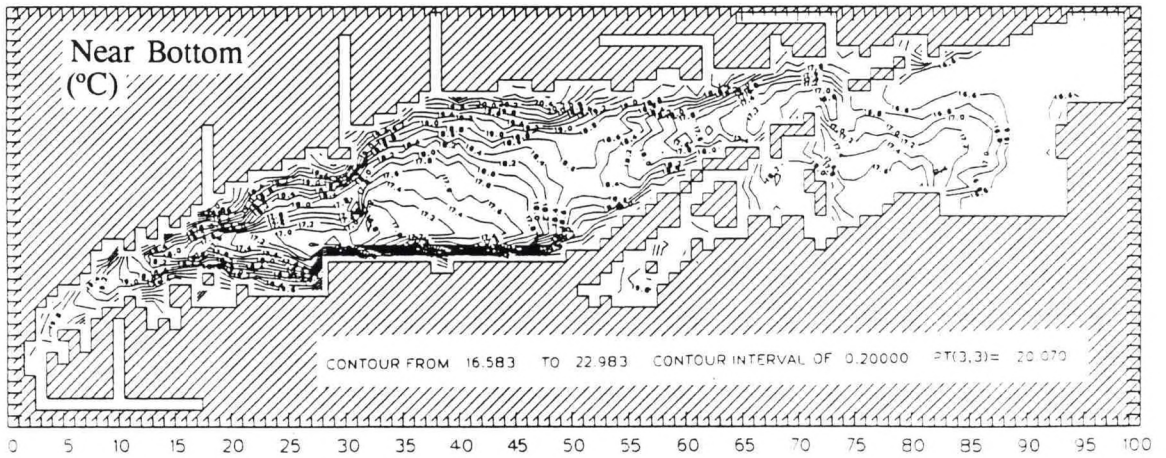

Figure 6.40. Simulated Near Surface and Near Bottom Temperature Fields: July 1989

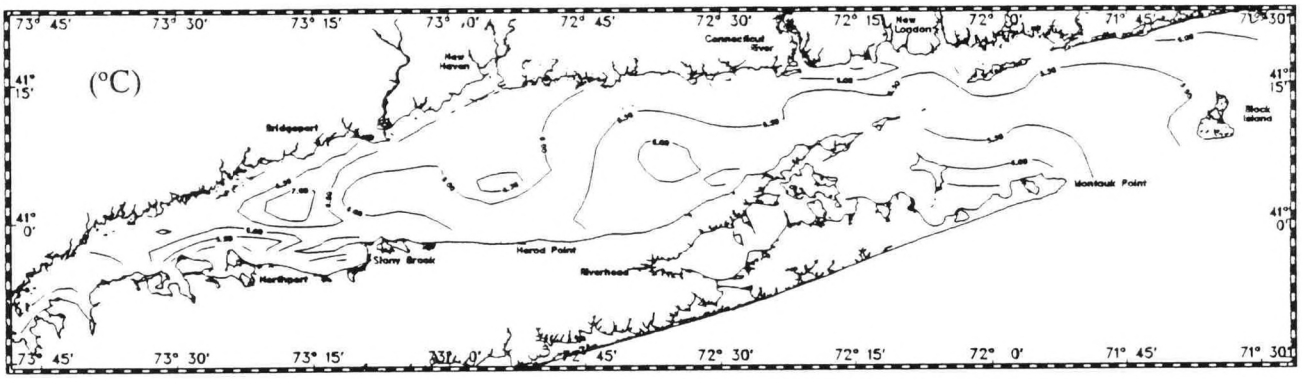

April 4 - 7, 1988

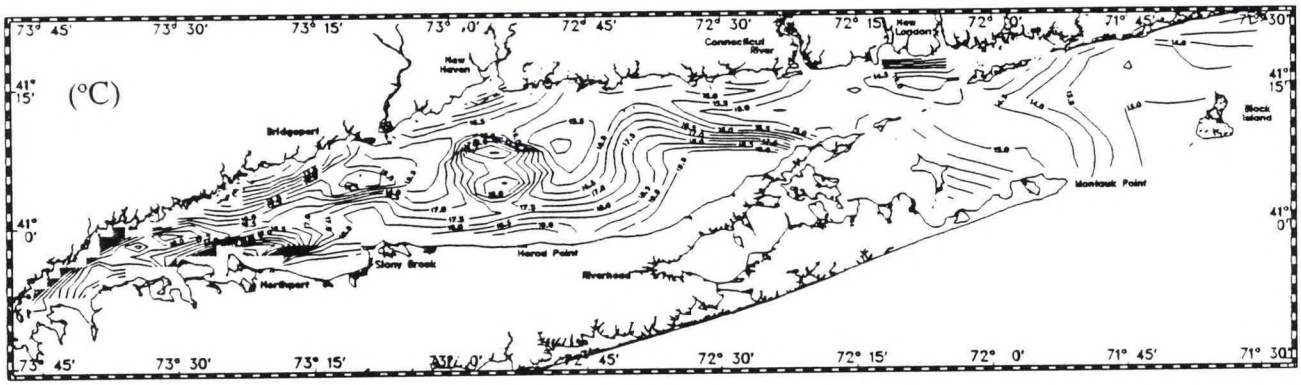

June 13 - 16, 1988

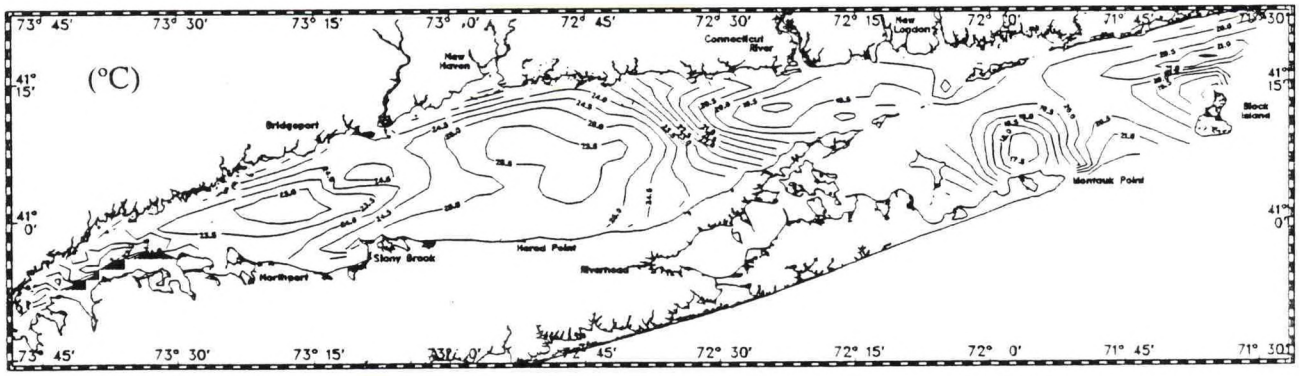

August 2 - 4, 1988

Figure 6.41. Observed Near Surface Temperature Fields: April 4-7, June 13-16, and August 2-4, 1988

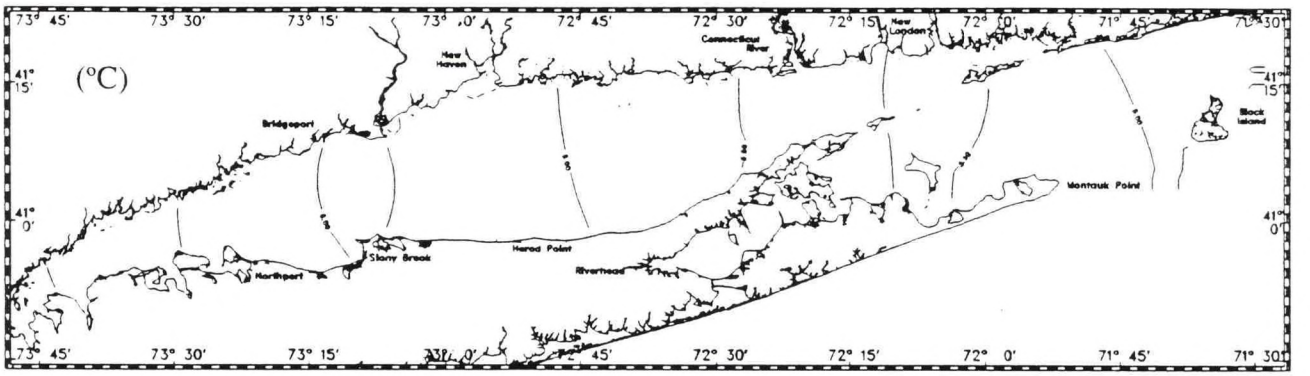

April 4 - 7, 1988

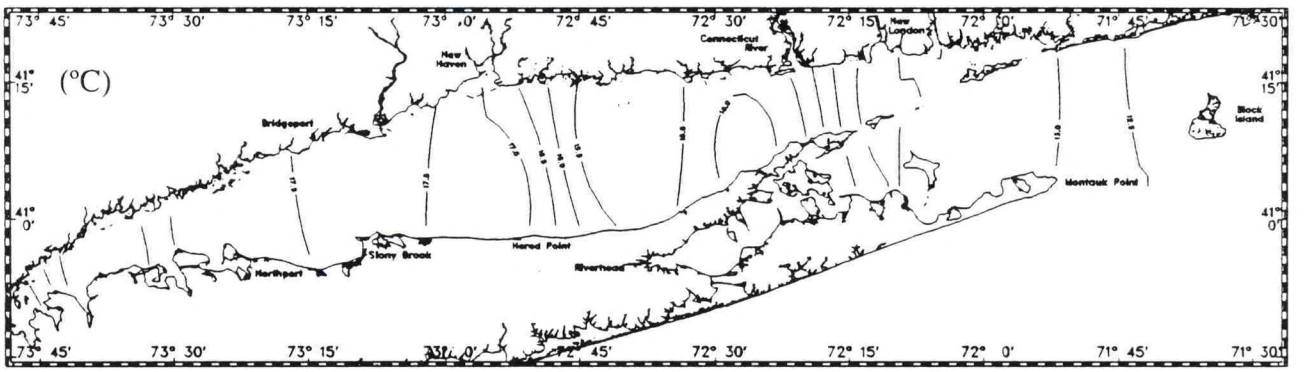

June 13 - 16, 1988

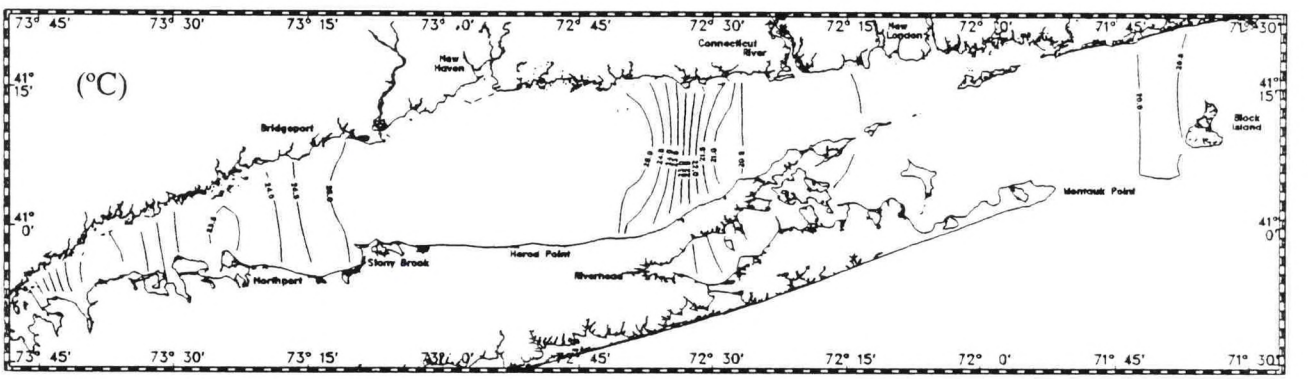

August 2 - 4, 1988

Figure 6.42. Simulated Near Surface Temperature Fields: April 4-7, June 13-16, and August 2-4,1988

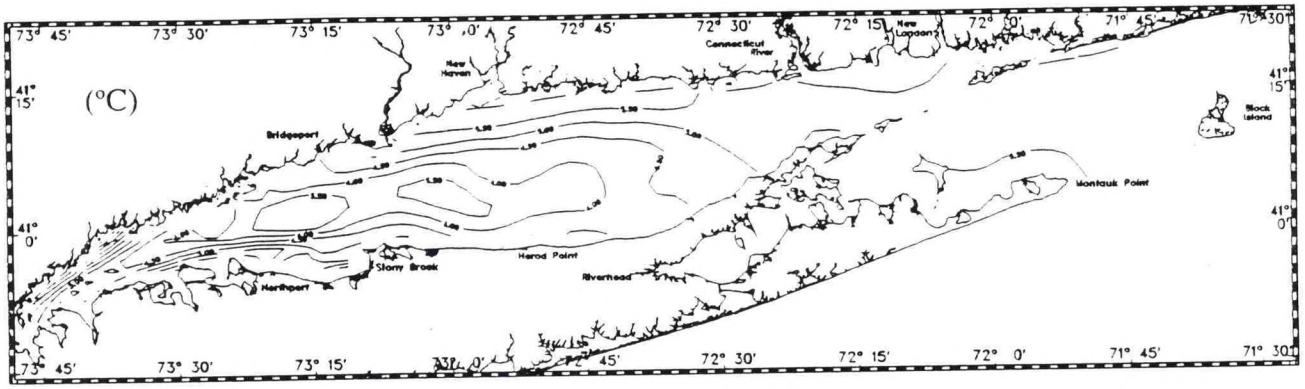

April 4 - 7, 1988

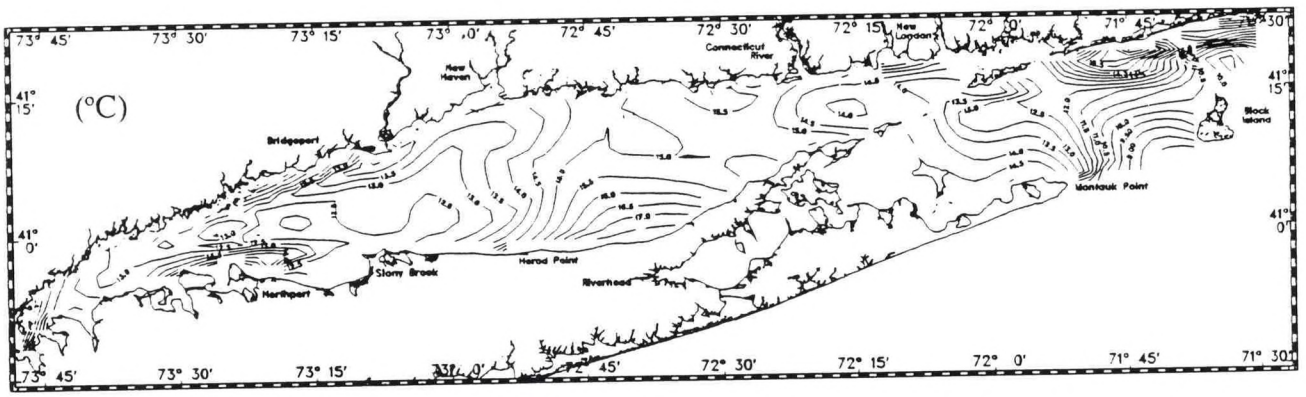

June 13 - 16, 1988

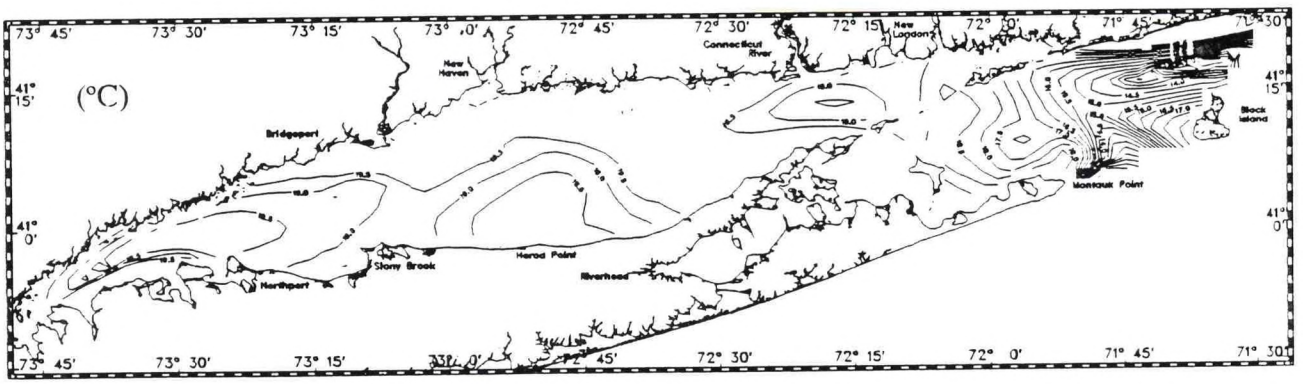

August 2 - 4, 1988

Figure 6.43. Observed Near Bottom Temperature Fields: April 4-7, June 13-16, and August 2-4, 1988

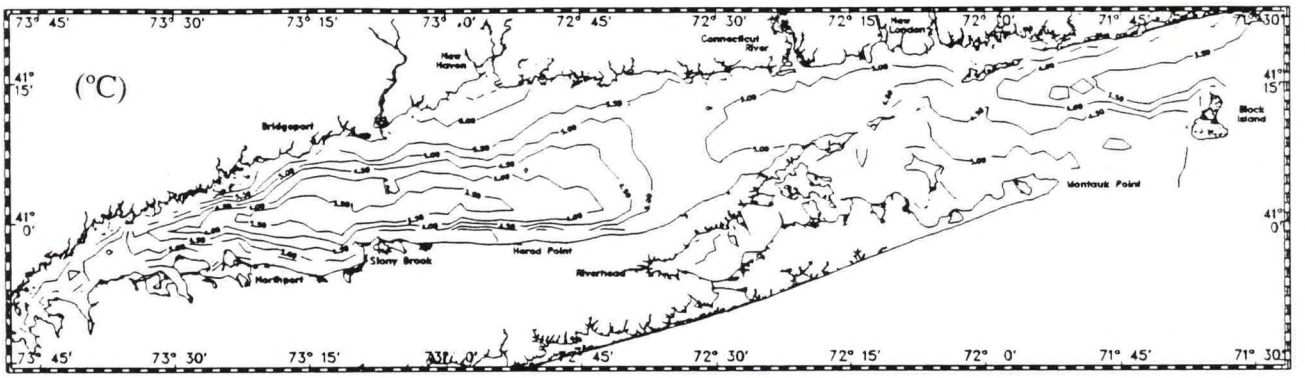

April 4 - 7, 1988

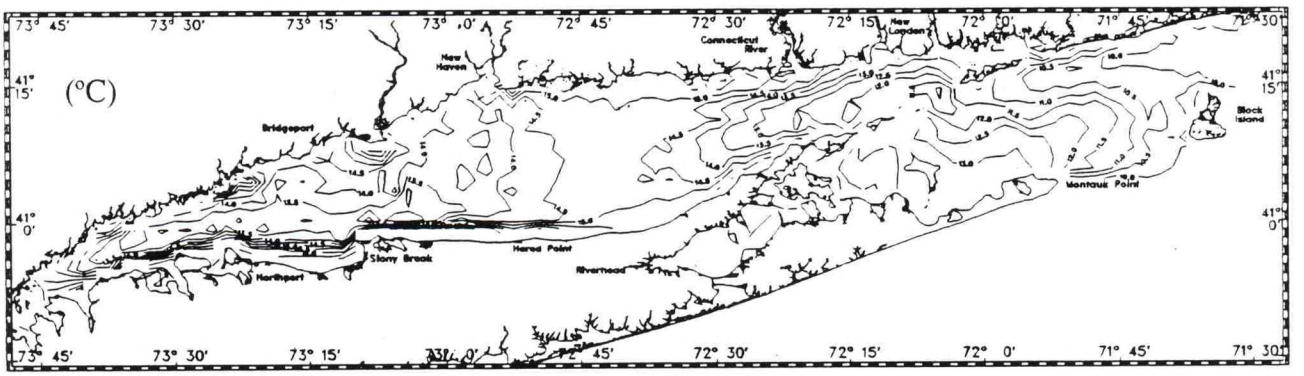

June 13 - 16, 1988

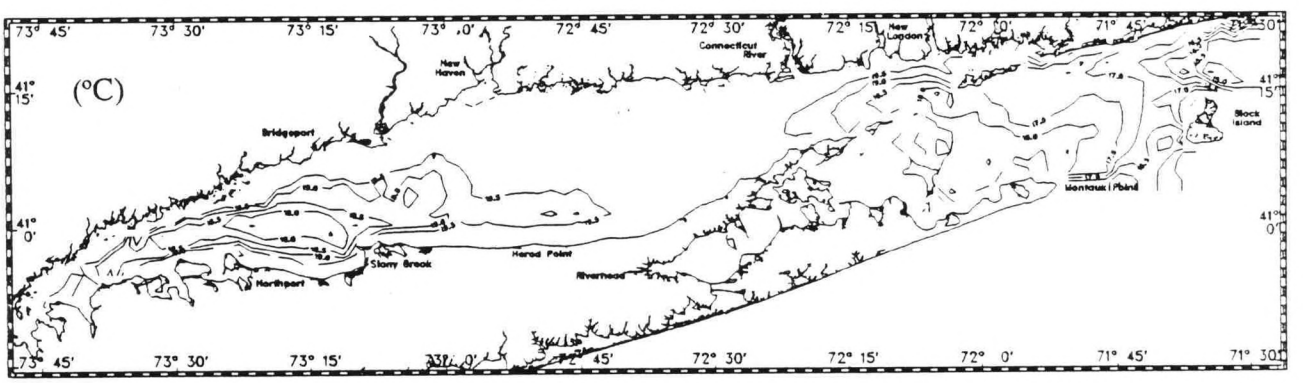

August 2 - 4, 1988

Figure 6.44. Simulated Near Bottom Temperature Fields: April 4-7, June 13-16, and August 2-4,1988

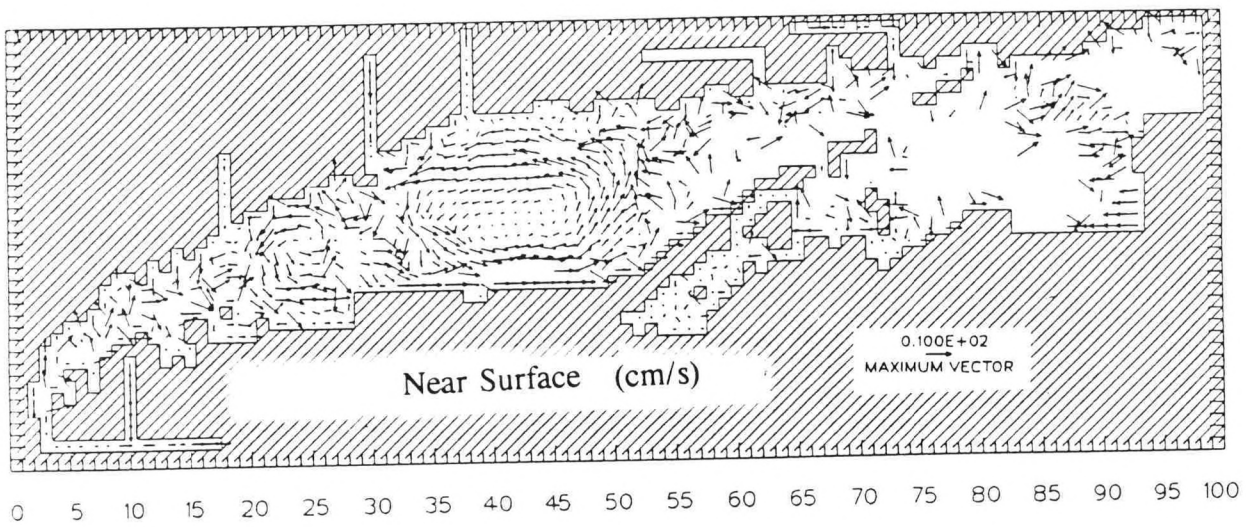

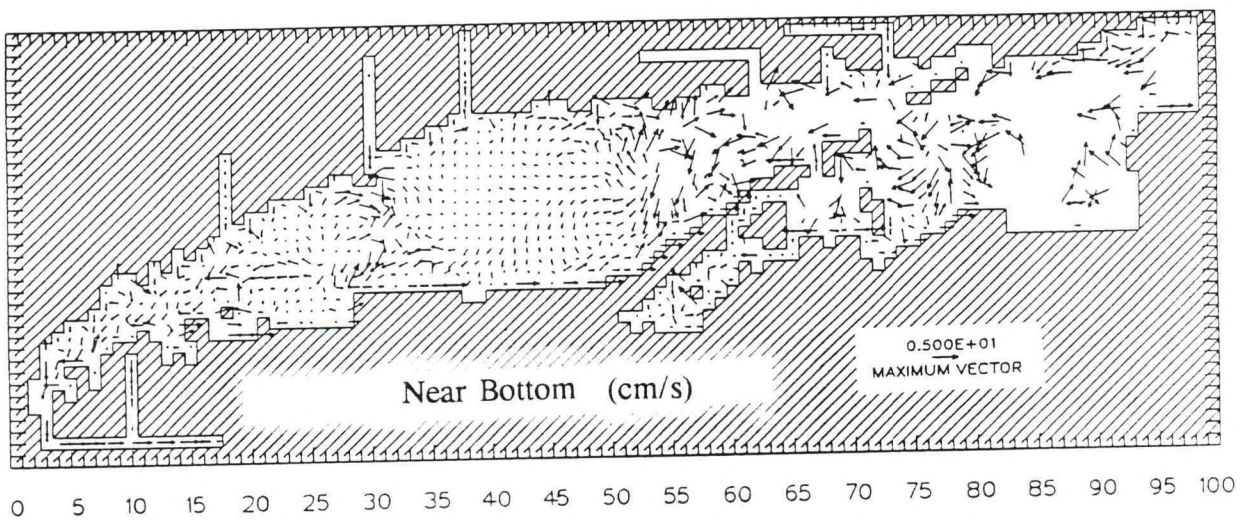

Figure 6.45. Simulated Near Surface and Near Bottom Astronomic Tide and Density Residual Circulation Fields (April 1988)

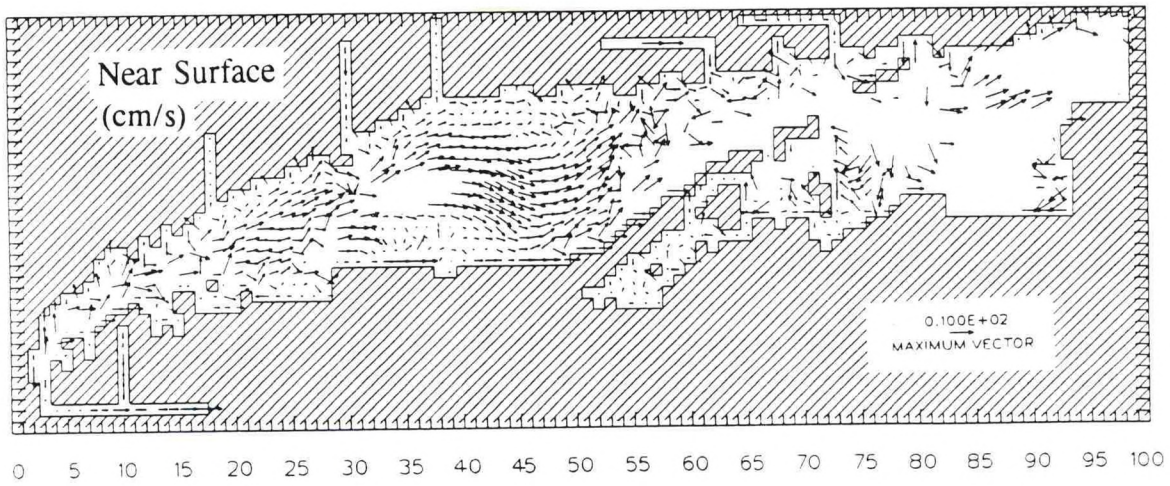

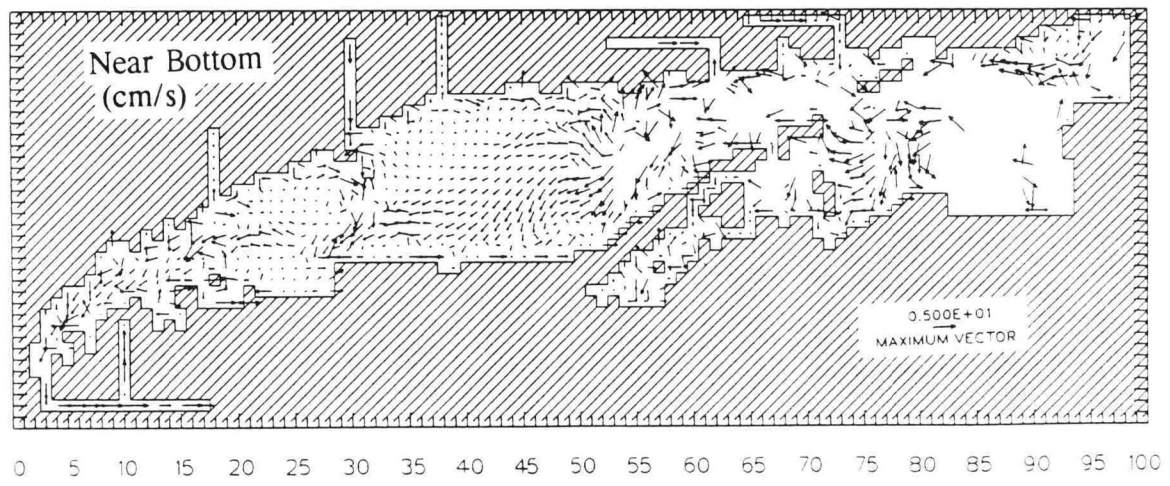

Figure 6.46. Simulated Near Surface and Near Bottom Residual Circulation: July 1988

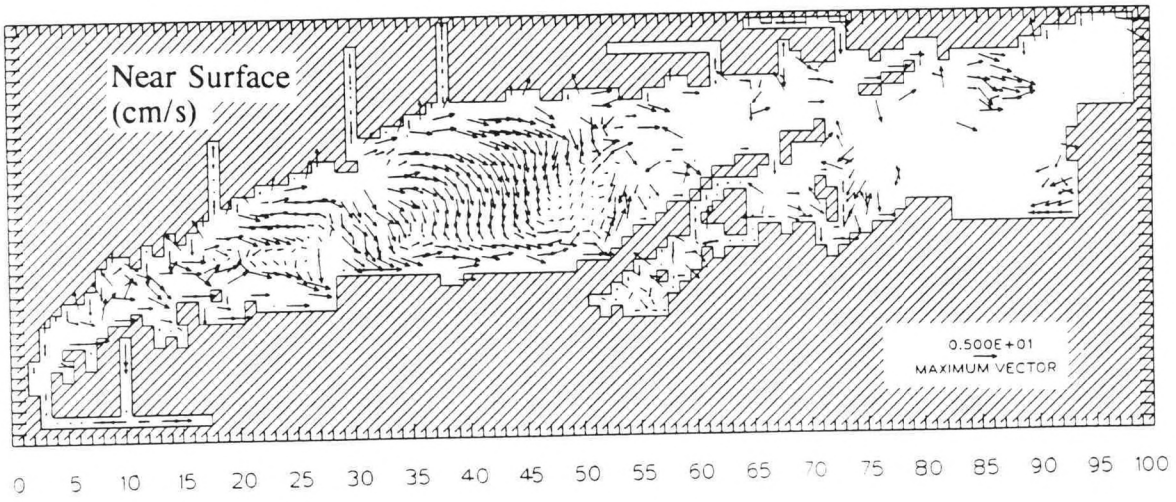

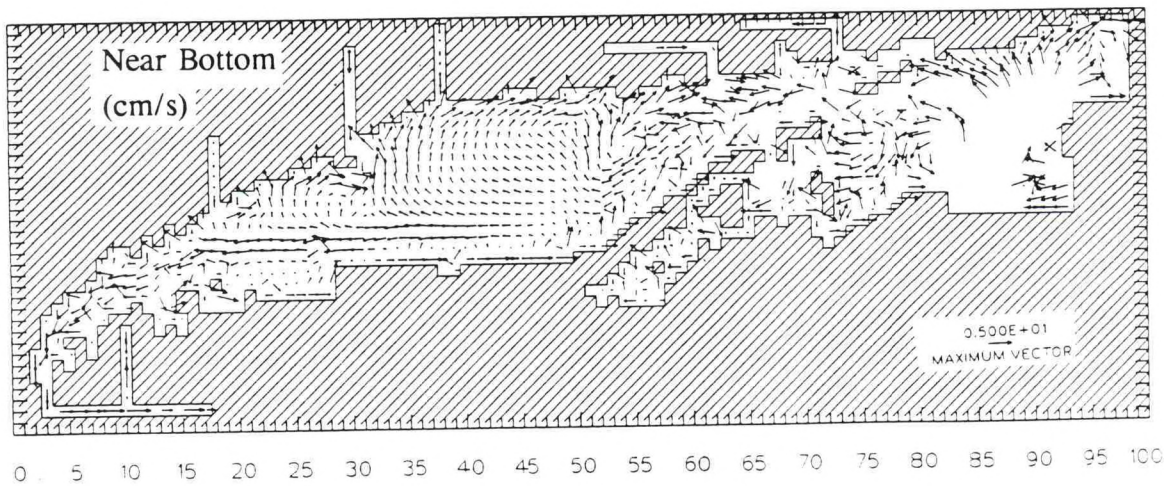

Figure 6.47. Simulated Near Surface and Near Bottom Residual Circulation: January 1989

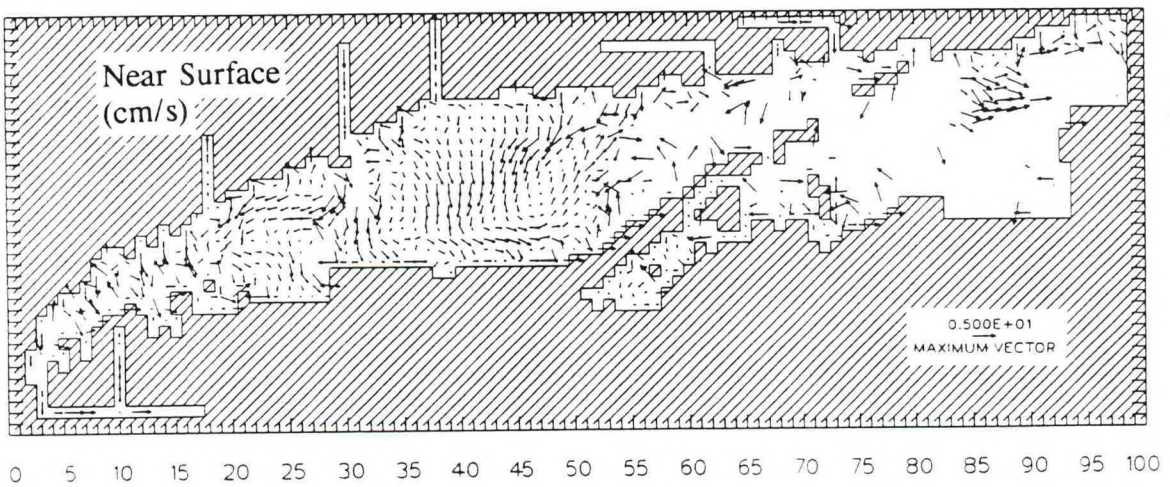

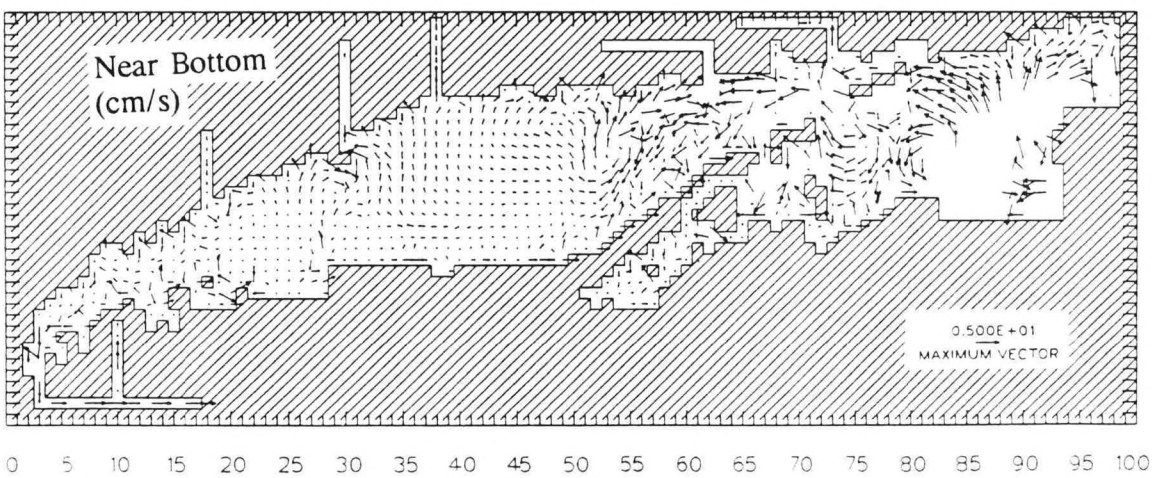

Figure 6.48. Simulated Near Surface and Near Bottom Residual Circulation: March 1989

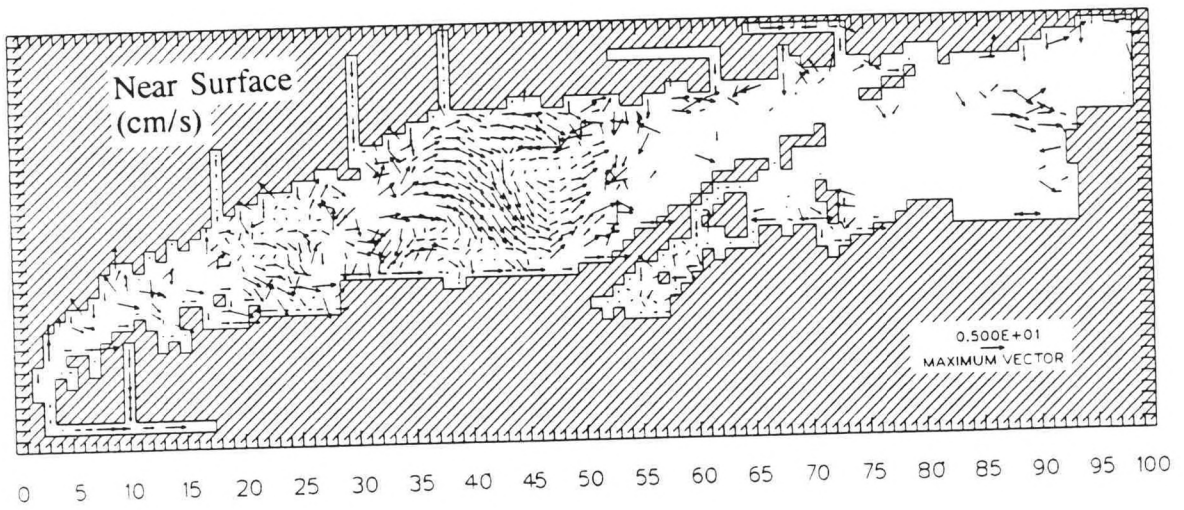

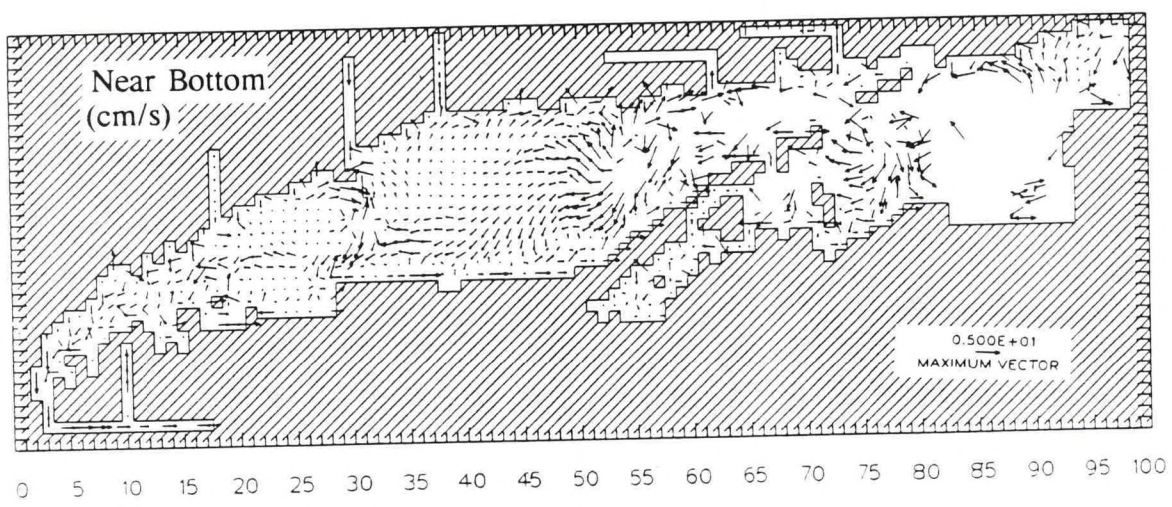

Figure 6.49. Simulated Near Surface and Near Bottom Residual Circulation: July 1989

7. CONCLUSIONS AND RECOMMENDATIONS

Here, we summarize and assess the data (observational and model forcing) and the overall ability of the hydrodynamic model to simulate conditions in Long Island Sound. Possible additional observational and model studies are recommended.

7.1. Data Assessment

Originally, only the period April - September 1988 was intended to be studied with CTD and CT, water level, current meter (bottom-mounted and towed ADCP), meteorological, and Sound inflow measurements. In order to further study the evolution and erosion of the pycnocline, the measurement program was extended an additional year until September 1989. Thus the evolution and erosion effects could be investigated for two successive Spring - Summer - Fall cycles. In addition, it was possible to obtain ADCP measurements at nine additional stations, in order to better define the residual circulation characteristics in the Sound. Additional ADCP stations 1 and 2 have been used to define nontidal flux targets in the East River.

Salinity and Temperature Data

CTD measurements were made during the extension at only the master stations along the thalweg of the Sound. North - south lateral sections were no longer occupied. CTD measurements were continued along the open ocean boundary in Block Island Sound but at less frequent intervals (monthly). CTD measurements made by New York City, Department of Conservation, were plagued by high concentrations of metals in the water column, making the determination of conductivity, and hence salinity, problematical. As a result, additional near surface amd bottom measurements in the vicinity of The Battery, NY, were used and correlated to Hudson River flow by EPA and supplied to NOS. Measurements at Spuyten Duyvil, NY, were also available at only two depths in the water column. These measurements are adequate to provide representative monthly variations in salinity and temperature at The Battery, NY, and Spuyten Duyvil, NY, but cannot be used to develop realistic vertical profiles during periods of significant stratification in either salinity (due to high river flows) or temperature (during the late spring and summer).

Water Surface Elevation Data

Hourly water level residuals determined at The Battery, NY, were transferred in unaltered form to Spuyten Duyvil, NY, further up the Hudson River. The long term solar semi- and solar annual, *Ssa* and *Sa*, tidal constituents determined at The Battery, NY, were assumed to hold at Spuyten Duyvil, NY. The mean sea level at Spuyten Duyvil, NY, was determined from only 1 month rather than over the full 18.6 year tidal epoch. On the open ocean boundary, water level residuals at Montauk, NY, were transferred to the other open boundary signals. The mean sea level at Point Judith, RI was assumed equal to the mean sea level at Newport, RI as determined over the full tidal epoch. Water level stations were also occupied at locations between the model boundaries and over the complete measurement period. Spatial and temporal coverage was

sufficient to determine and further advance tidal elevation characteristics in Long Island and Block Island Sounds.

Current Meter Data

In order to cover the entire Sound, ADCP instruments were deployed at most stations for approximately 35 days. Only at ADCP Station 1 near Throgs Neck, NY, were extensive current measurements made over the entire eighteen month measurement period. Due to the asymmetry noted in the towed ADCP sections above Throgs Neck, NY, a single ADCP is insufficient to resolve the lateral variations in flow. Thus the nontidal flux in the upper East River cannot be estimated from currently available ADCP measurements to within 400 - 500 m^3/s. Stations were occupied long enough to perform 29 day harmonic analyses of tidal currents and to estimate residual currents over approximately one month. These months were obviously not the same at all stations. Spatial coverage was sufficient to further confirm and develop characteristics of the tidal currents, particularly with respect to depth, in Long Island and Block Island Sounds. The high degree of variability in both tidal and residual currents was confirmed throughout the Sound particularly in the vicinity of The Race.

Meteorological and Inflow Data

Wind speed and direction were analyzed at only LaGuardia, NY, and assumed to represent conditions over the entire extent of the Sound. Barometric pressure anomalies were not considered. Hourly data were available throughout the eighteen month period but only to the nearest ten degrees in direction. River flow information were available on an average daily basis. Sewage treatment plant inflows were assumed constant, while combined sewer overflows were updated monthly. The total amount of freshwater entering the Sound was well represented. The short term temporal dynamics of storm events could not be accounted for in this methodology.

7.2. Model Assessment

In assessing the model's ability to simulate conditions in Long Island Sound, it is important to keep the intended use of the model in mind. The model grid was constructed as a 2 km square rectangular grid with seven vertical levels to allow long term simulation on presently available supercomputers (CRAY-YMP2/216). The East and Harlem Rivers are included in the present computational grid as one-dimensional sections. In the vicinity of the confluence of the East River and western Long Island Sound, geometrics are distorted due to the grid folding and only 3-4 grid cells cover the North-South width of the Sound. Grid resolution horizontally is insufficient in the vicinity of CTD stations A1 and A2 and ADCP Stations 1 and 4. In the highly energetic, topographically complex region near The Race, the 2 km grid resolution is not adequate to locally characterize tidal and residual flows. In the vertical, seven levels are employed in a sigma coordinate system. The first two layers represent one tenth of the water column. In the deeper regions of the Sound, the layer thicknesses approach 5 - 7 m and may not be adequate to resolve the surface mixed layer and near surface thermocline structure. In most of the Sound, the upper level thicknesses are on the order of 2 - 3 m and are adequate to resolve

general thermocline structure. Clearly, greater horizontal grid resolution is desirable, albeit at the expense of computer resources. The present grid represents a compromise between efficiency of long-term computation over a large water body (Long Island and Block Island Sounds) and higher spatial resolution.

Using the present grid, tidal heights are in agreement order 10 cm and thus volumetrics are adequate. Tidal currents and residual current comparisons at points or stations are more problematic. Overall residual current characteristics are in agreement with known patterns and appear to be reasonable. Salinity and temperature vertical profiles agree with CTD data collected by SUNY and UCONN to order 0.6 psu and 0.7 °C, respectively, and simulated horizontal distributions are in agreement with known spatial patterns. Thermocline and halocline evolution and erosion are adequately represented in the model for water quality investigations. Simulated East River nontidal fluxes at the confluence of western Long Island Sound average approximately 300 m^3/s into the river during the eighteen month period, April 1988 - September 1989. A two layer flow pattern is developed in the one-dimensional section of the model grid in agreement with known behavior in the upper East River. The magnitude of the nontidal fluxes are in agreement with EPA flux targets to within 100 m^3/s during the calibration period April - August 1989.

7.3. Additional Observational and Numerical Studies

In order to further refine observational estimates of nontidal fluxes within the East and Harlem River tidal straits, it is recommended that additional ADCP studies be undertaken. In the vicinity of North College Point and South Clason, three bottom mounted ADCP systems should be deployed across the East River. Each ADCP unit should also contain a pressure sensor in order to provide for non-ambiguous location of the recorded velocities in the vertical. Additional CTD measurements using refined instrument systems, which account for the presence of heavy metals in the water column, should be performed to provide for accurate determination of salinity in the East and Harlem Rivers. A Physical Oceanographic Real-time System (PORTS) concept might be developed for the East and Harlem River system. Bottom mounted ADCP with pressure sensors and ancillary meteorological measurements (wind speed, wind direction, barometric pressure, air temperature, surface water temperature, and relative humidity) should be made at The Battery, Spuyten Duyvil, Hell Gate, and Willets Point, NY. In addition, permanent water level measurement stations should be installed at Spuyten Duyvil, NY, and at Hell Gate, NY. Additional leveling lines should be run in order to more accurately determine vertical control between The Battery, Spuyten Duyvil, and Willets Point, NY. In order to address these issues, EPA is in the process of developing a long term monitoring program as part of a comprehensive Sound-wide water quality management plan.

The present computational grid provides a reasonable description of the general circulation patterns throughout Long Island Sound. Two areas of particular interest suggest nested refined curvilinear grids. Area one concerns the role of the Connecticut River plume in the overall salinity structure. While present model results show the influence of the plume to be confined to the immediate shoreline and propagation to the west in accord with general knowledge,

additonal finer resolution studies are warranted. In particular, an alternate passive constituent equation could be added to the model equation set to represent rhodyamine dye. Dye releases within the Connecticut River could be simulated to further elucidate plume dynamics on both the present and more refined curvilinear grid systems. The second area addresses the interaction between western Long Island Sound and the East-Harlem River tidal straits. It would be highly desirable to develop a refined orthogonal curvilinear coordinate grid extending from the western boundary of the Central Basin of Long Island Sound through the East and Harlem River tidal straits, including the Hudson River and New York Harbor systems. The present rectilinear grid model could be used to provide the Long Island Sound boundary condition. This approach would provide more accurate determination of the nontidal and salt fluxes within the East and Harlem Rivers and between western Long Island Sound than is presently possible. The opportunity would also exist to investigate the influence of the East and Harlem River tidal straits on both western Long Island and the lower Hudson - New York Harbor systems in support of water quality management of New York Harbor.

ACKNOWLEDGEMENTS

This work was performed in conjunction with the joint NOAA - EPA Long Island Sound Study during the period March 1988 to December 1993 within the Coastal and Estuarine Oceanography Branch, Office of Ocean and Earth Sciences under the supervision of Branch Chiefs Dr. Henry R. Frey (1988 - 1992) and Dr. Bruce B. Parker (1992 - 1993). Both provided counsel and leadership thereby in large part ensuring the successful completion of this project. Dr. Wayne L. Wilmot, Chief of the Scientific and Technical Applications Section, was instrumental in developing the NOS estimates of nontidal fluxes in the East River based on NOS ADCP measurements. Dr. Kurt W. Hess, Chief of the Oceanography Projects Section, provided many valuable suggestions and advice. Dr. Eugene J. Wei greatly assisted with many of the model computations and offered many valuable insights. Ms. Karen L. Earwaker and Mr. Richard W. Bourgerie performed the harmonic and residual water level analyses. Mr. John F. Cassidy developed the horizontal and vertical section graphics presented in both Chapters 3 and 6. Ms. Brenda W. Via assisted in developing the figures and prepared the final manuscript.

Assistance outside of NOAA is also greatfully acknowledged. Professor Emeritus Donald W. Pritchard was instrumental in the development of the coordinated modeling approach, which used the EPA high resolution East River model to provide East River flux targets for the NOAA Long Island Sound hydrodynamic model. Professor Pritchard provided an extraordinary thoroughly edited SUNY CTD dataset and a comprehensive review of the UCONN CTD dataset for use in the thermohaline validation. Both model developers, Professor George L. Mellor, Princeton University, and Dr. Alan F. Blumberg, HydroQual, Inc., actively participated in several model evaluation and assessment meetings and provided overall advice and assistance.

REFERENCES

Earwaker, K.L. (editor), 1990. Long Island Sound Oceanography Project: 1988 - 1990, **NOS Oceanographic Circulation Survey Report No. 10**, National Ocean Service, Silver Spring, MD.

Garvine, R.W., 1977. Observations of the motion field of the Connecticut River plume, **Journal of Geophysical Research**, 82,441-54.

Garvine, R.W., 1986. The role of brackish plumes in open shelf waters, in The role of Freshwater Outflow in Coastal Marine Ecosystems, **NATO ASI Series Vol. G7**, 47-65.

Gordon, R.B. and C.C. Pilbeam, 1975. Circulation in central Long Island Sound, **Journal of Geophysical Research**, 80,414-422.

Ianello, J.P., 1981. Tidally induced residual circulation in Long Island Sound, **Estuarine and Coastal Marine Science**, 12,177-191.

Jay, D.A. and M.J. Bowman, 1975. The physical oceanography and water quality of New York Harbor and western Long Island Sound, **MSRC Technical Report 23**, State University of New York, Stony Brook, NY, pp 71.

Larkin, R.R. and G. Riley, 1967. A drift bottle study in Long Island Sound, **Bulletin of Bingham Oceanographic Collection**, 19,62-71.

LeLacheur, E.A. and J.C. Sammons, 1932. Tides and currents in Long Island and Block Island sounds, **Coast and Geodectic Survey Special Publication 174**, Washington, DC, 187 pp.

Longuet - Higgins, M.S., 1969. On the transport of mass by time-varying ocean currents, **Deep-Sea Research**, 16, 431-447.

McClain, C.R. and H. Walden, 1979. On the performance of the Martin digital filter for high- and low-pass applications, **NASA Technical Memorandum 80593**, GSFC, Greenbelt, Maryland, pp 24.

Paskausky, D.F., 1977. Net drift in an atypical estuary, Long Island Sound, **Journal of Environmental Management**, 4,331-342.

Paskausky, D.F. and D.L. Murphy, 1976. Seasonal variation of residual drift in Long Island Sound, **Estuarine, Coastal and Shelf Science**, 4,513-522.

Pingree, R.D. and L. Maddock, 1979. The tidal physics of headland flows and offshore tidal bank formation, **International Journal of Marine Geology, Geochemistry, and Geophysics**, 32,269-289.

Redfield, A.C., 1950. The analysis of tidal phenomena in narrow embayments, **MIT and WHOI, Papers in Physical Oceanography and Meteorology**, 11:1-35.

Riley, G.A., 1952. Hydrography of Long Island and Block Island Sounds, **Bulletin of Bingham Oceanographic Collection**, 13,5-39.

Riley, G.A., 1956. Oceanography of Long Island Sound, 1952-1954, **Bulletin of Bingham Oceanographic Collection**, 15,15-46.

Robinson, I.S., 1983. Tidally induced residual flows, in **Physical Oceanography of Shelf Seas**, B. Johns ed., Elsevier, New York, NY.

Schmalz, R.A., 1992. Simulation of Three-Dimensional Hydrodynamics in Long Island Sound: Annual Timescales, **Proceedings, Second International Conference on Estuarine and Coastal Modeling**, Tampa, FL, November 13-15, 1991, 441-452.

Schmalz, R.A., 1993a. Sensitivity of Residual Circulation in Long Island Sound to Tidal Datums, **Proceedings, International Conference on Hydroscience and Engineering**, Washington, DC, June 8-11, 1993, 1475-1482.

Schmalz, R.A., 1993b. Numerical Decomposition of Eulerian Residual Circulation in Long Island Sound, Submitted to **Proceedings, Third International Conference on Estuarine and Coastal Modeling**, Oak Brook, IL, September 8-10, 1993, 15pp.

Schmalz, R.A., 1994a. Application and Documentation of the Long Island Sound Three-Dimensional Circulation Model, **Volume 1: Long Island Sound Oceanography Project Summary Report**, NOS, NOAA, Silver Spring, Maryland.

Schmalz, R.A., 1994b. Development of Long-term Three-Dimensional Hydrodynamics in Long Island Sound For Use in Water Quality Modeling, Submitted to **Proceedings, National Conference on Hydraulic Engineering**, Buffalo, NY, August 1-5, 1994, 5pp.

Sullivan, J., 1980. Accurate least-squares techniques using an orthogonal function approach, **NOAA Tech. Rept. EDIS 33**, Washington, DC, pp 64.

Wei, E.J., 1992. Simulation of Three-Dimensional Hydrodynamics in Long Island Sound: Seasonal Timescales, **Proceedings, Second International Conference on Estuarine and Coastal Modeling**, Tampa, FL, November 13-15, 1991, 430-440.

Wei, E.J., 1993. Development of a Long Island Sound Tidal Circulation and Water Level Atlas, **Proceedings, International Conference on Hydroscience and Engineering**, Washington, DC, June 8-11, 1993, 1483-1490.

Wilson, R.E., 1976. Gravitational circulation in Long Island Sound, **Estuarine and Coastal Marine Science**, 4,443-453.

Wison, R.E., 1990. Personal Communication.

Zilkoski, D.B. et al., 1992. Results of the general adjustment of the North American Vertical Datum of 1988, **Surveying and Land Information Systems**, 52,133-149.

Appendix A: Model vs Data Salinity Comparisons

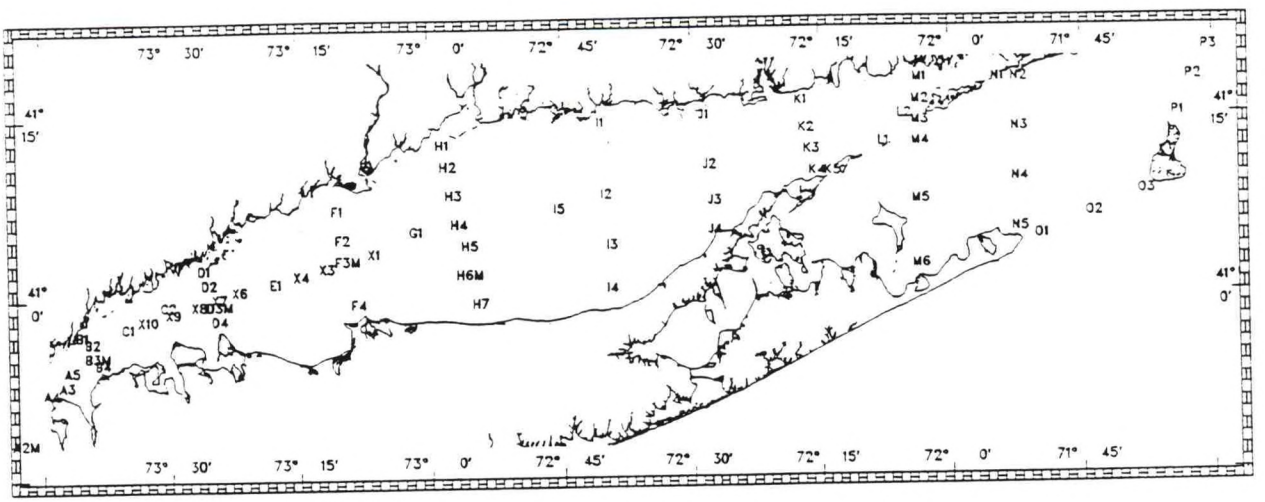

Station Locations.

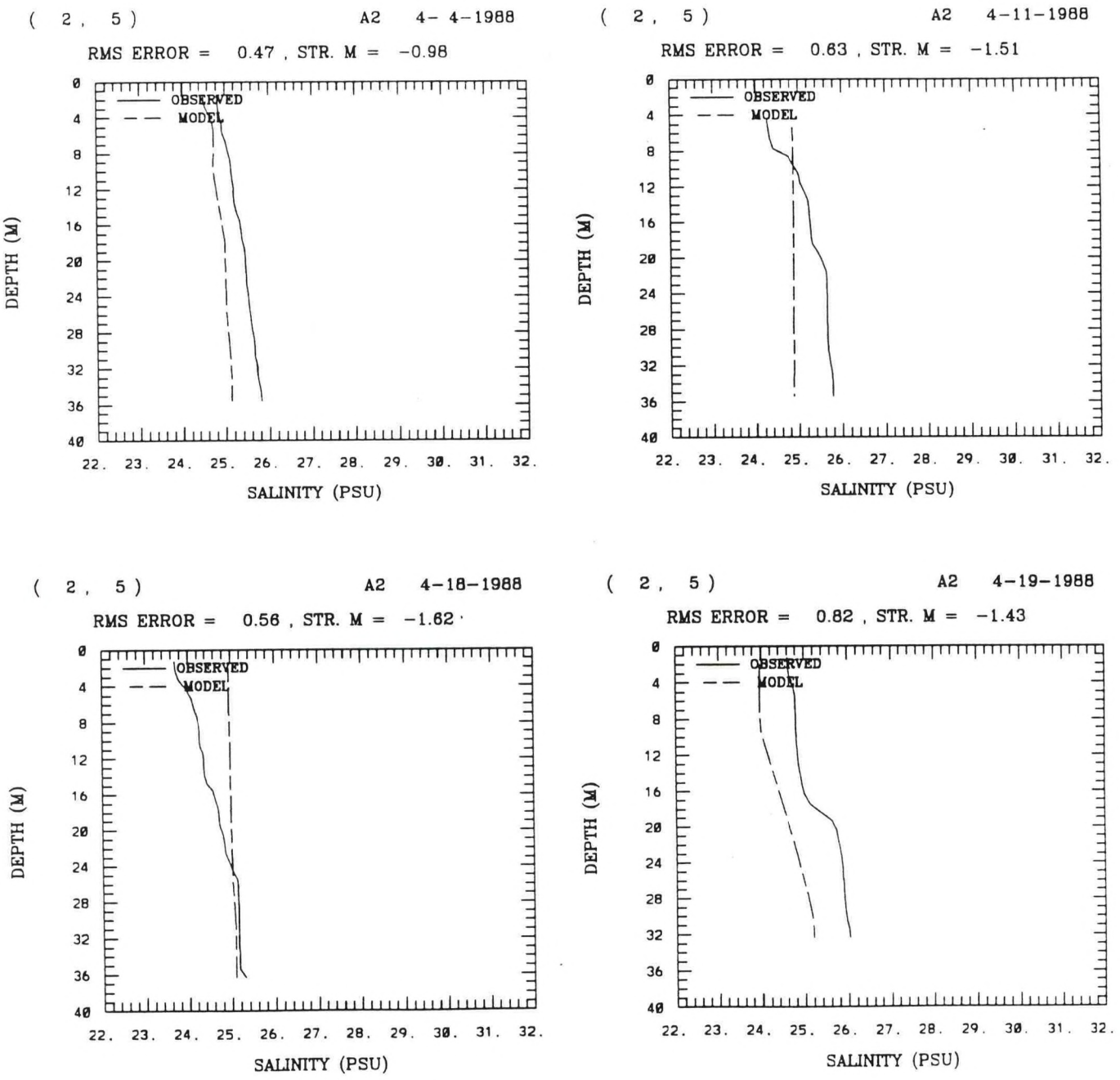

Figure A.1. Simulated versus Observed Vertical Salinity Profiles At Station: A2

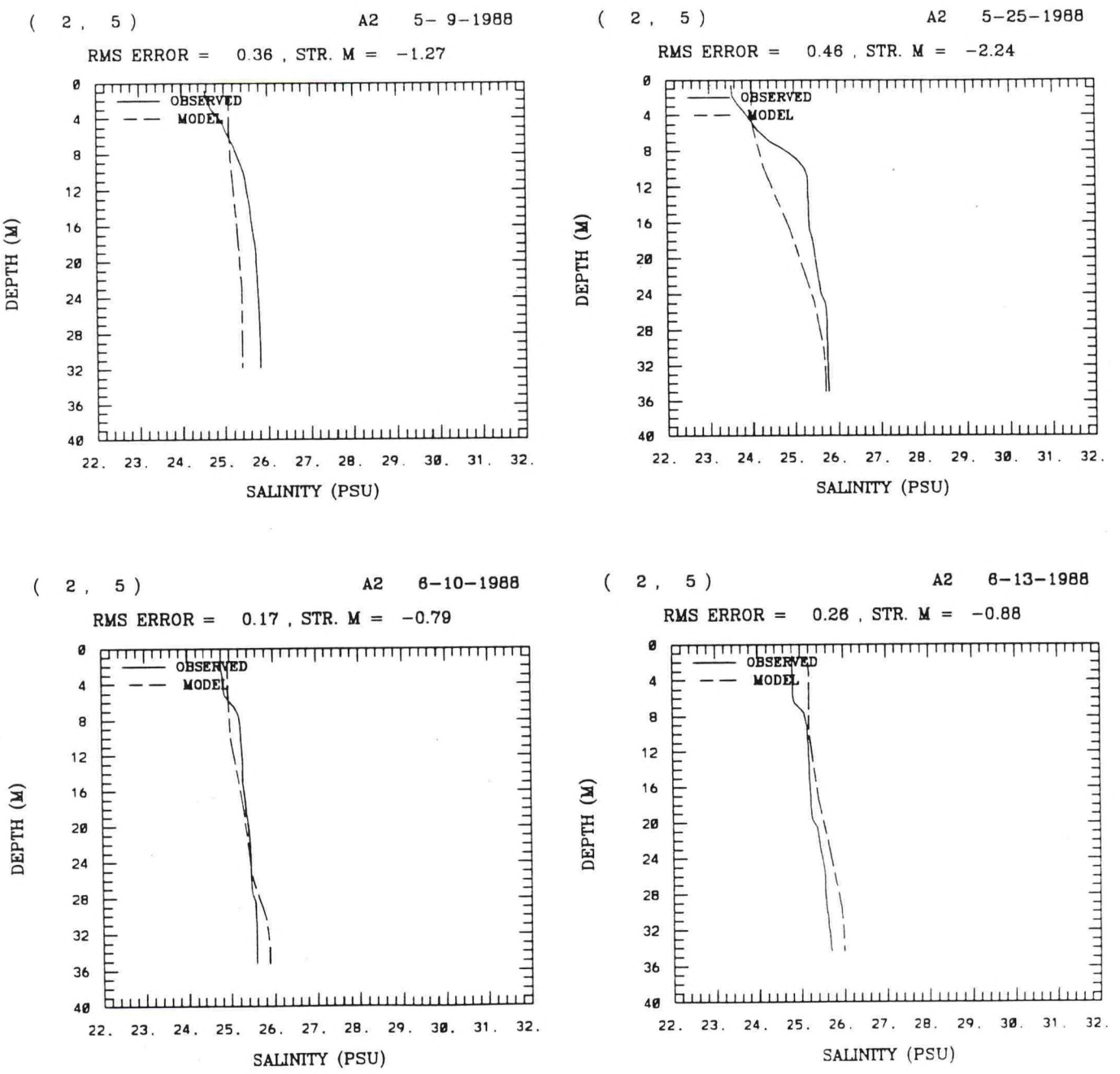

Figure A.1. (Cont.) Simulated versus Observed Vertical Salinity Profiles At Station: A2

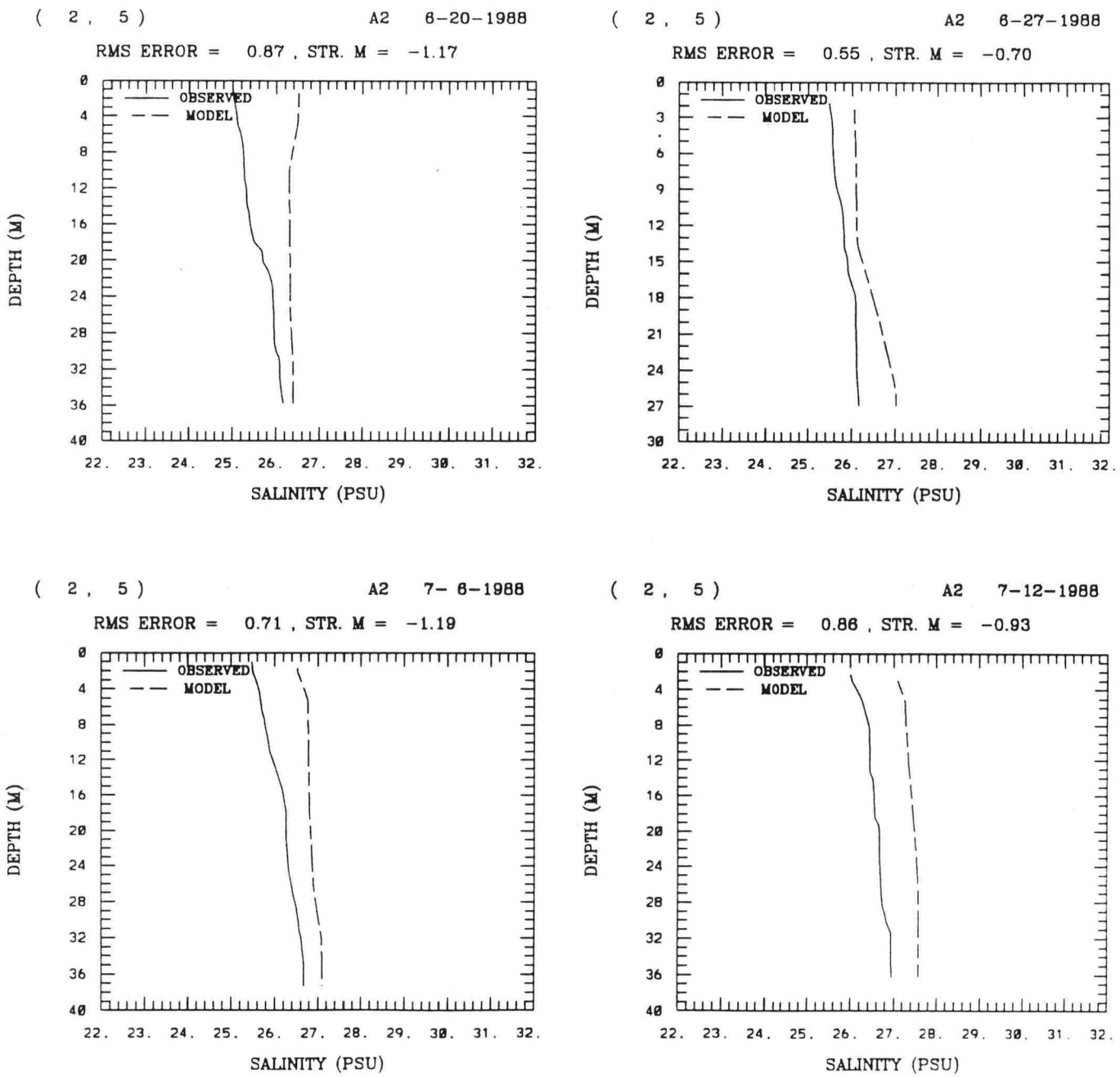

Figure A.1. (Cont.) Simulated versus Observed Vertical Salinity Profiles At Station: A2

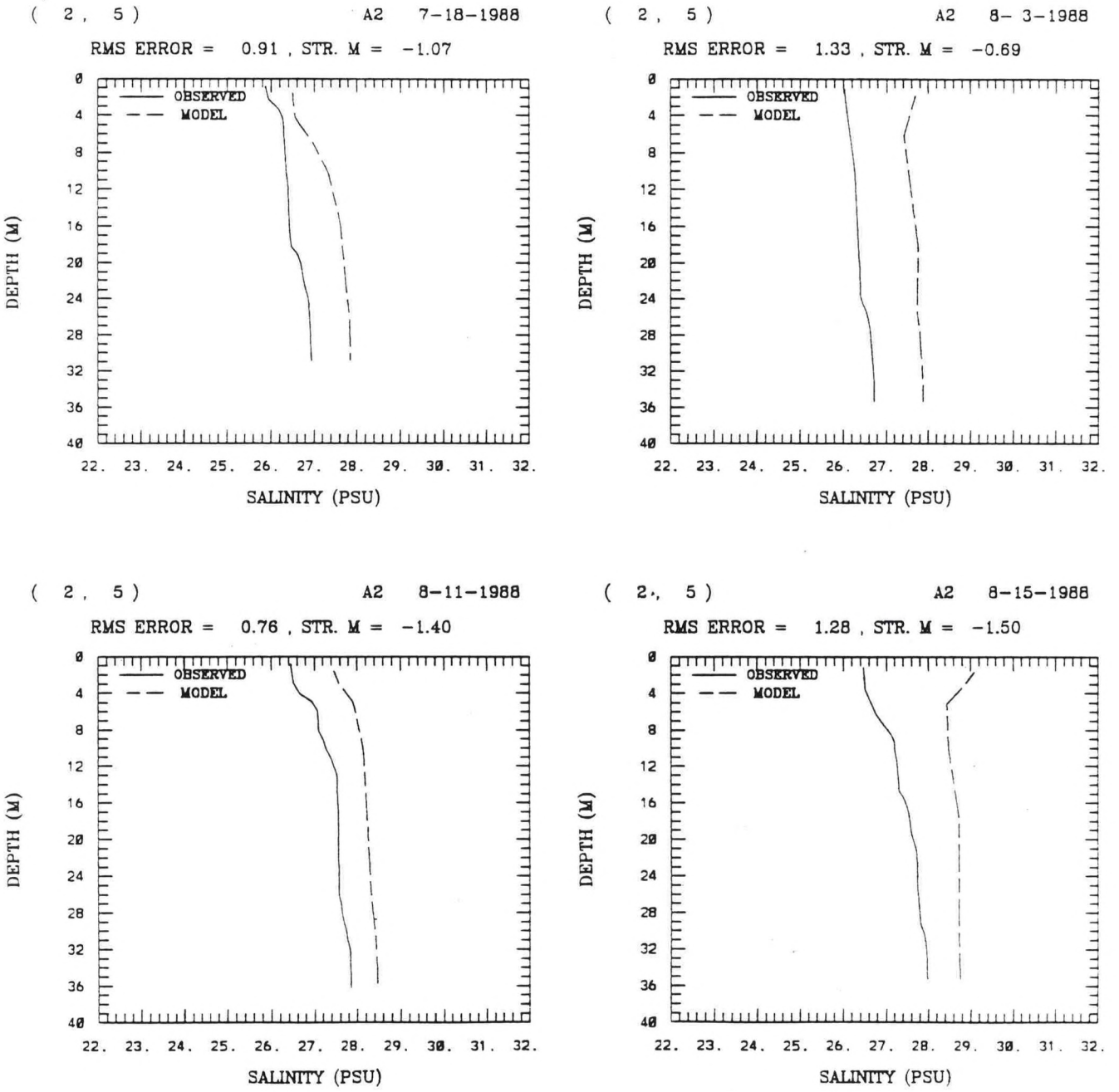

Figure A.1. (Cont.) Simulated versus Observed Vertical Salinity Profiles At Station: A2

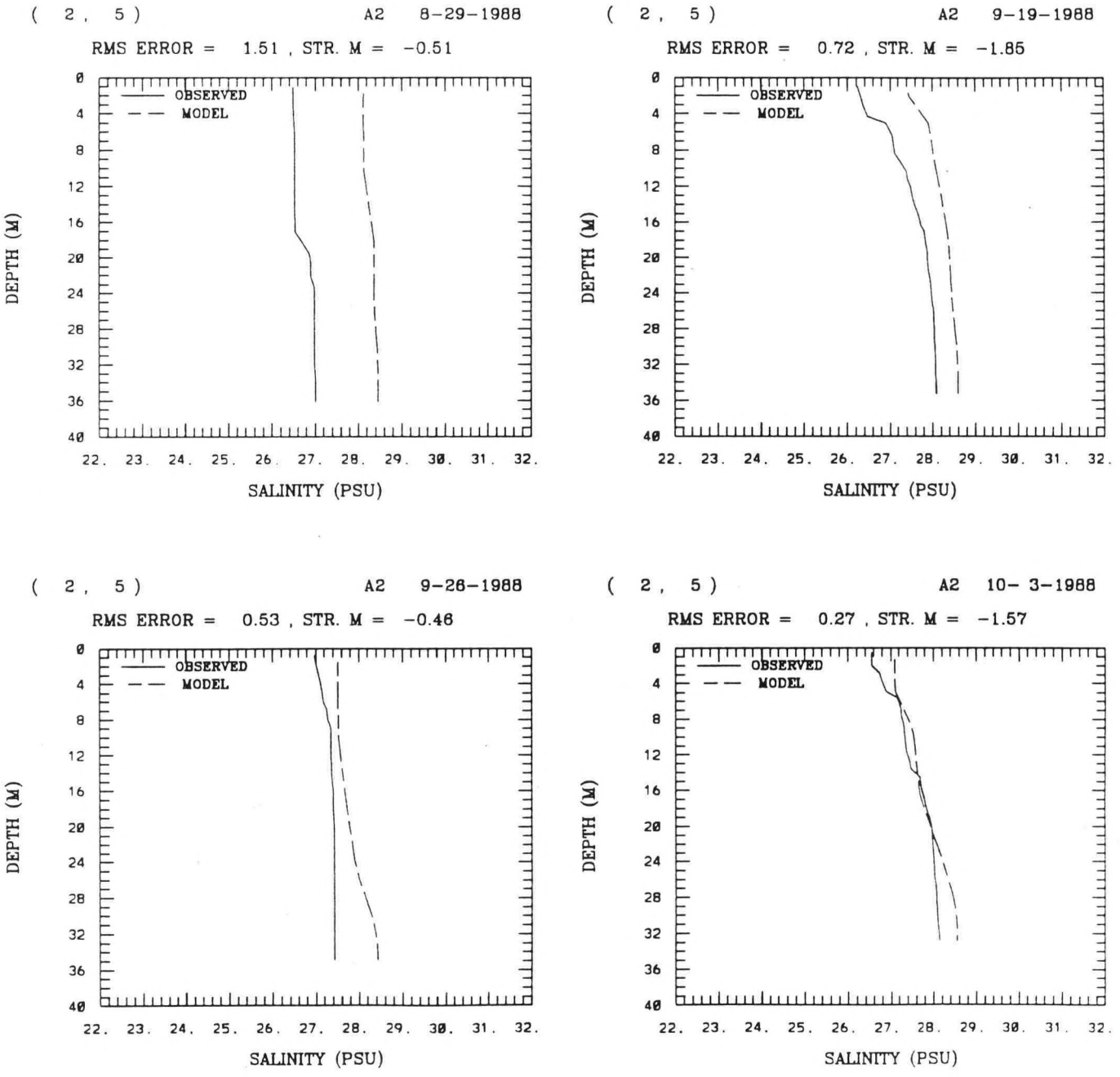

Figure A.1. (Cont.) Simulated versus Observed Vertical Salinity Profiles At Station: A2

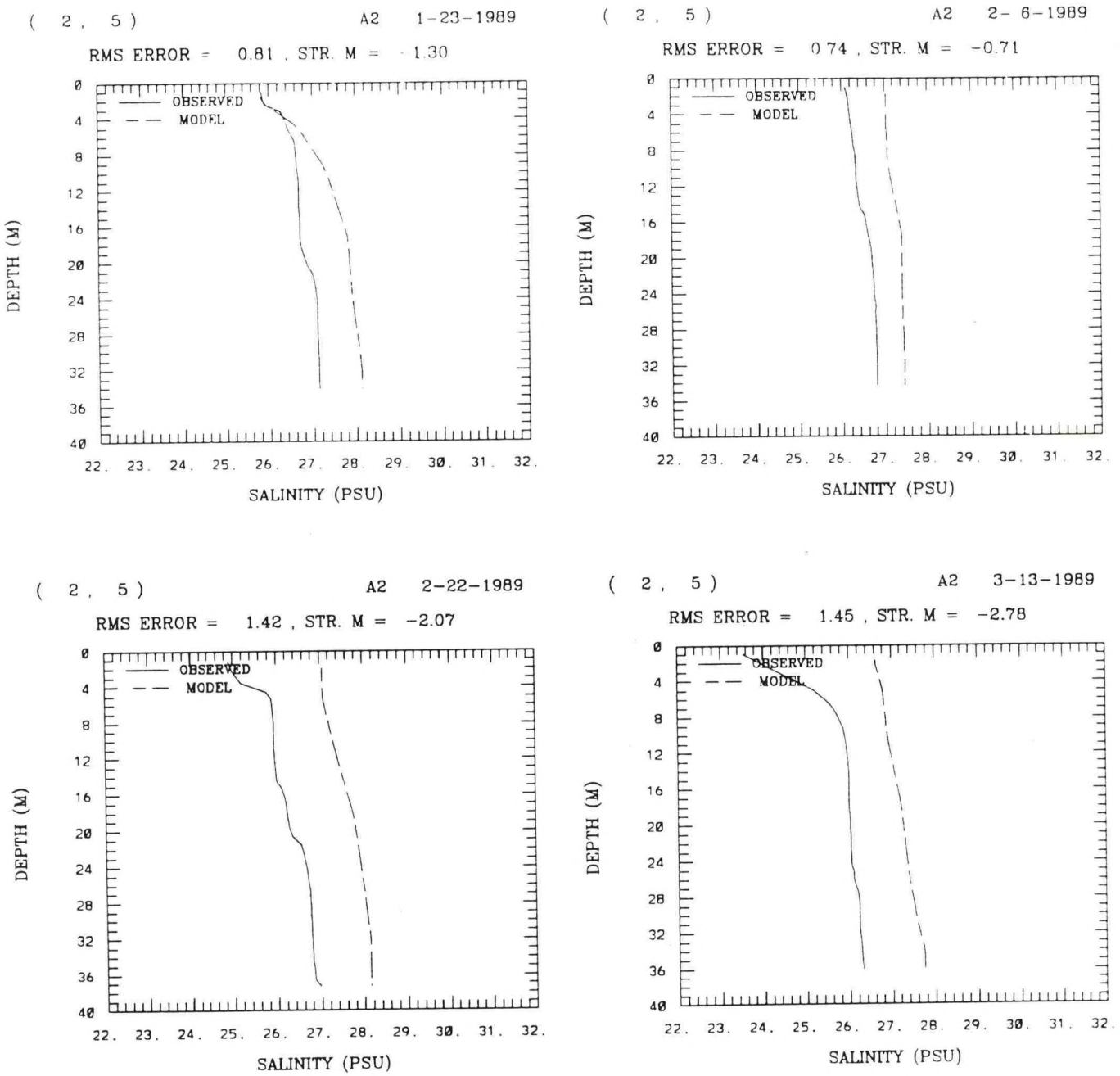

Figure A.1. (Cont.) Simulated versus Observed Vertical Salinity Profiles At Station: A2

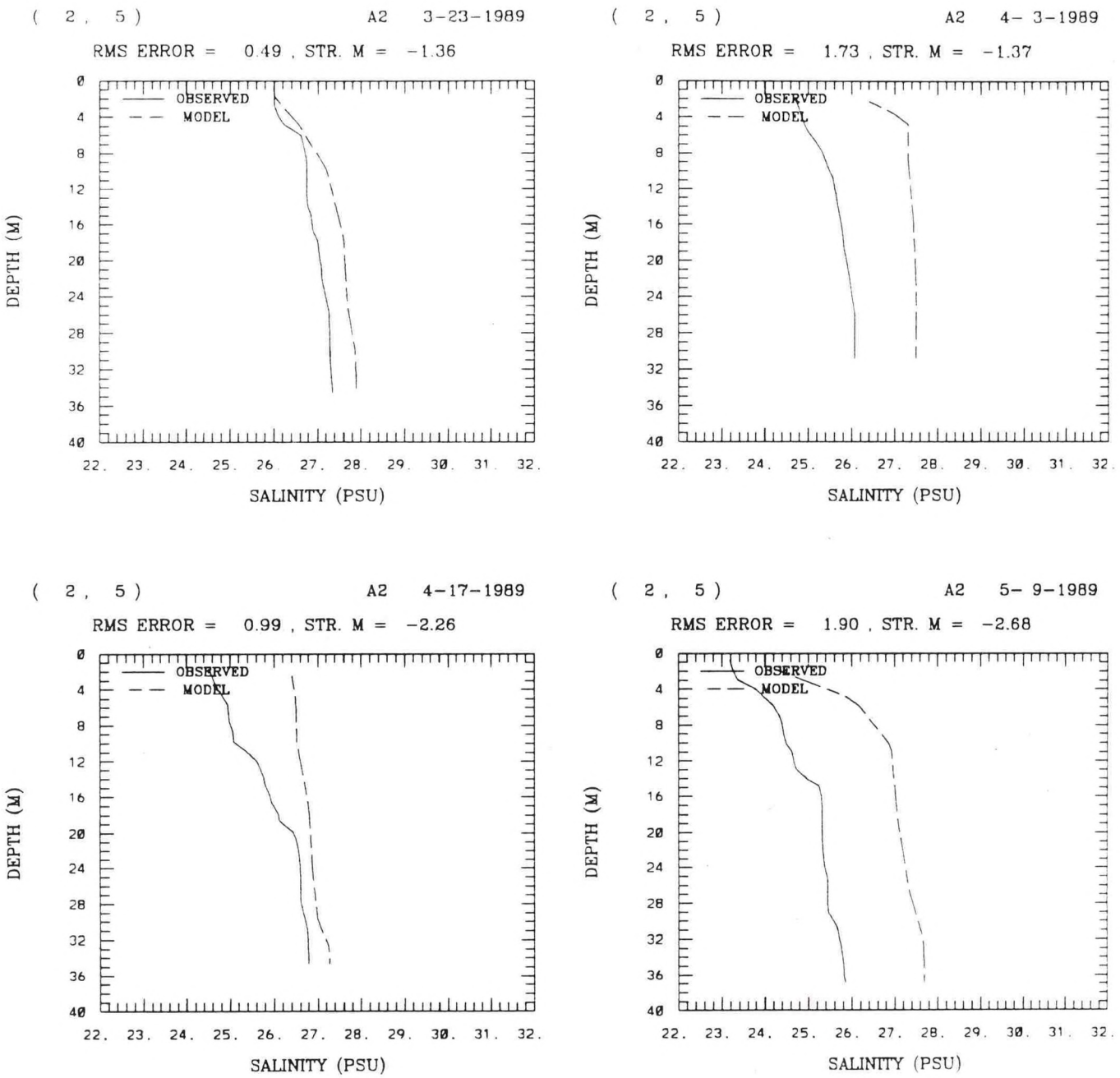

Figure A.1. (Cont.) Simulated versus Observed Vertical Salinity Profiles At Station: A2

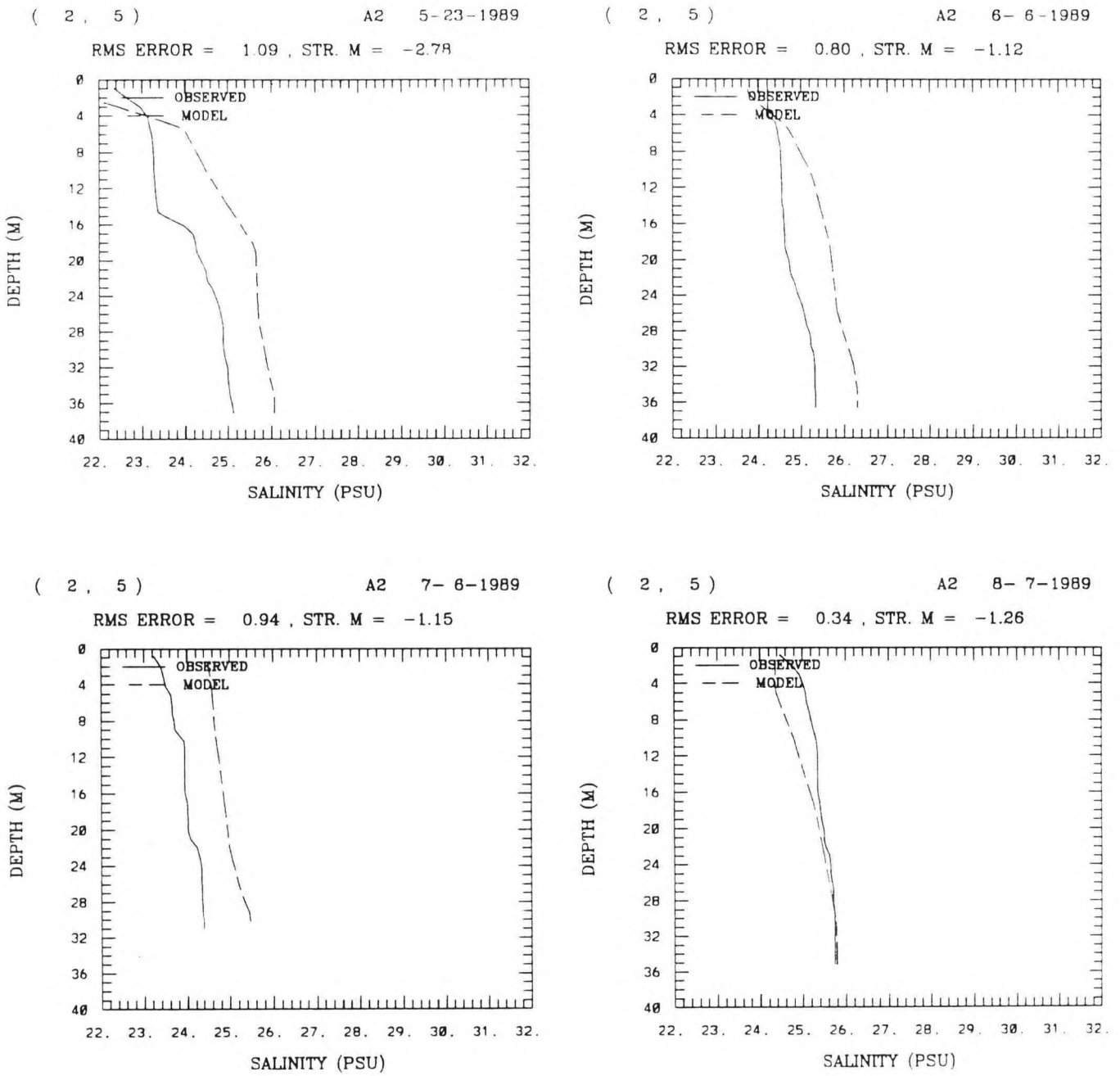

Figure A.1. (Cont.) Simulated versus Observed Vertical Salinity Profiles At Station: A2

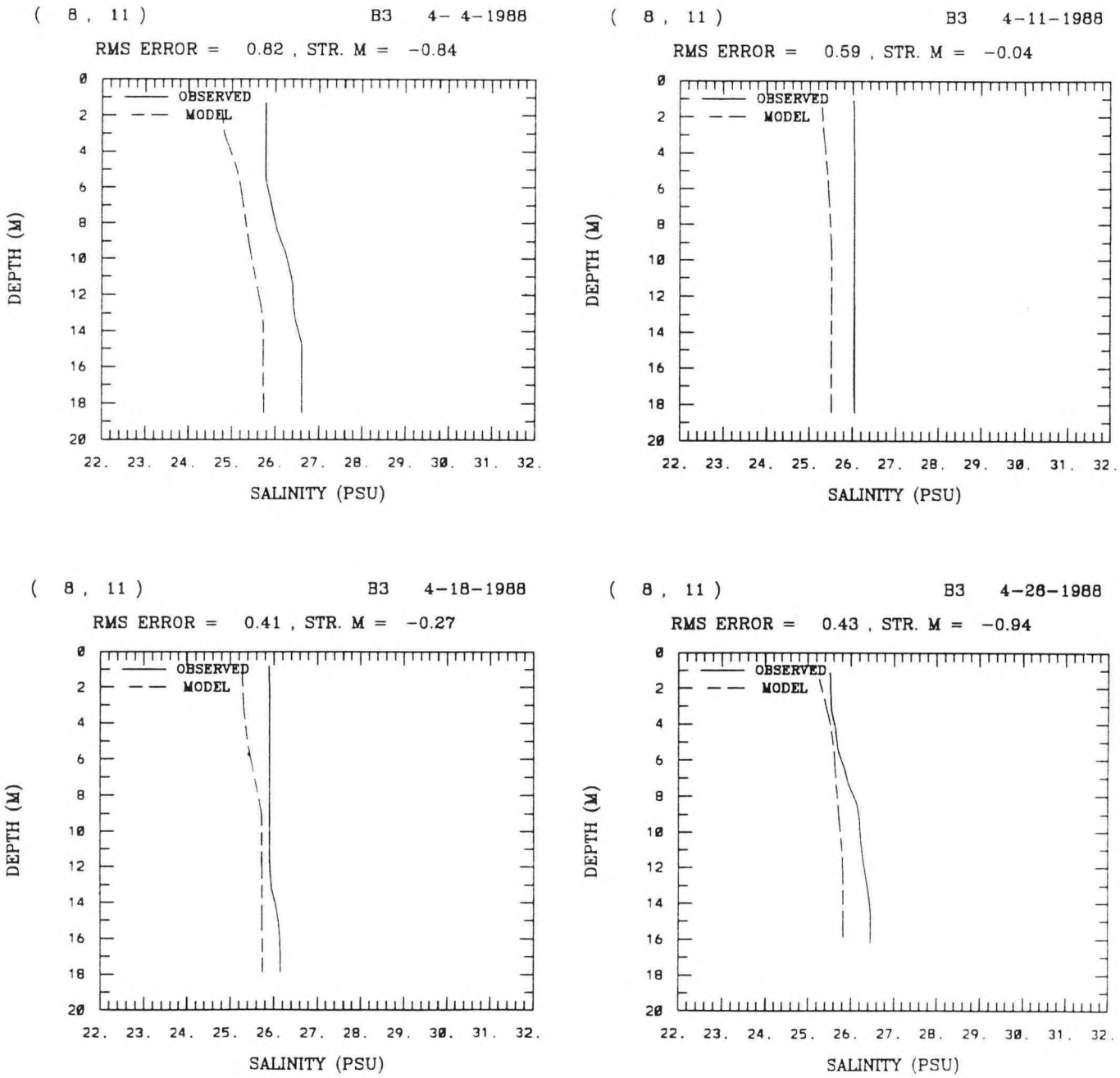

Figure A.2. Simulated versus Observed Vertical Salinity Profiles At Station: B3

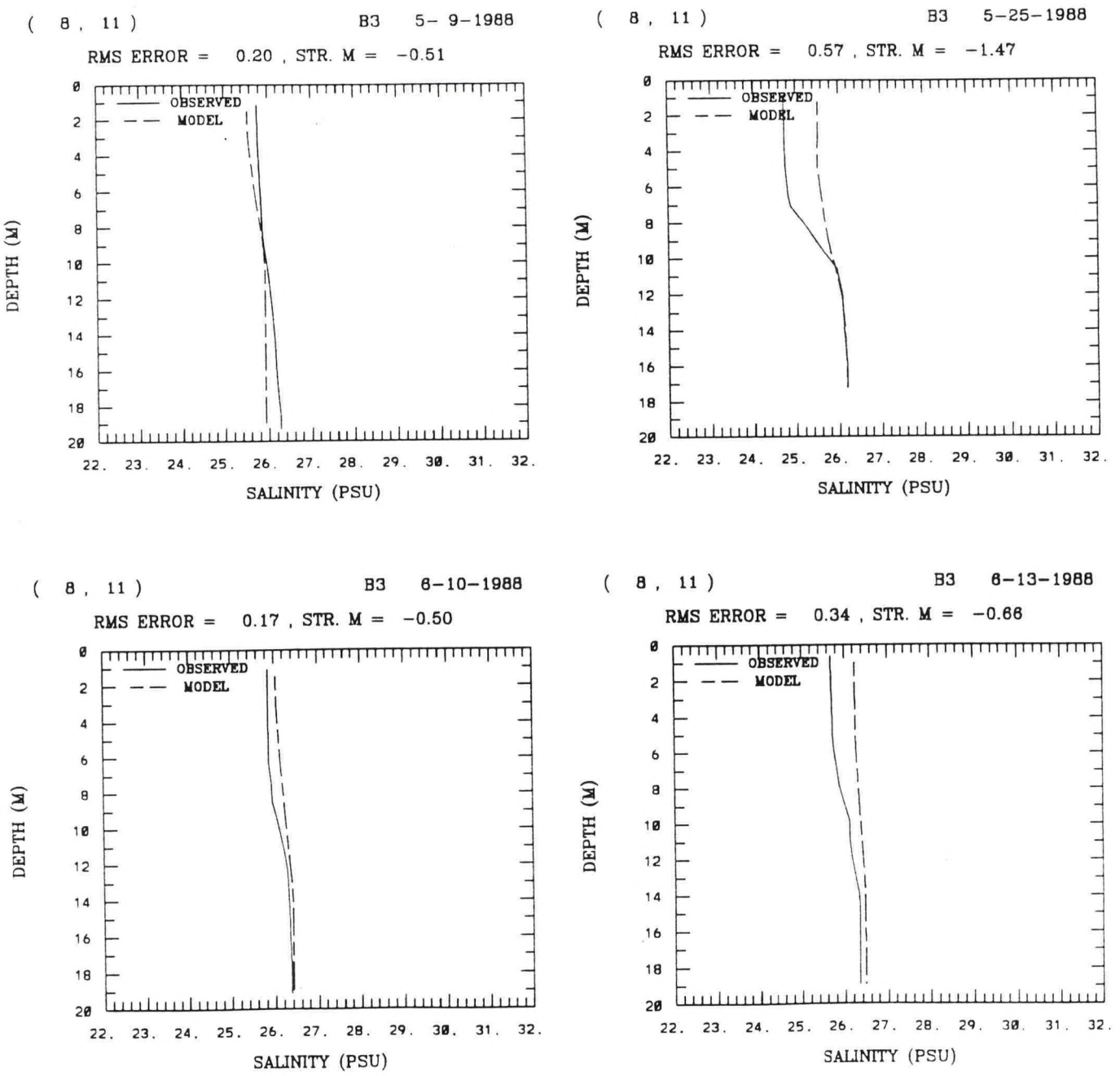

Figure A.2. (Cont.) Simulated versus Observed Vertical Salinity Profiles At Station: B3

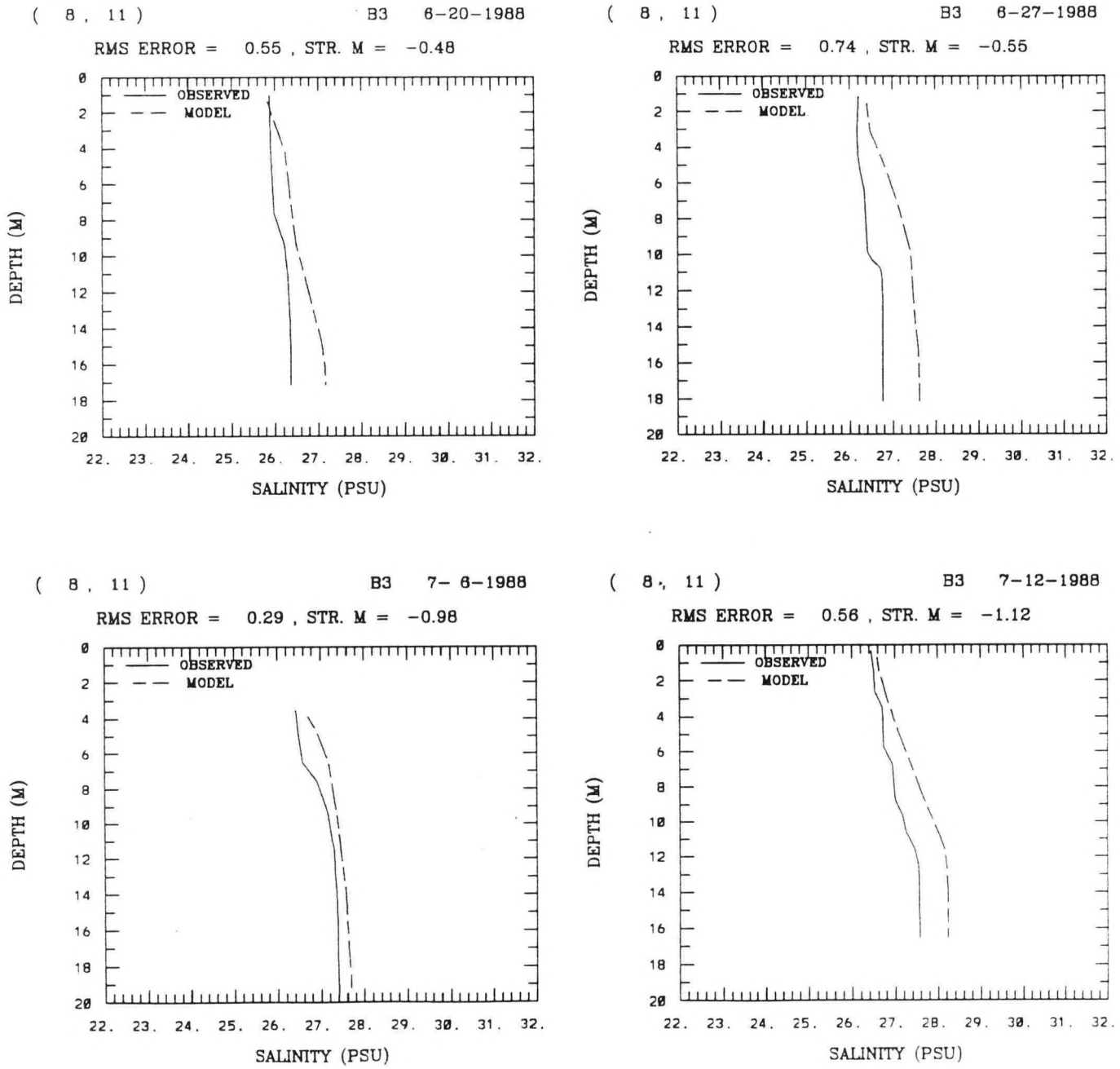

Figure A.2. (Cont.) Simulated versus Observed Vertical Salinity Profiles At Station: B3

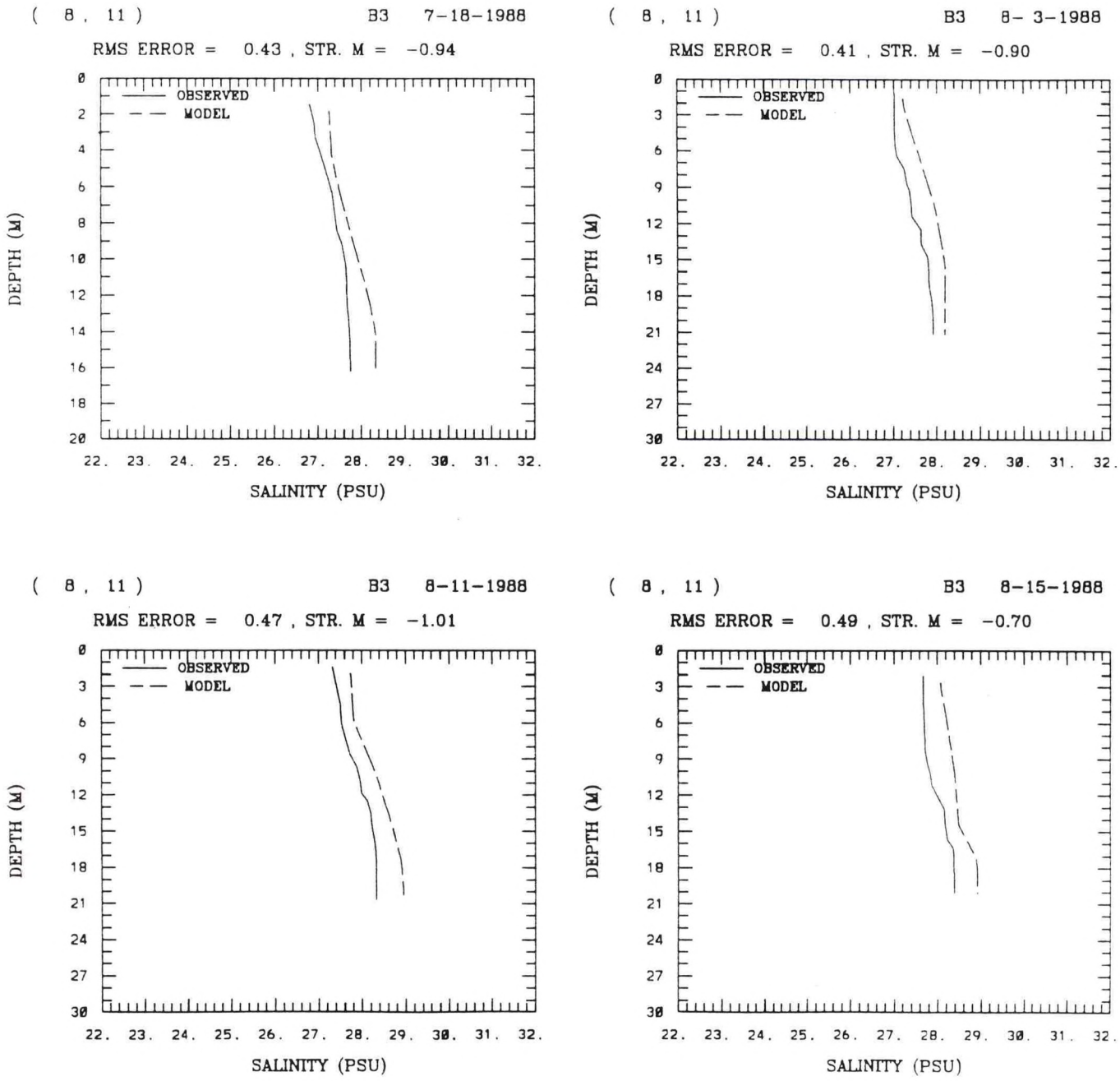

Figure A.2. (Cont.) Simulated versus Observed Vertical Salinity Profiles At Station: B3

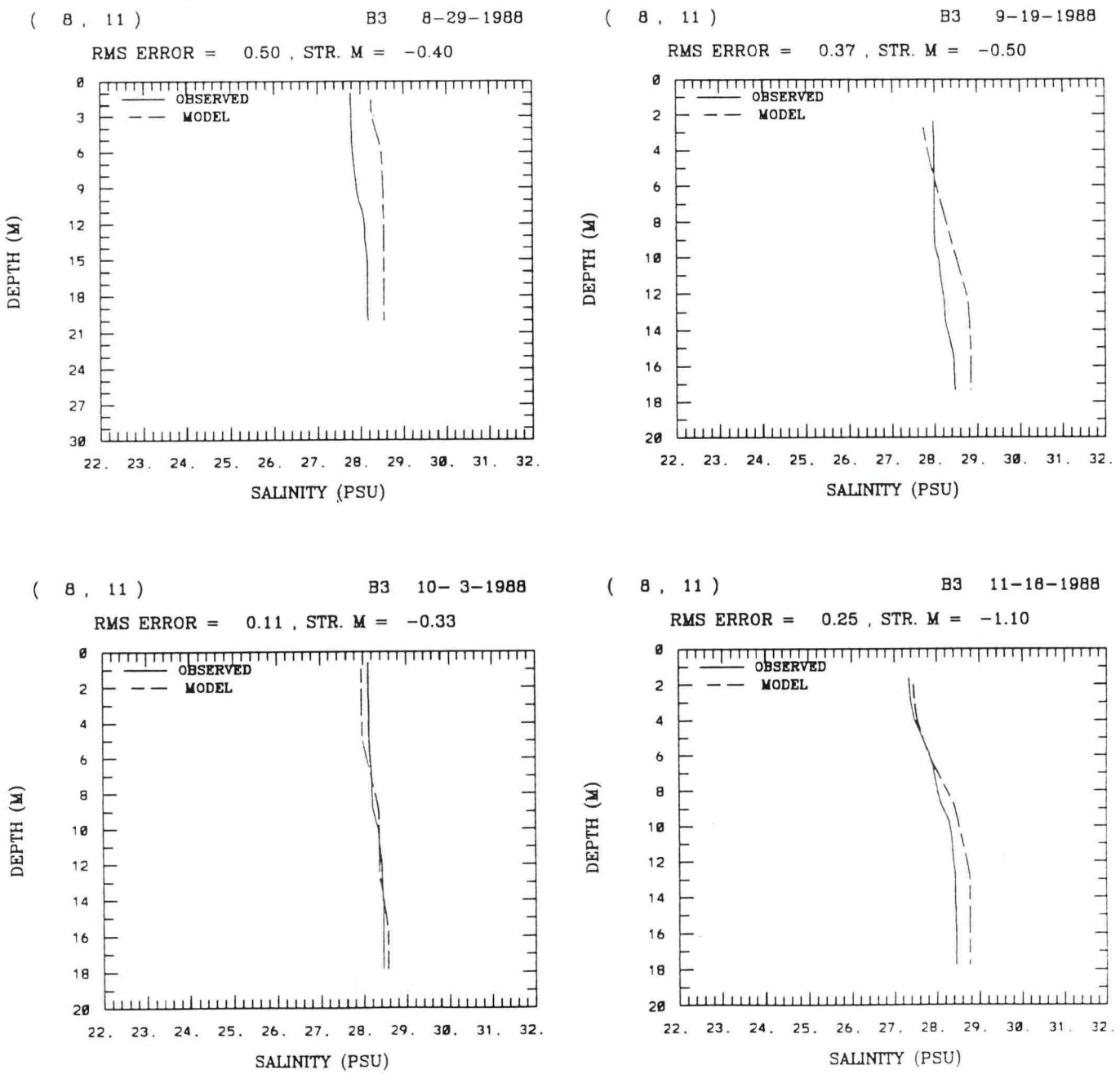

Figure A.2. (Cont.) Simulated versus Observed Vertical Salinity Profiles At Station: B3

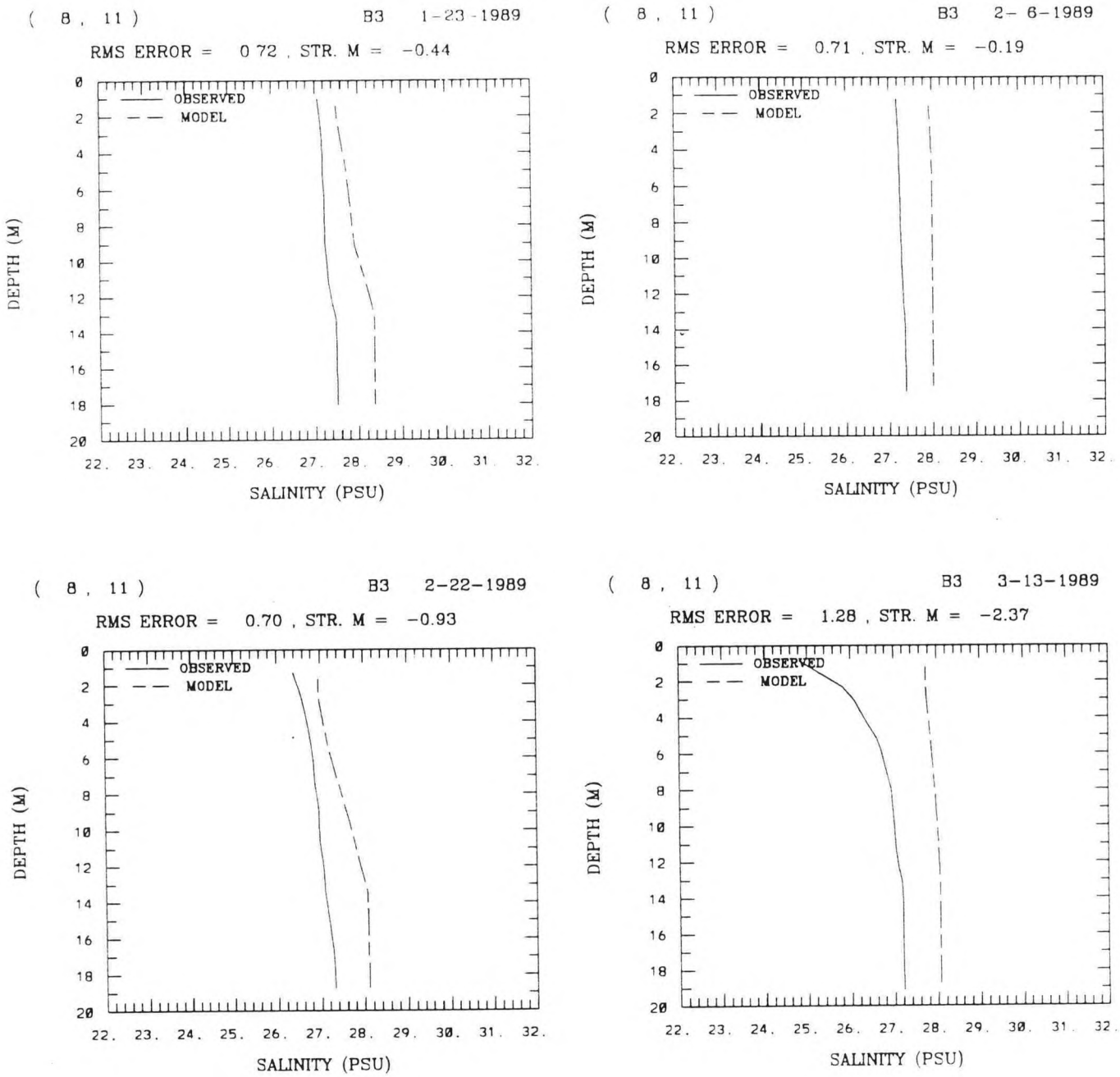

Figure A.2. (Cont.) Simulated versus Observed Vertical Salinity Profiles At Station: B3

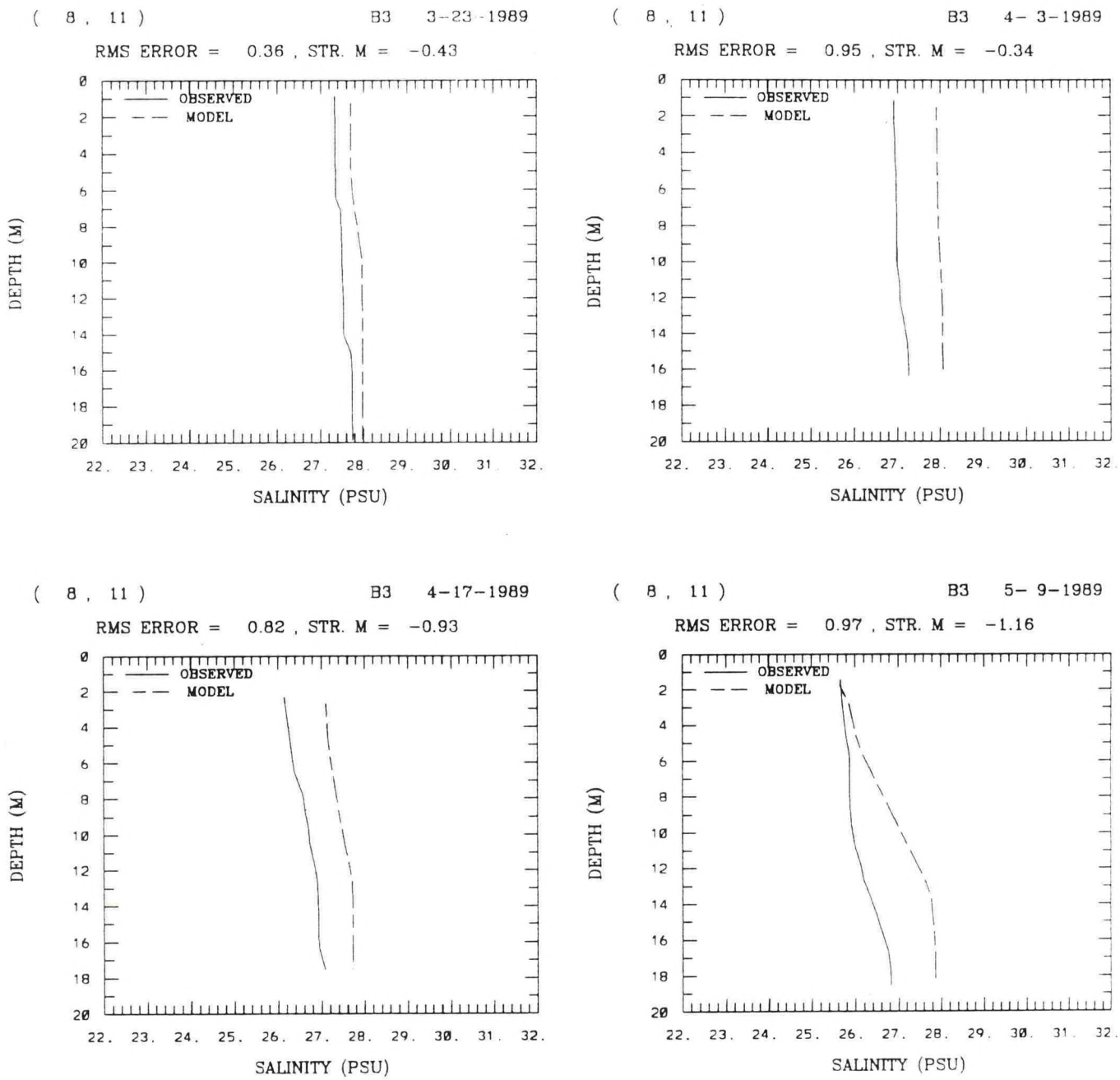

Figure A.2. (Cont.) Simulated versus Observed Vertical Salinity Profiles At Station: B3

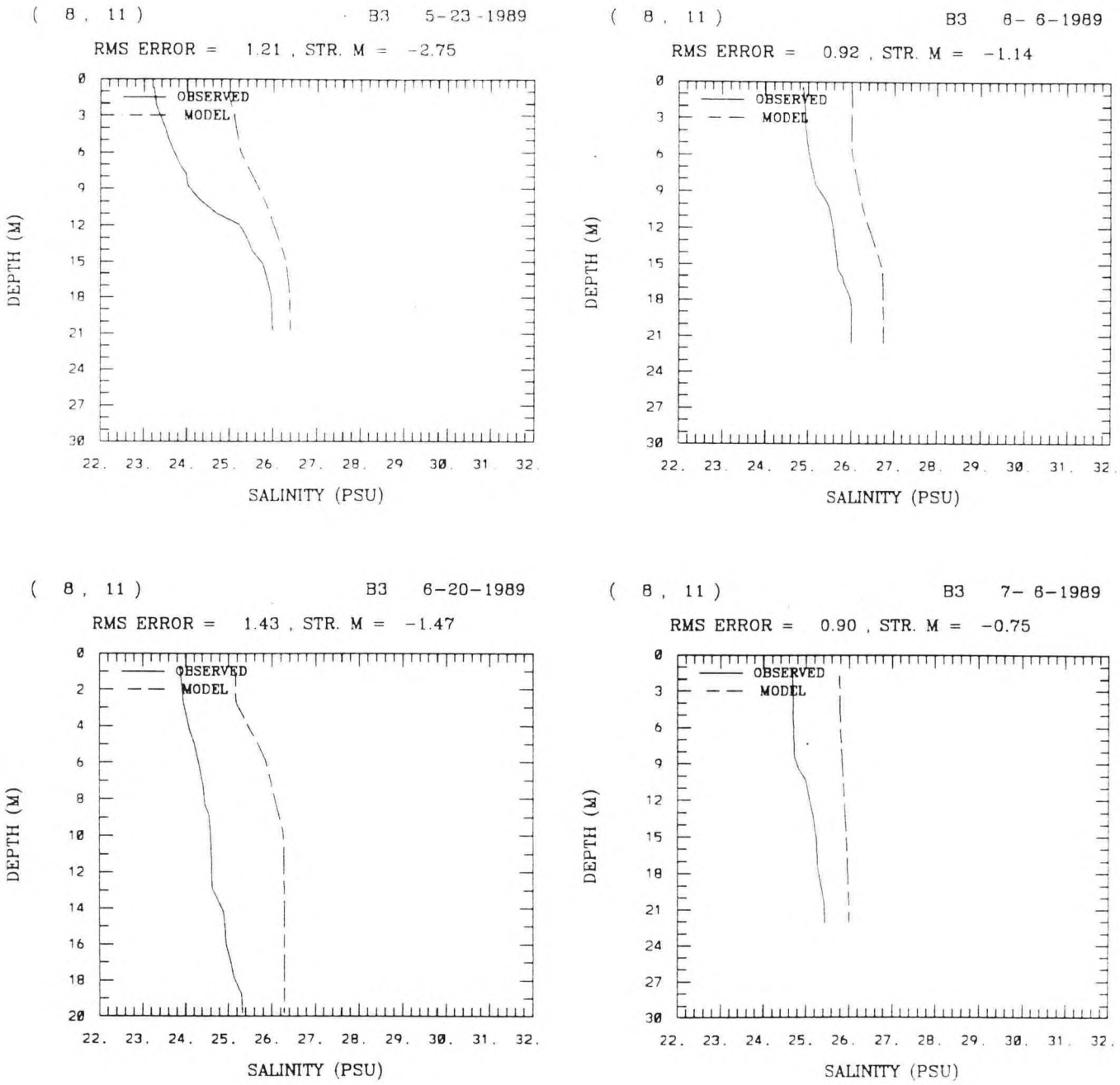

Figure A.2. (Cont.) Simulated versus Observed Vertical Salinity Profiles At Station: B3

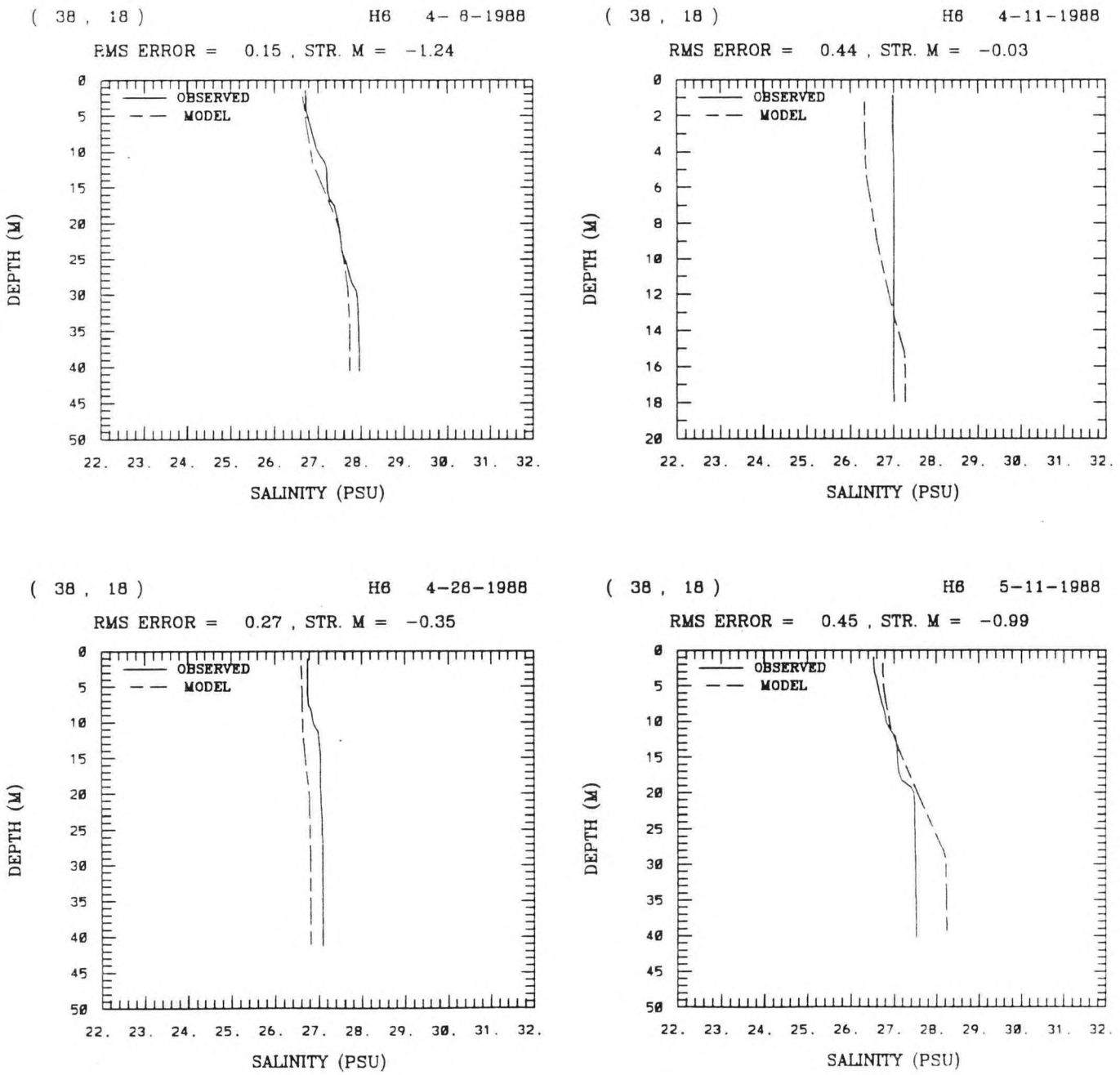

Figure A.3. Simulated versus Observed Vertical Salinity Profiles At Station: H6

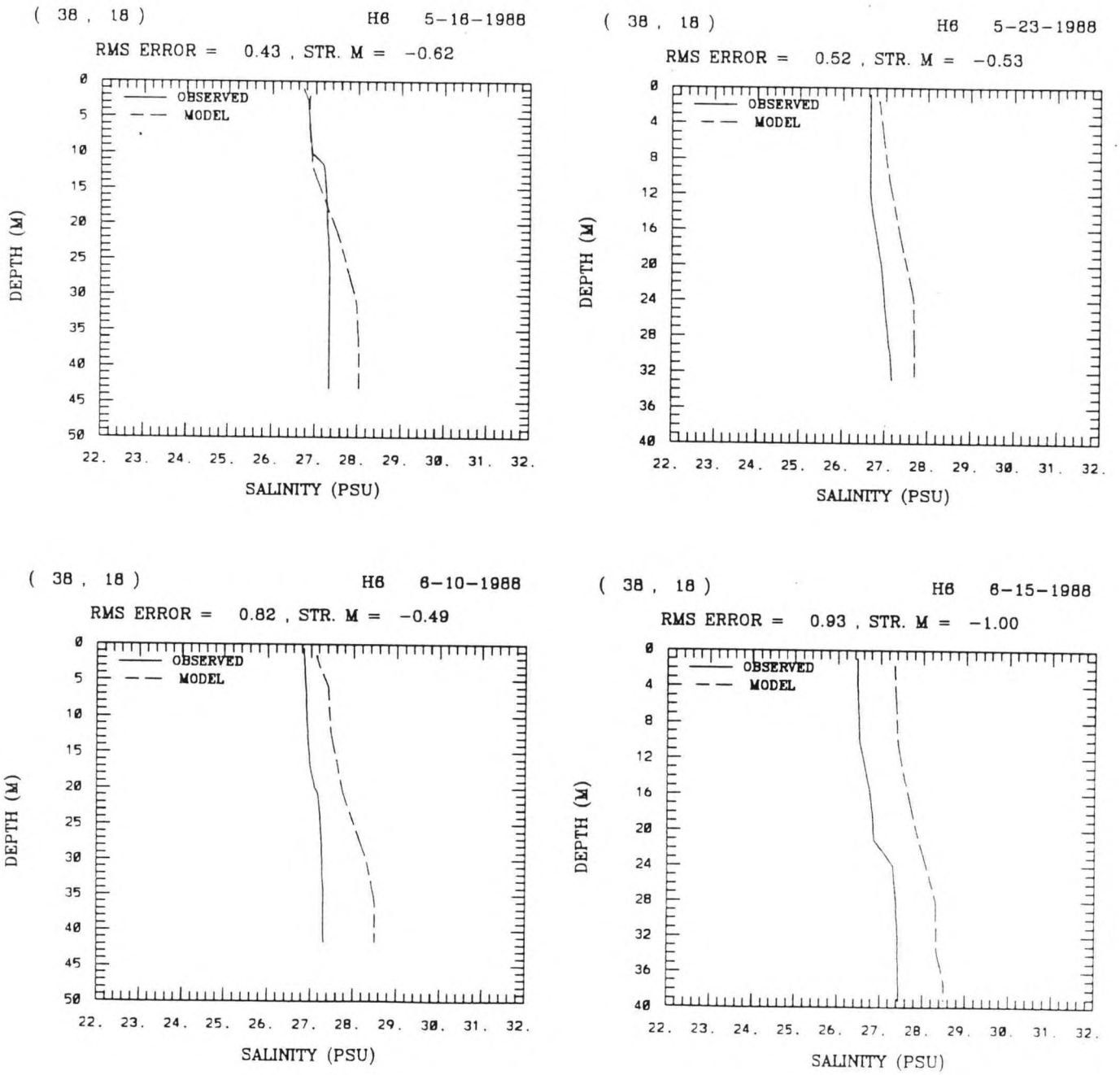

Figure A.3. (Cont.) Simulated versus Observed Vertical Salinity Profiles At Station: H6

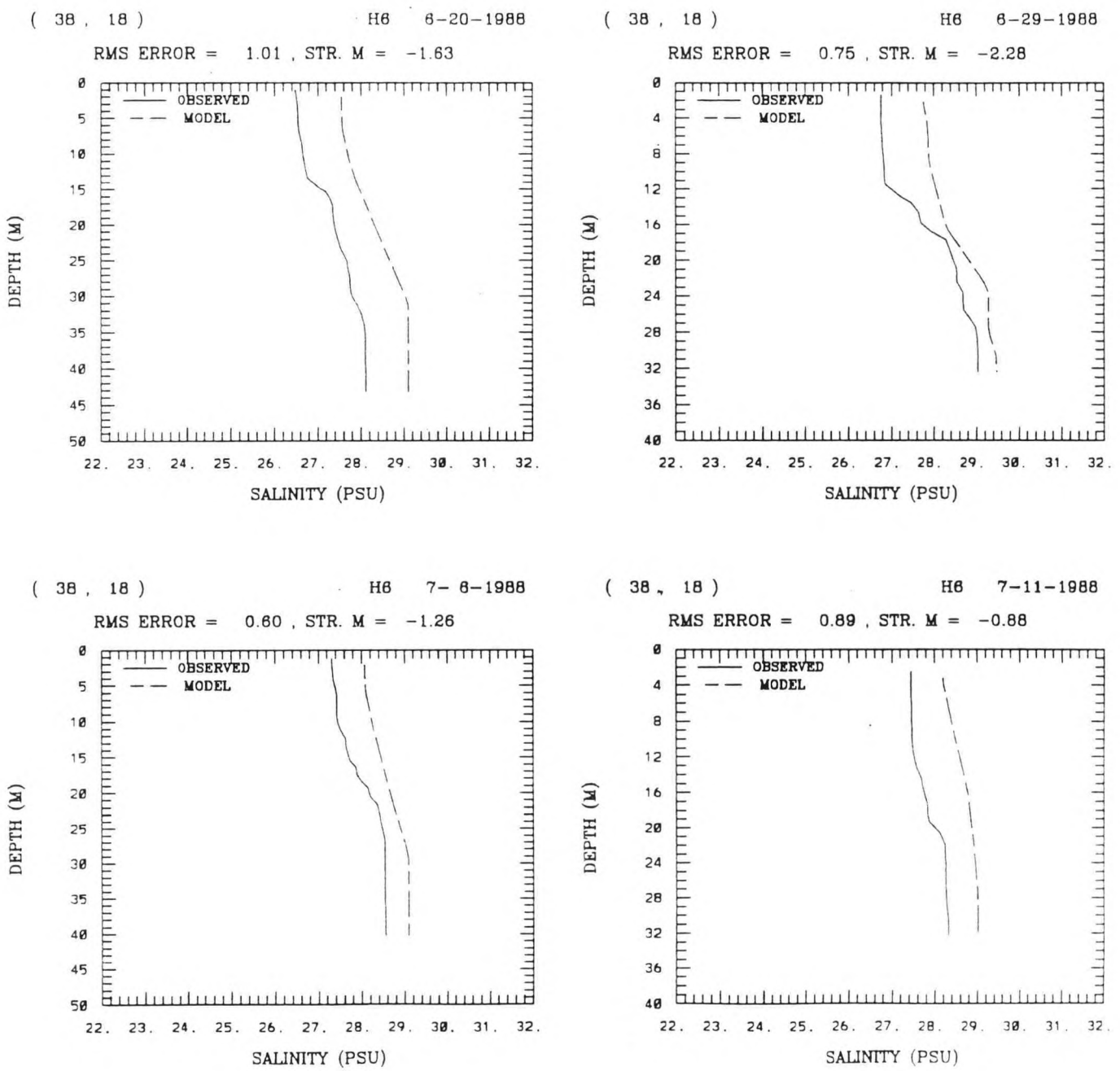

Figure A.3. (Cont.) Simulated versus Observed Vertical Salinity Profiles At Station: H6

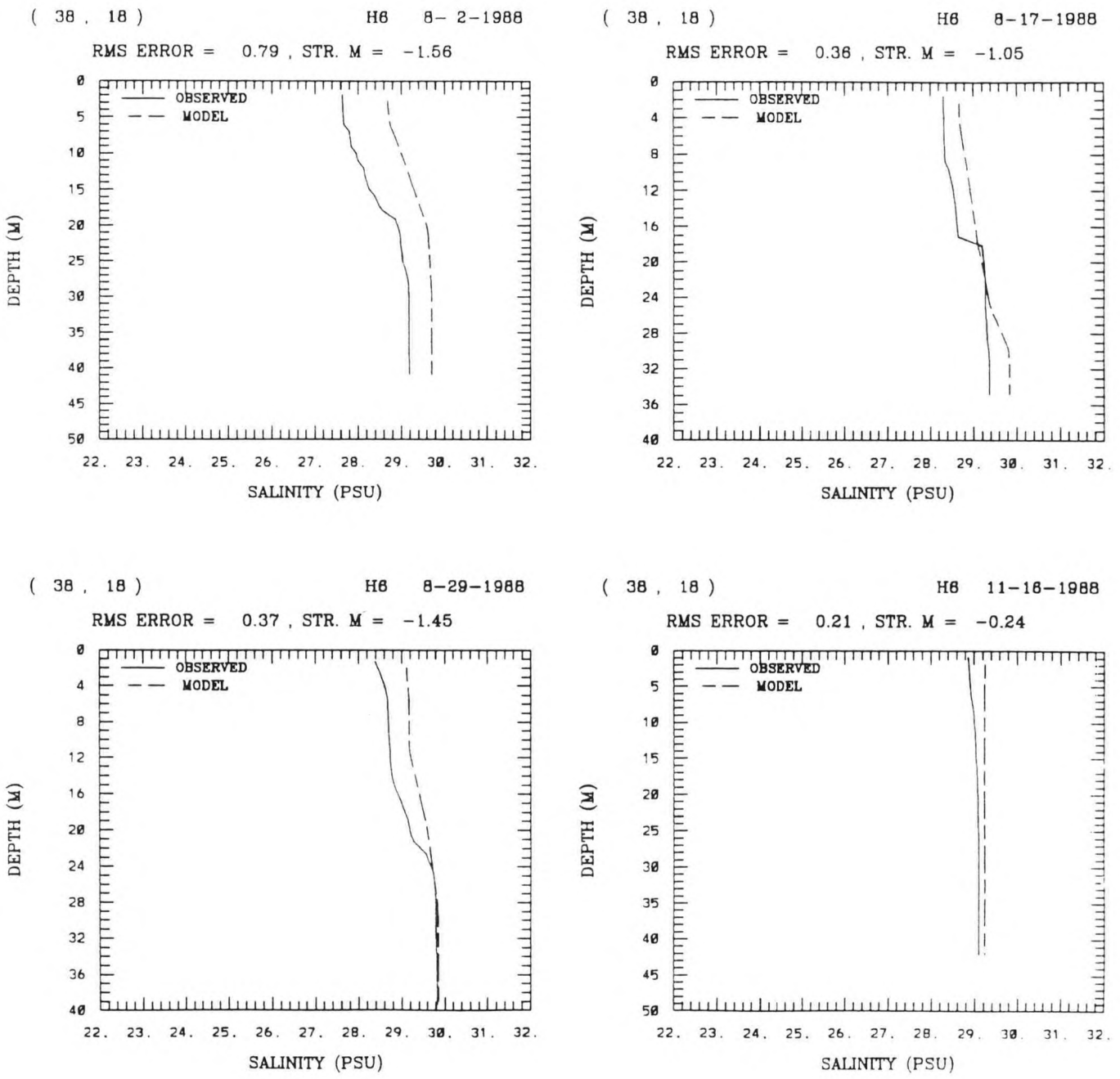

Figure A.3. (Cont.) Simulated versus Observed Vertical Salinity Profiles At Station: H6

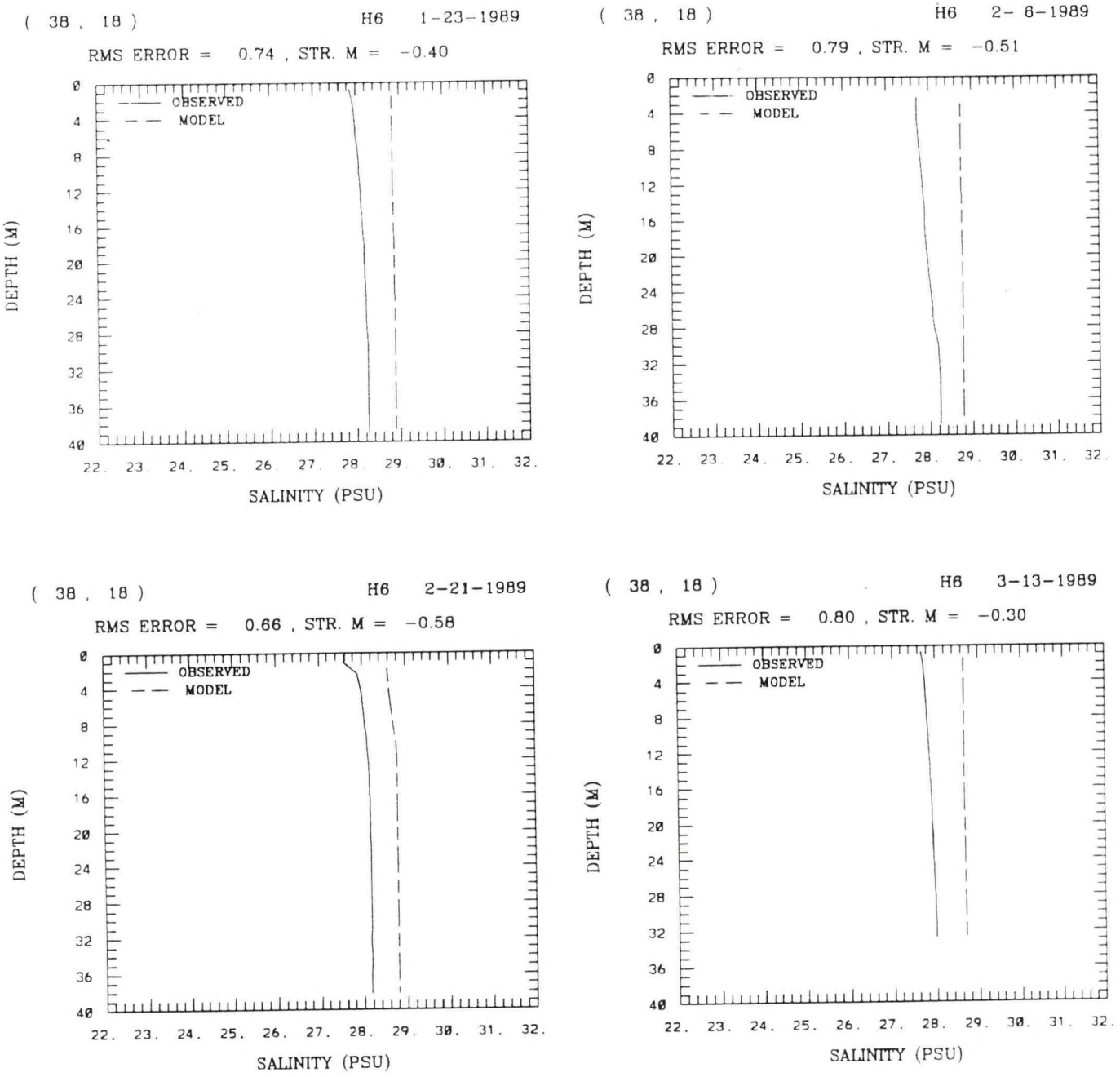

Figure A.3. (Cont.) Simulated versus Observed Vertical Salinity Profiles At Station: H6

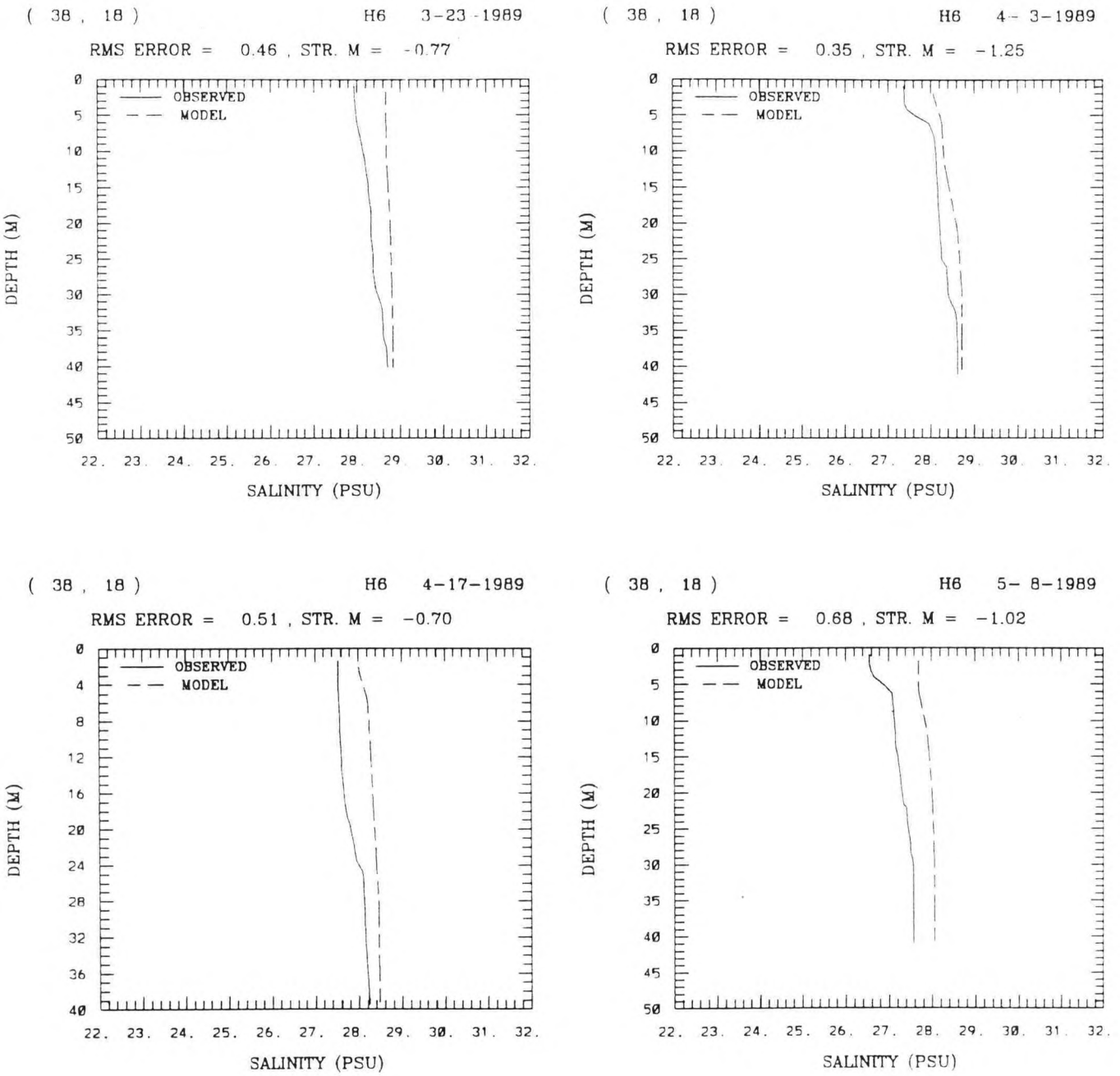

Figure A.3. (Cont.) Simulated versus Observed Vertical Salinity Profiles At Station: H6

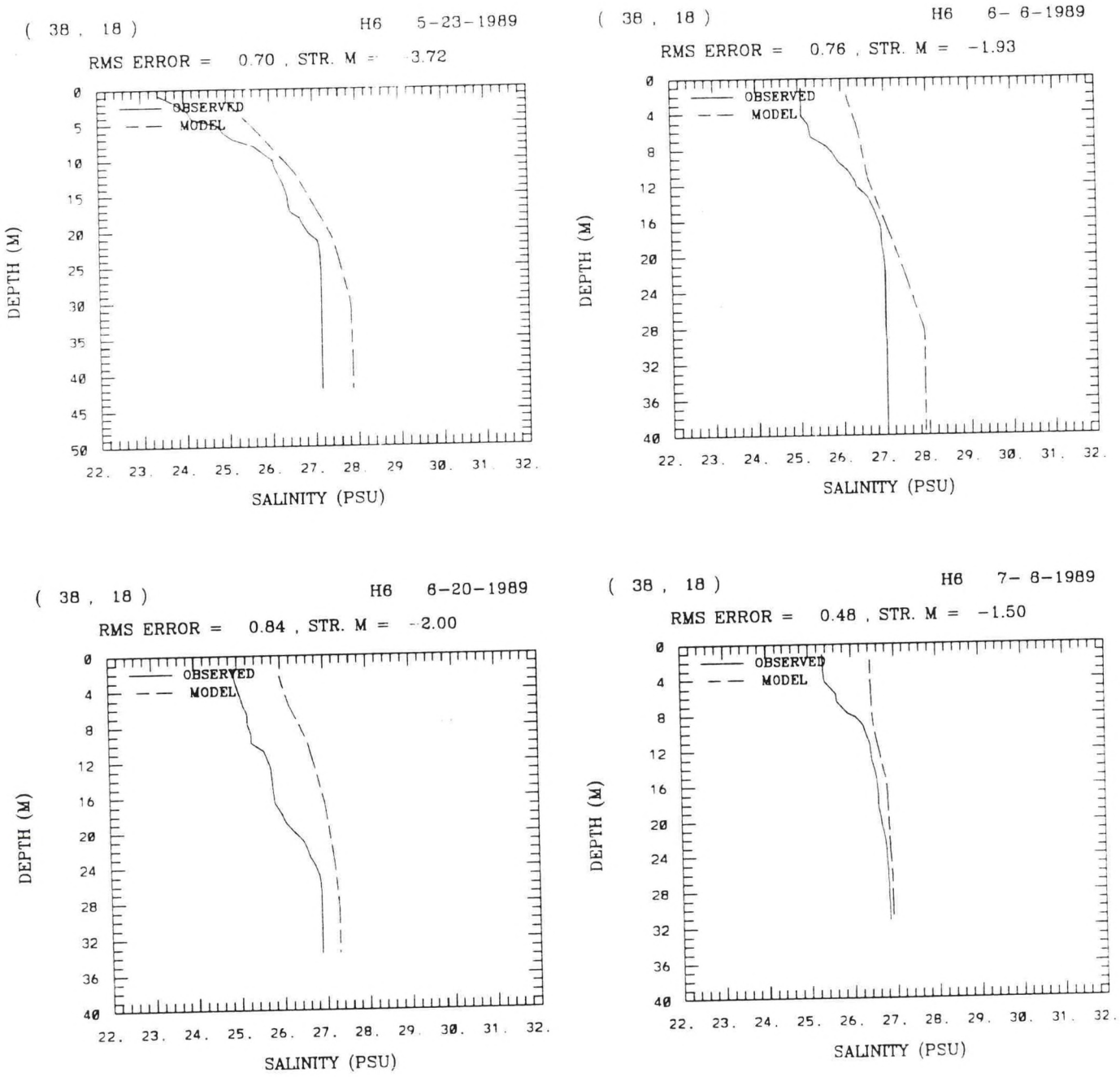

Figure A.3. (Cont.) Simulated versus Observed Vertical Salinity Profiles At Station: H6

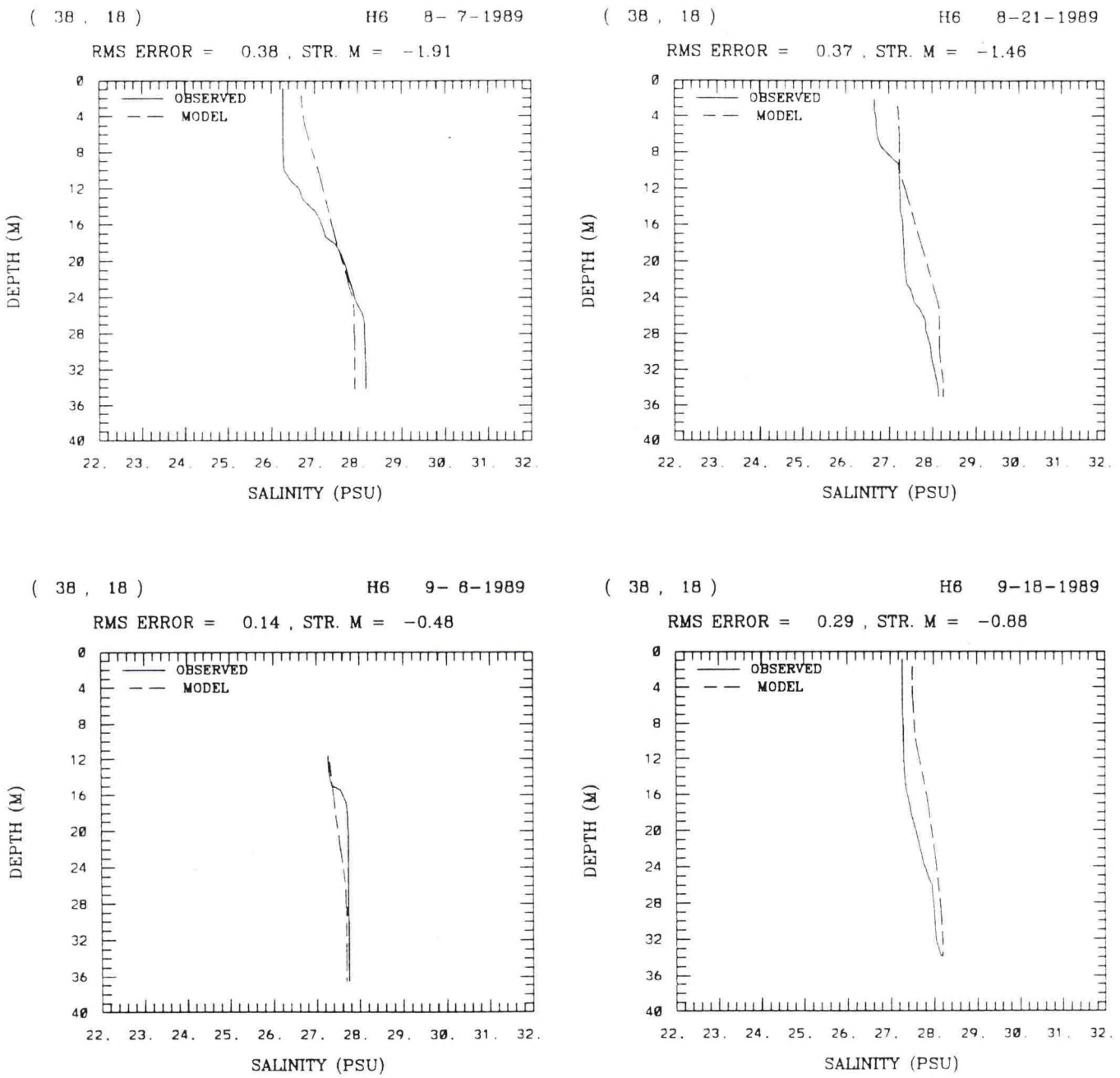

Figure A.3. (Cont.) Simulated versus Observed Vertical Salinity Profiles At Station: H6

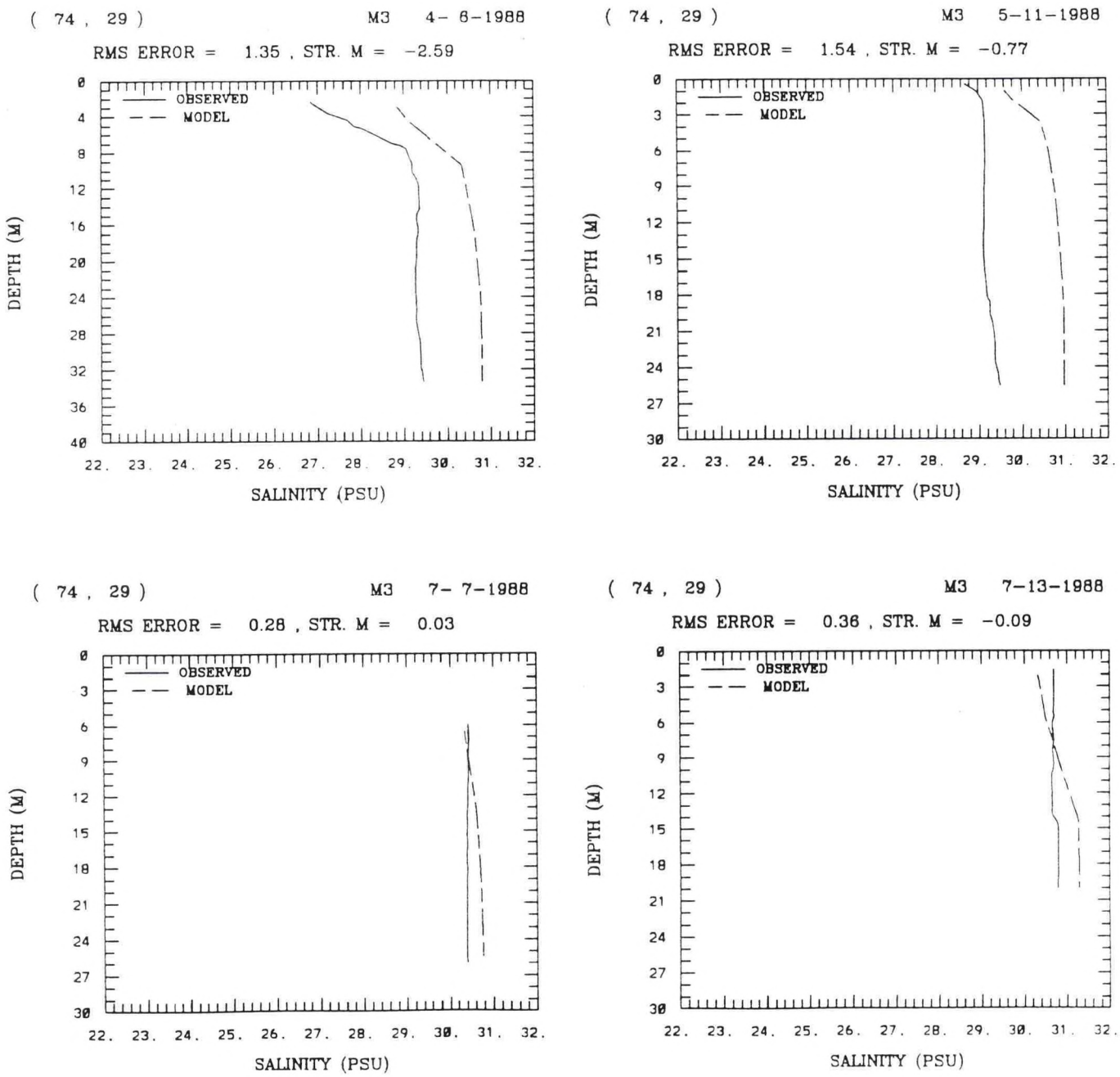

Figure A.4. Simulated versus Observed Vertical Salinity Profiles At Station: M3

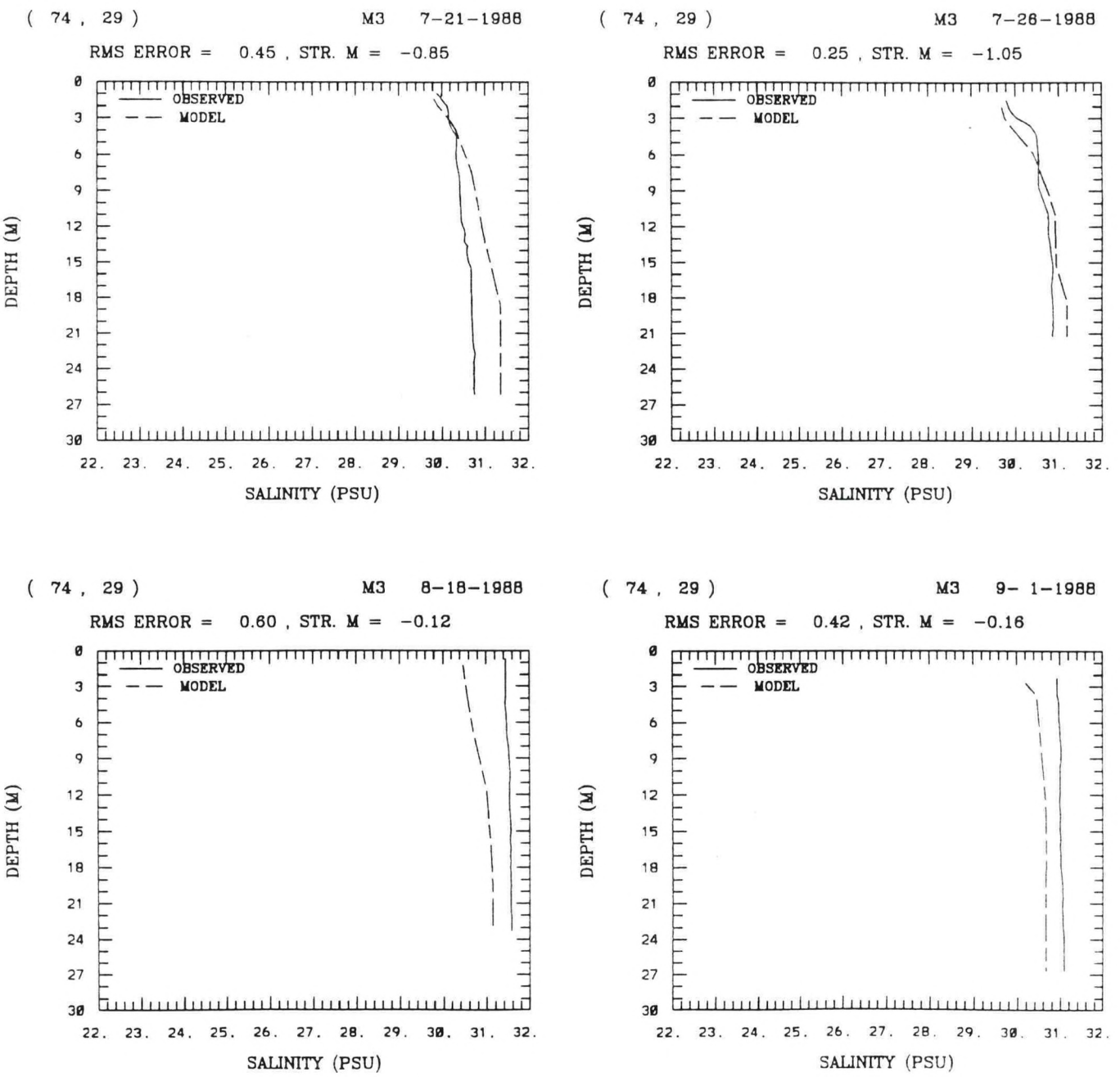

Figure A.4. (Cont.) Simulated versus Observed Vertical Salinity Profiles At Station: M3

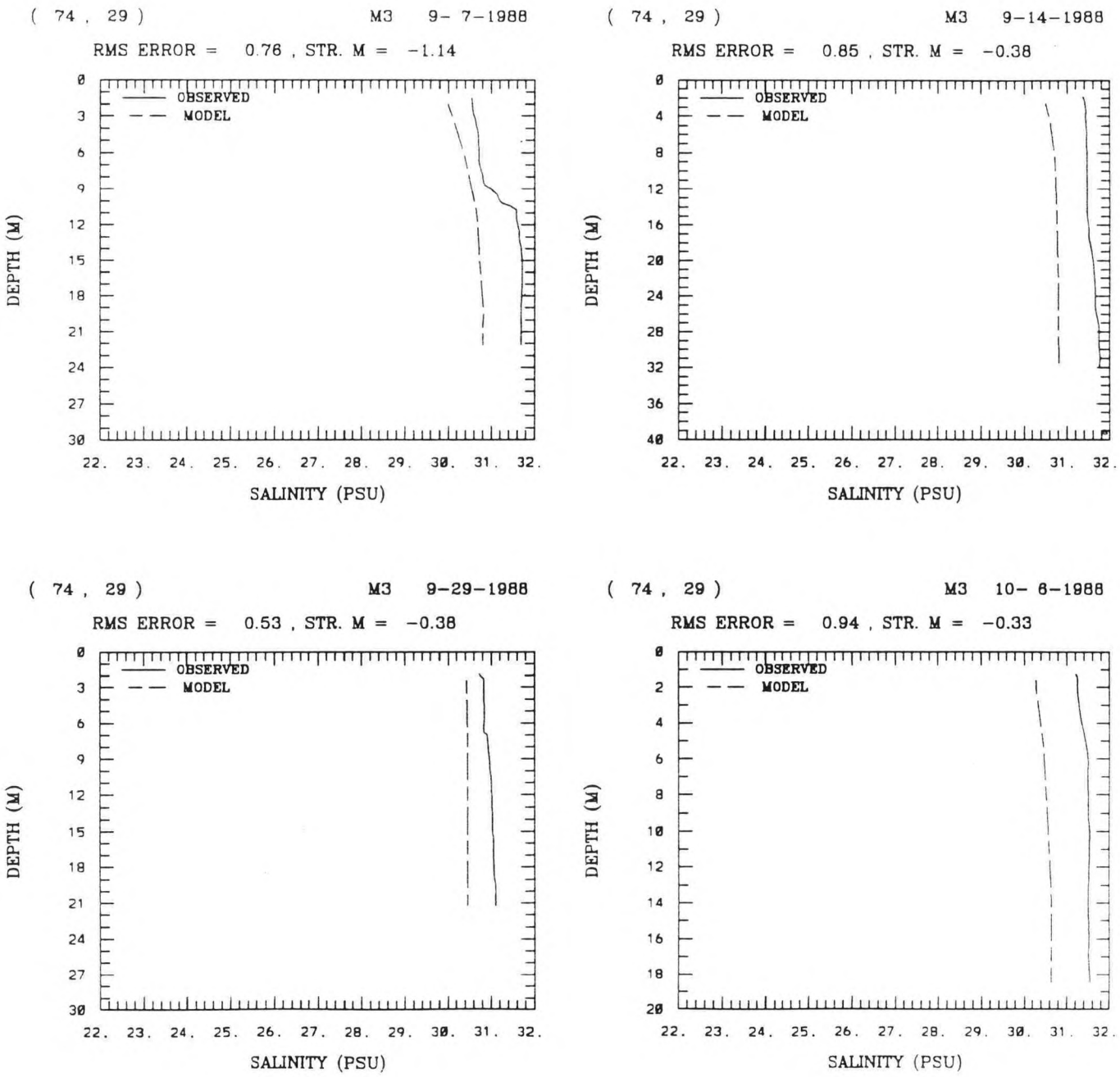

Figure A.4. (Cont.) Simulated versus Observed Vertical Salinity Profiles At Station: M3

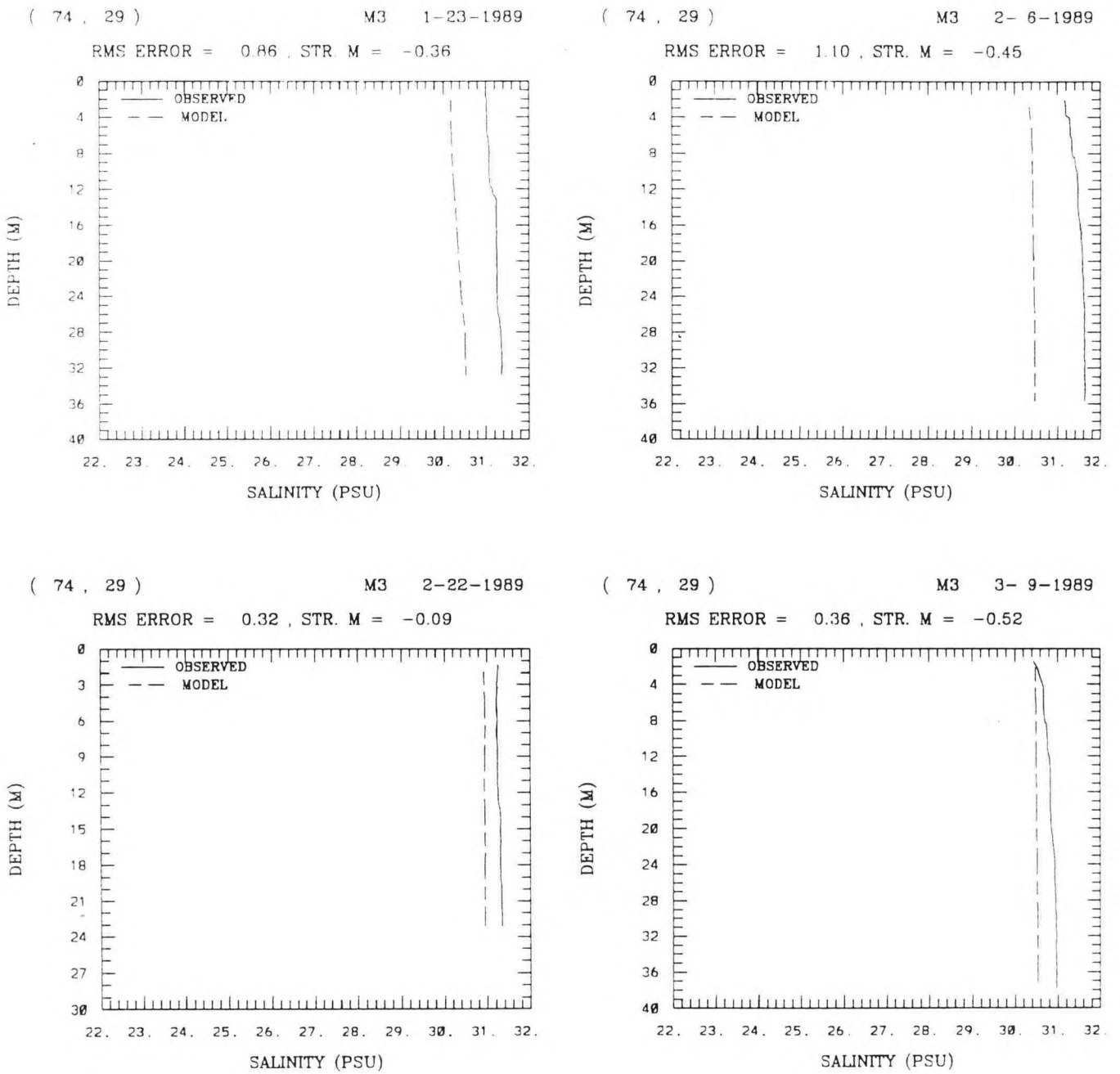

Figure A.4. (Cont.) Simulated versus Observed Vertical Salinity Profiles At Station: M3

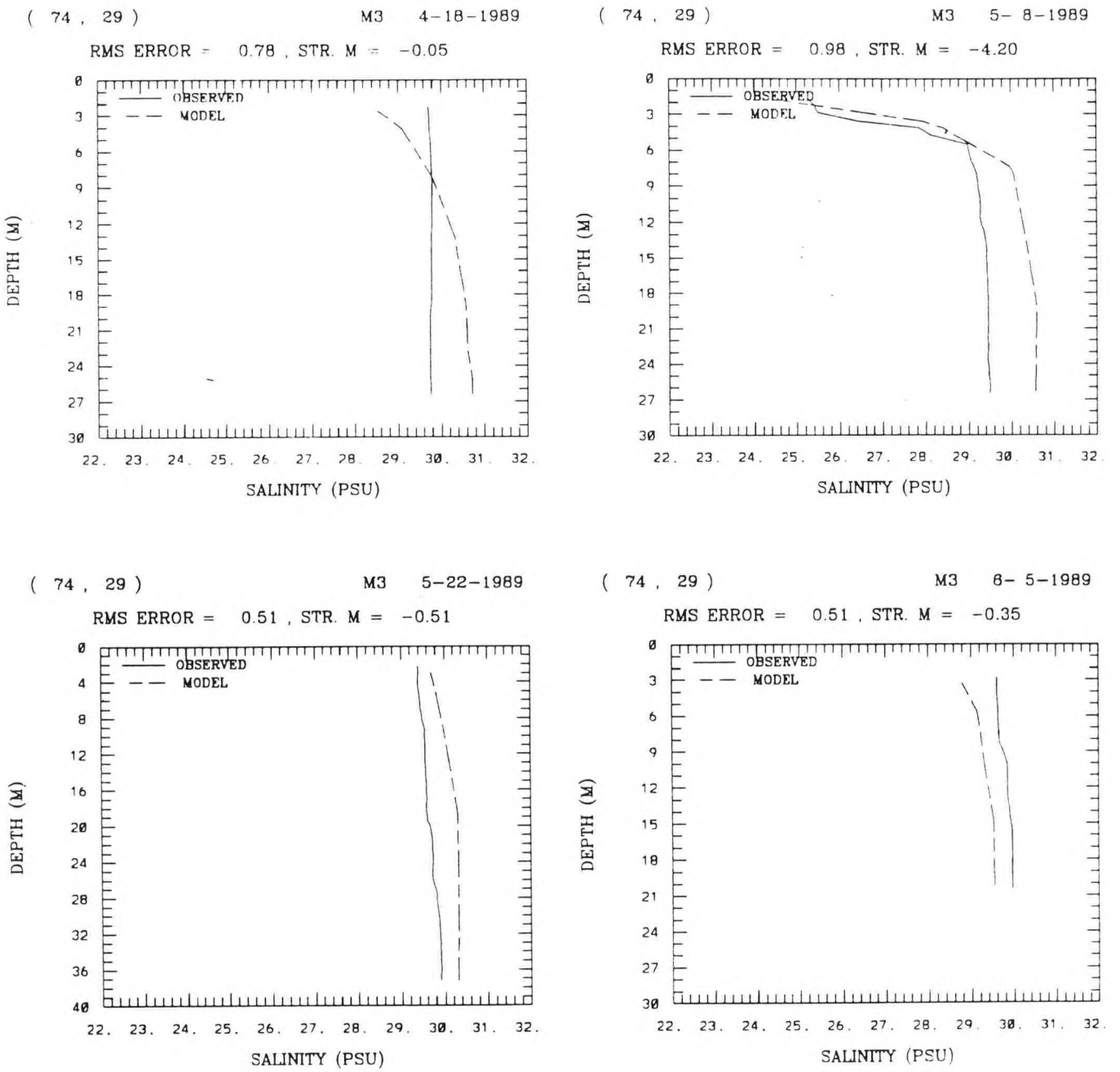

Figure A.4. (Cont.) Simulated versus Observed Vertical Salinity Profiles At Station: M3

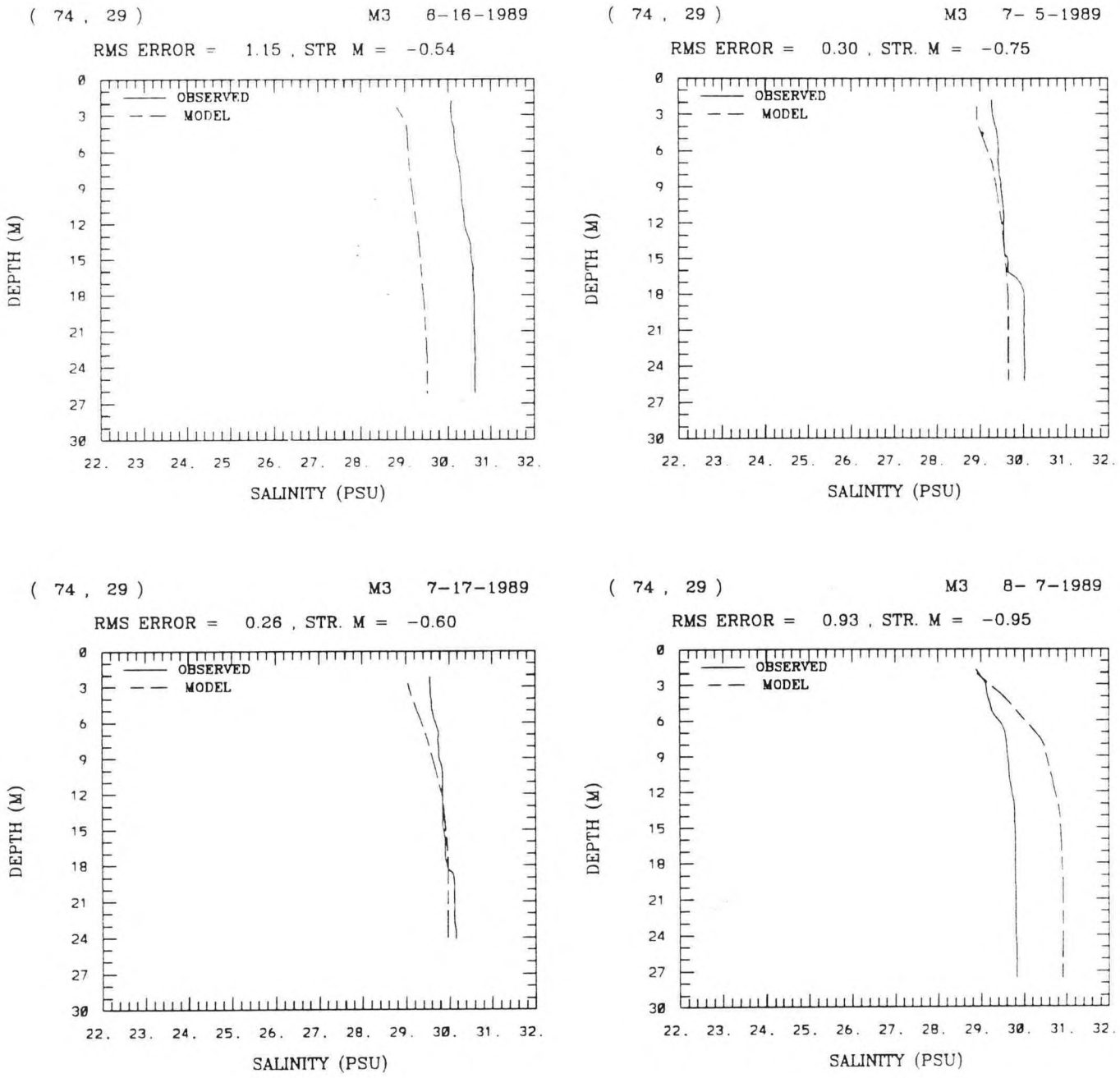

Figure A.4. (Cont.) Simulated versus Observed Vertical Salinity Profiles At Station: M3

Table A.1. Model versus Data Salinity Comparisons: Station A2

Calibration Period

SALINITY (PSU)

STATION	DATE	TIME	DEPTH (M)	RMS ERROR	SURFACE M	SURFACE D	BOTTOM M	BOTTOM D	STR. D	STR. M
A2	4/ 4/1988	12:43	35.55	0.47	24.46	24.83	25.13	25.81	-0.98	-0.67
A2	4/11/1988	11:16	35.45	0.63	24.87	24.27	24.88	25.78	-1.51	-0.01
A2	4/18/1988	11:45	36.32	0.56	24.96	23.69	25.09	25.31	-1.62	-0.13
A2	4/19/1988	11:16	32.40	0.82	23.98	24.61	25.19	26.04	-1.43	-1.22
A2	5/ 9/1988	11:31	31.83	0.36	25.11	24.54	25.39	25.81	-1.27	-0.27
A2	5/25/1988	11:45	34.93	0.46	24.01	23.53	25.70	25.77	-2.24	-1.69
A2	6/10/1988	10:47	35.24	0.17	24.96	24.80	25.89	25.59	-0.79	-0.92
A2	6/13/1988	11:31	34.36	0.26	25.20	24.82	25.99	25.70	-0.88	-0.79
A2	6/20/1988	11:16	35.76	0.87	26.52	25.00	26.40	26.17	-1.17	0.12
A2	6/27/1988	11:45	26.92	0.55	26.04	25.47	27.03	26.17	-0.70	-0.99
A2	7/ 6/1988	15:21	37.25	0.71	26.51	25.48	27.10	26.67	-1.19	-0.59
A2	7/12/1988	11:31	36.22	0.86	27.04	26.01	27.57	26.94	-0.93	-0.52
A2	7/18/1988	11: 2	30.90	0.91	26.49	25.87	27.85	26.94	-1.07	-1.36
A2	8/ 3/1988	11:45	35.34	1.33	27.71	26.03	27.87	26.72	-0.69	-0.16
A2	8/11/1988	11:16	36.22	0.76	27.40	26.45	28.46	27.85	-1.40	-1.06
A2	8/15/1988	12: 0	35.24	1.28	29.19	26.47	28.75	27.97	-1.50	0.44
A2	8/29/1988	10:47	36.12	1.51	28.12	26.50	28.45	27.01	-0.51	-0.33
A2	9/19/1988	11: 2	35.29	0.72	27.40	26.23	28.59	28.08	-1.85	-1.19
A2	9/26/1988	11:31	34.88	0.53	27.51	26.97	28.43	27.43	-0.46	-0.91
A2	10/ 3/1988	10:48	32.81	0.27	27.10	26.56	28.54	28.13	-1.57	-1.45
A2	10/18/1988	12: 0	34.00	0.64	27.98	26.95	28.00	27.68	-0.73	-0.02
A2	11/16/1988	14:52	34.15	0.63	26.14	25.56	28.23	27.62	-2.06	-2.09

Verification Period

SALINITY (PSU)

STATION	DATE	TIME	DEPTH (M)	RMS ERROR	SURFACE M	SURFACE D	BOTTOM M	BOTTOM D	STR. D	STR. M
A2	1/23/1989	16:33	34.05	0.81	25.72	25.83	28.11	27.13	-1.30	-2.40
A2	2/ 6/1989	17:16	34.31	0.74	27.04	26.09	27.44	26.80	-0.71	-0.40
A2	2/22/1989	12:57	37.25	1.42	27.07	24.90	28.14	26.97	-2.07	-1.07
A2	3/13/1989	15:21	36.01	1.45	26.62	23.54	27.76	26.32	-2.78	-1.14
A2	3/23/1989	15:35	34.67	0.49	26.00	25.99	27.89	27.35	-1.36	-1.88
A2	4/ 3/1989	16: 4	30.85	1.73	26.26	24.69	27.49	26.06	-1.37	-1.23
A2	4/17/1989	15:35	34.62	0.99	26.39	24.53	27.27	26.79	-2.26	-0.89
A2	5/ 9/1989	12:57	36.94	1.90	24.28	23.18	27.69	25.86	-2.68	-3.41
A2	5/23/1989	15:21	37.15	1.09	21.66	22.34	26.06	25.12	-2.78	-4.40
A2	6/ 6/1989	14:38	36.63	0.80	23.75	24.20	26.31	25.32	-1.12	-2.56
A2	7/ 6/1989	14:38	30.95	0.94	24.50	23.24	25.47	24.39	-1.15	-0.97
A2	8/ 7/1989	11: 2	35.24	0.34	24.35	24.48	25.79	25.74	-1.26	-1.44
A2	8/21/1989	12:28	36.63	0.87	25.43	24.28	25.47	25.03	-0.75	-0.03
A2	9/ 6/1989	15:21	35.55	0.15	24.69	24.61	25.56	25.52	-0.91	-0.87

Table A.2. Model versus Data Salinity Comparisons: Station B3

Calibration Period

			SALINITY (PSU)							
STATION	DATE	TIME	DEPTH (M)	RMS ERROR	SURFACE M	SURFACE D	BOTTOM M	BOTTOM D	STR. D	STR. M
B3	4/ 4/1988	16:47	18.55	0.82	24.76	25.78	25.73	26.62	-0.84	-0.97
B3	4/11/1988	12:28	18.45	0.59	25.28	26.02	25.51	26.06	-0.04	-0.23
B3	4/18/1988	16:19	17.88	0.41	25.28	25.89	25.73	26.16	-0.27	-0.45
B3	4/26/1988	12:28	16.22	0.43	25.22	25.52	25.82	26.46	-0.94	-0.60
B3	5/ 9/1988	14:52	19.33	0.20	25.55	25.76	25.93	26.27	-0.51	-0.38
B3	5/25/1988	16:33	17.20	0.57	25.53	24.72	26.18	26.19	-1.47	-0.65
B3	6/10/1988	12:14	19.12	0.17	26.05	25.87	26.42	26.37	-0.50	-0.37
B3	6/13/1988	14: 9	18.91	0.34	26.25	25.69	26.48	26.35	-0.66	-0.23
B3	6/20/1988	12:28	17.15	0.55	25.78	25.88	27.16	26.36	-0.48	-1.38
B3	6/27/1988	15: 7	18.14	0.74	26.40	26.21	27.62	26.76	-0.55	-1.22
B3	7/ 6/1988	13:55	19.53	0.29	26.62	26.43	27.69	27.41	-0.98	-1.07
B3	7/12/1988	14:38	16.53	0.56	26.57	26.45	28.24	27.57	-1.12	-1.67
B3	7/18/1988	12:28	16.22	0.43	27.25	26.81	28.32	27.75	-0.94	-1.08
B3	8/ 3/1988	15: 7	21.13	0.41	27.22	27.02	28.19	27.92	-0.90	-0.97
B3	8/11/1988	13:26	20.67	0.47	27.73	27.32	28.95	28.33	-1.01	-1.22
B3	8/15/1988	15:35	20.15	0.49	28.07	27.69	28.92	28.39	-0.70	-0.84
B3	8/29/1988	12: 0	20.05	0.50	28.24	27.77	28.54	28.17	-0.40	-0.29
B3	9/19/1988	12:14	17.31	0.37	27.71	27.97	28.84	28.47	-0.50	-1.13
B3	10/ 3/1988	12:14	17.83	0.11	27.95	28.12	28.56	28.45	-0.33	-0.61
B3	11/16/1988	13:11	17.77	0.25	27.45	27.35	28.77	28.45	-1.10	-1.32

Verification Period

			SALINITY (PSU)							
STATION	DATE	TIME	DEPTH (M)	RMS ERROR	SURFACE M	SURFACE D	BOTTOM M	BOTTOM D	STR. D	STR. M
B3	1/23/1989	14:52	18.08	0.72	27.48	27.07	28.37	27.51	-0.44	-0.89
B3	2/ 6/1989	15:21	17.52	0.71	27.92	27.18	28.00	27.37	-0.19	-0.08
B3	2/22/1989	11:45	18.76	0.70	26.97	26.39	28.09	27.32	-0.93	-1.12
B3	3/13/1989	13:55	19.12	1.28	27.75	24.84	28.07	27.21	-2.37	-0.32
B3	3/23/1989	14: 9	19.89	0.36	27.70	27.32	27.97	27.75	-0.43	-0.27
B3	4/ 3/1989	13:55	16.38	0.95	27.92	26.92	28.06	27.26	-0.34	-0.14
B3	4/17/1989	14: 9	17.52	0.82	27.10	26.15	27.73	27.08	-0.93	-0.63
B3	5/ 9/1989	11:31	18.55	0.97	25.59	25.66	27.86	26.82	-1.16	-2.27
B3	5/23/1989	13:55	20.77	1.21	24.93	23.24	26.39	25.99	-2.75	-1.45
B3	6/ 6/1989	12:43	21.60	0.92	26.01	24.87	26.75	26.01	-1.14	-0.74
B3	6/20/1989	13:55	19.79	1.43	25.15	23.86	26.29	25.33	-1.47	-1.14
B3	7/ 6/1989	13:26	22.17	0.90	25.78	24.69	26.01	25.44	-0.75	-0.23
B3	8/ 7/1989	12:43	16.17	0.25	25.27	25.10	26.45	26.81	-1.71	-1.18
B3	8/21/1989	11: 2	19.53	0.22	25.58	25.57	25.99	25.80	-0.23	-0.41
B3	9/ 6/1989	13:55	18.29	0.13	26.24	26.03	26.26	26.42	-0.39	-0.02

Table A.3. Model versus Data Salinity Comparisons: Station D3

Calibration Period

SALINITY (PSU)

STATION	DATE	TIME	DEPTH (M)	RMS ERROR	SURFACE M	SURFACE D	BOTTOM M	BOTTOM D	STR. D	STR. M
D3	4/ 5/1988	10:47	31.26	0.50	25.88	26.15	26.11	26.89	-0.74	-0.23
D3	4/11/1988	14: 9	30.23	0.19	26.13	26.22	26.15	26.69	-0.47	-0.02
D3	4/19/1988	11: 2	24.44	0.12	26.14	26.22	26.15	26.35	-0.13	-0.01
D3	4/26/1988	13:40	30.95	0.43	25.96	25.95	26.27	26.83	-0.88	-0.31
D3	5/10/1988	11:16	31.05	0.09	26.19	26.31	26.60	26.66	-0.35	-0.42
D3	5/16/1988	15:35	31.52	0.13	26.32	26.41	26.82	26.61	-0.20	-0.50
D3	5/26/1988	11:31	31.11	0.31	26.39	25.80	26.66	26.75	-0.95	-0.27
D3	6/10/1988	13:40	25.47	0.77	26.73	26.24	27.35	26.53	-0.29	-0.62
D3	6/14/1988	9: 7	30.69	0.68	26.94	26.08	27.52	26.64	-0.56	-0.57
D3	6/20/1988	13:55	30.07	0.62	26.79	26.20	27.57	26.89	-0.69	-0.78
D3	6/28/1988	8:24	30.12	0.58	27.34	26.48	28.46	27.86	-1.38	-1.12
D3	7/ 6/1988	11: 2	30.85	0.42	27.65	27.30	28.45	27.84	-0.54	-0.80
D3	7/13/1988	7:26	27.70	0.62	27.48	26.83	28.67	27.87	-1.04	-1.20
D3	7/18/1988	13:55	30.95	0.36	27.89	27.42	28.52	28.03	-0.61	-0.64
D3	8/ 3/1988	19:26	31.00	0.20	27.97	27.49	28.44	28.51	-1.02	-0.47
D3	8/16/1988	11:31	33.02	0.56	28.82	27.97	28.81	28.73	-0.76	0.01
D3	8/29/1988	13:26	32.14	0.65	28.92	28.01	28.92	28.37	-0.36	0.00
D3	10/ 3/1988	13:40	30.85	0.20	28.93	28.69	28.97	29.07	-0.38	-0.04
D3	11/16/1988	11:45	40.20	0.24	28.68	28.11	28.94	28.76	-0.65	-0.26

Verification Period

SALINITY (PSU)

STATION	DATE	TIME	DEPTH (M)	RMS ERROR	SURFACE M	SURFACE D	BOTTOM M	BOTTOM D	STR. D	STR. M
D3	1/23/1989	12:43	40.20	0.95	28.25	27.34	28.62	27.74	-0.40	-0.37
D3	3/13/1989	12: 0	39.17	0.96	28.38	27.37	28.38	27.44	-0.07	0.00
D3	3/23/1989	12: 0	40.66	0.49	28.31	27.67	28.31	28.10	-0.43	0.00
D3	4/ 3/1989	12: 0	41.28	0.72	28.30	27.48	28.31	27.67	-0.19	-0.01
D3	4/17/1989	12:14	42.16	0.79	28.10	26.89	28.24	27.70	-0.81	-0.13
D3	5/ 9/1989	9:35	39.58	0.78	27.48	26.67	27.88	27.13	-0.46	-0.40
D3	5/23/1989	12: 0	37.67	1.05	25.39	23.36	27.33	26.56	-3.20	-1.93
D3	6/ 6/1989	11: 2	38.49	0.72	26.10	24.85	27.06	26.52	-1.67	-0.97
D3	6/20/1989	12:14	36.43	0.95	26.36	24.68	26.68	26.01	-1.33	-0.32
D3	8/ 7/1989	14:52	38.29	0.51	26.31	25.89	26.85	27.33	-1.44	-0.54
D3	8/21/1989	9:36	38.86	0.15	26.41	26.25	26.58	26.62	-0.37	-0.17
D3	9/ 6/1989	12:14	38.13	0.17	26.73	26.75	26.89	27.05	-0.30	-0.17

Table A.4. Model versus Data Salinity Comparisons: Station F3

Calibration Period

			SALINITY (PSU)							
STATION	DATE	TIME	DEPTH (M)	RMS ERROR	SURFACE M	SURFACE D	BOTTOM M	BOTTOM D	STR. D	STR. M
F3	4/ 5/1988	14:52	28.37	0.23	26.30	26.41	27.35	27.38	-0.97	-1.05
F3	4/11/1988	15:50	26.87	0.54	26.27	26.82	26.57	27.01	-0.19	-0.29
F3	4/19/1988	14: 9	26.82	0.33	26.34	26.66	26.53	26.95	-0.29	-0.18
F3	4/26/1988	15: 7	26.35	0.32	26.37	26.68	26.52	26.90	-0.22	-0.16
F3	5/10/1988	14: 9	27.13	0.27	26.31	26.44	27.34	26.81	-0.37	-1.03
F3	5/16/1988	13:40	29.35	0.16	26.47	26.57	27.13	26.92	-0.35	-0.66
F3	5/26/1988	14: 9	24.91	0.35	26.46	25.78	27.23	26.81	-1.03	-0.77
F3	6/10/1988	15: 7	25.27	0.84	26.84	26.22	27.75	26.79	-0.57	-0.90
F3	6/14/1988	12:28	27.13	0.69	27.10	26.41	27.74	26.98	-0.57	-0.65
F3	6/20/1988	15:21	29.25	0.91	27.13	26.29	28.08	27.14	-0.85	-0.95
F3	6/28/1988	11:31	29.92	0.42	27.61	26.81	28.72	28.34	-1.53	-1.10
F3	7/ 6/1988	9: 7	28.32	0.48	27.79	27.10	28.71	28.18	-1.08	-0.92
F3	7/13/1988	10:47	28.88	0.39	28.02	27.53	28.61	28.20	-0.67	-0.59
F3	8/ 4/1988	11:45	28.37	0.36	28.18	27.43	28.88	28.78	-1.35	-0.70
F3	8/11/1988	16:19	28.78	0.31	28.30	27.77	29.06	28.75	-0.98	-0.76
F3	8/16/1988	13:40	29.97	0.43	28.90	28.30	29.23	28.89	-0.59	-0.33
F3	8/29/1988	15: 7	29.25	0.30	29.08	28.48	29.08	29.49	-1.01	0.01
F3	9/28/1988	7:55	24.75	0.04	29.09	29.04	29.12	29.19	-0.15	-0.03
F3	10/19/1988	12:43	25.32	0.10	29.11	29.10	29.14	29.26	-0.16	-0.03
F3	11/16/1988	9:50	39.11	0.33	29.08	28.67	29.08	28.79	-0.12	0.00

Verification Period

			SALINITY (PSU)							
STATION	DATE	TIME	DEPTH (M)	RMS ERROR	SURFACE M	SURFACE D	BOTTOM M	BOTTOM D	STR. D	STR. M
F3	1/23/1989	10:33	40.15	0.92	28.71	27.57	28.70	27.95	-0.38	0.01
F3	2/21/1989	10: 4	38.55	0.67	28.56	27.35	28.56	28.01	-0.66	0.00
F3	3/13/1989	10: 4	39.42	0.88	28.42	27.40	28.42	27.61	-0.21	0.00
F3	3/23/1989	10: 4	40.15	0.25	28.47	28.07	28.52	28.54	-0.47	-0.04
F3	4/ 3/1989	9:50	34.83	0.45	28.21	27.56	28.39	28.20	-0.64	-0.18
F3	4/17/1989	9:50	41.59	0.32	26.39	26.96	28.39	28.06	-1.10	-1.99
F3	5/ 8/1989	9:50	39.01	0.78	27.89	26.52	27.93	27.44	-0.92	-0.04
F3	5/23/1989	10: 4	41.44	0.50	25.34	24.02	27.40	26.95	-2.93	-2.06
F3	6/ 6/1989	9:21	40.51	0.50	26.25	25.00	27.10	26.73	-1.73	-0.86
F3	6/20/1989	10:19	39.06	0.79	26.34	24.44	26.84	26.76	-2.32	-0.49
F3	8/ 7/1989	16:33	39.01	0.59	26.46	26.17	27.08	27.86	-1.69	-0.62
F3	8/21/1989	7:55	38.75	0.26	26.79	26.29	27.22	27.17	-0.88	-0.44
F3	9/ 6/1989	9:36	37.41	0.24	27.12	26.93	27.17	27.53	-0.60	-0.05

Table A.5. Model versus Data Salinity Comparisons: Station H6

Calibration Period

SALINITY (PSU)

STATION	DATE	TIME	DEPTH (M)	RMS ERROR	SURFACE M	SURFACE D	BOTTOM M	BOTTOM D	STR. D	STR. M
H6	4/ 6/1988	12:57	40.61	0.15	26.65	26.72	27.74	27.96	-1.24	-1.09
H6	4/11/1988	17:16	17.98	0.44	26.33	26.99	27.29	27.02	-0.03	-0.95
H6	4/26/1988	16:19	41.28	0.27	26.61	26.75	26.82	27.10	-0.35	-0.21
H6	5/11/1988	12:28	40.20	0.45	26.74	26.53	28.24	27.52	-0.99	-1.50
H6	5/16/1988	12:43	43.14	0.43	26.86	26.73	28.04	27.35	-0.62	-1.18
H6	5/23/1988	13:55	32.86	0.52	26.85	26.64	27.70	27.17	-0.53	-0.85
H6	6/10/1988	16:33	41.65	0.82	27.14	26.83	28.50	27.32	-0.49	-1.36
H6	6/15/1988	13:12	39.17	0.93	27.33	26.45	28.51	27.45	-1.00	-1.18
H6	6/20/1988	17: 2	43.20	1.01	27.55	26.48	29.10	28.11	-1.63	-1.55
H6	6/29/1988	12:14	32.45	0.75	27.73	26.75	29.48	29.03	-2.28	-1.75
H6	7/ 6/1988	7:40	40.20	0.60	28.06	27.30	29.09	28.56	-1.26	-1.03
H6	7/11/1988	13:26	32.24	0.89	28.18	27.45	29.03	28.33	-0.88	-0.85
H6	8/ 2/1988	16:47	40.92	0.79	28.68	27.63	29.71	29.19	-1.56	-1.03
H6	8/17/1988	12:14	34.77	0.36	28.67	28.31	29.83	29.36	-1.05	-1.16
H6	8/29/1988	16:33	39.27	0.37	29.11	28.38	29.86	29.83	-1.45	-0.75
H6	11/16/1988	8: 9	42.06	0.21	29.25	28.87	29.25	29.11	-0.24	0.00

Verification Period

SALINITY (PSU)

STATION	DATE	TIME	DEPTH (M)	RMS ERROR	SURFACE M	SURFACE D	BOTTOM M	BOTTOM D	STR. D	STR. M
H6	1/23/1989	8:38	38.91	0.74	28.85	27.86	28.89	28.26	-0.40	-0.04
H6	2/ 6/1989	9: 7	38.80	0.79	28.74	27.72	28.76	28.23	-0.51	-0.02
H6	2/21/1989	8:24	38.18	0.66	28.59	27.58	28.80	28.16	-0.58	-0.22
H6	3/13/1989	8: 9	32.81	0.80	28.67	27.68	28.69	27.98	-0.30	-0.02
H6	3/23/1989	8: 9	40.20	0.46	28.67	27.93	28.83	28.70	-0.77	-0.16
H6	4/ 3/1989	7:55	41.18	0.35	28.06	27.36	28.72	28.61	-1.25	-0.66
H6	4/17/1989	7:55	39.42	0.51	27.98	27.53	28.47	28.23	-0.70	-0.49
H6	5/ 8/1989	7:55	41.08	0.68	27.70	26.56	28.07	27.58	-1.02	-0.36
H6	5/23/1989	8: 9	42.11	0.70	25.06	23.44	27.87	27.16	-3.72	-2.81
H6	6/ 6/1989	7:40	39.58	0.76	26.13	25.07	27.91	27.00	-1.93	-1.77
H6	6/20/1989	8:38	33.64	0.84	25.96	24.90	27.31	26.90	-2.00	-1.35
H6	7/ 6/1989	8: 9	31.36	0.48	26.45	25.34	26.92	26.84	-1.50	-0.47
H6	8/ 7/1989	18: 0	34.21	0.38	26.68	26.26	27.92	28.17	-1.91	-1.25
H6	8/21/1989	6: 0	35.14	0.37	27.20	26.67	28.25	28.13	-1.46	-1.06
H6	9/ 6/1989	8: 9	36.53	0.14	27.29	27.27	27.68	27.75	-0.48	-0.39
H6	9/18/1989	8:38	33.95	0.29	27.51	27.28	28.20	28.16	-0.88	-0.69

Table A.6. Model versus Data Salinity Comparisons: Station I2

Calibration Period

SALINITY (PSU)

STATION	DATE	TIME	DEPTH (M)	RMS ERROR	SURFACE M	SURFACE D	BOTTOM M	BOTTOM D	STR. D	STR. M
I2	5/10/1988	11:31	24.30	0.91	26.52	26.69	28.38	27.17	-0.48	-1.86
I2	7/ 7/1988	9:35	26.18	0.65	28.71	27.98	29.18	28.52	-0.54	-0.47
I2	7/20/1988	11:31	25.50	0.84	28.76	28.15	29.99	29.11	-0.96	-1.23
I2	8/ 4/1988	11:31	24.51	0.93	28.96	27.38	29.58	28.64	-1.26	-0.62
I2	8/12/1988	7:26	25.84	0.71	28.94	28.37	29.96	29.17	-0.80	-1.02
I2	8/18/1988	11:31	16.33	0.29	29.24	29.02	30.13	29.53	-0.51	-0.89
I2	9/ 1/1988	9: 7	25.35	0.56	29.60	28.89	29.62	29.14	-0.25	-0.02
I2	9/14/1988	9:35	25.84	0.49	29.56	29.00	29.56	29.10	-0.10	0.00
I2	10/19/1988	11:16	25.20	0.03	29.51	29.45	29.51	29.55	-0.10	0.00
I2	12/19/1988	13:26	24.56	0.42	29.25	28.70	29.28	28.88	-0.18	-0.02

Verification Period

SALINITY (PSU)

STATION	DATE	TIME	DEPTH (M)	RMS ERROR	SURFACE M	SURFACE D	BOTTOM M	BOTTOM D	STR. D	STR. M
I2	1/18/1989	12:43	24.91	0.20	29.03	28.83	29.03	28.83	0.00	0.00
I2	1/23/1989	8:52	25.64	0.21	28.85	28.68	28.91	28.75	-0.07	-0.06
I2	2/ 6/1989	12:43	25.59	0.32	29.02	28.31	29.01	29.11	-0.80	0.01
I2	3/ 9/1989	12: 0	27.16	0.16	29.16	29.04	29.15	28.99	0.05	0.01
I2	3/21/1989	10: 4	26.33	0.57	29.27	28.40	29.29	29.06	-0.66	-0.02
I2	4/18/1989	12: 0	26.67	0.51	27.29	27.90	28.49	27.85	0.05	-1.20
I2	5/ 8/1989	12:14	26.48	0.57	26.78	27.52	28.23	27.59	-0.07	-1.46
I2	5/22/1989	14: 9	27.26	0.48	26.29	26.82	27.76	27.21	-0.39	-1.47
I2	6/ 5/1989	12:14	27.50	0.92	27.18	25.94	27.63	26.93	-0.99	-0.45
I2	6/16/1989	11:31	27.41	0.27	25.85	25.85	27.63	27.19	-1.34	-1.78
I2	7/ 5/1989	12:28	27.21	0.63	26.75	25.47	27.24	27.60	-2.13	-0.49
I2	7/17/1989	10:33	27.60	0.97	27.22	26.29	28.34	28.55	-2.26	-1.11
I2	8/ 7/1989	12:43	27.31	0.36	27.55	27.07	28.78	28.58	-1.51	-1.24
I2	8/21/1989	12:14	27.41	0.27	27.73	27.41	28.08	27.87	-0.46	-0.35
I2	9/ 5/1989	12: 0	26.97	0.36	27.70	27.30	28.34	28.27	-0.97	-0.64
I2	9/18/1989	11: 2	26.38	0.44	28.36	27.73	28.37	28.19	-0.46	0.00

Table A.7. Model versus Data Salinity Comparisons: Station J2

Calibration Period

SALINITY (PSU)

STATION	DATE	TIME	DEPTH (M)	RMS ERROR	SURFACE M	SURFACE D	BOTTOM M	BOTTOM D	STR. D	STR. M
J2	4/ 7/1988	15:21	14.31	0.67	26.17	27.47	29.36	28.63	-1.16	-3.19
J2	5/10/1988	15:21	15.10	1.87	28.24	27.37	29.52	27.46	-0.09	-1.28
J2	7/14/1988	14:38	13.53	0.50	29.65	29.04	30.23	29.81	-0.77	-0.58
J2	8/ 4/1988	15:21	16.67	0.23	29.81	29.69	29.91	29.67	0.02	-0.11
J2	9/ 8/1988	14:52	13.24	0.18	29.47	29.78	30.10	30.02	-0.24	-0.63
J2	10/ 6/1988	11:31	23.29	0.35	29.70	29.12	29.63	30.01	-0.89	0.07
J2	10/19/1988	14:52	16.23	0.41	29.37	30.05	29.73	30.15	-0.10	-0.37
J2	12/19/1988	11:45	16.23	0.19	29.24	28.75	29.26	29.17	-0.42	-0.02

Verification Period

SALINITY (PSU)

STATION	DATE	TIME	DEPTH (M)	RMS ERROR	SURFACE M	SURFACE D	BOTTOM M	BOTTOM D	STR. D	STR. M
J2	1/18/1989	11:45	22.50	0.84	29.08	29.71	29.09	30.02	-0.31	-0.01
J2	1/23/1989	10:33	21.52	0.78	29.15	29.92	29.18	29.97	-0.05	-0.03
J2	2/ 6/1989	11:16	19.56	0.31	29.68	29.85	29.68	30.03	-0.18	0.00
J2	2/22/1989	11:45	21.67	0.45	29.33	30.07	29.63	30.05	0.02	-0.30
J2	3/ 9/1989	10:48	24.81	0.11	29.63	29.81	29.63	29.66	0.15	0.00
J2	3/21/1989	11:16	18.43	0.29	29.47	29.73	29.88	30.27	-0.54	-0.41
J2	4/18/1989	10:48	15.64	1.09	28.30	27.96	29.59	28.70	-0.74	-1.29
J2	5/ 8/1989	11:31	22.70	1.22	28.25	28.00	29.32	27.99	0.01	-1.07
J2	5/22/1989	12:43	16.03	1.32	28.10	25.80	28.90	28.77	-2.97	-0.80
J2	6/ 5/1989	11: 2	22.85	0.56	26.76	28.45	28.35	28.44	0.01	-1.59
J2	6/16/1989	10:19	16.08	0.27	26.34	26.54	28.38	28.64	-2.10	-2.04
J2	7/ 5/1989	11:16	21.62	0.37	28.01	28.49	28.13	28.49	0.00	-0.12
J2	7/17/1989	11:45	19.71	0.35	28.02	27.67	29.28	28.89	-1.22	-1.26
J2	8/ 7/1989	11:45	23.44	0.33	28.49	28.60	29.44	28.93	-0.33	-0.95
J2	8/21/1989	11: 2	19.07	0.32	28.41	28.06	28.38	28.08	-0.02	0.03
J2	9/ 5/1989	11: 2	22.16	0.10	28.42	28.74	28.78	28.80	-0.06	-0.36
J2	9/18/1989	10: 4	20.44	0.02	28.78	28.83	28.83	28.82	0.01	-0.05

Table A.8. Model versus Data Salinity Comparisons: Station M3

Calibration Period

SALINITY (PSU)

STATION	DATE	TIME	DEPTH (M)	RMS ERROR	SURFACE M	SURFACE D	BOTTOM M	BOTTOM D	STR. D	STR. M
M3	4/ 6/1988	7:55	33.38	1.35	28.74	26.85	30.80	29.44	-2.59	-2.06
M3	5/11/1988	15:21	25.54	1.54	29.61	28.71	30.98	29.48	-0.77	-1.37
M3	7/ 7/1988	11:16	25.94	0.28	30.33	30.42	30.75	30.39	0.03	-0.43
M3	7/13/1988	7:40	20.00	0.36	30.29	30.69	31.28	30.78	-0.09	-0.99
M3	7/21/1988	13:26	26.13	0.45	29.76	29.90	31.36	30.75	-0.85	-1.59
M3	7/26/1988	11:45	21.23	0.25	29.65	29.80	31.18	30.85	-1.05	-1.54
M3	8/18/1988	15: 7	23.29	0.60	30.46	31.45	31.14	31.57	-0.12	-0.68
M3	9/ 1/1988	11: 2	26.67	0.42	30.10	30.93	30.65	31.09	-0.16	-0.55
M3	9/ 7/1988	7:55	22.11	0.76	29.93	30.55	30.80	31.69	-1.14	-0.87
M3	9/14/1988	11:45	31.92	0.85	30.46	31.37	30.80	31.75	-0.38	-0.34
M3	9/29/1988	9: 7	21.23	0.53	30.42	30.72	30.45	31.10	-0.38	-0.03
M3	10/ 6/1988	7:55	18.48	0.94	30.26	31.21	30.64	31.54	-0.33	-0.37
M3	10/18/1988	8:24	27.01	0.96	30.30	31.30	30.52	31.52	-0.22	-0.22
M3	12/19/1988	8:24	46.33	0.60	30.13	30.68	30.46	31.33	-0.65	-0.33

Verification Period

SALINITY (PSU)

STATION	DATE	TIME	DEPTH (M)	RMS ERROR	SURFACE M	SURFACE D	BOTTOM M	BOTTOM D	STR. D	STR. M
M3	1/23/1989	12:57	32.90	0.86	30.18	30.99	30.52	31.35	-0.36	-0.33
M3	2/ 6/1989	9: 7	35.69	1.10	30.31	31.18	30.47	31.63	-0.45	-0.16
M3	2/22/1989	9:35	23.09	0.32	30.92	31.25	30.95	31.34	-0.09	-0.03
M3	3/ 9/1989	9: 7	37.85	0.36	30.49	30.44	30.54	30.96	-0.52	-0.05
M3	4/18/1989	8:38	26.43	0.78	28.40	29.71	30.71	29.76	-0.05	-2.32
M3	5/ 8/1989	9: 7	26.48	0.98	24.41	25.28	30.57	29.48	-4.20	-6.16
M3	5/22/1989	10:33	37.21	0.51	29.65	29.39	30.31	29.90	-0.51	-0.66
M3	6/ 5/1989	9: 7	20.44	0.51	28.73	29.61	29.54	29.96	-0.35	-0.80
M3	6/16/1989	8: 9	26.18	1.15	28.73	30.09	29.51	30.63	-0.54	-0.78
M3	7/ 5/1989	9:21	25.30	0.30	28.92	29.28	29.65	30.03	-0.75	-0.73
M3	7/17/1989	14: 9	24.12	0.26	29.01	29.56	29.96	30.16	-0.60	-0.95
M3	8/ 7/1989	9:21	27.60	0.93	28.79	28.89	30.91	29.84	-0.95	-2.11
M3	8/21/1989	8:52	26.97	0.35	29.40	28.70	29.86	29.66	-0.96	-0.46
M3	9/ 5/1989	8:38	29.91	0.19	29.43	29.87	30.15	30.24	-0.37	-0.72
M3	9/18/1989	7:55	27.41	0.14	29.88	29.91	30.00	30.14	-0.23	-0.12

Appendix B: Model vs Data Temperature Comparisons

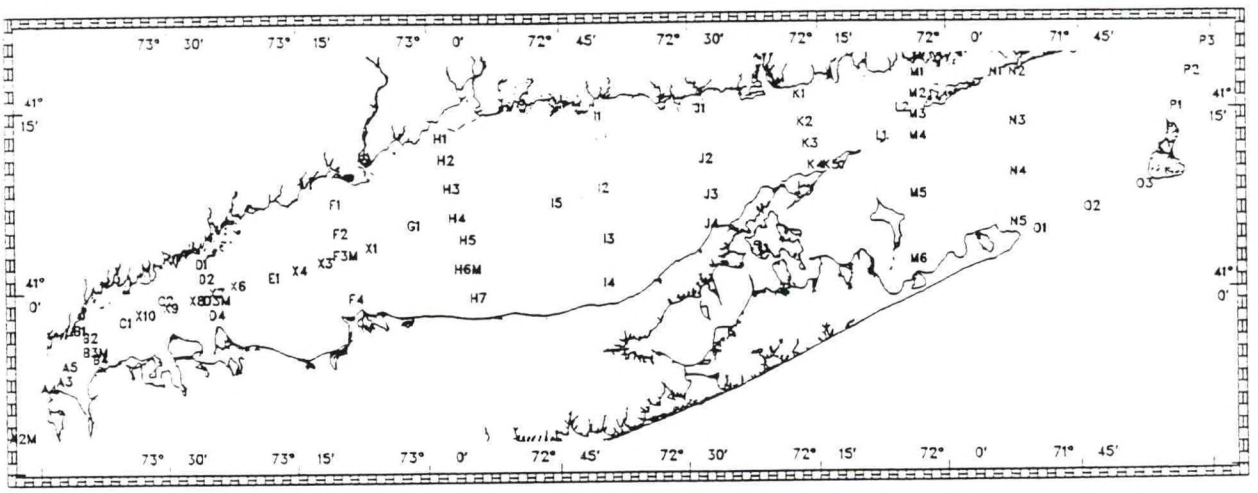

Station Locations.

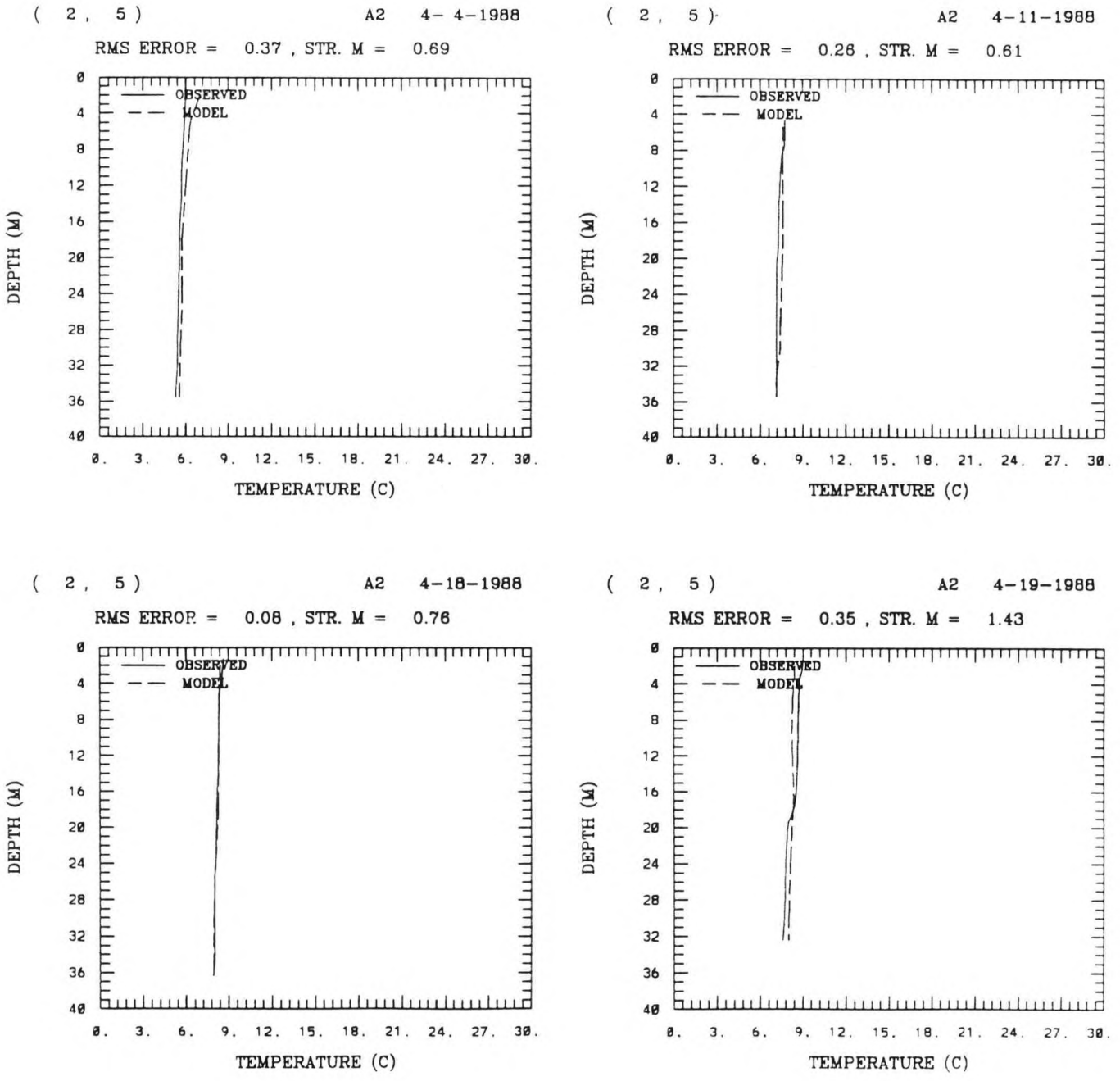

Figure B.1. Simulated versus Observed Vertical Temperature Profiles At Station: A2

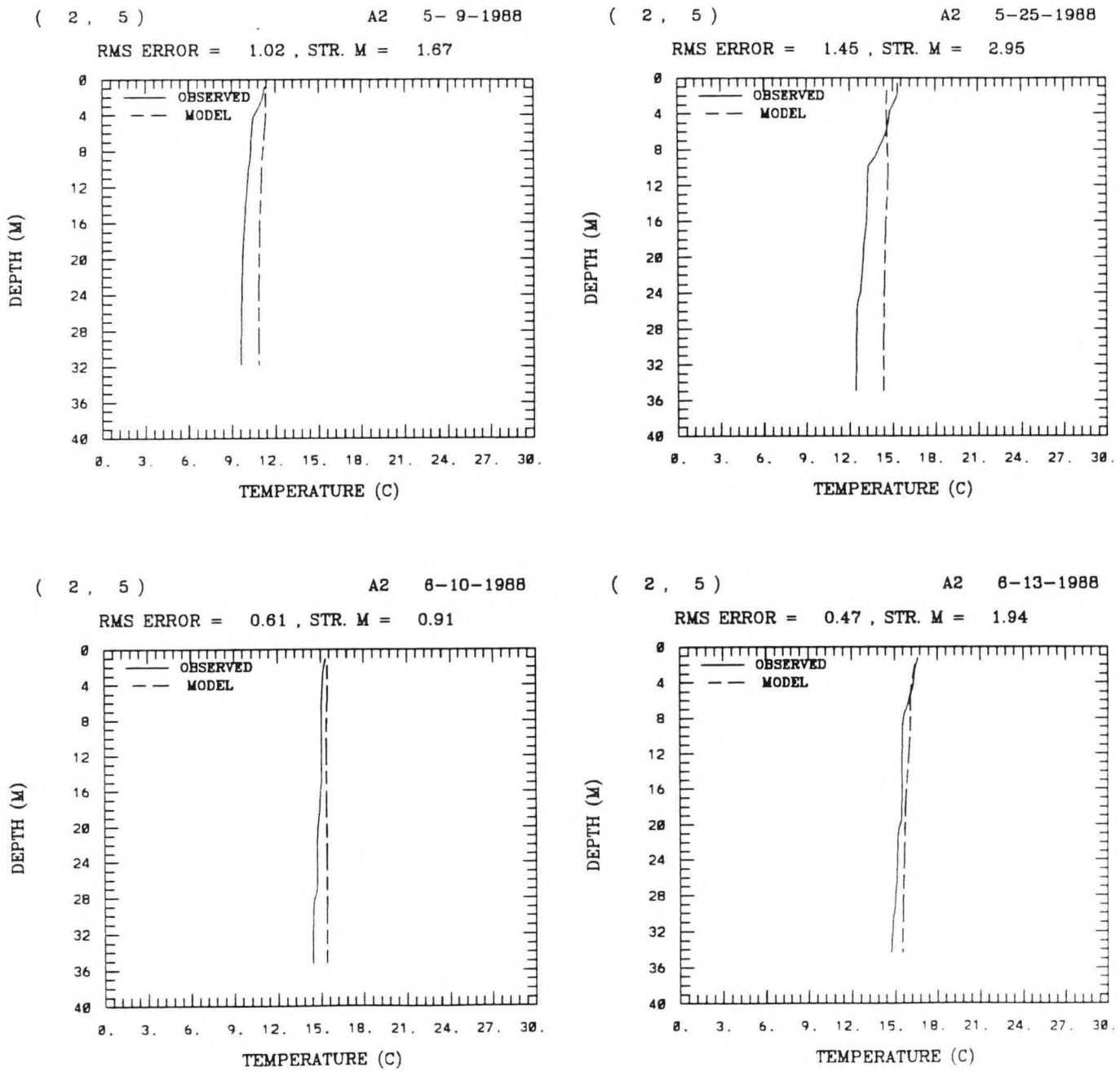

Figure B.1. (Cont.) Simulated versus Observed Vertical Temperature Profiles At Station: A2

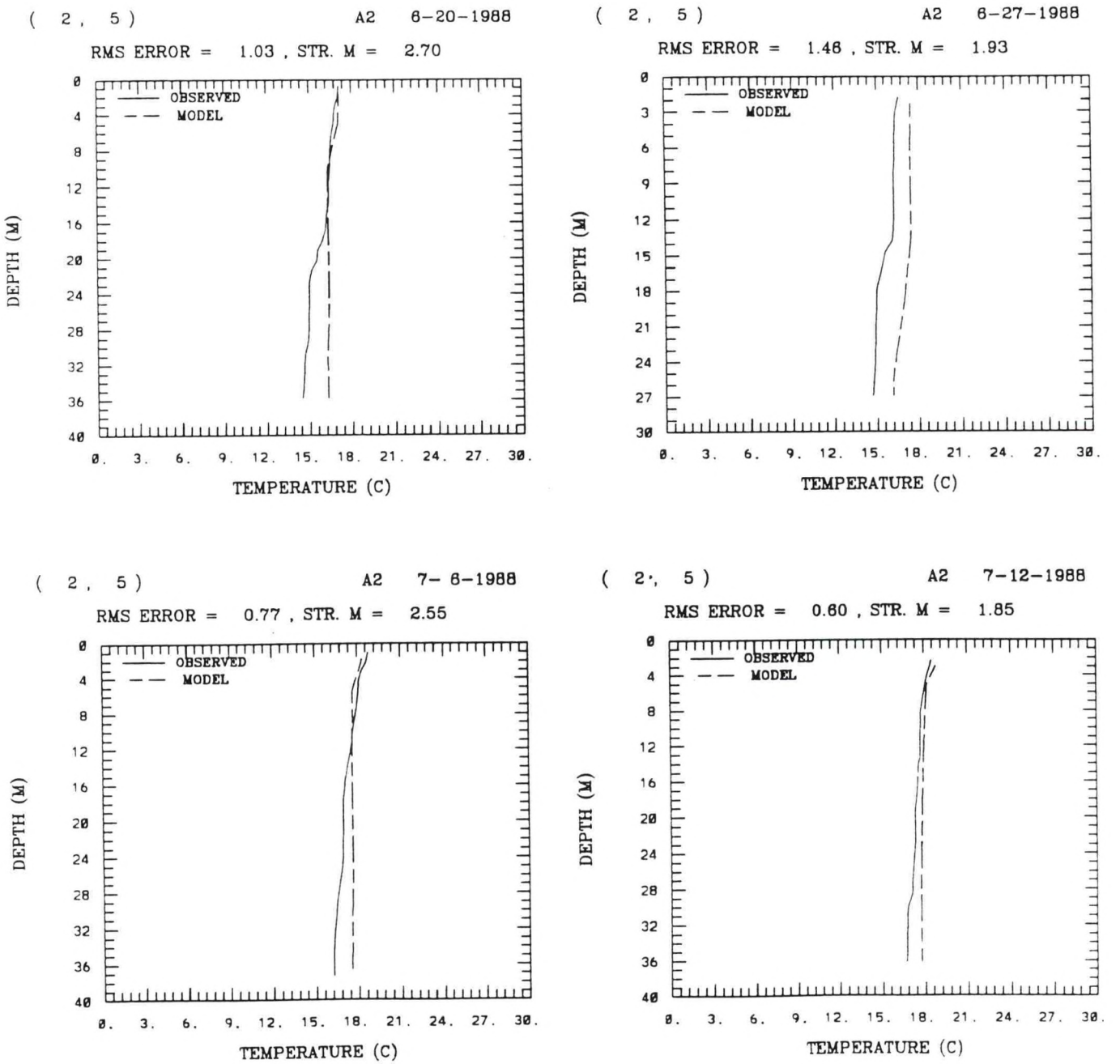

Figure B.1. (Cont.) Simulated versus Observed Vertical Temperature Profiles At Station: A2

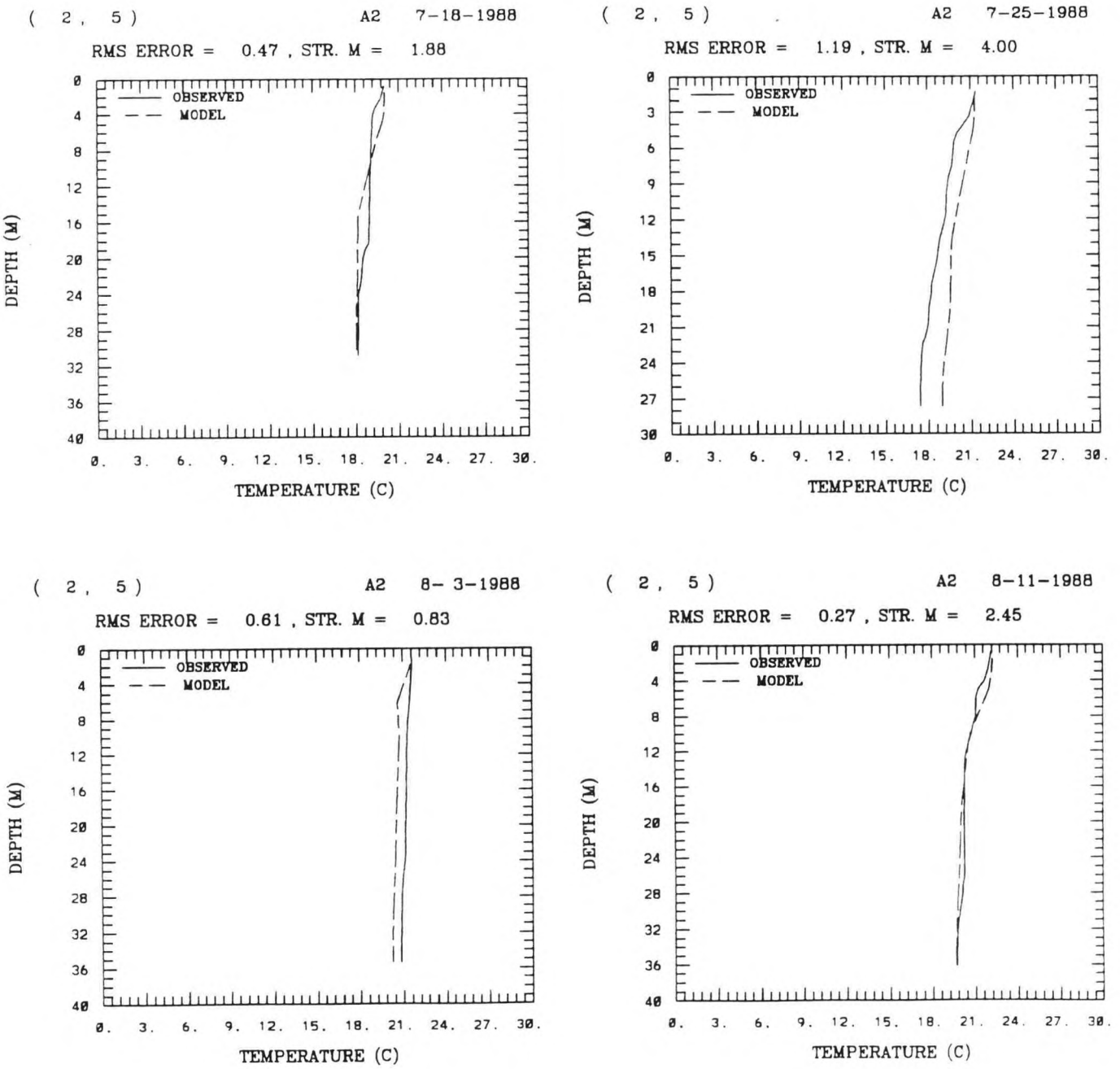

Figure B.1. (Cont.) Simulated versus Observed Vertical Temperature Profiles At Station: A2

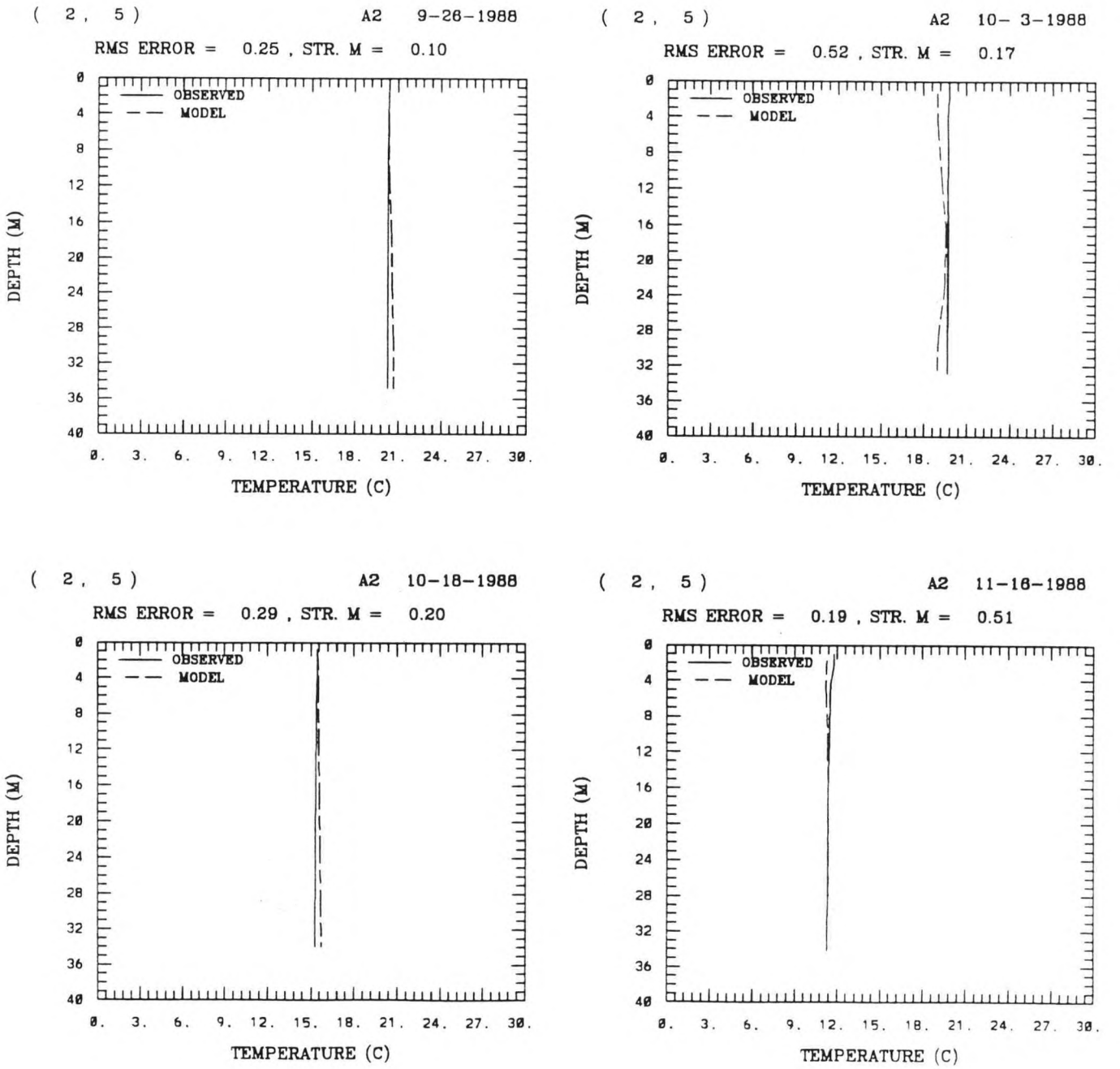

Figure B.1. (Cont.) Simulated versus Observed Vertical Temperature Profiles At Station: A2

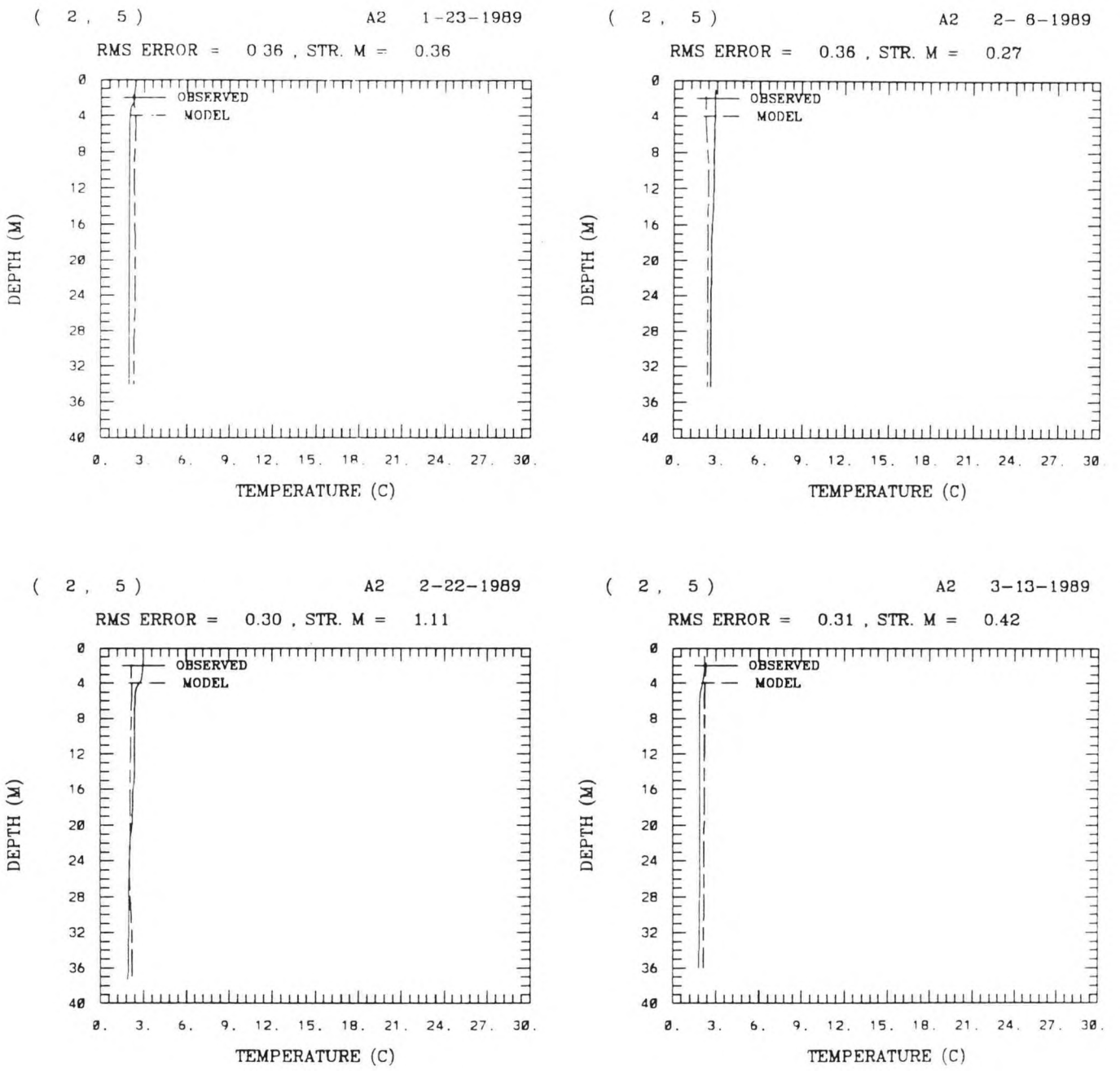

Figure B.1. (Cont.) Simulated versus Observed Vertical Temperature Profiles At Station: A2

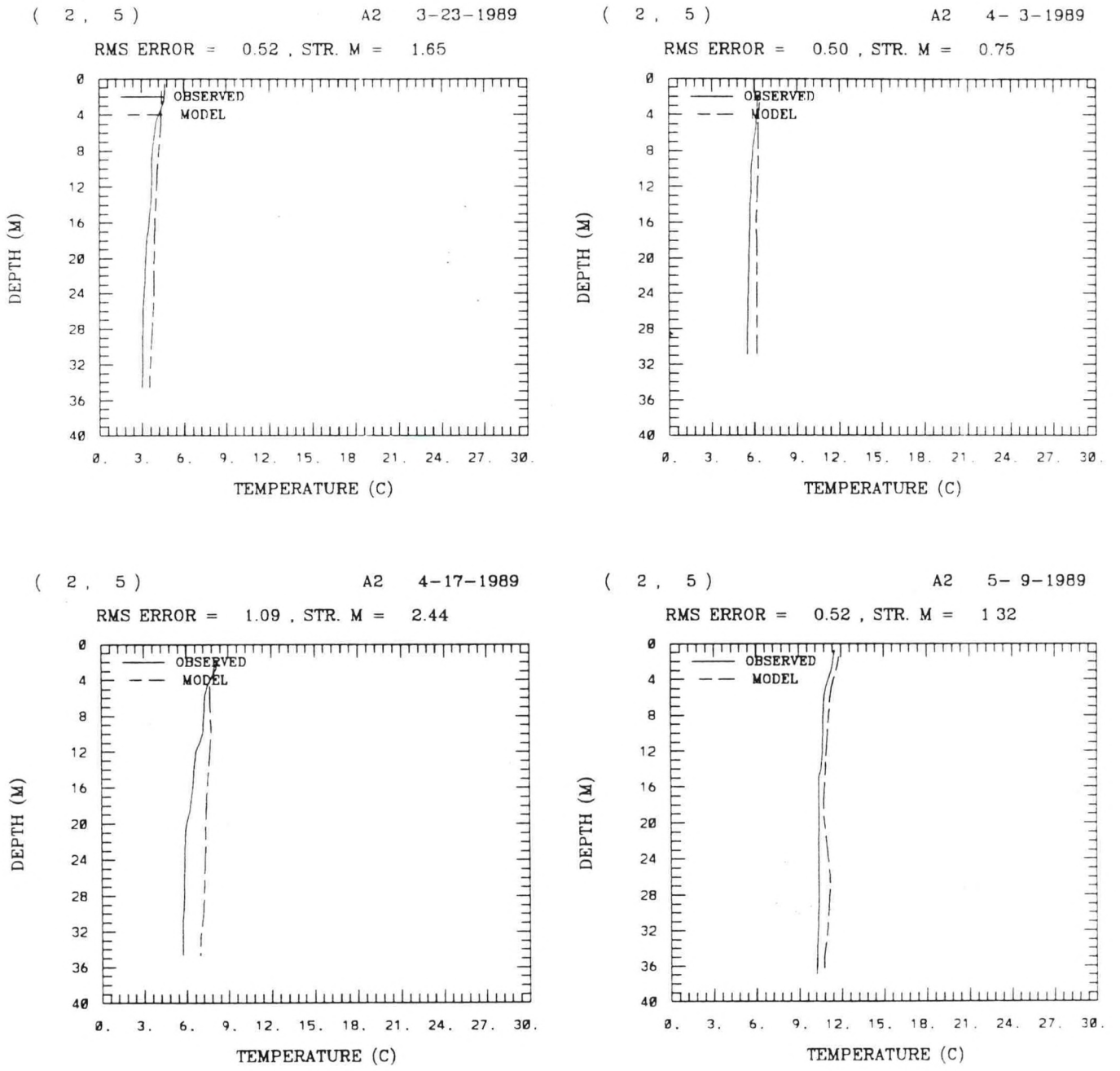

Figure B.1. (Cont.) Simulated versus Observed Vertical Temperature Profiles At Station: A2

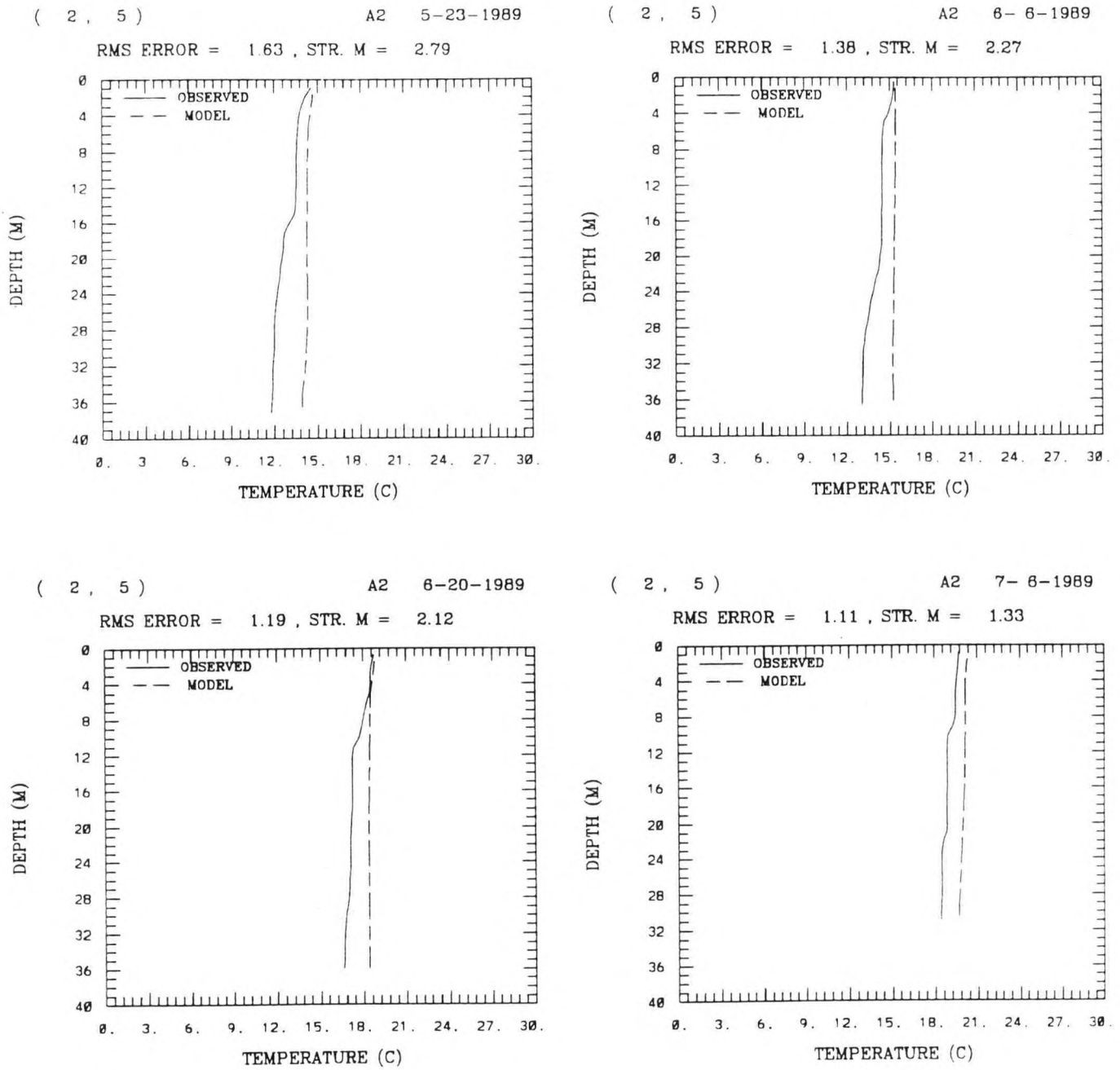

Figure B.1. (Cont.) Simulated versus Observed Vertical Temperature Profiles At Station: A2

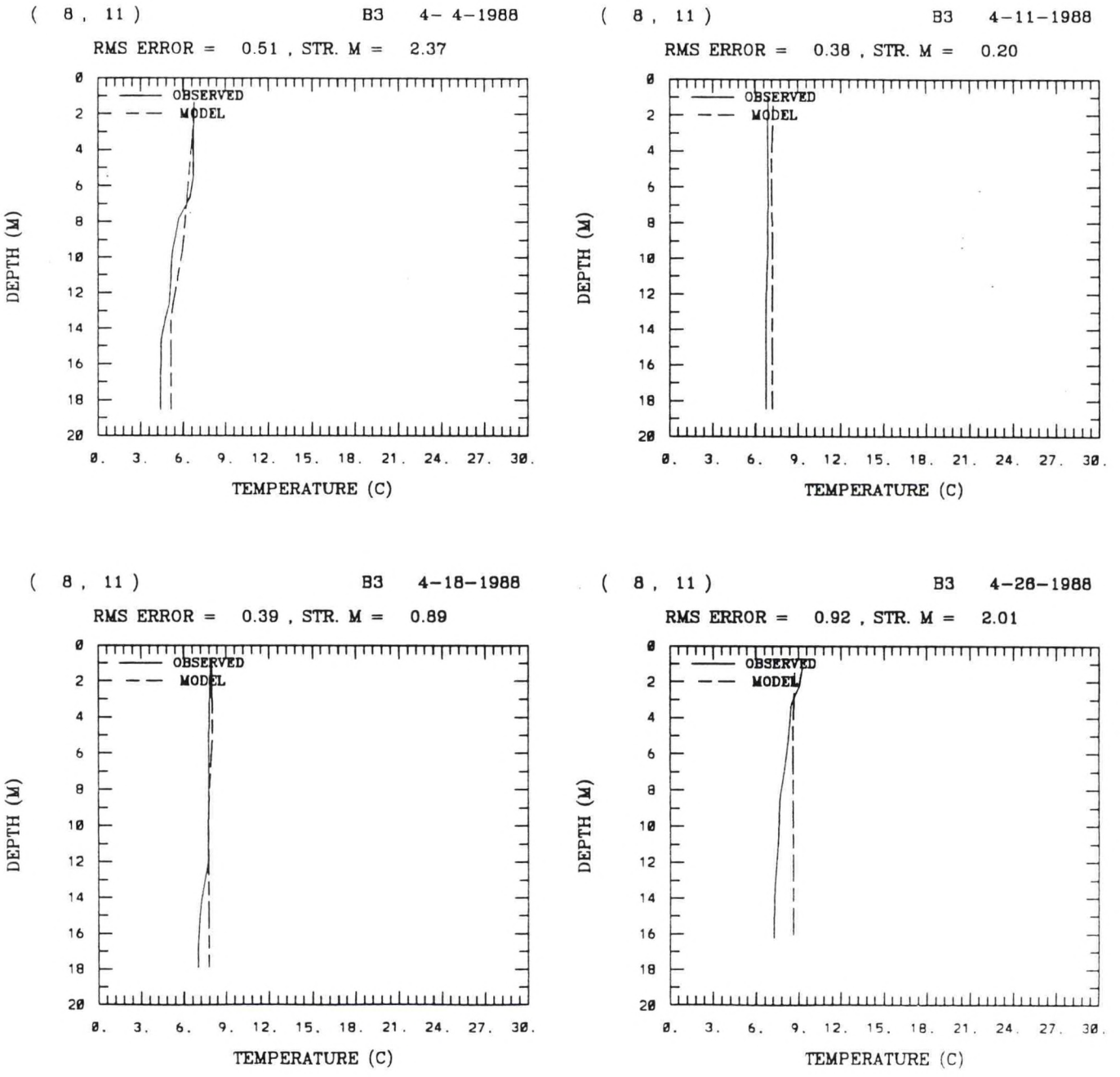

Figure B.2. Simulated versus Observed Vertical Temperature Profiles At Station: B3

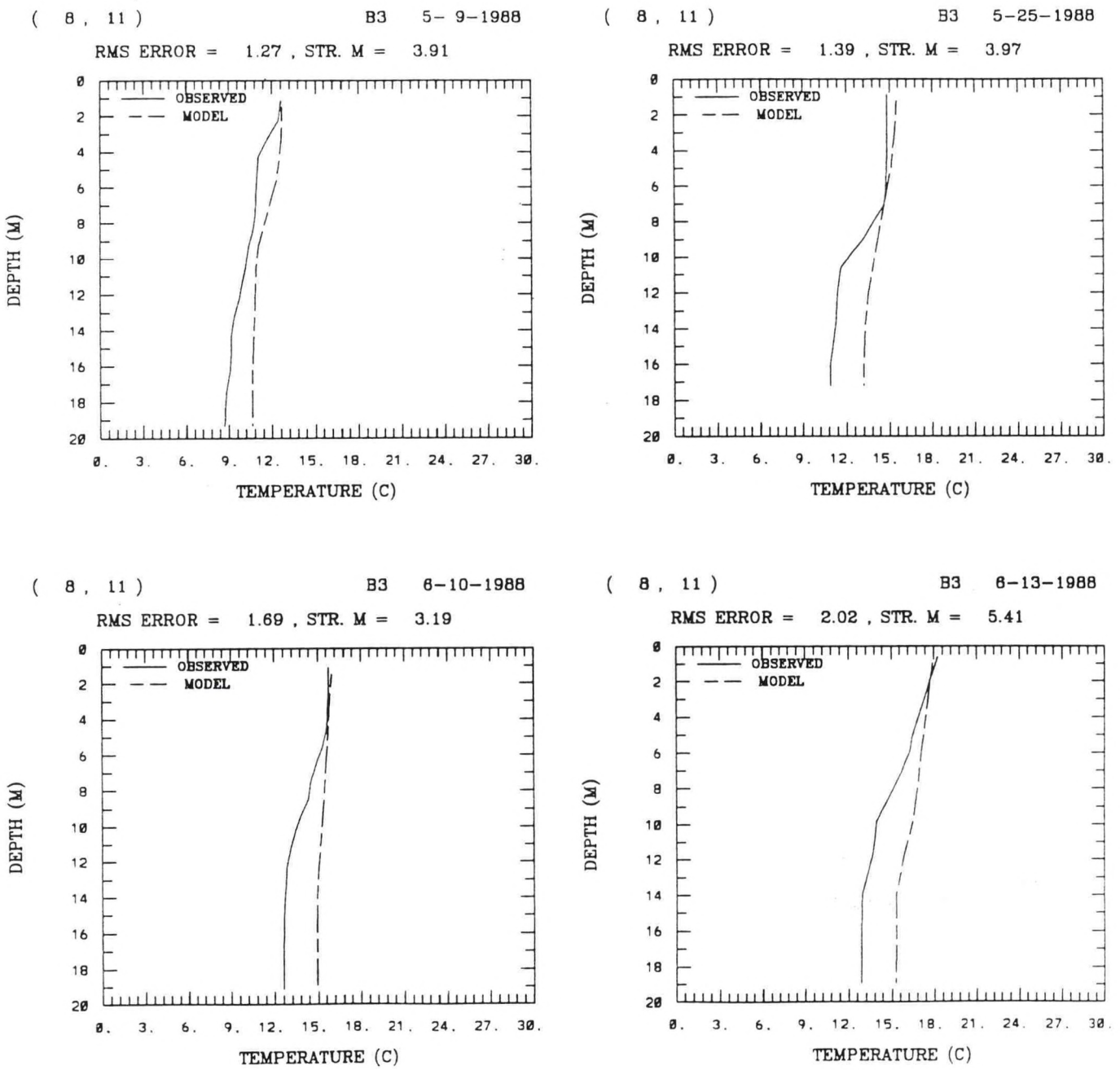

Figure B.2. (Cont.) Simulated versus Observed Vertical Temperature Profiles At Station: B3

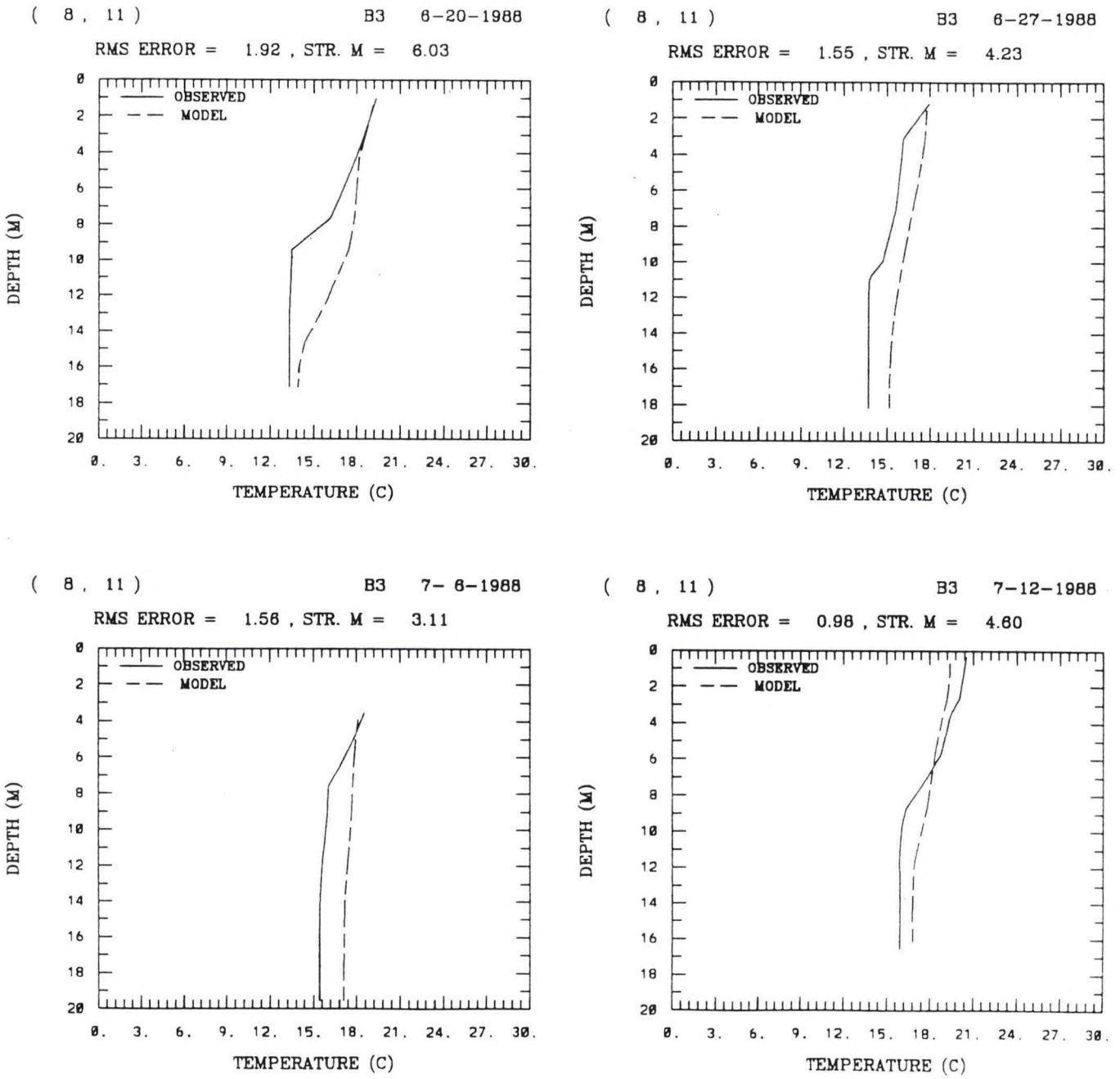

Figure B.2. (Cont.) Simulated versus Observed Vertical Temperature Profiles At Station: B3

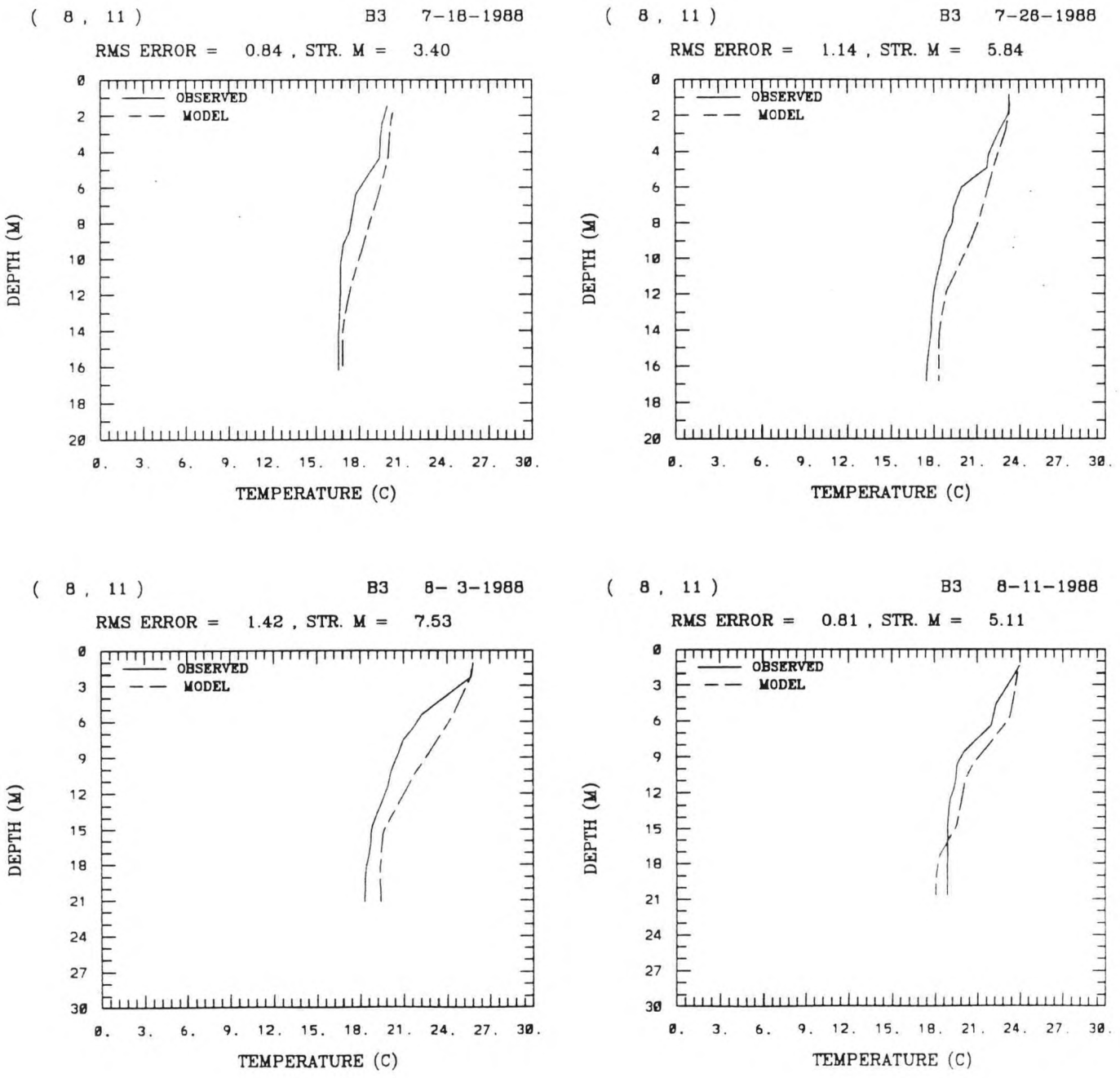

Figure B.2. (Cont.) Simulated versus Observed Vertical Temperature Profiles At Station: B3

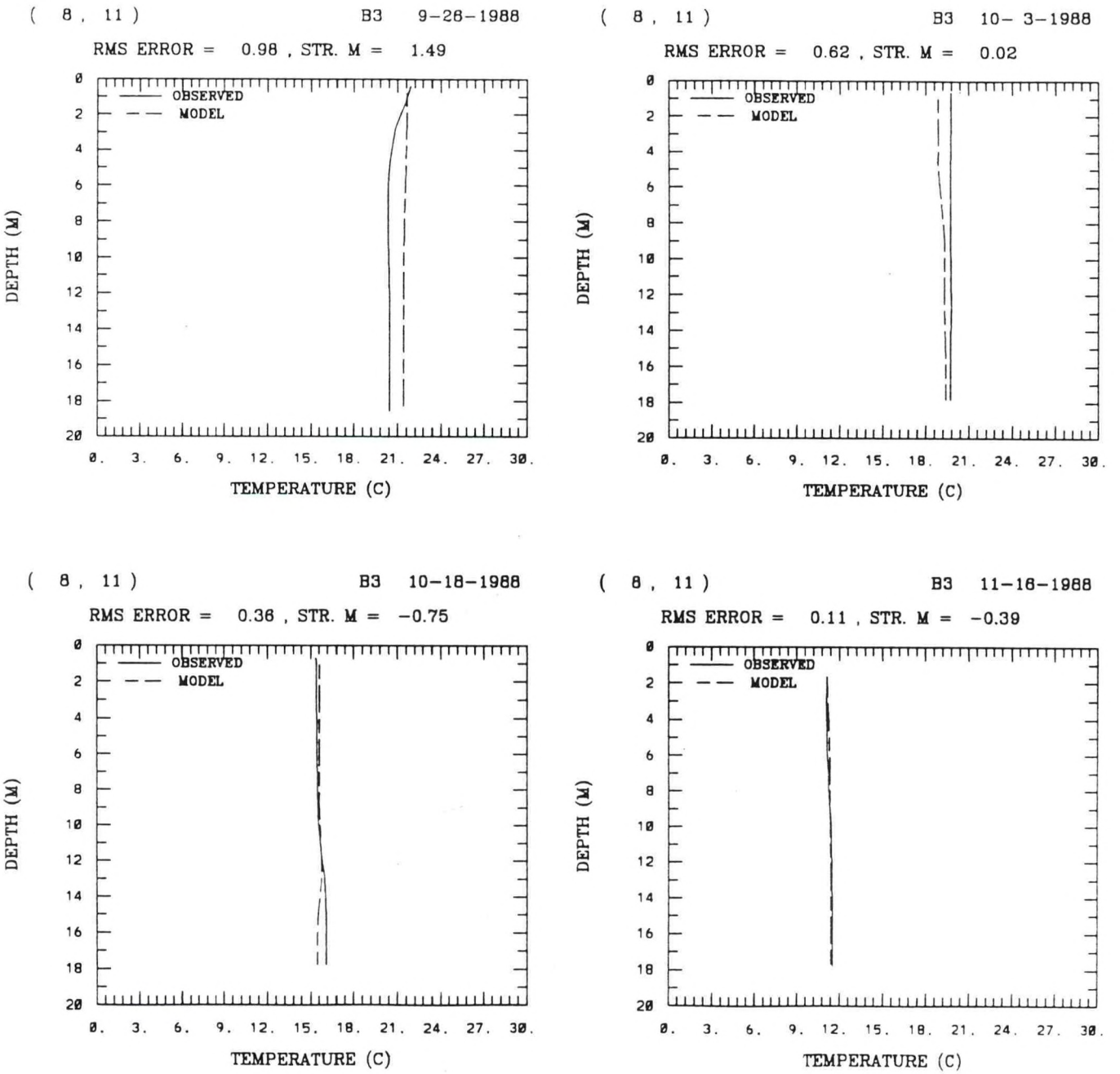

Figure B.2. (Cont.) Simulated versus Observed Vertical Temperature Profiles At Station: B3

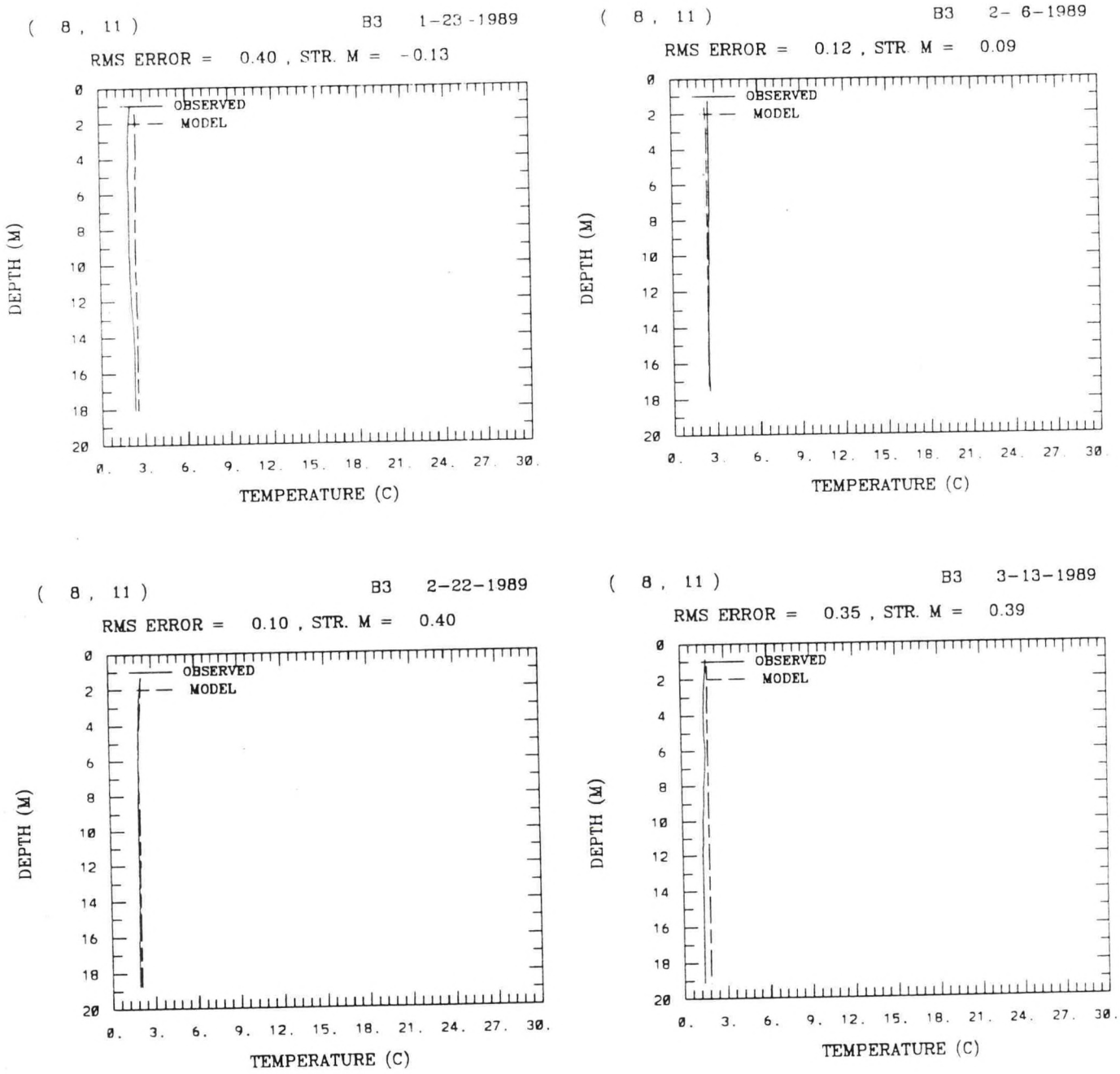

Figure B.2. (Cont.) Simulated versus Observed Vertical Temperature Profiles At Station: B3

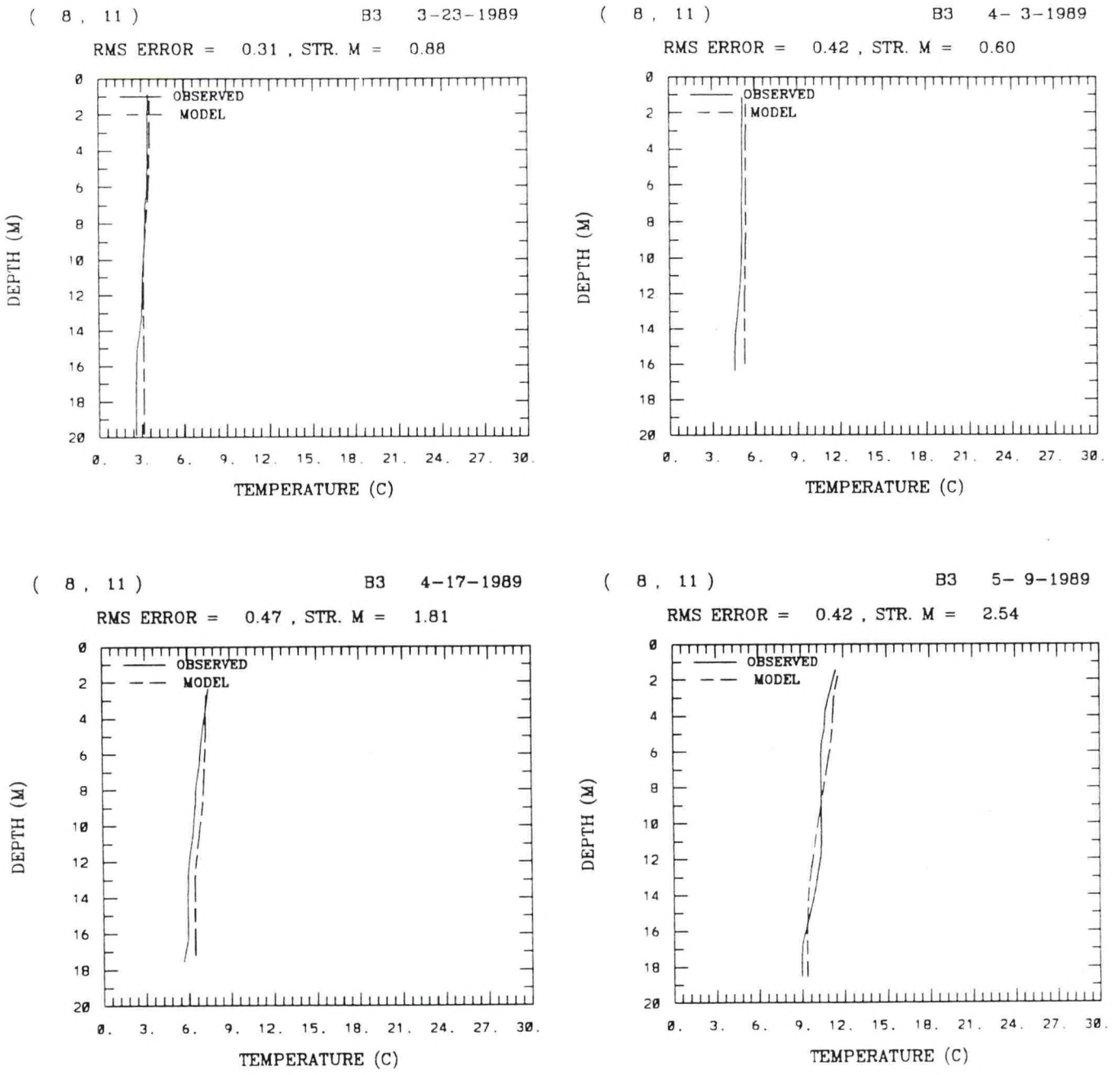

Figure B.2. (Cont.) Simulated versus Observed Vertical Temperature Profiles At Station: B3

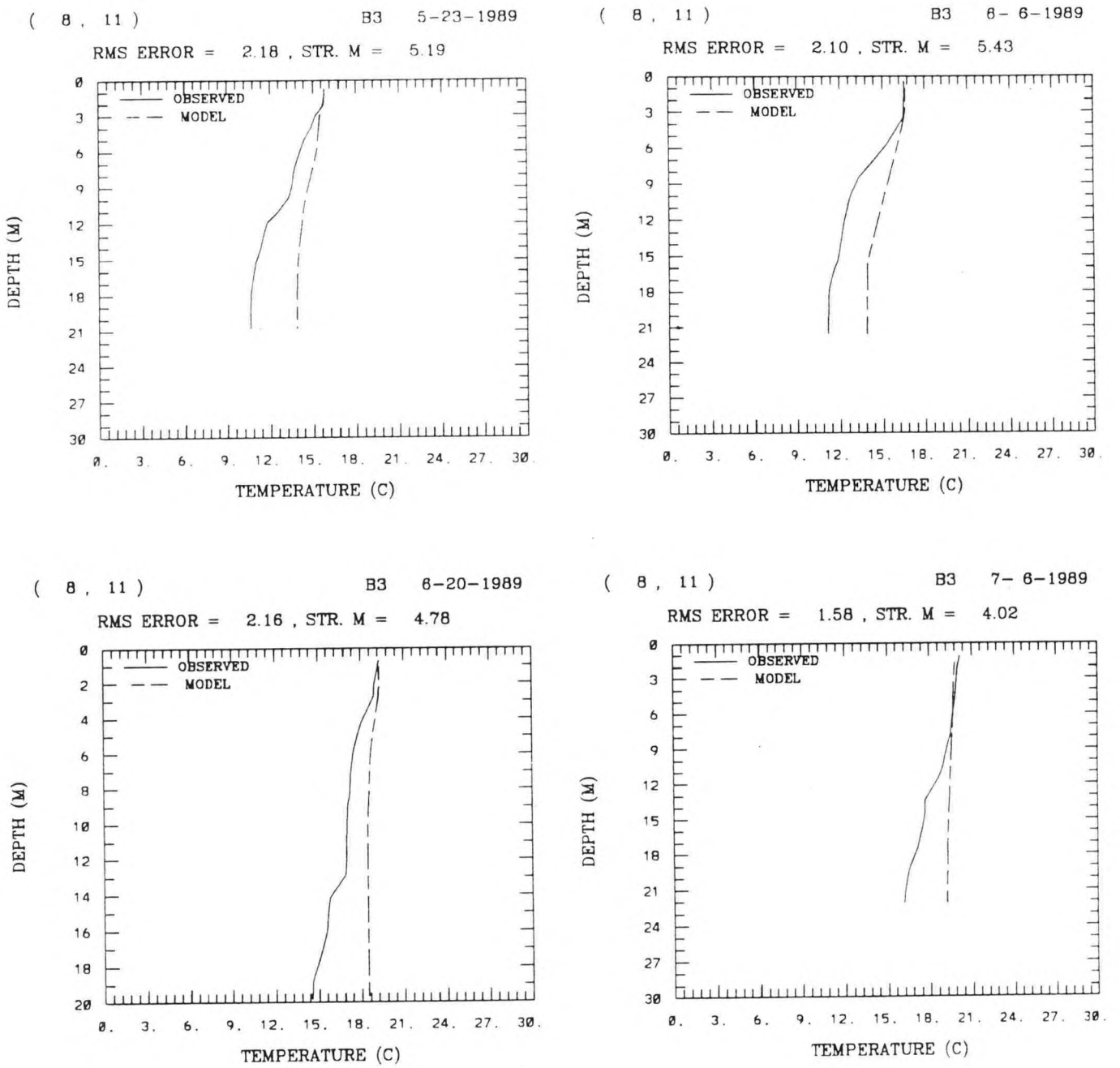

Figure B.2. (Cont.) Simulated versus Observed Vertical Temperature Profiles At Station: B3

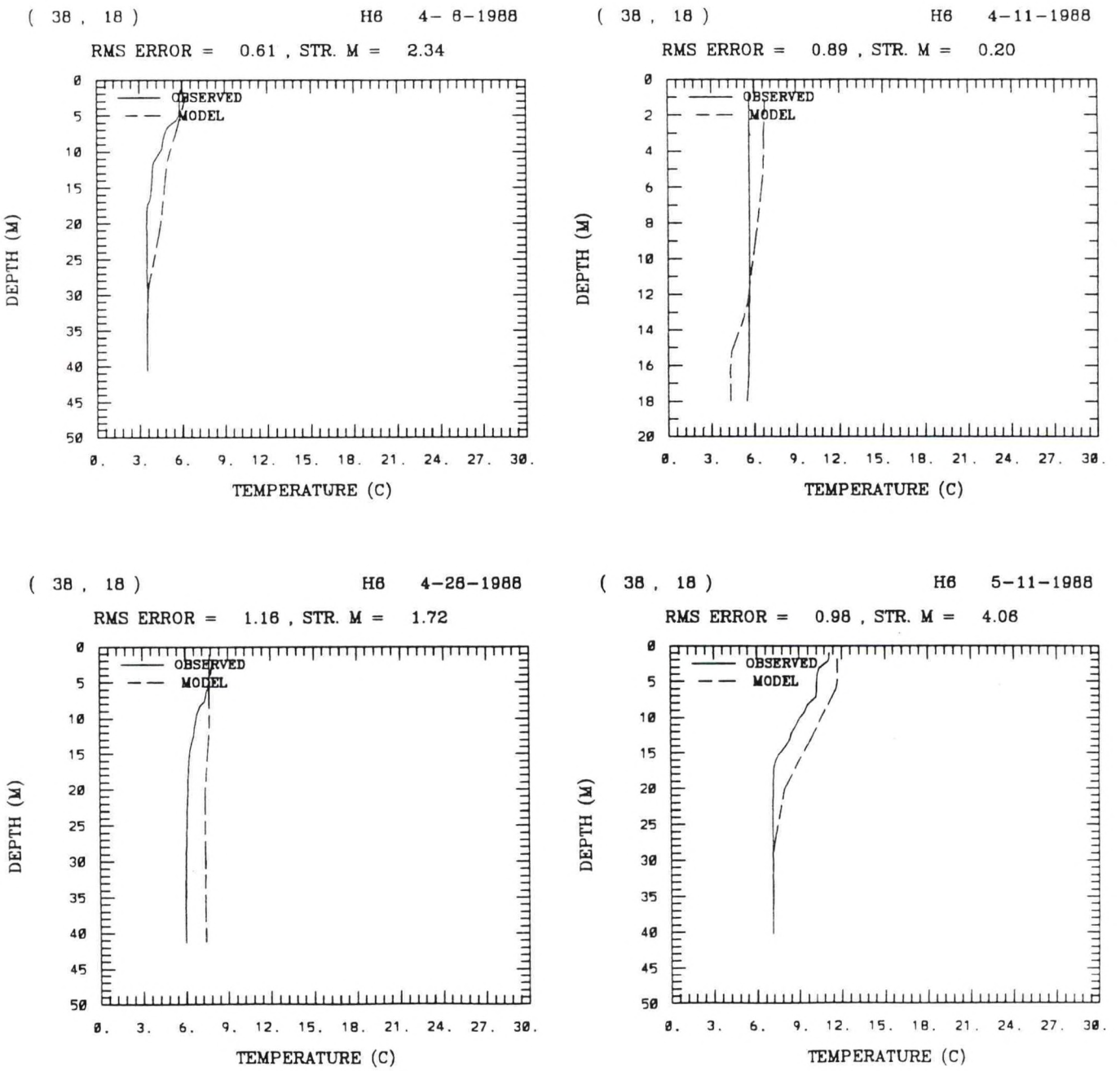

Figure B.3. Simulated versus Observed Vertical Temperature Profiles At Station: H6

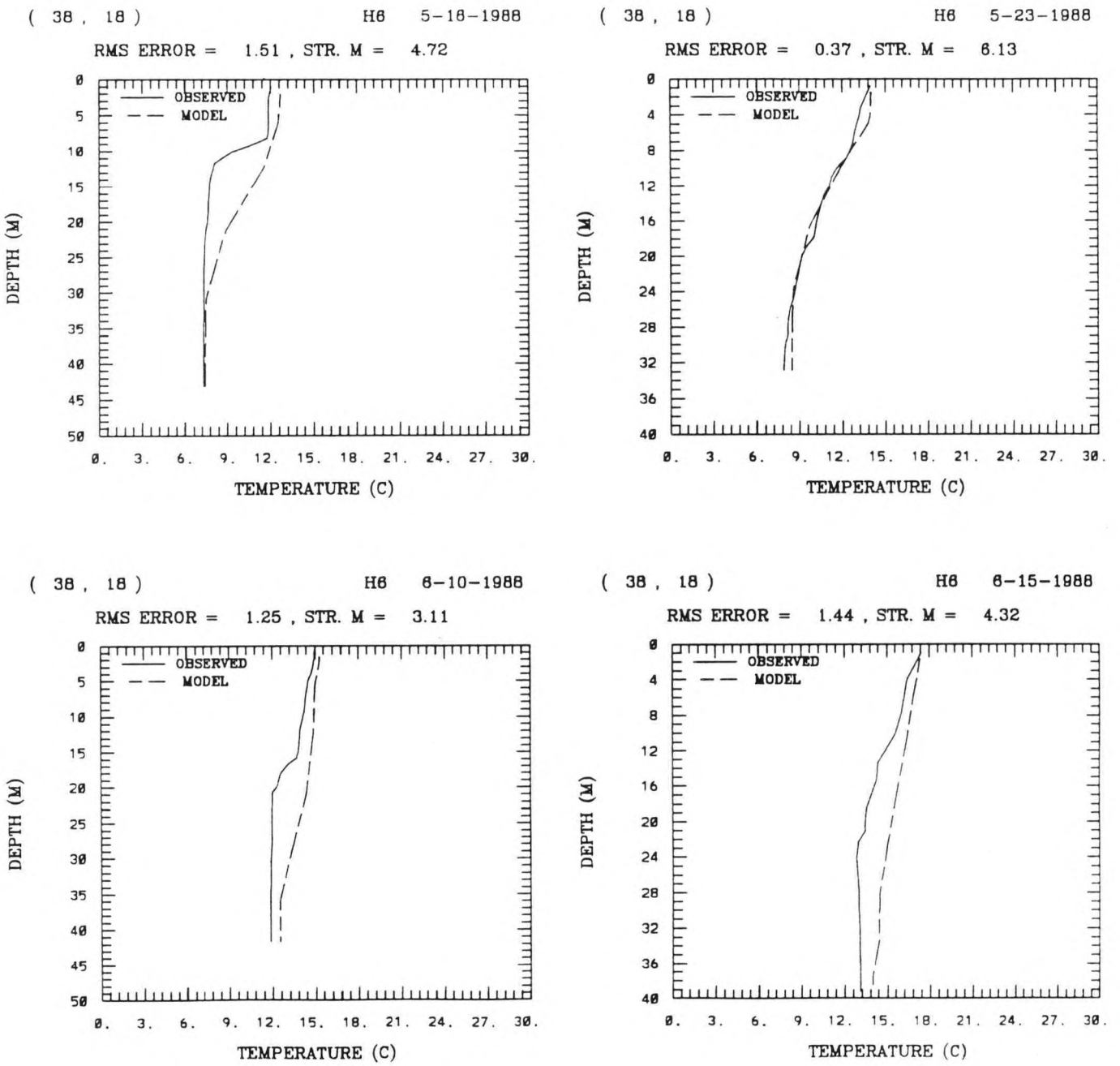

Figure B.3. (Cont.) Simulated versus Observed Vertical Temperature Profiles At Station: H6

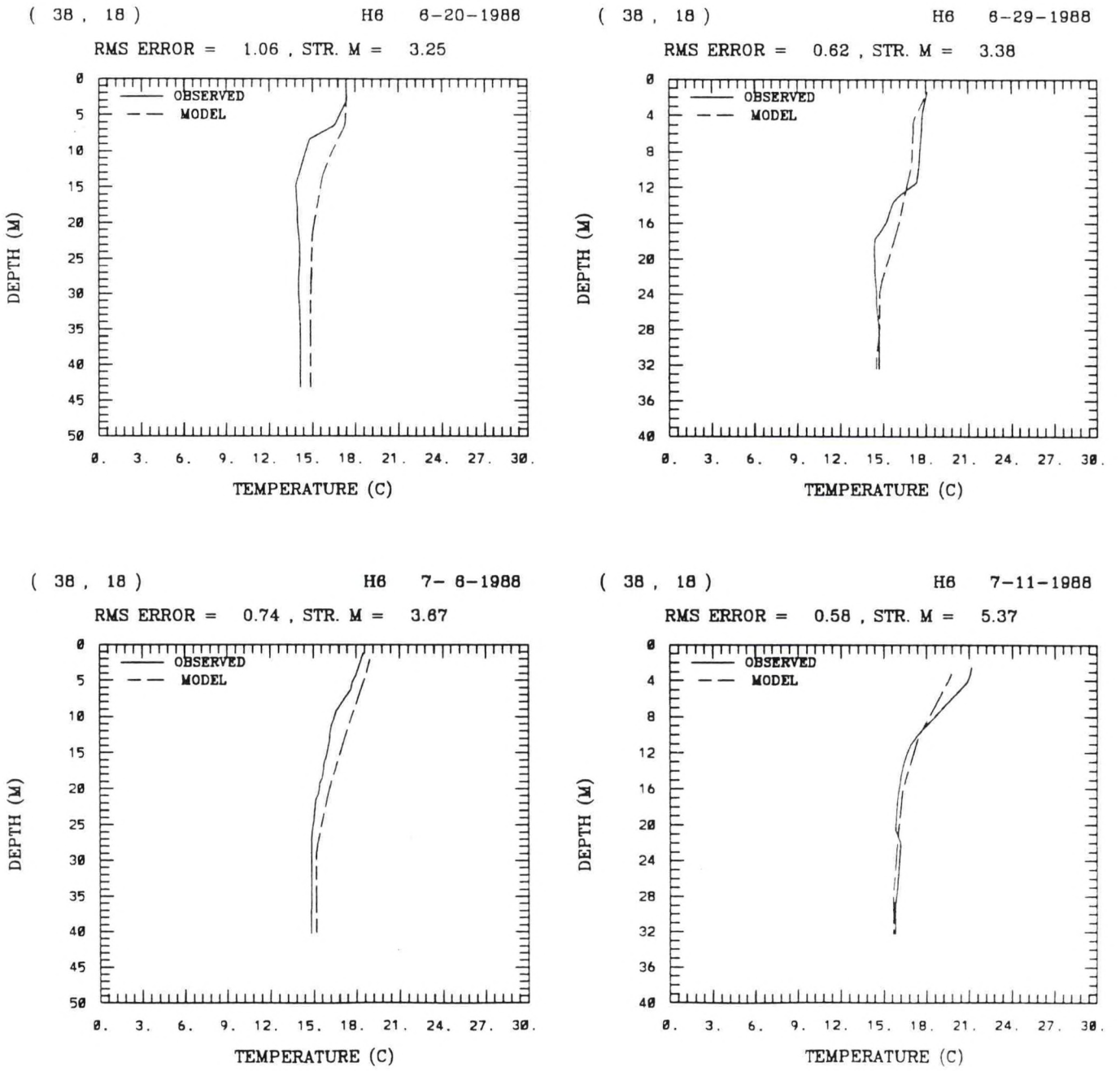

Figure B.3. (Cont.) Simulated versus Observed Vertical Temperature Profiles At Station: H6

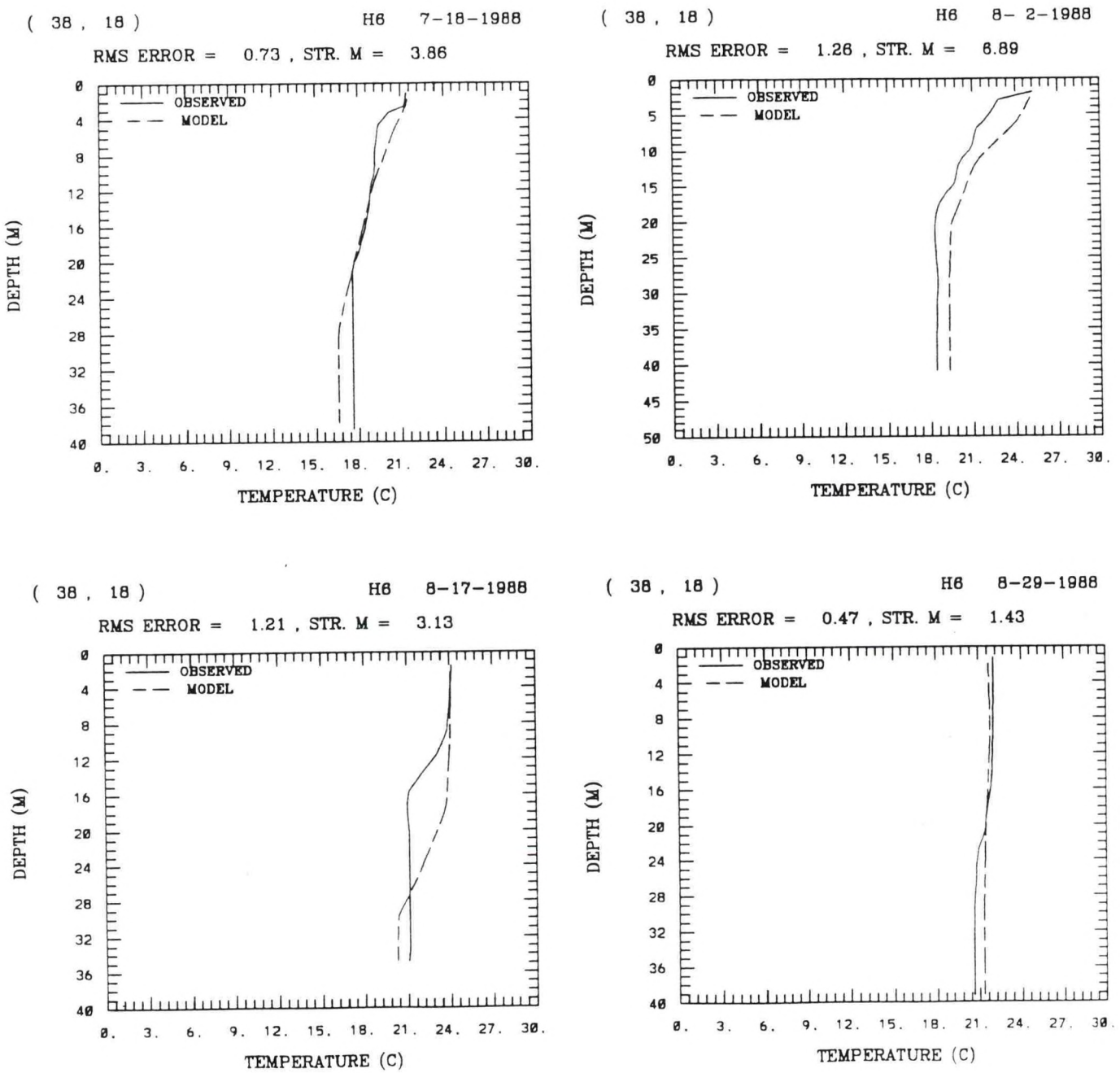

Figure B.3. (Cont.) Simulated versus Observed Vertical Temperature Profiles At Station: H6

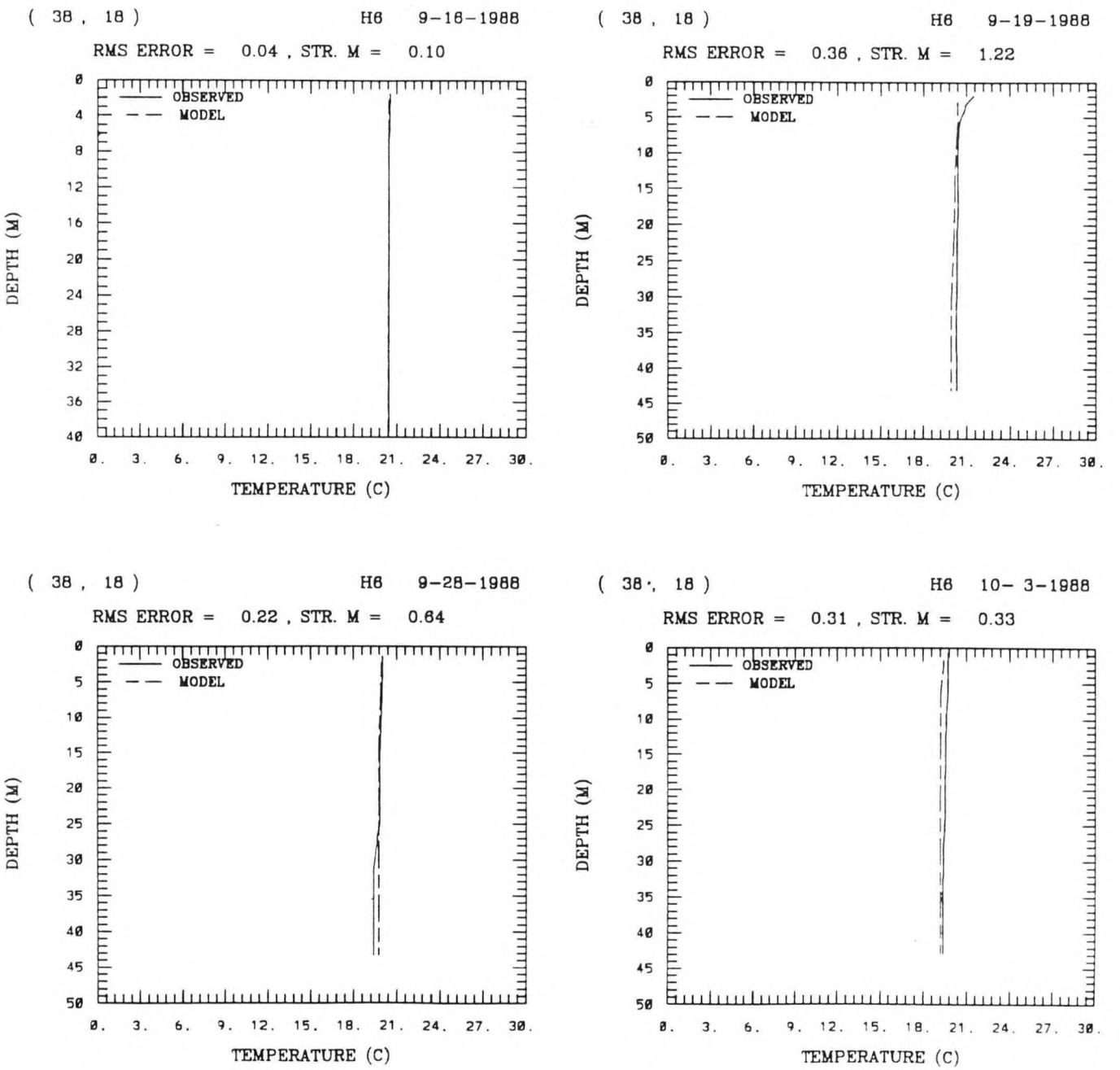

Figure B.3. (Cont.) Simulated versus Observed Vertical Temperature Profiles At Station: H6

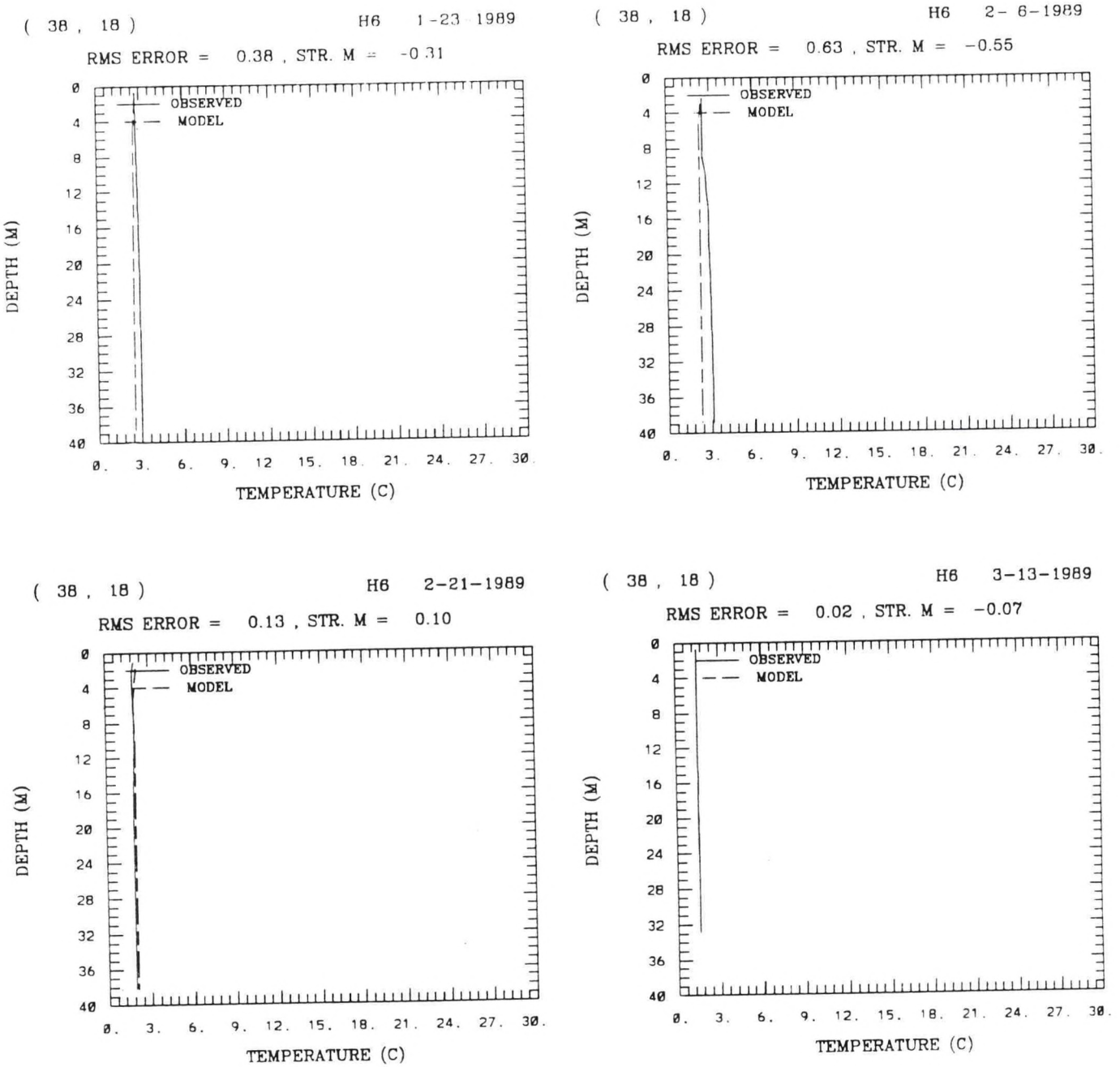

Figure B.3. (Cont.) Simulated versus Observed Vertical Temperature Profiles At Station: H6

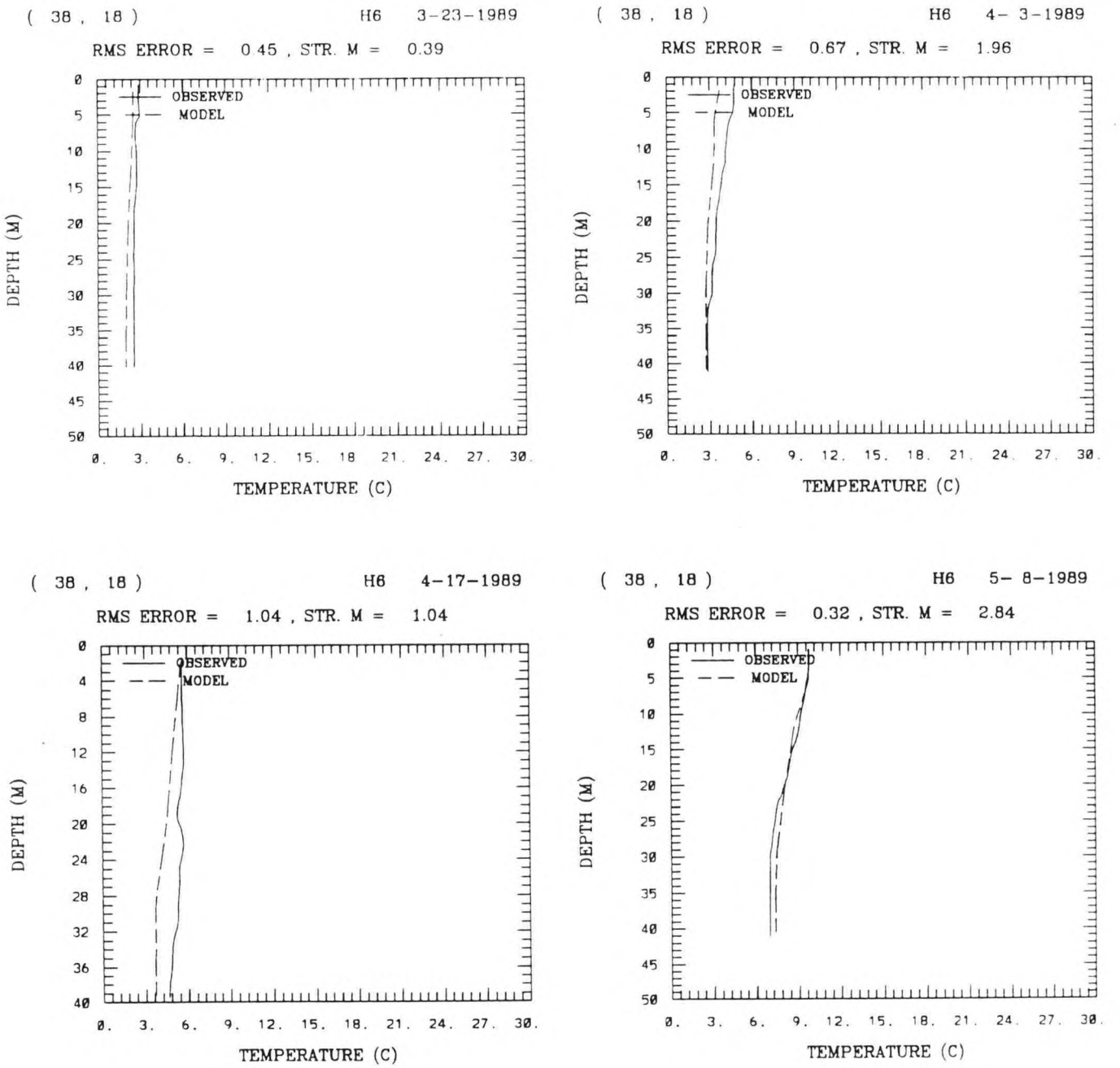

Figure B.3. (Cont.) Simulated versus Observed Vertical Temperature Profiles At Station: H6

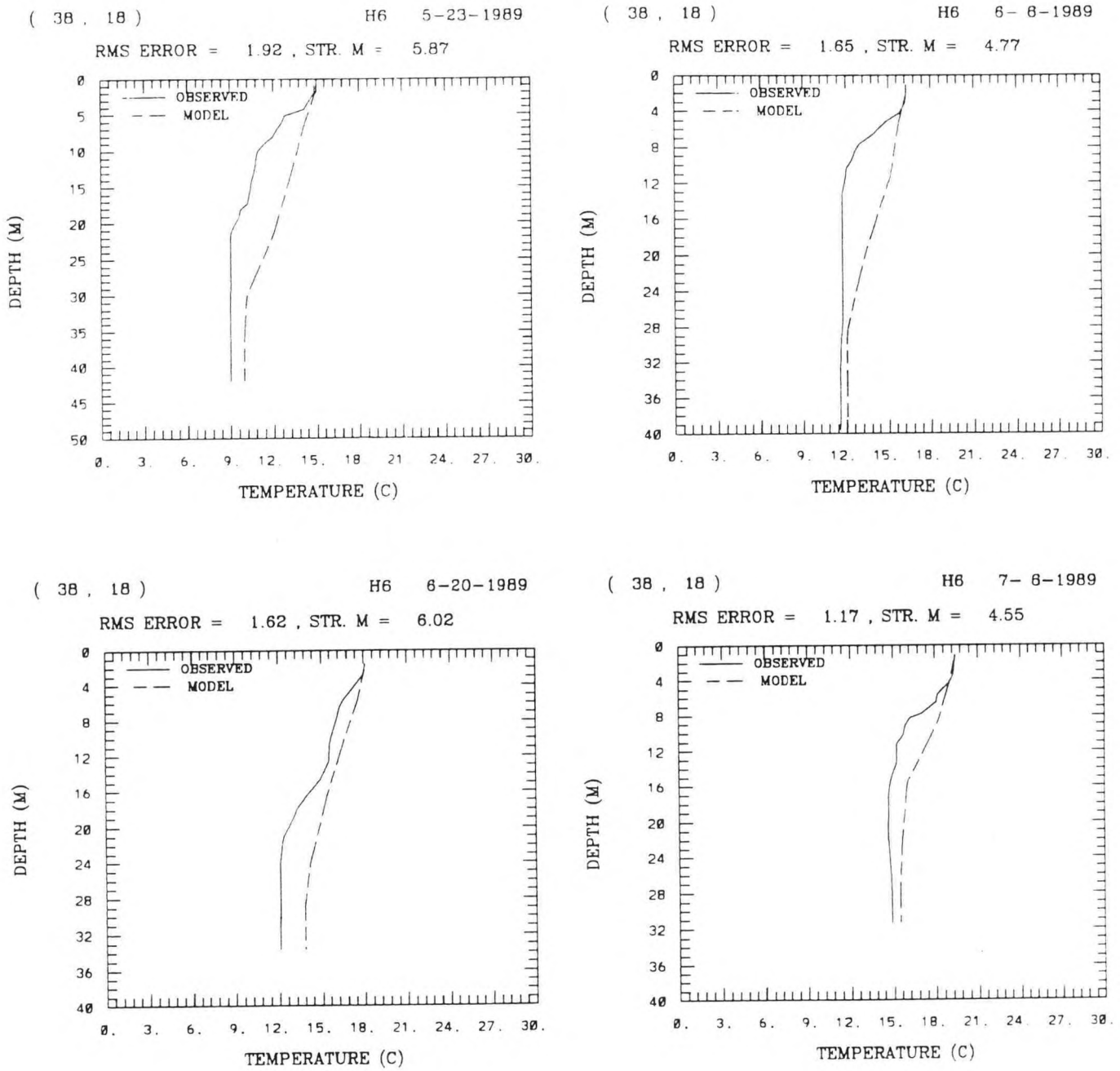

Figure B.3. (Cont.) Simulated versus Observed Vertical Temperature Profiles At Station: H6

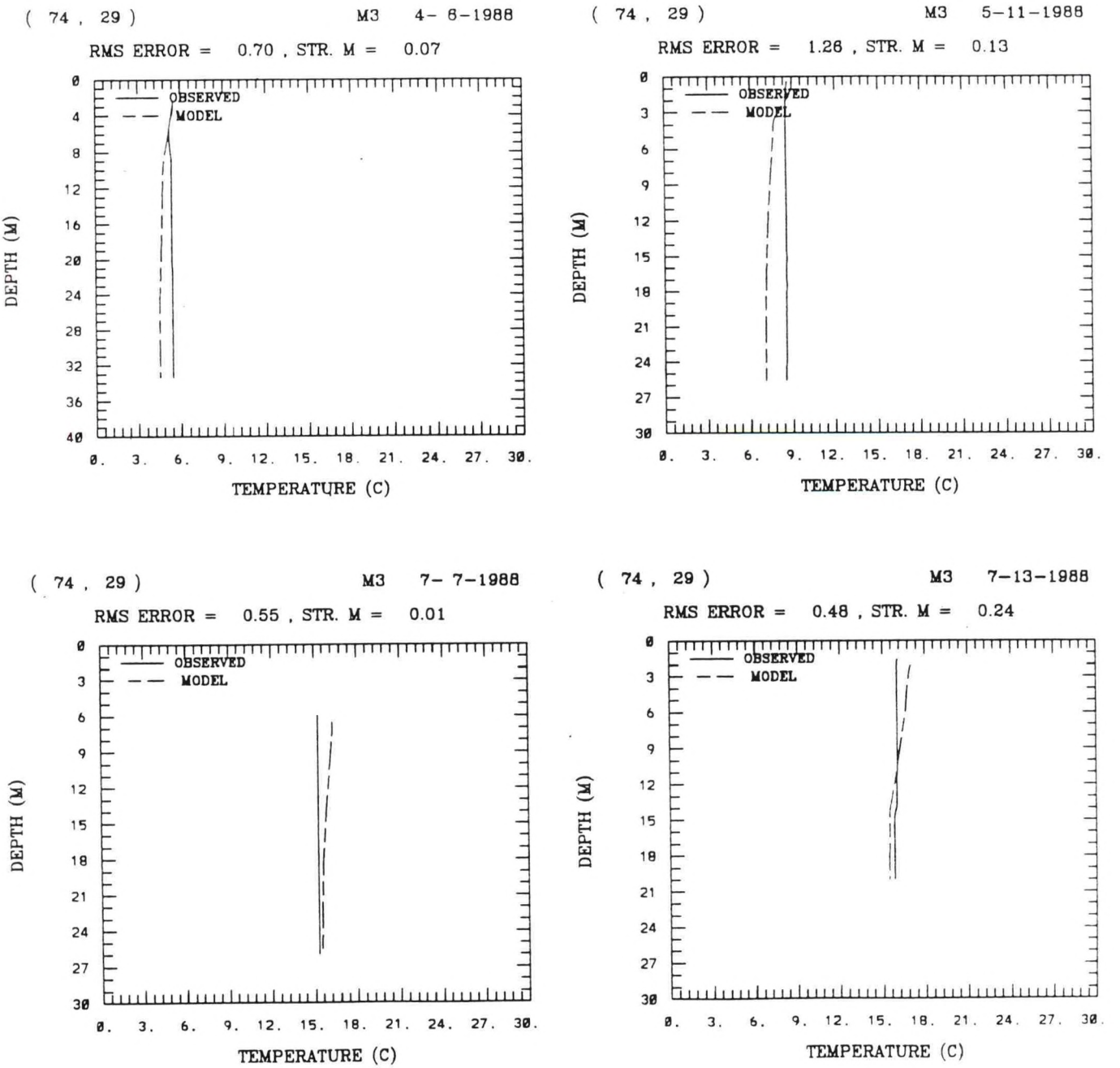

Figure B.4. Simulated versus Observed Vertical Temperature Profiles At Station: M3

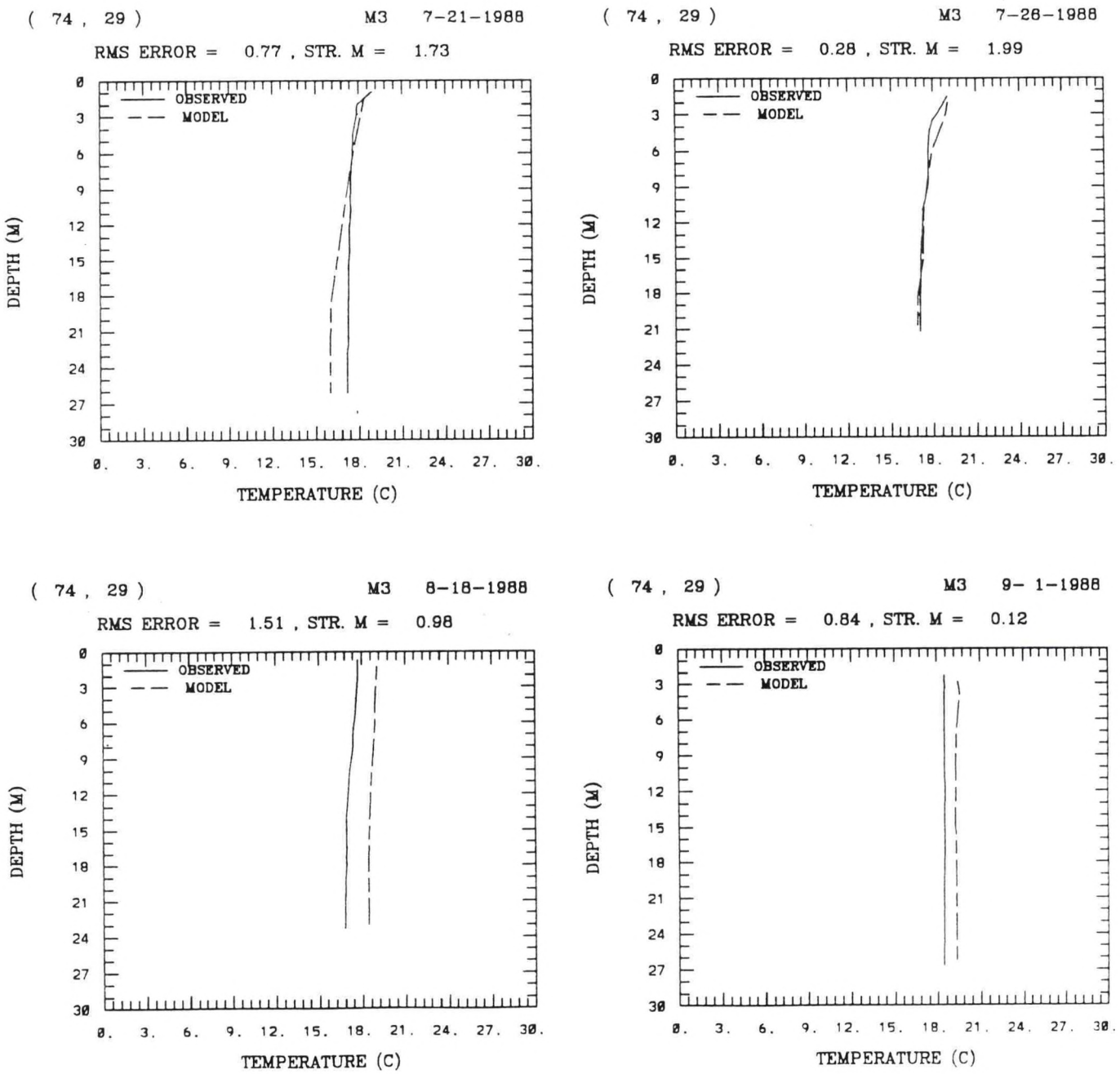

Figure B.4. (Cont.) Simulated versus Observed Vertical Temperature Profiles At Station: M3

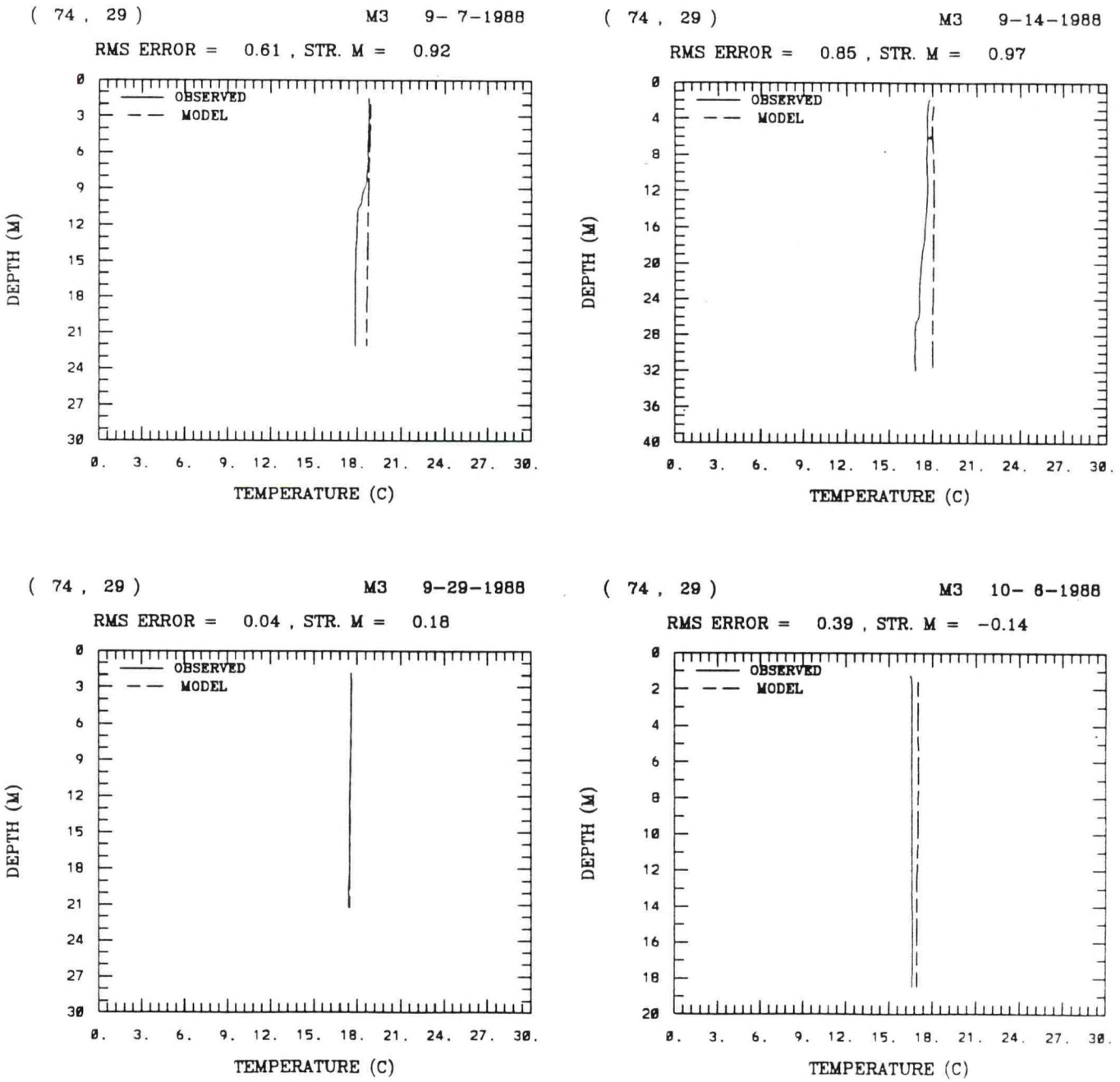

Figure B.4. (Cont.) Simulated versus Observed Vertical Temperature Profiles At Station: M3

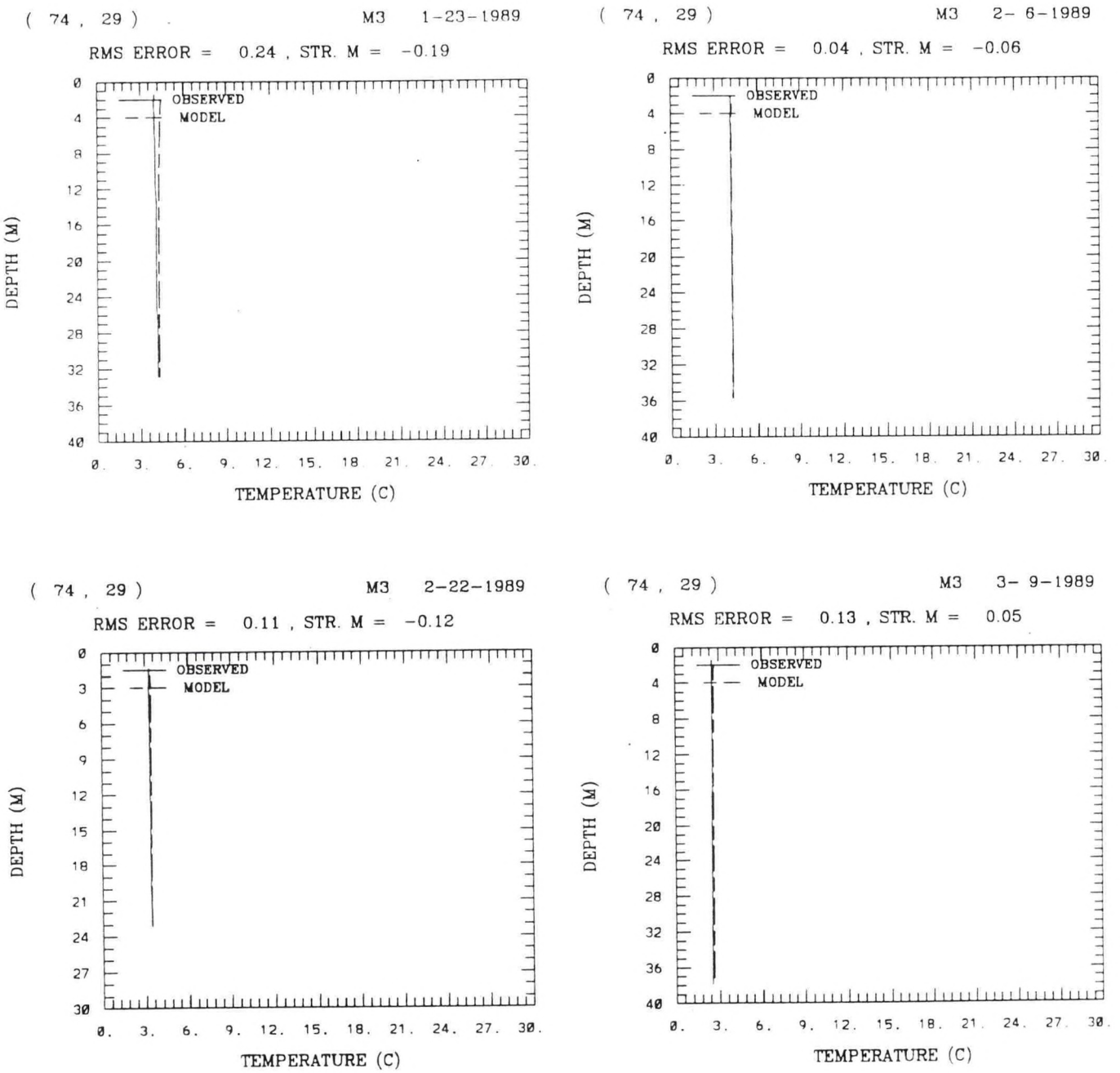

Figure B.4. (Cont.) Simulated versus Observed Vertical Temperature Profiles At Station: M3

Table B.1. Model versus Data Temperature Comparisons: Station A2

Calibration Period

			TEMPERATURE (C)							
STATION	DATE	TIME	DEPTH (M)	RMS ERROR	SURFACE M	SURFACE D	BOTTOM M	BOTTOM D	STR. D	STR. M
A2	4/ 4/1988	12:43	35.55	0.37	7.07	5.99	5.57	5.30	0.69	1.50
A2	4/11/1988	11:16	35.45	0.26	7.60	7.75	7.11	7.14	0.61	0.49
A2	4/18/1988	11:45	36.32	0.08	8.42	8.67	7.92	7.91	0.76	0.49
A2	4/19/1988	11:16	32.40	0.35	8.43	9.01	7.98	7.58	1.43	0.45
A2	5/ 9/1988	11:31	31.83	1.02	11.38	11.29	10.82	9.62	1.67	0.56
A2	5/25/1988	11:45	34.93	1.45	14.58	15.37	14.36	12.42	2.95	0.22
A2	6/10/1988	10:47	35.24	0.61	15.48	15.35	15.40	14.44	0.91	0.08
A2	6/13/1988	11:31	34.36	0.47	16.47	16.66	15.51	14.72	1.94	0.96
A2	6/20/1988	11:16	35.76	1.03	17.16	17.15	16.25	14.45	2.70	0.90
A2	6/27/1988	11:45	26.92	1.46	17.49	16.62	16.13	14.69	1.93	1.36
A2	7/ 6/1988	15:21	37.25	0.77	18.39	18.78	17.52	16.23	2.55	0.87
A2	7/12/1988	11:31	36.22	0.60	19.07	18.55	17.73	16.70	1.85	1.34
A2	7/18/1988	11: 2	30.90	0.47	20.05	19.98	17.98	18.10	1.88	2.07
A2	7/25/1988	11:45	27.70	1.19	21.30	21.40	18.92	17.40	4.00	2.38
A2	8/ 3/1988	11:45	35.34	0.61	21.65	21.66	20.20	20.83	0.83	1.46
A2	8/11/1988	11:16	36.22	0.27	22.30	22.15	19.64	19.70	2.45	2.67
A2	8/15/1988	12: 0	35.24	0.88	22.65	22.79	20.20	19.92	2.87	2.46
A2	8/29/1988	10:47	36.12	0.10	22.44	22.23	22.02	21.97	0.26	0.42
A2	9/13/1988	11:45	33.33	0.23	21.37	21.36	21.39	21.08	0.28	-0.01
A2	9/19/1988	11: 2	35.29	0.80	20.84	20.74	21.35	20.39	0.35	-0.52
A2	9/26/1988	11:31	34.88	0.25	20.36	20.40	20.72	20.30	0.10	-0.36
A2	10/ 3/1988	10:48	32.81	0.52	18.97	19.82	18.94	19.65	0.17	0.03
A2	10/18/1988	12: 0	34.00	0.29	15.52	15.48	15.73	15.28	0.20	-0.21
A2	11/16/1988	14:52	34.15	0.19	11.27	11.79	11.27	11.28	0.51	0.00

Verification Period

			TEMPERATURE (C)							
STATION	DATE	TIME	DEPTH (M)	RMS ERROR	SURFACE M	SURFACE D	BOTTOM M	BOTTOM D	STR. D	STR. M
A2	1/23/1989	16:33	34.05	0.36	2.23	2.34	2.31	1.98	0.36	-0.08
A2	2/ 6/1989	17:16	34.31	0.36	2.21	2.85	2.38	2.58	0.27	-0.17
A2	2/22/1989	12:57	37.25	0.30	2.17	3.00	2.22	1.89	1.11	-0.05
A2	3/13/1989	15:21	36.01	0.31	2.35	2.22	2.13	1.80	0.42	0.22
A2	3/23/1989	15:35	34.67	0.52	4.43	4.66	3.55	3.01	1.65	0.88
A2	4/ 3/1989	16: 4	30.85	0.50	6.45	6.26	6.15	5.51	0.75	0.29
A2	4/17/1989	15:35	34.62	1.09	8.09	8.14	6.93	5.70	2.44	1.16
A2	5/ 9/1989	12:57	36.94	0.52	11.86	11.56	10.76	10.24	1.32	1.10
A2	5/23/1989	15:21	37.15	1.63	14.69	14.56	13.92	11.77	2.79	0.77
A2	6/ 6/1989	14:38	36.63	1.38	15.44	15.31	15.19	13.04	2.27	0.25
A2	6/20/1989	15:21	35.96	1.19	18.82	18.74	18.35	16.62	2.12	0.47
A2	7/ 6/1989	14:38	30.95	1.11	20.34	19.73	19.69	18.40	1.33	0.65
A2	8/ 7/1989	11: 2	35.24	1.32	21.54	21.66	21.25	19.67	1.99	0.29
A2	8/21/1989	12:28	36.63	0.46	22.18	21.82	21.92	21.27	0.55	0.26
A2	9/ 6/1989	15:21	35.55	0.51	22.20	21.92	22.11	21.41	0.51	0.09

Table B.2. Model versus Data Temperature Comparisons: Station B3

Calibration Period

			TEMPERATURE (C)							
STATION	DATE	TIME	DEPTH (M)	RMS ERROR	SURFACE M	SURFACE D	BOTTOM M	BOTTOM D	STR. D	STR. M
B3	4/ 4/1988	16:47	18.55	0.51	6.72	6.78	5.15	4.41	2.37	1.56
B3	4/11/1988	12:28	18.45	0.38	7.32	6.93	7.17	6.73	0.20	0.15
B3	4/18/1988	16:19	17.88	0.39	7.97	7.86	7.75	6.97	0.89	0.22
B3	4/26/1988	12:28	16.22	0.92	8.75	9.27	8.60	7.26	2.01	0.15
B3	5/ 9/1988	14:52	19.33	1.27	12.70	12.62	10.61	8.71	3.91	2.09
B3	5/25/1988	16:33	17.20	1.39	15.50	14.84	13.18	10.87	3.97	2.31
B3	6/10/1988	12:14	19.12	1.69	16.05	15.79	14.93	12.60	3.19	1.12
B3	6/13/1988	14: 9	18.91	2.02	17.99	18.29	15.29	12.88	5.41	2.70
B3	6/20/1988	12:28	17.15	1.92	19.24	19.34	13.93	13.31	6.03	5.31
B3	6/27/1988	15: 7	18.14	1.55	17.81	17.92	15.16	13.69	4.23	2.65
B3	7/ 6/1988	13:55	19.53	1.56	18.15	18.52	17.09	15.41	3.11	1.06
B3	7/12/1988	14:38	16.53	0.98	19.41	20.51	16.82	15.91	4.60	2.59
B3	7/18/1988	12:28	16.22	0.84	20.46	19.97	16.85	16.57	3.40	3.60
B3	7/26/1988	7:12	16.84	1.14	23.40	23.32	18.33	17.48	5.84	5.07
B3	8/ 3/1988	15: 7	21.13	1.42	25.75	25.83	19.37	18.30	7.53	6.38
B3	8/11/1988	13:26	20.67	0.81	23.94	23.97	18.04	18.86	5.11	5.90
B3	8/15/1988	15:35	20.15	0.87	22.97	22.63	19.90	19.36	3.27	3.07
B3	8/29/1988	12: 0	20.05	0.48	21.41	22.15	21.27	21.28	0.87	0.14
B3	9/13/1988	14:38	17.15	0.35	21.50	21.06	21.30	21.04	0.02	0.19
B3	9/19/1988	12:14	17.31	0.95	21.63	20.53	21.08	20.49	0.04	0.55
B3	9/26/1988	14:52	18.55	0.98	21.65	21.92	21.41	20.43	1.49	0.23
B3	10/ 3/1988	12:14	17.83	0.62	18.88	19.76	19.38	19.74	0.02	-0.51
B3	10/18/1988	14:52	17.77	0.36	15.63	15.38	15.46	16.13	-0.75	0.17
B3	11/16/1988	13:11	17.77	0.11	11.15	11.14	11.40	11.53	-0.39	-0.25

Verification Period

			TEMPERATURE (C)							
STATION	DATE	TIME	DEPTH (M)	RMS ERROR	SURFACE M	SURFACE D	BOTTOM M	BOTTOM D	STR. D	STR. M
B3	1/23/1989	14:52	18.08	0.40	2.47	2.16	2.51	2.29	-0.13	-0.04
B3	2/ 6/1989	15:21	17.52	0.12	2.32	2.56	2.41	2.47	0.09	-0.09
B3	2/22/1989	11:45	18.76	0.10	2.22	2.28	2.03	1.88	0.40	0.19
B3	3/13/1989	13:55	19.12	0.35	1.87	1.78	1.81	1.39	0.39	0.06
B3	3/23/1989	14: 9	19.89	0.31	3.62	3.49	3.15	2.61	0.88	0.47
B3	4/ 3/1989	13:55	16.38	0.42	5.44	5.14	5.26	4.54	0.60	0.17
B3	4/17/1989	14: 9	17.52	0.47	7.29	7.44	6.45	5.63	1.81	0.84
B3	5/ 9/1989	11:31	18.55	0.42	11.74	11.48	9.33	8.94	2.54	2.41
B3	5/23/1989	13:55	20.77	2.18	15.90	15.82	13.84	10.63	5.19	2.06
B3	6/ 6/1989	12:43	21.60	2.10	16.66	16.57	13.85	11.14	5.43	2.81
B3	6/20/1989	13:55	19.79	2.16	19.31	19.31	18.45	14.53	4.78	0.86
B3	7/ 6/1989	13:26	22.17	1.58	19.88	20.19	19.18	16.17	4.02	0.70
B3	8/ 7/1989	12:43	16.17	1.39	21.32	22.27	20.27	18.71	3.56	1.04
B3	8/21/1989	11: 2	19.53	0.48	21.79	21.94	21.57	20.77	1.17	0.22
B3	9/ 6/1989	13:55	18.29	0.56	21.81	21.47	21.64	21.03	0.44	0.17

Table B.3. Model versus Data Temperature Comparisons: Station D3

Calibration Period

			TEMPERATURE (C)							
STATION	DATE	TIME	DEPTH (M)	RMS ERROR	SURFACE M	SURFACE D	BOTTOM M	BOTTOM D	STR. D	STR. M
D3	4/ 5/1988	10:47	31.26	0.81	6.29	5.75	5.46	4.09	1.66	0.84
D3	4/11/1988	14: 9	30.23	0.86	6.94	6.05	6.55	4.87	1.18	0.39
D3	4/19/1988	11: 2	24.44	0.62	7.72	6.93	7.34	6.65	0.28	0.39
D3	4/26/1988	13:40	30.95	1.23	8.39	8.54	7.88	6.17	2.37	0.51
D3	5/10/1988	11:16	31.05	0.60	10.48	10.20	8.79	7.69	2.51	1.69
D3	5/16/1988	15:35	31.52	0.84	11.70	10.98	9.16	8.70	2.28	2.54
D3	5/26/1988	11:31	31.11	1.86	13.72	14.41	11.84	9.29	5.12	1.88
D3	6/10/1988	13:40	25.47	0.44	15.38	15.16	13.24	12.25	2.91	2.15
D3	6/14/1988	9: 7	30.69	1.71	17.00	16.93	13.49	12.34	4.59	3.51
D3	6/20/1988	13:55	30.07	1.58	18.31	18.33	14.13	13.14	5.19	4.17
D3	6/28/1988	8:24	30.12	1.39	17.96	17.20	15.11	14.65	2.55	2.85
D3	7/ 6/1988	11: 2	30.85	1.15	18.35	19.02	16.22	15.52	3.50	2.13
D3	7/13/1988	7:26	27.70	0.60	19.44	20.18	16.04	15.97	4.21	3.40
D3	7/18/1988	13:55	30.95	1.47	20.01	20.10	16.63	16.54	3.56	3.38
D3	7/26/1988	11:45	33.33	1.16	19.48	19.17	17.53	16.75	2.42	1.95
D3	8/ 3/1988	19:26	31.00	1.58	23.48	23.46	18.83	18.12	5.34	4.65
D3	8/16/1988	11:31	33.02	1.91	22.75	22.72	22.54	19.52	3.20	0.21
D3	8/29/1988	13:26	32.14	0.28	21.16	21.52	21.02	21.19	0.33	0.15
D3	9/14/1988	9:35	25.89	0.21	20.76	20.88	20.70	20.98	-0.10	0.06
D3	9/19/1988	13:40	31.11	0.15	20.74	21.16	20.54	20.59	0.57	0.20
D3	9/26/1988	17:31	24.23	0.16	20.78	20.73	20.49	20.42	0.31	0.28
D3	10/ 3/1988	13:40	30.85	0.53	20.58	20.06	20.45	19.81	0.25	0.13
D3	10/18/1988	17:16	31.21	0.32	16.50	15.93	16.19	16.02	-0.09	0.31
D3	11/16/1988	11:45	40.20	0.51	11.03	11.56	11.26	11.81	-0.25	-0.23

Verification Period

			TEMPERATURE (C)							
STATION	DATE	TIME	DEPTH (M)	RMS ERROR	SURFACE M	SURFACE D	BOTTOM M	BOTTOM D	STR. D	STR. M
D3	1/23/1989	12:43	40.20	0.23	2.66	2.34	2.52	2.79	-0.45	0.15
D3	2/ 6/1989	13:11	38.29	0.24	2.47	2.60	2.36	2.66	-0.06	0.11
D3	2/22/1989	9:50	39.42	0.06	2.20	2.10	2.02	2.03	0.07	0.18
D3	3/13/1989	12: 0	39.17	0.40	1.91	1.87	1.89	1.46	0.41	0.03
D3	3/23/1989	12: 0	40.66	0.25	3.03	3.30	2.85	2.29	1.01	0.17
D3	4/ 3/1989	12: 0	41.28	0.15	4.28	4.25	3.99	3.81	0.44	0.29
D3	4/17/1989	12:14	42.16	0.74	6.27	6.35	5.44	4.73	1.62	0.84
D3	5/ 9/1989	9:35	39.58	1.00	10.39	9.75	9.31	8.12	1.63	1.08
D3	5/23/1989	12: 0	37.67	2.50	16.82	16.77	12.72	9.77	7.00	4.10
D3	6/ 6/1989	11: 2	38.49	2.45	16.95	16.88	12.75	10.69	6.19	4.20
D3	6/20/1989	12:14	36.43	3.44	19.30	19.35	15.89	12.86	6.49	3.42
D3	7/ 6/1989	11:45	31.67	1.24	18.91	19.38	17.51	15.96	3.42	1.39
D3	8/ 7/1989	14:52	38.29	1.52	22.35	22.43	19.57	18.60	3.83	2.79
D3	8/21/1989	9:36	38.86	0.43	21.45	21.55	21.27	20.34	1.21	0.17
D3	9/ 6/1989	12:14	38.13	0.35	20.64	21.23	20.73	20.95	0.28	-0.09

Table B.4. Model versus Data Temperature Comparisons: Station F3

Calibration Period

TEMPERATURE (C)

STATION	DATE	TIME	DEPTH (M)	RMS ERROR	SURFACE M	SURFACE D	BOTTOM M	BOTTOM D	STR. D	STR. M
F3	4/ 5/1988	14:52	28.37	0.24	5.93	5.65	3.47	3.57	2.08	2.47
F3	4/11/1988	15:50	26.87	0.77	6.55	5.64	5.22	4.97	0.67	1.33
F3	4/19/1988	14: 9	26.82	0.73	7.34	6.34	6.30	5.77	0.57	1.04
F3	4/26/1988	15: 7	26.35	0.95	8.05	8.45	7.30	6.19	2.26	0.75
F3	5/10/1988	14: 9	27.13	0.71	11.68	11.48	7.72	7.53	3.95	3.96
F3	5/16/1988	13:40	29.35	1.40	12.39	11.81	9.12	8.85	2.96	3.27
F3	5/26/1988	14: 9	24.91	0.81	13.55	13.51	9.87	9.69	3.82	3.68
F3	6/10/1988	15: 7	25.27	0.98	15.78	15.50	13.19	11.90	3.60	2.59
F3	6/14/1988	12:28	27.13	1.53	17.63	17.51	14.13	12.92	4.59	3.51
F3	6/20/1988	15:21	29.25	1.63	19.09	19.14	14.39	13.32	5.82	4.71
F3	6/28/1988	11:31	29.92	1.14	18.42	17.81	15.24	14.74	3.07	3.18
F3	7/ 6/1988	9: 7	28.32	1.30	18.89	19.07	15.86	15.38	3.69	3.03
F3	7/13/1988	10:47	28.88	0.60	20.17	19.86	16.62	16.13	3.73	3.55
F3	7/26/1988	14: 9	29.66	0.59	23.11	23.04	17.62	17.39	5.65	5.48
F3	8/ 4/1988	11:45	28.37	1.15	25.15	25.22	18.80	18.81	6.41	6.35
F3	8/11/1988	16:19	28.78	1.71	23.93	24.72	21.02	19.63	5.09	2.91
F3	8/16/1988	13:40	29.97	1.34	23.12	23.04	21.71	19.67	3.37	1.41
F3	8/29/1988	15: 7	29.25	0.60	20.94	21.88	20.93	21.20	0.68	0.01
F3	9/14/1988	12:28	21.65	0.65	20.30	21.14	20.27	20.87	0.27	0.03
F3	9/19/1988	15: 7	29.09	0.27	20.21	20.84	20.26	20.46	0.38	-0.05
F3	9/28/1988	7:55	24.75	0.25	20.51	20.07	20.27	20.04	0.03	0.25
F3	10/ 3/1988	15:21	27.95	0.43	20.45	19.85	19.92	19.48	0.37	0.54
F3	10/19/1988	12:43	25.32	0.49	15.87	16.35	15.85	16.35	0.00	0.02
F3	11/16/1988	9:50	39.11	0.70	11.07	11.73	11.03	11.72	0.01	0.04

Verification Period

TEMPERATURE (C)

STATION	DATE	TIME	DEPTH (M)	RMS ERROR	SURFACE M	SURFACE D	BOTTOM M	BOTTOM D	STR. D	STR. M
F3	1/23/1989	10:33	40.15	0.30	2.71	2.73	2.44	2.83	-0.10	0.27
F3	2/ 6/1989	11:16	37.98	0.37	2.61	2.60	2.32	2.79	-0.19	0.28
F3	2/21/1989	10: 4	38.55	0.09	2.28	1.97	1.96	1.99	-0.02	0.32
F3	3/13/1989	10: 4	39.42	0.09	1.55	1.51	1.53	1.44	0.07	0.01
F3	3/23/1989	10: 4	40.15	0.14	2.72	2.90	2.24	2.10	0.80	0.48
F3	4/ 3/1989	9:50	34.83	0.23	4.03	4.00	3.65	3.20	0.80	0.39
F3	4/17/1989	9:50	41.59	0.45	6.12	6.21	5.18	4.27	1.94	0.94
F3	5/ 8/1989	9:50	39.01	0.53	9.63	9.45	7.43	7.38	2.07	2.19
F3	5/23/1989	10: 4	41.44	3.70	16.63	16.60	11.76	8.91	7.69	4.87
F3	6/ 6/1989	9:21	40.51	2.72	15.75	15.65	12.98	10.67	4.98	2.77
F3	6/20/1989	10:19	39.06	2.84	19.69	19.73	15.39	12.11	7.62	4.30
F3	8/ 7/1989	16:33	39.01	1.47	22.98	22.85	20.26	19.06	3.79	2.72
F3	8/21/1989	7:55	38.75	1.45	22.09	21.72	21.47	19.70	2.02	0.62
F3	9/ 6/1989	9:36	37.41	0.25	21.25	20.97	21.18	20.81	0.16	0.07

Table B.5. Model versus Data Temperature Comparisons: Station H6

Calibration Period

			TEMPERATURE (C)							
STATION	DATE	TIME	DEPTH (M)	RMS ERROR	SURFACE M	SURFACE D	BOTTOM M	BOTTOM D	STR. D	STR. M
H6	4/ 6/1988	12:57	40.61	0.61	6.32	5.87	3.55	3.53	2.34	2.77
H6	4/11/1988	17:16	17.98	0.89	6.82	5.68	4.31	5.48	0.20	2.51
H6	4/26/1988	16:19	41.28	1.16	7.91	7.70	7.38	5.98	1.72	0.53
H6	5/11/1988	12:28	40.20	0.98	11.68	11.15	7.13	7.09	4.06	4.56
H6	5/16/1988	12:43	43.14	1.51	12.69	12.04	7.44	7.32	4.72	5.25
H6	5/23/1988	13:55	32.86	0.37	14.03	13.99	8.45	7.86	6.13	5.58
H6	6/10/1988	16:33	41.65	1.25	15.35	14.96	12.54	11.85	3.11	2.81
H6	6/15/1988	13:12	39.17	1.44	17.42	17.43	13.97	13.11	4.32	3.45
H6	6/20/1988	17: 2	43.20	1.06	17.43	17.40	14.87	14.15	3.25	2.56
H6	6/29/1988	12:14	32.45	0.62	18.07	18.11	14.53	14.73	3.38	3.54
H6	7/ 6/1988	7:40	40.20	0.74	19.11	18.50	15.20	14.83	3.67	3.91
H6	7/11/1988	13:26	32.24	0.58	19.92	21.18	15.65	15.81	5.37	4.28
H6	7/18/1988	16:47	38.60	0.73	21.60	21.44	16.55	17.58	3.86	5.04
H6	8/ 2/1988	16:47	40.92	1.26	25.24	25.24	19.30	18.35	6.89	5.94
H6	8/17/1988	12:14	34.77	1.21	24.09	24.18	20.25	21.05	3.13	3.84
H6	8/29/1988	16:33	39.27	0.47	21.73	22.04	21.31	20.61	1.43	0.42
H6	9/16/1988	11:16	39.68	0.04	20.47	20.56	20.40	20.46	0.10	0.07
H6	9/19/1988	16:48	43.04	0.36	20.41	21.54	19.92	20.32	1.22	0.49
H6	9/28/1988	11:45	43.30	0.22	19.97	20.03	19.75	19.39	0.64	0.22
H6	10/ 3/1988	16:48	42.89	0.31	19.45	19.72	19.20	19.39	0.33	0.25
H6	11/16/1988	8: 9	42.06	0.58	11.21	11.61	11.02	11.56	0.05	0.19

Verification Period

			TEMPERATURE (C)							
STATION	DATE	TIME	DEPTH (M)	RMS ERROR	SURFACE M	SURFACE D	BOTTOM M	BOTTOM D	STR. D	STR. M
H6	1/23/1989	8:38	38.91	0.38	2.67	2.68	2.52	2.99	-0.31	0.15
H6	2/ 6/1989	9: 7	38.80	0.63	2.47	2.52	2.27	3.07	-0.55	0.20
H6	2/21/1989	8:24	38.18	0.13	2.16	1.98	2.01	1.88	0.10	0.15
H6	3/13/1989	8: 9	32.81	0.02	1.51	1.48	1.55	1.55	-0.07	-0.04
H6	3/23/1989	8: 9	40.20	0.45	2.52	2.90	1.97	2.51	0.39	0.55
H6	4/ 3/1989	7:55	41.18	0.67	3.72	4.76	2.72	2.80	1.96	1.00
H6	4/17/1989	7:55	39.42	1.04	5.58	5.67	3.67	4.63	1.04	1.91
H6	5/ 8/1989	7:55	41.08	0.32	9.86	9.76	7.33	6.92	2.84	2.53
H6	5/23/1989	8: 9	42.11	1.92	14.94	14.87	9.94	9.00	5.87	5.00
H6	6/ 6/1989	7:40	39.58	1.65	16.34	16.31	12.07	11.54	4.77	4.27
H6	6/20/1989	8:38	33.64	1.62	18.12	18.10	13.81	12.08	6.02	4.31
H6	7/ 6/1989	8: 9	31.36	1.17	19.40	19.41	15.45	14.86	4.55	3.94
H6	8/ 7/1989	18: 0	34.21	1.77	23.31	22.88	21.34	19.77	3.11	1.97
H6	8/21/1989	6: 0	35.14	1.06	22.16	22.10	21.27	20.30	1.80	0.89
H6	9/ 6/1989	8: 9	36.53	0.32	21.02	21.13	21.28	20.80	0.33	-0.26
H6	9/18/1989	8:38	33.95	0.29	21.22	21.50	20.89	20.76	0.74	0.33

Table B.6. Model versus Data Temperature Comparisons: Station I2

Calibration Period

			TEMPERATURE (C)							
STATION	DATE	TIME	DEPTH (M)	RMS ERROR	SURFACE M	SURFACE D	BOTTOM M	BOTTOM D	STR. D	STR. M
I2	5/10/1988	11:31	24.30	0.26	10.77	10.57	7.55	7.92	2.65	3.21
I2	7/ 7/1988	9:35	26.18	0.26	17.10	16.80	16.86	16.68	0.12	0.23
I2	7/20/1988	11:31	25.50	0.64	22.15	21.80	18.65	18.53	3.27	3.50
I2	8/ 4/1988	11:31	24.51	1.03	24.02	25.43	21.09	19.92	5.51	2.93
I2	8/12/1988	7:26	25.84	0.96	23.89	24.71	20.19	21.08	3.63	3.70
I2	8/18/1988	11:31	16.33	0.71	22.79	23.00	19.93	21.50	1.50	2.86
I2	9/ 1/1988	9: 7	25.35	0.78	20.96	21.71	20.75	21.45	0.26	0.21
I2	9/14/1988	9:35	25.84	0.76	19.90	20.64	19.88	20.67	-0.03	0.02
I2	10/19/1988	11:16	25.20	0.24	15.21	15.47	15.26	15.50	-0.03	-0.05
I2	12/19/1988	13:26	24.56	0.62	6.11	5.44	6.06	5.46	-0.02	0.06

Verification Period

			TEMPERATURE (C)							
STATION	DATE	TIME	DEPTH (M)	RMS ERROR	SURFACE M	SURFACE D	BOTTOM M	BOTTOM D	STR. D	STR. M
I2	1/18/1989	12:43	24.91	0.39	2.96	3.35	2.95	3.34	0.01	0.01
I2	1/23/1989	8:52	25.64	0.08	2.83	2.80	2.96	2.95	-0.15	-0.13
I2	2/ 6/1989	12:43	25.59	0.53	2.50	2.97	2.51	3.13	-0.16	-0.01
I2	3/ 9/1989	12: 0	27.16	0.17	1.84	1.73	1.85	1.68	0.05	-0.01
I2	3/21/1989	10: 4	26.33	0.69	1.98	2.62	1.92	2.65	-0.03	0.06
I2	4/18/1989	12: 0	26.67	1.11	5.73	5.85	4.34	5.56	0.29	1.39
I2	5/ 8/1989	12:14	26.48	0.23	9.12	8.96	8.57	8.84	0.12	0.55
I2	5/22/1989	14: 9	27.26	0.83	14.09	14.59	9.93	10.80	3.79	4.16
I2	6/ 5/1989	12:14	27.50	0.48	14.68	15.45	13.43	13.26	2.19	1.25
I2	6/16/1989	11:31	27.41	0.57	15.17	15.07	13.74	13.83	1.24	1.43
I2	7/ 5/1989	12:28	27.21	0.50	20.07	20.81	17.95	17.80	3.01	2.13
I2	7/17/1989	10:33	27.60	0.84	19.98	20.00	17.97	18.44	1.56	2.01
I2	8/ 7/1989	12:43	27.31	0.51	22.99	23.27	20.56	20.35	2.92	2.43
I2	8/21/1989	12:14	27.41	0.45	22.12	21.82	21.32	20.83	0.99	0.79
I2	9/ 5/1989	12: 0	26.97	0.11	21.52	21.29	20.93	20.93	0.36	0.59
I2	9/18/1989	11: 2	26.38	0.49	21.09	21.17	20.52	21.04	0.13	0.57

Table B.7. Model versus Data Temperature Comparisons: Station J2

Calibration Period

			TEMPERATURE (C)							
STATION	DATE	TIME	DEPTH (M)	RMS ERROR	SURFACE M	SURFACE D	BOTTOM M	BOTTOM D	STR. D	STR. M
J2	4/ 7/1988	15:21	14.31	0.24	5.58	5.55	4.90	5.25	0.30	0.68
J2	5/10/1988	15:21	15.10	0.75	8.61	8.78	7.69	8.56	0.22	0.92
J2	7/14/1988	14:38	13.53	0.50	20.46	19.80	17.86	17.35	2.45	2.61
J2	8/ 4/1988	15:21	16.67	0.63	20.05	19.41	20.00	19.35	0.06	0.05
J2	9/ 8/1988	14:52	13.24	0.21	20.13	20.25	19.87	19.51	0.74	0.26
J2	10/ 6/1988	11:31	23.29	0.82	18.94	17.75	18.53	17.80	-0.05	0.41
J2	10/19/1988	14:52	16.23	0.15	15.43	15.16	15.35	15.20	-0.04	0.08
J2	12/19/1988	11:45	16.23	0.37	6.44	5.85	6.52	6.14	-0.29	-0.08

Verification Period

			TEMPERATURE (C)							
STATION	DATE	TIME	DEPTH (M)	RMS ERROR	SURFACE M	SURFACE D	BOTTOM M	BOTTOM D	STR. D	STR. M
J2	1/18/1989	11:45	22.50	0.32	4.33	3.92	4.30	4.06	-0.14	0.03
J2	1/23/1989	10:33	21.52	0.49	4.48	3.82	4.27	3.82	0.00	0.21
J2	2/ 6/1989	11:16	19.56	0.60	4.41	3.69	4.28	3.78	-0.09	0.13
J2	2/22/1989	11:45	21.67	0.42	3.45	2.92	3.31	2.90	0.02	0.15
J2	3/ 9/1989	10:48	24.81	0.27	2.36	2.03	2.37	2.14	-0.11	-0.01
J2	3/21/1989	11:16	18.43	1.00	2.09	3.29	2.06	3.02	0.27	0.03
J2	4/18/1989	10:48	15.64	1.24	5.57	6.34	4.26	5.40	0.94	1.31
J2	5/ 8/1989	11:31	22.70	0.34	8.24	8.14	7.76	8.14	0.00	0.48
J2	5/22/1989	12:43	16.03	0.78	10.29	11.53	9.24	9.71	1.82	1.06
J2	6/ 5/1989	11: 2	22.85	0.33	12.80	12.82	12.44	12.79	0.03	0.37
J2	6/16/1989	10:19	16.08	0.51	13.79	14.48	13.42	13.60	0.88	0.37
J2	7/ 5/1989	11:16	21.62	0.38	17.46	17.73	17.36	17.74	-0.01	0.11
J2	7/17/1989	11:45	19.71	0.78	19.58	19.60	17.22	18.38	1.22	2.37
J2	8/ 7/1989	11:45	23.44	0.41	20.53	21.72	20.27	20.57	1.15	0.26
J2	8/21/1989	11: 2	19.07	0.05	20.40	20.35	20.37	20.33	0.02	0.03
J2	9/ 5/1989	11: 2	22.16	0.11	20.22	20.33	20.35	20.23	0.10	-0.12
J2	9/18/1989	10: 4	20.44	0.45	19.92	20.32	19.86	20.33	-0.01	0.06

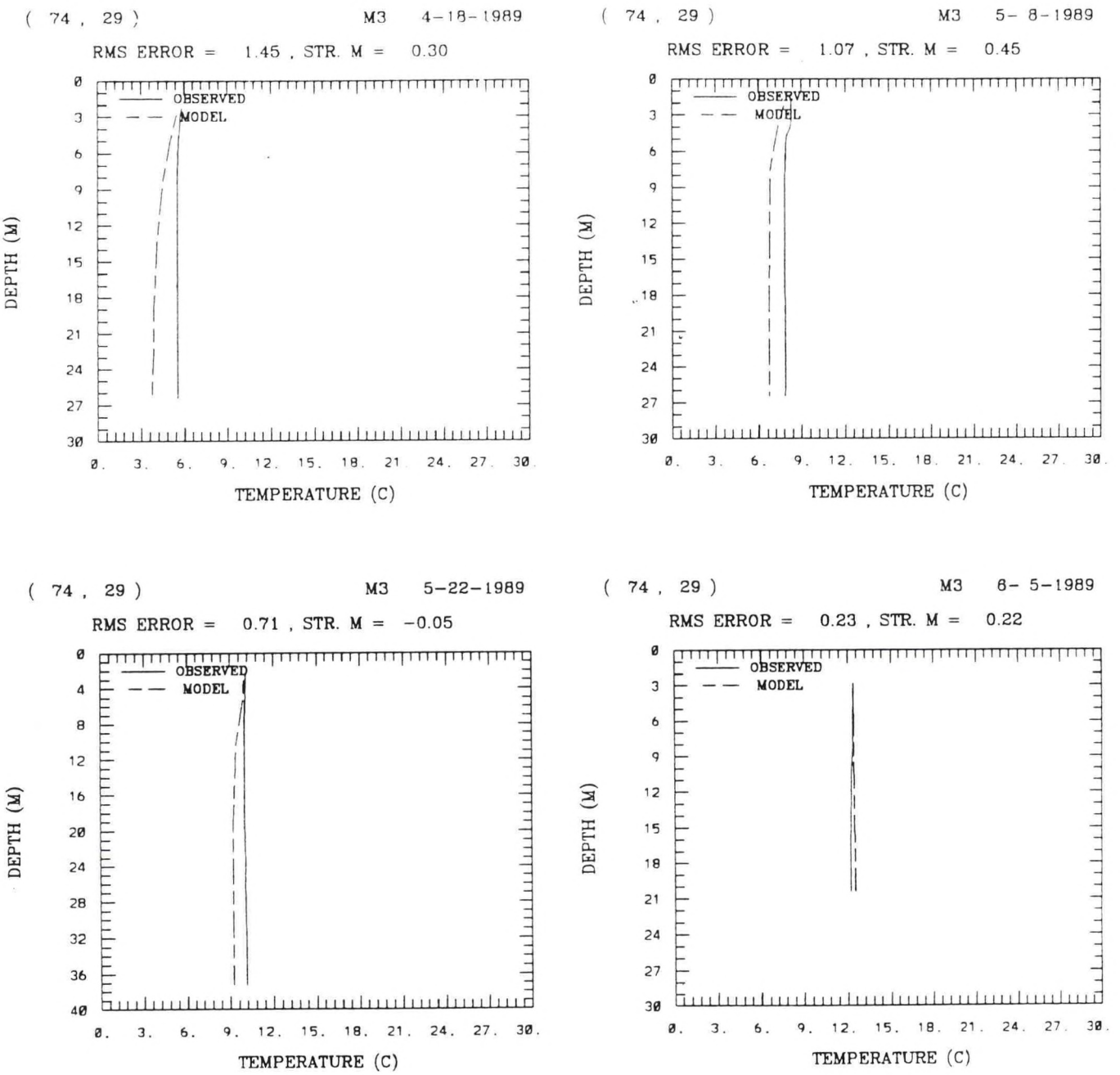

Figure B.4. (Cont.) Simulated versus Observed Vertical Temperature Profiles At Station: M3

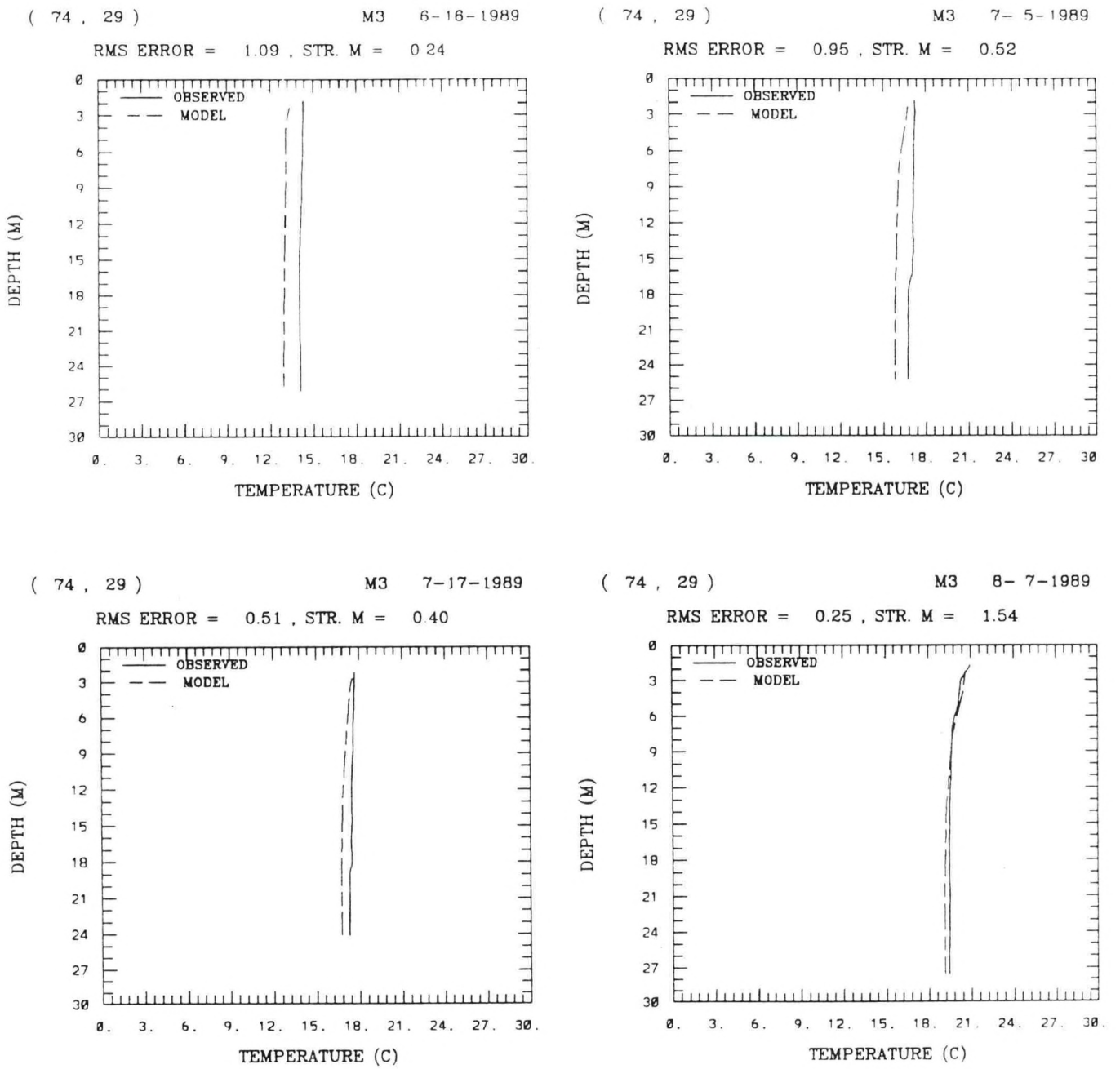

Figure B.4. (Cont.) Simulated versus Observed Vertical Temperature Profiles At Station: M3

Table B.8. Model versus Data Temperature Comparisons: Station M3

Calibration Period

TEMPERATURE (C)

STATION	DATE	TIME	DEPTH (M)	RMS ERROR	SURFACE M	SURFACE D	BOTTOM M	BOTTOM D	STR. D	STR. M
M3	4/ 6/1988	7:55	33.38	0.70	5.51	5.50	4.53	5.43	0.07	0.99
M3	5/11/1988	15:21	25.54	1.26	8.97	8.65	7.08	8.52	0.13	1.89
M3	7/ 7/1988	11:16	25.94	0.55	16.33	15.30	15.52	15.29	0.01	0.81
M3	7/13/1988	7:40	20.00	0.48	17.12	16.06	15.43	15.82	0.24	1.69
M3	7/21/1988	13:26	26.13	0.77	18.43	18.92	16.01	17.19	1.73	2.43
M3	7/26/1988	11:45	21.23	0.28	19.12	19.02	16.83	17.03	1.99	2.28
M3	8/18/1988	15: 7	23.29	1.51	19.09	17.76	18.41	16.78	0.98	0.68
M3	9/ 1/1988	11: 2	26.67	0.84	19.40	18.54	19.30	18.42	0.12	0.10
M3	9/ 7/1988	7:55	22.11	0.61	18.88	18.78	18.65	17.86	0.92	0.23
M3	9/14/1988	11:45	31.92	0.85	18.16	17.79	18.01	16.82	0.97	0.15
M3	9/29/1988	9: 7	21.23	0.04	17.63	17.57	17.48	17.39	0.18	0.15
M3	10/ 6/1988	7:55	18.48	0.39	17.04	16.47	16.94	16.61	-0.14	0.10
M3	10/18/1988	8:24	27.01	0.04	14.89	14.94	14.85	14.79	0.15	0.04
M3	12/19/1988	8:24	46.33	0.22	6.47	6.48	6.63	6.65	-0.17	-0.15

Verification Period

TEMPERATURE (C)

STATION	DATE	TIME	DEPTH (M)	RMS ERROR	SURFACE M	SURFACE D	BOTTOM M	BOTTOM D	STR. D	STR. M
M3	1/23/1989	12:57	32.90	0.24	4.43	3.99	4.27	4.18	-0.19	0.16
M3	2/ 6/1989	9: 7	35.69	0.04	4.28	4.16	4.24	4.22	-0.06	0.05
M3	2/22/1989	9:35	23.09	0.11	3.43	3.29	3.45	3.41	-0.12	-0.03
M3	3/ 9/1989	9: 7	37.85	0.13	2.70	2.55	2.65	2.50	0.05	0.05
M3	4/18/1989	8:38	26.43	1.45	5.60	5.82	3.77	5.52	0.30	1.83
M3	5/ 8/1989	9: 7	26.48	1.07	7.94	8.30	6.68	7.85	0.45	1.26
M3	5/22/1989	10:33	37.21	0.71	9.98	10.07	9.23	10.12	-0.05	0.75
M3	6/ 5/1989	9: 7	20.44	0.23	12.37	12.42	12.53	12.20	0.22	-0.16
M3	6/16/1989	8: 9	26.18	1.09	13.48	14.30	12.93	14.06	0.24	0.55
M3	7/ 5/1989	9:21	25.30	0.95	16.80	17.25	15.83	16.73	0.52	0.97
M3	7/17/1989	14: 9	24.12	0.51	17.63	17.69	16.78	17.29	0.40	0.85
M3	8/ 7/1989	9:21	27.60	0.25	20.68	20.98	19.14	19.44	1.54	1.54
M3	8/21/1989	8:52	26.97	0.60	20.35	20.60	20.02	19.35	1.25	0.33
M3	9/ 5/1989	8:38	29.91	0.72	19.90	19.33	19.70	18.91	0.42	0.20
M3	9/18/1989	7:55	27.41	0.47	19.24	19.52	18.81	19.38	0.14	0.43

Appendix C: Residual Circulation Model vs Data Comparisons

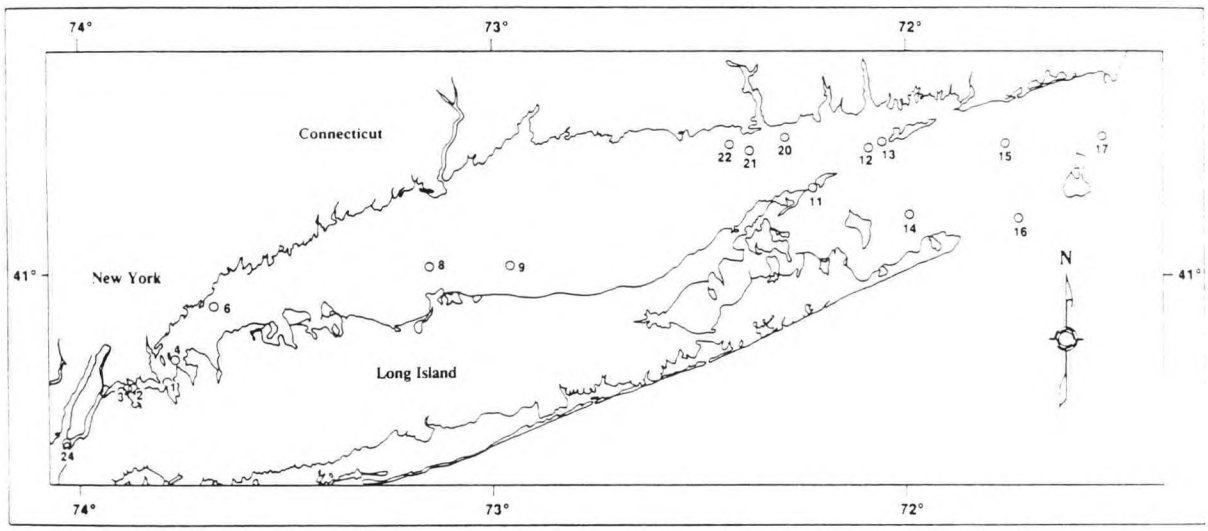

Station Locations

Table C.1. Average Monthly Residual Current Model versus Data Comparison
At Station: ADCP 4

Model (M) Period: 4/88 Data (D) Period: 5/3 - 6/1/88

DEPTH (M)	U (E-W) CMS		V (N-S) CMS	
	M	D	M	D
6.00	-1.97	2.34	3.72	-2.03
11.00	-2.46	-0.34	0.72	-3.89
16.00	-2.58	-1.63	-1.65	-5.67
21.00	-1.72	-2.19	-2.53	-6.75
26.00	-0.76	-2.38	-2.75	-5.62
29.00	-0.38	-0.25	-2.52	-0.65

DEPTH (M)	U-STD (E-W) CMS		V-STD (N-S) CMS	
	M	D	M	D
6.00	4.91	1.80	5.40	1.00
11.00	2.88	2.30	3.14	1.60
16.00	2.57	2.40	4.08	1.90
21.00	2.30	2.20	3.97	1.70
26.00	2.05	1.50	3.43	1.80
29.00	1.89	1.60	2.88	2.10

Table C.2. Average Monthly Residual Current Model versus Data Comparison
At Station: ADCP 6

Model (M) Period: 5/88 Data (D) Period: 5/3 - 6/1/88

DEPTH (M)	U (E-W) CMS		V (N-S) CMS	
	M	D	M	D
2.50	-0.26	0.11	5.13	0.28
5.50	-0.91	-2.39	3.67	-1.02
8.50	-1.41	-2.60	1.89	-2.19
11.50	-0.50	-1.16	0.09	-2.10
13.50	-0.45	0.17	-0.44	-1.39

DEPTH (M)	U-STD (E-W) CMS		V-STD (N-S) CMS	
	M	D	M	D
2.50	7.04	1.80	4.96	1.60
5.50	4.17	1.80	3.47	1.50
8.50	3.43	2.50	4.37	1.60
11.50	3.01	2.40	3.42	1.70
13.50	2.74	2.30	2.78	1.30

Table C.3. Average Monthly Residual Current Model versus Data Comparison At Station: ADCP 8

Model (M) Period: 8/88 Data (D) Period: 8/10 - 9/8/88

DEPTH (M)	U (E-W) CMS		V (N-S) CMS	
	M	D	M	D
9.00	-1.00	0.94	-2.77	2.21
14.00	-4.84	-1.62	-2.20	2.40
19.00	-6.20	-2.98	-1.59	0.37
24.00	-5.97	-3.40	-1.54	0.00
29.00	-4.68	-3.34	-1.86	0.65
34.00	-2.90	-2.26	-1.62	0.44
37.00	-1.95	0.99	-1.38	3.98

DEPTH (M)	U-STD (E-W) CMS		V-STD (N-S) CMS	
	M	D	M	D
9.00	5.68	3.00	4.84	2.50
14.00	6.15	3.60	4.30	1.90
19.00	7.51	2.00	3.95	1.40
24.00	7.45	2.40	3.30	2.20
29.00	6.46	3.00	2.45	2.60
34.00	5.10	3.10	2.07	1.60
37.00	4.13	2.90	1.91	1.50

Table C.4. Average Monthly Residual Current Model versus Data Comparison At Station: ADCP 9

Model (M) Period: 8/88 Data (D) Period: 8/10 - 9/8/88

DEPTH (M)	U (E-W) CMS		V (N-S) CMS	
	M	D	M	D
6.50	-3.64	3.20	0.59	0.11
11.50	-7.45	0.38	0.93	0.32
16.50	-7.68	-2.86	2.07	0.45
21.50	-7.44	-5.17	2.54	0.54
26.50	-6.50	-6.40	1.98	0.11
31.50	-4.77	-4.99	0.63	-0.26

DEPTH (M)	U-STD (E-W) CMS		V-STD (N-S) CMS	
	M	D	M	D
6.50	8.51	4.80	4.49	1.80
11.50	8.57	3.50	3.47	1.60
16.50	8.35	4.30	3.50	1.60
21.50	7.35	3.80	3.18	1.50
26.50	5.19	3.00	2.33	1.50
31.50	3.59	2.90	1.94	0.70

Table C.5. Average Monthly Residual Current Model versus Data Comparison
At Station: ADCP 11

Model (M) Period: 9/88 Data (D) Period: 9/14 - 10/13/88

DEPTH (M)	U (E-W) CMS		V (N-S) CMS	
	M	D	M	D
11.50	22.39	21.84	1.87	-7.52
17.50	19.56	18.85	0.95	-8.79
23.50	16.41	15.52	0.09	-9.70
29.50	13.18	11.58	-0.63	-9.05
35.50	9.73	8.63	-0.90	-6.99
41.50	6.56	6.63	-1.17	-4.30
47.50	4.38	5.72	-1.47	-1.43
51.50	3.47	4.71	-1.53	-0.92

DEPTH (M)	U-STD (E-W) CMS		V-STD (N-S) CMS	
	M	D	M	D
11.50	4.01	3.80	5.60	2.20
17.50	3.53	3.50	4.12	2.30
23.50	3.53	3.10	3.57	2.20
29.50	3.54	2.80	3.14	1.70
35.50	3.53	2.60	3.11	1.50
41.50	3.47	2.60	3.07	1.40
47.50	3.20	2.80	3.03	1.50
51.50	2.50	2.80	2.68	1.80

Table C.6. Average Monthly Residual Current Model versus Data Comparison
At Station: ADCP 12

Model (M) Period: 9/88 Data (D) Period: 9/14 - 10/13/88

DEPTH (M)	U (E-W) CMS		V (N-S) CMS	
	M	D	M	D
13.00	13.97	9.54	18.52	12.21
23.00	10.01	4.62	21.83	12.69
33.00	5.33	0.81	24.44	11.57
43.00	0.54	-2.89	26.96	10.09
53.00	-1.48	-7.01	24.81	8.35
63.00	-3.39	-12.04	22.37	6.95
73.00	-4.47	-16.74	17.99	5.44
81.00	-4.62	-14.18	13.22	4.88

DEPTH (M)	U-STD (E-W) CMS		V-STD (N-S) CMS	
	M	D	M	D
13.00	6.68	2.80	10.78	2.40
23.00	6.15	2.00	8.76	1.90
33.00	5.77	1.50	7.06	1.50
43.00	5.40	1.50	5.40	1.20
53.00	4.80	1.90	5.00	1.30
63.00	4.24	2.20	4.57	1.50
73.00	3.92	2.50	4.02	1.60
81.00	3.35	2.50	3.15	1.60

Table C.7. Average Monthly Residual Current Model versus Data Comparison At Station: ADCP 13

Model (M) Period: 12/88 Data (D) Period: 12/6/88 - 1/4/89

DEPTH (M)	U (E-W) CMS		V (N-S) CMS	
	M	D	M	D
18.50	0.65	3.75	-9.44	3.15
28.50	-4.97	-1.96	-8.66	0.42
38.50	-8.61	-6.63	-7.89	-2.81
48.50	-9.72	-8.65	-6.79	-4.60
58.50	-10.14	-9.43	-5.61	-4.40
68.50	-8.88	-11.36	-4.66	-0.99

DEPTH (M)	U-STD (E-W) CMS		V-STD (N-S) CMS	
	M	D	M	D
18.50	9.63	5.30	6.82	1.40
28.50	9.70	5.30	4.99	1.70
38.50	10.59	4.90	4.51	1.90
48.50	9.43	4.00	4.01	2.20
58.50	7.76	3.10	3.51	2.80
68.50	6.02	2.10	3.10	3.10

Table C.8. Average Monthly Residual Current Model versus Data Comparison At Station: ADCP 20

Model (M) Period: 4/89 Data (D) Period: 3/18 - 4/16/89

DEPTH (M)	U (E-W) CMS		V (N-S) CMS	
	M	D	M	D
8.50	-6.10	-2.77	-0.25	-1.60
13.50	-5.76	-3.42	-1.38	-1.67
18.50	-6.72	-3.44	-1.72	-1.05
21.50	-6.88	-3.61	-1.88	-0.83

DEPTH (M)	U-STD (E-W) CMS		V-STD (N-S) CMS	
	M	D	M	D
8.50	6.85	2.00	4.29	1.00
13.50	5.09	1.80	2.80	1.00
18.50	4.67	2.00	2.41	0.90
21.50	3.88	2.10	2.32	0.90

Table C.9. Average Monthly Residual Current Model versus Data Comparison
At Station: ADCP 21

Model (M) Period: 4/89 Data (D) Period: 3/18 - 4/16/89

DEPTH (M)	U (E-W) CMS		V (N-S) CMS	
	M	D	M	D
6.00	-7.18	-9.28	10.38	-9.95
11.00	-7.15	-5.06	6.76	-4.40
16.00	-5.77	-2.49	2.00	-1.05
21.00	-5.66	-2.77	1.45	0.39
26.00	-5.96	-2.90	1.76	1.96
29.00	-6.27	-3.52	1.72	4.35

DEPTH (M)	U-STD (E-W) CMS		V-STD (N-S) CMS	
	M	D	M	D
6.00	7.62	3.50	5.04	2.60
11.00	6.77	2.30	4.63	1.60
16.00	7.13	2.40	4.38	1.60
21.00	6.08	1.80	3.81	1.10
26.00	4.82	1.30	3.16	0.90
29.00	4.26	1.30	2.78	1.60

Table C.10. Average Monthly Residual Current Model versus Data Comparison
At Station: ADCP 22

Model (M) Period: 4/89 Data (D) Period: 3/18 - 4/16/89

DEPTH (M)	U (E-W) CMS		V (N-S) CMS	
	M	D	M	D
1.50	-0.79	2.45	1.21	1.14
4.50	2.91	8.59	3.96	0.45
7.50	4.34	8.49	2.37	-0.30
10.50	4.52	8.00	0.92	0.14
13.50	4.01	5.90	0.27	0.21

DEPTH (M)	U-STD (E-W) CMS		V-STD (N-S) CMS	
	M	D	M	D
1.50	10.62	11.60	9.63	4.70
4.50	5.23	3.80	3.69	1.10
7.50	3.76	2.20	3.42	0.80
10.50	2.97	1.90	3.70	0.90
13.50	2.41	1.60	3.41	0.70